



Investigation into mitochondrial function and energy metabolism and their connectivity with protumourigenic cellular processes in Barrett's oesophagus.

September 2015

James Phelan, M.Sc (DCU) PGD (TCD) B.Sc (TCD)

Student Number: 11266965

This thesis is submitted to Trinity College Dublin, the University of Dublin, in fulfilment for the degree of Doctor of Philosophy.

**Department of Surgery, Trinity College Dublin.
School of Medicine**

Thesis Supervisor: Dr. Jacintha O'Sullivan

DECLARATION

I declare that this thesis has not been submitted as an exercise for a degree at this or any other university and it is entirely my own work.

I agree to deposit this thesis in the University's open access institutional repository or allow the library to do so on my behalf, subject to Irish Copyright Legislation and Trinity College Library conditions of use and acknowledgement.

(James Phelan)

(Date)

ACKNOWLEDGEMENTS

First and foremost, I want to thank Dr. Jacintha O’Sullivan for all the endless hard work and dedication that she has put into my project throughout the duration of the Ph.D. It is without doubt that her overwhelming knowledge, commitment and passion for the research in the field has played a major role in driving me, this Ph.D project and additional collaborations that I have been allowed to get involved in. I simply can’t thank her enough for helping me to become, I feel, a better all-round scientist. In this field of research for which I want to pursue, she is my benchmark; I feel very privileged to have worked with her, and not for the last time I hope.

Within the Department of Surgery, I would like to single out Dr. Joanne Lysaght, Dr. Graham Pidgeon, Prof. Reynolds and Dr. Niamh Lynam-Lennon for all their constructive input and support throughout the Ph.D. I also would like to thank various past and present postdocs within the Surgery department. Within the Thoracic oncology research group, I would additionally like to acknowledge the help of Dr. Martin Barr and Dr. Stephen Gray since I started working in the IMM.

In addition, I also would like to acknowledge all the collaborators who directly contributed to this Ph.D thesis, in particular, Dr. Michael Quante (Technical University of Munich) and Dr. Finbar MacCarthy (Dept. Surgery, TCD).

To all the girls in the reading room; Aoife Cannon, Róisín Byrne, Gill Moore, Maria Kavanagh, Zivile Useckaite, Niamh Gilmartin, Michelle Lowry, Niamh Clarke and Nadia Rehill. You are all so amazing and talented at what you all do; the best of luck in all future endeavours and thank you for making the latter years of my Ph.D so enjoyable and a very entertaining experience.

To my soon-to-be wife, Andreea, my little rock, thanks for being so supportive and being there for me throughout the Ph.D. Similarly, to my soon-to-be new Da and Ma, Ivan and Angela, thank you so much for everything you’ve done for me up to now. I also want to say a big thanks to my father, my brother Brendan, my sister Catriona and my soon-to-be sister Alina for all their support throughout.

Moreover, to my late best friend James Carroll, thanks for everything; we did it.

Table of Contents

DECLARATION.....	ii
ACKNOWLEDGEMENTS.....	iii
THESIS OUTPUTS	x
Publications	x
Oral Presentations	xii
Poster Presentations.....	xii
Awards	xiv
Courses.....	xiv
THESIS ABSTRACT	xvi
ABREVIATIONS.....	xviii
LIST OF FIGURES	xxiii
LIST OF TABLES	xxviii
LIST OF APPENDICES	xxix
Chapter 1	1
1.1 BARRETT'S OESOPHAGUS AND OESOPHAGEAL CANCER	2
1.1.1. Oesophageal cancer prognosis and epidemiological trends.....	2
1.1.2 Barrett's Oesophagus.....	5
1.1.3 Dysplasia in Barrett's oesophagus.....	8
1.1.4 Surveillance in Barrett's oesophagus.....	9
1.1.5 The management and treatment of Barrett's oesophagus	10
1.1.6 Risks factors in the development of Barrett's oesophagus.....	15
1.1.6.1 GORD.....	15
1.1.6.2 Age, race and sex	16
1.1.6.3 Obesity and diet.....	17
1.1.6.4 Alcohol and smoking.....	18
1.1.6.5 Helicobacter pylori, medications and socioeconomic status	19
1.2 MITOCHONDRIA: THEIR ROLE IN DISEASE INITIATION, INFLAMMATION AND CANCER	20
1.2.1 Mitochondrial structure and the mitochondrial genome	20
1.2.2 Mitochondrial DNA damage in Barrett's oesophagus	21
1.2.3 The role of the electron transport complexes in disease progression	23
1.2.3.1 Complex I.....	23
1.2.3.2 Complex II.....	23

1.2.3.3	Complex III	24
1.2.3.4	Complex IV	24
1.2.3.5	Complex V	25
1.3	OXIDATIVE PHOSPHORYLATION AND GLYCOLYSIS IN CANCER.....	27
1.4	THE ROLE OF ENERGY METABOLISM IN DRIVING DISEASE PROGRESSION IN INFLAMMATORY, HYPOXIC AND ANGIOGENIC MICROENVIRONMENTS	30
1.4.1	Molecular mediators linking energy metabolism with inflammation, hypoxia and angiogenesis.	31
1.4.1.1	Conventional mediators linking energy metabolism with inflammation and hypoxia.	
1.4.1.1.1	HIF1 α	31
1.4.1.1.2	AMPK.....	32
1.4.1.1.3	p53	33
1.4.1.2	Novel mediators linking energy metabolism with inflammation, hypoxia and angiogenesis.....	35
1.4.1.2.1	NF κ B	35
1.4.1.2.2	VEGF and PFKFB3	36
1.4.1.2.3	mTOR, succinate and STAT3	37
1.4.2	Exploring the molecular mechanisms that link energy metabolism and hypoxia: Rheumatoid arthritis and circadian rhythms.	40
1.4.2.1	Glycolysis, hypoxia and rheumatoid arthritis	40
1.4.2.2	AMPK, hypoxia and circadian rhythms.....	41
1.4.3	Reciprocal mechanisms linking energy metabolism to inflammation in gastroenterological diseases.	43
1.4.4	Innovative metabolic-based treatments and multi-targeted therapies	45
1.4.5	Chapter 1 overview.....	48
1.5	AIMS AND OBJECTIVES	49
1.5.1	Overall hypothesis	49
1.5.2	Overall aim	49
1.5.3	Specific objectives.....	49
Chapter 2	50
2.1	INTRODUCTION	51
2.2	HYPOTHESIS AND AIMS OF CHAPTER TWO	53
2.3	MATERIALS AND METHODS	54
2.3.1	Chemicals and reagents	54

2.3.2	Metaplastic, dysplastic and adenocarcinoma cell line models	54
2.3.3	In-vitro cell culture.....	54
2.3.3.1	Cell line subculturing.....	54
2.3.3.2	Preparation of stable frozen stocks	55
2.3.3.3	Reconstitution of frozen cell stocks	55
2.3.3.4	Cell counting	55
2.3.4	Screening via qRT-PCR microarray analysis.....	56
2.3.5	In-vitro validation of gene targets	56
2.3.5.1	cDNA synthesis.....	56
2.3.5.2	Quantitative real-time PCR.....	56
2.3.6	In-vivo qRT-PCR validation of gene targets	56
2.3.7	In-vitro siRNA knockdown of gene targets.....	57
2.3.8	Exploring the functional effect of siRNA knockdown on reactive oxygen species production, mitochondrial mass and mitochondrial membrane potential in-vitro	58
2.3.9	Crystal Violet Assay	58
2.3.10	Characterising the metabolic effect of siRNA knockdown utilising the Seahorse XF ^E 24 analyser in-vitro	59
2.3.11	Statistical analysis	59
2.4	RESULTS	60
2.4.1	In-vitro screening using human PCR gene microarrays	60
2.4.2	In-vivo validation of gene targets	60
2.4.3	Functional effect of BAK1, FIS1 and SFN siRNA knockdown on reactive oxygen species (ROS) production, mitochondrial mass and mitochondrial membrane potential (MMP) in-vitro	61
2.4.4	Assessing the effect of BAK1, FIS1 and SFN siRNA knockdown on cellular metabolism in-vitro.....	70
2.5	DISCUSSION	72
Chapter 3	77
3.1	INTRODUCTION	78
3.2	HYPOTHESIS AND AIMS OF CHAPTER THREE.....	81
3.3	MATERIALS AND METHODS.....	82
3.3.1	Screening via qRT-PCR microarray analysis.....	82
3.3.2	In-vitro validation of gene targets	82
3.3.3	In-vivo validation of gene targets	82

3.3.4	ATP5B, Hsp60, PKM2 and GAPDH immunohistochemistry analysis using tissue microarrays	82
3.3.5	Characterising the metabolic plasticity of Barrett’s and adenocarcinoma cell lines utilising the Seahorse XF24 analyser	83
3.3.6	Statistical analysis	84
3.4	RESULTS	85
3.4.1	In-vitro screening using human PCR gene microarrays	85
3.4.2	In-vivo validation of gene targets	89
3.4.3	Oxidative phosphorylation and glycolytic activity across Barrett’s sequence	91
3.4.4	Characterisation of oxidative metabolic plasticity in the in-vitro Barrett’s sequence..	97
3.5	DISCUSSION	99
Chapter 4	103
4.1	INTRODUCTION.....	104
4.2	HYPOTHESIS AND AIMS OF CHAPTER 4	106
4.3	METHODS.....	107
4.3.1	Squamous, metaplastic, dysplastic and adenocarcinoma cell line models.....	107
4.3.2	Assessing the effect of deoxycholic acid, N-acetylcysteine and epigallocatechin gallate in-vitro utilising the Seahorse XF24 analyser	107
4.3.3	Investigating the effect of proton-pump inhibitor use in-vitro utilising the Seahorse XF24 analyser	107
4.3.4	Exploring the effect of Quininib in-vitro utilising the Seahorse XF24 analyser	108
4.3.5	Examining the effect of Quininib on inflammatory, angiogenic and metabolic profiles in ex-vivo Barrett’s explant tissue	108
4.3.5.1	Normal squamous and Barrett’s ex-vivo explant culture	108
4.3.5.2	Ex-vivo MSD multiplex ELISA analysis.....	108
4.3.5.3	Ex-vivo qRT-PCR analysis	109
4.3.6	Statistical analysis	109
4.4	RESULTS	110
4.4.1	Examining the effect of deoxycholic acid, N-acetylcysteine and epigallocatechin gallate on energy metabolism in-vitro.	110
4.4.2	Exploring the effect of omeprazole and lansoprazole on energy metabolism in-vitro.	114
4.4.3	Investigating the effect of Quininib on inflammatory, angiogenic and metabolic profiles in-vitro and ex-vivo.	114
4.5	DISCUSSION	127

Chapter 5	132
5.1 INTRODUCTION	133
5.2 HYPOTHESIS AND AIMS OF CHAPTER FIVE	136
5.3 MATERIALS AND METHODS	137
5.3.1 Patient selection.....	137
5.3.2 ATP5B, GAPDH, p53, IL1 β , SERPINA3 and HIF1 α immunohistochemistry analysis using tissue microarrays.....	137
5.3.3 Assessing the effect of hypoxia in an in-vitro model of Barrett’s oesophagus	138
5.3.3.1 Cell Culture	138
5.3.3.2 Gene Expression Analysis	138
5.3.3.3 Assessment of secreted inflammatory and angiogenic markers	138
5.3.4 Barrett’s ex-vivo explant culture	139
5.3.5 Ex-vivo qRT-PCR analysis.....	139
5.3.6 Ex-vivo MSD multiplex ELISA analysis	139
5.3.7 Statistical analysis.....	139
5.4 RESULTS	141
5.4.1 Linking energy metabolism, p53 and inflammation in the Barrett’s tissue microenvironment in-vivo	141
5.4.2 Linking hypoxia to energy metabolism, inflammation and p53 in Barrett’s oesophagus in-vitro and in-vivo.....	146
5.4.3 Linking energy metabolism to obesity and to the length of the Barrett’s segment in the Barrett’s tissue microenvironment in-vivo.....	147
5.4.4 Linking energy metabolism to p53, inflammation, hypoxia and angiogenesis in the Barrett’s tissue microenvironment ex-vivo	151
5.4.5 Linking inflammation, hypoxia, p53, BMI and angiogenesis in the Barrett’s tissue microenvironment ex-vivo	151
5.5 DISCUSSION	155
Chapter 6	161
6.1 INTRODUCTION.....	162
6.2 HYPOTHESIS AND AIMS OF CHAPTER SIX	165
6.3 MATERIALS AND METHODS	166
6.3.1 Wild-type and PL2-IL1 β mice.....	166
6.3.2 Maintenance of wild-type and PL2-IL1 β mice	167
6.3.3 Experimental design	167

6.3.4	Histopathological analysis	171
6.3.5	Immunohistochemical analysis of ATP5B, GAPDH, p53 and HIF1 α	171
6.3.6	Statistical analyses	172
6.4	RESULTS	174
6.4.1	Examining the effect of IL1 β overexpression and diet on glycolytic profiles in transgenic mice	174
6.4.2	Assessing the effect of IL1 β overexpression and diet on oxidative phosphorylation in transgenic mice	177
6.4.3	Examining the effect of IL1 β overexpression and diet on p53 expression in transgenic mice	182
6.4.4	Examining the effect of IL1 β overexpression and diet on hypoxia in transgenic mice.....	186
6.5	DISCUSSION	191
Chapter 7	197
7.1	DISCUSSION	198
7.2	FUTURE DIRECTIONS	204
Appendices	206
References	231

THESIS OUTPUTS

Publications

Published

- **Phelan, J.J.**, Feighery, R., Eldin, O.S., Meachair, S., Cannon, A., Byrne, R., MacCarthy, F., O'Toole, D., Reynolds, J.V. and O'Sullivan, J. 'Examining the connectivity between different cellular processes in the Barrett tissue microenvironment'. *Cancer Letters*. 2015.
- **Phelan J.J.**, O'Hanlon C., Reynolds J.V., O'Sullivan J. 'The role of energy metabolism in driving disease progression in inflammatory, hypoxic and angiogenic microenvironments'. *Gastro Open J*. 2015; 1(2): 44-58.
- **Phelan J.J.**, MacCarthy F., Feighery R., et al. 'Differential expression of mitochondrial energy metabolism profiles across the metaplasia-dysplasia-adenocarcinoma disease sequence in Barrett's oesophagus'. *Cancer Letters*. 2014; 354(1): 122-131. doi: 10.1016/j.canlet.2014.07.035.
- Lynam-Lennon N., Maher S.G., Maguire A., **Phelan J.J.**, Muldoon C., et al. (2014). 'Altered Mitochondrial Function and Energy Metabolism Is Associated with a Radioresistant Phenotype in Oesophageal Adenocarcinoma'. *PLOS ONE* 9(6): e100738. doi:10.1371/journal.pone.0100738.
- O'Sullivan K.E., **Phelan J.J.**, O'Hanlon C., Lysaght J., O'Sullivan J.N., Reynolds J.V. 'The role of inflammation in cancer of the oesophagus'. *Expert review of gastroenterology & hepatology*. 2014; 8(7): 749-760. doi: 10.1586/17474124.2014.913478.

Under review

- **Phelan, J.J.**, MacCarthy, F., Ravi, N., Reynolds, J.V. and O'Sullivan, J.N. '*BAK1, FIS1 and SFN modulate mitochondrial function and energy metabolism across the metaplasia-dysplasia-adenocarcinoma sequence in Barrett's oesophagus*'. Under review with *PLOS One*.
- Biniecka, M., Canavan M., Ng C.T., Gao W., McGarry T., Smith T., **Phelan J.J.**, Ryan J., O'Sullivan J., Veale DJ and Fearon U. 'Dysregulated Bioenergetics: A Key Regulator of Joint Inflammation'. Under review with *Arthritis and Rheumatology*.
- O'Farrell N.J., Feighery R., Picardo S.L., **Phelan J.J.**, Fox E.J., Biniecka M., Dunne C., Dunne B., Reynolds J.V., O'Sullivan J.N. '*Mitochondrial mutagenesis and dysfunction along the Barrett's oesophagus to adenocarcinoma sequence and the role of antioxidants in reversing this dysfunction*'. Under review with *BMC Cancer*.

- MacCarthy, F., Duggan, S., Quinn, E., **Phelan, J.J.**, Feighery, R., O'Sullivan, J.N., Kelleher, D., Reynolds, J.V. and O'Toole, D. 'IL1 β and SERPINA3 are markers of an aggressive Barrett's Esophagus phenotype identified using mRNA sequencing'. Submitted to *PLOS One*.
- Widdowson, W.M., McGowan, A., **Phelan, J.J.**, Boran, G., Reynolds, J.V., and Gibney, J. 'Intestinal cholesterol metabolic gene expression is associated with markers of early vascular disease and atherosclerosis.' Submitted to the *Journal of Clinical Endocrinology & Metabolism*.
- Dowling, C., **Phelan, J.J.**, Cathcart, M.C., Mehigan, B., McCormick, P., Dalton, T., Coffey, J.C., O'Sullivan, J. and Kiely, P.A. 'Protein Kinase C Beta II acts as a tumour suppressor in Colorectal Cancer'. Submitted to *EMBO Molecular Medicine*.

In preparation

- **Phelan, J.J.**, Stephens, N., Reynolds, J.V., Quante, M. and O'Sullivan, J.N. '*Investigating the functional effect of IL1 β overexpression and a high fat diet in a transgenic model of Barrett's oesophagus on cellular processes, specifically energy metabolism, p53 and hypoxia*'.
- **Phelan J.J.***, Dwyer, L.*, Cannon, A., Clarke, C., Ravi, N., O'Toole, Reynolds, JV and O'Sullivan. '*Exploring the role of the mitochondrial complexes across the metaplasia-dysplasia-adenocarcinoma sequence of oesophageal cancer*'. (*Joint first author)
- O' Sullivan, K.E., Cathcart, MC, O' Regan, E., Michaelson, J., Gilmartin, N., Cannon, A., Moore, G., Gao, W., **Phelan, J.J.**, U Fearon, J Lysaght, J O' Sullivan, JV Reynolds. '*Investigation of the role of STAT3 signalling in obesity-associated adenocarcinoma of the oesophagus*'.
- Malik, V., **Phelan, J.J.**, Johnston, C., O'Sullivan, J.V., Feighery, R., Claxton, Z., Muldoon, C. and Reynolds, J.V. '*Implication of F-FDG PET negative oesophageal carcinoma*'.
- Dunne, C., Tosetto, M., **Phelan, J.J.**, Biniacka, M., Mulcahy, H. and O'Sullivan, J. '*Manipulation of clusterin and cyclin D1 regulate mitochondrial cellular function and alter mitochondrial genes involved in mitochondrial biogenesis and respiration*'.
- Oficjalska, K., **Phelan, J.J.**, O'Sullivan, J.N. and Creagh, E. '*Elucidating the role of caspases 1, 4 and 5 across the intestinal metaplasia-adenocarcinoma disease sequence in Barrett's oesophagus*'.
- Dunne, M.R., Michielsen, A.J., **Phelan, J.J.**, Maguire, A.A., O'Sullivan, K.E., Feighery, R., Tosetto, M., Doyle, B., Cathcart, M.C., Watson, J., Kay, E., Sheahan, K., Hyland, J., Ravi, N.,

Reynolds, J.V., Ryan, E.J. and O'Sullivan, J.N. 'HLA-DR expression in tumour epithelia correlates with patient survival in upper and lower gastrointestinal cancers'.

Oral Presentations

Invited Oral Presentations (presenting author)

- "Metabolism and its link with the tissue microenvironment in the Barrett's to Oesophageal Cancer disease sequence". January 2015, Trinity College Dublin Cancer Review, TBSI, Trinity College Dublin, Dublin, Ireland.

Invited International Oral Presentations (presenting author)

- "Mitochondrial function and changes in energy metabolism across the disease state in Barrett's oesophagus". October 2012, Global engagement of graduate education: collaborative interactions in health sciences, University of Michigan, Ann Arbor, USA.

National Oral Presentations (presenting author)

- "Examining the link between metabolism, hypoxia, inflammation, p53 and obesity in Barrett's oesophagus". December 2014, 7th Trinity College Postgraduate Research Day, Trinity Centre for Sciences, Trinity College, Tallaght Hospital, Dublin, Ireland.
- "Elucidating the link between metabolism, hypoxia, inflammation, p53 and obesity in Barrett's oesophagus". November 2014, 17th Annual Meeting of the Institute of Molecular Medicine, Trinity Centre for Sciences, Trinity College, St. James's Hospital, Dublin, Ireland.
- "Changes in mitochondrial dysfunction and energy metabolism in the Barrett's oesophagus to adenocarcinoma disease sequence". March 2013, *Irish Association of Cancer Research (IACR)*, The Crown Plaza, Santry, Dublin, Ireland.
- "Early preneoplastic reprogramming of mitochondrial energy metabolism and mitochondrial gene function across the disease state in Barrett's oesophagus". November 2012, Irish Area Section of the Biochemical Society (IASBS): regulation of metabolism in cancer and immune cells, TBSI, Trinity College, Dublin, Ireland. **Awarded best oral presentation.**

Poster Presentations

International Poster Presentation (presenting author)

- "Deciphering the intrinsic link between metabolism, inflammation, hypoxia, p53 and obesity in the Barrett's Oesophagus microenvironment". April 2015, Research Progress in

Barrett's Oesophagus: 9th National Symposium, University College London (UCL), United Kingdom.

- "Shifts in mitochondrial energy metabolism are correlated with disease progression in Barrett's oesophagus." July 2014, European Association of Cancer Research (EACR23), Munich, Germany.
- "Alterations in mitochondrial energy metabolism across the disease sequence in Barrett's esophagus." March 2014, Keystone Tumor Metabolism (X6) (Metabolism and Angiogenesis X5), Whistler, Canada.
- "Alterations in Mitochondrial Energy Metabolism Profiles across the Metaplasia-Dysplasia-Adenocarcinoma Disease sequence in Barrett's Oesophagus". June 2013, Abcam's Cancer and Metabolism Conference, Amsterdam, Holland.
- "Barrett's oesophagus exhibits shifts in mitochondrial function and energy metabolism". April 2013, Research Progress in Barrett's Oesophagus: 7th National Symposium, University College London (UCL), United Kingdom.

National Poster Presentation (presenting author)

- "Investigating the intrinsic link between hypoxia, metabolism, inflammation, p53 and obesity in Barrett's oesophagus." May 2015, Keystone's Hypoxia- From Basic Mechanisms to Therapeutics, Dublin, Ireland.
- "Elucidating the link between metabolism, hypoxia, inflammation, p53 and obesity in Barrett's Oesophagus". Feb 2015, Irish Association of Cancer Research (IACR), Limerick, Ireland.
- "Elucidating the link between metabolism, hypoxia, inflammation, p53 and obesity in Barrett's oesophagus". November 2014, 17th Annual Meeting of the Institute of Molecular Medicine, Trinity Centre for Sciences, Trinity College, St. James's Hospital, Dublin, Ireland.
- "The association between metabolism, inflammation, p53, hypoxia and obesity in Barrett's oesophagus in-vivo." September 2014, 9th Annual Trinity College Dublin Cancer Conference, Dublin, Ireland.
- "Deoxycholic acid, antioxidants and proton-pump inhibitors induce alterations in mitochondrial energy metabolism in Barrett's oesophagus". Feb 2014, Irish Association of Cancer Research (IACR), Galway, Ireland.
- "Examining the functional role of DCA, antioxidants, proton-pump inhibitors and QB on mitochondrial metabolism in Barrett's Oesophagus". November 2013, School of Medicine Postgraduate Research Day, Trinity College Dublin, Ireland.

- “Alterations in mitochondrial energy metabolism are correlated with disease progression across the metaplasia-dysplasia-adenocarcinoma disease sequence in Barrett’s Oesophagus”. November 2013, School of Medicine Postgraduate Research Day, Trinity College Dublin, Ireland.
- “An investigation into the role of DCA, antioxidants, proton-pump inhibitors and QB on mitochondrial energy metabolism in Barrett’s Oesophagus”. November 2013, 16th Annual Meeting of the Institute of Molecular Medicine, Trinity Centre for Sciences, Trinity College, St. James’s Hospital, Dublin, Ireland.
- “Mitochondrial energy metabolism and mitochondrial gene function is reprogrammed early across the metaplastic-dysplastic-cancer sequence of events in Barrett’s Oesophagus”. November 2012, 15th Annual Meeting of the Institute of Molecular Medicine, Trinity Centre for Sciences Trinity College, St. James’s Hospital, Dublin, Ireland.
- “Mitochondrial energy metabolism and mitochondrial gene function is reprogrammed early across the metaplastic-dysplastic-cancer sequence of events in Barrett’s Oesophagus”. September 2012, School of Medicine Postgraduate Research Day, Trinity College Dublin, Ireland.
- “Altered pattern of energy metabolism during disease progression in Barrett’s Oesophagus”. September 2012, EACR-IACR Joint Conference: The Tumour Microenvironment, Burlington Hotel, Dublin, Ireland.
- “Mitochondrial energy metabolism and mitochondrial gene function is reprogrammed early across the metaplastic-dysplastic-cancer sequence of events in Barrett’s Oesophagus”. July 2012, UK Clinical Research Facilities Network, Trinity College Dublin, Ireland.

Awards

- **Best Oral Presentation**, November 2012, Irish Area Section of the Biochemical Society (IASBS): regulation of metabolism in cancer and immune cells, Trinity College Dublin, Ireland.
- **‘Honourable Mention’ for poster**, July 2012, UK Clinical Research Facilities Network, Trinity College Dublin, Ireland.

Courses

- **Postgraduate Diploma in Statistics (Level 9) (Distinction received)**, September 2012-May 2013, Trinity College Dublin, Ireland.

- **CSTAR's Statistics with SPSS: An Introductory Course**, March 2012, University College Dublin (UCD), Belfield, Ireland.
- **Certificate of Good Clinical Practice**, January 2015, Clinical Research Facility, St. James's hospital, Dublin, Ireland.

THESIS ABSTRACT

Introduction

Contemporary clinical management of Barrett's oesophagus has highlighted the lack of accurate predictors of neoplastic progression. Currently all Barrett's patients undergo surveillance, however, only a subset of patients progress to oesophageal adenocarcinoma (OAC). Understanding the biology of why only a subset of these patients with Barrett's oesophagus progress is a major clinical challenge. Abnormal mitochondrial function has long been linked with the development and progression of various cancers. Transitioning from a normal squamous cell to a malignant cancer cell is a multi-step pathogenic process which includes interactions between cancer-associated gene activation, metabolic reprogramming and tumour-induced changes in the microenvironment. The aim of this Ph.D thesis was to characterise mitochondrial function and energy metabolism across the Barrett's disease sequence, to assess if markers of metabolism could have diagnostic potential and to further investigate the connection between metabolism and other key cellular processes activated in the Barrett's tissue microenvironment, known to be previously linked with disease progression.

Methods

PCR microarrays were employed to identify gene changes associated with mitochondrial function and mitochondrial energy metabolism in Barrett's, dysplastic and OAC cells *in-vitro*. Upon identification, genes were validated in cell lines *in-vitro* and using *in-vivo* patient samples across the metaplastic-dysplastic-OAC disease sequence. Functional assessment of mitochondrial function genes were examined through a siRNA knockdown approach. Surrogate protein markers of oxidative phosphorylation (ATP5B/HSP60) and glycolysis (GAPDH/PKM2) were immunohistologically assessed across the metaplastic-dysplastic-OAC disease sequence *in-vivo* using tissue microarrays. Real-time metabolic profiles were challenged using Seahorse technology. The effect of the bile acid deoxycholic acid (DCA), proton pump inhibitors, antioxidants and a novel small molecule inhibitor (Quininib) on the modulation of cellular energetic was additionally assessed. The link between energy metabolism and other key cellular processes (inflammation, hypoxia, p53) in the Barrett's oesophagus microenvironment was examined immunohistologically by assessing the expression of surrogate markers (IL1 β /SERPINA3, HIF1 α , p53) of these processes in cell lines *in-vitro*, in tissue microarrays *in-vivo* and in Barrett's *ex-vivo* explant tissue. Furthermore, a transgenic mouse model of Barrett's oesophagus was utilised to elucidate if IL1 β overexpression and changes in dietary lifestyle could modulate

oxidative phosphorylation, glycolysis, HIF1 α and p53 thereby potentially promoting disease progression in Barrett's oesophagus.

Results

PCR microarrays identified 4 mitochondrial function genes (*BAK1*, *FIS1*, *SFN*, *CDKN2A*) and 3 mitochondrial metabolism genes (*ATP12A*, *COX4I2*, *COX8C*) differentially expressed across the metaplastic-dysplastic-OAC sequence *in-vitro*. Upon *in-vitro* validation of these gene targets, all genes exhibited differential expression profiles in *in-vivo* patient material. Altered expression was specific to Barrett's tissue compared to matched normal adjacent tissue. siRNA knockdown of the *BAK1*, *FIS1* and *SFN* genes resulted in significant decreases in mitochondrial membrane potential in Barrett's cells and altered metabolic profiles in OAC cells *in-vitro*. We also demonstrate significant increases in the metabolic markers ATP5B, HSP60, GAPDH and PKM2 in epithelial tissue across the metaplastic-dysplastic-OAC sequence *in-vivo*. In addition, we show that the oxidative metabolism marker, ATP5B, segregated Barrett's non progressors and progressors to neoplastic progression in first time surveillance biopsy tissue. Moreover, Seahorse analysis of oxidative metabolism in Barrett's cells illustrate that Barrett's cells rely significantly more on oxidative metabolism than to OAC cells. We also show that DCA decreases oxidative phosphorylation in Barrett's cells, however, increases both metabolic pathways in neoplastic cells *in-vitro*. Moreover, DCA treated Barrett's and OAC cells supplemented with the antioxidant EGCG exhibit significantly lower levels of oxidative phosphorylation and glycolysis respectively. The proton pump inhibitor lansoprazole and Quininib also exhibited anti-metabolic potential. Furthermore, we show that energy metabolism is linked with inflammation, hypoxia, p53 and obesity in the Barrett's tissue microenvironment *in-vivo* and *ex-vivo*. Using a transgenic mouse model of Barrett's oesophagus, we demonstrate that induction of inflammation through IL1 β manipulation and a high fat diet can modulate the expression levels of GAPDH, ATP5B, p53 and HIF1 α .

Discussion

This Ph.D thesis demonstrates, for the first time, that changes in mitochondrial function, oxidative phosphorylation and glycolysis play central roles in disease progression in Barrett's oesophagus. This thesis also identifies a marker of oxidative phosphorylation, ATP5B, with potential clinical utility in segregating those Barrett's patients at higher risk of neoplastic progression. The *in-vivo* and *ex-vivo* findings demonstrated in the Barrett's tissue microenvironment in patients and also in mice show that energy metabolism and its associated processes could potentially support disease progression in Barrett's oesophagus, thereby highlighting future potential therapeutic opportunities in the field.

ABREVIATIONS

18S – 18S ribosomal RNA

2-DG – 2-deoxy-D-glucose

5-FU - 5-fluorouracil

ADP - Adenosine diphosphate

AICAR - 5-aminoimidazole-4-carboxamide ribonucleoside

AKT – Protein kinase B

AMPK - AMP-activated protein kinase

ANG-1 – Angiopoietin 1

ATP – Adenosine triphosphate

ATP12A - ATPase, H⁺/K⁺ transporting, nongastric, alpha polypeptide

ATP5B – Adenosine triphosphate isoform 5B

B2M – β -2-microglobulin

BAK1 - Bcl-2 homologous antagonist killer

BCM – Barrett's conditioned media

BEBM – Bronchial Epithelial Cell Growth Medium

bFGF – Basic fibroblast growth factor

BMI – Body mass index

BPE – Bovine pituitary extract

CDKN2A – Cyclin-dependent kinase inhibitor 2A

cDNA – Complementary deoxyribonucleic acid

CO₂ – Carbon Dioxide

COX4I2 - Cytochrome c oxidase subunit 4 isoform 4

COX6C – Cytochrome c oxidase subunit 6

COX8C – Cytochrome c oxidase subunit 8

CRY1/2 – Cryptochrome protein 1/2

Ct – Cycle threshold

DAB - 3,3'-diaminobenzidine

DCA – Deoxycholic acid

dH₂O – Distilled water

DMSO – Dimethylsulfoxide

DNA – Deoxyribonucleic acid

ECAR – Extracellular acidification rate

EDTA - Ethylenediaminetetraacetic acid

EGCG - Epigallocatechin gallate

ERK – Extracellular signal-regulated kinase

ETS-1 – C-ets-1

F26B – Fructose-2,6-bisphosphate

FADH₂ – Flavin adenine dinucleotide

FBP - fructose-1,6-bisphosphatase

FBS – Fetal bovine serum

FBXL3 - F-box/LRR-repeat protein 3

FCCP - Trifluorocarbonyl cyanide phenylhydrazone

FIS1 – Mitochondrial fission 1 protein

GA-1000 – Gentamicin/Amphotericin-B

GAPDH – Glyceraldehyde 3-phosphate dehydrogenase

GI – Gastrointestinal

GLUT1 - Glucose transporter 1

GORD – Gastroesophageal reflux disease

GRO α - GRO-alpha

HC – Hydrocortisone

hEGF – Human epidermal growth factor

HGD – High-grade dysplasia

HIF1 α – Hypoxia-inducible factor 1-alpha

HSP60 – Heat shock protein 60

IBD – Inflammatory bowel disease

ICAM-1 – Intercellular adhesion molecule-1

IgG – Immunoglobulin G

IL-12p70 – Interleukin-12

IL1 β – Interleukin-1 β

IL-2/4/6/8/10 – Interleukin-2/4/6/8/10

IxP – Intensity multiplied by percentage positivity

LDH – Lactate dehydrogenase

LGD – Low-grade dysplasia

LKB1 – Liver kinase B1

LPS – Lipopolysaccharide

MCP-1 - Monocyte chemoattractant protein-1

MCT1 – Monocarboxylate transporter 1

MIP3 α – Macrophage inflammatory protein-3 alpha

MMP – Mitochondrial membrane potential

MMP2/9 - Matrix metalloproteinase 2/9

mtDNA – Mitochondrial DNA

mTOR – Mammalian target of rapamycin

NAC - N-acetylcysteine

NADH - nicotinamide adenine dinucleotide

NADPH – Nicotinamide adenine dinucleotide phosphate

NFκB – Nuclear factor kappa-light-chain-enhancer of activated B cells

OAC – Oesophageal adenocarcinoma

OCR – Oxygen consumption rate

OSCC - Oesophageal squamous cell carcinoma

OXPPOS – Oxidative phosphorylation

p53 – Tumour protein p53

PAI-1 – Plasminogen activator inhibitor-1

PBS – Phosphate-buffered saline

PCR – Polymerase chain reaction

PK-2 – Pyruvate dehydrogenase kinase 2

PFK1 – Phosphofructose kinase 1

PFKFB3 - 6-phosphofructo-2-kinase/fructose-2,6-bisphosphatase-3

PHD2 – Prolyl hydroxylase domain protein 2

PI3K - phosphoinositide 3-kinase

PKM2 – Pyruvate kinase isoform 2

PPP – Pentose phosphate pathway

qRT-PCR – Quantitative/real-time reverse transcription polymerase chain reaction

rcf – Relative centrifugal force

RNA – Ribonucleic acid

ROS – Reactive oxygen species

RPMI – Roswell Park Memorial Institute Medium

RT-PCR – Reverse transcription polymerase chain reaction

SCJ – Squamocolumnar junction

SCO2 - Synthesis of cytochrome c oxidase 2

SERPINA3 - Alpha-1-antichymotrypsin/Serpin A3

SFN – Stratifin

SIM – Specialised intestinal metaplasia

siRNA – Small interfering RNA

SIRT1 - Silent mating type information regulation 2 homolog 1

STAT3 - Signal transducer and activator of transcription 3

TIGAR – TP53-induced glycolysis and apoptosis regulator

TMA – Tissue microarrays

TNF α – Tumour necrosis factor alpha

TORC1 – Rapamycin complex 1

VCAM-1 - Vascular cell adhesion molecule-1

VEGF – Vascular endothelial growth factor

VEGFR2 – Vascular epithelial growth factor receptor 2

LIST OF FIGURES

Figure 1. The incidence of oesophageal cancer in the Irish population between the years 1994-2012.

Figure 2. The 5-year age-standardised survival rates of those with oesophageal cancer within the Irish population between the years 1994-2012.

Figure 3. The endoscopic detection and histology of Barrett's oesophagus.

Figure 4. The management and treatment algorithm for patients with Barrett's oesophagus.

Figure 5. The mitochondrial genome and its role in cancer.

Figure 6. The mitochondrial electron transport chain.

Figure 7. The differences between oxidative phosphorylation, anaerobic glycolysis and aerobic glycolysis (the Warburg effect).

Figure 8. Conventional mediators linking energy metabolism with inflammation and hypoxia.

Figure 9. Novel mediators linking energy metabolism with inflammation, hypoxia and angiogenesis.

Figure 10. Human PCR gene microarray screen across the Barrett's cell lines.

Figure 11. *In-vitro* validation of global mitochondrial function gene targets found to be differentially expressed across the Barrett's cell lines.

Figure 12. Global mitochondrial function gene expression across the disease sequence in diseased versus matched normal adjacent *in-vivo* samples.

Figure 13. Assessing the effect of *BAK1*, *FIS1* and *SFN* siRNA knockdown on cell number in QH and OE33 cells *in-vitro* using a crystal violet assay.

Figure 14. Functional effect of *BAK1* siRNA knockdown on reactive oxygen species production, mitochondrial mass and mitochondrial membrane potential in the QH and OE33 cell lines *in-vitro*.

Figure 15. Functional effect of *FIS1* siRNA knockdown on reactive oxygen species production, mitochondrial mass and mitochondrial membrane potential in the QH and OE33 cell lines *in-vitro*.

Figure 16. Functional effect of *SFN* siRNA knockdown on reactive oxygen species production, mitochondrial mass and mitochondrial membrane potential in the QH and OE33 cell lines *in-vitro*.

Figure 17. Investigating the metabolic effect of siRNA-induced knockdown of *BAK1*, *FIS1* and *SFN* in the QH and OE33 cell lines *in-vitro*.

Figure 18. ‘Differential expression of mitochondrial energy metabolism profiles across the metaplasia–dysplasia–adenocarcinoma disease sequence in Barrett’s oesophagus’.

Figure 19. Human PCR gene microarray screen across the Barrett’s cell lines.

Figure 20. *In-vitro* validation of mitochondrial energy metabolism gene targets differentially expressed across Barrett’s oesophagus and OAC cell lines.

Figure 21. Mitochondrial energy metabolism gene expression across the disease sequence in diseased versus matched normal adjacent *in-vivo* samples.

Figure 22. Epithelial immunohistochemical tissue expression of the oxidative phosphorylation protein biomarkers, ATP5B and Hsp60, across the metaplasia-dysplasia-adenocarcinoma disease sequence.

Figure 23. Epithelial and stromal immunohistochemical tissue expression of the glycolytic protein markers, PKM2 and GAPDH, across the metaplasia-dysplasia-adenocarcinoma disease sequence.

Figure 24. Longitudinal immunohistochemical assessment of mean ATP5B, HSP60, PKM2 and GAPDH tissue microarray expression in Barrett’s non-progressors and progressors to OAC.

Figure 25. Seahorse assessment of mitochondrial respiration, ATP synthesis maximal respiratory capacity, non electron transport respiration and proton leak between the Barrett’s and adenocarcinoma *in-vitro* cell lines.

Figure 26. Investigating the effect of deoxycholic acid on oxidative phosphorylation and glycolysis across the *in-vitro* squamous-metaplasia-dysplasia-adenocarcinoma sequence.

Figure 27. Examining the effect of the antioxidants N-acetylcysteine and epigallocatechin gallate on deoxycholic acid-induced alterations in oxidative phosphorylation and glycolysis across the *in-vitro* squamous-metaplasia-dysplasia-adenocarcinoma sequence.

Figure 28. Assessing the effect of the antioxidant epigallocatechin gallate on deoxycholic acid-induced alterations in OCR and ECAR across the *in-vitro* squamous-metaplasia-dysplasia-adenocarcinoma sequence.

Figure 29. Exploring the effect of the proton pump inhibitors omeprazole and lansoprazole on oxidative phosphorylation and glycolysis across the *in-vitro* squamous-metaplasia-dysplasia-adenocarcinoma sequence.

Figure 30. Investigating the effect of the novel small molecular inhibitor, Quininib, on oxidative phosphorylation and glycolysis across the *in-vitro* squamous-metaplasia-dysplasia-adenocarcinoma sequence.

Figure 31. Characterisation of untreated and Quininib treated matched normal adjacent and Barrett's tissue.

Figure 32. Characterising the expression of an array of secreted inflammatory and angiogenic mediators in an *ex-vivo* model of Barrett's oesophagus.

Figure 33. Assessing the expression of an array of secreted inflammatory and angiogenic mediators in an *ex-vivo* model of Barrett's oesophagus.

Figure 34. Investigating the inflammatory and angiogenic profile of an *ex-vivo* model of Barrett's oesophagus subsequent to treatment with the small molecule inhibitor Quininib.

Figure 35. Characterising the expression of an array of secreted inflammatory and angiogenic mediators in an *ex-vivo* model of Barrett's oesophagus subsequent to treatment with the small molecule inhibitor Quininib.

Figure 36. Investigating the metabolic gene profile of an *ex-vivo* model of Barrett's oesophagus subsequent to treatment with the small molecule inhibitor Quininib.

Figure 37. Assessing secreted lactate and SMAC/Diablo levels in an *ex-vivo* model of Barrett's oesophagus subsequent to treatment with the small molecule inhibitor Quininib.

Figure 38. The link between energy metabolism and p53 in Barrett's oesophagus *in-vivo*.

Figure 39. Linking p53 and inflammation in Barrett's oesophagus *in-vivo*.

Figure 40. The association between energy metabolism and inflammation in Barrett's oesophagus *in-vivo*.

Figure 41. Investigating the effect of hypoxia on metabolic, inflammatory and angiogenic profiles in an *in-vitro* model of Barrett's oesophagus.

Figure 42. Linking hypoxia to energy metabolism, inflammation and p53 in Barrett's oesophagus *in-vivo*.

Figure 43. Linking energy metabolism to obesity and to the length of the Barrett's segment in Barrett's oesophagus *in-vivo*.

Figure 44. The Barrett's oesophagus microenvironment.

Figure 45. The Epstein Bar virus IL1 β construct.

Figure 46. Study protocol.

Figure 47. Anatomy of all male mice within the study post treatment prior to formalin fixation and paraffin embedding.

Figure 48. Anatomy of all female mice within the study post treatment prior to formalin fixation and paraffin embedding.

Figure 49. Histology of PL2-IL1 β and wild-type mice.

Figure 50. Examining the functional effect of IL1 β induction on glycolytic profiles between transgenic wild-type and IL1 β mice.

Figure 51. Investigating the effect of a high fat diet on glycolytic profiles in transgenic wild-type and IL1 β mice.

Figure 52. Examining the functional effect of IL1 β induction on oxidative phosphorylation between transgenic wild-type and IL1 β mice.

Figure 53. Investigating the effect of a high fat diet on oxidative phosphorylation in transgenic wild-type and IL1 β mice.

Figure 54. Summarising the effect of IL1 β manipulation on metabolism in mice fed chow and high fat (B) diets.

Figure 55. Summarising the effect of a high fat diet on metabolism in wild-type and PL2-IL1 β mice.

Figure 56. Examining the functional effect of IL1 β induction on p53 expression between transgenic wild-type and IL1 β mice.

Figure 57. Investigating the effect of a high fat diet on p53 in transgenic wild-type and IL1 β mice.

Figure 58. Summarising the effect of IL1 β overexpression and a high fat diet on p53 expression in wild type and PL2-IL1 β mice.

Figure 59. Examining the functional effect of IL1 β induction on HIF1 α expression between transgenic wild-type and IL1 β mice.

Figure 60. Investigating the effect of a high fat diet on HIF1 α in transgenic wild-type and IL1 β mice.

Figure 61. Summarising the effect of IL1 β manipulation and diet on HIF1 α expression in wild type and transgenic mice.

Figure 62. Investigating the interaction between transgenic mouse models and diet and their effect on glycolysis.

LIST OF TABLES

Table 1. Categories of dysplasia: Histological features and endoscopic surveillance

Table 2. Metabolic-based compounds.

Table 3. Mitochondrial function gene microarray screen between QH and OE33 cell lines

Table 4. Energy Metabolism Gene Microarray Screen between QH and OE33 Cell Lines

Table 5. A summary of the inhibitory effect of Quininib on markers of angiogenesis, inflammation and metabolism *ex-vivo*.

Table 6. Comparing the association between metabolism, inflammation, hypoxia, p53, obesity and the length of the Barrett's segment *in-vivo* using Spearman ρ and multiple regression analyses.

Table 7. The association between metabolism and inflammation, hypoxia, p53 and angiogenesis in Barrett's *ex-vivo* explant tissue.

Table 8. The association between inflammation, hypoxia, p53, BMI and angiogenesis in Barrett's *ex-vivo* explant tissue.

LIST OF APPENDICES

Appendix A. Mitochondrial function gene microarray screen between GO and QH cell lines.

Appendix B. Mitochondrial function gene microarray screen between GO and OE33 cell lines.

Appendix C. Energy Metabolism Gene Microarray Screen between GO and QH Cell Lines.

Appendix D. Energy Metabolism Gene Microarray Screen between GO and OE33 Cell Lines.

Appendix E. *In-vitro* and *in-vivo* validation of *COX6C*.

Appendix F. Stromal immunohistochemical tissue expression of the oxidative phosphorylation protein markers, ATP5B and HSP60, across the metaplasia-dysplasia-adenocarcinoma disease sequence.

Appendix G. Epithelial and stromal immunohistochemical tissue intensity of the oxidative phosphorylation protein markers, ATP5B and HSP60, across the metaplasia-dysplasia-adenocarcinoma disease sequence.

Appendix H. Epithelial immunohistochemical tissue expression of the glycolytic protein biomarkers, PKM2 and GAPDH, across the metaplasia-dysplasia-adenocarcinoma disease sequence in matched normal adjacent tissue.

Appendix I. Epithelial and stromal immunohistochemical tissue intensity of the glycolytic protein biomarkers, PKM2 and GAPDH, across the metaplasia-dysplasia-adenocarcinoma disease sequence.

Appendix J. Stromal immunohistochemical positivity of the oxidative phosphorylation protein markers, ATP5B and HSP60, and the glycolytic protein biomarkers, PKM2 and GAPDH, across the metaplasia-dysplasia-adenocarcinoma disease sequence in matched normal adjacent tissue.

Appendix K. Characterising real-time metabolism at baseline in QH and OE33 cell lines.

Appendix L. Investigating the real-time effect of complex V (ATP synthase) inhibition on glycolysis in the Barrett's (QH) and adenocarcinoma (OE33) cell lines *in-vitro*.

Appendix M. *In-vitro* and *in-vivo* validation of *ETS-1*.

Appendix N. Investigating the association between ATP5B and the transcription factor ETS-1 across the squamous-metaplasia-dysplasia-adenocarcinoma disease sequence *in-vivo*.

Appendix O. Investigating the effect of two Quininib analogues, CC8 and OS-1, on metabolism between metaplasia and adenocarcinoma cell lines *in-vitro*.

Appendix P. Longitudinal immunohistochemical assessment of p53 and ATP5B expression in Barrett's non-progressors and progressors to LGD and HGD.

Appendix Q. Investigating the effect of hypoxia on inflammatory and angiogenic profiles in an *in-vitro* model of Barrett's oesophagus.

Appendix R. Investigating the effect of hypoxia on cell number in the Barrett's QH cell line *in-vitro*.

Appendix S. Examining the expression of p53, HIF1 α and ATP5B in initial and most recent matched longitudinal Barrett's tissues.

Appendix T. Linking obesity to p53 status, HIF1 α and IL1 β in Barrett's oesophagus *in-vivo*.

Appendix U. Assessing the dependencies between factors taking into account the combined effect of all factors *in-vivo*.

Appendix V. Characterisation of matched normal adjacent and Barrett's tissue.

Appendix W. The association between metabolism, inflammation, angiogenesis and BMI in matched normal adjacent tissue from patients with Barrett's oesophagus *ex-vivo*.

Appendix X. The association between angiogenesis, inflammation and SMAC/Diablo in matched normal adjacent tissue from patients with Barrett's oesophagus *ex-vivo*.

Chapter 1

Introduction

1.1 BARRETT'S OESOPHAGUS AND OESOPHAGEAL CANCER

1.1.1. Oesophageal cancer prognosis and epidemiological trends

Oesophageal cancer is one of the most rapidly increasing malignancies in the world (1). The overall 5-year survival rate in those with oesophageal carcinoma ranges from 15% to 25% worldwide with positive prognosis associated with earlier diagnosis (2). Squamous-cell carcinoma is the pre-dominant histological type of oesophageal carcinoma worldwide, however, the incidence of oesophageal adenocarcinoma (OAC) in countries such as the United Kingdom, United States, Australia and some western European countries, including Ireland, now exceeds that of squamous-cell carcinoma (2). For example, while the incidence rates for most cancers continues to decline in the United States, the incidence of OAC has increased greater than six-fold over the past four decades (3).

With on average 386 new cases of oesophageal cancer diagnosed in Ireland per year, the current incidence of oesophageal carcinoma remains steady (figure 1A) with a 2.17 fold predominance in males compared to females according to the National Cancer Registry of Ireland (figure 1B) (4). For OAC, this ratio increases to 3.6 (792 cases male; 220 cases female) in Ireland between the years 2006-2011 (4). Age is additionally associated with increased incidence of oesophageal cancer in the Irish population (4). The period 2006-2012 has additionally seen an increase of 6% in the 5-year survival rate in those with oesophageal carcinoma compared to the period 1994-2005 (figure 2A) making the current 5-year survival rate approximately 18.1% in Ireland (figure 2B) (4). In those with OAC in Ireland, 5-year survival rates are noticeably stage dependent and are currently 84.2%, 42.4%, 12% and 3.5% for stages 1-4 respectively (figure 2C) (4). For cases in the period 2006-2011, the estimated 5-year survival for squamous cell carcinoma and OAC in Ireland is currently 15.4% and 7.4% respectively (4). In Ireland, oesophageal cancer is responsible for 376 deaths per year and now ranks 6th amongst the most common invasive cancer causing deaths (4).

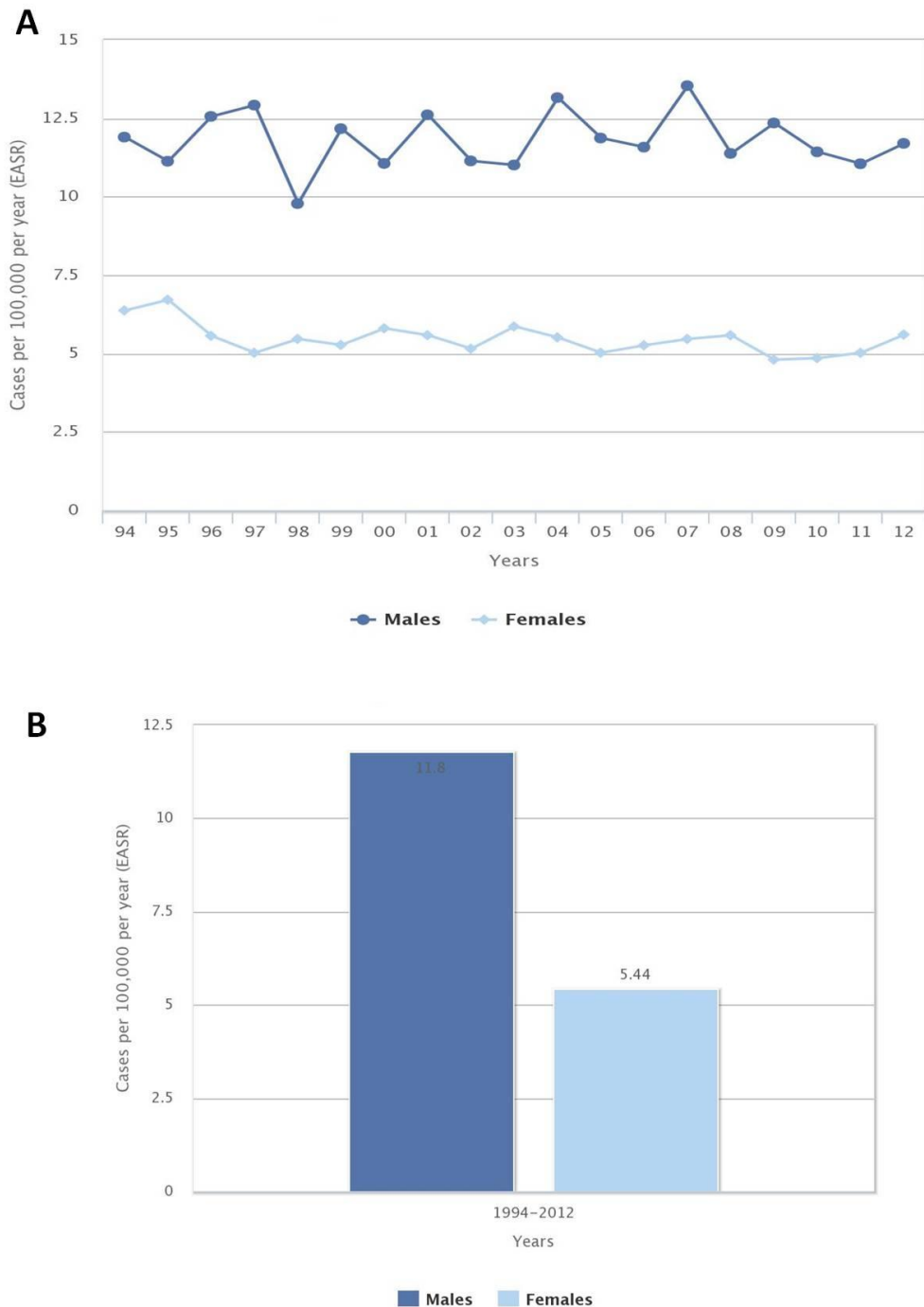


Figure 1. The incidence of oesophageal cancer in the Irish population between the years 1994-2012. (A) Overall, the incidence of oesophageal cancer in the Irish population remains steady with the current annual percentage change in incidence rates of -0.9% in females and 0.0% in males. **(B)** There is a 2.17 fold predominance in the incidence of oesophageal cancer in males versus females in Ireland (compared to 3.6 for OAC). Data obtained from the National Cancer Registry of Ireland (NCRI) database.

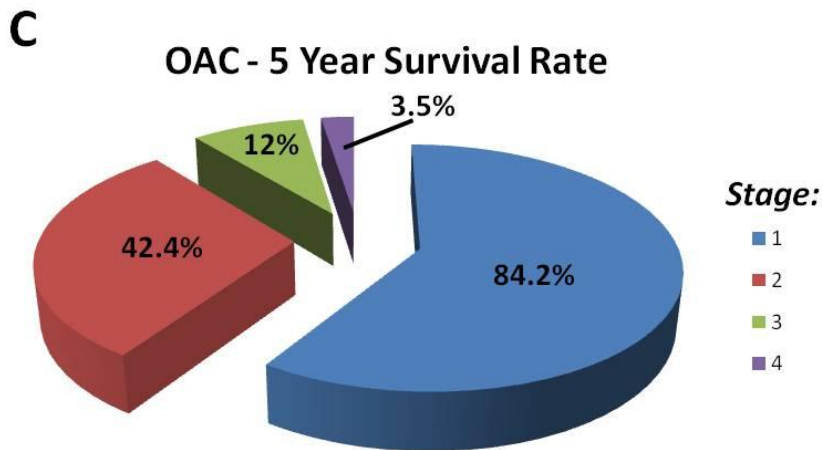
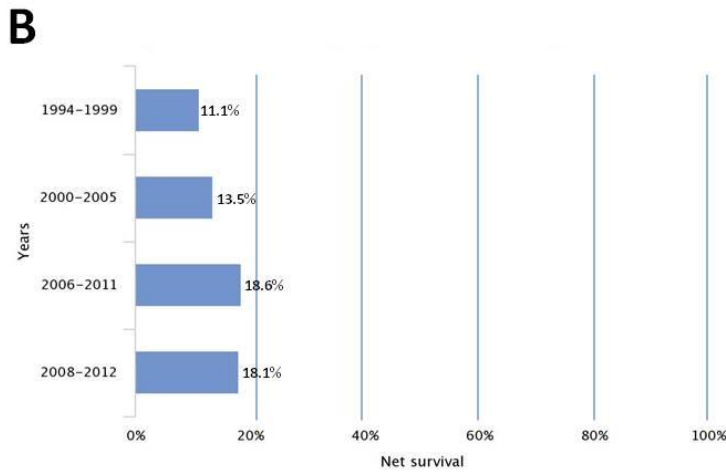
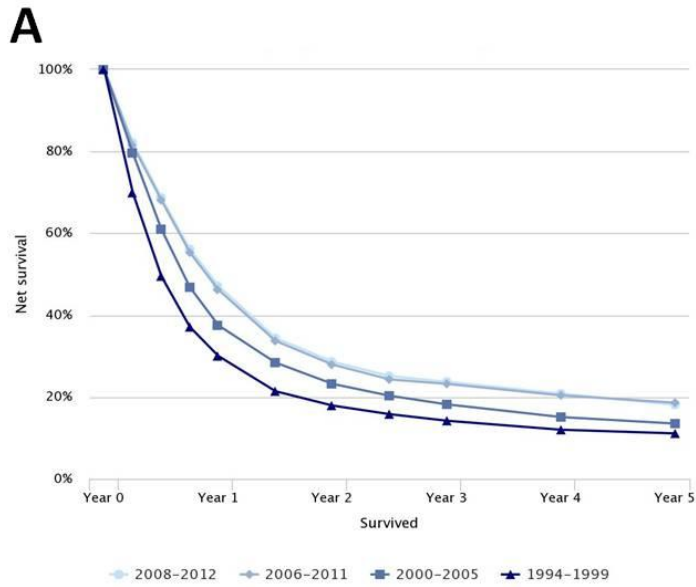


Figure 2. The 5-year age-standardised survival rates of those with oesophageal cancer within the Irish population between the years 1994-2012. (A) There has been an increase in the 5-year survival rate of approximately 6% between the years ranging from 1994-2005 and 2006-2012. **(B)** The current 5-year survival rate in the Irish population in those with oesophageal cancer is 18.1%. **(C)** 5-year survival rates in those with stage 1-4 oesophageal adenocarcinoma are 84.2%, 42.4%, 12% and 3.5% respectively. Data obtained from the National Cancer Registry of Ireland (NCRI) database.

1.1.2 Barrett's Oesophagus

Barrett's oesophagus, defined as intestinal metaplasia of the distal oesophagus, predominantly arises from gastroesophageal reflux disease (GORD) and is a precursor lesion in the majority of patients with oesophageal and gastroesophageal adenocarcinoma (5, 6). The risk of developing OAC is approximately 30-40 times greater among patients with Barrett's oesophagus compared to those without intestinal metaplasia making it the greatest risk factor for OAC and the only recognised precursor for OAC (6, 7). Barrett's oesophagus is diagnosed in approximately 10-15% of patients with reflux who are undergoing endoscopy, however, it is still reported in patients without chronic reflux symptoms thereby making diagnosis of Barrett's oesophagus a greater clinical problem. One study reported that among 556 patients who never had reflux symptoms, the prevalence of Barrett's oesophagus was 5.6% (8).

Specifically, Barrett's oesophagus is a metaplastic alteration in the oesophageal cell lining from a squamous epithelial mucosa to a columnar-lined epithelium (figure 3A). In normal individuals, the squamocolumnar junction (SCJ) and the gastroesophageal junction are situated in the same place, however, the SCJ is displaced proximally in patients with Barrett's oesophagus (6). In Barrett's patients, the SCJ is evident endoscopically as a transition from a light-pink squamous epithelium to a salmon-pink columnar-lined epithelium characterised as Barrett's oesophagus (figure 3A) (6).

Historically, Barrett's oesophagus was classified as either a short-segment disease, less than 3 cm, or a long-segment disease, greater than 3 cm, according to the length of the metaplastic epithelium during endoscopy (6). Despite this, it is not evident that such classification is clinically meaningful or affects the management of these patients (9). However, studies have linked long segment lengths with a greater risk of neoplastic progression (10). One of the main reasons for the 3 cm requirements in early definitions of Barrett's oesophagus was the difficulty in assessing the SCJ and gastroesophageal junction with fiberoptic endoscopy (11). The difference in short-segment Barrett's oesophagus and intestinal metaplasia of the gastric cardia is important as the risk of progression to OAC requires further surveillance of short-segment Barrett's oesophagus (11). Therefore, endoscopy examination documents the location of the SCJ and gastroesophageal junction and biopsies are excised from lesions suspected of Barrett's oesophagus, i.e. from any proximal displacement from the SCJ (12).

Histologically, the surface and crypts in Barrett's oesophagus are typically composed of various cells including mucinous cells, goblet cells, enterocytes, endocrine cells and Paneth cells (figure 3B) (11). Glandular tissue may be composed of mucous glands, oxyntic glands or a mixture of

both. Moreover, Barrett's oesophagus can exhibit mesenchymal and stromal alterations such as the duplication of the muscularis mucosae, an increase in the number of blood vessels and changes in constituent inflammatory cells (11). The diagnosing criteria for Barrett's oesophagus varies worldwide (13). The primary differential factor for diagnosing Barrett's oesophagus concerns the requirement for histological confirmation of intestinal metaplasia, characterised by goblet cells (13). In the United States, the presence of intestinal metaplasia (goblet cells) in biopsies obtained from areas of columnar-lined epithelium is required for the diagnosis of Barrett's oesophagus (14). Conversely, the British Society of Gastroenterology only requires proof of metaplastic columnar lined-mucosa, without the presence of goblet cells (15).

During the past few decades, columnar-lined epithelium with goblet cells represents a premalignant lesion as it was shown to contain DNA abnormalities, however, metaplastic columnar-lined epithelium without goblet cells shows very similar DNA content abnormalities suggesting that the non-goblet cell phenotype also possesses equal neoplastic potential (16). One study, however, showed an increase in the presence of DNA abnormalities in non-goblet cell metaplasia compared to goblet cell metaplasia (17). Conversely, using 8522 patients with Barrett's oesophagus in a large population-based study, the reported risk for developing OAC was 0.07% in patients without goblet cells compared to 0.38% in patients with goblet cells (18).

Chronic reflux can lead to chronic inflammation and ulceration of the distal oesophagus, and if persistent, may induce metaplastic conversion of the normal squamous epithelium to a columnar-lined epithelium (11). This metaplastic process requires the activation of multiple genes and transcription factors involved in cell differentiation and proliferation. Upon exposure of gastric refluxate in squamous epithelial cells, inflammation and injury activates various differentiation and inflammatory signalling pathways that subsequently leads to the expression of Cdx1, Cdx2 and Sox9, all known to induce columnar metaplasia (14). Barrett's oesophagus, or early stage intestinal differentiation, can be detected through the use of various proteins or transcription factors that are specific to the intestine, such as villin and some intestine-specific mucopolysaccharides, however, some markers are expressed specifically at different stages of the metaplastic process (19, 20). For example, MUC5AC and MUC6 are significantly expressed earlier in Barrett's oesophagus prior to the onset of a columnar-lined epithelial phenotype characterised with goblets cells, whereas MUC2 expression can be detected late in the metaplastic process during the onset of goblet cells (19).

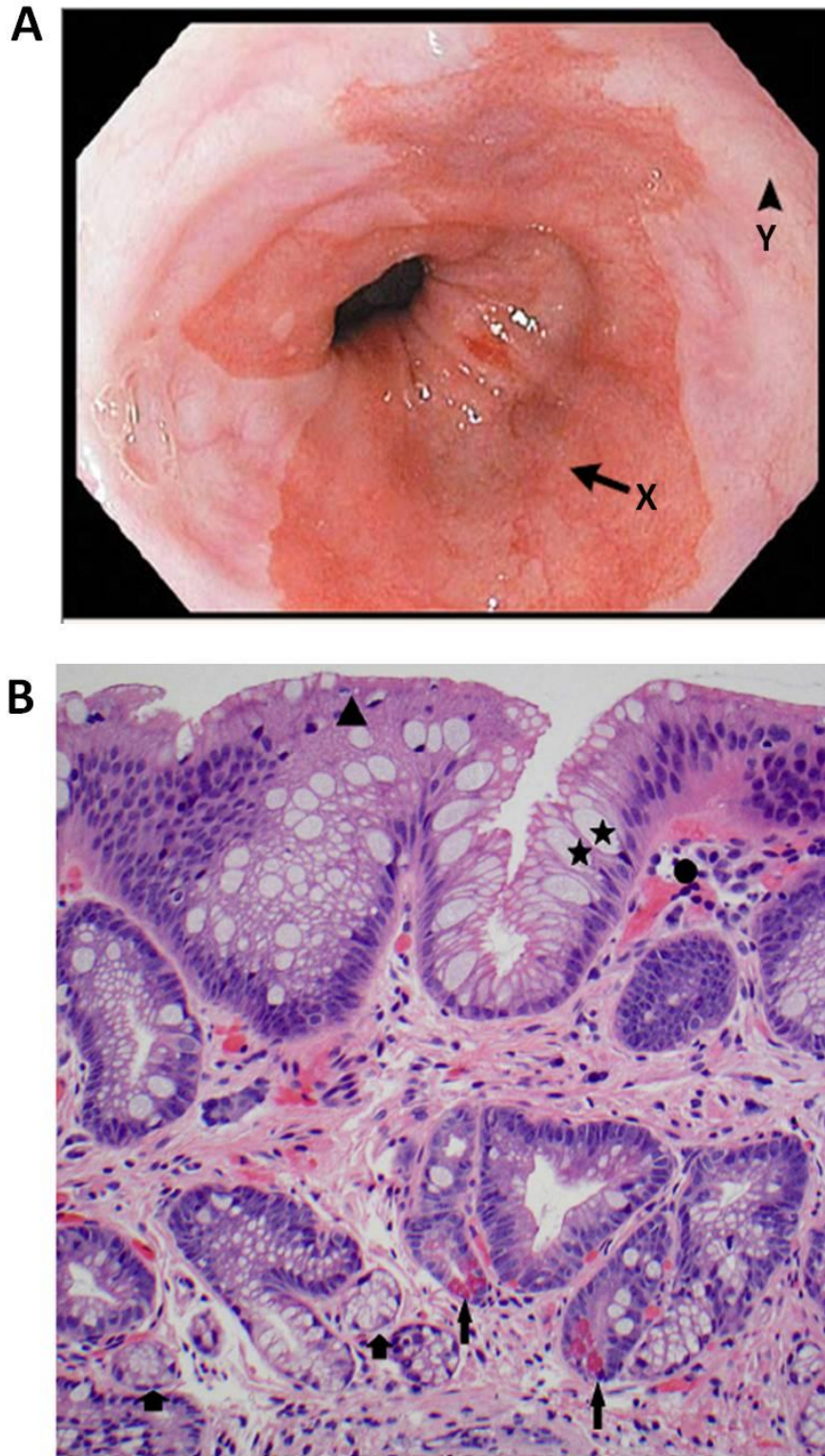


Figure 3. The endoscopic detection and histology of Barrett's oesophagus. (A) The salmon-pink, columnar-lined oesophagus (X), and the contrast between the light-pink squamous epithelium (Y) are characteristic of Barrett's oesophagus. **(B)** The epithelium consists of columnar epithelium with goblet cells (star asterisks) and non-goblet cells (arrowheads). Paneth cells may also be present (arrows). The epithelial crypts show slight architectural budding and distortion. The lamina propria additionally shows some evidence of lymphoplasmacytic infiltrate (circle). Furthermore, some mucous glands are present in the basal mucosa (wide arrow). Endoscopic image: Sharma, (2009) (6). Image and histological description: Naini *et al.* (2015) (11).

1.1.3 Dysplasia in Barrett's oesophagus

Barrett's oesophagus progresses to OAC in a sequential manner from intestinal metaplasia through low-grade dysplasia (LGD), high-grade dysplasia (HGD) followed by OAC (21). According to the 7th edition of the American Joint Committee on Cancer, HGD is now considered early oesophageal cancer (22). Dysplasia is defined as neoplastic epithelium that is confined within the basement membrane of the gland from which it arises, thereby differentiating it from adenocarcinoma (23). LGD is characterised by the relative preservation of glandular architecture in conjunction with cellular abnormalities ranging from nuclear hyperchromatism, pleomorphism, mucin depletion and absence of goblet cells (24). HGD involves a greater degree of cytologic and architectural abnormalities including increased crypt crowding, branching and cribriform formation with marked nuclear pleomorphism, round nuclei with prominent nucleoli, loss of polarity and frequent mitotic figures (11). LGD can be significantly more difficult to diagnose among pathologists, particularly for non-gastrointestinal pathologists (24). For example, inflammation and ulceration of the epithelium can mimic LGD, therefore, guidelines issued by the British Society of Gastroenterology now recommend that pathologists who are experts in oesophageal histopathology should confirm the diagnosis of dysplasia in Barrett's oesophagus (15, 25). Two large population-based studies demonstrate that the risk of neoplastic progression from LGD is between 0.5% and 1.4% compared to 0.12% per year in those with non-dysplastic Barrett's oesophagus (5, 18). Moreover, even though a high degree of inter-observer variability is observed in the histological diagnosis of LGD, a consensus of LGD among pathologists suggests a significantly increased risk of progression from LGD to HGD or OAC (26).

Due to the ambiguous nature of LGD, some studies have attempted to identify molecular markers to help predict the risk of progression to OAC. Co-localisation of the tumour suppressor protein p53 with LGD increases the risk of progression to OAC (27). Hypermethylation of cyclin-dependent kinase inhibitor 2A (CDKN2A), runt-related transcription factor and tomoregulin-2 in LGD have been shown to be independent risk factors for disease progression (28). The presence of aneuploidy or tetraploidy in LGD is additionally associated with progression to OAC (29, 30). Despite an increase in the number of potential prognostic and diagnostic biomarkers, many biomarkers are not in use as they have not been validated across multi-centres and many lack statistical power. There are also some limitations in the implementation of biomarker use, particularly in clinical practice, including costing issues, the requirement for complex analytical techniques such as immunohistochemistry, polymerase chain reaction (PCR) or flow cytometry, and issues regarding reproducibility between laboratories are additional concerns (24).

Nevertheless, biomarkers possess significant future prognostic and diagnostic potential in dysplasia within Barrett's oesophagus.

1.1.4 Surveillance in Barrett's oesophagus

Due to the high number of patients who present with advanced oesophageal disease, endoscopic surveillance has been established in an effort to diagnose disease earlier, thereby allowing patients to be treated at an earlier stage. Even though GORD is the biggest risk factor for the development of Barrett's oesophagus, the presence of GORD alone may not be sufficient to undergo endoscopic screening (31). Endoscopic screening for Barrett's oesophagus is additionally based on the presence of various other risks factors including age, sex, race, abdominal fat distribution and hiatal hernias (31). Moreover, as Barrett's oesophagus progresses in a sequential stepwise manner to OAC, this makes Barrett's metaplasia ideal to undergo surveillance (21). Surveillance of patients with Barrett's oesophagus is recommended worldwide by all major gastroenterological experts and societies including the British Society of Gastroenterology (15). Early surveillance programs investigating the outcome of patients with OAC arising from a background of Barrett's oesophagus reported that patients had a better clinical outcome compared to non-surveyed patients (32). Patients with surveillance-detected OAC diagnosed at an earlier stage have also been shown to have a better prognosis than those who present with symptomatic tumours (33). Moreover, surveillance leads to better 5-year survival (34). Despite surveillance identifying low-stage disease and improving survival, some believe that surveillance is still unlikely to significantly impact the population's mortality from oesophageal cancers, therefore, better methods are needed to identify at risk patients, for example, through the use of biomarker screening (35). Diagnosis of Barrett's oesophagus is based on both endoscopic and histological evaluation of biopsied tissue. Additional surveillance is necessary for those with indefinite dysplasia or LGD with clinical follow up tailored to individual patients with HGD (table 1) (31).

Several factors can limit the benefits of surveillance strategies. These include the low incidence of OAC in patients with Barrett's oesophagus, the complete absence of Barrett's oesophagus or LGD in patients with either advanced HGD or OAC and the ambiguity that can ensue between pathologists in the diagnosis of dysplasia (6, 9). Moreover, with the relatively low risk of progression to OAC, patients diagnosed with LGD often do not have evidence of dysplasia on subsequent endoscopy (26). In addition, studies have questioned the need for such arduous surveillance when the risk of not developing OAC in Barrett's oesophagus could be as high as 99.88% (5). Nevertheless, as Barrett's oesophagus remains the main risk factor for OAC, the main

clinical challenge is to identify those Barrett's patients at high risk of developing OAC, thereby supporting current surveillance strategies.

1.1.5 *The management and treatment of Barrett's oesophagus*

Depending on the presence and grade of dysplasia, worldwide gastroenterological societal guidelines recommend endoscopic surveillance for all patients with Barrett's oesophagus. Generally, patients with no dysplasia on their first surveillance endoscopy undergo subsequent surveillance within one year (31). If the same patient is negative for dysplasia a second time, then subsequent follow up at 3 years is suggested. Patients who present with LGD, identified and then confirmed with an expert gastroenterological pathologist, undergo further surveillance endoscopy every 6-12 months to rule out HGD (36). Patients who have progressed to HGD undergo more routine endoscopic surveillance to rule out cancer (36). Once identified, it is recommended that HGD be confirmed by an expert gastroenterological pathologist and a repeat exam be taken within 3 months. Those patients who are indefinite for dysplasia are treated similar to patients who have LGD. As table 1 illustrates, the surveillance intervals undertaken are predominantly dependent on the histological and pathological results as suggested by ACG guidelines (31, 37).

Table 1. Categories of dysplasia: Histological features and endoscopic surveillance (31). Depending on the presence and grade of dysplasia, worldwide gastroenterological societal guidelines recommend endoscopic surveillance for all patients with Barrett’s oesophagus. Surveillance intervals undertaken are predominantly dependent on the histological and pathological results. Histology is dependent on tissue architecture, cellular cytology and maturation status.

Category	Histology		Follow Up
Negative for dysplasia	<i>Architecture</i>	Normal – well spaced glands.	Repeat OGD* within 1 year. OGD* every 3 years.
	<i>Cytology</i>	Regular nuclei, smooth membranes.	
	<i>Maturation</i>	Complete.	
Indefinite for dysplasia	<i>Architecture</i>	Inflamed, mild distortion.	Repeat *OGD within 6 months, follow up as indicated by results. PPI** prior to repeat biopsy if significant inflammation present.
	<i>Cytology</i>	Hyperchromasia, overlapping nuclei, irregular nuclear borders.	
	<i>Maturation</i>	Complete when intact surface epithelium is present.	
Low-grade dysplasia	<i>Architecture</i>	Normal to mild distortion, gland crowding.	Repeat OGD* within 6 months to rule out HGD with expert pathologist confirmation. Early OGD until no dysplasia.
	<i>Cytology</i>	Minimal pleomorphism, maintained polarity, increased mitotic activity.	
	<i>Maturation</i>	Minimal to done.	
High-grade dysplasia	<i>Architecture</i>	Mild to marked distortion, crowded glands, cribriform/budding glands.	Repeat OGD* within 3 months to rule out cancer with expert pathologist confirmation. Mucosal irregularity- EMR***. Individualised follow up and treatment plan.
	<i>Cytology</i>	Loss of polarity, enlarged nuclei, prominent pleomorphism, atypical mitoses.	
	<i>Maturation</i>	None.	

*OGD: Oesophagogastroduodenoscopy, **PPI: Proton pump inhibitor, *** EMR: Endoscopic mucosal resection

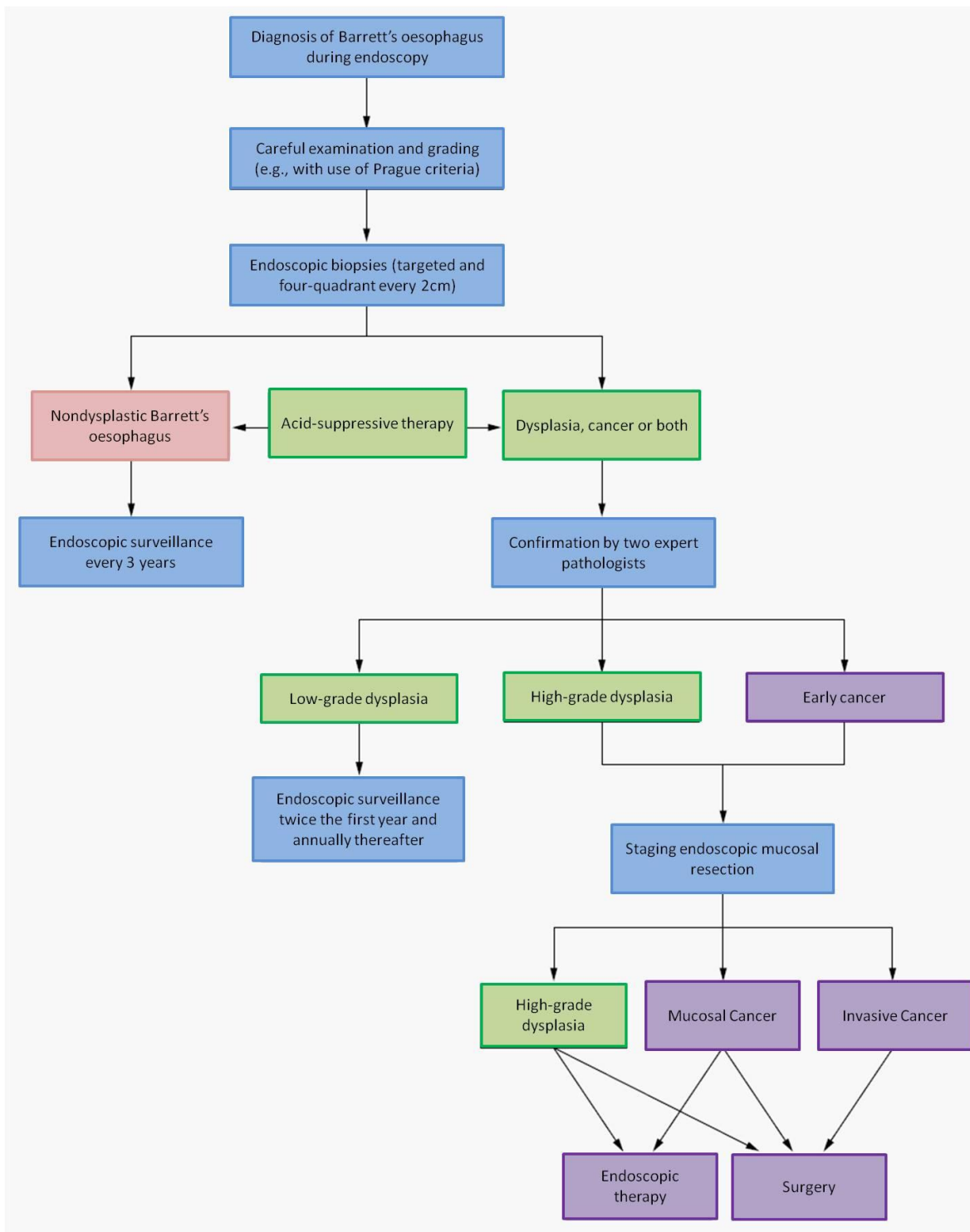


Figure 4. The management and treatment algorithm for patients with Barrett's oesophagus. Patients with no dysplasia on their first surveillance endoscopy undergo subsequent surveillance within one year. Upon confirmation of dysplasia or cancer by two expert pathologists, those with low-grade dysplasia undergo subsequent surveillance within one year. Those with high-grade dysplasia or cancer undergo staged endoscopic mucosal resection. If staging suggests high-grade dysplasia or mucosal cancer upon subsequent inspection, the patient will undergo either endoscopic therapy, such as HALO ablative therapy, or surgery depending on an interdisciplinary collaboration of experts. Those with invasive cancer undergo surgery. Image adapted from Sharma, P., (2009). (6).

Figure 4 illustrates the management and treatment algorithm for patients with Barrett's oesophagus (6). Treatment is predominantly tailored for individuals based on their preferences, their suitability for each treatment regime and the experience of the treating physician (31, 37). The primary treatments for patients with Barrett's oesophagus includes the administration of H₂-receptor antagonists, proton pump inhibitors, prokinetics and antacids that aim to control symptoms of reflux and promote the healing of the oesophageal mucosa (38). Some patients additionally opt to have antireflux surgery, however, outcomes for those who opt to undergo antireflux surgery are similar to those patients with chronic reflux indicating that Barrett's oesophagus shouldn't be viewed as an indication for antireflux surgery (39). In a multicentre clinical trial, 554 patients with chronic reflux and Barrett's oesophagus, were randomly assigned to either antireflux surgery or proton pump inhibitor treatment groups. Despite the surgery group having better oesophageal pH control, symptoms and quality-of-life measures did not statistically differ between the antireflux surgery and proton pump inhibitor treatment regimes (40). Use of proton pump inhibitors, the most common treatment of Barrett's oesophagus, has been shown to be associated with reduced risk of progression to dysplasia and OAC (41, 42). Conversely, normalisation of oesophageal pH with high-dose proton pump inhibitor use has been shown to be unsuccessful at regressing the metaplastic columnar-lined epithelium in Barrett's oesophagus (43). Moreover, a meta-analysis of over 30 studies found no significant difference in the risk of OAC between patients who received antireflux surgery and those who received medical treatment (44). The use of some of these treatments may be another cause for concern. For example, could proton pump inhibitor use be ameliorating acid reflux, regressing intestinal metaplasia and reducing patient risk or could they be exacerbating circumstances and promoting unwanted cellular side effects? Studies are lacking, however, investigating such associations.

Treating neoplastic Barrett's oesophagus requires a more aggressive approach. Increased detection of HGD and cancer incidence is thought to have been attributed to the introduction of more rigorous surveillance programmes (45). Endoscopic mucosal resection (EMR) is employed to remove all visible neoplastic tissue followed by the removal of residual metaplastic epithelium through the use of mucosal ablative therapies such as photodynamic therapy, radiofrequency ablation, cryoablation and argon plasma coagulation (46). Oesophagectomy used to be one of the primary treatments in patients with HGD due to the high reported prevalence of coexisting OAC of approximately 40%, however, in the absence of visualisation of abnormal mucosal abnormalities, the prevalence is now thought to be about 3% (47). However, the use of endoscopic eradication therapy in patients with HGD has been shown to be beneficial. EMR in conjunction with radiofrequency ablation has been shown to be an acceptable alternative to

surgery (48). In a clinical trial investigating the efficacy of photodynamic therapy, more patients significantly remained free of HGD for five years in the group randomly assigned to photodynamic therapy supplemented with the proton pump inhibitor omeprazole compared to those who were randomly assigned omeprazole alone (49). Moreover, a sham-controlled trial showed that the rate of complete eradication of HGD in those assigned radiofrequency ablation was significantly higher compared to the sham-control group (50). In those with OAC, however, it is recommended that such endoscopic eradication therapies be utilised with predominantly mucosal neoplasia, where the rate of lymph node metastasis is low. In one such trial, 200 patients with mucosal OAC who underwent endoscopic eradication therapy displayed a 5-year survival rate of 87% (51). With the overall low risk of OAC progression in Barrett's oesophagus, endoscopic eradication therapy is not recommended in patients with non-dysplastic Barrett's. In addition to potential complications that could result from endoscopic eradication therapy, it is estimated that 250 cases of non-dysplastic Barrett's oesophagus would need to be treated to prevent one case of OAC (6).

In our centre within the Department of Surgery (St. James's hospital, Dublin), interdisciplinary collaboration of experts including gastroenterologists, surgeons, pathologists and radiologists is mandatory in achieving optimum outcomes (48). In our centre, HALO® ablative treatment is undertaken in Barrett's patients with HGD and intramucosal cancer. HALO® ablative technology involves delivering heat in a very precise and highly controlled manner and therefore achieves complete removal of diseased tissue without damage to underlying tissue. If staging suggests HGD or mucosal cancer upon subsequent inspection, the patient will undergo either endoscopic therapy, such as EMR and HALO® ablative therapy, or surgery depending on an interdisciplinary collaboration of experts. Treatment with EMR ± ablation appears an acceptable alternative to surgery in our centre as morbidity has been shown to be higher in the surgery group compared to those who obtained EMR ± ablative therapy (48). Moreover, after approximately 13 months, EMR ± ablative therapy offered 100% disease control, 72% had no endoscopic or histological evidence of Barrett's oesophagus (48). However, upon progression to OAC, oesophagectomy remains the primary gold standard treatment approach (52). While neoadjuvant therapy prior to surgery is increasingly utilised for the treatment of locally advanced OAC, preoperative and postoperative chemotherapy is predominantly employed in the majority of European countries including Ireland and Britain (52). Such treatment regimes are currently employed based on successful clinical trials showing that preoperative chemotherapy followed by surgical resection improved survival compared to those who received surgery alone (53, 54). Moreover, combining chemotherapy and radiation therapy prior to surgery has also been shown to have positive outcomes (48, 52).

1.1.6 Risks factors in the development of Barrett's oesophagus

Various studies in the last few decades have investigated the aetiology of and the risk factors that contribute to the development of Barrett's oesophagus and its subsequent progression to OAC. There is a general consensus, based on such studies, that the main risk factors include GORD, medications, age, race, sex, diet, obesity, alcohol, smoking, socioeconomic status, and *Helicobacter pylori* status (55, 56).

1.1.6.1 GORD

Early evidence suggested that gastric acid and refluxate in GORD played a causative role in the pathogenesis of Barrett's oesophagus (57). Various studies have since shown that GORD plays an important role in the aetiology of Barrett's oesophagus. It is estimated that approximately 10% of individuals with GORD will develop Barrett's oesophagus (58). Moreover, a pooled meta-analysis showed that the association between GORD and OAC is significantly strong (59). The risk of OAC increases with increasing duration and frequency of symptoms (60). One landmark study showed that the risk of developing OAC with any history of reflux had an odds ratio of 7.7, however, this odds ratio increased to 43.5 in those with frequent and chronic symptoms (61). Another study showed that a 1-5 year history of reflux increased the odds of having Barrett's oesophagus by 3, whereas patients with a greater than 10 year history of reflux exhibited odds of 6.4 (62).

Some individuals possess a genetic predisposition to GORD (63). Even though many studies support familial and genetic origins, the mechanisms linking these genetic components to the development of GORD still remain unknown (63). However, there are various mechanisms in which GORD can promote the metaplastic transformation of squamous epithelium. It is thought that chronic GORD-induced damage to the squamous epithelium results in the regeneration of a metaplastic columnar epithelium, thought to be mediated by GORD as it has been well established that GORD can increase the rate of proliferation thereby facilitating in the regeneration of new epithelia (64). For example, in biopsy specimens of squamous mucosa from patients with severe reflux, cells in the basal zone demonstrate increased rates of proliferation compared to those from patients with no or mild reflux symptoms (65). In addition, acidic pH has been shown to activate the MAP kinase pathway, the pathway known to regulate cell proliferation (66). Moreover, acid perfusion of squamous epithelium *in-vivo* activates the pro-proliferative kinase ERK1/2 in GORD patients without Barrett's oesophagus but not in those with Barrett's oesophagus (67). It is also thought that GORD causes oesophagitis and promotes Barrett's oesophagus through a cytokine-mediate mechanism (68). Using a rat model of reflux oesophagitis, one study found that oesophageal inflammation was prominent in the submucosal

layer which promoted an immune infiltrate comprised of T lymphocytes and neutrophils suggestive that GORD causes epithelial cells to produce cytokines, subsequently thought to be IL-8 and IL1 β (68). Furthermore, conditioned media caused a significant increase in the migratory potential of T lymphocytes and neutrophils and subsequent supplementation with an IL-8 blocking antibody prevented migration of neutrophils strongly implicating IL-8 in the recruitment of neutrophils (68). In a transgenic mouse model of Barrett's oesophagus, the development of Barrett's oesophagus and OAC is accelerated by exposure to bile acids (69). Deoxycholic acid, or DCA, one of the main components of bile acid has additionally been shown to play a major role in the development of Barrett's oesophagus and in its subsequent progression to OAC (70-74). It is plausible, therefore, that GORD-induced inflammation plays some role in the initiation and development of Barrett's oesophagus. Despite a significant amount of evidence implicating GORD in the development of Barrett's oesophagus throughout the literature, it remains to be determined why only 10% of these patients with reflux progress towards a metaplastic phenotype.

1.1.6.2 Age, race and sex

The incidence of Barrett's oesophagus and OAC increases with age, however, as Barrett's oesophagus can be asymptomatic, determining when it first developed can be difficult (75). As the mean age for diagnosing Barrett's oesophagus in Europe is in the 60s, this suggests many individuals have unrecognised Barrett's oesophagus for years prior to diagnosis (56). In the United Kingdom, the mean age for Barrett's associated OAC is approximately 64.7 for men compared to 74 years for women. In the United States, there was been a significant increase in incidence among younger individuals between the ages 45-65 which may be linked to dietary lifestyle (76). In a review of Ireland's national Barrett's registry of 1033 patients, the median age of patients was 59 with a 2:1 male to female ratio (77).

Barrett's oesophagus is more common in men than women with a male:female ratio of approximately 2:1 (56). Interestingly, as Barrett's oesophagus progresses to OAC, this ratio can increase up to between 3:1 or 8:1 suggesting that men are not only likely to get Barrett's oesophagus, but once they do, they are more likely to progress to OAC (78, 79). The disproportion of males to females in some studies may mean that some studies are insufficiently powered to address specific risk factors by gender thereby biasing overall population associated risks.

Barrett's oesophagus is more common in Caucasians (56). Moreover, the proportion of Caucasians affected increases with the development of OAC (78). Some evidence additionally

suggests an increase in Hispanics in the United States (80). An increasing prevalence of Barrett's oesophagus in Taiwan has also emerged proposing that Westernisation of diet and lifestyle are the primary factors in this increase (81). Whether non-Caucasians who have a greater genetic variation that is protective against the development of Barrett's and changes in environmental factors, such as diet, are starting to predispose themselves to the development of Barrett's remains to be seen.

1.1.6.3 Obesity and diet

Obesity is strongly associated with the increase in incidence of Barrett's oesophagus and OAC (82, 83). Debate exists, however, as to whether obesity can directly promote GORD. In a cross-sectional population based study of in excess of 10,000 subjects, obesity increased the likelihood of having heartburn and refluxate by 3 fold (84). Body mass index (BMI) is also a known risk factor for GORD (85). In a case-control study, all measures of central adiposity were significantly associated to Barrett's oesophagus, particularly to long segment Barrett's oesophagus (86). In one study utilising standard anthropometry and bioimpedance analysis of total fat, high total body fat was linked to increased risk of Barrett's oesophagus (83). In the first genome-wide study on Barrett's oesophagus, it was found that single nucleotide polymorphism alleles predisposing to obesity increase the risk for developing Barrett's oesophagus (87). In a large genetic susceptibility study, obesity was independently associated with Barrett's oesophagus (82). Individuals with a high genetic propensity to obesity had significantly higher risks of metaplasia and neoplasia compared to people with low genetic propensity (82). Moreover, in Ireland's National Barrett's Registry that links five national hospitals, 72% of patients with Barrett's oesophagus are overweight and exhibit body mass indices above 25 (unpublished).

Evidence suggests that dietary intervention influences the risk of Barrett's oesophagus. Based on a number of studies, specific dietary factors and patterns influence the risk of developing Barrett's oesophagus and OAC. Polyunsaturated fat, omega-3-fatty acids, fibre, fruit, vegetables, dietary vitamin C, vitamin E amongst others, lower the risk of Barrett's oesophagus (88, 89). In a study comparing 'health-conscious' and 'Western' dietary patterns, the health-conscious diet was inversely associated with Barrett's oesophagus whereas the Western diet was associated with adverse effects (90). A review of the literature suggests that patients at higher risk for Barrett's oesophagus and OAC may benefit from a reduction in the consumption of red meat and an increase in the consumption of fruits and vegetables (91). Dietary nitrosamines are also implicated in oesophageal carcinogenesis as dietary nitrate is converted to the free radical nitric oxide which can be toxic. The development of Barrett's and OAC is accelerated upon exposure to

nitrosamines in a transgenic mouse model (69). Antioxidant rich foodstuffs are also associated with decreased risk of Barrett's oesophagus (92). High levels of the trace element selenium, naturally present in many foods and known to exhibit antioxidant potential, have also been shown to be associated with reduced risk of OAC among patients with Barrett's oesophagus (93). Addition of selenium in Barrett's oesophagus is believed to act primarily at the latter stages of progression towards OAC, thereby promoting the idea of supranutritional antioxidant supplementation in patients with Barrett's oesophagus (93).

1.1.6.4 Alcohol and smoking

Studies investigating the link between Barrett's oesophagus and alcohol have found inconsistent findings. The United Kingdom Barrett's oesophagus registry shows no association between alcohol consumption in patients with Barrett's oesophagus (94). Some studies have also investigated the association between alcohol and oesophageal cancer using patients with Barrett's oesophagus as a control group (56). In a review examining the association between alcohol consumption and Barrett's oesophagus, 54.5% of studies found some association (56). Most of these associations were reported to be '*weak*', however, one study reported an odds ratio of 2.3 fold (95). One study in particular showed that beer and liquor consumption was not associated with cancer development, however, the risk was decreased for drinking wine (96). A meta-analysis of observational studies found no association between alcohol consumption and the risk of Barrett's, therefore, it is plausible that alcohol does not increase the risk of Barrett's oesophagus and if it does the effect is quite small (97). One of the main issues with most of these studies, however, is defining what moderate and excessive drinking is. Moreover, it is possible that different alcohol types encompass different risks.

Various studies have shown that smoking is associated with an increased risk of Barrett's oesophagus (98, 99). Smokers also have an increased risk of developing OAC, with increased risk associated with per pack years smoked (100). Similar to alcohol, however, the risk of smoking in the development of Barrett's oesophagus is additionally controversial. Various small studies have found no association between smoking and Barrett's oesophagus but such studies seem limited by sample size (94). Moreover, one study showed that patients with non-dysplastic Barrett's oesophagus were more likely to be non-smokers than patients with severe oesophagitis and OAC (101). The genotoxicity of tobacco smoke, the increased prevalence of GORD among smokers and the presence of significant amounts of free radical nitrosamines in tobacco smoke are potential biological instigators in the initiation and progression of neoplastic tissue. Generally, there are

more positive studies implicating smoking in the development of Barrett's oesophagus and OAC, however, the risk of smoking is higher in squamous cell carcinoma compared to OAC (56).

1.1.6.5 Helicobacter pylori, medications and socioeconomic status

Helicobacter pylori decreases the risk of Barrett's oesophagus (102-104). It is thought that the reason for this inverse association may in part be the reduced risk of GORD symptoms among patients with *H. pylori* (104). Furthermore, it is thought that *H. pylori* protects against the development of Barrett's oesophagus and OAC, therefore, debate exists whether to eradicate *H. pylori* infection based on data suggesting that its eradication increases reflux symptoms in these patients (105). As all these studies show associations, future studies need to examine the role of *H. pylori* to prove causality perhaps through the use of model systems. Much interest has additionally focused on the potential pathogenic role of medications in promoting neoplastic progression. Studies have speculated that lower oesophageal sphincter (LES) relaxing medications such as nitroglycerins, anticholinergics, beta-adrenergic agonists, aminophyllines and benzodiazepines may contribute to the increasing incidence of OAC (96). The estimated incident rate ratio of OAC in long term LES medication users was 3.8 compared to individuals who never used the drugs (96). The increased use of these medications has also coincided with the increased incidence of OAC (56). Extraordinarily, it is estimated that 10% of OAC in the population may be attributed to the use of LES medication (96). Furthermore, in a retrospective case-control study, higher socioeconomic status was shown to be an independent risk factor for Barrett's oesophagus (106). Developing OAC is also associated with higher socioeconomic status, however, inverse associations have also been documented (107, 108).

Throughout the literature, the mitochondria have been documented to play significant roles in disease initiation, inflammation and cancer. Research investigating the role of mitochondria in Barrett's oesophagus has additionally highlighted mutations in the mitochondrial genome to be important in instigating neoplastic progression (109). However, little is known about how alterations in mitochondrial function and mitochondrial energy metabolism promote neoplastic progression in Barrett's oesophagus.

1.2 MITOCHONDRIA: THEIR ROLE IN DISEASE INITIATION, INFLAMMATION AND CANCER

1.2.1 *Mitochondrial structure and the mitochondrial genome*

Mitochondria are semi-autonomous organelles composed of specialised compartments including the outer membrane, the intermembrane space, the inner membrane, the cristae and the matrix. Mitochondria are involved in a range of cellular functions including energy generation, the regulation of signalling, cellular differentiation, cell death, cell growth and the control of cell cycle (110, 111). The outer membrane consists of a phospholipid bilayer consisting of porins that allow the movement of certain molecules of about 10kDa or less such as ions and adenosine triphosphate (ATP). The inner membrane is permeable only to oxygen (O₂), carbon dioxide (CO₂) and water, and contains integral proteins for the active transport of specific metabolites across the membrane in a highly regulated manner (110). In addition, the inner mitochondrial membrane contains components of the electron transport chain and the ATP synthase complex which are involved in cellular respiration and energy production, specifically oxidative phosphorylation (110, 111). Oxidative phosphorylation is the final step of aerobic cellular respiration in which ATP is formed following the transfer of electrons from nicotinamide adenine dinucleotide (NADH) or flavin adenine dinucleotide (FADH₂) to produce O₂ by a series of electron carriers located in the inner membrane (110). In addition to oxidative phosphorylation, the citric acid cycle takes place in the mitochondrial matrix where it functions in the chemical conversion of carbohydrates, fats and proteins into CO₂, water, guanosine triphosphate, ATP and NADH (110). Within the mitochondrial matrix, the mitochondrial genome resides.

Human mitochondrial DNA (mtDNA) forms 5µm circles, composed of 16,569 base pairs (figure 5A) (112). Even though the number of mitochondria per cell varies with cell type, it is estimated that each mitochondrion contains between 2 and 10 copies of mtDNA. MtDNA is somewhat able to maintain genomic independence from the nucleus, however, the majority of mitochondrial proteins are encoded by nuclear DNA and imported into mitochondria (111). mtDNA encodes for 13 of 87 proteins required for oxidative phosphorylation in addition to 12S, 16S ribosomal RNAs and 22 transfer RNAs required for protein synthesis in the mitochondria (111). The overall biogenesis of mitochondria keeps pace with ongoing cellular proliferation and growth. One of the main features between the nuclear and mitochondrial genomes is their inherent susceptibilities to cellular damage (111).

1.2.2 Mitochondrial DNA damage in Barrett's oesophagus

MtDNA is significantly more vulnerable to mutations than nuclear DNA (111). This is due to its lack of histone protection, limited repair capacity and its close proximity to the electron transport chain which constantly generates superoxide radicals, such as reactive oxygen species (ROS) (111). Moreover, mtDNA lacks introns, therefore, most mutations occur in coding sequences that are more likely to be of biological consequence (113). Various studies have identified many mitochondrial regions that harbour common mutations in different cancer sites in a multitude of cancer types. (114). MtDNA mutations are regarded as oncogenic factors (109).

The accumulation of mutations in mtDNA, leading to mitochondrial dysfunction, has been implicated in the etiology of aging, various degenerative pathologies and carcinogenesis based on the presence of novel hetero- and homoplasmies (115). In one study, 53% of patients with Barrett's oesophagus exhibited significantly higher mtDNA mutations in Barrett's tissue compared with matched normal adjacent tissue (109). This was paralleled with significant levels of ROS in Barrett's tissue compared to normal tissue (109). Therefore, high levels of ROS early in Barrett's oesophagus may contribute to the development of mtDNA mutations, alterations in mitochondrial function and play a crucial role in further disease progression and tumourigenesis (109). Another study investigating mutations in the D-loop region of mtDNA supports the hypothesis that oxidative damage may be a mechanism for the induction of OAC in Barrett's oesophagus (116). A paired exome analysis of Barrett's oesophagus and OAC suggests that on average 62.5% of OACs emerge not through the gradual accumulation of tumour-suppressor alterations but through a more direct mechanism where a p53-mutant cell undergoes genome doubling followed by the acquisition of oncogenic amplications (117). In a recent case-control study, the mutational load, a measure of genetic instability assessed by measuring loss of heterozygosity and microsatellite instability, predicted progression to HGD and OAC in patients with non-dysplastic Barrett's oesophagus and LGD (118). Therefore, high mutational load may be able to identify patients with Barrett's oesophagus with a greater risk of progression to OAC.

PCR amplification of the mtDNA 4977bp deletion across the Barrett's-dysplastic-OAC disease sequence also showed significant clinical utility for the assessment of dysplastic severity, but not OAC as the frequency of the 4977bp deletion reduced sharply in OAC specimens (119). This is in accordance with other studies that have shown HGD to exhibit widespread chromosomal instability implicating chromosomal variation seen at the HGD stage to be the source of specific karyotypes that progress to OAC (120). Furthermore, mtDNA mutations have been identified in a variety of human preneoplastic and neoplastic tissues (figure 5B) (111, 121).

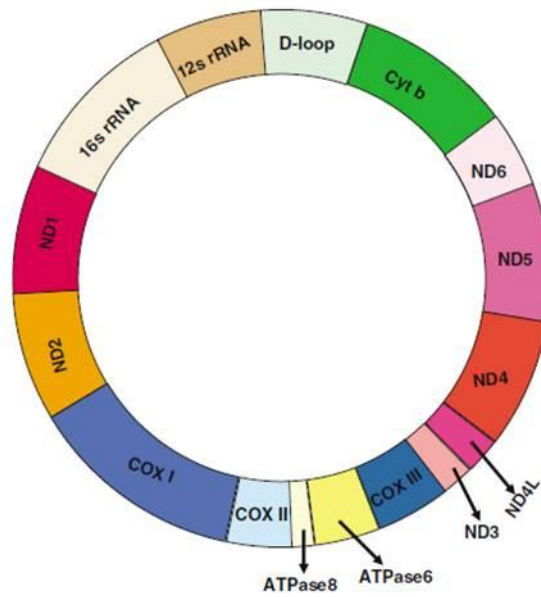
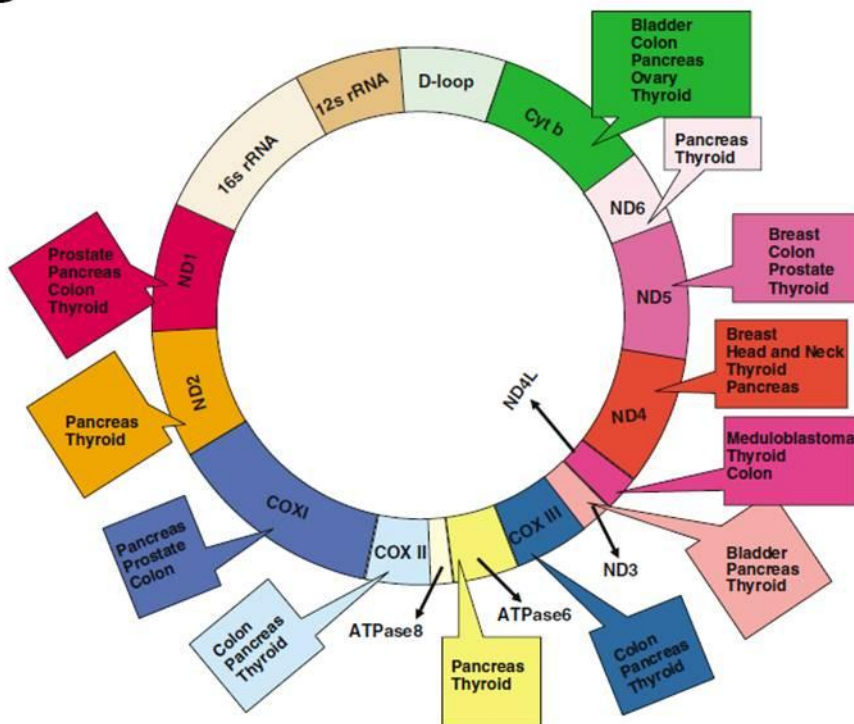
A**B**

Figure 5. The mitochondrial genome and its role in cancer. (A) A schematic presentation of the wild-type mitochondrial genome. **(B)** The mitochondrial genome is more vulnerable to mutations than nuclear DNA. Various studies have identified many mitochondrial regions that harbour common mutations in different cancer sites in a multitude of cancer types. Image: Chatterjee *et al.* (2006) (114).

1.2.3 The role of the electron transport complexes in disease progression

1.2.3.1 Complex I

As figure 6 illustrates, the electron transport chain plays a central role in oxidative phosphorylation and it has long been known that respiratory impairment plays a key role in tumourigenesis (122). As the entry point for most electrons into the respiratory chain, complex I has been suggested as the rate-limiting step in electron transfer (123). In the recent decade, mtDNA mutations in genes encoding complex I subunits have been found in various cancer cells (124). Complex I defective cells carrying a heteroplasmic mutation in the ND5 subunit exhibit increased tumourigenic potential thought to be mediated by ROS and/or resistance to apoptosis (125). Moreover, this defect could be reversed by bypassing the defective complex, and furthermore, suppression of complex I with rotenone enhanced tumourigenesis through AKT activation (123). Interestingly, antioxidant supplementation ameliorated ROS-mediated AKT activation and reversed the tumourigenicity of complex I defective cells (123). It is also speculated that genetic changes that alter complex I structure and function may alter a cell's ability to respond to low oxygen concentrations and consolidate hypoxia rescue mechanisms, thereby contributing to resistance to chemotherapeutic agents (126). Moreover, complex I deficiency is associated with an increased inflammatory phenotype that can potentially enhance the metastatic potential of tumour cells (127, 128). Deficits in complex I are additionally associated with the more protumourigenic glycolytic phenotype (129). Differential expression of various complex I subunits has also been documented between Barrett's and OAC cells *in-vitro* (130). On the other hand, as increased mitochondrial ATP synthesis is characteristic of many tumours, the targeting of ATP synthesis has recently exhibited significant promise. Various studies targeting complex I utilising metformin, the anti-diabetic drug, have found that metformin directly inhibits complex I and limits the ability of cancer cells to cope with energetic stress (131). One recent study has shown that metformin and phenformin, another biguanide analogue, inhibit angiogenesis and the metastatic growth of breast cancer *in-vitro* and *in-vivo* by targeting both neoplastic and microenvironmental cells (132). Past clinical trials have shown significant promise for metformin-induced complex I inhibition and its role as an adjuvant therapeutic in various cancers, therefore, its anti-cancer promise still continues to be investigated (133-137).

1.2.3.2 Complex II

Complex II deficiency gives rise to cancer (138). It is also speculated that complex II subunits function as tumour suppressors (138). One particular study reported that the activity of complex II in gastrointestinal stromal tumours bearing complex II mutations is compromised (139).

Expression levels of the complex II subunits *SDHA*, *SDHC* and *SDHD* has also been shown to be decreased in OAC cells compared to Barrett's cells *in-vitro* (130). As complex II converts succinate to fumarate, defects in complex II leads to succinate accumulation resulting in the inhibition of prolyl hydroxylase enzymes which marks hypoxia-inducible factor (HIF) for proteasomal degradation (140). As such, *in-situ* and *in-vivo* analyses have shown that complex II-deficient tumours accumulate succinate which stabilises HIF1 α and results in various protumourigenic effects (140). Indeed, many studies do exhibit increases in HIF1 α expression in complex II-deficient tumours (141). Moreover, in pheochromocytoma-paraganglioma syndromes, the most aggressive tumours are those deficient or malfunctioning in the *SDHB* subunit of complex II (142). In addition, the immunohistochemical absence of the *SDHB* subunit in pheochromocytoma-paraganglioma biopsies has been suggested as a surrogate marker for the presence of mutations in other complex II subunits (143). In addition to the anti-oxidant properties of vitamin E and vitamin E analogues, complex II is additionally used as a target for anti-cancer agents, primarily due to its role in metabolism and its role in the early stages of the apoptotic process (138, 144). For example, the complex II inhibitors malonate and 3-nitropropionic acid increase ROS levels and subsequently induce apoptosis (145, 146).

1.2.3.3 Complex III

Although the majority of studies document complexes I, II, IV and V in carcinogenesis, some evidence also links complex III with a role in carcinogenesis. An increase in superoxide radicals inactivates complex III resulting in the impairment of mitochondrial respiration in rat hepatomas (147). Various respiratory chain diseases have since been accredited to complex III deficiency (148). Not only have complex III mutations been identified in patients with a spectrum of clinical manifestations, complex III mutations have been attributed to breast, colorectal and ovarian cancer (149-151). The 4977bp deletion of complex III is frequent in the mtDNA of patients with oesophageal squamous cell carcinoma and increases in frequency from Barrett's oesophagus to HGD (119, 152). Moreover, expression levels of the complex III subunits *UQCR11*, *UQCRC1*, *UQCR2* and *UQCRQ* were decreased in OAC cells compared to Barrett's cells *in-vitro* (130).

1.2.3.4 Complex IV

More and more studies are beginning to associate alterations and defects in complex IV with disease progression. The complex IV subunits *COX4I2* and *COX8C* have been shown to be differentially altered across the *in-vitro* and *in-vivo* metaplastic-dysplastic-OAC sequence in Barrett's oesophagus (130). Chronic pancreatitis has been linked with complex IV deficiency (153). Parathyroid cell metaplasia is additionally characterised by somatic mtDNA mutations in complex

IV activity-impairing genes (154). In a study investigating the deficiency of a complex IV subunit in colonic epithelium, it was shown that deficiencies increased in frequency with age and clusters of deficient epithelial crypts were associated with, and may give rise to, colon cancer (155). It is also thought that about 11-12% of all prostate cancer patients harbour mutations in subunit 1 of complex IV (156). Loss of the tumour suppressor p53, known to regulate complex IV indirectly through synthesis of cytochrome c oxidase 2 (SCO2), has been well documented throughout the literature and is associated with a shift from oxidative phosphorylation to glycolysis, characteristic of many cancers (157).

1.2.3.5 Complex V

Like complex IV, studies have linked defects in complex V to disease progression. One study introduced a pathogenic mtDNA mutation of the complex V subunit ATP6 into a prostate cancer cell line and tested for tumour growth in nude mice (156). As a result, tumours were up to 7 times larger and generated significantly more ROS than wild-type mice demonstrating that mutations in complex V play an important role in the etiology of prostate cancer (156). Furthermore, increased expression of the complex V subunit ATP5B has been shown to be significantly increased in patients who have a poor pathological response to neoadjuvant chemoradiation therapy for the treatment of OAC suggesting a role for complex V, mitochondrial alterations and oxidative phosphorylation in the radioresistance of OAC (158). Expression of various complex V subunits have been shown to be differentially expressed across the metaplastic-dysplastic-OAC sequence in Barrett's oesophagus *in-vitro* (130). The subunit, *ATP12A* has been shown to decrease across the same disease sequence *in-vivo* (130). As a surrogate marker of oxidative phosphorylation, the complex V subunit ATP5B protein marker, has been shown to be significantly increased across the oesophagitis-metaplasia-dysplasia-OAC sequence, thereby reflecting the role of a highly oxidative microenvironment in Barrett's oesophagus and in the progression of OAC (130). Furthermore, using first time surveillance biopsy material, protein levels of ATP5B were significantly higher in Barrett's patients who progressed to HGD and OAC compared to those who did not progress highlighting the applicability of this marker in the clinical setting (130).

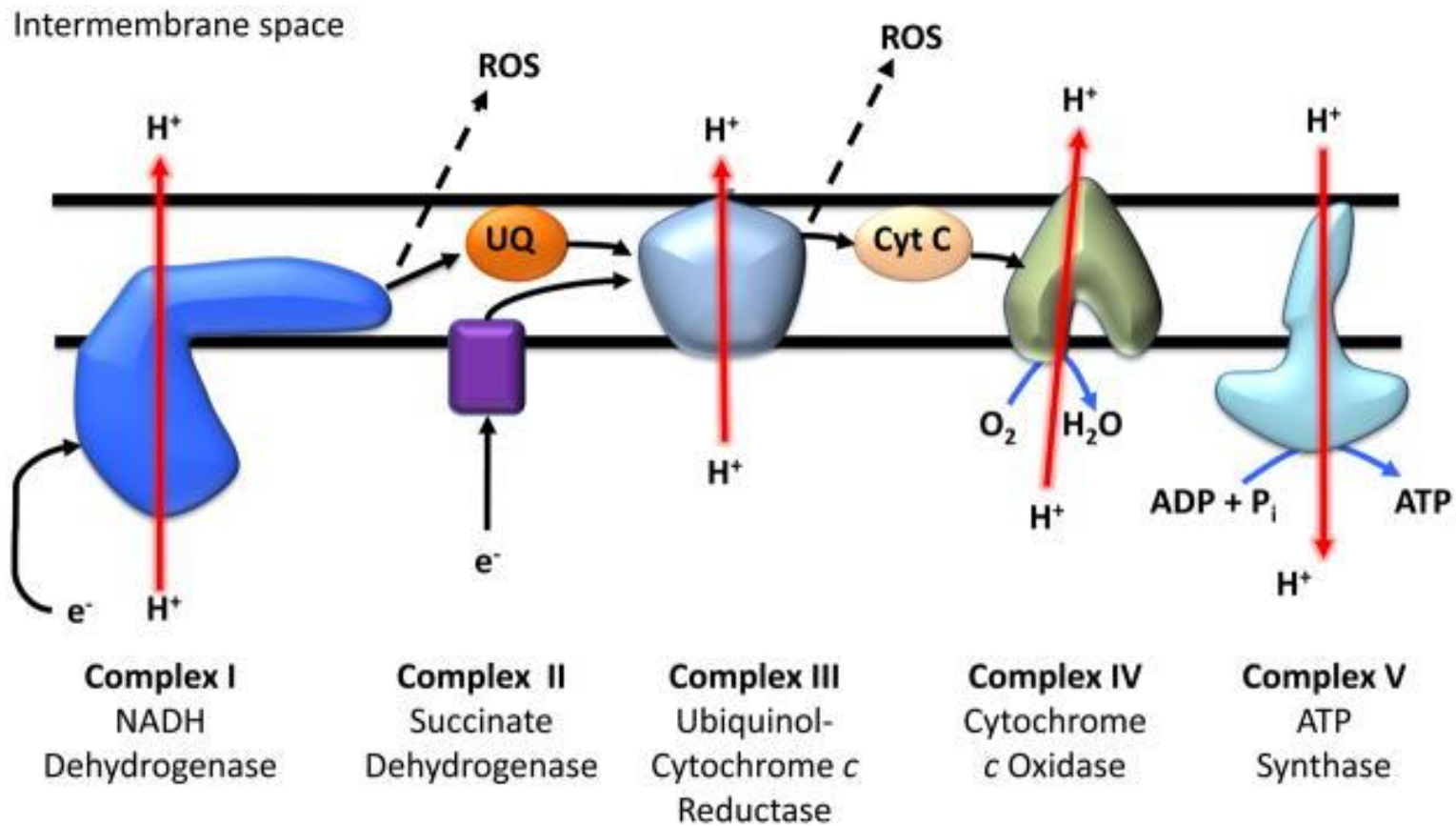


Figure 6. The mitochondrial electron transport chain. Composed of five mitochondrial protein complexes, the electron transport chain extrudes hydrogen ions into the intermembrane space to produce an electrochemical gradient. The subsequent influx of hydrogen ions from the intermembrane space into the mitochondrial matrix through complex V produces ATP thereby playing a central role in mitochondrial respiration. Image: Ghouleh *et al.* 2011 (159).

1.3 OXIDATIVE PHOSPHORYLATION AND GLYCOLYSIS IN CANCER

Altered metabolism is now a universal feature of most, if not all, cancer cells (160). Transitioning from a normal cell to a malignant cancer cell is a multi-step pathogenic process which includes a permanent interaction between cancer-associated gene activation, metabolic reprogramming and tumour-induced changes in the microenvironment (161). As figure 7 illustrates, in contrast to normal cells which primarily rely on oxidative phosphorylation to generate the ATP needed for cellular function, most cancer cells instead rely on aerobic glycolysis, a phenomenon termed the Warburg effect (162). Even though aerobic glycolysis is an inefficient way to generate ATP, it encompasses many advantages for anabolic purposes. Cancer cells, and proliferating cells, adapt to facilitate the uptake of nutrients into ATP, nucleotides, amino acids, and lipids, all components necessary in proliferating cancer cells (162). Increased glucose consumption in the majority of cancer cells is devoted to lactate conversion and anabolic biosynthesis and is thought to be uncoupled from oxidative metabolism (160). Glycolytic intermediates play a more vital role than the final product pyruvate as cancer cells use a variety of mechanisms to slow down the final step of glycolysis (161). Even though alterations in oncogenes and tumour suppressors drive inappropriate cell proliferation, they can also rewire cell bioenergetics to meet the biosynthetic demands of neoplastic tissue (160).

While the majority of studies demonstrate a reduction of oxidative phosphorylation metabolism in different cancer cells, other analyses have revealed contradictory modifications with the upregulation of oxidative phosphorylation (163). Some studies have challenged the Warburg effect hypothesis showing that mitochondria in cancer cells are not inactive, but function at low capacity (164). Some studies in cancer cells, however, have shown that oxidative phosphorylation supplies the majority of cellular ATP (165). Various glioma cell lines are highly dependent on oxidative phosphorylation (166). Moreover, glioma, breast, hepatoma, and pancreatic cells that prefer glycolytic metabolism exhibit metabolic plasticity and switch to oxidative metabolism upon glucose starvation highlighting that both metabolic pathways work in tandem during times of stress thus targeting both pathways together may be clinically appealing (161, 167). One study showed that the magnitude of oxidative phosphorylation contributing to cellular ATP supply in HeLa cells was 79% (165). Other studies have tried to mimic the inner layers of solid human cervical tumours, where substrates and oxygen are limited, and revealed that these limitations did not affect the levels of oxidative phosphorylation or cellular ATP levels (165). Furthermore, the growth of HeLa cells and breast cancer cells in aglycemia and/or hypoxia has additionally been shown to trigger a compensatory increase in oxidative phosphorylation capacity (163, 167). Two models of sequential oncogenesis have additionally shown the importance of active oxidative

phosphorylation in the initiation of tumorigenesis. In one model, the transformation of human mesenchymal stem cells increases their dependency on oxidative phosphorylation, while in another model, fibroblast cells expressing oncogenic RAS display an increase in mitochondrial mass, mtDNA and ROS prior to senescent cell cycle arrest (168, 169). These studies demonstrate the interplay between both oxidative phosphorylation and glycolysis within neoplastic cells, to adapt their cellular mechanisms of energy production to endogenous microenvironmental requirements. Therefore, a better understanding of the mechanistic links between cellular metabolism, associated tumorigenic processes, the microenvironment and neoplastic growth may result in better treatments for human cancers.

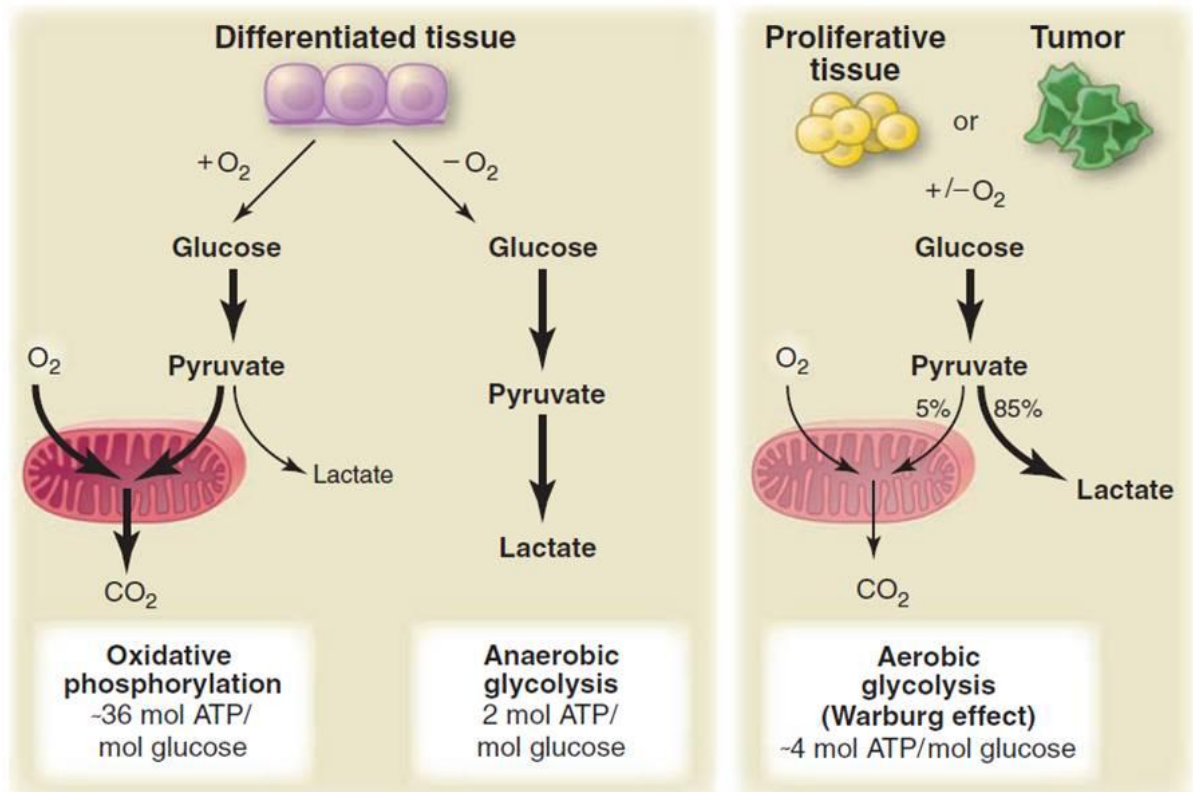


Figure 7. The differences between oxidative phosphorylation, anaerobic glycolysis and aerobic glycolysis (the Warburg effect). In the presence of oxygen, non-proliferating normal tissues metabolise glucose to pyruvate via glycolysis, and subsequently, oxidise the majority of the pyruvate in the mitochondria during oxidative phosphorylation. When oxygen is limited, cells redirect pyruvate away from oxidative phosphorylation by generating lactate (anaerobic glycolysis). The continued production of lactate allows the generation of glycolysis to continue by recycling NADH back to NAD⁺ but results in minimal production of ATP. Warburg observed that cancer cells convert the majority of glucose to lactate regardless if oxygen is present (aerobic glycolysis). Image: Vander Heiden *et al.*, (2009) (162).

1.4 THE ROLE OF ENERGY METABOLISM IN DRIVING DISEASE PROGRESSION IN INFLAMMATORY, HYPOXIC AND ANGIOGENIC MICROENVIRONMENTS

Otto Warburg's initial observation in 1956 demonstrated that tumours exhibit increased levels of aerobic glycolysis (170). This observation has since resulted in numerous studies investigating the role of mitochondrial energy metabolism in disease progression across many disease entities. As a reflection of its importance in the development of various cancers, the reprogramming of cellular energetics is now beginning to establish itself as one of the new hallmarks of cancer (171, 172). In addition to significant quantities of ATP, metabolically demanding tumours require glucose for lipid and protein synthesis and *de novo* synthesis of nucleotides for rapid proliferation (173). More importantly, this altered metabolic phenotype allows tumours to maintain higher proliferative rates and resist apoptosis orchestrated by increased oxidative damage (174). Moreover, these metabolic phenotypes persist and are sometimes altered in distinct metabolically demanding microenvironments. Therefore, elucidating how diverse metabolic processes converse with distinct functional inflammatory, hypoxic and angiogenic pathways may infer significant insights into how several heterogeneous malignancies arise and subsequently advance beyond therapeutic intervention. It has been widely documented that inflammation, hypoxia and angiogenesis all play independent roles in disease prevalence and in its subsequent stepwise progression. Some studies, however, have uncovered close associations between energy metabolism and these extensive processes. Therefore, the remaining section of this introduction chapter, having been published in *Gastro Open Journal*, predominantly focuses on the primary molecular mechanisms that link energy metabolism with inflammation, hypoxia and angiogenesis in the tissue microenvironment (175).

1.4.1 Molecular mediators linking energy metabolism with inflammation, hypoxia and angiogenesis.

1.4.1.1 Conventional mediators linking energy metabolism with inflammation and hypoxia.

1.4.1.1.1 HIF1 α

HIF1 α is an oxygen sensitive transcription factor subunit involved in various cellular processes including hypoxia, angiogenesis, cell survival, inflammation and energy metabolism (176). Interestingly, cells in hypoxic regions tend to be more resistant to the effects of radiotherapy and other conventional chemotherapeutic agents (177). As a result, these more resistant cells have been implicated in disease resistance and recurrence, and can lead to more aggressive phenotypes and contribute to subsequent metastasis (177, 178). It is important to note, however, that hypoxia-induced alterations in energy metabolism are physiologically normal, for example, cardiomyocytes upregulate glycolytic ATP production under hypoxic stress (179). As figure 8 shows, hypoxia affects metabolism by inducing the overexpression of various glycolytic enzymes, lactate dehydrogenase (LDH) and carbonic anhydrase in addition to inhibiting pyruvate dehydrogenase, a key enzyme that converts pyruvate into acetyl-CoA for subsequent oxidative metabolism (180). However, it has been shown that hypoxia, specifically HIF1 α , plays a key role on T-cell function by modulating T-cell metabolism.

Upon activation, the metabolic demands of T-cells increase dramatically since activated T-cells are highly anabolic and exhibit marked increases in glycolytic metabolism (181, 182). Interestingly, one study hypothesises that one possible mechanism responsible for T-cell anergy is failure to upregulate key metabolic machinery, since blocking energy metabolism mitigates T-cell activation and inhibition of these metabolic pathways during activation leads to anergy in Th1 cells (181). Hypoxia has differential effects on T-cell function, however, as lack of glucose in human CD4⁺ T lymphocytes results in increased dead cell numbers and increased reactive oxygen species under normoxia but not under hypoxic conditions (183). Hypoxia also stimulates increased levels of interleukin-1 β (IL1 β), IL-10 and IL8 in these cells, but the lack of glucose reduces secretions of these cytokines, implying that CD4⁺ T cells are highly metabolically adaptable allowing for proper immune function under highly fluctuating bioenergetic microenvironments (183). HIF1 α also regulates the balance between regulatory T cell and helper T cell differentiation (184). This differentiation has been shown to be regulated in both regulatory T cells and helper T cells via the glycolytic pathway in a HIF1 α -dependent manner (185). In stimulated T_H17 cells, glycolysis and various glycolytic enzymes were actively upregulated, although blocking glycolysis inhibited T_H17 development while promoting T_{REG} differentiation (185). HIF1 α activity is key for mediating glycolytic activity and subsequently contributes to lineage choices between T_H17 and T_{REG} cells,

whereas lack of HIF1 α results in reduced T_H17 development but enhances T_{REG} differentiation (185). Some evidence suggests that HIF1 α mediates this effect through mammalian target of rapamycin (mTOR) (185, 186). These studies support the view that hypoxia mediates T-cell function and drives chronic inflammation through HIF1 α by regulating T-cell metabolism.

1.4.1.1.2 AMPK

AMP-activated protein kinase, or AMPK, is a sensor of cellular energy metabolism and exhibits anti-Warburg effects by promoting fatty acid oxidation, mitochondrial biogenesis and the expression of genes necessary for oxidative metabolism (figure 8) (187-190). As aerobic glycolysis is a common entity in many cancer types, it is exciting to speculate that drugs that activate AMPK might therefore have therapeutic and clinical utility. Any metabolic imbalance that either inhibits the generation of ATP or accelerates ATP consumption results in increases in the ADP/ATP ratio resulting in AMPK activation due to the accumulation of ADP (187). As a result, activated AMPK acts to switch off ATP-consuming anabolic processes and restores energy imbalances by switching on alternative catabolic pathways that increase cellular ATP (187, 191). One of these mechanisms involves down-regulating protein synthesis. For example, AMPK down-regulates protein synthesis of target of rapamycin complex 1 (TORC1), which is known to promote HIF1 α translation, thereby reducing HIF1 α expression and decreasing the expression of key glycolytic and glucose transporters required for aerobic glycolysis (192). Using a mouse model of Peutz-Jeghers syndrome, deficiency of either AMPK or liver kinase B1 (LKB1), the protein kinase responsible for induction of AMPK activation, led to the upregulation of HIF1 α , hexokinase 2 and glucose transporter member 1 (GLUT1) (193).

Activated immune cells tend to favour aerobic glycolysis whereas quiescent cells preferentially utilise oxidative metabolism (181, 182). Therefore, agents that activate AMPK may have anti-inflammatory effects. LPS-induced activation of dendritic cells results in reduced activation of AMPK, whereas knockdown of AMPK leads to the maturation of dendritic cells that exhibit increased glucose uptake (194). Interestingly, AMPK downregulation in macrophages results in increased expression of various proinflammatory cytokines whereas expression of AMPK had the reverse effect (195). Therefore, AMPK promotes macrophage polarisation towards an anti-inflammatory M2 phenotype rather than the proinflammatory M1 phenotype. In addition, AMPK has been shown to monitor metabolic stress in cytotoxic T lymphocytes and control the differentiation switch from metabolically active cytotoxic T lymphocytes to metabolically quiescent CD8⁺ T cells, highlighting the important role of AMPK in various metabolic, immune and inflammatory processes (196).

1.4.1.1.3 p53

As figure 8 illustrates, the transcription factor p53 regulates metabolism by lowering aerobic glycolysis and promoting oxidative phosphorylation through a variety of molecular mechanisms (197, 198). p53 primarily supports oxidative phosphorylation by functioning as a mitochondrial checkpoint protein, regulating mitochondrial DNA copy number and mediating mitochondrial biogenesis (199, 200). p53 promotes mitochondrial health via the p53-inducible protein MIEAP that controls mitochondrial quality by repairing or eliminating unhealthy mitochondria (201). In intestinal metaplasia patients with progressive disease, oxidative-induced damage results in telomere shortening and mutations in the p53 gene abrogate p53's role as the checkpoint of proliferation and apoptosis (202). Other studies have also shown that p53 plays a vital role in the synthesis of key components of the electron transfer chain (203-205).

p53 mediates its central metabolic role through TP53-induced glycolysis and apoptosis regulator, or TIGAR (197, 206). TIGAR acts as a phosphatase and degrades fructose-2,6-bisphosphate (F26B) thereby decreasing the activity of phosphofructose kinase 1 (PFK1), a key enzyme of the glycolytic pathway (197). p53, via TIGAR, decreases glycolysis by diverting glycolytic intermediates into the pentose phosphate pathway (PPP) (207). p53 also negatively regulates the expression of pyruvate dehydrogenase kinase 2 (PDK-2) thereby activating the pyruvate dehydrogenase complex responsible for converting pyruvate to acetyl-CoA (208). Thus p53, activating the pyruvate dehydrogenase complex, favours oxidative phosphorylation through the production of acetyl-CoA (208). Furthermore, p53 directly downregulates the expression of GLUT1 and GLUT4 (209).

The role of p53 is highlighted in hypoxic microenvironments. Through a hypoxia-induced HIF1 α dependent mechanism, TIGAR has been shown to form a complex with hexokinase 2 at the mitochondria resulting in an increase in hexokinase 2 activity (206). This complex reduces glycolytic flux supporting pentose phosphate pathway activity, generates NADPH in the process and promotes antioxidant function thereby limiting reactive oxygen species-associated apoptosis and autophagy (206). p53 also represses the expression of monocarboxylate transporter 1 (MCT1) preventing the efflux of lactate under hypoxic conditions (210). It has been speculated that aberrant p53 expression may even promote tumour progression as some evidence suggests that p53 may enhance aerobic glycolysis rather than inhibit it (197, 198, 211). In addition, the mechanism by which p53 regulates the glycolytic pathway may be tissue and context specific which is thought to reflect different types of cellular stress, that is, metabolic, oxidative and hypoxic stress (197, 212).

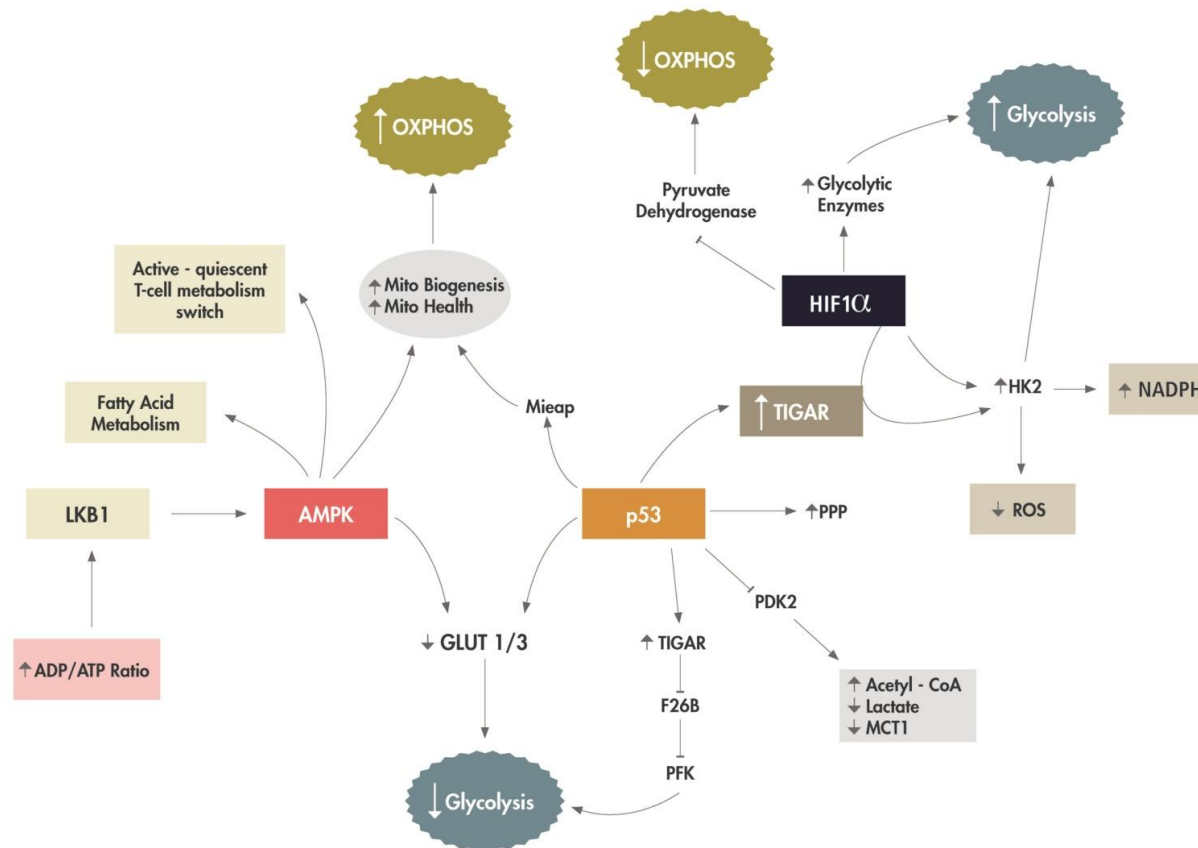


Figure 8. Conventional mediators linking energy metabolism with inflammation and hypoxia. p53, through HIF1 α , enhances aerobic glycolysis. Hypoxia, through HIF1 α , affects metabolism by inducing the overexpression of a host of glycolytic enzymes, for example, hexokinase 2. HIF1 α also depresses OXPHOS by inhibiting pyruvate dehydrogenase, the enzyme known to convert pyruvate into acetyl-CoA. Through p53 and a HIF1 α -dependent mechanism, TIGAR has been shown to form a complex with hexokinase 2 at the mitochondria resulting in an increase in hexokinase 2 activity supporting the production of NADPH and limiting reactive oxygen species. p53, through Mieap, supports OXPHOS by mediating mitochondrial health and biogenesis. p53, via TIGAR, reduces glycolysis by degrading F26B, thereby decreasing the activity of PFK, a key glycolytic enzyme and diverts glycolytic intermediates into the pentose phosphate pathway. p53 also negatively regulates PDK-2 promoting acetyl-CoA production, decreases lactate production and represses the expression of MCT1. p53, like AMPK, downregulates the expression of GLUT1 and GLUT3. Moreover, any ADP/ATP ratio imbalance that affects ATP production or its consumption can result in LKB1-induced activation of AMPK. AMPK can subsequently promote OXPHOS by promoting fatty acid oxidation, mitochondrial biogenesis and mitochondrial health. AMPK has also been documented to control the differentiation switch from active glycolytic cytotoxic T lymphocytes to metabolically quiescent CD8⁺ T cells that preferentially utilise OXPHOS. Image: Phelan *et al.*, (2015) (175).

1.4.1.2 Novel mediators linking energy metabolism with inflammation, hypoxia and angiogenesis.

1.4.1.2.1 NFκB

Despite some early studies linking nuclear factor kappa B (NFκB) with energy metabolism, recent studies have increasingly shown NFκB to possess an equally important central role in various metabolic and pathological diseases (213). Inflammation is a key factor in the development of metabolic diseases such as atherosclerosis, insulin resistance, type 2 diabetes and obesity (213-215). The central role of NFκB in immunity, inflammation and carcinogenesis has been well documented (216-218). NFκB activation, thought to be mediated by PI3K/AKT-IKKα/β-ERK1/2, is also increased in Barrett's oesophagus and adenocarcinoma (219, 220).

NFκB regulates cellular respiration in a p53-dependent manner (figure 9) (221). Translocation of the NFκB family member RelA to mitochondria is inhibited by p53, however, in the absence of p53, RelA is transported into mitochondria and recruited to the mitochondrial genome where it represses mitochondrial gene expression, oxygen consumption and cellular ATP levels, thereby contributing to the switch to glycolysis (221). Indeed, it was reported that the RelA subunit also upregulates transcription of GLUT3 resulting in increases in glucose uptake and glycolytic flux (222). The elevated glycolytic flux stimulates further IKK/NFκB pathway activity in a positive feedback loop that subsequently promotes H-Ras-induced oncogenic transformation in mouse embryonic fibroblasts (222). This was the first functional study to show that NFκB promotes cell growth and carcinogenesis by metabolic manipulation, but crucially, p53 was central to this pathway, as introduction of p53 disrupted the link between NFκB and glycolysis (222).

Intriguingly, the role of NFκB is reversed in normal mouse embryonic fibroblasts upon glucose starvation, whereby NFκB inhibition causes cellular reprogramming to aerobic glycolysis (223). The role of NFκB in upregulating mitochondrial respiration in this circumstance involves the p53-mediated upregulation of mitochondrial SCO2, a key component of complex IV of the electron transport chain (223). Hence, NFκB can act as a focal checkpoint of metabolic homeostasis in conjunction with AMPK and p53 to regulate the response to low cellular ATP levels (223). Therefore, despite its prominent role in the Warburg effect, the metabolic plasticity of NFκB confers adaptivity in cells to adapt to fluctuating oxidative and hypoxic microenvironments.

1.4.1.2.2 VEGF and PFKFB3

In response to hypoxia-induced pro-angiogenic stimuli, endothelial cells rapidly switch from a metabolically inactive state of quiescence to an active migratory and proliferative state (224). Effective vascular sprouting relies on coordinated navigating tip cells and on proliferating stalk cells that elongate the sprout. Until recently, only genetic signals were known to play a role in this angiogenic switch. However, the angiogenic switch also requires a change in endothelial cell metabolism (224). Interestingly, endothelial cells are thought to be addicted to glycolysis as they rely minimally on oxidative phosphorylation for ATP generation (224, 225). For instance, the glycolytic inhibitor 2-deoxy-D-glucose induces significant endothelial cell death (226).

Endothelial cells increase their glycolytic rate by upregulating a range of glycolytic constituents including GLUT1, LDH and 6-phosphofructo-2-kinase/fructose-2,6-bisphosphatase-3 (PFKFB3) (224). PFKFB3 has been shown to be critical for angiogenic sprouting, and its inactivation reduces endothelial cell proliferation and migration, and impairs motility and formation of endothelial cell lamellipodia and filopodia (226). Conversely, PFKFB3 overexpression stimulates the sprouting of mitotically-inactivated endothelial cells and promotes tip cell formation (226). This entire process of tip and stalk cell differentiation, however, is under tight control of vascular epithelial growth factor (VEGF) and Notch signalling (figure 9) (225).

VEGF promotes tip cell induction and filopodia formation inducing the expression of the Notch ligand Delta-like 4 (DLL4) (225). One of the main genetic signals of vessel sprouting is orchestrated through Notch (227). DLL4 subsequently activates Notch signalling in neighbouring cells and suppresses VEGF receptor 2 expression and tip cell behaviour (225). Therefore, the activation of VEGF receptor 2 in tip cells upregulates PFKFB3 levels and glycolysis but induces the expression of the Notch ligand DLL4 in neighbouring stalk cells activating Notch signalling, lowering VEGF receptor 2 expression resulting in lower PFKFB3 expression and glycolytic flux (225). Interestingly, overexpression of PFKFB3 overcomes the pro-stalk activity of Notch signalling, thereby promoting tip cell behaviour, indicating that highly glycolytic endothelial cells can overcome inhibitory genetic signals (226).

VEGF also controls angiogenesis through the glycolytic metabolite lactate (224). Once taken up by endothelial cells through MCT1, lactate competitively inhibits the oxygen-sensing prolyl hydroxylase domain protein 2 (PHD2), resulting in activation of HIF1 α and an increase in VEGF receptor 2 expression (228). Lactate signalling also induces VEGF expression (229). In addition to

its angiogenic role, lactate also indirectly releases NF κ B inducing IL8 expression, another promoter of angiogenesis (230). VEGF has also been shown to induce the production of IL8 in endothelial cells (231). In addition to promoting aerobic glycolysis, VEGF stimulates mitochondrial biogenesis through Akt-dependent signalling, and plays a significant role in fatty acid metabolism (232-234). These studies demonstrate a close relationship between VEGF-induced metabolism, hypoxia, angiogenesis and inflammation in endothelial cells and highlight how stressed endothelial cells adapt to an altering milieu that could potentially favour tumour progression.

1.4.1.2.3 *mTOR, succinate and STAT3*

mTOR is a serine/threonine kinase that controls cell proliferation and metabolism in response to a range of extracellular stimuli such as the availability of nutrients, growth factors and stress (235). mTOR plays an important role in the modulation of both innate and adaptive immune function (figure 9) (236). As discussed, activated T cells switch to an anabolic metabolism using aerobic glycolysis as a major supply of ATP to fuel the rapid synthesis of proteins, nucleotides and other biosynthetic products (235). TORC1, one of two currently recognised signalling forms of mTOR, has been shown to be heavily involved in the up-regulation of enzymes involved in glycolysis, glutaminolysis, the pentose phosphate pathway, surface expression of GLUT1 and expression of the glutamine transporter, SNAT-2 (237-239). Similarly, inhibition of mTOR results in a metabolic bias towards oxidative phosphorylation and has been shown to produce a larger CD8 memory T cell pool (240). Ongoing clinical trials investigating the efficacy of mTOR inhibitors suggest that mTOR-mediated metabolism does play a central role in regulating biological outcomes within immune cells, however, a key question remaining is how mTOR-mediated metabolism is coupled to immune function (174).

Increasing evidence also proposes that succinate, a citric acid cycle metabolite that accumulates due to succinate dehydrogenase mutations, transmits an oncogenic signal from the mitochondria to the cytosol, directly inhibiting PHD and resulting in HIF1 α stabilization under normoxic conditions, with resultant increased expression of genes that facilitate angiogenesis, metastasis and glycolysis (figure 9) (241). By adding succinate to glioblastoma multiforme-derived cells cultured under hypoxic conditions, HIF1 α stabilization is induced which increases stem cell fractions and preserves the tumour stem cell niche thereby promoting tumour survival (242). Recently, it has been reported that succinate as a metabolite in innate immune function enhances IL1 β production during inflammation through HIF1 α , thereby promoting disease progression (243).

The signal transducer and activator of transcription factors (STATs) are a family of transcription factors that regulate cell growth, survival, differentiation and motility (244). One of the STAT members, STAT3, has long been recognised as a critical regulator of tumour cells (244). STAT3 has been recently found to act as one of the central mediators of aerobic glycolysis through both HIF1 α and independent mechanisms (figure 9) (244, 245). Upon translocation to the mitochondria, serine phosphorylation of STAT3 contributes to tumour cell transformation and tumourigenesis (246-248).

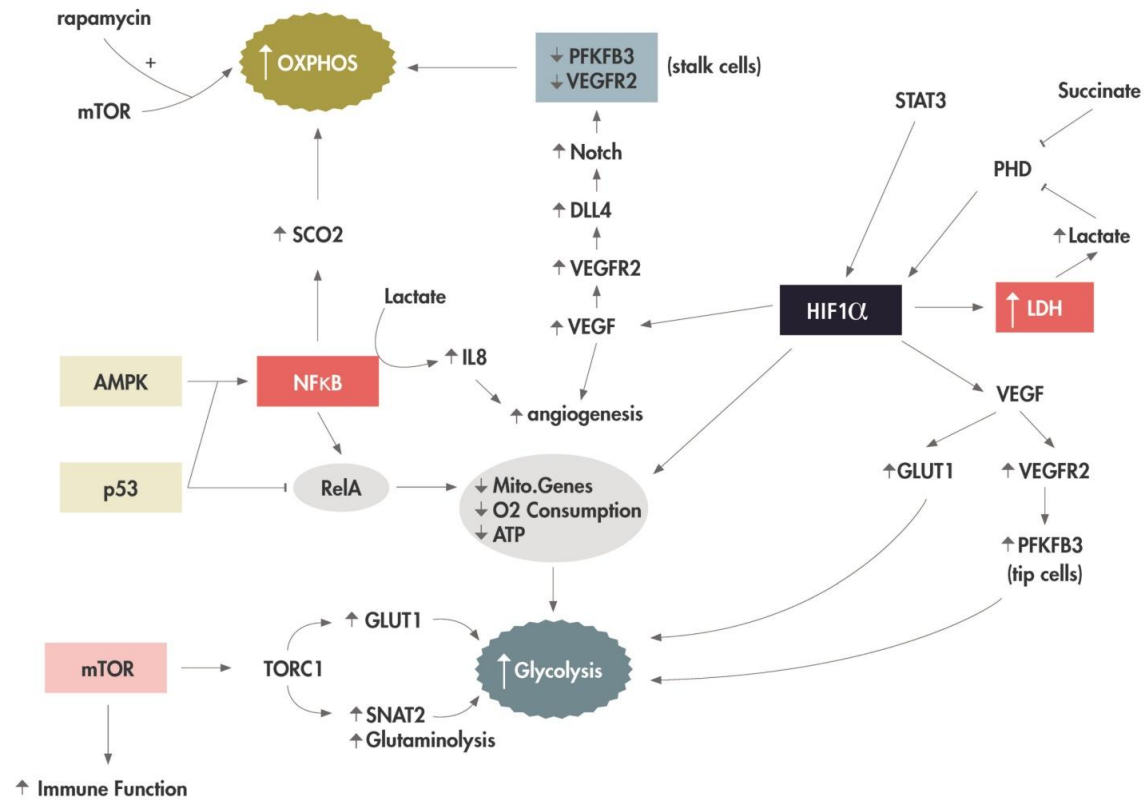


Figure 9. Novel mediators linking energy metabolism with inflammation, hypoxia and angiogenesis. NFκB regulates cellular respiration in a p53-dependent manner. In the absence of p53, the NFκB family member, Rel A, represses mitochondrial gene expression, oxygen consumption and cellular ATP levels thereby promoting glycolysis. NFκB promotes OXPHOS through an AMPK-p53-mediated mechanism by upregulating SCO2. Furthermore, endothelial tip cells increase their glycolytic rate and promote angiogenesis by upregulating numerous glycolytic constituents such as LDH and GLUT1, through HIF1α, VEGF, VEGFR2 and PFKFB3 signalling. The activation of VEGFR2 in tip cells induces the expression of Notch ligand DLL4 in neighbouring stalk cells activating Notch signalling. As a result, this reduces VEGF2 and PFKFB3 expression thereby lowering glycolytic flux and promoting OXPHOS in stalk cells. VEGF can also control angiogenesis through the glycolytic metabolite lactate, as lactate inhibits PHD resulting in HIF1α activation subsequently promoting OXPHOS and glycolysis. In addition, lactate has been shown to induce the production of IL8. mTOR, succinate and STAT3 can also mediate metabolism. mTOR plays an important role in the modulation of both adaptive and innate immune function. TORC1, one of mTOR's signalling forms, upregulates glycolysis, glutaminolysis and the expression of SNAT-2. Moreover, mTOR inhibition results in a metabolic bias towards OXPHOS. Succinate can mediate metabolism through the inhibition of PHD and HIF1α. Similarly, STAT3 can regulate tumour cell metabolism through HIF1. Image: Phelan *et al.*, (2015) (175).

1.4.2 Exploring the molecular mechanisms that link energy metabolism and hypoxia: Rheumatoid arthritis and circadian rhythms.

1.4.2.1 Glycolysis, hypoxia and rheumatoid arthritis

It has been 35 years since the link between increased glycolytic activity and rheumatoid arthritis (RA) was first established (249). In normal synovial tissue, glycolysis is the primary pathway for mitochondrial substrate oxidation of pyruvate (250). Levels of two major glycolytic enzymes glyceraldehyde 3-phosphate dehydrogenase (GAPDH) and LDH were significantly increased in the synovial cells between fresh non-rheumatoid and rheumatoid synovial tissue (249). More recently, one study detected elevated lactate and reduced glucose levels in the synovial fluid in RA (251). Moreover, it is plausible that metabolic alterations that favour aerobic glycolysis are a result of hypoxia-induced mitochondrial mutagenesis and dysfunction (252). Despite studies lacking strong evidence of a direct relationship between inflammation and glycolysis in RA, it is interesting that some glycolytic components are characterised as autoantigens, for example, glucose-6-phosphate isomerase, aldolase and enolase (250). However, studies need to be undertaken to examine the role of metabolic autoantigens in cancer initiation and progression.

On the other hand, the link between hypoxia and inflammation has been well documented *in-vivo* (253-256). Significantly higher levels of synovial fluid tumour necrosis factor- α (TNF α), IL1 β , interferon- γ and macrophage inflammatory protein-3 α in combination with low partial oxygen pressures of <20mm Hg were found in patients with inflammatory arthritis (256). Interestingly, TNF α blocking therapy reverses joint inflammation and hypoxia (255). Another study also demonstrated that hypoxia-induced IL-17A expression is localised to neutrophils, mast cells and T cells within inflamed synovial tissue supporting the concept that IL-17A is a key mediator in inflammatory arthritis (253).

Numerous mechanistic processes within the inflammatory joint may alter energy metabolism profiles. RA is associated with increased levels of HIF1 α and HIF2 α (257, 258). HIF1 also induces the expression of GLUT1 and GLUT3 (259). Furthermore, HIF has been shown to regulate the levels of hexokinase 2, GAPDH, LDH and cytochrome oxidase in the inflammatory synovium (259-263). RA is also commonly associated with mutations in p53 (264-266). As discussed, p53 can regulate glucose metabolism through NF κ B, however, loss of p53 promotes the positive feedback cycle between the IKK-NF κ B pathway and glycolysis, thereby promoting oncogenic transformation (222, 267). It is also plausible that angiogenic factors, such as VEGF, within the hypoxic inflammatory joint may induce alterations in energy metabolism profiles (268, 269). Therefore, it may be enticing to speculate that metabolic perturbations within the inflammatory joint are a

consequence of the combined contribution of many reciprocal mechanisms, for example, aberrantly expressed HIF1 α , HIF2 α , VEGF, NF κ B and mutations in p53.

1.4.2.2 AMPK, hypoxia and circadian rhythms

Significant time-of-day oscillations in glucose metabolism are observed in both humans and rodent models, at both the whole body and cellular level (270). It has been speculated that various mitochondrial functions may be regulated by the circadian clock, thereby serving as a central coordinator between the clock and cellular energy metabolism (271). For example, cytochrome c oxidase activity is increased in the brains of 2 month old wistar rats during wakefulness compared to sleep to meet increased energy demands (272). AMPK is one of the main metabolic sensors responsible for transmitting energy dependent signals to the mammalian clock (273).

A molecular oscillator exists whereby the transcription factors CLOCK and BMAL1 work together to drive the expression of many genes responsible for the mammalian molecular clock, including those encoding their own inhibitors, the period (PER1, PER2 and PER3) and cryptochrome (CRY 1 and CRY2) proteins (273). CRY1 and CRY2 are transcriptional repressors that are necessary for circadian clock function (274). The E3 ligase component F-box/LRR-repeat protein 3 (FBXL3) catalyzes the polyubiquitination of CYR1 and CRY2 and thus stimulates their proteosomal degradation (275). AMPK-mediated serine phosphorylation of CRY1 and CRY2 initiates the interaction between CRY1, CRY2 and FBXL3 and stimulates the degradation of both cryptochromes (276). Casein kinases, CKI ϵ and CKI δ , are also important modulators of circadian rhythm in mammals (273). Genetic disruption or pharmacological inhibition of these casein kinases alters behavioural and cellular circadian rhythms in mice (277). Casein kinases phosphorylate serines in PER2, however, AMPK was reported to phosphorylate CKI ϵ at serine 389, thereby increasing its enzymatic activity and indirectly leading to destabilisation of PER2 and alterations in circadian rhythm (278).

AMPK has also been implicated in circadian rhythm entrainment in mice as pharmacological activation of AMPK by intraperitoneal injection of both 5-aminoimidazole-4-carboxamide rib nucleoside (AICAR) or metformin causes a phase shift of the liver clock (276, 278). In addition, AICAR stimulation altered clock gene expression in wild type mice but not in mice lacking the AMPK γ 3 subunit implying that AMPK activation may play a role in circadian entrainment (279). Furthermore, AMPK possesses a close relationship with silent mating type information regulation 2 homolog 1 (SIRT1), another fuel-sensing molecule key to nutritional status and circadian regulation. AMPK not only enhances SIRT1 activity by increasing NAD⁺ levels but activation of

SIRT1 causes AMPK phosphorylation via LBK1 activation (280, 281). AMPK is also associated with regulating other metabolic sensors known to have key roles in circadian regulation such as poly(ADP-ribose) polymerase 1 and nicotinamide phosphoribosyltransferase (282, 283). These studies suggest that the effectiveness of widely prescribed drugs that regulate glucose homeostasis, such as metformin, may be ameliorated by altering the timing of treatment through AMPK-mediated control of circadian function by pharmacological intervention.

1.4.3 Reciprocal mechanisms linking energy metabolism to inflammation in gastroenterological diseases.

It is apparent thus far, that the combined effect of various molecular processes, can act in tandem to significantly alter the local microenvironment and attenuate disease progression. Little is known about how energy metabolism profiles cooperate with inflammatory processes to facilitate metaplastic progression in gastroenterological disease entities. However, some recent research has provided some insight on metabolic signatures in Barrett's oesophagus, oesophageal adenocarcinoma, inflammatory bowel disease (IBD), gastritis and gastric cancer (284-288).

Our research has demonstrated that both oxidative phosphorylation and glycolysis are reprogrammed early in the inflamed Barrett's disease sequence and may act mutually to promote disease progression in Barrett's oesophagus (130). Subsequent to screening 84 genes using a PCR microarray, validations utilising *in-vitro* and *in-vivo* models found that 3 genes associated with mitochondrial energy metabolism, *ATP12A*, *COX4I2* and *COX8C*, were differentially expressed across the Barrett's sequence (130). In addition, tissue microarrays demonstrated significant epithelial and stromal alterations using surrogate protein markers of oxidative phosphorylation, ATP synthase subunit 5 beta and heat shock protein 60, or *ATP5B* and *HSP60* respectively (130). Moreover, significant alterations across the Barrett's sequence were also demonstrated using surrogate protein markers of glycolysis, pyruvate kinase isozyme M2 and glyceraldehydes 3-phosphate dehydrogenase, or *PKM2* and *GAPDH* respectively (130). Interestingly, *ATP5B* in sequential follow up surveillance biopsy material segregated Barrett's non progressors and progressors to HGD and OAC, thereby highlighting the prognostic advantage of metabolic profiles in these preneoplastic patients (130). Finally, utilising the *in-vitro* model, the authors present evidence that Barrett's and adenocarcinoma cells exhibit significantly altered levels of various oxidative parameters, whereby the adenocarcinoma cell line maintains an equilibrium between both metabolic pathways while the Barrett's cell line favours a more detrimental oxidative phenotype that may be selected for during early stages of disease progression (130).

Other studies, although mostly indirectly, link inflammation to energy metabolism. IL-6, documented to be increased in myofibroblasts of Crohn's disease patients, has also been shown to increase the expression of hexokinase 2 and *PFKFB3* in murine embryonic fibroblasts (289, 290). Moreover, increased secreted and immunological levels of IL-6 have been found in Barrett's tissue compared to matched normal adjacent squamous epithelium (291). Aberrant expression of p53 is also associated with an increased risk of neoplastic progression in patients with Barrett's oesophagus (292). Therefore, since mutated p53 enhances IL-6 promoter activity in renal cell carcinoma, it may be plausible that p53, known to modulate oxidative phosphorylation and

glycolysis, simultaneously alters inflammatory and metabolic profiles in pre-neoplastic and neoplastic microenvironments of the oesophagus (222, 293). Similarly, HIF1 α , known to mediate hypoxia-induced alterations in glycolytic metabolism and to possess an intrinsic relationship with p53, has been shown to be differentially expressed across the Barrett's sequence (176, 206).

Interestingly, despite increased oxidative phosphorylation in Barrett's oesophagus, ulcerative colitis is associated with low levels of this metabolic pathway (286, 294). Loss of oxidative phosphorylation precedes the development of dysplasia in ulcerative colitis and thus could potentially be utilised to predict cancer (286). Furthermore, following neoplastic progression, cancer cells restore mitochondria indicative of an increase in energy demands for growth and proliferation (286). In addition, one study showed that increasing mucosal levels of ATP can protect mice from colitis and thus increasing ATP synthesis could be a plausible therapeutic approach for ulcerative colitis (294). Such reductions in oxidative phosphorylation, thought to be caused by defects in complex I of the electron transport chain, have also been reported in atrophic and active chronic gastritis (287, 295). Gastric cancer is additionally associated with a complex I-induced defective electron transport chain (296). As well as decreased mitochondrial respiration, gastric cancer exhibits shifts to glycolysis (285, 297). Decreased fructose-1,6-bisphosphatase (FBP), the enzyme which functions to antagonise glycolysis through NF κ B, has been shown to be decreased in both gastric cell lines and gastric carcinomas thereby promoting glycolysis (298, 299). PDK-1 and PKM2 are also overexpressed in gastric and colorectal tumour tissue and their expression is associated with poor survival (300-302). Moreover, knockdown of PKM2 has been shown to repress the proliferative and migratory capabilities of colorectal cancer cells (301).

IBD patients are known to have high levels of HIF1 α and HIF2 α (303). IBD patients also exhibit increased colonic expression of various glycolytic enzymes and these alterations in metabolism are thought to be triggered by hypoxic stress (304). Such extensive regulation of various glycolytic intermediates could be mediated by central regulators of metabolism known to associate with HIF, for example, PFKFB. One study in gastric cancer cell lines and tissue found that both PFKFB3 and PFKFB4 significantly responded to hypoxia through HIF1 α and this subsequently promoted the Warburg effect (305). Interestingly, alterations in the gut microbiome, as demonstrated by the fucosyltransferase 2 polymorphism in Crohn's disease patients for example, could also affect the host mucosal state and thus increase disease susceptibility (306). Therefore, further studies directly linking inflammation with energy metabolism profiles through these distinct processes would enhance our understanding on the mechanisms involved in inflammatory-induced neoplastic progression in gastrological diseases.

1.4.4 Innovative metabolic-based treatments and multi-targeted therapies

In order to replicate and divide, tumour cells need to possess the ability to acquire large quantities of proteins, lipids and nucleotides (174). As these processes are highly metabolically demanding, cells additionally require vast quantities of ATP. Consequently, targeting glucose metabolism and nucleotide biosynthesis could have significant advantages in combating metabolic transformation. In addition, altering the metabolism of susceptible or predisposed pre-neoplastic or neoplastic tissue may prevent subsequent disease progression.

Table 2 highlights some of the diverse therapeutic strategies currently being employed to target various aspects of energy metabolism. Significant research has begun to focus on targeting upstream regulators of metabolic pathways such as HIF, phosphoinositide 3-kinase (PI3K), Akt, mTOR and AMPK (174). For example, PI3K inhibitors such as BEZ235 have been shown to target metabolism leading to cancer regression in Kras-mutant murine lung adenocarcinomas (307). The AMPK activator metformin, primarily used to treat patients with type 2 diabetes, has been shown to be protective as those treated with metformin were cancer free over 8 years compared to those on alternative treatment regimes (308). Additional AMPK activators are also being investigated for their potential therapeutic use (309). Interestingly, methotrexate, a chemotherapeutic known to target nucleotide biosynthesis, enhances the antianabolic and antiproliferative effects of AICAR, an alternative AMPK agonist (310). Moreover, targeting nucleotide biosynthesis may be more favourable as nucleotide building blocks necessary for proliferating tumour cells can be synthesised by endogenous glucose and glutamine due to poor vascularisation (174). Therefore, blocking ribose-5-phosphate synthesis, with 5-fluorouracil (5-FU) for example, could provide a better therapeutic window. Dichloroacetate, an inhibitor of PDK-1, has also been shown to re-sensitise gastric cancer cells with hypoxia-induced resistance to 5-FU through the alteration of glycolysis (311).

Therapeutic agents that target the glycolytic pathway such as 2-deoxyglucose, ionidamine, 3-bromopyruvate and TLN-232 have also shown significant promise (174). Despite not showing substantial effects on tumour growth as monotherapeutic drugs, their use in conjunction with other chemotherapeutic reagents seems to sensitise tumours by reducing ATP levels and perhaps by indirectly limiting the availability of macromolecules synthesised through anapleurotic interactions (312). In addition to being combined with radiotherapy, some glycolytic inhibitors are currently being used in phase I, II and III clinical trials (174, 313). Inhibitors that target glucose transport across the plasma membrane, such as phloridzin and phloretin, have also shown efficacy in inhibiting *in-vitro*, xenograft and *in-vivo* tumour growth (314-316). Inhibition of PFKFB3

with 3-(3-pyridinyl)-1-(4-pyridinyl)-2-propen-1-one, or 3-PO, known to be a selective agent against neoplastic cells, has been shown to reduce cellular lactate, ATP, NAD⁺ and other cellular metabolites within several human malignant hematopoietic and adenocarcinoma cell lines (317).

Additional therapeutic modalities that can be exploited include targeting HIF1 α , lactate transporters, amino acid metabolism and lipid metabolism (174). Altering diet is also a unique and beneficial therapeutic approach. For example, a ketogenic diet relies on food that does not increase plasma glucose but produces ketone bodies that can be used as a carbon source thereby bypassing glycolysis (318). Even though the ketogenic diet has been shown to have mixed results, further studies may reveal that it is a cancer specific therapy (318). More recently, micro RNAs have shown promise at targeting cancer metabolic pathways. A recent study demonstrated that mir-122 targets PKM2 and affects metabolism in hepatocellular carcinoma (319). Despite the encouraging evolution of metabolic-based treatments and multi-targeted therapies, more work is required to understand which pathways are activated in distinct tumour types, thereby allowing the identification of pharmacological targets that can avert disease progression and alleviate tumour burden.

Table 2. Metabolic-based compounds.

<i>Drug</i>	<i>Target</i>	<i>Mechanism</i>	<i>Reference(s)</i>
<i>2-deoxyglucose</i>	Glycolytic Pathway	Inhibits the production of glucose-6-phosphate	(174, 313)
<i>3-bromopyruvate</i>	Glycolytic Pathway	Inhibits GAPDH	(174)
<i>3-PO</i>	Glycolytic Pathway	Inhibits PFKFB3	(317)
<i>5-FU</i>	Nucleotide Biosynthetic Pathway	Inhibits cell proliferation	(174)
<i>BEZ235</i>	PI3K/mTOR Pathways	Inhibits PI3K signalling & mTORC1/mTORC2	(307)
<i>Dichloroacetate</i>	Glycolytic Pathway	Inhibits PDK-1	(311)
<i>Lonidamine</i>	Glycolytic Pathway	Inhibits hexokinase and mitochondrial respiration	(174)
<i>Metformin</i>	AMPK agonist	Activates AMPK	(308)
<i>Methotrexate</i>	AMPK / Nucleotide Biosynthetic Pathway	Activates AMPK	(174, 310)
<i>Phloretin</i>	Glucose Transport	Inhibits sodium-glucose transporters 1 & 2	(314, 315)
<i>Phloridzin</i>	Glucose Transport	Inhibits sodium-glucose transporters 1 & 2	(314, 315)
<i>PX-478</i>	HIF1 α	Inhibits HIF signalling	(174)
<i>Salicylate</i>	AMPK agonist	Activates AMPK	(309)
<i>TLN-232</i>	Glycolytic Pathway	Inhibits PKM2	(174)
<i>WZB117</i>	Glucose Transport	Small molecule inhibitor of GLUT1	(316)

1.4.5 Chapter 1 overview

Mitochondria and cellular energy metabolism play a crucial role in inflammatory, hypoxic and angiogenic microenvironments by supporting malignant progression in a range of disease entities. Preneoplastic and neoplastic tissue must use a diverse range of molecular components to alter their metabolism to adapt to fluctuating oxidative, hypoxic and metabolic stresses. This involves exploiting various molecular elements such as HIF1 α , AMPK or p53 that have the potential to function rapidly to acute onsets of stress. It is evident from ongoing research, however, that tumour cells can survive these stresses by adjusting their metabolism through a range of alternative pathways and novel mediators such as NF κ B, VEGF and mTOR. Substantiating the reciprocal relationship between energy metabolism in inflammatory and hypoxic diseases is evident in RA and circadian rhythms. In addition, it is clear that the inflammatory environment in Barrett's oesophagus presents clear indication of some of these mutual associations. Therefore, understanding the underlying mechanisms that permit premalignant cells to transform, survive, thrive and subsequently adapt in response to a range of metabolic-based therapies will aid considerably in the development of effective and specific multi-targeted therapies.

1.5 AIMS AND OBJECTIVES

1.5.1 Overall hypothesis

Mitochondrial function and energy metabolism are important in driving disease progression in Barrett's oesophagus, and defects in mitochondrial biology link with other cellular processes within the Barrett's microenvironment.

1.5.2 Overall aim

The overall aim of this thesis is to characterise mitochondrial function and energy metabolism across the Barrett's disease sequence, assess if markers of metabolism can identify Barrett's oesophagus patients who progress to oesophageal adenocarcinoma and investigate the connection between metabolism and other key cellular processes known to be previously linked with disease progression.

1.5.3 Specific objectives

1. Assess mitochondrial function across the metaplasia-dysplasia-adenocarcinoma sequence using *in-vitro* and *in-vivo* models of Barrett's oesophagus.
2. Characterise mitochondrial energy metabolism across the metaplasia-dysplasia-adenocarcinoma sequence using *in-vitro* and *in-vivo* models of Barrett's oesophagus.
3. Investigate if deoxycholic acid and proton-pump inhibitors alter energy metabolism profiles across the normal squamous-metaplasia-dysplasia-adenocarcinoma sequence, and if antioxidants and a novel small molecule inhibitor can modulate metabolic profiles.
4. Examine if energy metabolism acts in tandem with key cellular processes (inflammation, hypoxia, p53 and obesity) in the Barrett's oesophagus microenvironment.
5. Elucidate if an inflammatory microenvironment and changes in diet can modulate energy metabolism and other key cellular processes to promote disease progression in a mouse model of Barrett's oesophagus.

Chapter 2

***BAK1, FIS1* and *SFN* modulate mitochondrial function and energy metabolism across the metaplasia-dysplasia-adenocarcinoma sequence in Barrett's oesophagus.**

2.1 INTRODUCTION

Despite numerous multimodality therapies, Barrett's oesophagus still lacks any proven therapeutic strategy. In addition, contemporary clinical management of Barrett's oesophagus has highlighted the need of accurate predictors of disease progression to oesophageal cancer. Moreover, the prognosis for individuals with Barrett's associated OAC still remains inadequate with a survival rate of 9-15%, however, some cancer centres report survival in patients treated with curative intent to be approximately between 35-50% (320, 321). Reliable prognostic markers would allow the tailoring of personalised medicine, influence personalised treatment regimes for individual patients and may prospectively determine if patients who have subsequently progressed to OAC would benefit from such physically demanding therapies such as radiation and chemoradiation therapy. In the last decade, the mitochondria have displayed potential in the early diagnosis, prognosis and treatment response of various cancers (322-324).

The mitochondria have been implicated in cancer since the nineteenth century (325). Early studies investigating the role of mitochondria in tumour cells concluded that the mitochondria were dysfunctional compartments, however, they are now known to play a supportive role or even trigger disease progression (325). Many studies also suggest that increases in mitochondrial activity are an important step for the generation of disseminated tumour cells, thereby contributing to metastases (326, 327). In normal cells, mitochondria play several roles in various anabolic and catabolic pathways including the maintenance of calcium homeostasis, the synthesis of ATP, the buffering of the redox potential within the cytosol and as a protagonist of apoptosis (325, 328). It is through these cellular mechanisms that mitochondria can support the initiation, transformation, differentiation and aggressive proliferation of tumour cells in both preneoplastic and neoplastic microenvironments.

Aerobic glycolysis has been shown to be the primary source of ATP in the majority of cancers, however, both oxidative phosphorylation and glycolysis have both been shown to be reprogrammed across the disease sequence in Barrett's oesophagus (130). In addition, we have shown a marker of mitochondrial respiration, ATP5B, segregated Barrett's patients who progressed to HGD/OAC from non-progressors, highlighting the possible prognostic advantage of screening for mitochondrial dysfunction in these preneoplastic Barrett's patients (130). Increased reactive oxygen species (ROS) is also implicated in the impairment of mitochondrial acetoacetyl-CoA thiolase in ulcerative colitis (329). Differential expression of the electron transport chain complexes is associated with the development of ulcerative colitis (286, 330-332). S100 calcium-binding protein P, carbamoyl-phosphate synthase 1, transcription factor Sp1, peroxisome proliferator-activated receptor-gamma coactivator-1 α and c-myc are other mitochondrial

associated proteins known to be involved in neoplastic progression in ulcerative colitis (286, 333). In addition, overexpression of mitochondrial translocator protein in ulcerative colitis and Crohn's disease has been demonstrated as having potential diagnostic and treatment value (334). Moreover, there is a significant lack of assessment of these mitochondrial parameters in Barrett's oesophagus.

Mitochondrial dysfunction can also contribute to the development of chemoresistance in cancer (335). To support a role of mitochondrial dysfunction in cancer drug resistance, studies with cells chemically depleted of mitochondrial DNA become less sensitive to chemotherapeutic drugs (336, 337). Mitochondrial dysfunction also promotes resistance to the induction of apoptosis, thought to be attributed to the mislocalisation of pro-apoptotic factors (338). Studies have additionally investigated a plausible role of ROS-mediated apoptosis through the regulation of redox balance (339). In addition, various genetic and metabolic mitochondrial alterations have been implicated in the modulation of drug sensitivity in a range of cancer cells (335, 340). Moreover, mitochondrial mutations are associated with increased metastasis and adverse prognosis (150, 341). Conversely, increased mitochondrial DNA has been shown to induce acquired resistance to docetaxel in head and neck cancer cells (342). Furthermore, increased expression of ATP5B has been shown to be significantly increased in patients who have a poor pathological response to neoadjuvant chemoradiation therapy in OAC suggesting a role for mitochondria in the radioresistance of OAC (158). Interestingly, one study shows evidence of mitochondrial mutations below a threshold level being associated with tumour growth, however, when mutations reach a critically high frequency, the opposite effect is observed, thereby illustrating biphasic oncogenic and anti-tumourigenic phenotypes indicative of mitochondrial adaptability (335, 343).

Therefore, the aim of this study was to examine mitochondrial function across the disease sequence *in-vitro* and *in-vivo* in Barrett's oesophagus. We have identified genes associated with mitochondrial function that are differentially expressed across the metaplastic-dysplastic-OAC disease sequence both *in-vitro* and *in-vivo*. We demonstrate through functional manipulation of these mitochondrial genes alterations in cellular bioenergetics and mitochondrial function; specifically mitochondrial mass, ROS production and mitochondrial membrane potential (MMP). Obtaining a better understanding of mitochondrial function may reveal potential biological mechanisms that promote disease progression that could be exploited for improved targeted drug development.

2.2 HYPOTHESIS AND AIMS OF CHAPTER TWO

We hypothesise that mitochondrial function is differentially expressed across the metaplasia-dysplasia-adenocarcinoma sequence in *in-vitro* and *in-vivo* models of Barrett's oesophagus.

Specific aims of chapter 2;

- 1) Identify, using specific mitochondrial arrays, gene changes involved in mitochondrial function across the Barrett's disease sequence *in-vitro*.
- 2) Validate the expression of the identified mitochondrial function target genes across the disease sequence *in-vivo*.
- 3) Examine the functional effect of knocking down mitochondrial gene targets using siRNA on mitochondrial mass, ROS production and mitochondrial membrane potential *in-vitro*.
- 4) Investigate the effect of knocking down mitochondrial gene targets using siRNA on cellular metabolism *in-vitro* utilising the Seahorse XF^E24 analyser.

2.3 MATERIALS AND METHODS

2.3.1 Chemicals and reagents

All laboratory chemicals and reagents were purchased from Sigma-Aldrich (USA) unless otherwise stated and were prepared and stored according to the manufacturer's specifications. Chemicals and reagents were weighed using a Radwag fine electronic balance (Radwag AS110.R2) and solubilised in double distilled water unless otherwise stated. The pH of solutions was measured using an Accumet pH metre (Fisher Scientific, AB150) subsequent to calibration using buffers at pH 4, pH 7 and pH 10. Labnet pipettes (p1000, p200, p20 and p10) were used to transfer liquid volumes up to 1mL, electronic pipette aids (Drummond, PA, USA) and disposable pasteur pipettes (Starstedt Ltd., Wexford, Ireland) were used for liquid volumes greater than 1mL and graduated cylinders were used for volumes greater than 10mL.

2.3.2 Metaplastic, dysplastic and adenocarcinoma cell line models

QH (Barrett's), GO (dysplasia) and OE33 (OAC) cell lines, representing stages of the Barrett's disease sequence, were grown to 70% confluency in BEBM medium (OE33 in RPMI, 2mM glutamine, 10% FBS, 1% penicillin-streptomycin L-glutamine) supplemented with BEBM SingleQuots (2mL BPE, 0.5mL insulin, 0.5mL HC, 0.5mL GA-1000, 0.5mL retinoic acid, 0.5mL transferrin, 0.5mL triiodothyronine, 0.5mL adrenaline and 0.5mL hEGF per 500ml media). QH and GO cell lines were obtained from American Type Culture Collection (ATCC) (LGC Standards, Middlesex, UK). The OE33 cell line was sourced from the European Collection of Cell Cultures (Sailsbury, UK). Cell RNA extractions were subsequently performed using RNeasy Mini Kit (Qiagen) following manufacturer's instructions. RNA content and quality was quantified and assayed respectively and RNA reverse transcribed using the RT² PCR array first strand kit (SABiosciences).

2.3.3 In-vitro cell culture

2.3.3.1 Cell line subculturing

All culturing was carried out using an aseptic technique in a grade II laminar air flow cabinet, cleaned and sterilised monthly. The unit, all equipment, chemicals and reagents used within the laminar hood were swabbed with 70% (v/v) industrial methylated spirits (Lennox Laboratory Supplies, Dublin, Ireland) before and after use. Cell lines (section 2.3.2) were examined daily using an inverted phase contrast microscope (Optika, XDS-1R) and subcultured upon reaching approximately 70-80% confluency. 1-2mL of trypsin ethylene diamine tetra acetic acid (EDTA) (0.05% (w/v) trypsin, 0.02% (w/v) EDTA) was added to the cell monolayer of the flask until cells detached and were in solution. The same volume (1-2mL) of complete media (containing 10%

FBS) was added to inactivate the trypsin, cells counted (section 2.3.3.4) and cells seeded at the appropriate densities as desired according to the experimental setup. Excess cells, along with 10mL complete media, were transferred into a 75cm² flask to maintain the cell line and cultured at 37°C in a CO₂ incubator.

2.3.3.2 Preparation of stable frozen stocks

Frozen stocks were prepared from cell lines growing in the exponential growth phase at 70-80% confluency. Cells were trypsinised as described above (section 2.3.3.1) and 5mL of complete media was added to inactivate the trypsin. Cells were centrifuged at 1500 X rcf for 3 minutes, the supernatant decanted and the pelleted cells resuspended in FBS containing 10% dimethylsulfoxide (DMSO). The cell suspension was subsequently divided into 1.25mL aliquots and cryovials were transferred to a -80°C freezer for short term storage or under liquid nitrogen for long term storage.

2.3.3.3 Reconstitution of frozen cell stocks

Frozen stocks were thawed rapidly at 37°C, centrifuged at 1500 X rcf for 2 minutes, the supernatant decanted, the cell pellet resuspended in 1mL complete media and transferred to a 75cm² and incubated overnight at 37°C and 5% CO₂. The media was replaced the following day and cell subculturing was continued as described above (see section 2.3.3.1).

2.3.3.4 Cell counting

Cells were counted using a haemocytometer (Supe Rior, Germany). Cells were trypsinised as described above (section 2.3.3.1), added to 5mL of complete media and centrifuged at 1500 x rcf for 3 minutes. The supernatant was decanted and the cell pellet resuspended in 1mL complete media. 20µL of the cell suspension was added to 180µL trypan blue (0.4% w/v) solution and mixed well by repeated pipetting. 20µL of this cell suspension was added to the counting chamber of the haemocytometer and the number of viable cells in five grids (the four corner and centre grids) were counted. The number of cells per millilitre was calculated using the following equation:

$$(N/5) \times 10^4 \text{ and } 10 \text{ (dilution factor)} = \text{Cells per 1 millilitre}$$

(where,

N = Total numbers of cells in 5 grids

5 = Number of grids counted

10^4 = Haemocytometer constant

10 = Trypan Blue Dilution factor).

2.3.4 Screening via qRT-PCR microarray analysis

A catalogued human mitochondrial function PCR gene microarray (Qiagen) was used to simultaneously quantify the expression of 84 mitochondrial genes across the *in-vitro* sequence using the beta-2-microglobulin (B2M) gene as the endogenous control gene. PCR was performed using the RT² Real-time SYBR Green PCR mix (SABiosciences) on a 7900HT Fast Real-time PCR Light-Cycler System (Applied Biosystems). Data were analysed utilising the $2^{-\Delta\Delta Ct}$ method. First, threshold cycle (Ct) values were converted to 2^{-Ct} in order to be proportional to the amount of transcripts in all samples. Next, $2^{-\Delta Ct}$ values were calculated by normalising the data to a housekeeping gene, B2M, as follows: $2^{-\Delta Ct} = 2^{-Ct}(\text{sample}) / 2^{-Ct}(\text{B2M})$. In order to compare the data between cell line models, $2^{-\Delta\Delta Ct}$ values were calculated by normalising the experimental data by reference data. For example, data from the calibrator QH cell line was normalised to the GO cell line as follows: $2^{-\Delta\Delta Ct} = 2^{-\Delta Ct}(\text{QH}) / 2^{-\Delta Ct}(\text{GO})$. Differentially expressed genes were defined as those that changed by >4-fold.

2.3.5 In-vitro validation of gene targets

2.3.5.1 cDNA synthesis

Cell lines were cultured (see section 2.3.3) and RNA extracted as above (see section 2.3.2). Per sample, 1 μ g of RNA and 1 μ L 0.5 μ g/ μ L random hexamers (Invitrogen), made up to 12 μ L with RNase/DNase free dH₂O, was heated at 70°C for 10 minutes and put immediately on ice. To each sample, 1 μ L 10mM dNTPs (Invitrogen), 4 μ L 5xbuffer (Bioline), 2 μ L RNase/DNase free dH₂O, 0.5 μ L 0.2 μ g RNase out (Invitrogen) and 0.5 μ L Bioscript reverse transcriptase enzyme (Bioline) was then added, vortexed, gently centrifuged and heated at 37°C for 1.5 hours followed by 70°C for 10 minutes using a Peltier thermocycler (MJ Research, Peltier Thermal Cycler, PTC-200). cDNA samples were subsequently stored at -20°C prior to undertaking real-time PCR.

2.3.5.2 Quantitative real-time PCR

Gene primer probes for *BAK1*, *CDKN2A*, *FIS1*, *SFN* and *18S* (Applied Biosystems) were purchased and real-time PCR was performed in triplicate using Taqman mastermix (Applied Biosystems). Each well of the qPCR reaction consisted of 10 μ L Taqman mastermix, 8 μ L RNase/DNase free dH₂O, 1 μ L of the transcribed cDNA from the sample of interest and 1 μ L of primer probe specific to the gene of interest. Data were analysed utilising the $2^{-\Delta\Delta Ct}$ method as before (see section 2.3.4).

2.3.6 In-vivo qRT-PCR validation of gene targets

The expression of these four genes was analysed in independent groups of tissue across the Barrett's sequence. Real-time qRT-PCR was performed and all genes validated across the diseased

Barrett's sequence *in-vivo* utilising normal squamous ($n=10$), metaplasia ($n=34$), LGD ($n=13$), HGD ($n=12$) and OAC ($n=8$) cases. The median age of the patients was 61 years and there was a 1.52-fold male predominance. Ethical approval to conduct all aspects of this work was granted by the Adelaide and Meath Hospital (AMNCH), Tallaght, Dublin (REC 200110405). All cases were prospectively recruited at our national referral centre for upper GI malignancy. Written informed consent was obtained in accordance with local institutional ethical guidelines. All patients attending with histologically confirmed Barrett's esophagus or OAC arising in Barrett's were considered for inclusion. Patients with a prior history of treated OAC (including *in-situ* carcinoma post endomucosal resection), other malignancy of any type, ablative therapy (Radiofrequency ablation, Argon plasma coagulation, cryoablation) were excluded.

Endoscopic examination consisting of white light and chromoendoscopy (FICE (fujinon) or NBI (olympus)) was performed in all cases. The Barrett's segment was assessed and measured as per the Prague classification system. Suspicious sites were biopsied using large capacity forceps in the first instance, with mapping biopsies performed thereafter as per international guidelines. Matched squamous samples were taken at least 5cm superior to the proximal border of Barrett's mucosa.

Normal control samples, demonstrating normal squamous mucosa, were taken from individuals attending for upper GI endoscopy without symptoms to suggest GORD or other inflammatory aetiology. Cancer samples were taken from individuals undergoing assessment for a new diagnosis of OAC arising in a setting of Barrett's esophagus. All samples were placed in RNAlater at the time of endoscopy. Barrett's tissue was characterised by assessing the expression of columnar epithelium molecular markers, cytokeratin 8 and villin by RTPCR (undertaken by Dr. Finbar MacCarthy).

Patient tissue was homogenised using a Tissue-Lyser (Qiagen) for 5 mins at a frequency of 25 pulses per second, RNA extracted, reverse transcribed (Bioline), RNA quantified (NanoDrop, Technologies, Wilmington, DE) and sample quality assessed using the RNA Nano 6000 kit (Agilent technologies, Santa Clara, CA).

2.3.7 *In-vitro* siRNA knockdown of gene targets

QH (Barrett's) and OE33 (OAC) cell lines, representing Barrett's metaplasia and OAC respectively, were grown and cultured to 70% confluency as above (see section 2.3.3). Both cell lines were seeded for mitochondrial function and metabolic Seahorse assays at 15,000 cells per well (96 well format) and simultaneously reverse transfected with previously optimised 10nM HLC purified

27mer Dicer-substrate siRNA duplexes specific to *BAK1*, *FIS1* and *SFN* with an adequate universal scrambled negative control siRNA duplex (Origene). Moreover, QH and OE33 cells were treated with 10ul and 20ul of siTran 1.0 transfection reagent (Origene) respectively per 10nM siRNA treatment and were incubated at 37°C in a CO₂ incubator for 24 hours prior to commencing mitochondrial function and metabolic Seahorse assays. QH and OE33 cells were reverse transfected similarly to characterise knockdown efficiency through qRT-PCR. qRT-PCR was undertaken as described in section 2.3.5 using specific Taqman primer probes for *BAK1*, *FIS1* and *SFN* (Applied Biosystems).

2.3.8 Exploring the functional effect of siRNA knockdown on reactive oxygen species production, mitochondrial mass and mitochondrial membrane potential in-vitro

QH and OE33 cells were seeded at 15,000 cells per well in a 96-well cell culture plate, reverse transfected as described above (see section 2.3.7) and allowed to incubate for 24 hours. The cells were washed with 100ul PBS/Mg²⁺ buffer (130mM Na²Cl, 5mM KCl, 1mM Na²PO₄, 1mM CaCl₂, 1mM MgCl₂ and 25mM HEPES, pH 7.4) and incubated for 30 mins at 37°C with 100ul 5µM 2',7'-dichlorofluorescein (Invitrogen), 0.3µM mitotracker (Invitrogen) or 5µM rhodamine (Sigma) to assess reactive oxygen species production, mitochondrial mass and mitochondrial membrane potential respectively. Cells were washed with 200ul PBS/Mg²⁺ buffer, the buffer discarded, 100ul fresh buffer added and fluorescence read with excitation and emission wavelengths of 485nm and 538nm respectively (Thermo Scientific, Fluoroskan Ascent FL). All measurements were normalised to cell number using the crystal violet assay (see section 2.3.9).

2.3.9 Crystal Violet Assay

All assays undertaken were normalised to cell number using a crystal violet assay. Cell growth media was removed carefully from cells and 50µL 1% glutaraldehyde (Sigma) (in PBS) per well was added to cells in a 96 well plate for 15 minutes at room temperature. The glutaraldehyde was removed and gently washed with 1x PBS twice. 50µL 0.1% crystal violet (Sigma) (in dH₂O) was added to each well for 30 minutes at room temperature, all wells gently washed with tap water and the plate left inverted to dry overnight. 40µL of 1% triton-X (Sigma) (in PBS) was added to each well and the plate put on a plate shaker for 15 minutes at room temperature. Each corresponding well solution was then transferred into a new 96 well plate and the absorbance read at 590nm using a Versa-max spectrophotometer (Molecular Devices).

2.3.10 Characterising the metabolic effect of siRNA knockdown utilising the Seahorse XF^E24 analyser *in-vitro*

Oxygen consumption rate (OCR) and extracellular acidification rate (ECAR), reflecting oxidative phosphorylation and glycolysis respectively, were measured before and subsequent to treatment with oligomycin (2 $\mu\text{g}\cdot\text{mL}^{-1}$, Sigma), trifluorocarbonylcyanide phenylhydrazone (FCCP) (2 μM , Sigma), antimycin-A (2 μM , Sigma) and 2-DG (100mM, Seahorse Biosciences) using the Seahorse XF^E24 analyser (Seahorse Biosciences). QH and OE33 cells were seeded at 15,000 cells per well in a 24-well cell culture XF microplate (Seahorse Biosciences), reverse transfected as described above (see section 2.3.7) and allowed to incubate for 24 hours. Cells were rinsed with assay medium (unbuffered DMEM supplemented with 10mM glucose, 5mM sodium pyruvate and 1mM L-glutamine, pH 7.4) before incubation with assay medium for 1 hour at 37°C in a non-CO₂ incubator. Three baseline OCR and ECAR measurements were obtained over 21 minutes before injection of specific metabolic inhibitors. Three OCR and ECAR measurements were obtained over 15 minutes following injection with oligomycin, FCCP, antimycin-A and 2-DG. Percentage non-mitochondrial respiration was calculated by expressing residual OCR post antimycin-A injection as a percentage of baseline OCR. Oligomycin-induced compensatory glycolysis was calculated by plotting ECAR as a percentage of baseline ECAR post oligomycin injection. The experiment was repeated four times with technical replicates. All measurements were normalised to cell number using the crystal violet assay (see section 2.3.9).

2.3.11 Statistical analysis

Data were analysed using Graph Pad Prism software (Graph Pad Prism, San Diego, CA). One-way ANOVA was used to investigate differences in *BAK1*, *CDKN2A*, *FIS1* and *SFN* expression across the *in-vitro* Barrett's sequence (Bonferroni post-hoc test; unpaired *t*-test). qRT-PCR *in-vivo* data were normalised using the $2^{-\Delta\Delta\text{Ct}}$ method and statistically analysed using a Kruskal-Wallis test (Dunns post-hoc test; Mann-Whitney U). qRT-PCR target genes were statistically analysed (Wilcoxon Sign Rank) in matched patient samples to explore if observed gene expression changes were an effect seen in the Barrett's tissue compared to the surrounding mucosa. Student's paired *t*-tests were utilised to compare differences in control and siRNA treated groups for all *in-vitro* mitochondrial and Seahorse assays. Differences of $P < 0.05$ (*), $P < 0.01$ (**) and $P < 0.001$ (***) were considered statistically significant.

2.4 RESULTS

2.4.1 *In-vitro* screening using human PCR gene microarrays

To analyse the expression of 84 human genes associated with global mitochondrial function across the disease sequence *in-vitro*, fold expression of all target genes was normalised relative to the Barrett's metaplastic cell line model, QH. The cut-off for differential gene expression was defined by either a relative 4-fold upregulation or 4-fold downregulation. 4 of the 84 mitochondrial function gene targets (*BAK1*, *FIS1*, *CDKN2A* and *SFN*) were differentially expressed across the metaplastic-dysplastic-OAC cell line sequence. These 4 gene targets identified were subsequently validated *in-vitro* and *in-vivo* using patient samples.

Figure 10 shows the *in-vitro* PCR gene microarray screen between the Barrett's, dysplastic and OAC cells. Using a 4-fold cut-off, 3 gene targets were differentially expressed between QH and GO cells (figure 10A). Using a 4-fold cut-off, 13 gene targets were differentially expressed between QH and OE33 cells (figure 10B). Using a 4-fold cut-off, 12 gene targets were differentially expressed between the GO and OE33 cells (figure 10C). Table 3 summarizes the relative expression of all 84 genes screened between QH and OE33 cell lines (see appendices A and B for additional PCR microarray screen results between GO and QH and between GO and OE33 cells respectively).

Figure 11 shows the *in-vitro* validation of the 4 mitochondrial function gene targets. While *BAK1* (figure 11A) and *FIS1* (figure 11B) expression was not statistically significant across the Barrett's sequence, *SFN* ($P=0.0011$) expression significantly decreased between Barrett's and OAC cell lines but significantly increased between GO and OAC cell lines (figure 11C). *CDKN2A* ($P=0.0158$) expression significantly increased across the *in-vitro* Barrett's sequence (figure 11D).

2.4.2 *In-vivo* validation of gene targets

Figure 12 illustrates mitochondrial function gene expression of the 4 gene targets across the disease sequence in diseased and matched normal adjacent tissue samples. *BAK1* (figure 12A) ($P<0.05$), *FIS1* (figure 12C) ($P<0.05$), *SFN* (figure 12E) ($P<0.0001$) and *CDKN2A* (figure 12G) ($P<0.01$) were differentially expressed across the Barrett's sequence. Field effect changes in gene expression of these targets in diseased versus matched normal adjacent biopsies was examined. *BAK1* (figure 12B) ($P<0.01$), *FIS1* (figure 12D) ($P<0.01$) and *SFN* (figure 12F) ($P<0.001$) were differentially expressed across the Barrett's disease sequence suggesting this effect was specific to the pathological diseased tissue (Barrett's, LGD, HGD/OAC) compared to the matched surrounding matched mucosa. Moreover, as no significant difference in *CDKN2A* (figure 12H)

($P>0.05$) expression was found between pathological diseased tissue and the matched surrounding matched mucosa, the functional effect of *BAK1*, *FIS1* and *SFN* gene manipulation was further examined *in-vitro*.

2.4.3 Functional effect of *BAK1*, *FIS1* and *SFN* siRNA knockdown on reactive oxygen species (ROS) production, mitochondrial mass and mitochondrial membrane potential (MMP) *in-vitro*

BAK1, *FIS1* or *SFN* knockdown did not affect cell number in QH (figure 13A) or OE33 cells (figure 13B). Figure 14 shows the functional effect of *BAK1* siRNA knockdown on ROS production, mitochondrial mass and MMP in the Barrett's and OAC cell lines. siRNA-induced knockdown of *BAK1* resulted in a significant reduction in *BAK1* expression in the QH (figure 14A) ($P=0.019$) and OE33 (figure 14B) ($P=0.003$) cell lines of 81.9% and 56.9% respectively compared to unscrambled control treated cells. Knockdown of *BAK1* in QH cells significantly increased ROS levels (figure 14C) ($P=0.0248$) and significantly decreased MMP (figure 14G) ($P=0.045$) while not affecting mitochondrial mass (figure 14E). In contrast, knockdown of *BAK1* in OE33 cells had no effect on ROS levels (figure 14D), mitochondrial mass (figure 14F) or MMP (figure 14H). Thus, changes induced by *BAK1* knockdown were specific to Barrett's cells.

Figure 15 shows the functional effect of *FIS1* siRNA knockdown on ROS production, mitochondrial mass and MMP in the Barrett's and OAC cell lines. siRNA-induced knockdown of *FIS1* resulted in a significant reduction in *FIS1* expression in both the QH (figure 15A) ($P=0.0242$) and OE33 (figure 15B) ($P=0.0037$) cell lines of 75.9% and 54.8% respectively compared to unscrambled control treated cells. Knockdown of *FIS1* in QH cells significantly decreased MMP (figure 15G) ($P=0.019$) but not alter ROS levels (figure 15C) or mitochondrial mass (figure 15E). In contrast, knockdown of *FIS1* in OE33 cells significantly increased mitochondrial mass (figure 15F) ($P=0.0316$), however, ROS levels (figure 15D) and MMP (figure 15H) remained unchanged.

Figure 16 shows the functional effect of *SFN* siRNA knockdown on ROS production, mitochondrial mass and MMP in the Barrett's and OAC cell lines. siRNA-induced knockdown of *SFN* resulted in a significant reduction in *SFN* expression in both the QH (figure 16A) ($P=0.0495$) and OE33 (figure 16B) ($P=0.0247$) cell lines of 73% and 41% respectively compared to unscrambled control treated cells. Knockdown of *SFN* in QH cells significantly decreased MMP (figure 16G) ($P=0.049$) but did not alter ROS levels (figure 16C) or mitochondrial mass (figure 16E). Similarly, knockdown of *SFN* in OE33 cells significantly decreased MMP (figure 16H) ($P=0.0224$) without affecting ROS levels (figure 16D) or mitochondrial mass (figure 16F).

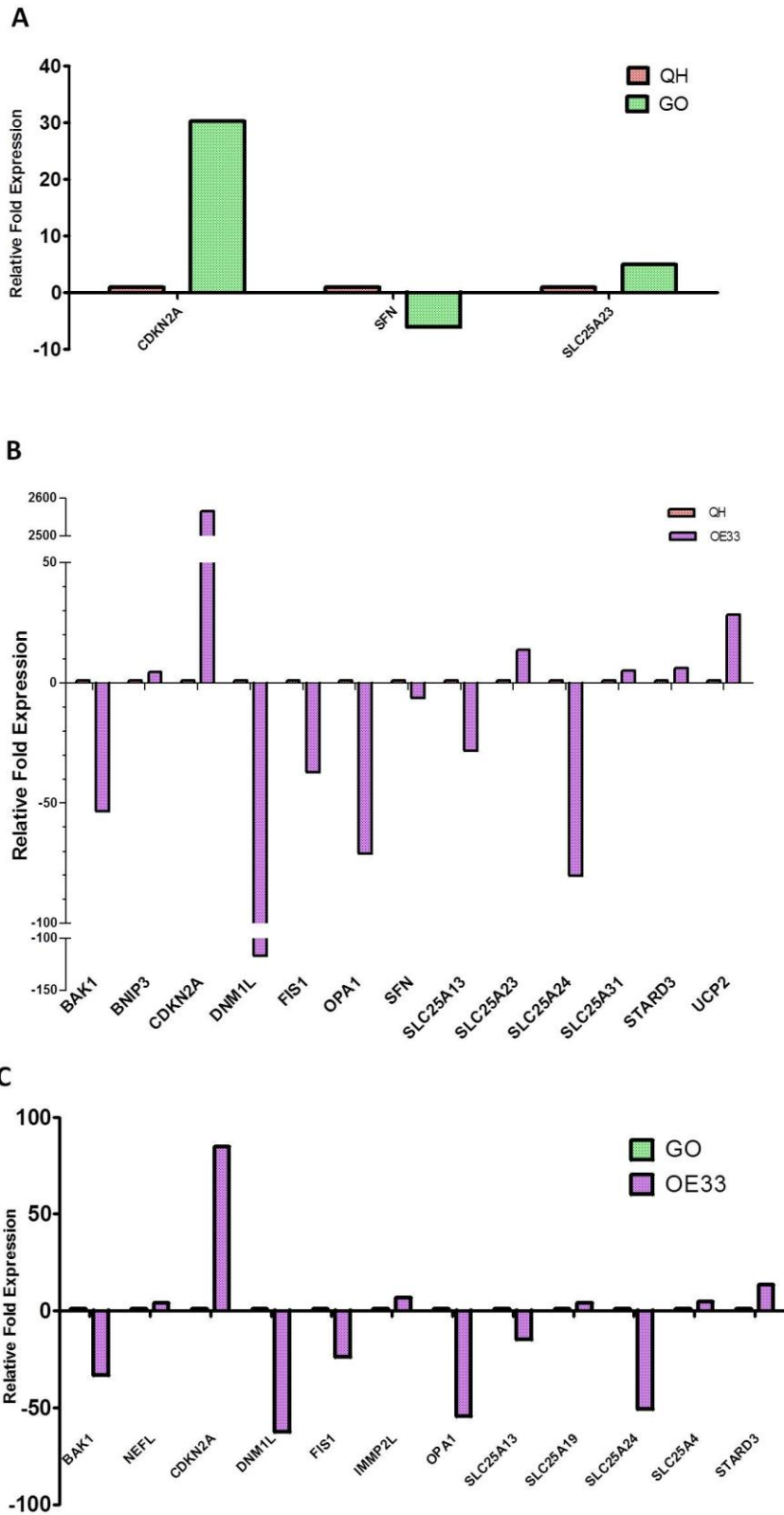


Figure 10. Human PCR gene microarray screen across the Barrett's cell lines. (A) Using a 4-fold cut-off, 3 gene targets were differentially expressed between the Barrett's (QH) and dysplastic (GO) cell lines. **(B)** Using a 4-fold cut-off, 13 gene targets were differentially expressed between the Barrett's (QH) and adenocarcinoma (OE33) cell lines. **(C)** Using a 4-fold cut-off, 12 gene targets were differentially expressed lines between the dysplastic (GO) and adenocarcinoma (OE33) cell lines. Arrays were performed in duplicate.

Table 3. Mitochondrial function gene microarray screen between QH and OE33 cell lines

Gene	Expression*	Gene	Expression*	Gene	Expression*
<i>AIFM2</i>	4.16	<i>NEFL</i>	6.63	<i>SLC25A4</i>	1.63
<i>AIP</i>	-1.17	<i>OPA1</i>	-70.93	<i>SLC25A5</i>	1.11
<i>BAK1</i>	-53.37	<i>PMAIP1</i>	-1.20	<i>SOD1</i>	-1.63
<i>BBC3</i>	-2.13	<i>RHOT1</i>	1.59	<i>SOD2</i>	-1.85
<i>BCL2</i>	1.22	<i>RHOT2</i>	-1.14	<i>STARD3</i>	6.13
<i>BCL2L1</i>	1.28	<i>SFN</i>	-6.38	<i>TAZ</i>	1.52
<i>BID</i>	1.80	<i>SH3GLB1</i>	-1.01	<i>TIMM10</i>	1.57
<i>BNIP3</i>	4.49	<i>SLC25A1</i>	-1.78	<i>TIMM17A</i>	-1.30
<i>CDKN2A</i>	2565.37	<i>SLC25A10</i>	1.54	<i>TIMM17B</i>	1.28
<i>COX10</i>	-1.88	<i>SLC25A12</i>	-1.94	<i>TIMM22</i>	-2.57
<i>COX18</i>	-1.90	<i>SLC25A13</i>	-28.33	<i>TIMM23</i>	1.52
<i>CPT1B</i>	-1.15	<i>SLC25A14</i>	-3.91	<i>TIMM44</i>	1.04
<i>CPT2</i>	-1.85	<i>SLC25A15</i>	-1.19	<i>TIMM50</i>	-1.46
<i>DNAJC19</i>	1.03	<i>SLC25A16</i>	1.42	<i>TIMM8A</i>	-1.14
<i>DNM1L</i>	-116.76	<i>SLC25A17</i>	1.20	<i>TIMM8B</i>	-1.44
<i>FIS1</i>	-37.17	<i>SLC25A19</i>	1.69	<i>TIMM9</i>	-1.34
<i>FXC1</i>	-2.54	<i>SLC25A2</i>	1.03	<i>TOMM20</i>	-2.14
<i>GRPEL1</i>	-1.56	<i>SLC25A20</i>	-1.54	<i>TOMM22</i>	-1.27
<i>HSP90AA1</i>	1.24	<i>SLC25A21</i>	1.90	<i>TOMM34</i>	-1.63
<i>HSPD1</i>	1.46	<i>SLC25A22</i>	-1.12	<i>TOMM40</i>	1.26
<i>IMMP1L</i>	-1.23	<i>SLC25A23</i>	13.68	<i>TOMM40L</i>	-1.65
<i>IMMP2L</i>	2.82	<i>SLC25A24</i>	-80.21	<i>TOMM70A</i>	-1.30
<i>LRPPRC</i>	-2.28	<i>SLC25A25</i>	2.13	<i>TP53</i>	-2.55
<i>MFN1</i>	-1.22	<i>SLC25A27</i>	-3.30	<i>TSPO</i>	-1.52
<i>MFN2</i>	-2.52	<i>SLC25A3</i>	-1.07	<i>UCP1</i>	3.32
<i>MIPEP</i>	-1.63	<i>SLC25A30</i>	1.20	<i>UCP2</i>	28.32
<i>MSTO1</i>	-1.65	<i>SLC25A31</i>	5.04	<i>UCP3</i>	2.06
<i>MTX2</i>	1.12	<i>SLC25A37</i>	-1.29	<i>UXT</i>	-1.15

B2M = Endogenous Control Gene

* Relative Expression (e.g. expression of *AIFM2* is 4.16 times greater in OE33 than QH cells)

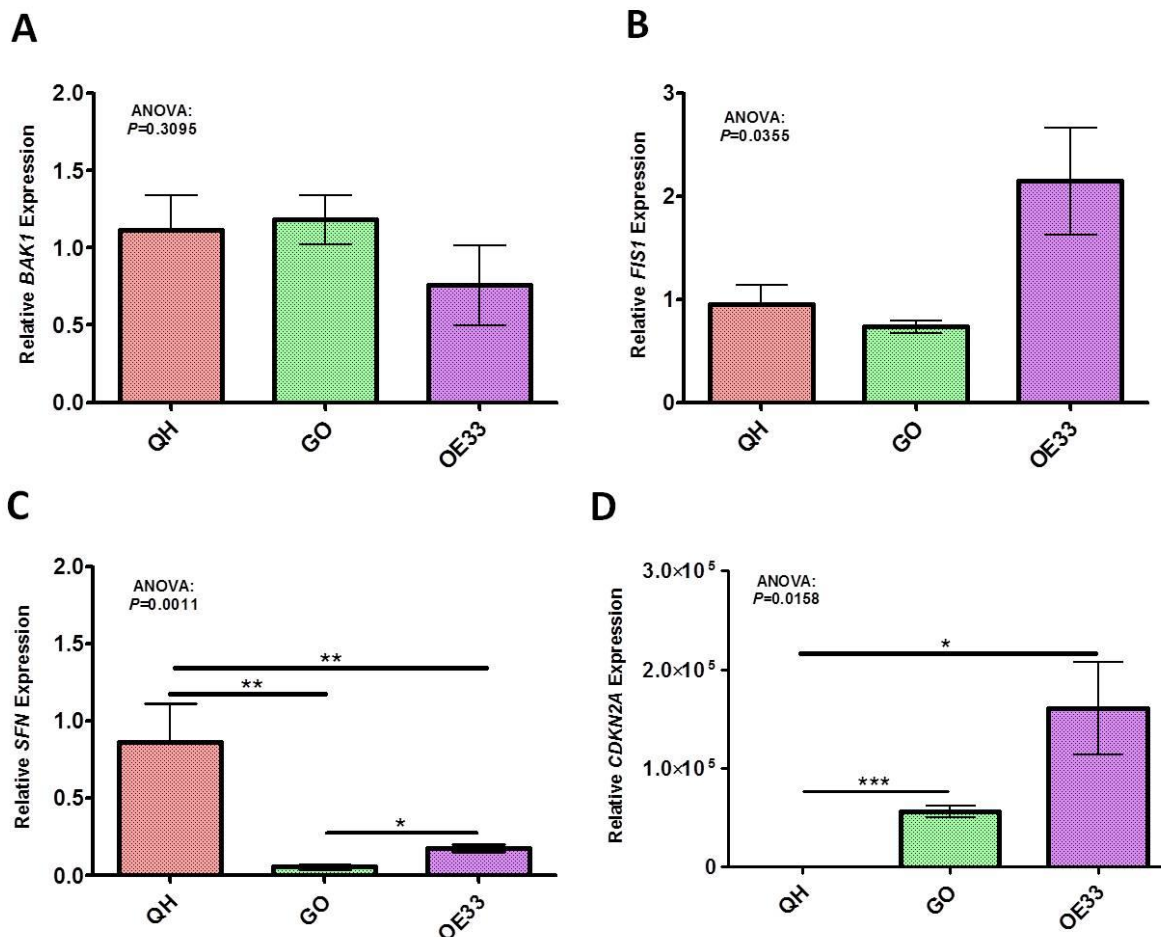


Figure 11. *In-vitro* validation of global mitochondrial function gene targets found to be differentially expressed across the Barrett's cell lines. (A) *BAK1* ($P>0.05$), (B) *FIS1* ($P>0.05$), (C) *SFN* ($P<0.05$) and (D) *CDKN2A* ($P<0.05$) were differentially expressed between the *in-vitro* Barrett's cell lines (unpaired *t*-test; Bonferroni post-hoc test). One-way ANOVA was used to investigate differences across the *in-vitro* Barrett's sequence for *BAK1* ($P=0.3095$), *FIS1* ($P=0.0355$), *SFN* ($P=0.0011$) and *CDKN2A* ($P=0.0158$). Bars denote mean \pm SEM.

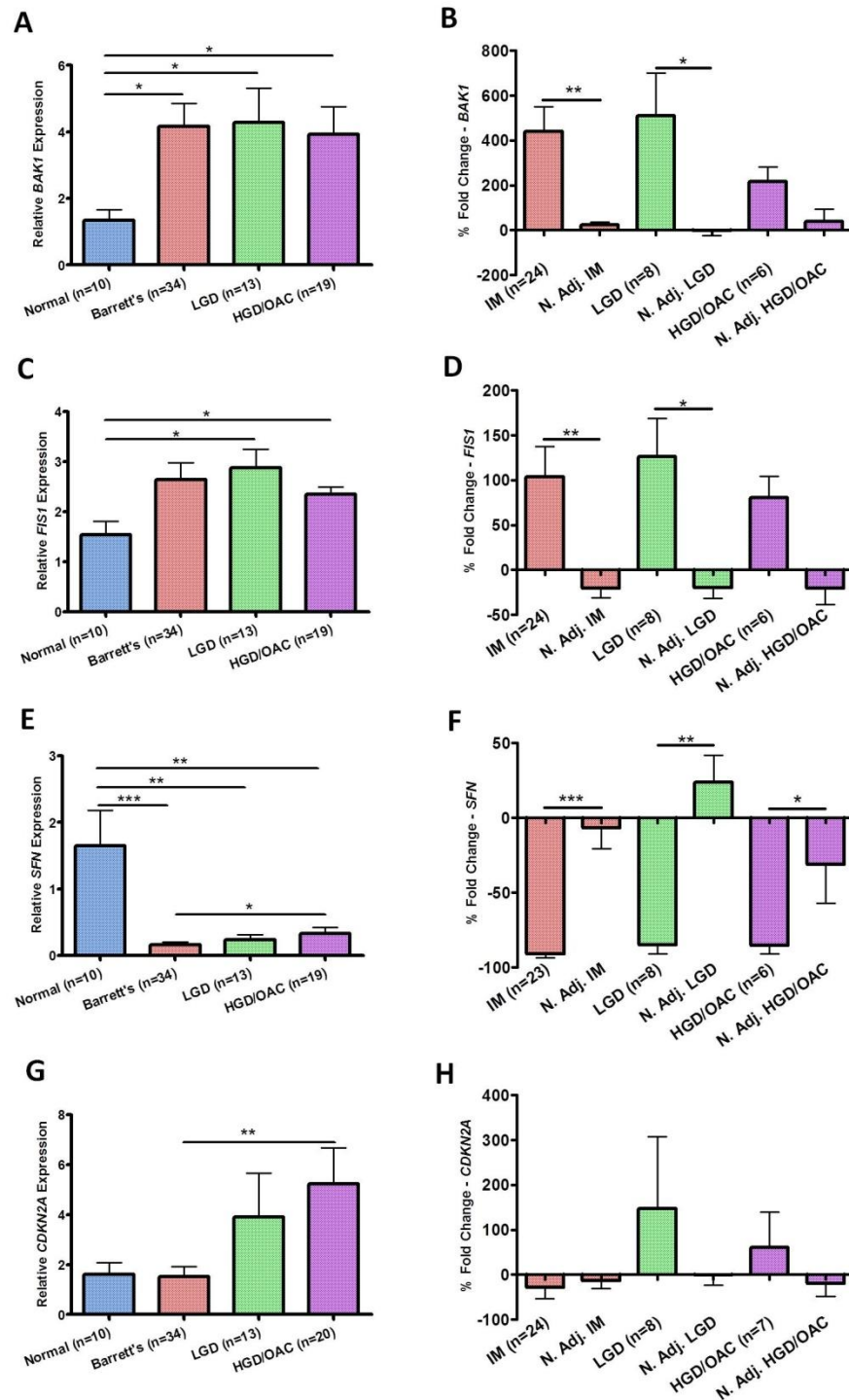


Figure 12. Global mitochondrial function gene expression across the disease sequence in diseased (A, C, E and G) versus matched normal adjacent (B, D, F and H) *in-vivo* samples. (A) *BAK1* ($P<0.05$), (C) *FIS1* ($P<0.05$), (E) *SFN* ($P<0.0001$) and (G) *CDKN2A* ($P<0.01$) were found to be differentially expressed between independent groups in the Barrett's disease sequence (Mann Whitney U) (Dunns post-hoc test). Kruskal-Wallis tests were used to investigate differences across the *in-vitro* Barrett's sequence for *BAK1* ($P=0.037$), *FIS1* ($P=0.108$), *SFN* ($P<0.0001$) and *CDKN2A* ($P=0.0152$). (B) *BAK1* ($P<0.01$), (D) *FIS1* ($P<0.01$), (F) *SFN* ($P<0.001$) and (H) *CDKN2A* ($P>0.05$) were found to be differentially expressed across the Barrett's disease sequence compared to matched normal adjacent samples (Wilcoxon Sign Rank). Bars denote mean \pm SEM. IM: Intestinal metaplasia.

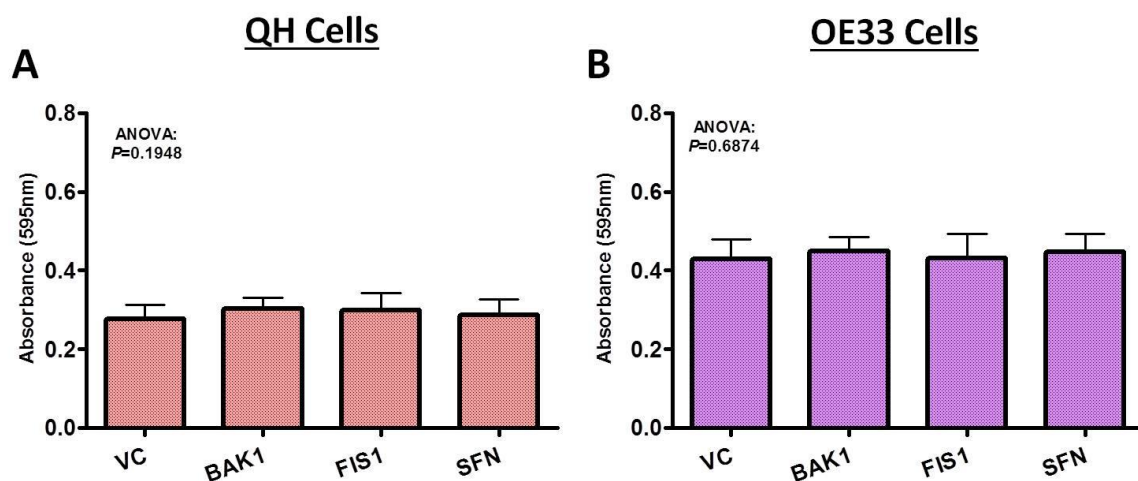


Figure 13. Assessing the effect of *BAK1*, *FIS1* and *SFN* siRNA knockdown on cell number in QH and OE33 cells *in-vitro* using a crystal violet assay. (A). Knockdown of *BAK1*, *FIS1* and *SFN* had no significant effect on cell number in QH cells ($P=0.1948$). **(B)** Knockdown of *BAK1*, *FIS1* and *SFN* had no significant effect on cell number in OE33 cells ($P=0.6874$) (One way ANOVA; Dunnett's multiple comparison post-hoc test). Bars denote mean \pm SEM.

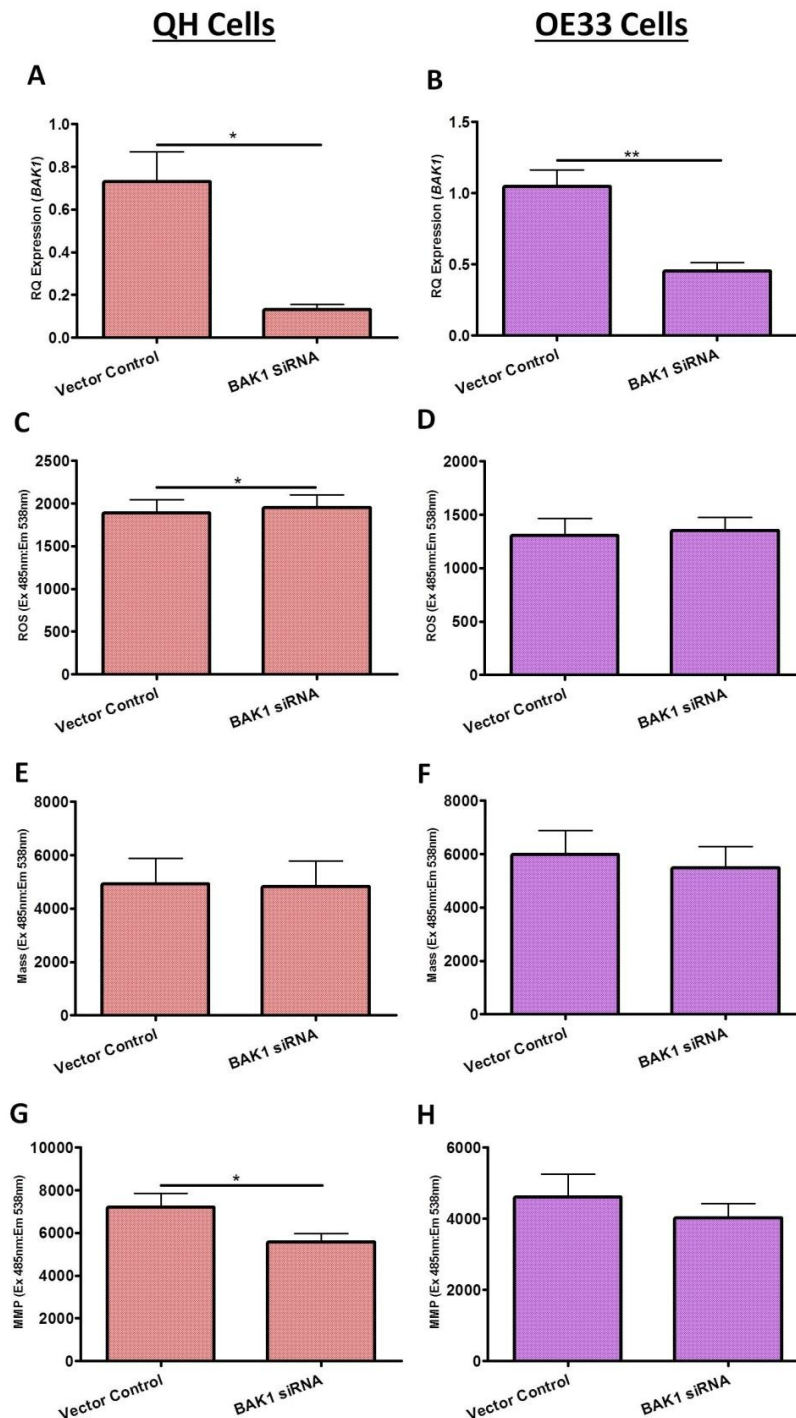


Figure 14. Functional effect of *BAK1* siRNA knockdown on reactive oxygen species (ROS) production, mitochondrial mass and mitochondrial membrane potential (MMP) in the QH (Barrett's) and OE33 (adenocarcinoma) cell lines *in-vitro*. (A) *BAK1* gene expression was significantly knocked down (81.9%) in the *BAK1*-siRNA treated QH cell line ($P=0.0191$). (B) *BAK1* gene expression was significantly knocked down (56.9%) in the *BAK1*-siRNA treated OE33 cell line ($P=0.0030$). (C) *BAK1* knockdown significantly increased ROS production in the QH cell line ($P=0.0248$) (D) but had no significant effect on ROS production in the OE33 cell line ($P=0.5723$). (E) *BAK1* knockdown had no significant effect on mitochondrial mass in QH ($P=0.8269$) or (F) OE33 cell lines ($P=0.1114$). (G) *BAK1* knockdown significantly decreased MMP in the QH cell line ($P=0.0454$) (H) but had no significant effect on MMP in the OE33 cell line ($P=0.3080$). Paired *t*-tests assessed statistical differences between vector control and siRNA treated QH ($n=4$) and OE33 ($n=4$) cells. Bars denote mean \pm SEM.

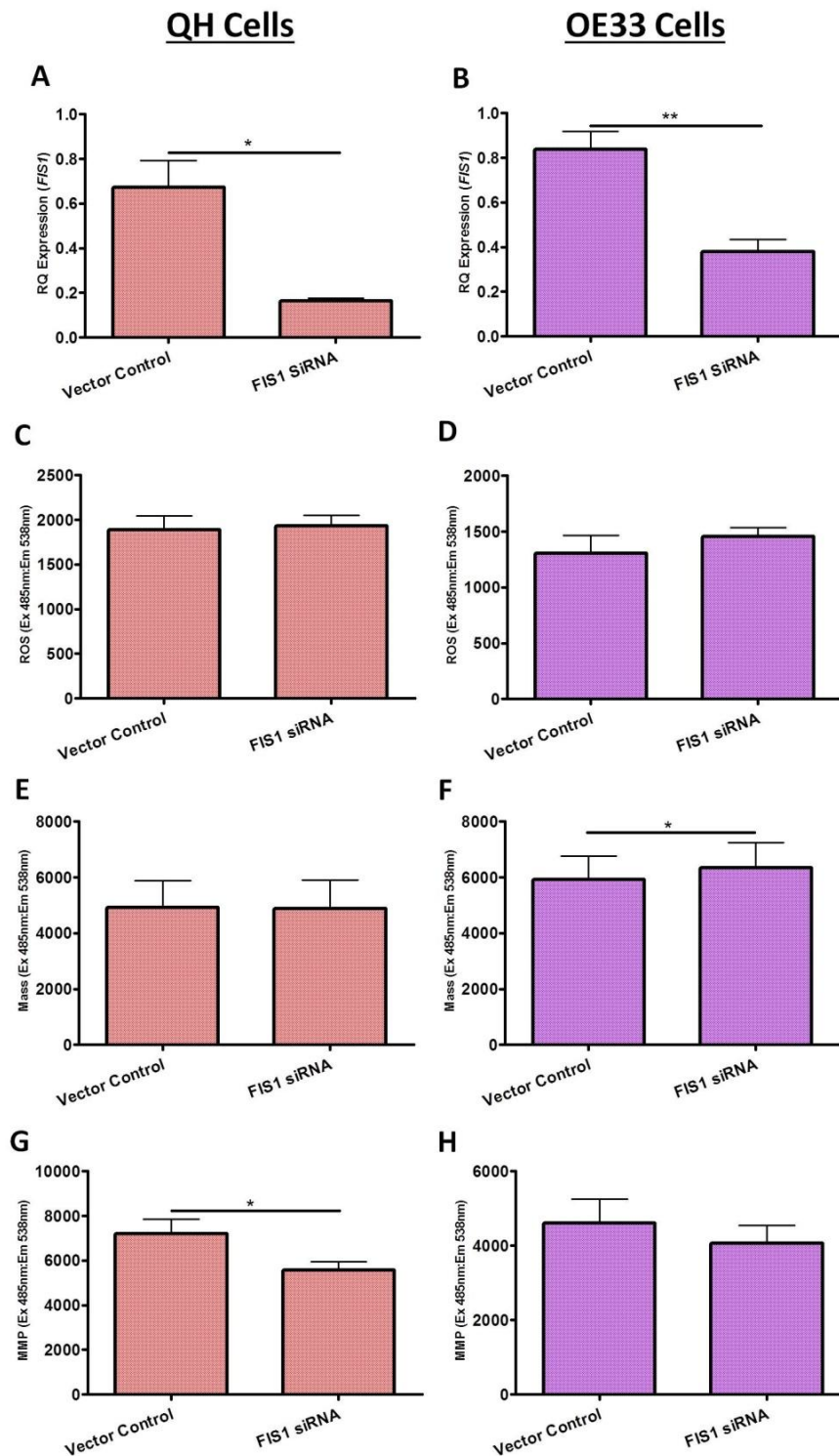


Figure 15. Functional effect of *FIS1* siRNA knockdown on reactive oxygen species (ROS) production, mitochondrial mass and mitochondrial membrane potential (MMP) in the QH (Barrett's) and OE33 (adenocarcinoma) cell lines *in-vitro*. (A) *FIS1* gene expression was significantly knocked down (75.9%) in the *FIS1*-siRNA treated QH cell line ($P=0.0242$). (B) *FIS1* gene expression was significantly knocked down (54.8%) in the *FIS1*-siRNA treated OE33 cell line ($P=0.0037$). (C) *FIS1* knockdown had no significant effect on ROS production in QH ($P=0.4112$) and (D) OE33 cell lines ($P=0.2401$). (E) *FIS1* knockdown had no significant effect on mitochondrial mass in the QH cell line ($P=0.9245$) but (F) significantly increased mitochondrial mass in the OE33 cell line ($P=0.0316$). (G) *FIS1* knockdown significantly decreased MMP in the QH cell line ($P=0.0190$) but (H) had no significant effect on MMP in the OE33 cell line ($P=0.3124$). Paired *t*-tests assessed statistical differences between vector control and siRNA treated QH ($n=4$) and OE33 ($n=4$) cells. Bars denote mean \pm SEM.

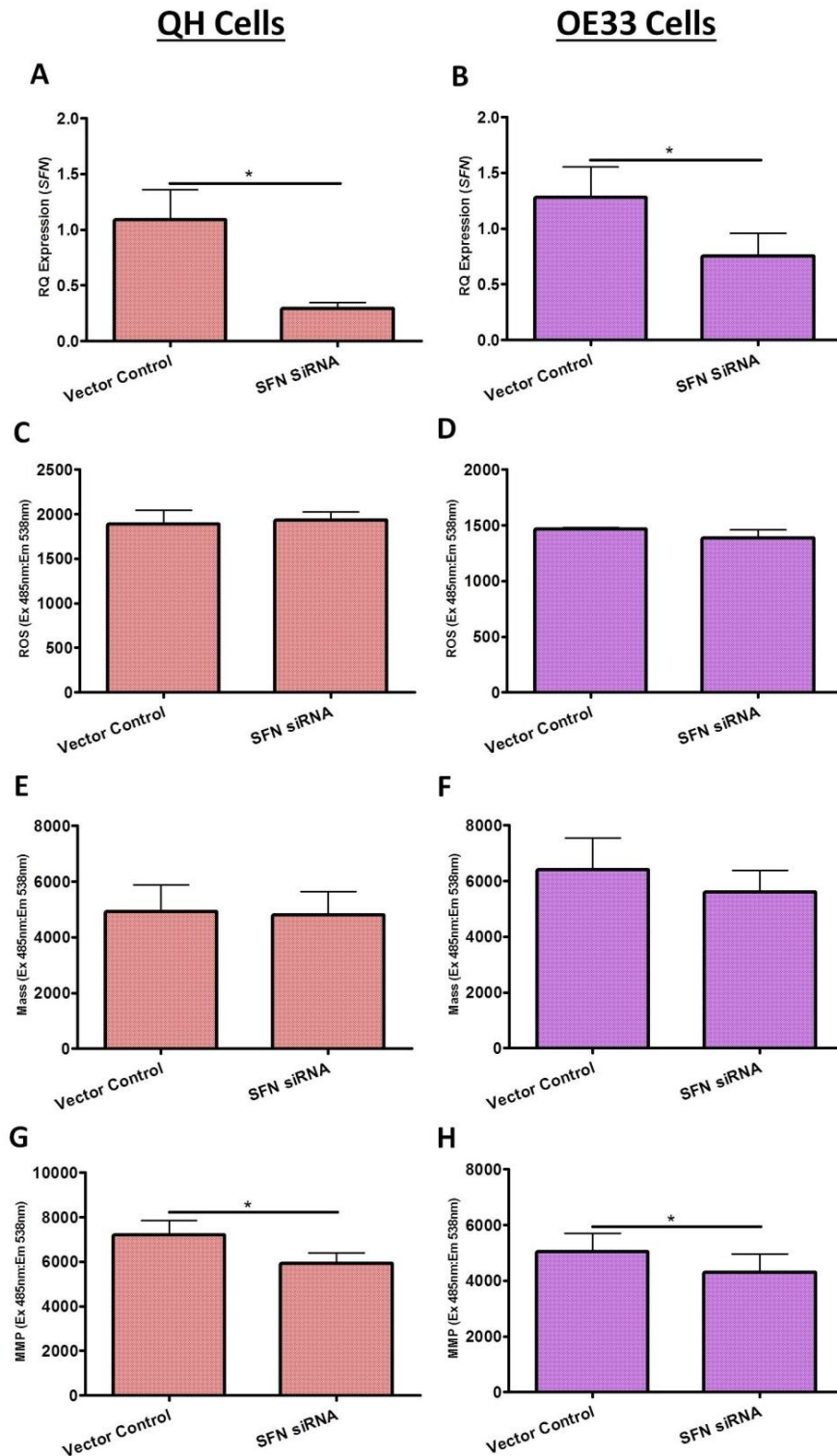


Figure 16. Functional effect of *SFN* siRNA knockdown on reactive oxygen species (ROS) production, mitochondrial mass and mitochondrial membrane potential (MMP) in the QH (Barrett's) and OE33 (adenocarcinoma) cell lines *in-vitro*. (A) *SFN* gene expression was significantly knocked down (73%) in the *SFN*-siRNA treated QH cell line ($P=0.0495$). (B) *SFN* gene expression was significantly knocked down (41%) in the *SFN*-siRNA treated OE33 cell line ($P=0.0247$). (C) *SFN* knockdown had no significant effect on ROS production in QH ($P=0.5619$) or (D) OE33 cell lines ($P=0.3371$). (E) *SFN* knockdown had no significant effect on mitochondrial mass in QH ($P=0.7858$) or (F) OE33 cell lines ($P=0.1431$). (G) *SFN* knockdown significantly decreased MMP in the QH ($P=0.049$) and (H) OE33 cell lines ($P=0.0224$). Paired *t*-tests assessed statistical differences between vector control and siRNA treated QH ($n=4$) and OE33 ($n=3$) cells. Bars denote mean \pm SEM.

2.4.4 Assessing the effect of *BAK1*, *FIS1* and *SFN* siRNA knockdown on cellular metabolism in-vitro

In conjunction with ROS, mitochondrial mass and MMP assays, the effect of *BAK1*, *FIS1* and *SFN* knockdown on cellular metabolism was assessed. Oxygen consumption rate (OCR) and extracellular acidification rate (ECAR) were assessed throughout as surrogate measures of oxidative phosphorylation and glycolysis respectively. Figure 17 demonstrates the effect of *BAK1*, *FIS1* and *SFN* knockdown on non-mitochondrial respiration, oligomycin-induced compensatory glycolysis and baseline ECAR in QH and OE33 cells respectively. *BAK1* knockdown significantly decreased non-mitochondrial respiration in the OE33 cell line (figure 17B) ($P=0.0433$) but not in the QH cell line (figure 17A). Upon complex V inhibition with oligomycin, unscrambled control treated OE33 cells increased their glycolytic levels to compensate for the lack of oxidative phosphorylation activity, however, *FIS1* knockdown significantly decreased oligomycin-induced compensatory glycolysis in OE33 cells (figure 17D) ($P=0.0065$). Such observations were not seen in the QH cell line (figure 17C). Interestingly, *SFN* knockdown significantly decreased baseline levels of ECAR, or glycolysis, in OE33 cells (figure 17F) ($P=0.0271$) but failed to have any effect in QH cells (figure 17E). No significant effect of *BAK1*, *FIS1* or *SFN* knockdown was observed on baseline OCR, ATP synthesis or proton leak in both cell lines (data not shown) ($P>0.05$). All mitochondrial function and metabolism assays were normalised to cell number using the crystal violet assay (figure 13).

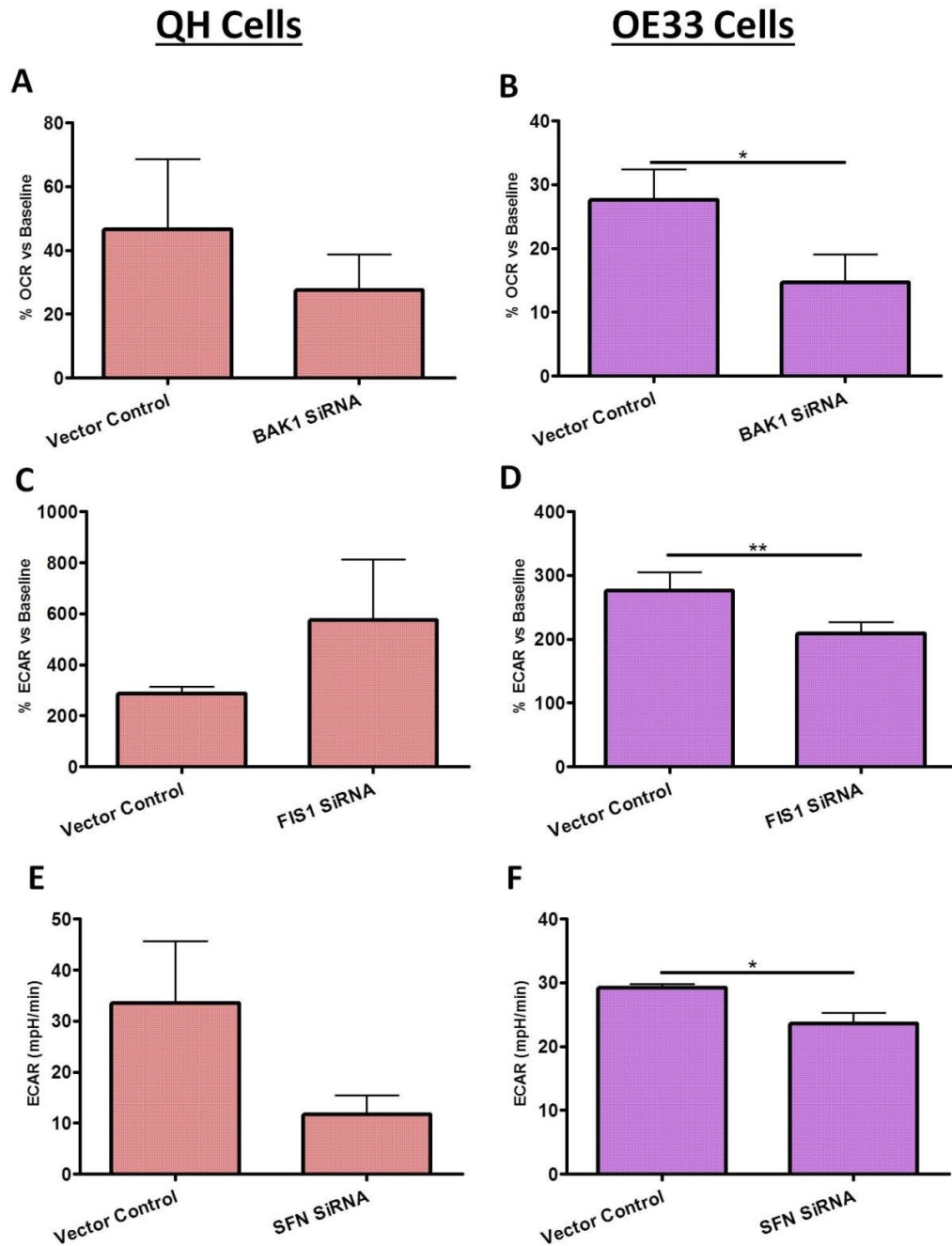


Figure 17. Investigating the metabolic effect of siRNA-induced knockdown of *BAK1*, *FIS1* and *SFN* in the QH (Barrett's) and OE33 (adenocarcinoma) cell lines *in-vitro*. **(A)** *BAK1* knockdown did not affect non-mitochondrial respiration in the QH cell line ($P=0.5148$). **(B)** *BAK1* knockdown significantly decreased non-mitochondrial respiration in the OE33 cell line ($P=0.0433$). **(C)** *FIS1* knockdown did not affect oligomycin-induced compensatory glycolysis in the QH cell line ($P=0.3230$). **(D)** *FIS1* knockdown significantly decreased oligomycin-induced compensatory glycolysis in the OE33 cell line ($P=0.0065$). **(E)** *SFN* knockdown did not affect baseline ECAR (glycolysis) in the QH cell line ($P=0.1034$). **(F)** *SFN* knockdown significantly decreased ECAR (glycolysis) glycolysis in the OE33 cell line ($P=0.0271$). Paired *t*-tests assessed statistical differences between vector control and siRNA treated QH ($n=4$) and OE33 ($n=4$) cells. Bars denote mean \pm SEM.

2.5 DISCUSSION

Mitochondria play an important role in the initiation and progression of a variety of cancers (325). As such, mitochondria are now considered a potential therapeutic target in cancer (344). Identifying and targeting specific mitochondrial genes that modulate cellular function and metabolism may offer significant therapeutic benefit. Moreover, obtaining a better understanding on how mitochondria contribute to tumour development and growth and deciphering the mechanisms that mitochondria exploit to support the progression of Barrett's oesophagus to OAC may affect how some of these patients are managed. A better comprehension on how these mechanisms are intrinsically linked and how they functionally differ between preneoplastic and neoplastic tissue may provide further insight on how to treat these patients. We have shown for the first time that mitochondrial function is altered across the normal-metaplasia-dysplasia-adenocarcinoma sequence of events in Barrett's oesophagus. These alterations in mitochondrial function may increase the risk of neoplastic progression from Barrett's metaplasia to OAC.

In this study, a human PCR gene microarray identified four genes associated with mitochondrial function differentially expressed between Barrett's and OAC cells *in-vitro*. One of these genes was associated with mitochondrial fission (fission 1, or *FIS1*), one with apoptosis (bcl-2 homologous antagonist killer, or *BAK1*) and two with tumour suppression (stratifin and cyclin-dependent kinase inhibitor 2A, or *SFN* and *CDKN2A* respectively).

We demonstrate that expression of the *BAK1* gene significantly increases across the disease sequence *in-vivo*. This increase in expression was shown to be localised specifically in the Barrett's tissue compared to the surrounding matched normal mucosa. Induction of apoptosis through *BAK1* activation has been shown to be beneficial in many studies. For example, one study demonstrated that *BAK1* overexpression resulted in decreased *in-vitro* growth, decreased cell cycle G0/G1 arrest and in the induction of apoptosis of gastric cancer cells, thereby suggesting it may be a therapeutic approach (345). Such *BAK1* mediated apoptosis was shown to correlate with caspase-3 activation and exerted its apoptotic effect independent of p53 (345). Infliximab-induced apoptosis in monocytes from patients with Crohn's disease and TRAIL-induced apoptosis in colon cancer cells has also been shown to be mediated by activation of BAK (346, 347). Conversely, one study investigating *BAK1* in tumour and non-tumour lesions in matched head and neck cancer patients found that loss of *BAK1* predicted a non-tumour phenotype (348). Moreover, although deletion of BAK significantly inhibited hepatocyte apoptosis in Mcl-1 knockout mice, deletion resulted in reduced incidences of liver cancer, reductions in TNF α production, oxidative stress and oxidative DNA damage in non-cancerous livers (349). *BAK1* expression has also been shown to

maintain a pro-oxidant state during periods of stress by regulating cytochrome c oxidase activity and mitochondrial respiration possibly indicating a novel anti-apoptotic role of BAK1 in conferring resistance to human leukaemia and cervical cancer cells (350). Moderate expression levels of *BAK1*, therefore, may play a role in Barrett's patients by conferring resistance to potential cancer cell candidates by regulating cytochrome c oxidase and mitochondrial energy metabolism, known to be differentially altered across the normal-metaplasia-dysplasia-adenocarcinoma disease sequence in Barrett's oesophagus (130).

In this study, *FIS1*, known to play important roles in apoptosis and mitochondrial fission, was shown to significantly increase across the disease sequence and this change was only seen in the Barrett's tissue compared to matched surrounding mucosa. *FIS1* is a novel gene target associated with poor prognosis in pretreatment patients with acute myeloid leukaemia (351). It is also upregulated in patients with non-metastatic prostate cancer (352). Moreover, *FIS1* has been shown to play a role in cisplatin resistance in tongue squamous cell carcinoma with cisplatin sensitivity being restored upon knockdown of *FIS1* (353). It is also plausible that increased levels of *FIS1* promotes mitophagy to eliminate defective mitochondria following cellular stress and perhaps support functional oxidative phosphorylation known to be associated with progression to OAC in Barrett's oesophagus (130, 354). In addition, *FIS1* may be a marker of chemotherapeutic resistance in OAC although future studies are necessary to examine this link. Therefore, increased *FIS1* in Barrett's associated OAC may be indicative of mitochondrial dysfunction, enhanced mitophagy and oxidative stress.

We have shown a loss of *SFN* expression across the normal-metaplastic-dysplastic-cancer sequence. Loss of *SFN* expression was shown to be specific to the Barrett's tissue compared to the surrounding matched normal adjacent mucosa. Similar *SFN* expression patterns were found in breast cancer cell lines and primary breast carcinomas (355). Significant loss of *SFN* expression has been documented in human hepatocellular carcinoma, lung cancer, oral cancer, prostate cancer, ovarian cancer and gliomas (356-358). Some studies, however, have found *SFN* expression to be increased in some head and neck cancers and have demonstrated *SFN* as an independent prognostic marker for poor survival in colorectal cancer patients (357, 359). In oesophageal squamous cell carcinoma (OSCC), downregulation of *SFN* has been shown to be associated with β -catenin expression, proliferation, invasion depth, lymph node metastasis and has been shown to have potential to be utilised as a prognostic biomarker for OSCC (360-362). Reduced *SFN* expression also functions as an independent prognostic factor for poor survival in patients with OAC and may be a potential target for more effective therapy and a potential predictor for the effect of chemoradiation therapy outcomes in patients with OAC (363, 364). Along with such

evidence and the loss of *SFN* demonstrated across the Barrett's disease sequence in this study, *SFN* may have future promise as a prognostic biomarker in OAC.

CDKN2A has been extensively studied throughout the literature as having a significant role to play in the progression of numerous neoplasms and cancers including OAC (365-368). Results demonstrated in this study are in accordance with other studies investigating *CDKN2A* across disease progression. *CDKN2A* was significantly reduced in Barrett's patients compared to OAC individuals in both the Barrett's tissue and the surrounding mucosa suggesting an overall field effect. This finding is interesting as previous studies have shown *CDKN2A* expression to be decreased, through the accumulation of somatic genetic abnormalities and during DNA promoter hypermethylation of *CDKN2A*, across the same disease sequence (367, 369). Despite being frequently downregulated in tumours, overexpression has also been described in several other studies associated with cancer such as breast, colorectal, head and neck, breast, astrocytic and various sarcomic cancers (370-372). Interestingly, analysis of the genetic progression of Barrett's has also identified abnormalities in *CDKN2A* as critical in the evolution of OAC (369). Gastrointestinal stromal tumours have also been recently noted for *CDKN2A* overexpression analogous to that seen in the current study (372). Interestingly, new models of neoplastic progression in Barrett's oesophagus currently include loss of *CDKN2A* models highlighting the importance of *CDKN2A* in disease progression (373). In addition, functional studies have examined the role of upstream mediators of *CDKN2A* (374-376). Therefore, elucidating the precise role that *CDKN2A* plays in the progression from Barrett's to OAC and other diseases may have significant therapeutic potential and clinical application.

To gain a better functional understanding of *BAK1*, *FIS1* and *SFN*, these genes were knocked down in the Barrett's and OAC cell lines *in-vitro* as their expression was elevated *in-vivo* from Barrett's oesophagus. Moreover, their expression was shown to be specific to the Barrett's tissue compared to the surrounding matched normal adjacent mucosa. ROS, mitochondrial mass, MMP and energy metabolism assays were undertaken upon siRNA-induced knockdown to assess the functional effect of manipulation of these gene targets.

We show that knockdown of *BAK1*, *FIS1* and *SFN* resulted in significant decreases in MMP in Barrett's cells. Little is known about the precise role of the MMP in preneoplastic tissue but studies have documented elevated MMP in carcinomas compared to their matched normal controls, therefore, developing agents that target MMP, and thus apoptosis, are clinically appealing (377, 378). Delocalised lipophilic cations are concentrated into mitochondria by cells in response to negative transmembrane potentials. Therefore, their selective accumulation within

the mitochondria of cancer cells results in mitochondrial toxicity and a basis for selective cancer cell killing (377). Such increases in MMP in the mitochondria of cancer cells can be targeted using positively charged ions that induce apoptosis (379). Common consequences of apoptosis include decreases in MMP, release of pro-apoptotic proteins, increases in stress-induced ROS and arrest of cellular bioenergetics (378, 380, 381). In addition to finding significant decreases in MMP in *BAK1* siRNA-treated Barrett's cells, knockdown resulted in significantly increased levels of ROS.

Furthermore, for all genes, we found significant alterations in cellular energetics in siRNA treated OAC cells but not in Barrett's cells. We show that loss of *BAK1* decreased non-mitochondrial OCR, therefore increasing OCR. This may also explain the increased levels of ROS, as increased oxidative phosphorylation is associated with increased ROS production attributed to increased activity of the electron transport chain. Loss of *FIS1* may also negate mitochondrial fission thus promoting mitochondrial fusion and thereby increasing mitochondrial mass, as demonstrated in OAC cells in this study. This loss of *FIS1*, therefore, may favour a shift from glycolysis to oxidative metabolism. Furthermore, we demonstrate that loss of *SFN* in OAC cells is associated with lower levels of MMP and glycolysis. Moreover, as OAC is known to be associated with high levels of glycolysis, targeting *SFN* may be beneficial (130). These observations may suggest that therapies directed at these gene targets with a view to additionally influencing cellular energetics may be a better therapeutic approach in the neoplastic setting.

Moreover, as decreased MMP is an indicator of apoptosis, we investigated if knockdown of *BAK1*, *FIS1* or *SFN* had an effect on cell number (382). We found that siRNA-induced knockdown of *BAK1*, *FIS1* and *SFN* had no significant effect on cell number in both Barrett's and OAC cells. Despite no significant effect on cell number, decreases in MMP, increases in ROS, increases in mitochondrial mass and alterations in cellular bioenergetics may be due to undetectable levels of apoptosis and thus consequences of independent knockdown of *BAK1*, *FIS1* and *SFN* alone. The combined effect of *BAK1*, *FIS1* and *SFN* knockdown, however, may have a more substantial effect on mitochondrial function, cell viability and thus apoptosis at different time points. The extent of siRNA-induced knockdown of one of these genes alone may not reduce the MMP sufficiently to induce cellular apoptosis but may induce cellular alterations in mitochondrial function and cellular bioenergetics as we have demonstrated. Therefore, reagents that target *BAK1*, *FIS1* and *SFN* may need to be used in combination to assist in other routine treatment regimes.

SFN has also been shown to regulate cell cycle arrest rather than apoptosis via p53, another tumour suppressor known to be associated with neoplastic progression in Barrett's oesophagus and mediate cellular metabolism under oxidative stress microenvironments (175, 202, 292, 383).

In glioblastoma cells, cellular senescence is also induced through the regulation of *SFN* (384). Therefore, despite observations that loss of *SFN* may be indicative of a poor prognosis in some cancer types, increased expression may be the equivalent in OAC. Based on previous studies investigating the role of *BAK1*, *FIS1*, and *SFN*, therefore, one primary function of these three genes in Barrett's oesophagus and in Barrett's associated OAC may indeed be in conferring therapeutic resistance to cells, however, further studies are necessary to explore this relationship. Moreover, these genes may help to assist, sculpt and maintain a hostile oxidative microenvironment with the capability of adapting to various multimodal therapies thereby facilitating in cancer progression (350, 353, 363).

We have shown for the first time that global mitochondrial gene expression is differentially expressed across the normal-metaplastic-dysplastic-adenocarcinoma disease sequence in Barrett's oesophagus *in-vitro* and *in-vivo*. These mitochondrial changes activated in the disease sequence may increase the risk of progression from Barrett's oesophagus to OAC. Examining whether these genes promote chemotherapeutic resistance and oxidative stress and the cellular mechanisms behind such functionality may provide some insight into how screening for the levels of these genes can be utilised clinically in the future.

Chapter 3

Differential expression of mitochondrial energy metabolism profiles across the metaplasia-dysplasia-adenocarcinoma disease sequence in Barrett's oesophagus.

3.1 INTRODUCTION

In chapter two, we identified genes associated with mitochondrial function that were differentially expressed across the metaplastic-dysplastic-OAC disease sequence *in-vitro* and *in-vivo*. Moreover, we demonstrated that functional manipulation of these mitochondrial genes altered mitochondrial function, specifically mitochondrial membrane potential. We also found evidence that manipulation of these genes resulted in changes in cellular metabolism, specifically in neoplastic tissue. These *in-vitro* results imply that alterations in cellular metabolism may play an important role in neoplastic progression in Barrett's oesophagus, which we examine in this chapter.

Research in recent years has focused on the mitochondria as been primary instigators of tumour progression. First reported by Otto Warburg in 1926, and thus coined the Warburg effect, cancer cells produce the majority of their ATP through aerobic glycolysis to support the extensive transformation, differentiation and aggressive proliferation of malignant cells (385). These transformed cells convert the majority of incoming glucose to lactate rather than metabolising it through oxidative phosphorylation. Furthermore, despite aerobic glycolysis being more rapid at ATP production, it is far less efficient in terms of ATP produced per molecule of glucose and therefore glucose uptake demands can function at abnormally high rates (385). Glycolysis also allows the shunting of intermediates for anapleurotic reactions such as in biosynthetic or nucleotide pathways that are vital in neoplastic proliferation and differentiation (162).

Studies investigating cancer metabolism have documented metabolic shifts from oxidative phosphorylation to aerobic glycolysis to generate energy. In human breast, gastric, squamous oesophageal and lung carcinomas, expression of mitochondrial and glycolytic protein markers varied significantly in carcinomas when compared with paired normal tissue (386). It is speculated that this metabolic shift occurs as an adaptation to defects in oxidative phosphorylation in the mitochondria since mitochondria lack DNA repair enzymes and are adjacent to cancer causing free radicals (387). In the colonic mucosa of ulcerative colitis patients, mitochondrial complex activity is decreased between 50-60% compared to healthy controls (330). This profile has also been documented in human kidney, liver and colonic carcinomas in tandem with increases in key glycolytic enzymes (388). Moreover, loss of oxidative phosphorylation precedes the development of dysplasia in ulcerative colitis (286). However, some studies report that mitochondrial function is crucial for transformation in some tumours (389). For example, a more recent study has found that fidelity of the mitochondrial genome in fact increases in human colorectal cancer in conjunction with a shift in glucose metabolism from oxidative phosphorylation to glycolysis (390).

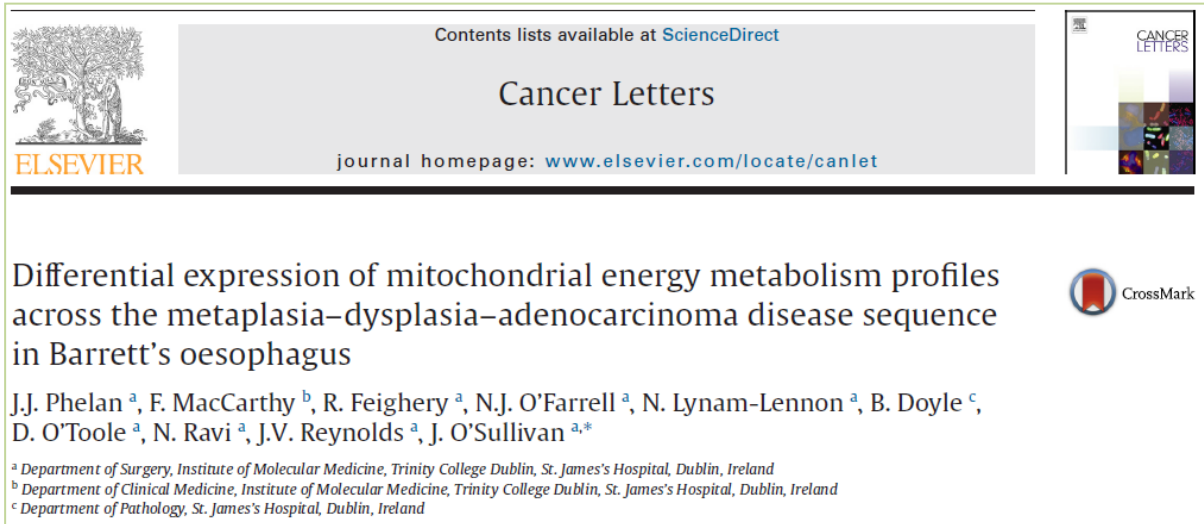
The focus on the mitochondria as primary instigators of tumour progression is of great interest. The production of lactate during glycolysis may also facilitate tumour invasion and metastasis (173). Other studies report that mitochondrial function is crucial for transformation in some tumour progression systems (389). As previously alluded to in the introduction, oxidative phosphorylation has also been reported to supply the majority of ATP in certain cancer tissues; some studies have subsequently demonstrated an upregulation of oxidative phosphorylation in neoplastic tissue (165, 166).

Despite innovative strategies in tumour detection and monitoring, for example, in fluorodeoxyglucose positron emission tomography imaging and glycolytic pathway inhibitors, a thorough understanding of the molecular mechanisms mediating tumour progression, particularly in Barrett's oesophagus and its progression to OAC is warranted (174). Barrett's oesophagus also lacks accurate predictors of disease progression. Accordingly, more accurate predictors of disease progression should be validated, thus allowing early preneoplastic detection of such molecular mechanisms offering a greater insight into the risk of disease progression.

Some studies have attempted to characterise glucose metabolism in Barrett's oesophagus. Cell lines derived from patients with advanced genetically unstable Barrett's oesophagus exhibit significantly higher glycolysis compared to a cell line with early genetically stable Barrett's oesophagus (391). Interestingly, however, all cell lines show active mitochondria and an upregulation of oxidative phosphorylation in response to glucose via the Crabtree effect (391). Moreover, pyruvate kinase isoform 2 (PKM2) expression has been shown to be significantly increased along the metaplasia-dysplasia-OAC sequence, however, it was not shown to be a specific marker of Barrett's associated OAC but a marker of transformed and highly proliferating cells during cancer progression (392). No study to date has investigated differential gene and protein expression associated with mitochondrial energy metabolism in Barrett's patients in such a sequential, retrospective and longitudinal manner.

Therefore, the aim of this study was to examine mitochondrial energy metabolism gene changes across the disease sequence *in-vitro* and *in-vivo* and to assess glucose metabolism across the disease sequence utilising two oxidative phosphorylation and two glycolytic protein markers *in-vivo*. We have shown that genes associated with mitochondrial energy metabolism are differentially expressed across the metaplasia-dysplasia-OAC sequence both *in-vitro* and *in-vivo*. Furthermore, the Barrett's disease sequence exhibits significant alterations in the expression of oxidative phosphorylation and glycolytic proteins. Interestingly, levels of the oxidative phosphorylation protein ATP5B in sequential follow up material could significantly segregate

Barrett's non progressors and progressors to cancer. Aspects of this chapter have been published in *Cancer Letters* (see figure 18) (130).



Contents lists available at ScienceDirect

Cancer Letters

journal homepage: www.elsevier.com/locate/canlet

Differential expression of mitochondrial energy metabolism profiles across the metaplasia–dysplasia–adenocarcinoma disease sequence in Barrett's oesophagus

J.J. Phelan^a, F. MacCarthy^b, R. Feighery^a, N.J. O'Farrell^a, N. Lynam-Lennon^a, B. Doyle^c, D. O'Toole^a, N. Ravi^a, J.V. Reynolds^a, J. O'Sullivan^{a,*}

^a Department of Surgery, Institute of Molecular Medicine, Trinity College Dublin, St. James's Hospital, Dublin, Ireland
^b Department of Clinical Medicine, Institute of Molecular Medicine, Trinity College Dublin, St. James's Hospital, Dublin, Ireland
^c Department of Pathology, St. James's Hospital, Dublin, Ireland

Figure 18. 'Differential expression of mitochondrial energy metabolism profiles across the metaplasia–dysplasia–adenocarcinoma disease sequence in Barrett's oesophagus'. Aspects of chapter three have been published in *Cancer Letters* (130).

3.2 HYPOTHESIS AND AIMS OF CHAPTER THREE

We hypothesise that mitochondrial energy metabolism is differentially expressed across the metaplasia-dysplasia-adenocarcinoma sequence in *in-vitro* and *in-vivo* models of Barrett's oesophagus.

Specific aims of chapter 3;

- 1) Identify and validate gene changes involved in mitochondrial energy metabolism across the Barrett's disease sequence *in-vitro* and *in-vivo*.
- 2) Examine the levels of oxidative phosphorylation and glycolysis across the same disease sequence *in-vivo* by screening surrogate protein markers of both metabolic pathways.
- 3) Investigate the predictive role of metabolic protein screening in segregating Barrett's non-progressors and progressors to high grade dysplasia and adenocarcinoma *in-vivo*.
- 4) Explore the realtime metabolic plasticity of Barrett's and adenocarcinoma cell lines *in-vitro* utilising the Seahorse XF24 analyser.

3.3 MATERIALS AND METHODS

3.3.1 Screening via qRT-PCR microarray analysis

Cell lines representing Barrett's metaplasia (QH), HGD (GO) and OAC (OE33) were employed and subcultured as before (see sections 2.3.2 and 2.3.3). A catalogued human mitochondrial energy metabolism PCR gene microarray (Qiagen) was used to simultaneously quantify the expression of 84 mitochondrial genes across the *in-vitro* sequence using the *B2M* gene as the endogenous control gene similar to as previously described (see section 2.3.4). PCR was performed using the RT² Real-time SYBR Green PCR mix (SABiosciences) on a 7900HT Fast Real-time PCR Light-Cycler System (Applied Biosystems) as before (see section 2.3.4). Data were analysed utilising the $2^{-\Delta\Delta Ct}$ method as previously described (see section 2.3.4). Differentially expressed genes were defined as those that changed by >4-fold.

3.3.2 In-vitro validation of gene targets

Cell lines were cultured and RNA extracted as described in chapter two (see section 2.3.2). cDNA synthesis was undertaken as described before (see section 2.3.5.1) prior to undertaking real-time PCR. Gene primer probes for *COX8C*, *COX4I2*, *ATP12A* and *18S* (Applied Biosystems) were purchased and real-time PCR was performed in triplicate using Taqman mastermix (Applied Biosystems) as previously undertaken (see section 2.3.5.2). Data were analysed utilising the $2^{-\Delta\Delta Ct}$ method as before (section 2.3.4).

3.3.3 In-vivo validation of gene targets

The expression of these three genes was analysed in independent groups of tissue across the Barrett's sequence. Real-time qRT-PCR was performed as before (see section 2.3.6) and all three genes validated across the diseased Barrett's sequence *in-vivo* utilising the same patient cohort as previously described; normal squamous ($n=10$), metaplasia ($n=34$), LGD ($n=13$), HGD ($n=12$) and OAC ($n=8$) cases (see section 2.3.6). The median age of the patients was 61 years and there was a 1.52-fold male predominance. Data were analysed utilising the $2^{-\Delta\Delta Ct}$ method as before (section 2.3.4). Barrett's tissue was characterised by assessing the expression of columnar epithelium molecular markers, cytokeratin 8 and villin by RTPCR (undertaken by Dr. Finbar MacCarthy).

3.3.4 *ATP5B*, *Hsp60*, *PKM2* and *GAPDH* immunohistochemistry analysis using tissue microarrays

Immunohistochemistry was performed utilising normal squamous ($n=17$), oesophagitis (41), metaplasia ($n=66$), LGD ($n=32$), HGD ($n=12$) and OAC ($n=20$) cases. The areas of interest on the

diagnostic biopsy blocks were marked by a histopathologist and 0.6 mm cores were taken from the blocks and tissue microarrays (TMAs) were constructed. Immunohistochemistry was performed on tissue microarrays (TMAs) utilising the Vectastain Kit (Elite). All sections were processed and stained on the same day. Endogenous peroxidases were quenched in 3% hydrogen peroxide (in methanol) for 30 mins and slides blocked for 30 mins. Primary oxidative phosphorylation antibodies included a mouse anti-ATP5B IgG (SantaCruz Biotechnology) and a mouse anti-HSP60 IgG (Abcam) diluted 1:1000 and 1:400 in PBS respectively. Primary glycolytic antibodies used were a rabbit anti-PKM2 IgG (Abgent) and a rabbit anti-GAPDH IgG (AbDserotec Division of MorphoSys) both diluted 1:100 in PBS. Staining was undertaken with adequate negative controls (PBS only without primary antibody). Slides were incubated with primary antibody for 1 hour, biotinylated antibody for 30 minutes, incubated with avidin-biotin complex for 30 minutes and DAB substrate for 2-15 minutes. DAB was rinsed off slides upon colour development and haematoxylin added for 30 seconds. Lastly, slides were dehydrated and mounted using DPX. Slides were scanned (Aperio Scanscope XT digital scanner, University College Dublin) and immunoreactivity was assessed digitally under 40X magnification in a semi-quantitative manner for each protein by observers who were blinded to the pathological and clinical diagnosis of all patients in the study while scoring. For each protein, both epithelial and stromal cells were evaluated for both percentage positivity and intensity of cytoplasmic staining. Intensity was graded as 0 (negative), 1 (weak), 2 (moderate) and 3 (strong) and positivity was categorised as 0%, 10%, 25%, 50%, 75%, 90% or 100%.

Moreover, we investigated if screening for these metabolic proteins using first surveillance biopsies could predict neoplastic progression. Barrett's non-progressors ($n=15$) and progressors ($n=11$) were separated with the primary end-point being progression to OAC. The median age of patients with intestinal metaplasia was 58 years and there was a 3.3-fold male predominance. There was no significant difference in age between progressors and non-progressors ($P=0.6404$). Median time of progression to cancer was 2.6 years. TNM staging for progressors was as follows: 20% T₁N₀M₀, 20% T₃N₁M_x, 20% T_{1S}N₀M₀, 10% T_{1S}N₀M₀, 10% T₃N₀M₀, 10% T₃N₁M₀ and 10% T₃N₁M₁. The non-progressor group was followed for a median of 5.4 years and had no evidence of conversion to HGD and/or OAC.

3.3.5 Characterising the metabolic plasticity of Barrett's and adenocarcinoma cell lines utilising the Seahorse XF24 analyser

Oxygen consumption rate (OCR) and extracellular acidification rate (ECAR), reflecting oxidative phosphorylation and glycolysis respectively, were measured before and subsequent to treatment

with oligomycin ($2 \mu\text{g}\cdot\text{mL}^{-1}$, Seahorse Biosciences), trifluorocarbonylcyanide phenylhydrazine (FCCP) ($5\mu\text{M}$, Seahorse Biosciences) and antimycin-A ($2 \mu\text{M}$, Seahorse Biosciences) using the Seahorse XF24 analyser (Seahorse Biosciences) similar to as above (see section 2.3.10). QH and OE33 cells were seeded at 20,000 cells per well in a 24-well cell culture XF microplate (Seahorse Biosciences) and allowed to adhere for 24 hours. Cells were rinsed with assay medium (unbuffered DMEM supplemented with 10mM glucose and 20mM sodium pyruvate, pH 7.4) before incubation with assay medium for 1 hour at 37°C in a non- CO_2 incubator. Four baseline OCR and ECAR measurements were obtained over 28 minutes before injection of specific metabolic inhibitors. Three OCR and ECAR measurements were obtained over 15 minutes following injection with oligomycin, FCCP and antimycin-A. Percentage ATP synthesis was calculated by subtracting the OCR post oligomycin injection from baseline OCR prior to oligomycin addition and expressing residual OCR as a percentage of baseline OCR. Proton leak was calculated by subtracting percentage OCR versus baseline post antimycin-A addition from percentage ATP synthesis. The experiment was repeated five times with technical replicates. All measurements were normalised to cell number using the crystal violet assay as previously described (see section 2.3.9).

3.3.6 Statistical analysis

Data were analysed using Graph Pad Prism (Graph Pad Prism, San Diego, CA) and SPSS (PASW [Predictive Analytics Software] version 18) (IBM, Armonk, New York, USA) software. qRT-PCR data were normalised using the $2^{-\Delta\Delta\text{Ct}}$ method and statistically analysed (Kruskal-Wallis, Mann-Whitney U). qRT-PCR target genes were statistically analysed (Wilcoxon Sign Rank) in matched patient samples to explore if observed gene expression changes were an effect seen in the Barrett's tissue compared to the surrounding mucosa. Immunohistochemical differences between individual histological groups (Mann-Whitney U) and across the Barrett's sequence (Kruskal-Wallis) were statistically analysed. Categorical differences between Barrett's metaplasia progressors and non-progressors was analysed using Chi-square tests, and Mann-Whitney U tests were used to determine differences between percentage positivity. Student's unpaired *t*-test was utilised to compare Seahorse metabolics in two groups of normally distributed independent groups. Differences of $P < 0.05$ (*), $P < 0.01$ (**) and $P < 0.001$ (***) were considered statistically significant.

3.4 RESULTS

3.4.1 *In-vitro* screening using human PCR gene microarrays

To analyse the expression of 84 human mitochondrial energy metabolism genes across the disease sequence *in-vitro*, fold expression of all target genes was normalised relative to the Barrett's metaplastic cell line model, QH. The cut-off for differential gene expression was defined by either a relative 4-fold upregulation or 4-fold downregulation. 3 of the 84 mitochondrial energy metabolism gene targets (*ATP12A*, *COX4I2* and *COX8*) were differentially expressed across the metaplastic-dysplastic-OAC cell line sequence. These 3 gene targets identified were subsequently validated *in-vitro* and *in-vivo* using patient samples.

Figure 19 shows the *in-vitro* PCR gene metabolism microarray screen between the Barrett's, dysplastic and OAC cells. Using a 4-fold cut-off, 6 gene targets were differentially expressed between QH and GO cells (figure 19A). Using a 4-fold cut-off, 2 gene targets were differentially expressed between GO and OE33 cells (figure 19B). Using a 4-fold cut-off, 6 gene targets were differentially expressed between the QH and OE33 cells (figure 19C). Table 4 summarizes the relative expression of all 84 genes screened between QH and OE33 cell lines (see appendices C and D for additional PCR microarray screen results between GO and QH and between GO and OE33 cells respectively).

Figure 20 shows the *in-vitro* validation of the 3 mitochondrial energy metabolism gene targets. *ATP12A* ($P < 0.05$) expression significantly decreased across the Barrett's sequence (figure 20A). *COX4I2* expression decreased, however, this was not statistically significant (figure 20B). *COX8C* ($P < 0.05$) expression significantly increased between Barrett's and dysplastic cell lines ($P < 0.05$) but subsequently decreased between dysplastic and OAC cell lines, however, this was not statistically significant (figure 20C).

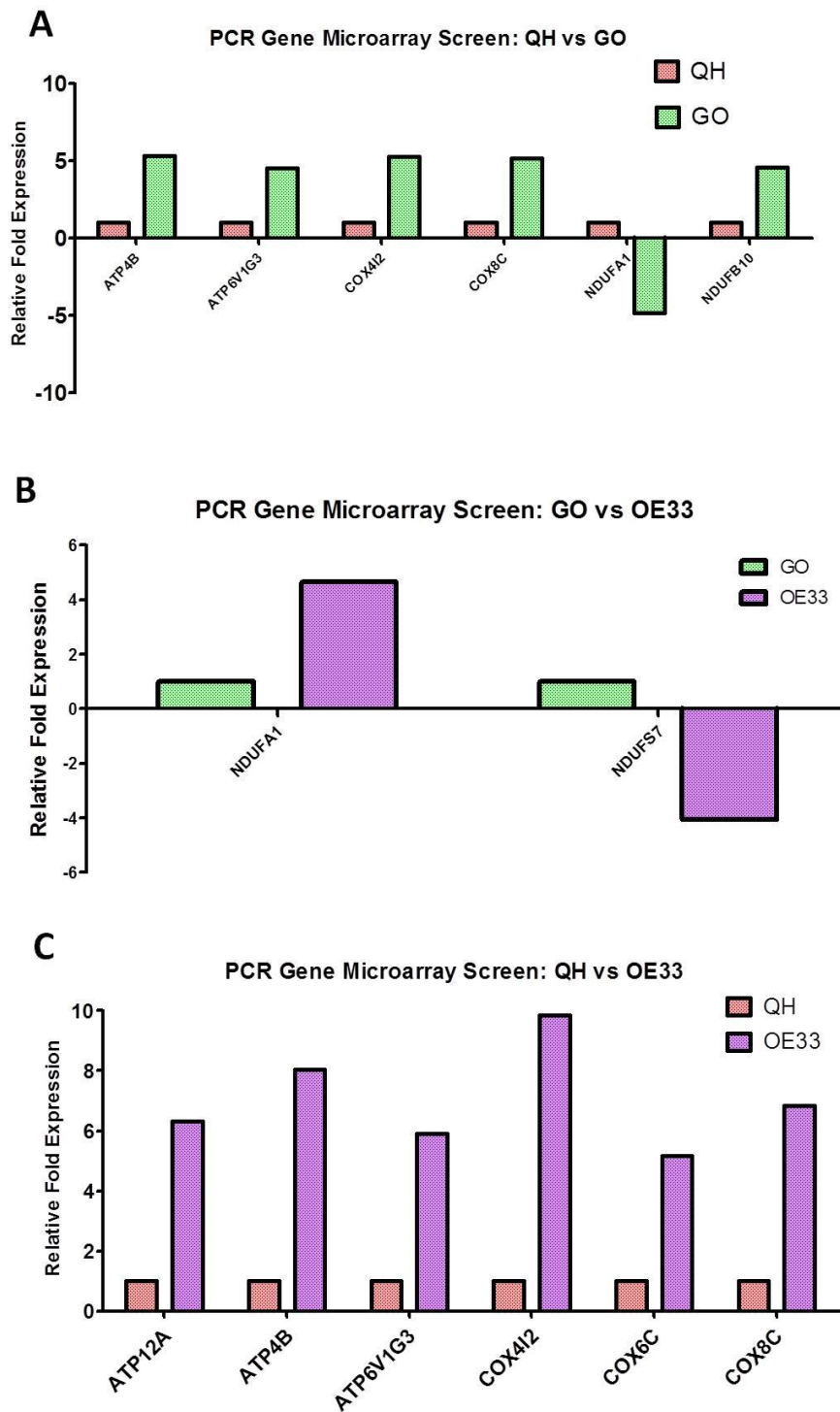


Figure 19. Human PCR gene microarray screen across the Barrett's cell lines. (A) Using a 4-fold cut-off, 6 gene targets were differentially expressed between the Barrett's (QH) and dysplastic (GO) cell lines. **(B)** Using a 4-fold cut-off, 2 gene targets were differentially expressed between the dysplastic (GO) and adenocarcinoma (OE33) cell lines. **(C)** Using a 4-fold cut-off, 6 gene targets were differentially expressed between the Barrett's (QH) and adenocarcinoma (OE33) cell lines. Arrays were performed in duplicate.

Table 4. Energy Metabolism Gene Microarray Screen between QH and OE33 Cell Lines

Gene	Expression*	Gene	Expression*	Gene	Expression*
<i>ATP4A</i>	3.67	<i>COX6B1</i>	1.25	<i>NDUFB8</i>	1.34
<i>ATP4B</i>	8.05	<i>COX6B2</i>	1.33	<i>NDUFB9</i>	1.1
<i>ATP5A1</i>	-1.07	<i>COX6C</i>	5.17	<i>NDUFC1</i>	-1.02
<i>ATP5B</i>	1.04	<i>COX7A2</i>	1.13	<i>NDUFC2</i>	1.53
<i>ATP5C1</i>	1.33	<i>COX7A2L</i>	-1.06	<i>NDUFS1</i>	1.22
<i>ATP5F1</i>	1.28	<i>COX7B</i>	1.49	<i>NDUFS2</i>	-2.01
<i>ATP5G1</i>	-1.69	<i>COX8A</i>	1.49	<i>NDUFS3</i>	1.26
<i>ATP5G2</i>	-1.40	<i>COX8C</i>	6.84	<i>NDUFS4</i>	-1.45
<i>ATP5G3</i>	-2.00	<i>CYC1</i>	1.13	<i>NDUFS5</i>	-1.55
<i>ATP5H</i>	-1.03	<i>LHPP</i>	1.38	<i>NDUFS6</i>	1.93
<i>ATP5I</i>	-1.59	<i>NDUFA1</i>	-1.04	<i>NDUFS7</i>	-1.59
<i>ATP5J</i>	-1.70	<i>NDUFA10</i>	1.09	<i>NDUFS8</i>	1.22
<i>ATP5J2</i>	3.83	<i>NDUFA11</i>	-1.48	<i>NDUFV1</i>	1.57
<i>ATP5L</i>	-1.11	<i>NDUFA2</i>	-1.37	<i>NDUFV2</i>	-1.71
<i>ATP5O</i>	-1.44	<i>NDUFA3</i>	1.1	<i>NDUFV3</i>	1.03
<i>ATP6V0A2</i>	2.21	<i>NDUFA4</i>	1.04	<i>OXA1L</i>	-1.24
<i>ATP6V0D2</i>	1.54	<i>NDUFA5</i>	-1.92	<i>PPA1</i>	2.17
<i>ATP6V1C2</i>	2.21	<i>NDUFA6</i>	1.53	<i>PPA2</i>	-1.1
<i>ATP6V1E2</i>	1.66	<i>NDUFA7</i>	-1.6	<i>SDHA</i>	1.94
<i>ATP6V1G3</i>	5.92	<i>NDUFA8</i>	-1.3	<i>SDHB</i>	-1.78
<i>ATP12A</i>	6.32	<i>NDUFAB1</i>	1.52	<i>SDHC</i>	-2.30
<i>BCS1L</i>	1.04	<i>NDUFB10</i>	3.98	<i>SDHD</i>	-1.67
<i>COX4I1</i>	-1.21	<i>NDUFB2</i>	-1.42	<i>UQCRC1</i>	-1.27
<i>COX4I2</i>	9.84	<i>NDUFB3</i>	-1.04	<i>UQCRC1</i>	-2.13
<i>COX5A</i>	1.16	<i>NDUFB4</i>	1.15	<i>UQCRC2</i>	1.8
<i>COX5B</i>	1.22	<i>NDUFB5</i>	1.01	<i>UQCRC1</i>	1.02
<i>COX6A1</i>	1.06	<i>NDUFB6</i>	-1.33	<i>UQCRC1</i>	-1.88
<i>COX6A2</i>	2.57	<i>NDUFB7</i>	-1.18	<i>UQCRC1</i>	1.44

B2M = Endogenous Control Gene

* Relative Expression (e.g. expression of *ATP4A* is 3.67 times greater in OE33 than QH cells)

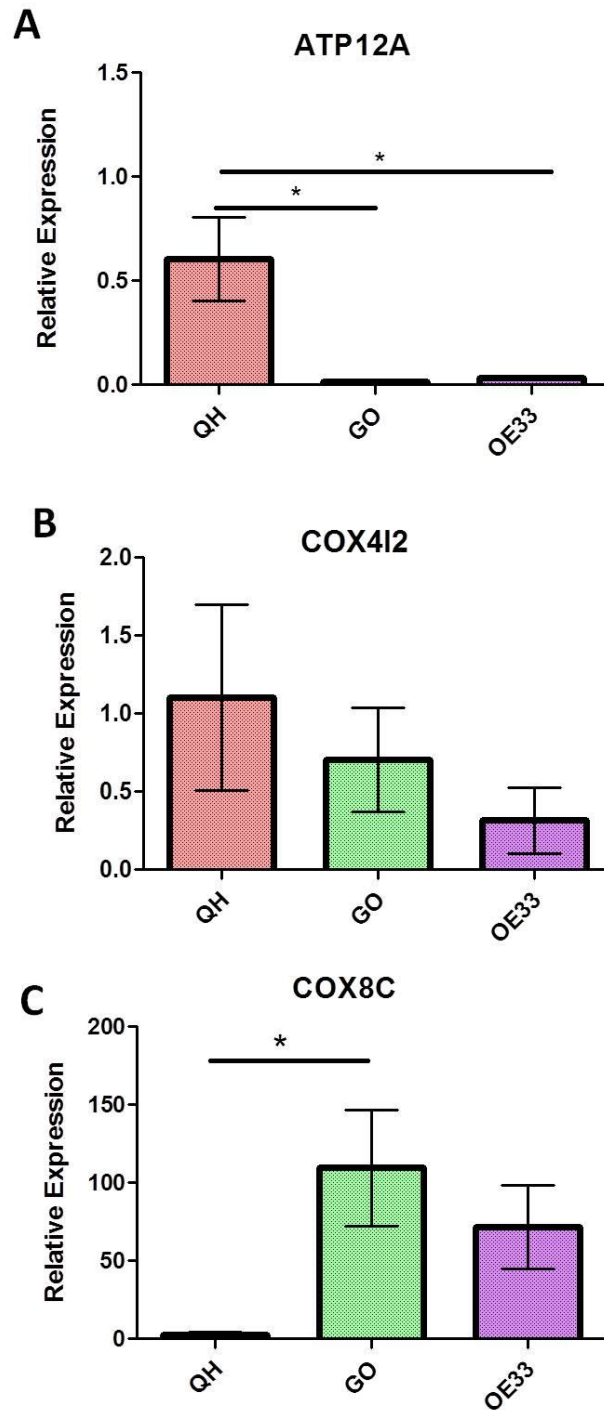


Figure 20. *In-vitro* validation of mitochondrial energy metabolism gene targets differentially expressed across Barrett's oesophagus and OAC cell lines. (A) *ATP12A* ($P < 0.05$), (B) *COX4I2* ($P > 0.05$) and (C) *COX8C* ($P < 0.05$) were differentially expressed between the *in-vitro* Barrett's cell lines (unpaired *t*-test) (Bonferroni post-hoc test). One-way ANOVA was used to investigate differences across the *in-vitro* Barrett's sequence for *ATP12A* ($P < 0.05$), *COX4I2* ($P > 0.05$) and *COX8C* ($P = 0.072$) ($n = 3$). Bars denote mean \pm SEM.

3.4.2 *In-vivo validation of gene targets*

Figure 21 illustrates mitochondrial energy metabolism gene expression of the 3 gene targets across the disease sequence in diseased and matched normal adjacent tissue samples. *ATP12A* (figure 21A) ($P<0.001$), *COX4I2* (figure 21C) ($P<0.01$) and *COX8C* (figure 21E) ($P<0.05$) were differentially expressed across the Barrett's sequence. Field effect changes in gene expression of these targets in diseased versus matched normal adjacent biopsies was examined. *ATP12A* (figure 21B) ($P<0.001$), *COX4I2* (figure 21D) ($P<0.01$) and *COX8C* (figure 21F) ($P<0.01$) were differentially expressed across the Barrett's disease sequence suggesting this effect was specific to the pathological diseased tissue (Barrett's, LGD, HGD/OAC) compared to the matched surrounding matched mucosa. In addition to the three genes screened in the PCR microarrays and found to be differentially expressed across the sequence *in-vitro* and *in-vivo*, a fourth gene, *COX6C*, was additionally validated *in-vitro* and *in-vivo*, however, due to lack to patient material *COX6C* expression could not be assessed in matched normal adjacent tissue across the disease sequence (see appendix E).

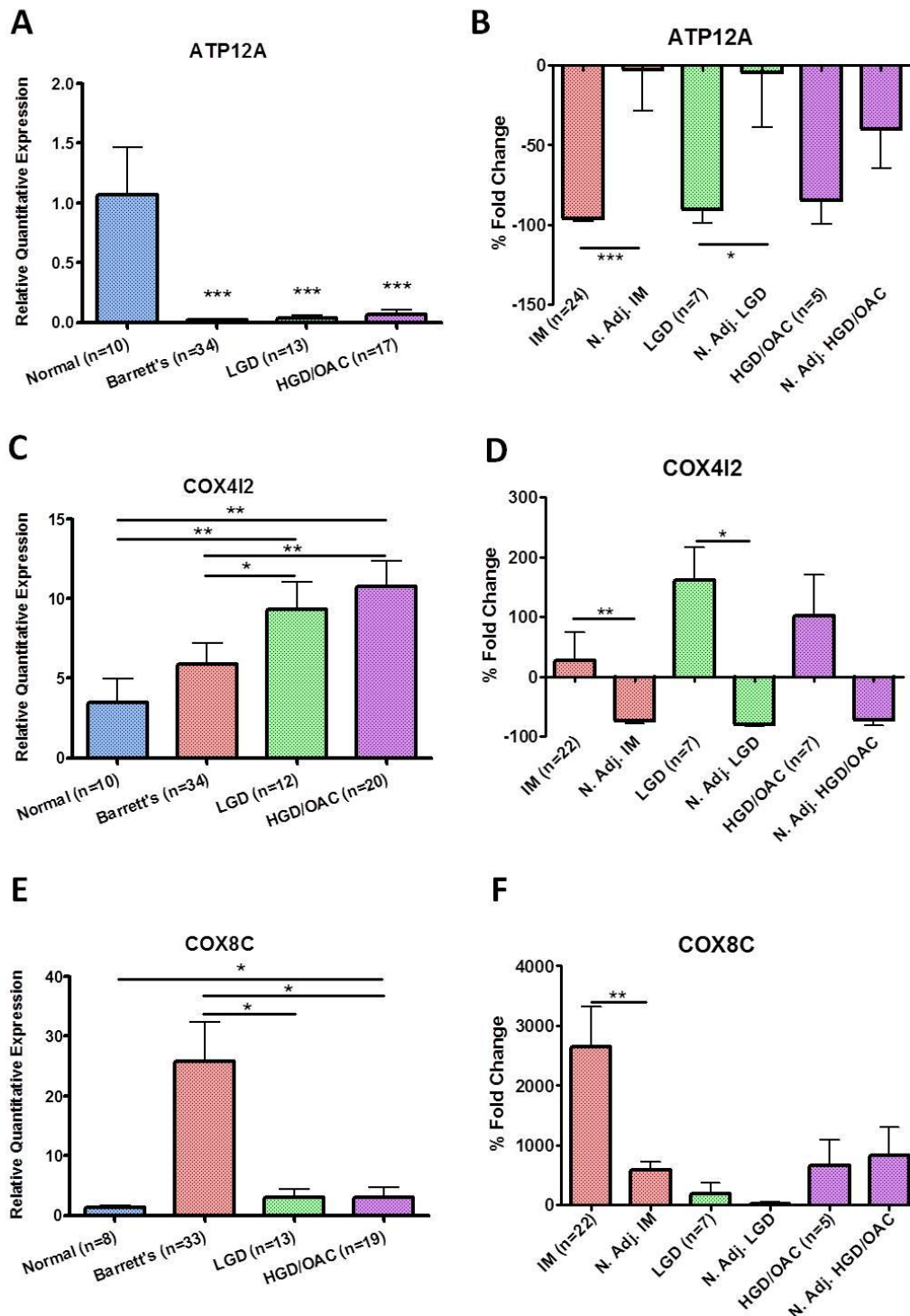


Figure 21. Mitochondrial energy metabolism gene expression across the disease sequence in diseased (A, C and E) versus matched normal adjacent (B, D and F) *in-vivo* samples. (A) *ATP12A* ($P<0.001$), (C) *COX4I2* ($P<0.01$) and (E) *COX8C* ($P<0.05$) were differentially expressed across the Barrett's disease sequence (Kruskal-Wallis test, Mann Whitney U). (B) *ATP12A* ($P<0.001$), (D) *COX4I2* ($P<0.01$) and (F) *COX8C* ($P<0.01$) were differentially expressed across the Barrett's disease sequence (Wilcoxon Sign Rank). Bars denote mean \pm SEM.

3.4.3 Oxidative phosphorylation and glycolytic activity across Barrett's sequence

To assess oxidative phosphorylation at the protein level, levels of ATP5B and HSP60 were assessed as no reliable antibodies to ATP12A, COX4I2 and COX8C have yet been developed. Even though ATP5B is a direct component of the electron transport chain and thus an effective determinant of oxidative phosphorylation, HSP60 is increasingly being used as a surrogate marker for mitochondrial function and for the assessment of oxidative mitochondrial metabolism due to its role as an active mitochondrial chaperone (130, 390, 393). Figure 22 shows immunohistochemical expression of these oxidative phosphorylation protein biomarkers across the metaplasia-dysplasia-OAC disease sequence. Figures 22A and 22B show representative images of ATP5B expression in oesophagitis and OAC tissue respectively. Figures 22C and 22D show representative images of Hsp60 expression in oesophagitis and HGD tissue respectively. Epithelial ATP5B positivity across the Barrett's disease sequence was increased significantly (figure 22E) ($P=0.0003$). Moreover, epithelial Hsp60 positivity across the Barrett's disease sequence was increased significantly (figure 22F) ($P<0.0001$). Interestingly, no significant changes in the levels of both oxidative phosphorylation markers ATP5B and HSP60 were detected in stromal tissue across the Barrett's sequence (see appendix F). Moreover, figures 22G and 22H respectively show that epithelial expression levels of ATP5B ($P<0.0001$) and HSP60 ($P<0.05$) were significantly altered across the Barrett's disease sequence in matched normal adjacent tissue. Although epithelial HSP60 intensity was significantly increased across the Barrett's sequence, no significant differences in intensity were found for epithelial ATP5B, stromal ATP5B or stromal HSP60 (see appendix G).

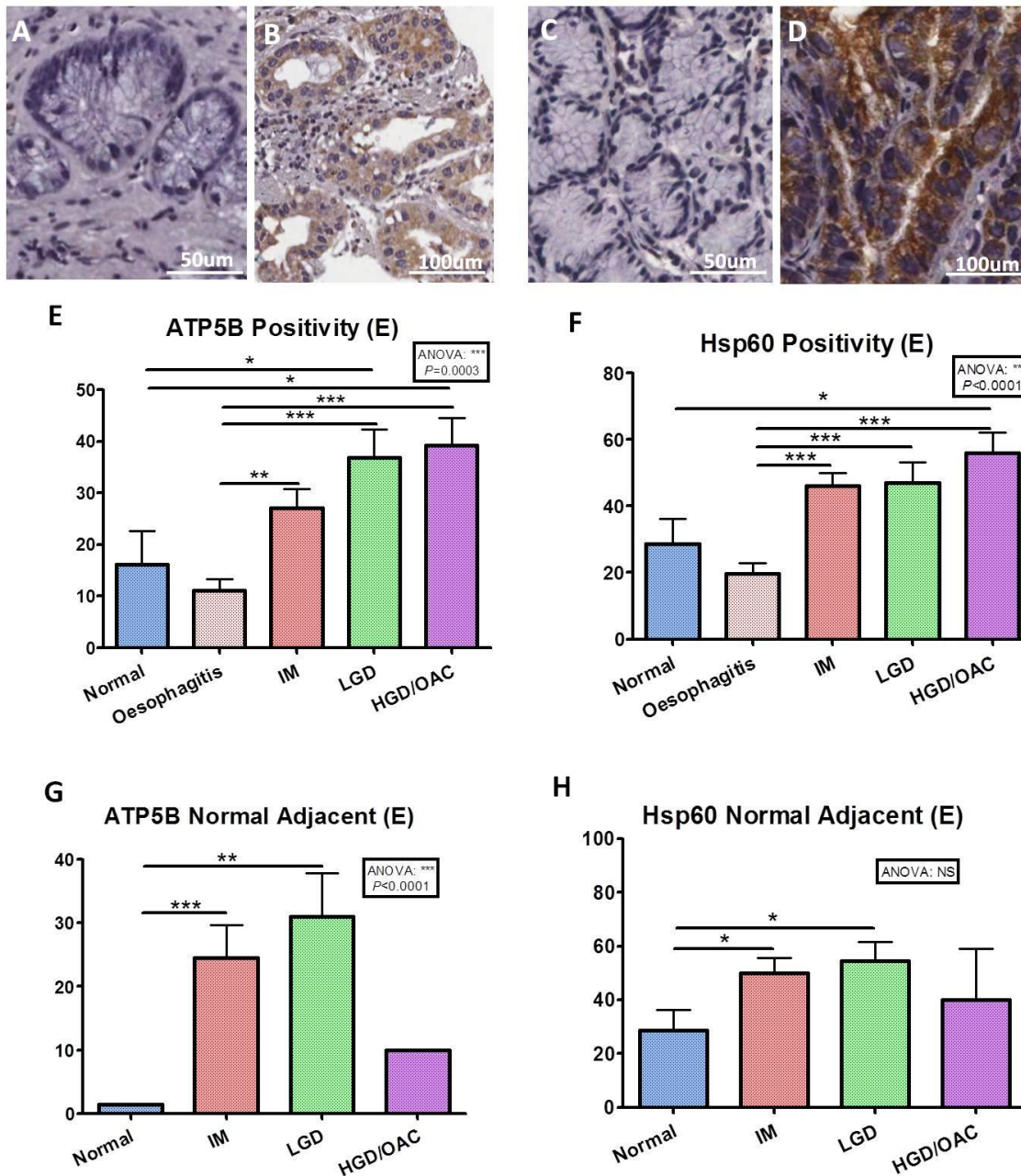


Figure 22. Epithelial immunohistochemical tissue expression of the oxidative phosphorylation protein biomarkers, ATP5B (A, B, E and G) and HSP60 (C, D, F and H), across the metaplasia-dysplasia-adenocarcinoma disease sequence. (A) Tissue section from an oesophagitis patient negative for levels of epithelial ATP5B staining. **(B)** Tissue section from an OAC patient positive for levels of ATP5B staining in epithelium. **(C)** Tissue section from an oesophagitis patient with negative levels of epithelial Hsp60 staining. **(D)** Tissue section from a HGD patient exhibiting positive levels of HSP60 staining in epithelium. **(E)** Epithelial ATP5B positivity across the Barrett’s disease sequence was shown to increase significantly ($P<0.001$, Mann Whitney U) (ANOVA; $P=0.0003$). **(F)** Epithelial HSP60 positivity across the Barrett’s disease sequence increased significantly ($P<0.001$, Mann Whitney U) (ANOVA; $P<0.0001$). **(G)** Epithelial ATP5B positivity early across the Barrett’s disease sequence in matched normal adjacent tissue was shown to increase significantly ($P<0.0001$, Mann Whitney U) (ANOVA; $P<0.0001$). **(H)** Epithelial HSP60 positivity early across the Barrett’s disease sequence in matched normal adjacent tissue increased significantly ($P<0.05$, Mann Whitney U).

Figure 23 illustrates epithelial and stromal tissue expression of the glycolytic protein markers, PKM2 and GAPDH, across the metaplastic-dysplastic-OAC disease sequence. Figures 23A and 23B show representative images of epithelial PKM2 expression in oesophagitis and HGD tissue respectively. Figures 23C and 23D show representative images of epithelial GAPDH expression in Barrett's and OAC tissue respectively. Epithelial PKM2 positivity across the Barrett's disease sequence was shown to increase significantly (figure 23E) ($P=0.0003$). Epithelial GAPDH positivity also increased significantly across the Barrett's disease sequence (figure 23F) ($P=0.0002$). In contrast to the markers of oxidative phosphorylation in the stromal compartment, stromal tissue expression of the glycolytic protein markers, PKM2 (figure 23G) ($p=0.03$) and GAPDH (figure 23H) ($P=0.0007$), decreased significantly across the metaplastic-dysplastic-OAC disease sequence. Moreover, although both PKM2 and GAPDH expression increased across the sequence in matched normal adjacent tissue, only the latter was statistically significant (see appendix H). Furthermore, although epithelial PKM2 intensity was significantly increased across the Barrett's sequence in diseased tissue, no significant differences in intensity were found for epithelial GAPDH, stromal PKM2 or stromal GAPDH (see appendix I). It is may also be noteworthy to mention that stromal GAPDH intensity was significantly altered across the Barrett's sequence in matched normal adjacent tissue but no significant differences in intensity were found for stromal PKM2, ATP5B or HSP60 (see appendix J).

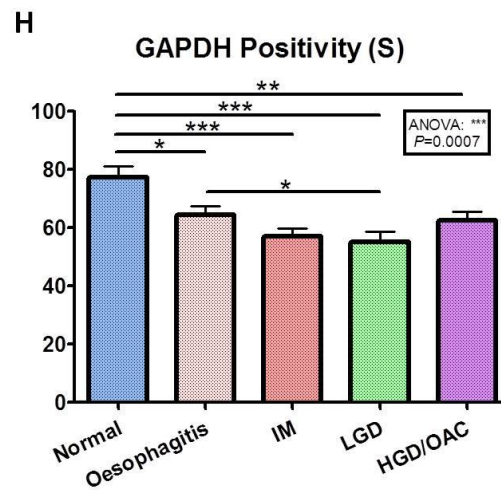
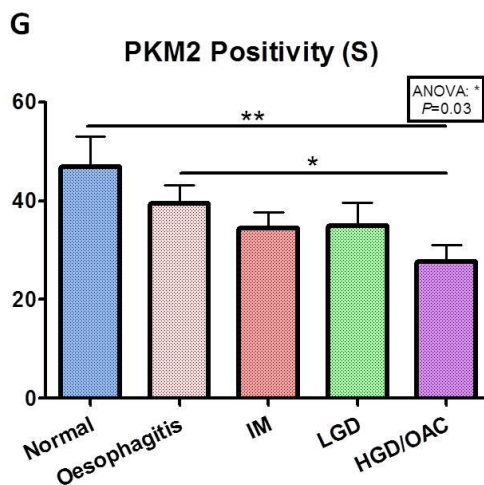
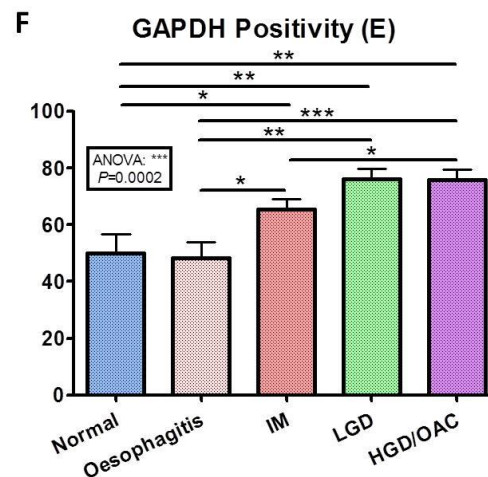
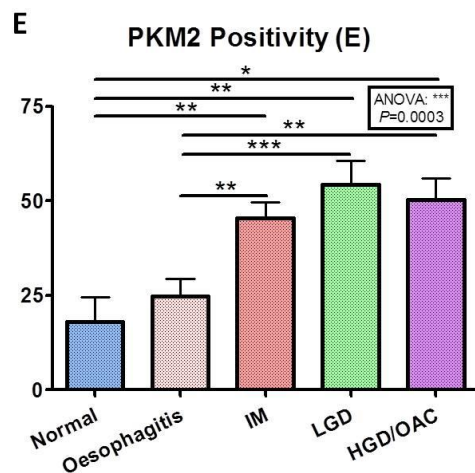
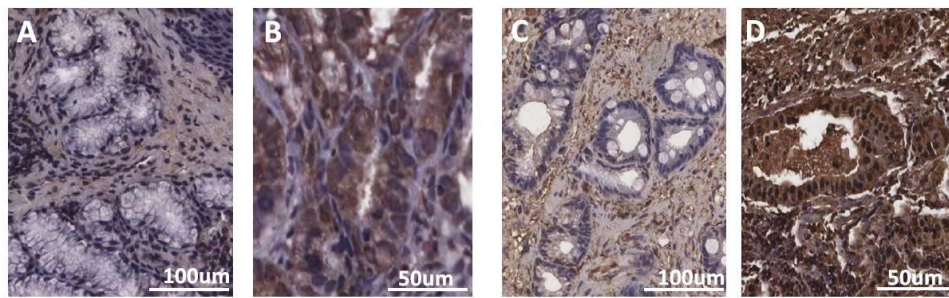


Figure 23. Epithelial and stromal immunohistochemical tissue expression of the glycolytic protein markers, PKM2 (A, B, E and G) and GAPDH (C, D, F, H), across the metaplasia-dysplasia-adenocarcinoma disease sequence. (A) Tissue section from an oesophagitis patient negative for levels of epithelial PKM2 staining. **(B)** Tissue section from a HGD patient positive for levels of PKM2 staining in epithelium. **(C)** Tissue section from a Barrett's esophagus patient exhibiting minimal baseline levels of epithelial GAPDH staining. **(D)** Tissue section from an OAC patient exhibiting strong positive levels of GAPDH staining in epithelium. **(E)** Epithelial PKM2 positivity across the Barrett's disease sequence was shown to increase significantly ($P<0.001$, Mann Whitney U) (ANOVA; $P=0.0004$). **(F)** Epithelial GAPDH positivity increased significantly across the Barrett's disease sequence ($P<0.001$, Mann Whitney U) (ANOVA; $P=0.0001$). **(G)** Stromal PKM2 positivity across the Barrett's disease sequence was shown to decrease significantly ($P<0.01$, Mann Whitney U) (ANOVA; $P=0.03$). **(H)** Stromal GAPDH positivity decreased significantly across the Barrett's disease sequence ($P<0.001$, Mann Whitney U) (ANOVA; $P=0.0007$).

In addition to analysing the expression of the protein markers ATP5B and HSP60 in independent groups of tissue across the Barrett's sequence, we also assessed their expression in sequential longitudinal material from Barrett's non progressors and progressors to investigate if screening for the metabolic proteins using first surveillance biopsies could predict neoplastic progression. Figure 24 illustrates the longitudinal tissue microarray expression of the metabolic biomarkers ATP5B, HSP60, PKM2 and GAPDH between Barrett's patients who did and did not progress using initial first-time surveillance biopsies from these patients. Interestingly, there was a significant increase in percentage positivity of stromal cytoplasmic ATP5B in Barrett's patients who prospectively progressed to OAC (figure 24A) ($P < 0.01$). This predictive expression pattern was specific to ATP5B and not detected with the other metabolic markers (figures 24B-D).

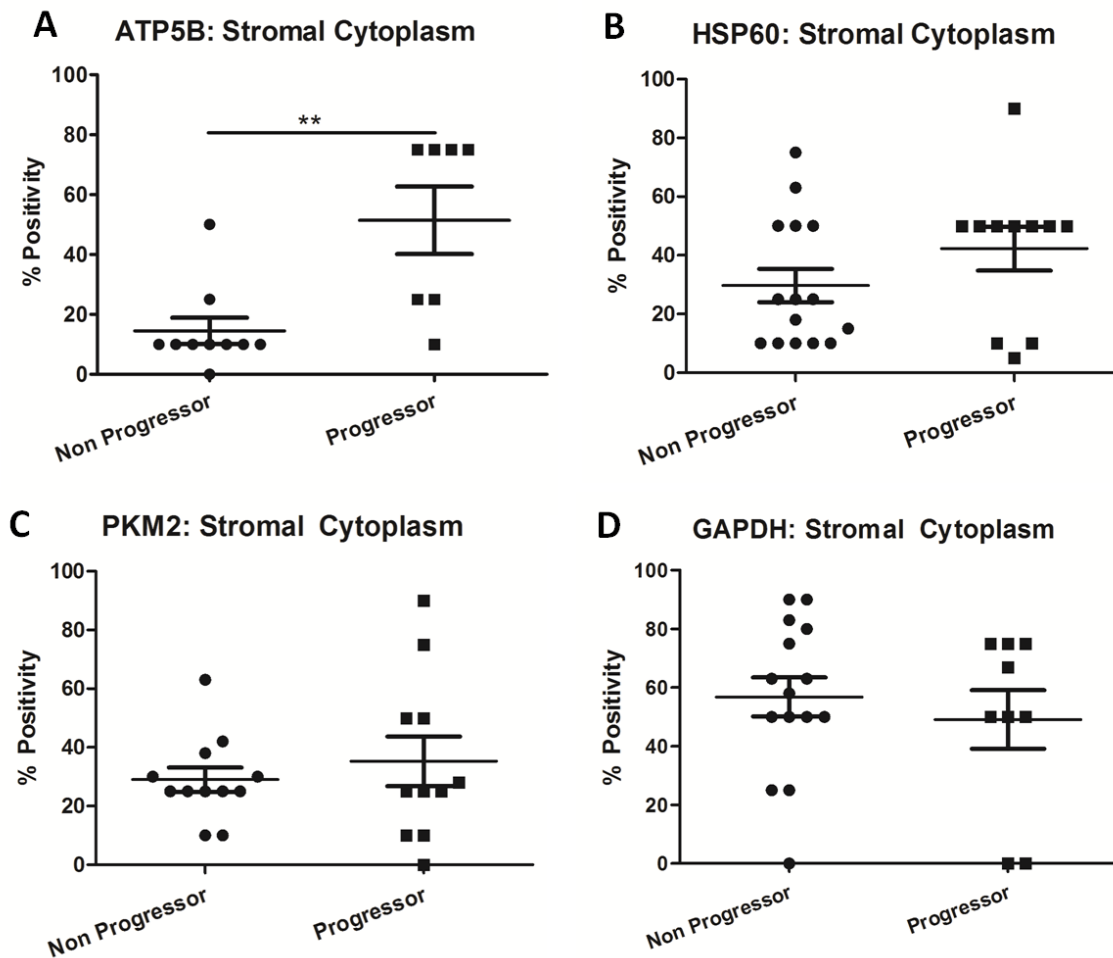


Figure 24. Longitudinal immunohistochemical assessment of mean ATP5B (A), HSP60 (B), PKM2 (C) and GAPDH (D) tissue microarray expression in Barrett's non-progressors and progressors to OAC. Barrett's non-progressors ($n=15$) and progressors ($n=11$) were separated with the primary end-point being progression to OAC. **(A)** Barrett's patients who prospectively progressed to OAC exhibited significantly increased levels of ATP5B ($P=0.007$, Mann Whitney U). **(B)** HSP60 expression was not significantly different between Barrett's non-progressors and progressors to OAC ($P>0.05$, Mann Whitney U). **(C)** PKM2 levels were not significantly different between Barrett's non-progressors and progressors to OAC ($P>0.05$, Mann Whitney U). **(D)** GAPDH expression was not significantly different between Barrett's non-progressors and progressors to OAC ($P>0.05$, Mann Whitney U). The median age of patients with intestinal metaplasia was 58 years and there was a 3.3-fold male predominance. There was no significant difference in age between progressors and non-progressors ($P=0.6404$). Median time of progression to cancer was 2.6 years. TNM staging for progressors was as follows: 20% $T_1N_0M_0$, 20% $T_3N_1M_x$, 20% $T_{15}N_0M_0$, 10% $T_{15}N_0M_0$, 10% $T_3N_0M_0$, 10% $T_3N_1M_0$ and 10% $T_3N_1M_1$. The non-progressor group was followed for a median of 5.4 years and had no evidence of conversion to HGD and/or OAC. For ATP5B and GAPDH, 7 and 9 progressors were deemed scorable respectively. Bars denote mean \pm SEM.

3.4.4 Characterisation of oxidative metabolic plasticity in the in-vitro Barrett's sequence

As ATP5B, the marker of oxidative phosphorylation, was predictive in segregating Barrett's non progressors and progressors, we examined how metaplastic and OAC cells would behave when challenged with mitochondrial inhibitors known to alter metabolic reprogramming. Figure 25 illustrates different metabolic parameters examined subsequent to challenging QH and OE33 cell lines with oligomycin, FCCP and antimycin-A using the Seahorse XF24 flux analyser. Figures 25A-F illustrate relative mitochondrial respiration in QH and OE33s cells, ATP synthesis, maximal respiratory capacity, non electron transport chain respiration and proton leak between the QH and OE33 cell lines, respectively. Approximately 80% of total OCR accounted for mitochondrial respiration in the QH cell line (figure 25A) and 64.7% of total OCR accounted for mitochondrial respiration in the OE33 cell line (figure 25B). Levels of oxygen consumed by the electron transport chain in both cell lines was significantly higher versus oxygen consumed for non electron transport chain purposes (figures 25A-B) ($P < 0.001$). QH cells (63%) exhibited higher levels of ATP synthesis compared to the OE33 (50.6%) cells (figure 25C) ($P < 0.05$). Upon mitochondrial uncoupling with FCCP, OE33 cells exhibited a significantly greater spare respiratory capacity of 33% compared to QH cells (figure 25D) ($P < 0.01$). OE33 cells demonstrated 15.2% higher levels of OCR, attributed to non electron transport chain processes, compared to QH cells (figure 25E) ($P < 0.05$). No significant difference in proton leak was observed between QH and OE33 cells (figure 25F). Interestingly, we found baseline oxidative phosphorylation and glycolysis to be higher in QH cells compared to OE33 cells with high levels of ECAR reaching statistical significance (see appendix K).

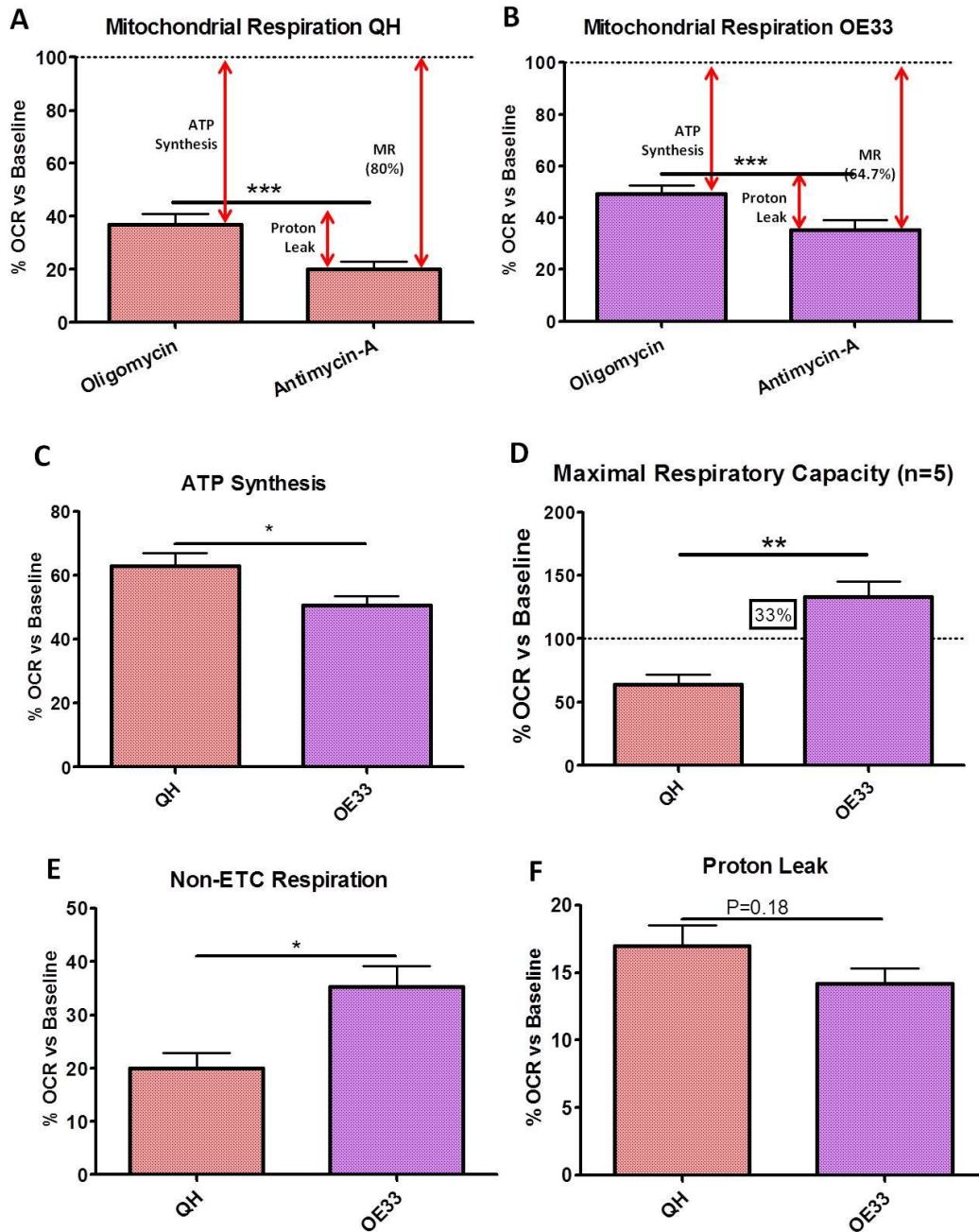


Figure 25. Seahorse assessment of mitochondrial respiration (A-B), ATP synthesis (C), maximal respiratory capacity (D), non electron transport respiration (E) and proton leak (F) between the Barrett's (QH) and adenocarcinoma (OE33) *in-vitro* cell lines. (A) Measurement of mitochondrial respiration (37%) and proton leak (17%) in the Barrett's metaplasia cell line, QH ($P < 0.001$). (B) Measurement of mitochondrial respiration (49.4%) and proton leak (14.2%) in the OAC cell line, OE33 ($P < 0.001$). (C) Graph shows the percentage of oxygen consumption versus baseline reflecting ATP production attributed to ATP synthase after ATP synthase inhibition via oligomycin. QH cells (63%) utilise significantly higher levels of oxygen for oxidative phosphorylation ($P < 0.05$) in contrast to OE33 cells (50.6%). (D) Graph illustrates the percentage of oxygen consumption versus baseline upon mitochondrial uncoupling via trifluorocarbonylcyanide phenylhydrazine (FCCP). OE33 cells exhibited a greater spare respiratory capacity (33%) compared to the QH cell line ($P < 0.01$). (E) The OE33 cell line (35.2%) demonstrated significantly higher non-electron transport chain respiration levels compared to the QH cell line (20%) ($P < 0.05$). (F) The Barrett's QH cell line (17%) exhibited higher cells of proton leak across the inner mitochondrial membrane versus the adenocarcinoma OE33 cell line (14.2%) ($P = 0.18$). Bars denote mean \pm SEM.

3.5 DISCUSSION

Understanding the underlying molecular mechanisms that support the progression of Barrett's oesophagus to cancer would significantly affect the clinical management of these patients. We have shown for the first time that mitochondrial energy metabolism is altered across the normal-metaplasia-dysplasia-OAC sequence of events in Barrett's oesophagus and these early changes in metabolic alterations, specifically oxidative phosphorylation, are associated with an increased risk of disease progression from Barrett's metaplasia to OAC.

In this study, a human PCR gene microarray identified three genes associated with mitochondrial energy metabolism differentially expressed between Barrett's and OAC cells. Few studies have associated *COX4I2*, *COX8C*, and *ATP12A* with cancer progression and their role in energy metabolism. We have shown a significant increase in *COX8C* expression in Barrett's patients compared to normal squamous tissue. Interestingly, the increase in *COX8C* expression in Barrett's tissue was subsequently followed by a significant decrease in *COX8C* expression in LGD and HGD/OAC tissue. This increase in *COX8C* expression was specific to Barrett's tissue compared to matched surrounding mucosa. No studies to date have reported a role for *COX8C* in tumourigenesis, therefore, we hypothesise that *COX8C* may play an important role in Barrett's patients by increasing basal oxidative phosphorylation levels, altering energy metabolism and subsequently promoting neoplastic progression.

We have also shown *in-vivo* a significant increase in *COX4I2* expression across the Barrett's sequence. *COX8C* and *COX4I2* pertain to the one protein complex and both have different expression patterns – *COX8C* increases and subsequently decreases while *COX4I2* increases and maintains its expression pattern. Interestingly, both complex IV genes are upregulated despite a significant downregulation in a subunit of their downstream associate complex, ATP synthase. This downregulation of *ATP12A* was also shown to be specific to Barrett's tissue compared to the matched surrounding mucosa. It is noteworthy to mention that *ATP12A* expression differed *in-vitro* using PCR microarrays and through subsequent *in-vitro* validation between QH and OE33 cells. Two possible reasons for this discrepancy is the presence of genomic DNA due to the lack of a DNA elimination step and the use of the SYBR green PCR probe in the PCR microarray kit. Implementation of routine quality control procedures, such as utilisation of a Taqman PCR probe, avoided such issues upon subsequent *in-vitro* and *in-vivo* validation. Moreover, it is important to mention the differential decrease and increase in *COX4I2* expression *in-vitro* and *in-vivo* respectively. Barrett's tissue is complex, primarily due to its rich cell diversity. For example, they contain various cell types including epithelial, stromal, endothelial, immune, inflammatory and fibroblast cells among others. However, the Barrett's cell line are solely epithelial cells and,

therefore, both models are considerably different biologically which may explain their differential expression patterns.

COX4I2 and *ATP12A* have been ascribed to few pathologies. A single base mutation in the *ATP12A* subunit results in complex V deficiency (394). Immunological ATP12A expression in normal and benign prostate hyperplasia and cancerous prostate tissue have been shown to be altered in luminal cells of the glandular epithelium (395). More recently, in a study proposing a protective role for decreased ATP levels analysing the function of lung-specific *COX4I2 in-vitro* and in *COX4I2*-knockout mice *in-vivo*, it was found that cytochrome *c* oxidase activity and ATP levels were significantly reduced in knockout mice (396). In addition, decreased oxidative phosphorylation in cancer development is commonly associated with a parallel increase in glycolysis (164, 397-400). This decrease in oxidative phosphorylation is frequently linked with defects in complex I and III, for example, in renal, leukaemia and fibroblast cell lines (397, 398, 400). One possible explanation for the dysregulation of these three genes is in the microenvironment they reside. MtDNA is highly prone to oxidative damage as it is situated on the inner mitochondrial membrane (401). Moreover, it is in close proximity to the electron transport chain and the levels of oxidized bases are estimated to be 2-3 times greater than nuclear DNA (401). The increased oxidative microenvironment demonstrated in this study may strengthen this hypothesis in Barrett's oesophagus.

Next, we examined the expression of different oxidative phosphorylation and glycolytic proteins across the Barrett's sequence, investigated if the metabolic phenotype at the protein level reflected these metabolic profiles seen at the gene level and investigated if a metabolic marker could segregate Barrett's non-progressors and progressors to cancer using established markers of oxidative phosphorylation (ATP5B and HSP60) and glycolysis (PKM2 and GAPDH) (390, 402, 403).

We have shown that both epithelial ATP5B and HSP60 positivity significantly increased across the Barrett's sequence, consistent with a metabolic shift in glucose metabolism to a more actively oxidative metabolic level. Moreover, the expression levels of ATP5B and HSP60 were significantly altered between Barrett's diseased tissue and the matched surrounding mucosa. This increase in oxidative phosphorylation is analogous to *COX4I2* and *COX8C* discussed above. One recent study showed a similar trend in glucose metabolism whereby human breast tumours demonstrated increased epithelial enzymatic activity in various complexes (404). To recall, HSP60 positivity significantly increased across the Barrett's sequence. HSP60 expression has been previously shown to be increased in various cancer types (405-407). This increase in oxidative phosphorylation complex IV genes and associated proteins highlighted may be a compensatory mechanism to counteract the significant downregulation of complex IV's main downstream

protein complex, complex V, namely attributed to *ATP12A* as this loss can lead to complete mitochondrial dysfunction (394). Therefore, we hypothesise that cancer cells may act as 'metabolic parasites', secreting hydrogen peroxide into the local microenvironment, inducing oxidative stress in normal host cells resulting in autophagy, mitophagy and aerobic glycolysis. As a result, high-energy glycolytic nutrients such as ketones, L-lactate and glutamine may fuel the anabolic growth of tumour cells through oxidative phosphorylation.

The epithelial expression of both glycolytic biomarkers, PKM2 and GAPDH, were significantly increased across the Barrett's sequence and concur with an elevation in epithelial glycolysis, a common entity shown in other cancers (390, 408, 409). PKM2 is more abundant during aerobic glycolysis in many tumour types, including the Barrett's sequence in non-sequential tissue (392). Interestingly, in contrast to the increased epithelial expression of both glycolytic makers, the expression of these markers are significantly decreased in matched stromal tissue. However, the proliferation status of the epithelium may in part exacerbate the degree of aerobic glycolysis. Interestingly, our longitudinal analysis demonstrates that Barrett's patients with increased levels of the oxidative phosphorylation marker ATP5B are more likely to progress to OAC. This novel finding indicates a crucial and pivotal role for oxidative phosphorylation in OAC progression in the Barrett's disease sequence. Increased levels of ATP5B, and thus oxidative phosphorylation, are fuelled by the greater availability of high-energy nutrients through increased glycolysis. As a result, the subsequent oxidative state may make local tissue more amenable to the anabolic growth of tumour cells, tumour differentiation and progression. Subsequent validation of ATP5B in different patient cohorts from different clinical institutions would potentially strengthen the applicability of this marker in the clinical setting as this assessment could be undertaken efficiently on formalin fixed paraffin embedded tissue.

It is evident from this study that oxidative phosphorylation at both the gene and protein level play a vital role in exacerbating disease progression in Barrett's oesophagus. It was necessary, therefore, to decipher elements of oxidative phosphorylation, specifically the complexes of the electron transport chain that play an important role. Using the Seahorse technology, we challenged the mitochondria to gain insight into the oxidative capabilities in both cell types as this could not be performed *in-vivo*. We investigated basal oxidative phosphorylation, basal glycolysis, mitochondrial respiration, ATP synthesis, spare respiratory capacity, non electron transport chain respiration and proton leak in both QH and OE33 cell lines. We demonstrate that metaplastic cells are more energy demanding compared to OAC cells suggesting an early metabolic advantage for differentiation, metastatic transformation and subsequent proliferation due to an increased capacity to generate ATP for anabolic purposes.

When the oxidative capacity of the QH and OE33 cells was challenged, mitochondrial respiration differed between the two cell types and the degree of ATP synthesis and proton leak attributed to mitochondrial respiration was also substantially different. The OE33 cell line maintains an equilibrium between both metabolic pathways, thereby demonstrating metabolic plasticity while the QH cell line favours a more detrimental oxidative phenotype that may be selected during early stages of disease progression. Interestingly, when oxidative metabolism is inhibited, both QH and OE33 cells can adapt metabolically by increasing their glycolytic metabolism, thereby illustrating further metabolic plasticity (see appendix L).

In an exploratory analysis of the gene encoding the protein C-ets-1, *ETS-1*, a transcription factor identified as being able to regulate *ATP5B* and known to mediate metabolism in neoplastic tissue, we examined the expression of *ETS-1 in-vitro* and *in-vivo* and investigated its link with *ATP5B in-vivo* at the gene level (410, 411). Despite no significant change in *ETS-1* expression in QH and OE33 cell lines, we found a significant increase in *ETS-1* expression across the squamous-metaplasia-dysplasia-OAC sequence *in-vivo* (see appendix M). Moreover, we found that *ATP5B* positively associated with *ETS-1* in metaplastic, dysplastic and OAC tissue with the strongest link being in the setting of Barrett's oesophagus possibly highlighting a role for *ETS-1* in Barrett's associated tumourigenesis (see appendix N).

Overall, we have shown in this study that metabolic reprogramming is active during disease progression in Barrett's and specifically, markers of oxidative phosphorylation can segregate Barrett's non progressors from progressors to cancer. This needs to be further examined using different patient cohorts from multicentres to establish clinical utility.

Chapter 4

An investigation into the role of deoxycholic acid, antioxidants, proton-pump inhibitors and the small molecule inhibitor, Quininib, on energy metabolism profiles in Barrett's oesophagus.

4.1 INTRODUCTION

Gastroesophageal reflux disease, or GORD, plays a central role in the development of Barrett's oesophagus and is one of the biggest risks of neoplastic progression in Barrett's associated OAC (412-414). It is estimated that Barrett's oesophagus is found in approximately 5-10% of GORD patients undergoing endoscopy due to heartburn or oesophagitis related symptoms (415). Gastric acid, bile acid and pepsin in the refluxate play a predominant role in the initiation of oesophageal injury and inflammation (415, 416). As a result, prolonged exposure of this refluxate to normal squamous epithelium and variations in pH promote the generation of columnar lined epithelium (416). Clinical studies show that intra-oesophageal bile acid concentrations are higher in patients with Barrett's oesophagus compared to those with uncomplicated GORD (417).

Interestingly, different bile acids exhibit distinct biological effects (418). Deoxycholic acid (DCA) and chenodeoxycholic acid cause morphological changes characteristic of apoptosis, ursodeoxycholic acid inhibits cell proliferation, increases antioxidant expression and prevents DNA damage whereas the bile acid cholic acid does not seem to affect cells (418, 419). DCA, however, has been extensively shown to play a major role in the development of Barrett's oesophagus and in its subsequent progression to OAC (70-74). Physiological levels of DCA have been shown to activate NF κ B and induce the expression of the chemokine IL-8 in OE33 cells (74). Interestingly, activation of NF κ B occurs at neutral pH and not at an acidic pH, however, acidic conditions do induce the expression of c-myc (74).

DCA also demonstrates chromosomal damage and mutation induction in the human p53 gene at both neutral and acidic pH (73). Furthermore, DCA-induced release of reactive oxygen species (ROS) has been shown to be linked to the genotoxicity of DCA in a ROS dependent manner (72, 73). Through NF κ B activation in Barrett's epithelial cells, DCA can cause DNA damage while inducing apoptotic resistance (71). In addition to IL-8, DCA-induced secretion of another chemokine, MIP3 α , and the upregulation of the farnesoid X receptor, the receptor involved in the regulation of bile acid synthesis, transport and absorption, suggests that bile acids actively induce the inflammatory response in Barrett's epithelium by recruiting immune cells (420). In addition to its role in promoting an inflammatory microenvironment, DCA has been linked to angiogenesis as DCA treated OE33 cells have also been shown to express significantly higher expression levels of VEGF (70).

Proton-pump inhibitors are thought to protect against Barrett's associated OAC as they help alleviate the chronic inflammation associated with GORD and decrease epithelial exposure to acid

refluxate (421). Proton-pump inhibitor use, prescribed for approximately 95-98% of patients with Barrett's oesophagus, is associated with reduced incidence of dysplasia and OAC in Barrett's oesophagus (41, 422, 423). Conversely, proton-pump inhibitors reduce the expression of various risk markers for HGD and OAC in Barrett's oesophagus, thereby confounding surveillance strategies for patients, however, the use of proton-pump inhibitors is still justified due to the lower risk of progression to OAC associated with proton-pump inhibitor use (424). For example, patients without prior treatment with proton-pump inhibitors are 3.4 times more likely to have a macroscopic marker or LGD compared to those on proton-pump inhibitors (424). Moreover, proton-pump inhibitor use is associated with increased risks of bone fractures and *Clostridium difficile* infections (425, 426). In the neoplastic setting, proton-pump inhibition has been shown to induce autophagy as a survival mechanism following oxidative stress (427).

Our research has demonstrated that oxidative phosphorylation and glycolysis are reprogrammed early across the metaplasia-dysplasia-adenocarcinoma disease sequence *in-vivo* (see section 2) (130). Since inflammation and cellular energetics are intrinsically linked, such alterations in cellular metabolism may be linked with DCA-induced alterations in the Barrett's microenvironment (428). No study to our knowledge has examined the effect of DCA and proton-pump inhibitor use on oxidative phosphorylation and glycolytic profiles. Therefore, this chapter assesses the effect of the bile reflux component DCA and two clinical proton-pump inhibitors, omeprazole and lansoprazole, on mitochondrial energy metabolism profiles across the *in-vitro* Barrett's disease sequence. The study also investigates if antioxidant supplementation with N-acetylcysteine (NAC) and epigallocatechin gallate (EGCG) can reverse DCA-induced metabolic changes. Furthermore, we examine if mitochondrial energy metabolism in Barrett's oesophagus and OAC can be modulated by a novel small molecule inhibitor, Quininib, which has previously been shown to exhibit anti-oxidative phosphorylation properties in *in-vitro* and *in-vivo* (unpublished).

4.2 HYPOTHESIS AND AIMS OF CHAPTER 4

We hypothesise that DCA and proton-pump inhibitors alter energy metabolism profiles across the normal squamous-metaplasia-dysplasia-adenocarcinoma sequence *in-vitro* and antioxidants and a novel small molecule inhibitor can modulate metabolic function.

Specific aims of chapter 4;

- 1) Investigate the effect of DCA on real-time metabolism and assess if antioxidants can rescue DCA-induced metabolic alterations *in-vitro* utilising the Seahorse XF24 analyser.
- 2) Examine the effect of the clinical proton-pump inhibitors omeprazole and lansoprazole on realtime metabolism *in-vitro* utilising the Seahorse XF24 analyser.
- 3) Examine the effect of the small molecule inhibitor, Quininib, on inflammatory, angiogenic and metabolic profiles *in-vitro* and using *ex-vivo* human Barrett's explants.

4.3 METHODS

4.3.1 *Squamous, metaplastic, dysplastic and adenocarcinoma cell line models*

QH, GO and OE33 cell lines were utilised and subcultured as before (see sections 2.3.2 and 2.3.3). HET1A cells, representing the normal squamous epithelium, were also grown to 70% confluency in BEBM medium supplemented with BEBM SingleQuots (2mL BPE, 0.5mL insulin, 0.5mL HC, 0.5mL retinoic acid, 0.5mL transferrin, 0.5mL triiodothyronine, 0.5mL adrenaline and 0.5mL hEGF per 500ml media). Unlike QH cells, HET1A cells were cultured without FBS and not supplemented with GA-1000 for optimal growth conditions, therefore, additional centrifugation and decantation steps were undertaken to remove and neutralise trypsin during subculturing. HET1A cells were obtained from American Type Culture Collection (ATCC) (LGC Standards, Middlesex, UK).

4.3.2 *Assessing the effect of deoxycholic acid, N-acetylcysteine and epigallocatechin gallate in-vitro utilising the Seahorse XF24 analyser*

Oxygen consumption rate (OCR) and extracellular acidification rate (ECAR), reflecting oxidative phosphorylation and glycolysis respectively, were measured using the Seahorse XF24 analyser (Seahorse Biosciences) as before (see section 2.3.10). OCR and ECAR were measured at baseline in response to treatment with DCA (100 μ M, Sigma), NAC (10 μ M, Sigma) and EGCG (40 μ M, Sigma). HET1A, QH, GO and OE33 cells were seeded at 20,000 cells per well in a 24-well cell culture XF microplate (Seahorse Biosciences), allowed to adhere for 24 hours and treated for an additional 24 hours with either control media, DCA, DCA+NAC or DCA+EGCG. Four baseline OCR and ECAR measurements were obtained over 28 minutes. The experiment was repeated three times with technical replicates. All measurements were normalised to cell number using the crystal violet assay (see section 2.3.9).

4.3.3 *Investigating the effect of proton-pump inhibitor use in-vitro utilising the Seahorse XF24 analyser*

Experimental protocol was followed as described before (see section 2.3.10). OCR and ECAR were measured at baseline in response to treatment with omeprazole (12 μ M, Sigma) and lansoprazole (12 μ M, Sigma). HET1A, QH, GO and OE33 cells were seeded at 20,000 cells per well in a 24-well cell culture XF microplate (Seahorse Biosciences), allowed to adhere for 24 hours, treated for an additional 24 hours with either control media, 12 μ M omeprazole or 12 μ M lansoprazole and the experiment carried out as per section 2.3.10.

4.3.4 *Exploring the effect of Quininib in-vitro utilising the Seahorse XF24 analyser*

Experimental protocol was followed as described above (see section 2.3.10). OCR and ECAR were measured at baseline in response to treatment with 10 μ M Quininib (patent number PCT/IE2012/000002). HET1A, QH, GO and OE33 cells were seeded at 20,000 cells per well in a 24-well cell culture XF microplate (Seahorse Biosciences), allowed to adhere for 24 hours, treated for an additional 24 hours with either control media or Quininib and the experiment carried out as per section 2.3.10.

4.3.5 *Examining the effect of Quininib on inflammatory, angiogenic and metabolic profiles in ex-vivo Barrett's explant tissue*

4.3.5.1 *Normal squamous and Barrett's ex-vivo explant culture*

All fresh *ex-vivo* Barrett's intestinal metaplasia and matched normal adjacent squamous tissue were prospectively recruited at our national referral centre for upper GI malignancy. The median age of patients ($n=9$) with intestinal metaplasia was 62 years and there was an 8-fold male predominance. Matched normal squamous and Barrett's explant tissue was subsequently transferred into 1mL M199 media (10% FBS, 1% Pen/Strep, 1mg/mL insulin) (Gibco) supplemented with or without 10 μ M Quininib and cultured for 24 hours at 5% CO₂ at 37°C. Following 24 hour incubation, the conditioned medium was collected and explant tissue snap frozen in liquid nitrogen. Both media and tissue were stored at -80°C for future use.

4.3.5.2 *Ex-vivo MSD multiplex ELISA analysis*

Conditioned medium was screened for the levels of the multiplex inflammatory and angiogenic proteins (Meso Scale Discovery Multi-Array technology). The inflammatory proteins assessed were GRO-alpha (GRO α), IL1 β , IL-10, IL-2, IL-6, monocyte chemoattractant protein-1 (MCP-1), macrophage inflammatory protein 3 alpha (MIP3 α), matrix metalloproteinase 2 (MMP2), MMP9 and TNF α . The angiogenic proteins assessed were angiopoietin 1 (ANG-1), basic fibroblast growth factor (bFGF), plasminogen activator inhibitor-1 (PAI-1), vascular cell adhesion molecule-1 (VCAM-1), ICAM-1 (intracellular cell adhesion molecule-1) and VEGF. Protein standards were produced by adding 10 μ L of each cytokine stock to 990 μ L M199 media to yield 8 standards with the following highest standards; ANG-1/VCAM-1/ICAM-1: 100,000pg/ml, MMP2/MMP9/PAI-1: 50,000pg/ml, TNF α /MIP3 α /IL-6/IL-2/VEGF/bFGF: 10,000pg/ml, MCP-1/IL-10/IL1 β : 2500pg/ml and GRO α : 5000pg/ml. 25 μ L diluent 2 solution (Meso Scale) was added to all wells for 30 minutes followed by 25 μ L of samples and standards for 2 hours. Plates were washed using PBS tween-20 (250 μ L Sigma Tween in 500ml PBS), 25 μ L of detection antibody solution added (Meso Scale, 60 μ L stock in diluent 3 solution) and left to incubate at room temperature for 2 hours. Plates were

subsequently washed with PBS tween-20, 150µL 2x read buffer (Meso Scale) added to each well and cytokines concentrations recorded with the SECTOR imager (Meso Scale). Secreted lactate levels were also assessed in the conditioned media. Total protein extracted above (Qiagen) was assayed utilising a bicinchonic acid assay (Thermo Scientific) and secreted protein levels of these secreted factors in all samples were normalised to total protein.

4.3.5.3 *Ex-vivo qRT-PCR analysis*

Matched normal squamous and Barrett's explant tissue was homogenised using a Tissue-Lyser (Qiagen) for 2.5 mins at a frequency of 25 pulses per second, RNA and protein extracted simultaneously (Qiagen), RNA quantified and RNA quality assessed (Nanodrop®, 8-Sample Spectrophotometer, ND-800). RNA was reverse transcribed using Bioscript enzyme (Bioline) as previously described (see section 2.3.5.1). Gene primer probes for *ATP5B*, *HSP60*, *GAPDH*, *PKM2*, and *18S* (Applied Biosystems) were purchased and real-time PCR was performed using Taqman mastermix (Applied Biosystems) as previously described (see section 2.3.5.2). Data were analysed utilising the $2^{-\Delta\Delta Ct}$ method as before (see section 2.3.4). All 9 matched normal squamous and Barrett's explant tissue was characterised by assessing the expression of the columnar epithelium molecular marker villin using RT-PCR; all Barrett's explant tissue was positive for the presence of villin and all matched adjacent normal squamous tissue was negative for villin.

4.3.6 *Statistical analysis*

Data were analysed using Graph Pad Prism software (Graph Pad Prism, San Diego, CA). Student's paired *t*-test was used to compare Seahorse parameters within HET1A, QH, GO and OE33 cell lines treated with DCA, NAC, EGCG, omeprazole, lansoprazole and Quininiib. Secreted levels of inflammatory and angiogenic mediators between *ex-vivo* explant tissue were statistically analysed using Wilcoxon signed rank tests. qRT-PCR data were normalised using the $2^{-\Delta\Delta Ct}$ method and statistically analysed (Wilcoxon signed rank test). Differences of $P < 0.05$ (*), $P < 0.01$ (**) and $P < 0.001$ (***) were considered statistically significant.

4.4 RESULTS

4.4.1 Examining the effect of deoxycholic acid, N-acetylcysteine and epigallocatechin gallate on energy metabolism *in-vitro*.

HET1A, QH, GO and OE33 cell lines, representing normal squamous epithelium, Barrett's metaplasia, HGD and OAC, were examined for DCA-induced alterations in OCR and ECAR, reflecting changes in oxidative phosphorylation and glycolysis respectively. Figure 26 shows the effect of the bile acid component DCA on OCR and ECAR across the *in-vitro* squamous-metaplasia-dysplasia-adenocarcinoma cell line sequence. DCA induced significant increases in OCR in both the GO ($P=0.0001$) and OE33 ($P=0.027$) cell lines with a significant concomitant decrease in OCR being exhibited in the QH cell line ($P=0.0018$) (figure 26A). DCA had no significant effect on OCR in the HET1A cell line (figure 26A). DCA significantly increased ECAR in the OE33 cells ($P=0.001$) while having no effect on ECAR levels in the HET1A, QH and GO cell lines (figure 26B).

As DCA altered energy metabolism profiles, we examined if the dietary antioxidants N-acetylcysteine (NAC) and epigallocatechin gallate (EGCG) could reverse these DCA-induced alterations in oxidative phosphorylation and glycolysis across the *in-vitro* squamous-metaplasia-dysplasia-OAC sequence. DCA exhibited no effect on OCR or ECAR in HET1A cells, however, in the presence of EGCG, both OCR (figure 27A) ($P=0.003$) and ECAR (figure 27E) ($P<0.0001$) were significantly decreased. NAC significantly rescued DCA-induced decreases in OCR in QH cells (figure 27B) ($P=0.033$). Moreover, EGCG significantly rescued DCA-induced increases in OCR in GO cells (figure 27C) ($P=0.005$) and OE33 cells (figure 27D) ($P<0.0001$). DCA exhibited no effect on ECAR in QH cells, however, in the presence of EGCG, ECAR significantly decreased (figure 27F) ($P=0.002$). DCA in combination with NAC or EGCG had no effect on ECAR in GO cells (figure 27G) ($P>0.05$). NAC significantly exacerbated DCA-induced increases in ECAR in OE33 cells (figure 27H) ($P=0.041$). Figure 28 shows the effect of EGCG on DCA-induced alterations in OCR and ECAR across the *in-vitro* sequence. EGCG treatment significantly affected OCR in DCA treated HET1A, GO and OE33 cells, without affecting OCR in QH cells ($P<0.0001$) (figure 28A). EGCG treatment significantly affected ECAR in DCA treated cells across the *in-vitro* sequence ($P=0.0003$) (figure 28B).

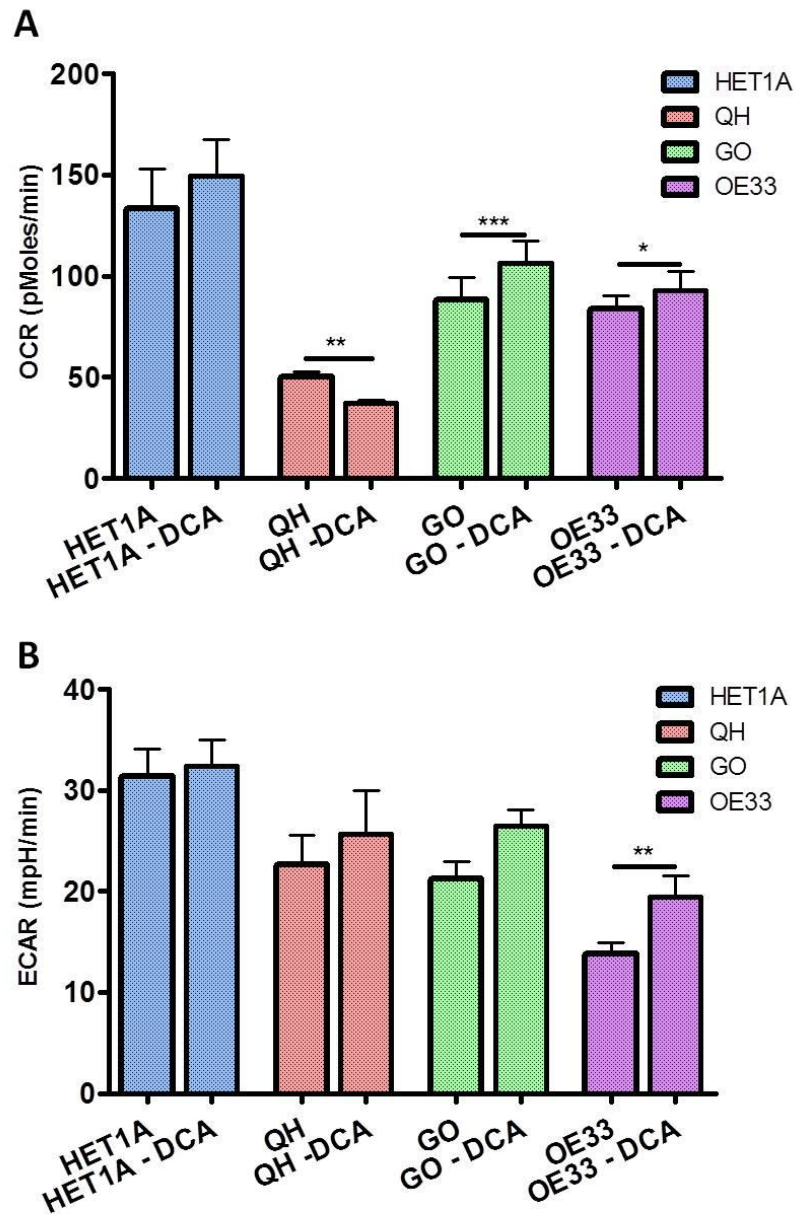


Figure 26. Investigating the effect of deoxycholic acid (DCA) on oxidative phosphorylation (A) and glycolysis (B) across the *in-vitro* squamous-metaplasia-dysplasia-adenocarcinoma sequence. (A) DCA induced significant increases in OCR in both GO ($P=0.0001$) and OE33 ($P=0.027$) cell lines with a significant concomitant decrease in OCR being exhibited in the QH cell line ($P=0.0018$). DCA had no significant effect on OCR in the HET1A cell line. (B) DCA significantly increased ECAR in the OE33 cell line ($P=0.001$) without affecting ECAR in the HET1A, QH and GO cell lines. Paired *t*-tests assessed differences between treatment groups ($n=3$). Bars denote mean \pm SEM.

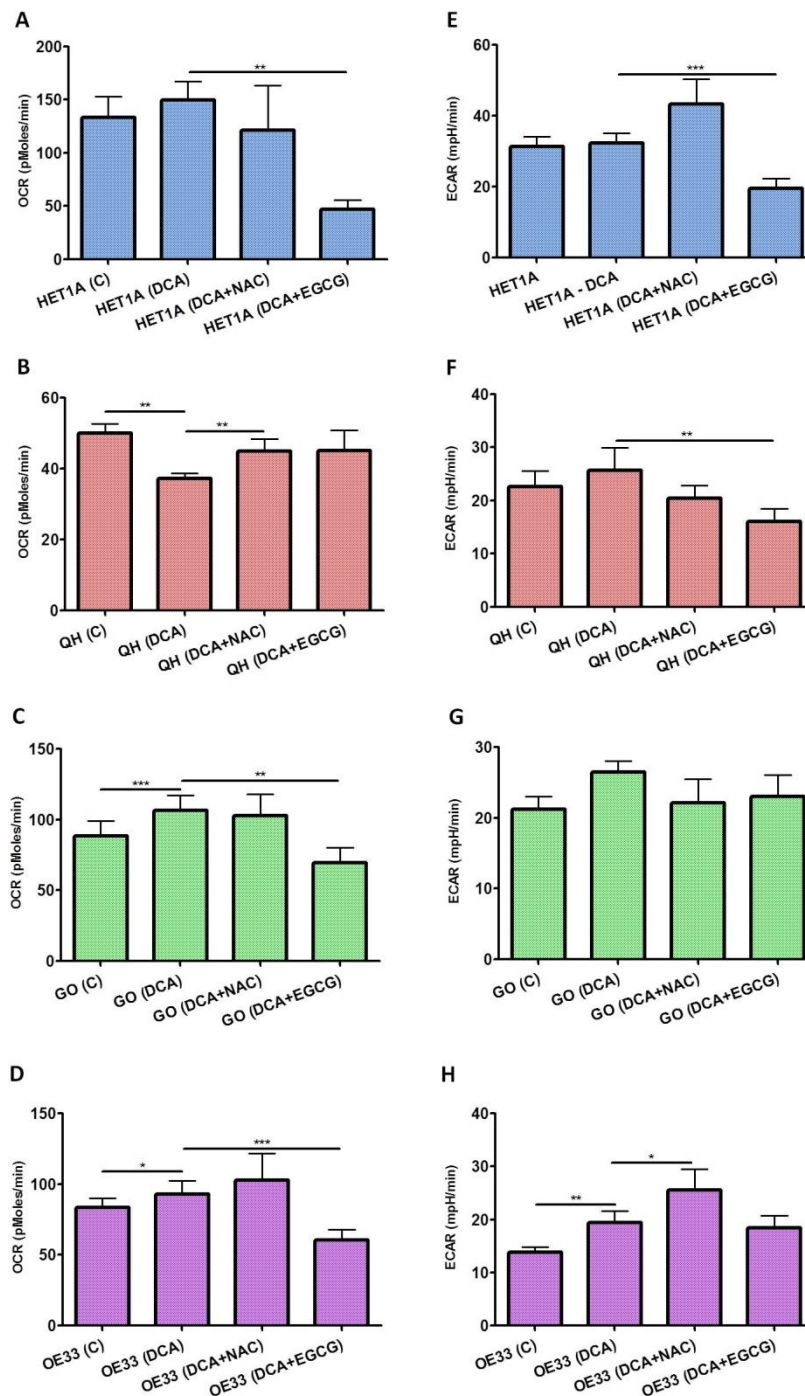


Figure 27. Examining the effect of the antioxidants N-acetylcysteine (NAC) and epigallocatechin gallate (EGCG) on deoxycholic acid (DCA)-induced alterations in oxidative phosphorylation (A-D) and glycolysis (E-H) across the *in-vitro* squamous-metaplasia-dysplasia-adenocarcinoma sequence. (A) DCA exhibited no effect on OCR in HET1A cells, however, in the presence of EGCG, OCR significantly decreased ($P=0.003$). **(B)** NAC significantly rescued DCA-induced decreases in OCR in QH cells ($P=0.033$). **(C)** EGCG significantly rescued DCA-induced increases in OCR in GO cells ($P=0.005$). **(D)** EGCG significantly rescued DCA-induced increases in OCR in OE33 cells ($P<0.0001$). **(E)** DCA exhibited no effect on ECAR in HET1A cells, however, in the presence of EGCG, ECAR significantly decreased ($P<0.0001$). **(F)** DCA exhibited no effect on ECAR in QH cells, however, in the presence of EGCG, ECAR significantly decreased ($P=0.002$). **(G)** DCA in combination with NAC or EGCG had no effect on ECAR in GO cells ($P>0.05$). **(H)** NAC significantly exacerbated DCA-induced increases in ECAR in OE33 cells ($P=0.041$). Paired *t*-tests assessed differences between treatment groups ($n=3$). Bars denote mean \pm SEM.

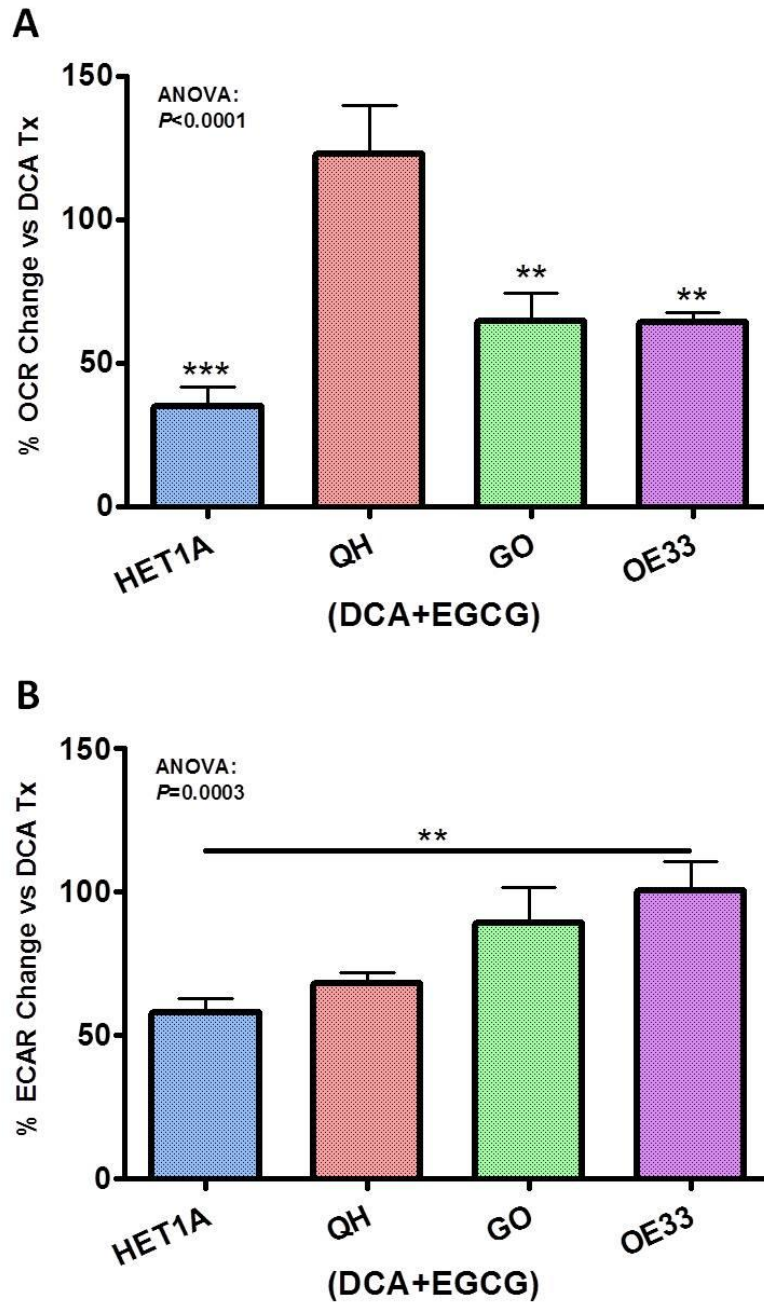


Figure 28. Assessing the effect of the antioxidant epigallocatechin gallate (EGCG) on deoxycholic acid (DCA)-induced alterations in OCR (A) and ECAR (B) across the *in-vitro* squamous-metaplasia-dysplasia-adenocarcinoma sequence. (A) EGCG treatment significantly affected OCR in DCA treated HET1A, GO and OE33 cells, without affecting OCR in QH cells ($P < 0.0001$). (B) EGCG treatment significantly affected ECAR in DCA treated cells across the *in-vitro* sequence ($P = 0.0003$). One way ANOVA assessed for differences across all cell lines ($n = 3$). A Bonferroni multiple comparison test assessed for differences between cell lines. Bars denote mean \pm SEM.

4.4.2 Exploring the effect of omeprazole and lansoprazole on energy metabolism *in-vitro*.

Next, we explored if two proton-pump inhibitors, omeprazole and lansoprazole, commonly prescribed clinically for GORD and Barrett's oesophagus to attenuate gastric acid production, could mediate energy metabolism profiles. Figure 29 shows the effect of omeprazole and lansoprazole treatment on OCR and ECAR across the *in-vitro* squamous-metaplasia-dysplasia-OAC sequence. Lansoprazole treated HET1A cells exhibited significantly reduced levels of OCR (figure 29A) ($P=0.016$) while levels of ECAR remained unchanged (figure 29E). However, omeprazole ($P>0.05$) had no effect on ECAR in HET1A cells (figure 29E). Lansoprazole treated QH cells exhibited significantly higher levels of OCR (figure 29B) ($P=0.019$), however, QH cells exhibited significantly reduced levels of ECAR (figure 29F) ($P=0.007$). Omeprazole ($P=0.0001$) and lansoprazole ($P<0.0001$) treated GO cells demonstrated significantly lower levels of OCR (figure 29C). Conversely, lansoprazole treated GO cells exhibited significantly higher levels of ECAR (figure 29G) ($P=0.015$). Omeprazole ($P>0.05$) and lansoprazole ($P>0.05$) had no effect on OCR in OE33 cells (figure 29D), however, omeprazole ($P=0.018$) and lansoprazole ($P=0.0002$) treated OE33 cells exhibited significantly higher levels of ECAR (figure 29H).

4.4.3 Investigating the effect of Quininib on inflammatory, angiogenic and metabolic profiles *in-vitro* and *ex-vivo*.

Furthermore, we investigated if energy metabolism profiles could be modulated by a novel molecular inhibitor, Quininib (our novel patented, small molecule inhibitor), known to previously exhibit anti-inflammatory potency in our laboratory. Figure 30 illustrates the effect of Quininib on OCR and ECAR across the *in-vitro* squamous-metaplasia-dysplasia-OAC sequence. Even though Quininib significantly increased OCR in HET1A cells (figure 30A) ($P=0.022$), Quininib exhibited significant anti-oxidative phosphorylation potential in QH cells (figure 30B) ($P=0.006$), GO cells (figure 30C) ($P=0.031$) and OE33 cells (figure 30D) ($P<0.0001$). Moreover, Quininib did not affect ECAR in HET1A (figure 30E) ($P>0.05$) or GO (figure 30G) ($P>0.05$) cell lines, however, Quininib exhibited anti-glycolytic potential and was demonstrated to significantly reduce ECAR in both QH (figure 30F) ($P=0.006$) and OE33 (figure 30H) ($P=0.039$) cell lines. In addition, CC8, an analogue of parental Quininib, was assessed in QH and OE33 cells and exhibited significant anti-oxidative phosphorylation potential in OE33 cells (see appendix O). Another Quininib analogue, OS-1, did not alter metabolism in QH or OE33 cells (see appendix O).

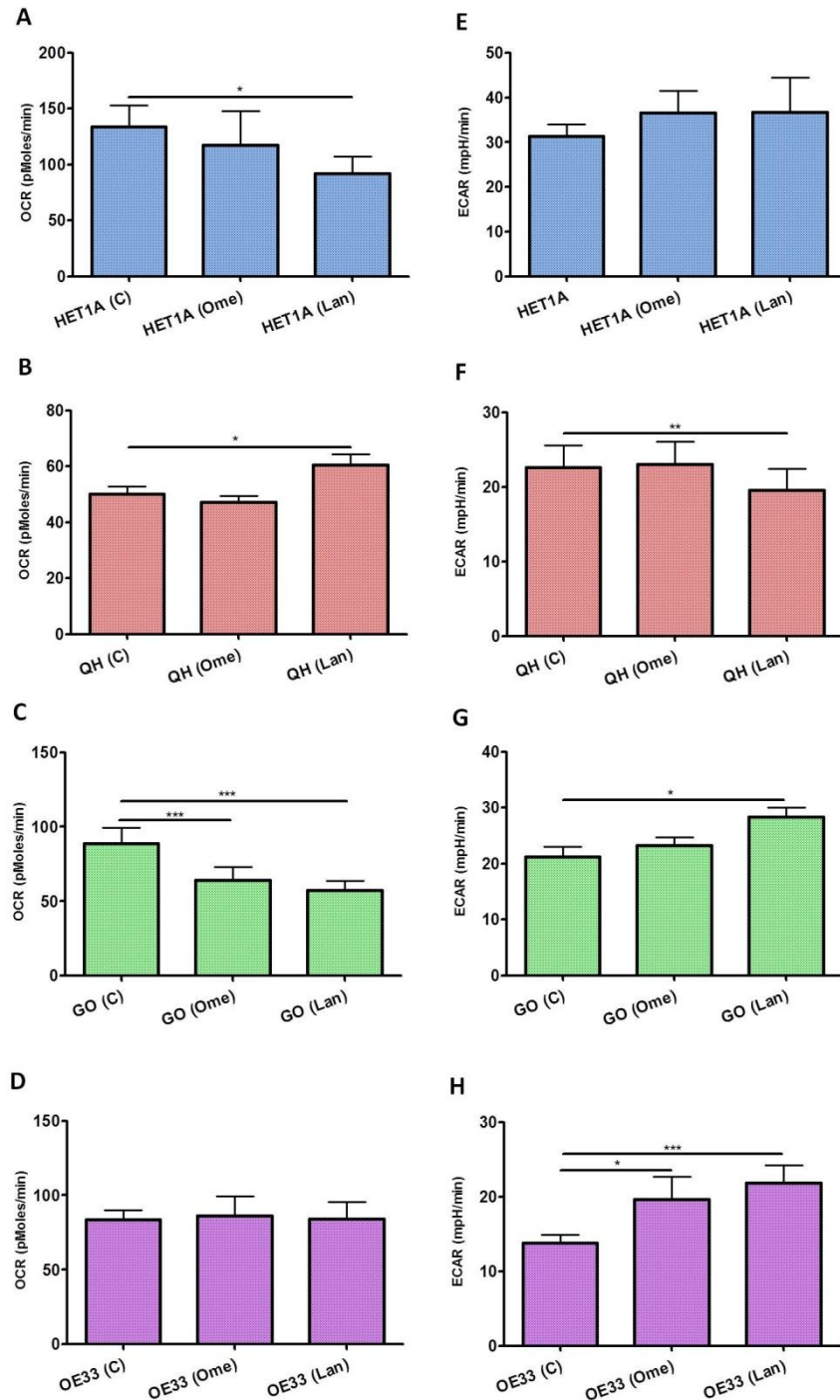


Figure 29. Exploring the effect of the proton pump inhibitors omeprazole and lansoprazole on oxidative phosphorylation (A-D) and glycolysis (E-H) across the *in-vitro* squamous-metaplasia-dysplasia-adenocarcinoma sequence. (A) Lansoprazole treated HET1A cells exhibited significantly reduced levels of OCR ($P=0.016$). **(B)** Lansoprazole treated QH cells exhibited significantly higher levels of OCR compared to untreated QH cells ($P=0.019$). **(C)** Omeprazole ($P=0.0001$) and lansoprazole ($P<0.0001$) treated GO cells exhibited significantly lower levels of OCR. **(D)** Omeprazole ($P>0.05$) and lansoprazole ($P>0.05$) had no effect on OCR in OE33 cells. **(E)** Omeprazole ($P>0.05$) and lansoprazole ($P>0.05$) had no effect on ECAR in HET1A cells. **(F)** Lansoprazole treated QH cells exhibited significantly reduced levels of ECAR ($P=0.007$). **(G)** Lansoprazole treated GO cells exhibited significantly higher levels of ECAR ($P=0.015$). **(H)** Omeprazole ($P=0.018$) and lansoprazole ($P=0.0002$) treated OE33 cells exhibited significantly higher levels of ECAR. Paired *t*-tests assessed differences between treatment groups ($n=3$). Bars denote mean \pm SEM.

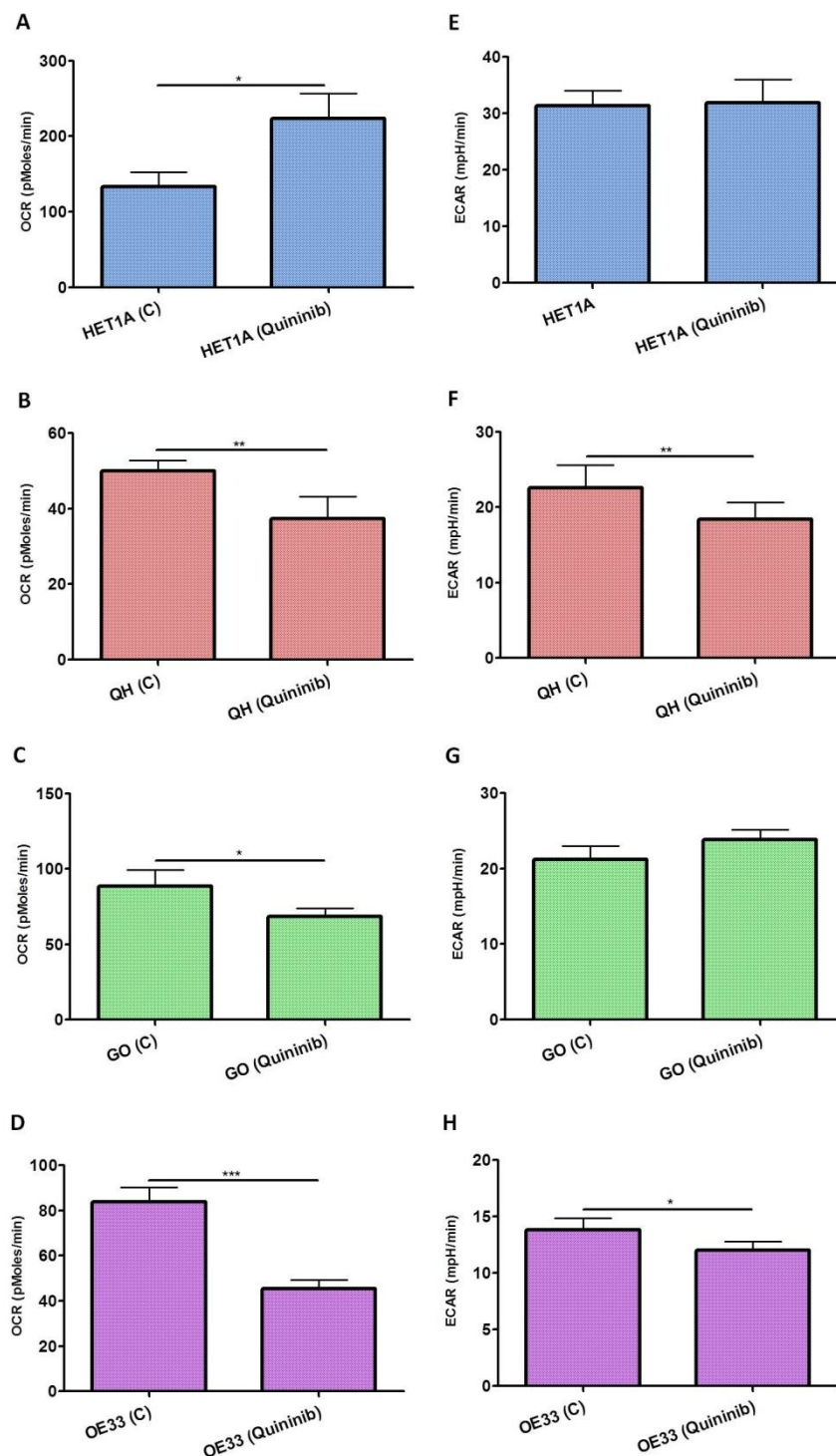


Figure 30. Investigating the effect of the novel small molecular inhibitor, Quininib, on oxidative phosphorylation (A-D) and glycolysis (E-H) across the *in-vitro* squamous-metaplasia-dysplasia-adenocarcinoma sequence. (A) Quininib treated HET1A cells demonstrated significantly higher levels of OCR ($P=0.022$). **(B)** Quininib treated QH cells exhibited significantly lower levels of OCR ($P=0.006$). **(C)** Quininib treated GO cells demonstrated significantly lower levels of OCR ($P=0.031$). **(D)** Quininib treated OE33 cells demonstrated significantly lower levels of OCR ($P<0.0001$). **(E)** Quininib treatment did not affect ECAR levels in HET1A cells ($P>0.05$). **(F)** Quininib treated QH cells demonstrated significantly lower levels of ECAR ($P=0.006$). **(G)** Quininib treatment did not affect ECAR levels in GO cells ($P>0.05$). **(H)** Quininib treated OE33 cells demonstrated significantly lower levels of ECAR ($P=0.039$). Paired *t*-tests assessed differences between treatment groups ($n=3$). Bars denote mean \pm SEM.

As Quininib exhibited significant anti-metabolic potential in an *in-vitro* model of Barrett's oesophagus, we investigated if we could recapitulate these results in an *ex-vivo* explant model of Barrett's oesophagus. As figure 31 illustrates, all explant tissue was characterised prior to analyses; all Barrett's explant tissue was positive for the presence of the molecular marker villin and all matched adjacent normal squamous tissue was negative for villin. Prior to Quininib treatment, we characterised the inflammatory and angiogenic profile of Barrett's and matched normal adjacent squamous tissue by screening an array of secreted inflammatory and angiogenic markers. Figure 32 shows the secretory profile of some of these inflammatory and angiogenic mediators from nine patients with Barrett's oesophagus. Secreted levels of IL-6 (figure 32A) ($P=0.008$), IL1 β (figure 32B) ($P=0.04$) and bFGF (figure 32E) ($P=0.016$) were significantly elevated in Barrett's explant tissue compared to matched normal adjacent squamous tissue. Interestingly, levels of VEGF ($P=0.004$) were significantly lower in Barrett's tissue compared to matched normal adjacent squamous tissue (figure 32D). Despite being elevated, no significant differences in the secreted levels of MMP9 (figure 32C), ICAM-1 (figure 32F), PAI-1 (figure 32G) or VCAM-1 (figure 32H) were found between Barrett's and matched normal squamous tissue ($P>0.05$). Moreover, no significant differences in the secreted levels of TNF α (figure 33A), MMP2 (figure 33B), MIP3 α (figure 33C), MCP-1 (figure 33D), IL-10 (figure 33E), IL-2 (figure 33F), GRO α (figure 33G) or ANG-1 (figure 33H) were found between Barrett's and matched normal squamous tissue ($P>0.05$).

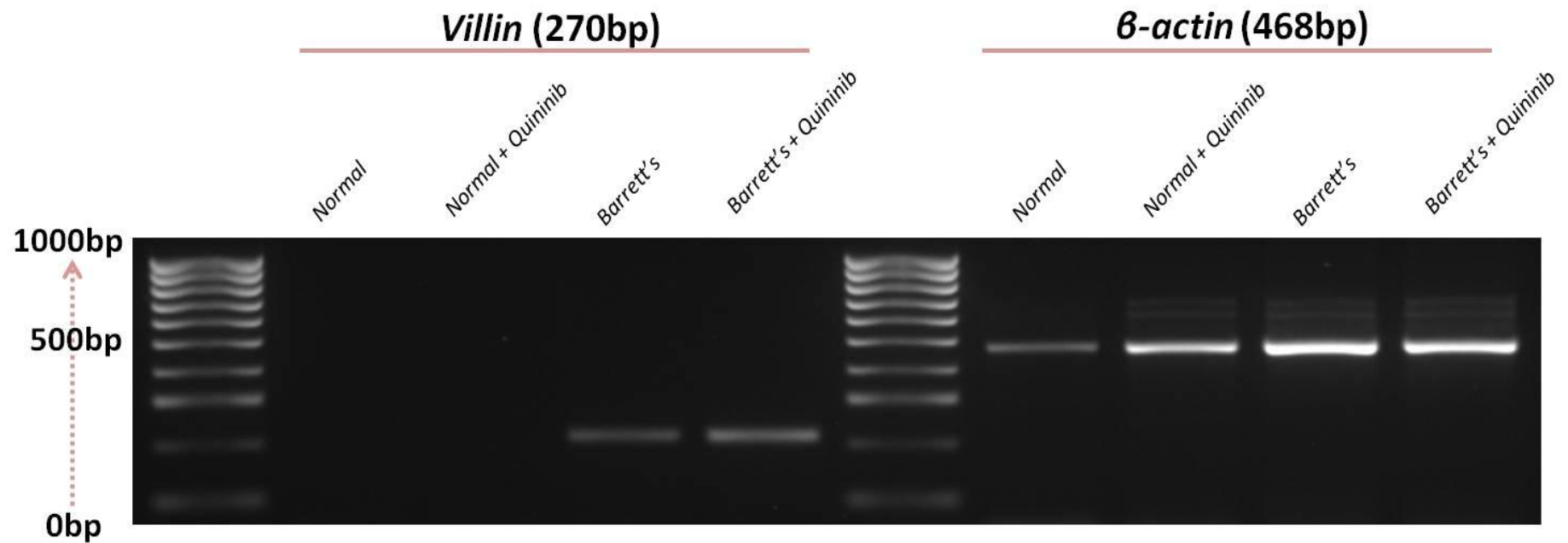


Figure 31. Characterisation of untreated and Quininib treated matched normal adjacent and Barrett's tissue. A representative image from a RT-PCR gel showing the absence of the intestinal metaplasia molecular marker, villin (270bp), in matched normal adjacent tissue and the presence of the same marker in Barrett's tissue. Both tissue types were simultaneously confirmed for the presence of β -actin (468bp). Upon synthesis of cDNA from mRNA, villin and β -actin were amplified in a PCR reaction utilising 2 μ L of cDNA with the melting temperatures (T_m°) of 62 $^\circ$ and 58 $^\circ$ respectively for 38 cycles. Primer sequences were as follows: **Villin forward** - 5'-AATGGCCACCATGGAGAACA-3'; **Villin reverse** - 5'-ACCACAATTCTGTCTTTACGG-3'; **β -actin forward** - 5'-TGAGAGGGAAATCGTGCGTG-3'; **β -actin reverse** - 5'-TGCTTGCTGATCCACATCTGC-3'. Each PCR reaction contained 10 μ L of 1x Mangomix (Bioline), 2 μ L 10 μ M forward primer, 2 μ L 10 μ M reverse primer, 5 μ L RNase/DNase free dH₂O and 2 μ L cDNA. PCR was performed for 95 $^\circ$ C for 5 minutes, followed by 38 cycles of 95 $^\circ$ C for 1 minute, 62 $^\circ$ C for 1 minute (58 $^\circ$ C for β -actin) and 72 $^\circ$ C for 1 minute. Lastly, PCR was heated to 72 $^\circ$ C for 10 minutes and PCR products ran on a 2% agarose gel containing 10mg/mL ethidium bromide at 80V for 1 hour and the gel imaged through UV exposure. Analogous images were obtained for all 9 *ex-vivo* Barrett's explant tissues used throughout this study.

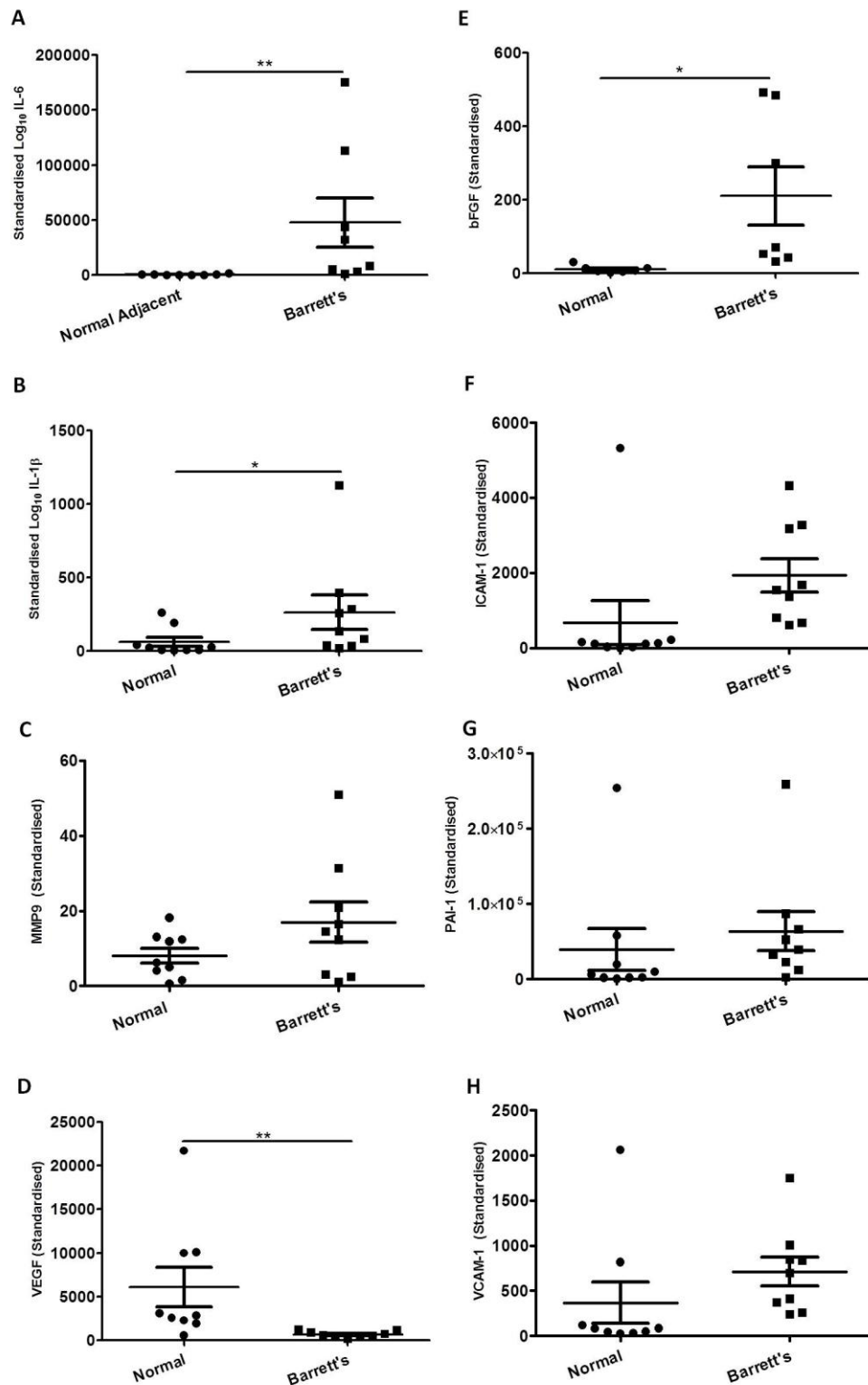


Figure 32. Characterising the expression of an array of secreted inflammatory and angiogenic mediators in an *ex-vivo* model of Barrett's oesophagus. Secreted levels of **(A)** IL-6 ($P=0.008$), **(B)** IL1 β ($P=0.04$) and **(E)** bFGF ($P=0.016$) were significantly elevated in Barrett's explant tissue compared to matched normal adjacent squamous tissue. **(D)** Levels of VEGF ($P=0.004$) were significantly lower in Barrett's tissue compared to matched normal adjacent squamous tissue. Despite being elevated, no significant differences in the secreted levels of **(C)** MMP9, **(F)** ICAM-1, **(G)** PAI-1 or **(H)** VCAM-1 were found between Barrett's and matched normal squamous tissue ($P>0.05$). Wilcoxon signed rank tests assessed differences between Barrett's and matched normal squamous tissue ($n=9$). Bars denote mean \pm SEM.

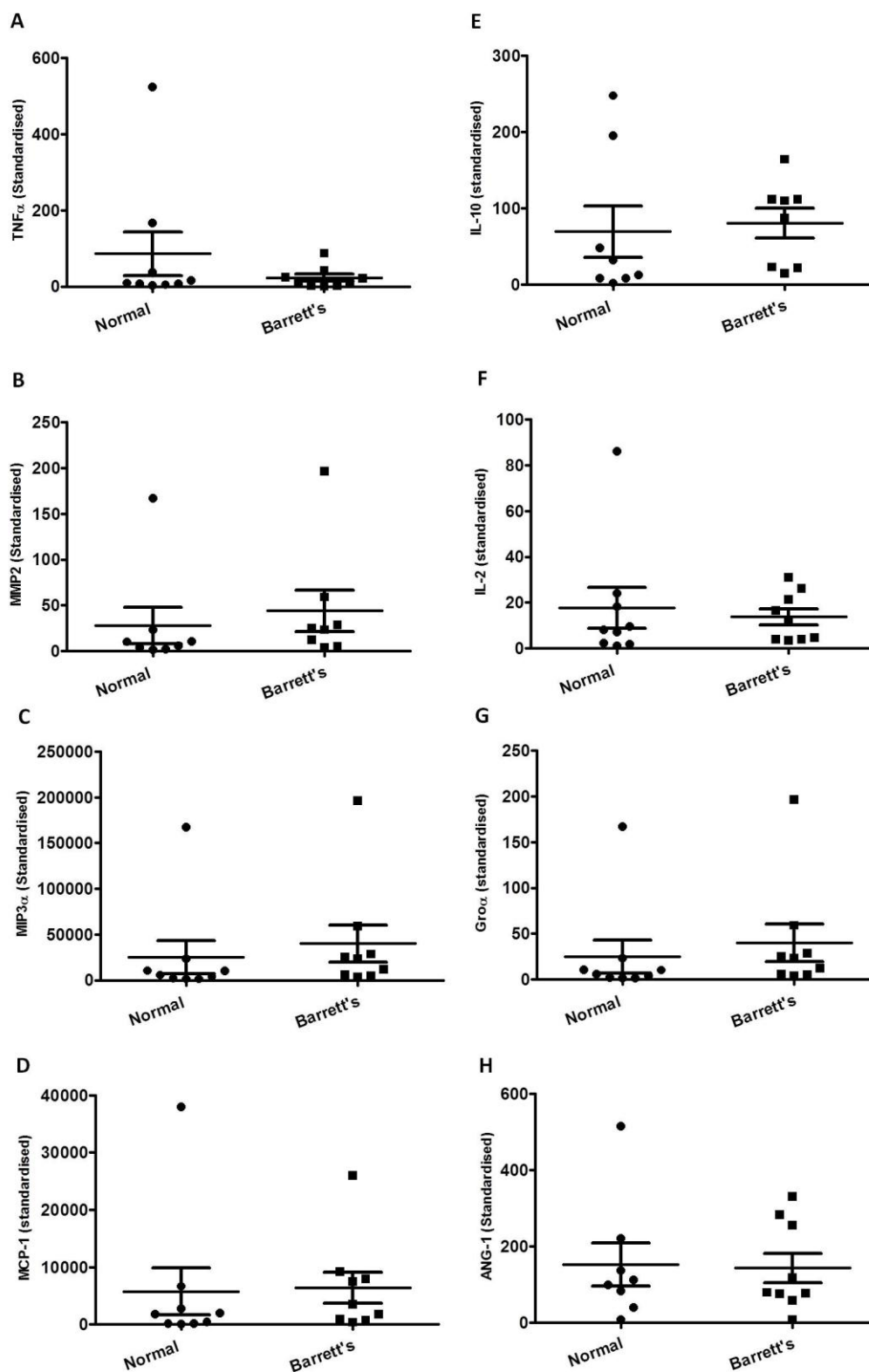


Figure 33. Assessing the expression of an array of secreted inflammatory and angiogenic mediators in an *ex-vivo* model of Barrett's oesophagus. No significant differences in the secreted levels of (A) TNF α , (B) MMP2, (C) MIP3 α , (D) MCP-1, (E) IL-10, (F) IL-2, (G) GRO α or (H) ANG-1 were found between matched normal squamous and Barrett's explant tissue ($P > 0.05$). Wilcoxon signed rank tests assessed differences between Barrett's and matched normal squamous tissue ($n=9$). Bars denote mean \pm SEM.

Next we examined if Quininib could modulate the inflammatory, angiogenic and metabolic profiles of the Barrett's explant tissue within the same nine patients. Figure 33 shows the inflammatory and angiogenic profile of the Barrett's tissue subsequent to treatment with or without Quininib. No significant differences in the secreted levels of IL-6 (figure 34A), IL1 β (figure 34B), MMP9 (figure 34C), VEGF (figure 34D), bFGF (figure 34E), ICAM-1 (figure 34F), PAI-1 (figure 34G) or VCAM-1 (figure 34H) were found between matched untreated and Quininib treated Barrett's explant tissue ($P>0.05$). Furthermore, even though no significant differences in the secreted levels of TNF α (figure 35A), MMP2 (figure 35B), MIP3 α (figure 35C), MCP-1 (figure 35D), IL-10 (figure 35E), GRO α (figure 35G) or ANG-1 (figure 35H) were found between matched untreated and Quininib treated Barrett's explant tissue ($P>0.05$), Quininib did significantly increase the levels of IL-2 (figure 35F) ($P<0.05$). Figure 36 shows the metabolic gene expression profile of the Barrett's tissue subsequent to treatment with or without Quininib. No significant differences in the expression levels of *ATP5B* (figure 36A), *HSP60* (figure 36B), *GAPDH* (figure 36C) or *PKM2* (figure 36D) were found between untreated and Quininib treated Barrett's explant tissue ($P>0.05$). Moreover, no significant differences in the secreted levels of lactate (figure 37A) or SMAC/Diablo (figure 37B) were found between matched untreated and Quininib treated normal squamous and Barrett's explant tissue ($P>0.05$). Although Quininib had no significant effect in reducing angiogenic, inflammatory and angiogenic profiles in all nine explant tissues, table 5 suggests that the effect of Quininib may be patient specific. For example, Quininib exhibited anti-angiogenic, anti-inflammatory and anti-metabolic potential by reducing the levels of the markers ANG-1, IL1 β /MCP-1 and *ATP5B* in 44.4%, 33.3% and 55.5% of the Barrett's explant tissues respectively. Quininib also reduced SMAC/Diablo in 66.7% of Barrett's explant tissues.

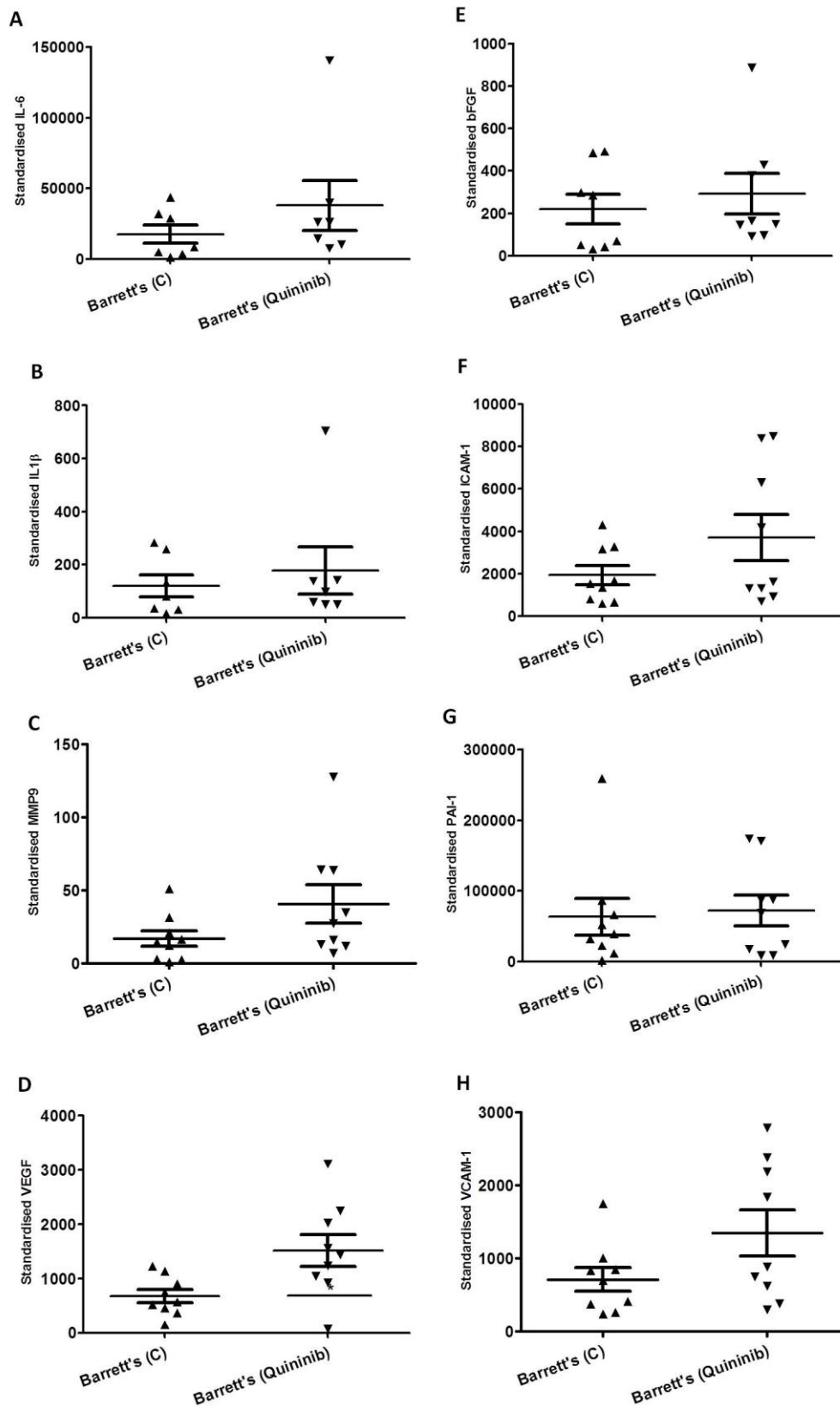


Figure 34. Investigating the inflammatory and angiogenic profile of an *ex-vivo* model of Barrett's oesophagus subsequent to treatment with the small molecule inhibitor Quininib. No significant differences in the secreted levels of **(A)** IL-6, **(B)** IL1 β , **(C)** MMP9, **(D)** VEGF, **(E)** bFGF **(F)** ICAM-1, **(G)** PAI-1 or **(H)** VCAM-1 were found between matched untreated (C=M199 media) and Quininib treated Barrett's explant tissue ($P>0.05$). Wilcoxon signed rank tests assessed differences between both treated groups ($n=9$). Bars denote mean \pm SEM.

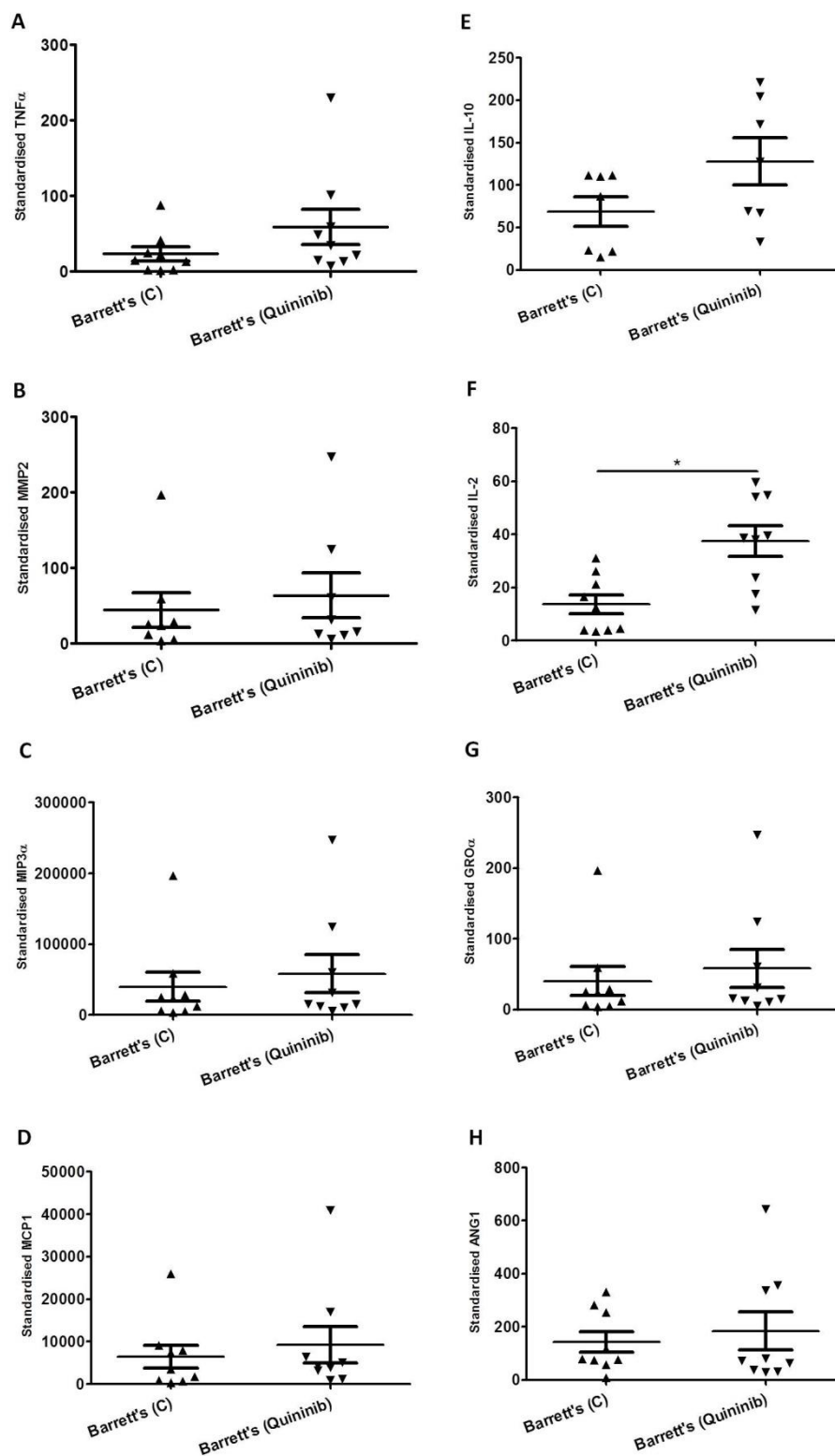


Figure 35. Characterising the expression of an array of secreted inflammatory and angiogenic mediators in an *ex-vivo* model of Barrett's oesophagus subsequent to treatment with the small molecule inhibitor Quininib. No significant differences in the secreted levels of **(A)** TNF α , **(B)** MMP2, **(C)** MIP3 α , **(D)** MCP-1, **(E)** IL-10, **(G)** GRO α or **(H)** ANG-1 were found between matched untreated (C=M199 media) and Quininib treated Barrett's explant tissue ($P>0.05$). **(F)** Quininib induced a significant increase in IL-2 in Quininib treated versus untreated Barrett's tissue ($P=0.012$). Wilcoxon signed rank tests assessed differences between Barrett's and matched normal squamous tissue ($n=9$). Bars denote mean \pm SEM.

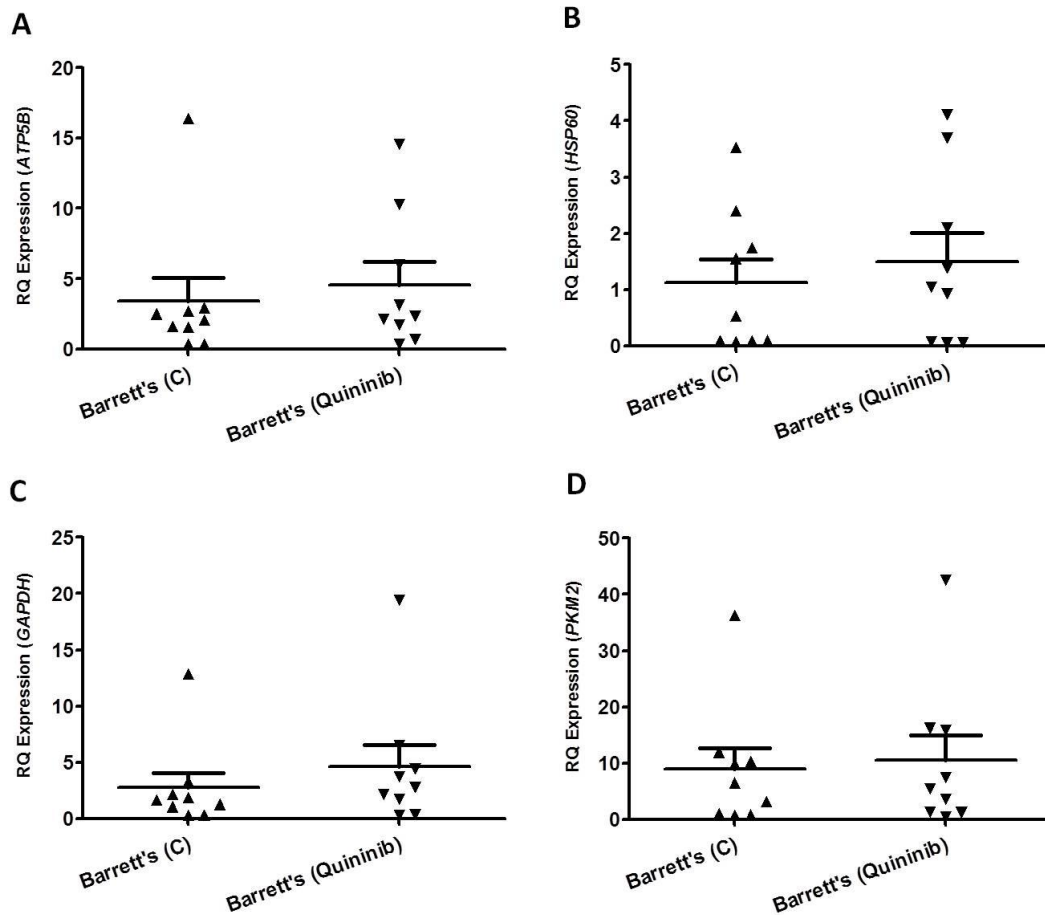


Figure 36. Investigating the metabolic gene profile of an *ex-vivo* model of Barrett's oesophagus subsequent to treatment with the small molecule inhibitor Quininib. No significant differences in the expression levels of **(A) *ATP5B***, **(B) *HSP60***, **(C) *GAPDH*** or **(D) *PKM2*** were found between matched untreated (C=M199 media) and Quininib treated Barrett's explant tissue ($P>0.05$). Wilcoxon signed rank tests assessed differences between both treatment groups ($n=9$). Bars denote mean \pm SEM.

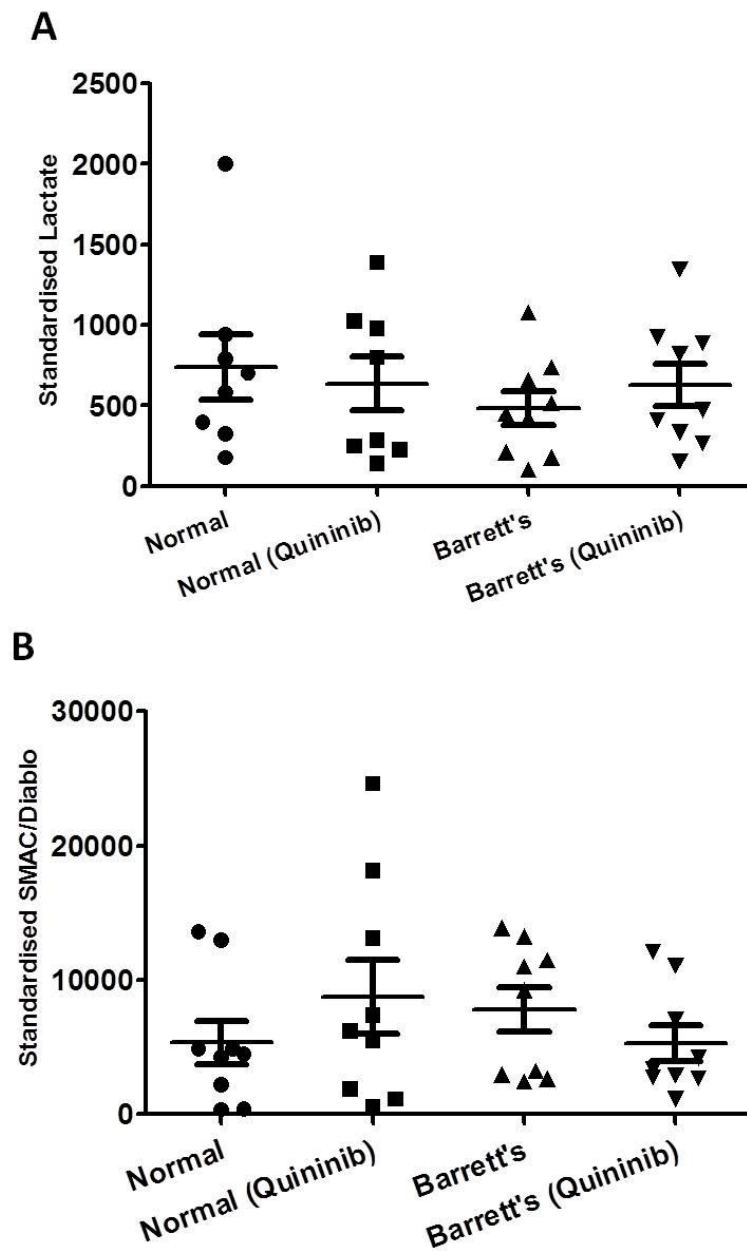


Figure 37. Assessing secreted lactate and SMAC/Diablo levels in an *ex-vivo* model of Barrett's oesophagus subsequent to treatment with the small molecule inhibitor Quininib. No significant differences in the secreted levels of **(A)** lactate or **(B)** SMAC/Diablo were found between matched untreated and Quininib treated normal squamous and Barrett's explant tissue ($P>0.05$). Wilcoxon signed rank tests assessed differences between both treated groups ($n=9$). Bars denote mean \pm SEM.

Table 5. A summary of the inhibitory effect of Quininib on markers of angiogenesis, inflammation and metabolism *ex-vivo*. Quininib had differential effects within different Barrett's patients. Quininib induced the greatest angiogenic, inflammatory and metabolic inhibitory effects on ANG-1, IL1 β /MCP-1 and *ATP5B* of 44.4%, 33.3% and 55.5% of the total *ex-vivo* cohort. Quininib reduced SMAC/Diablo in 66.7% of all Barrett's explant tissues.

Process	Angiogenic, Inflammatory and Metabolism Markers	Percentage of total cohort (n=9) that Quininib induced an inhibitory effect in (%)
Angiogenesis	ANG-1	44.4
	bFGF	33.3
	PAI-1	33.3
	ICAM-1	33.3
	VCAM-1	33.3
	VEGF	22.2
	Inflammation	GRO α
IL1 β		33.3
IL-10		11.1
IL-2		11.1
IL-6		22.2
MCP-1		33.3
MIP3 α		11.1
MMP2		22.1
MMP9		22.2
TNF α		11.1
Metabolism		<i>ATP5B</i>
	<i>HSP60</i>	33.3
	<i>GAPDH</i>	22.2
	<i>PKM2</i>	33.3
	Lactate	22.2
Mitochondrial Function	SMAC/Diablo	66.7

4.5 DISCUSSION

In this chapter, we have shown that DCA, a common GORD constituent, and two proton-pump inhibitors commonly prescribed for GORD, induce differential alterations in mitochondrial energy metabolism across the *in-vitro* squamous-metaplasia-dysplasia-OAC sequence. We further demonstrate that the antioxidants, NAC and EGCG, can rescue these DCA-induced metabolic perturbations. In addition, a novel small molecule inhibitor, Quininib, previously shown to illicit anti-inflammatory, anti-angiogenic and anti-metabolic effects in neoplastic tissue, exhibited anti-metabolic potential *in-vitro* possibly highlighting its potential role as an effective therapeutic agent.

Several exogenous risk factors have been documented as playing an important role in Barrett's associated OAC. Smoking status is known to be positively associated with erosive oesophagitis, Barrett's oesophagus and oesophageal-oesophagogastric junction adenocarcinomas (98, 412, 429). Age and diabetes mellitus status can also predict progression from Barrett's oesophagus (430). Some recent evidence additionally suggests a role of the oesophageal microbiome in the development of Barrett's oesophagus and OAC, although further in-depth studies are required to prove causality (431-433). Interestingly, many studies conclude a negligible link between alcohol and neoplastic progression in Barrett's oesophagus (434-436). Moreover, GORD, known to play an important pathogenic role in the development of Barrett's oesophagus, is one of the biggest risks of neoplastic progression in Barrett's associated OAC (412-414). However, the consequences of GORD on cellular bioenergetics, known to be altered early in Barrett's oesophagus and contribute to Barrett's associated OAC, remain unidentified (130, 391).

DCA is extensively thought to play a major role in the development of Barrett's oesophagus and in its subsequent progression to OAC (70, 71, 73, 74). We investigated if DCA could modulate energy metabolism across the normal squamous-metaplasia-dysplasia-OAC sequence *in-vitro*. We demonstrate that DCA alters cellular metabolism *in-vitro*, thereby potentially conferring Barrett's cells with a metabolic advantage for neoplastic progression. Interestingly, GO and OE33 cells treated with DCA exhibit significantly higher levels of OCR, however, these increases in OCR in neoplastic GO and OE33 cells could be reversed by treatment with the antioxidant EGCG. We also show that QH cells treated with DCA exhibited significantly lower OCR than its untreated control. This result is similar to a previous study showing that deoxycholate treated gastric mucosa cells exhibited reduced oxygen uptake and ATP levels subsequently implicating the impairment of energy metabolism in the mechanism of bile salt injury to gastric mucosa (437). Moreover, further treatment with the common dietary antioxidant, NAC, rescued the DCA-induced decrease in OCR

in QH cells. DCA significantly increased ECAR in OE33 cells but this increase could not be rescued by addition of NAC or by addition of the green tea antioxidant, EGCG. Interestingly, the antioxidant EGCG significantly lowered OCR in DCA-EGCG treated HET1A cells, ECAR in DCA-EGCG treated HET1A cells and ECAR in DCA-EGCG treated QH cells despite DCA having no effect on cellular metabolism providing some evidence that dietary EGCG supplementation alone may be beneficial.

We have demonstrated that DCA has both pro-glycolytic and anti-oxidative phosphorylation activity in the OE33 and QH cell lines respectively. Since the Warburg effect can potentially confer cells with several metabolic advantages for disease progression, perhaps the decrease in oxidative phosphorylation exhibited in the DCA-treated QH cells allows the shunting of high energy metabolic intermediates into glycolysis. Moreover, it may be noteworthy to mention that DCA's effect on metabolism may be tissue specific; for example, DCA decreased OCR in the preneoplastic QH cells but increased OCR in both neoplastic GO and OE33 cells. These results illustrating DCA's pro-glycolytic and pro-oxidative potential in the OAC cell line, therefore, indicate that DCA can indeed exacerbate disease progression in Barrett's associated tumourigenesis, as previously shown, but may do so in part by altering energy metabolism (413).

In this study, we show that DCA-treated QH and OE33 cells supplemented with NAC exhibited significantly higher OCR and ECAR levels respectively. This implies that NAC may in fact promote glycolysis. Despite the majority of studies reporting the protective role of NAC, one particular recent study found that NAC accelerated lung cancer in a mouse model (438). In this study, NAC treated cells seem to exacerbate disease progression by increasing the availability of energy through oxidative phosphorylation and glycolysis. Alternatively, NAC may attenuate disease progression by increasing oxidative phosphorylation using high energy intermediates for oxidative purposes initially destined for glycolytic-dependant tumour cells. These results are in contrast with DCA-EGCG treated QH and neoplastic cells (GO and OE33) that exhibited significantly lower ECAR and OCR levels respectively. No role for EGCG as an anti-glycolytic has been documented. EGCG is known to activate AMP-protein kinase (AMPK), known to decrease glycolysis. Activation of AMPK increases ATP levels by increasing fatty acid oxidation, lipolysis and glycolysis (439). EGCG, however, is increasingly being highlighted as an effective universal anti-cancer agent (440). It is clear that additional studies investigating the role of NAC and EGCG will offer more insight into their potential benefits, particularly in Barrett's metaplasia and OAC. However, the additional role of the antioxidant EGCG in the neoplastic setting, as displayed in GO and OE33 cells in this

study, holds promise as an antagonist of oxidative phosphorylation, known to be enhanced in Barrett's associated OAC (130).

The primary treatment for Barrett's metaplasia is the normalisation of oesophageal reflux acid exposure with proton pump inhibitors, which reduces the risk of development and progression in patients with Barrett's oesophagus (441-443). Proton-pump inhibitors can confer many additional benefits beyond acid suppression, however (442). We have shown that lansoprazole significantly reduces ECAR and OCR in QH and GO cell lines respectively. Furthermore, we demonstrate that omeprazole treated GO cells exhibit reduced OCR levels. These results suggest that proton-pump inhibitors may help to suppress cellular metabolism prior to cancer occurrence in the metaplastic and dysplastic settings and thus offer added benefit in addition to their role in acid suppression. Omeprazole and lansoprazole are known to exhibit antioxidant properties (444, 445). Both proton-pump inhibitors have also been shown to attenuate neutrophil adherence to endothelial cells by inhibiting the expression of the adhesion molecules ICAM-1 and VCAM-1 suggestive of anti-inflammatory activity (446). Lansoprazole has additionally been implicated in mediating the anti-inflammatory and anti-apoptotic effect in gastric mucosal cells (447, 448). Studies also highlight similar benefits of proton-pump inhibitors in the neoplastic setting (449, 450). No studies to our knowledge implicate omeprazole and lansoprazole in the modulation of glycolysis, however, as inhibitors of gastric H⁺K⁺ATPases, the inhibition of intracellular proton extrusion associated with higher rates of glycolysis in neoplastic tissue by lansoprazole has been shown to induce apoptosis and inhibit tumourigenesis in murine xenografts (451). Therefore, manipulation of mitochondrial membrane potential, and thus apoptosis, through proton-pump inhibitor treatment may be an additional benefit early in Barrett's metaplasia and dysplasia (452). Furthermore, chemoprevention with the use of proton-pump inhibitors in patients with Barrett's oesophagus may be cost-effective (453).

We have further demonstrated that proton-pump inhibitors augment cellular metabolism. Lansoprazole increased ECAR in GO and OE33 cells respectively while concomitantly increasing OCR in QH cells. Moreover, omeprazole promoted glycolysis in OE33 cells. It is plausible that alterations in glycolysis are due to perturbations in oxidative phosphorylation. For example, increased ECAR in GO cells may be the result of lansoprazole negatively affecting oxidative phosphorylation as basal glycolysis has been shown to be dependent on basal levels of oxidative phosphorylation (see appendix L). It is also possible that an increase in OCR is a stress induced consequence of H⁺K⁺ATPase inhibition. Moreover, with differential effects across cell types in this study, the effect of proton-pump inhibitors on metabolism may be a tissue specific effect as

proton-pump inhibitors have been shown to have differential results in erosive oesophagitis and non-erosive reflux disease (454). Despite promoting cellular metabolism and potentially conferring metabolic advantages to preneoplastic and neoplastic cells, future studies should investigate whether the additional benefits of proton pump inhibitors, taking into account potential tissue specific effects, outweigh undesirable increases in metabolism.

Ongoing translational research and clinical trials are currently attempting to identify multifunctional compounds with the capability of targeting many key cellular processes simultaneously. Such processes include inflammation, angiogenesis and more recently, energy metabolism. Therefore, we investigated if our novel patented small molecule inhibitor, Quininib, could modulate inflammatory, angiogenic and metabolic profiles across the *in-vitro* normal squamous-metaplasia-dysplasia-adenocarcinoma sequence. Quininib, which has patents filed and published nationally, in Europe and in the USA, has previously been shown to exhibit anti-inflammatory and anti-angiogenic activity in zebrafish, in *ex-vivo* human explants and in mice (455). Quininib significantly decreased levels of IL-6, IL1 β and various angiogenic markers in *ex-vivo* human colorectal cancer tissue (455). Moreover, Quininib decreased tumour growth, metastasis and angiogenic factors in murine studies (455). We found that Quininib significantly reduced OCR in the QH, GO, and OE33 cell lines. We additionally demonstrate that Quininib significantly reduces ECAR in both QH and OE33 cells. As Quininib has previously been shown to display anti-inflammatory and anti-angiogenic capabilities and has exhibited potent anti-oxidative and anti-glycolytic potential across the metaplastic-dysplastic-adenocarcinogenic sequence *in-vitro* in this study, we examined if we could recapitulate these anti-inflammatory, anti-angiogenic and anti-metabolic effects in an *ex-vivo* Barrett's explant model.

Prior to investigating the effect of Quininib, we characterised the inflammatory and angiogenic secretory profiles of Barrett's explant tissue compared to matched normal squamous tissue. Analogous to other studies, we found that Barrett's tissue demonstrates higher levels of various inflammatory and angiogenic markers, including IL-6, IL1 β and bFGF (219, 288, 456-458). Interestingly, a previous study utilising the only murine model of Barrett's oesophagus showed the importance of IL1 β and IL-6 in Barrett's associated cancer (69). Overexpression of IL1 β was shown to be sufficient to induce Barrett's oesophagus and neoplastic progression with the development of Barrett's and OAC reversed with IL-6 deficiency (69). Conversely, we have shown significantly reduced levels of VEGF in Barrett's tissue compared to matched normal adjacent tissue despite previous studies implicating VEGF in Barrett's oesophagus and neoplastic Barrett's

tissue (458-460). Moreover, various angiogenic markers in this study were increased in Barrett's tissue so this may explain in part the redundancy in increasing VEGF expression.

Next, we examined if Quininib could reduce the enhanced levels of inflammation and angiogenesis exhibited in the Barrett's explant tissue. We found that Quininib treatment did not alter the levels of secreted inflammatory and angiogenic markers. Moreover, Quininib had no significant effect on lactate levels or on genomic expression of *ATP5B*, *HSP60*, *GAPDH* or *PKM2*. These results indicate that Quininib may be unsuitable for use in Barrett's tissue to reduce inflammation and metabolism unlike previous results in *ex-vivo* colorectal cancer tissue. However, analogues of Quininib, known to display less toxic effects, may demonstrate more promise in Barrett's explant tissue (appendix O). This was the first study using Quininib in a preneoplastic setting; Quininib has since exhibited potential as an anti-inflammatory, anti-angiogenic and anti-metabolic agent in *ex-vivo* OAC explant tissue (currently been undertaken by Róisín Byrne), however, examining whether Quininib can recapitulate these effects in preneoplastic Barrett's *ex-vivo* tissue requires further investigation. Moreover, Quininib induced differential anti-inflammatory, anti-angiogenic and anti-metabolic effects in specific Barrett's explant tissues thereby highlighting its future potential. Therefore, employing similar Quininib analogues *ex-vivo* may have more promising outcomes. We acknowledge limitations in this work, however. In the presence of DCA, the proton pump inhibitors lansoprazole and omeprazole may have induced differential metabolic effects to what we have shown. Moreover, the additive effect of additional bile acids in conjunction with DCA may differentially modulate energy metabolism profiles.

In summary, we have shown for the first time that DCA, omeprazole and lansoprazole induce differential alterations in mitochondrial energy metabolism across the *in-vitro* normal squamous-metaplasia-OAC sequence. We have additionally shown that the antioxidants NAC and EGCG rescue DCA-induced metabolic alterations thereby highlighting potential benefit in antioxidant supplementation. Furthermore, we demonstrate that Quininib significantly decreased both oxidative phosphorylation and glycolysis in metaplastic and neoplastic cells *in-vitro* possibly highlighting its potential role as an effective metabolic therapeutic agent.

Chapter 5

Examining the connectivity between different cellular processes in the Barrett's tissue microenvironment: energy metabolism, hypoxia, inflammation, p53 and obesity.

5.1 INTRODUCTION

In chapter two, we showed that mitochondrial function is altered in Barrett's oesophagus. Moreover, manipulation of genes known to be differentially expressed between Barrett's oesophagus and OAC *in-vitro* and *in-vivo* resulted in significant alterations in MMP and ROS levels in Barrett's cells. In OAC cells, manipulation of these genes altered energy metabolism profiles thereby implicating altered cellular energetics in disease progression. In chapter three we demonstrated that both oxidative phosphorylation and glycolysis are in fact differentially altered across the metaplasia-dysplasia-OAC disease sequence *in-vitro* and *in-vivo*. In addition, using first surveillance biopsies from Barrett's patients, we found that Barrett's patients who went on to progress to OAC had significantly higher levels of the oxidative phosphorylation marker ATP5B. Moreover, in chapter four we show that DCA and proton inhibitors may modulate these metabolic pathways to promote disease progression. Numerous studies have implicated various cellular processes, such as inflammation, hypoxia, p53 and obesity, in disease progression in Barrett's oesophagus. No study, however, has investigated the link between metabolism and its links with the above cellular processes in the Barrett's oesophagus tissue microenvironment.

It is established that key cellular processes, with distinctive functional roles, are involved in promoting disease progression in Barrett's oesophagus. Some of these processes include inflammation, hypoxia and angiogenesis (69, 176, 457, 459, 461-463). Hypoxia, mediated through hypoxia-inducible factor-1 alpha (HIF1 α), is associated with the inflammatory reaction in Barrett's oesophagus, however, little is known on how it links with other cellular mediators (176). Increased HIF1 α and HIF2 α expression has been demonstrated across the metaplastic-dysplastic-OAC sequence (461). Barrett's-associated inflammation, through canonical proinflammatory mediators such as interleukin-6 (IL-6), IL1 β and signal transducer and activator of transcription 3 (STAT3), have additionally been shown to exacerbate inflammation and promote OAC (69, 462). A recent study showed that neoplastic and non-neoplastic Barrett's cells expressing VEGF and VEGFR2 mRNA and protein, promoted cell proliferation through a phospholipase C gamma1-protein kinase C-ERK pathway subsequent to VEGF-VEGFR2 activation (459). Moreover, sunitinib-induced VEGF inhibition reduced the weight and volume in mouse xenografts tumours from transformed Barrett's cells (459).

Obesity has further been implicated in disease progression in Barrett's oesophagus (82, 83). Individuals with central or visceral obesity, measured by waist circumferences, are at an increased risk of developing Barrett's oesophagus (83). Furthermore, individuals with a greater propensity to obesity have higher risks of intestinal metaplasia, thereby showing obesity is independently

associated with Barrett's oesophagus and its subsequent progression to OAC (82). Epidemiological studies have also shown a link between leptin and reduced adiponectin, both characteristic of obesity and Barrett's oesophagus (464-467). However, how obesity and associated changes in adipokines, cytokines, insulin, insulin-growth-factor-1 axis, immune mechanisms and their downstream signalling pathways influences Barrett's oesophagus and Barrett's tumourigenesis at the cellular level is currently unknown.

Alterations in energy metabolism is one of the new emerging hallmarks of cancer and disease progression (172, 288). Previous research from our group has demonstrated that both oxidative phosphorylation and glycolysis are reprogrammed early in the inflamed Barrett's disease sequence and may act mutually to promote disease progression in Barrett's oesophagus (130). In addition, levels of ATP5B, a marker of oxidative phosphorylation, in first time surveillance biopsy material segregated Barrett's patients who progressed to HGD/OAC from non-progressors, highlighting the possible prognostic advantage of assessing metabolic profiles in these preneoplastic patients (130). Moreover, Barrett's cells were shown to favour the more detrimental oxidative phenotype that may be selected for during the early stages prior to disease progression (130). Various studies linking energy metabolism with inflammation, hypoxia and angiogenesis highlight how reciprocal processes act jointly to significantly alter the local microenvironment and attenuate disease progression (185, 215, 226, 468). However, despite recent insight into energy metabolism profiles in Barrett's oesophagus, less is known about how energy metabolism and other key cellular processes cooperate in the Barrett's microenvironment. Interestingly, p53 overexpression is associated with an increased risk of neoplastic progression in patients with Barrett's oesophagus, however, the risk is greater with loss of p53 expression (292). Moreover, in inflamed Barrett's oesophagus patients with progressive disease, oxidative-induced damage results in telomere shortening and mutations in the p53 gene abrogate p53's role as the checkpoint of proliferation and apoptosis (202). In addition to obesity and p53 status, the length of the Barrett's segment has been shown to be a risk factor in the development of Barrett's associated OAC (10, 469, 470).

The aim of this study was to examine the link between energy metabolism, hypoxia, inflammation, p53 and obesity in the Barrett's tissue microenvironment *in-vivo* and *ex-vivo*. We report herein that oxidative phosphorylation and p53 status positively correlated with hypoxia. Moreover, levels of oxidative phosphorylation are positively linked to p53 expression whereas levels of glycolysis are negatively associated with p53 expression. In addition, oxidative phosphorylation and glycolysis are positively associated with inflammation. Interestingly, we

demonstrated that obesity was negatively associated with oxidative phosphorylation but positively associated with glycolysis. Analogous correlations were exhibited in *ex-vivo* explant tissue between metabolism, p53, hypoxia, inflammation and angiogenesis.

Aspects of this chapter have been published in *Cancer Letters*.

'Examining the connectivity between different cellular processes in the Barrett tissue microenvironment' (2015). **Phelan J.J.**, Feighery, R., Eldin, O.S., Ó Meachair, S., Cannon, A., Byrne, R., MacCarthy, F., O'Toole, D., Reynolds, J.V and O'Sullivan, J.N.

5.2 HYPOTHESIS AND AIMS OF CHAPTER FIVE

We hypothesise that energy metabolism acts in tandem with key cellular processes in the Barrett's oesophagus microenvironment.

Specific aims of chapter 5;

- 1) Investigate the association between p53 and metabolism in *in-vivo* and *ex-vivo* models of Barrett's oesophagus.
- 2) Examine the link between inflammation (IL1 β /SERPINA3) and p53 in *in-vivo* and *ex-vivo* models of Barrett's oesophagus.
- 3) Assess the association between metabolism and inflammation in *in-vivo* and *ex-vivo* models of Barrett's oesophagus.
- 4) Investigate the links between hypoxia, metabolism, inflammation and p53 in *in-vitro*, *in-vivo* and *ex-vivo* models of Barrett's oesophagus.
- 5) Investigate the association between metabolism, obesity status and the length of the Barrett's segment in Barrett's oesophagus.
- 6) Examine the link between metabolism and angiogenesis in an *ex-vivo* model of Barrett's oesophagus.

5.3 MATERIALS AND METHODS

5.3.1 Patient selection

Ethical approval to conduct all aspects of this work was granted by the Adelaide and Meath Hospital (AMNCH), Tallaght, Dublin (REC 200110405). All cases were prospectively recruited at our national referral centre for upper GI malignancy and written informed consent was obtained in accordance with local institutional ethical guidelines. All patients attending with histologically confirmed Barrett's esophagus were considered for inclusion. Patients with a prior history of dysplasia or carcinoma, other malignancy of any type, ablative therapy (radiofrequency ablation, argon plasma coagulation, cryoablation) were excluded. Endoscopic examination consisting of white light and chromoendoscopy (FICE (fujinon) or NBI (olympus)) was performed in all cases. The Barrett's segment was assessed and measured as per the Prague classification system and biopsied using large capacity forceps.

Patients with intestinal metaplasia were identified from our Barrett's tissue database and immunohistochemistry was performed. The median age of patients ($n=29$) with intestinal metaplasia was 65 years, there was a 2.22-fold male predominance and all patients were followed for a median of 7.5 years. The areas of interest on the diagnostic biopsy blocks were marked by a pathologist, 0.6 mm cores were taken from the blocks and tissue microarrays (TMAs) were constructed and pathology of the tissue re-evaluated prior to antibody staining.

Waist circumference and Barrett's segment length demographics were available on 15 and 22 patients respectively from the 29 patients who participated in the study. Expression of all protein markers was subsequently correlated to waist circumference and to the length of the Barrett's segment. 15 patients were used to assess the link between ATP5B, GAPDH and waist circumference; the median age of patients with intestinal metaplasia was 65 years, there was a 2.75-fold male predominance and patients had a median waist circumference of 104cm. 22 patients were used to assess the link between ATP5B, GAPDH and the length of the Barrett's segment; the median age of patients ($n=22$) with intestinal metaplasia was 61.5 years, there was a 2.14-fold male predominance and patients had a median Barrett's segment length of 5cm.

5.3.2 *ATP5B, GAPDH, p53, IL1 β , SERPINA3 and HIF1 α immunohistochemistry analysis using tissue microarrays*

Immunohistochemistry was performed utilising the Vectastain Kit (Elite) as before (see section 3.3.4). Primary antibodies used were a mouse anti-ATP5B IgG (SantaCruz Biotechnology) (1:1000), a rabbit anti-GAPDH IgG (AbDserotec Division of MorphoSys) (1:300), a rabbit anti-p53 IgG

(Abcam) (1:150), a rabbit anti-IL1 β IgG (Abcam) (1:200), a rabbit anti-SERPINA3 IgG (Abcam) (1:200) and a rabbit anti-HIF1 α IgG (Abcam) (1:200) diluted in PBS. Slides were incubated with primary antibody for 1 hour, then biotinylated antibody for 30 minutes, avidin-biotin complex for 30 minutes and DAB substrate for 2-15 minutes. Slides were scanned (Philips Digital Pathology Solutions) and immunoreactivity was assessed as before (see section 3.3.4). For each protein, both epithelial and stromal cells were evaluated for both percentage positivity and intensity of cytoplasmic staining. A third score, designated IxP, was obtained by multiplying intensity by positivity. Using these three parameters, the scoring and analysis was undertaken as described in section 3.3.4.

5.3.3 *Assessing the effect of hypoxia in an in-vitro model of Barrett's oesophagus*

5.3.3.1 *Cell Culture*

Cell culture was undertaken as described before (sections 2.3.2 and 2.3.3). QH cells were seeded 50,000 in 12 well plates and subsequently cultured under normoxia (21% oxygen) and hypoxia (0.5%) conditions for 24 hours. RNA extraction was subsequently performed using RNeasy Mini Kit (Qiagen) following manufacturer's instructions (see section 2.3.2), RNA content and quality was quantified and assayed respectively (Nanodrop[®], 8-Sample Spectrophotometer, ND-800) and RNA reverse transcribed using Bioscript enzyme (Bioline) as before (see section 2.3.5.1).

5.3.3.2 *Gene Expression Analysis*

qPCR was undertaken as before (see section 2.3.5.2). Gene primer probes for *VEGFA*, *ATP5B*, *p53*, *PKM2*, *IL1 β* , *AMPK*, *GAPDH*, *HSP60* and *18S* (Applied Biosystems) were purchased and real-time PCR was performed using Taqman mastermix on a 7900HT Fast Real-time PCR Light-Cycler System (Applied Biosystems). PCR data were analysed utilising the $2^{-\Delta\Delta Ct}$ method as before (section 2.3.4) (130).

5.3.3.3 *Assessment of secreted inflammatory and angiogenic markers*

QH cell supernatant, previously exposed to normoxia and hypoxia conditions, was screened for a panel of secreted inflammatory and angiogenic markers as previously described in section 4.3.5.2 (Meso Scale Discovery Multi-Array technology). The inflammatory markers assessed were IL-10, IL-12p70, IL-13, IL-2, IL-6, IL-4, IL-8 and TNF α . The angiogenic markers assessed were ANG2, bFGF, ICAM-1, PAI-1 and VEGF (Meso Scale Discovery Multi-Array technology). Secreted lactate levels were additionally assessed (Sigma). All *in-vitro* data were normalised to cell number using the crystal violet assay (see section 2.3.9).

5.3.4 Barrett's ex-vivo explant culture

All fresh *ex-vivo* Barrett's intestinal metaplasia tissue was prospectively recruited at our national referral centre for upper GI malignancy and obtained as above. The median age of patients ($n=9$) with intestinal metaplasia was 62 years and there was an 8-fold male predominance. Barrett's explant tissue was subsequently transferred into 1mL M199 media (10% FBS, 1% Pen/Strep, 1mg/mL insulin) (Gibco) and cultured for 24 hours at 5% CO₂ at 37°C. Following 24 hour incubation, the Barrett's conditioned medium (BCM) was collected and explant tissue snap frozen in liquid nitrogen. Both media and tissue were stored at -80°C for future use.

5.3.5 Ex-vivo qRT-PCR analysis

Ex-vivo qRT-PCR analysis was undertaken as described in section 2.3.5.2. RNA was reverse transcribed (Bioline), gene primer probes for *ATP5B*, *HSP60*, *GAPDH*, *PKM2*, *p53*, *HIF1A* and *18S* (Applied Biosystems) were purchased and real-time PCR performed using Taqman mastermix (Applied Biosystems). Data were analysed utilising the $2^{-\Delta\Delta Ct}$ method as above (see section 2.3.4). All 9 Barrett's explant tissue was characterised by assessing the expression of the columnar epithelium molecular marker villin using RT-PCR; all Barrett's explant tissue was positive for the presence of villin and all matched adjacent normal squamous tissue was negative for villin.

5.3.6 Ex-vivo MSD multiplex ELISA analysis

BCM was screened for the levels of the multiplex inflammatory and angiogenic proteins (Meso Scale Discovery Multi-Array technology) as previously described in section 4.3.5.2. Secreted lactate levels were also assessed in the BCM. Subsequent to screening for these secreted inflammatory and angiogenic proteins, *HIF1 α* and *p53* expression levels were evaluated through RT-qPCR and all factors were subsequently correlated to metabolism (*ATP5B*, *HSP60*, *GAPDH* and *PKM2*) at the gene level. Total protein extracted above (Qiagen) was assayed utilising a bicinchonic acid assay (Thermo Scientific) and secreted protein levels of these secreted factors in all samples were normalised to total protein.

5.3.7 Statistical analysis

Data were analysed using Graph Pad Prism software (Graph Pad Prism, San Diego, CA). Paired *t*-tests were utilised to assess if hypoxia had a metabolic or inflammatory effect using the *in-vitro* QH Barrett's cell line at the gene and protein level. *In-vivo* immunohistochemical expression profiles of *ATP5B* and *GAPDH* were correlated to *p53*, IL1 β , SERPINA3, *HIF1 α* , waist circumference and to the length of the Barrett's segment using Spearman ρ analyses. Multiple regression

analyses were undertaken to investigate associations between two factors taking into account other factors *in-vivo* (R statistical software, package 'abn'). In addition, additive Bayesian networks were implemented to assess the dependencies between factors taking into account the combined effect of all factors *in-vivo* (R statistical software, package 'abn'). Majority consensus was constructed over 5000 iterations to select a best-fitting network representation of the relations between markers. Secreted protein levels and gene expression levels in *ex-vivo* explant tissue were correlated similarly (Spearman ρ correlation). Moreover, BMI was correlated to all *ex-vivo* factors (Spearman ρ correlation). Differences of $P < 0.05$ (*), $P < 0.01$ (**), and $P < 0.001$ (***) were considered statistically significant.

5.4 RESULTS

5.4.1 Linking energy metabolism, p53 and inflammation in the Barrett's tissue microenvironment *in-vivo*

To assess oxidative phosphorylation and glycolysis at the protein level, levels of ATP5B and GAPDH respectively, were assessed in *in-vivo* Barrett's patient tissue. Figure 38 shows immunohistochemical expression of these metabolic markers and investigates the link between energy metabolism and p53 in the Barrett's tissue microenvironment. ATP5B intensity is positively correlated with p53 intensity in the epithelium (figure 38A) ($R= 0.53$, $P= 0.0031$). This association, illustrated by representative images, shows that Barrett's patients exhibiting low p53 expression (figure 38C) showed low ATP5B intensity (figure 38E), however, low p53 expression was associated with high intensity x positivity (IxP) GAPDH expression levels (figure 38G). Stromal GAPDH IxP expression significantly negatively correlated to p53 IxP expression (figure 38B) ($R= -0.39$, $P=0.0357$). This association, illustrated by representative images, shows that Barrett's patients exhibiting high p53 expression (figure 38D) displayed high ATP5B intensity (figure 38F), however, high p53 expression was associated with low IxP GAPDH expression levels (figure 38H). Levels of ATP5B and p53 were additionally found to be significantly higher in sequential longitudinal material in Barrett's tissue from non progressors and progressors to LGD and HGD (see appendix P).

Figure 39 investigates the relationship between p53 and inflammation in the Barrett's tissue microenvironment. IL1 β IxP expression significantly positively correlated to levels of p53 IxP expression in the epithelium (figure 39A) ($R= 0.43$, $P= 0.02$). This association, illustrated by representative images, shows that Barrett's patients exhibiting low epithelial p53 expression (figure 39C) demonstrated low IxP IL1 β expression (figure 39E) and low SERPINA3 positivity levels (figure 39G). SERPINA3 positivity significantly positively correlated to p53 positivity in the epithelium (figure 39B) ($R= 0.536$, $P=0.0033$). This association, illustrated by representative images, shows that Barrett's patients exhibiting high epithelial p53 expression (figure 39D) displayed high IxP IL1 β expression (figure 39F) and high SERPINA3 (figure 39H) positivity levels.

Next, the association between energy metabolism and inflammation in the Barrett's tissue microenvironment was investigated. Figure 40 investigates the association between energy metabolism and inflammation in the Barrett's tissue microenvironment. Epithelial ATP5B positivity significantly positively correlated to epithelial IL1 β positivity (figure 40A) ($R= 0.8$, $P< 0.0001$). Furthermore, epithelial GAPDH positivity significantly positively correlated to epithelial IL1 β positivity (figure 40B) ($R= 0.43$, $P= 0.022$). In addition, GAPDH expression did not significantly

correlate to levels of SERPINA3 in the epithelium, however, ATP5B IxP expression did significantly correlate to IxP expression levels of SERPINA3 in the epithelium ($R= 0.6644$, $P= 0.0001$) (data not shown).

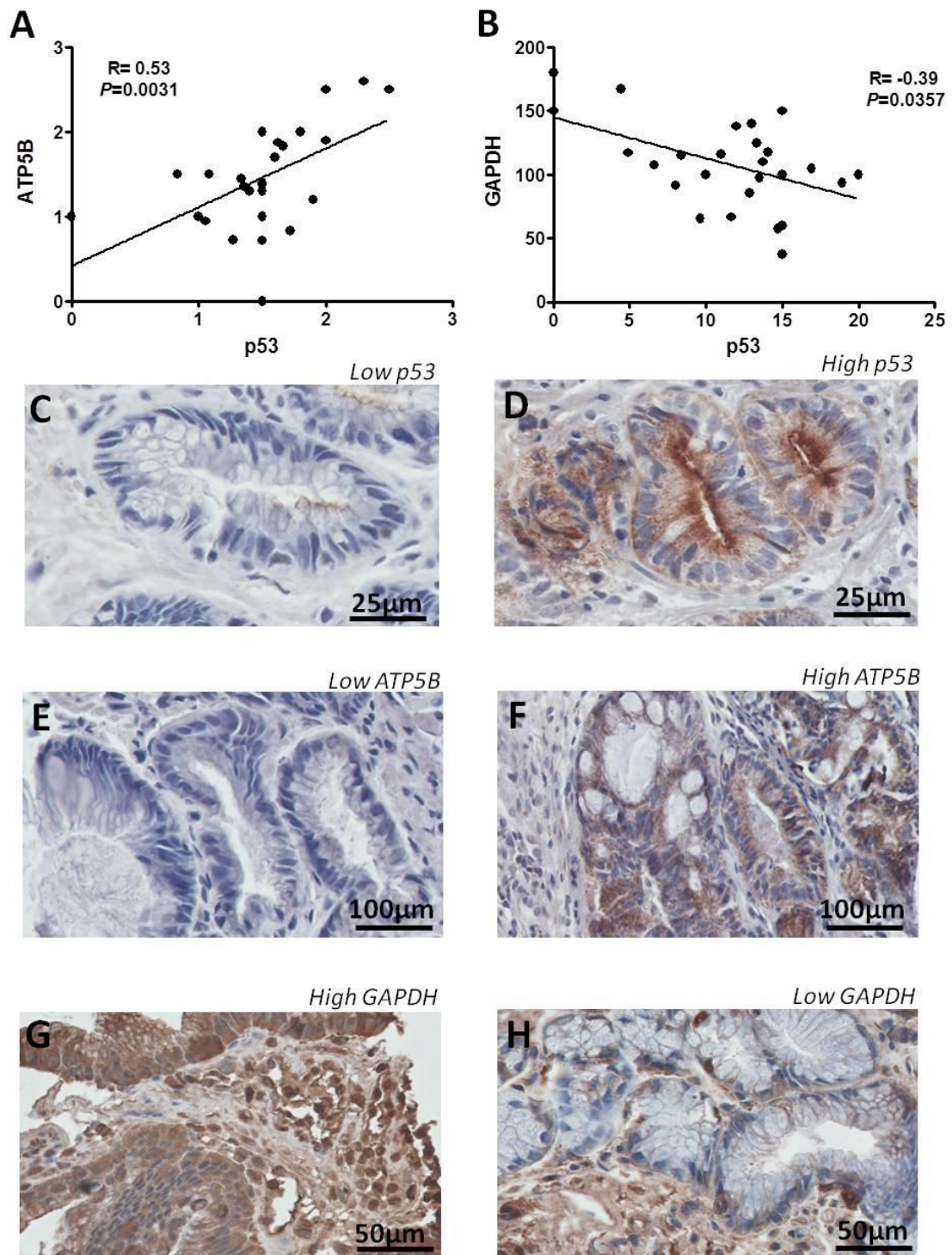


Figure 38. The link between energy metabolism and p53 in Barrett's oesophagus *in-vivo*. (A) Epithelial ATP5B intensity significantly positively correlated to epithelial p53 intensity ($R=0.53$, $P=0.0031$). (B) GAPDH IxP expression significantly negatively correlated to levels of p53 IxP expression in the stroma ($R=-0.39$, $P=0.0357$). (C) Barrett's patients displaying low levels of p53 expressed low intensity levels of ATP5B (E) and high IxP expression levels of GAPDH (G) respectively. (D) Barrett's patients displaying high levels of p53 expressed high intensity levels of ATP5B (F) and low IxP expression levels of GAPDH (H) respectively. R denotes Spearman ρ correlation (IxP= intensity by positivity).

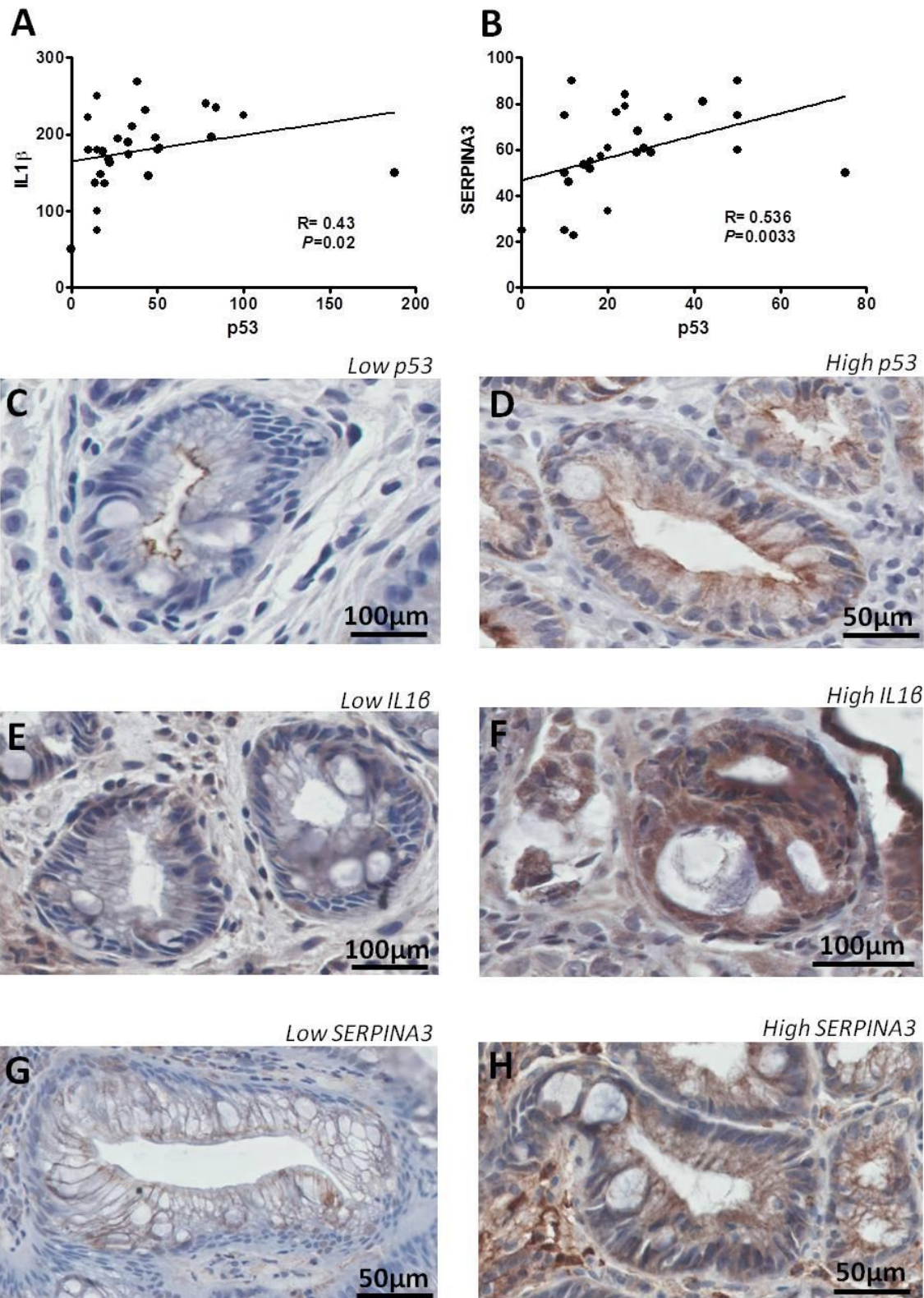


Figure 39. Linking p53 and inflammation in Barrett's oesophagus *in-vivo*. (A) Epithelial IL1 β IxP expression significantly positively correlated to levels of epithelial p53 IxP expression (R=0.43, P=0.02). (B) SERPINA3 positivity significantly positively correlated to p53 positivity in the epithelium (R=0.536, P=0.0033). (C) Barrett's patients displaying low epithelial levels of p53 expressed low epithelial IxP expression levels of IL1 β (E) and low epithelial positivity levels of SERPINA3 (G). (D) Barrett's patients displaying high epithelial levels of p53 expressed high epithelial IxP expression levels of IL1 β (F) and high epithelial positivity levels of SERPINA3 (H). R denotes Spearman ρ correlation (IxP= intensity by positivity).

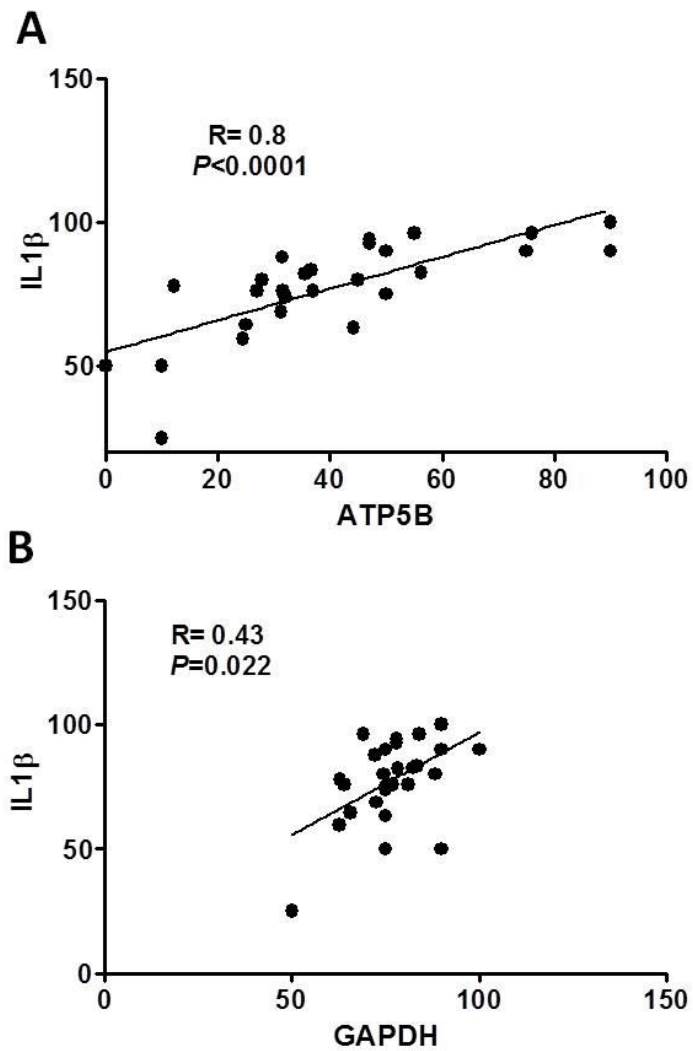


Figure 40. The association between energy metabolism and inflammation in Barrett's oesophagus *in-vivo*. (A) Epithelial ATP5B positivity significantly positively correlated to epithelial IL1 β positivity ($R=0.8$, $P<0.0001$). (B) Epithelial GAPDH positivity significantly positively correlated to epithelial IL1 β positivity ($R=0.43$, $P=0.022$). R denotes Spearman ρ correlation.

5.4.2 Linking hypoxia to energy metabolism, inflammation and p53 in Barrett's oesophagus *in-vitro* and *in-vivo*

Firstly, to investigate if hypoxia is potentially associated with mediating energy metabolism and inflammation, QH cells, an *in-vitro* model of Barrett's oesophagus, were exposed to normoxic (21% oxygen) and hypoxic (0.5% hypoxia) conditions. Levels of mRNA for *ATP5B* (figure 41A), *GAPDH* (figure 41B), *PKM2* (figure 41C), *VEGFA* (figure 41D) and *IL1 β* (figure 41E) were significantly differentially expressed in Barrett's QH cells under normoxic and hypoxic conditions. In addition, secreted levels of lactate (figure 41F), VEGF (figure 41G), IL-8 (figure 41H) and PAI-1 (figure 41I) were differentially altered in those Barrett's cells exposed to normoxia (21% oxygen) and hypoxia (0.5% hypoxia). Hypoxia had no significant effect on secreted levels of TNF α , IL-6, IL-10, IL-4, IL-2, IL-12p70, IL-13, bFGF or ICAM-1 (see appendix Q). Hypoxia was shown to significantly affect cell number (see appendix R). As we found differential hypoxia-induced alterations in various metabolic and inflammatory profiles *in-vitro*, we next investigated the effect of hypoxia *in-vivo*.

To assess if the relationship between hypoxia and these cellular processes can be recapitulated *in-vivo*, protein levels of HIF1 α were assessed. Figure 42 investigates the effect of hypoxia on energy metabolism, inflammation and p53 in the Barrett's tissue microenvironment. Focusing on the exact same area within the Barrett's tissue, Barrett's patients with low IxP HIF1 α expression (figure 42A) exhibited low IxP expression levels of ATP5B (figure 42C). Similarly, patients with high HIF1 α IxP expression (figure 42B) exhibited high IxP expression levels of ATP5B (figure 42D). HIF1 α IxP expression significantly positively correlated to ATP5B IxP expression in the epithelium (figure 42E) ($R= 0.71$, $P< 0.0001$). However, HIF1 α IxP expression ($R=0.06$, $P= 0.7$) did not significantly correlate to levels of GAPDH IxP expression in the epithelium as shown in figure 42F. HIF1 α IxP expression significantly positively correlated to levels of SERPINA3 IxP expression in the epithelium (figure 42G) ($R= 0.522$, $P= 0.0044$). Epithelial HIF1 α IxP expression significantly positively correlated to levels of epithelial p53 IxP expression (figure 42H) ($R= 0.455$, $P= 0.015$). It is also noteworthy to mention that the expression of p53, ATP5B and HIF1 α was differentially expressed between initial and most recently biopsied matched longitudinal Barrett's tissue (see appendix S).

5.4.3 Linking energy metabolism to obesity and to the length of the Barrett's segment in the Barrett's tissue microenvironment *in-vivo*

Figure 43 investigates the link between energy metabolism, obesity and the length of the Barrett's segment in the Barrett's tissue microenvironment. Stromal ATP5B IxP expression significantly negatively correlated to waist circumference (figure 43A) ($R = -0.6016$, $P = 0.0177$). Epithelial GAPDH intensity significantly positively correlated to waist circumference (figure 43B) ($R = 0.743$, $P = 0.0015$). No significant link was found between p53 and waist circumference, however, HIF1 α and IL1 β were negatively associated with waist circumference (see appendix T). ATP5B and GAPDH were also correlated to the length of the Barrett's segment. Stromal GAPDH intensity significantly positively correlated to the length of the Barrett's segment (figure 43C) ($R = 0.5192$, $P = 0.0133$), however, ATP5B did not.

Importantly, to ascertain a more comprehensive understanding between factors without the influence of other endogenous factors *in-vivo*, multiple regression analyses were undertaken. Table 6 compares the associations between metabolism, inflammation, hypoxia, p53, obesity and the length of the Barrett's segment *in-vivo* using both Spearman ρ and multiple regression analyses. ATP5B was significantly associated with p53 ($P = 0.03$), IL1 β ($P = 0.019$) and HIF1 α ($P = 0.002$). GAPDH was significantly linked with p53 ($P = 0.007$) and waist circumference ($P = 0.003$). All other pairings did not reach statistical significance. In addition, construction of Additive Bayesian Networks from multiple regressions showed some evidence of interdependencies between markers (see appendix U).

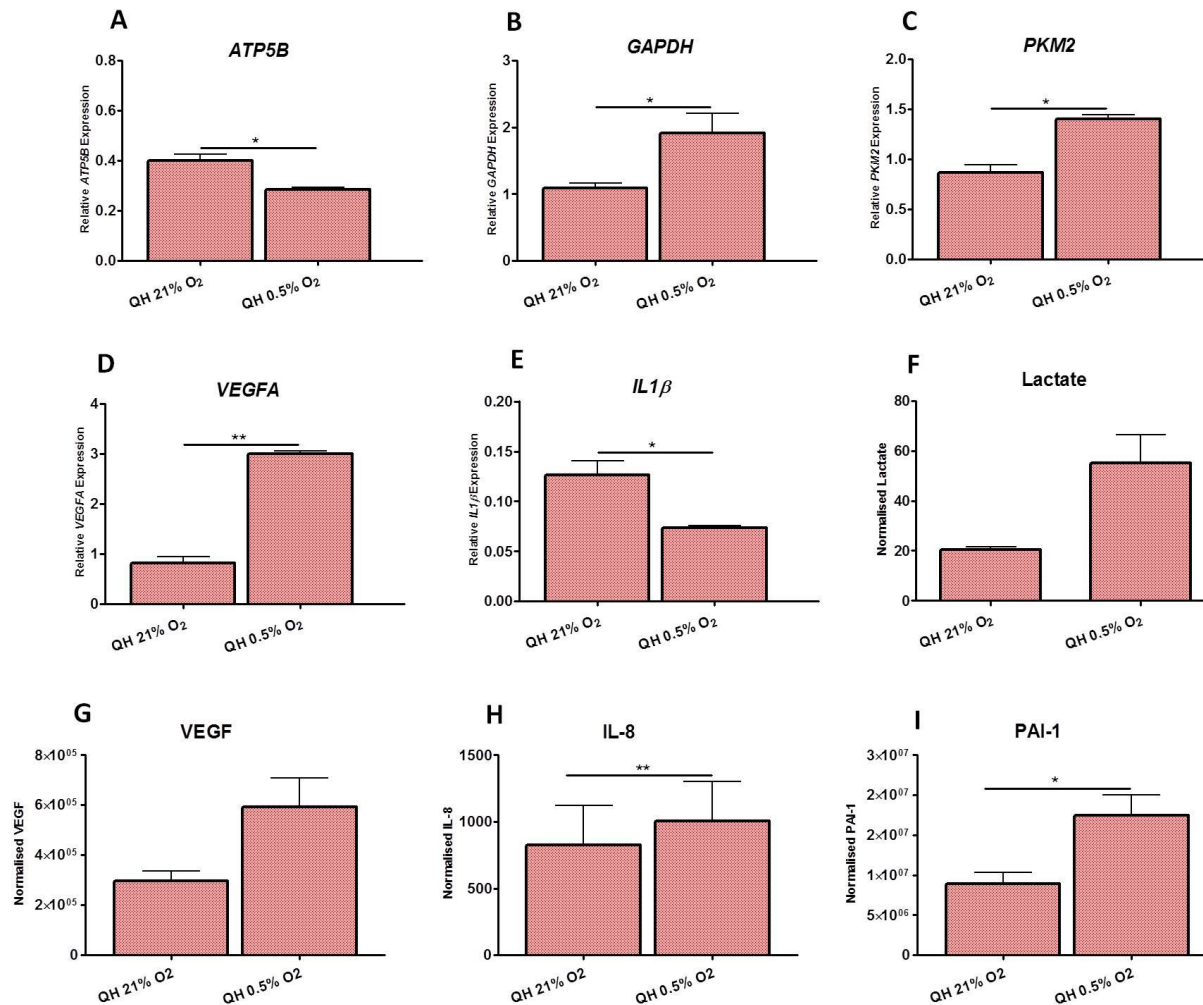


Figure 41. Investigating the effect of hypoxia on metabolic, inflammatory and angiogenic profiles in an *in-vitro* model of Barrett's oesophagus. Levels of genomic *ATP5B* (A), *GAPDH* (B), *PKM2* (C), *VEGFA* (D) and *IL1 β* (E) were significantly differentially expressed in Barrett's cells exposed to normoxia (21% oxygen) and hypoxia (0.5% hypoxia). Secreted levels of lactate (F), VEGF (G), IL-8 (H) and PAI-1 (I) were differentially altered in Barrett's cells exposed to normoxia (21% oxygen) and hypoxia (0.5% hypoxia). Bars denote mean \pm SEM.

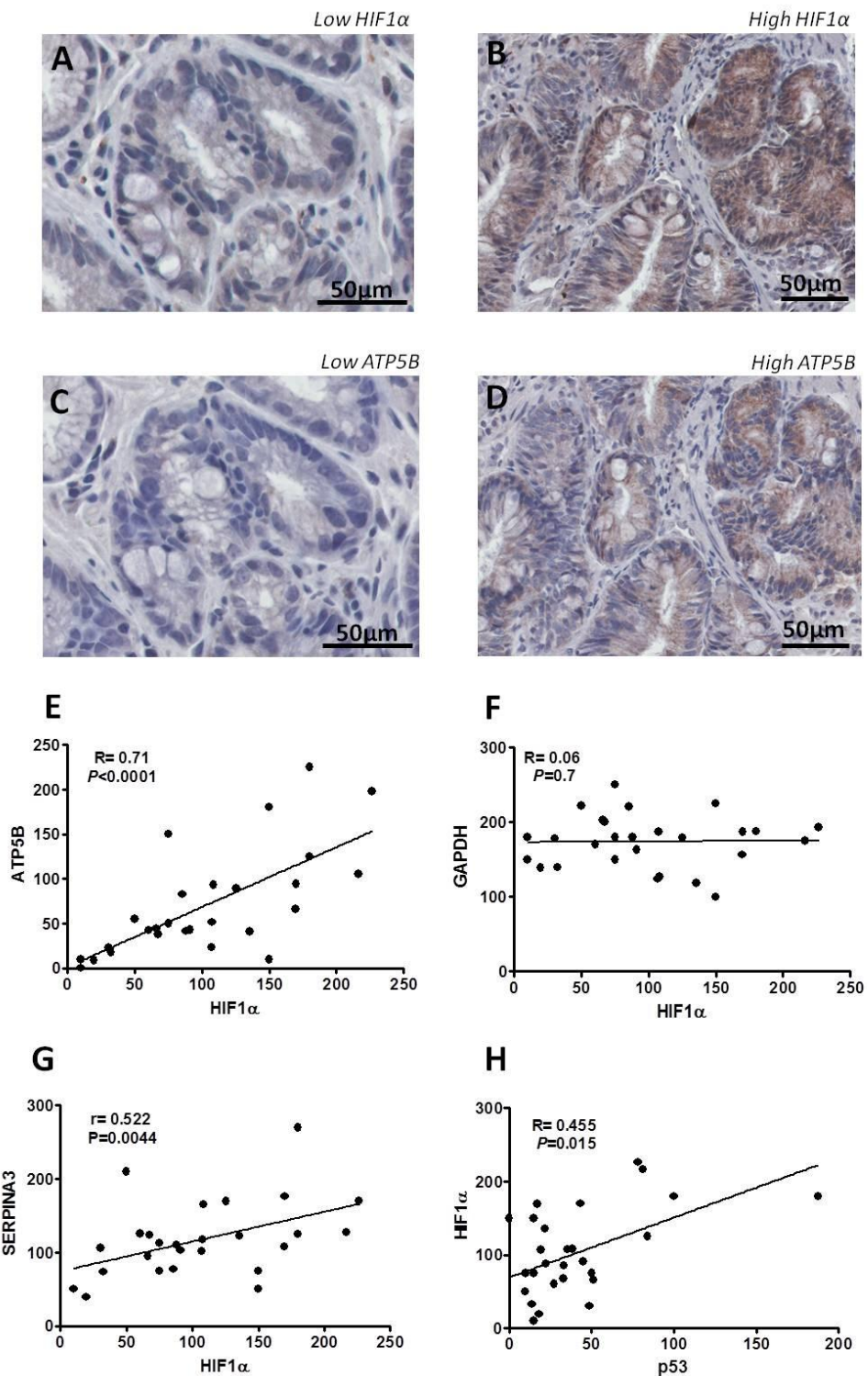


Figure 42. Linking hypoxia to energy metabolism, inflammation and p53 in Barrett's oesophagus *in-vivo*.

(A) A Barrett's patient, displaying low IxP expression levels of HIF1α also expressed low epithelial IxP expression levels of ATP5B (C) within the same glandular tissue area of the Barrett's tissue microenvironment. (B) A Barrett's patient, displaying high epithelial IxP expression levels of HIF1α also expressed high epithelial IxP expression levels of ATP5B (D) within the same glandular tissue area of the Barrett's tissue microenvironment. (E) Epithelial ATP5B IxP expression significantly positively correlated to levels of epithelial HIF1α IxP expression ($R=0.71$, $P<0.0001$). (F) HIF1α IxP expression did not correlate to levels of GAPDH IxP expression in the epithelium ($R=0.06$, $P=0.7$). (G) HIF1α IxP expression significantly positively correlated to levels of SERPINA3 IxP expression in the epithelium ($R=0.522$, $P=0.0044$). (H) p53 IxP expression significantly positively correlated to levels of HIF1α IxP expression in the epithelium ($R=0.455$, $P=0.015$). R denotes Spearman ρ correlation (IxP= intensity by positivity).

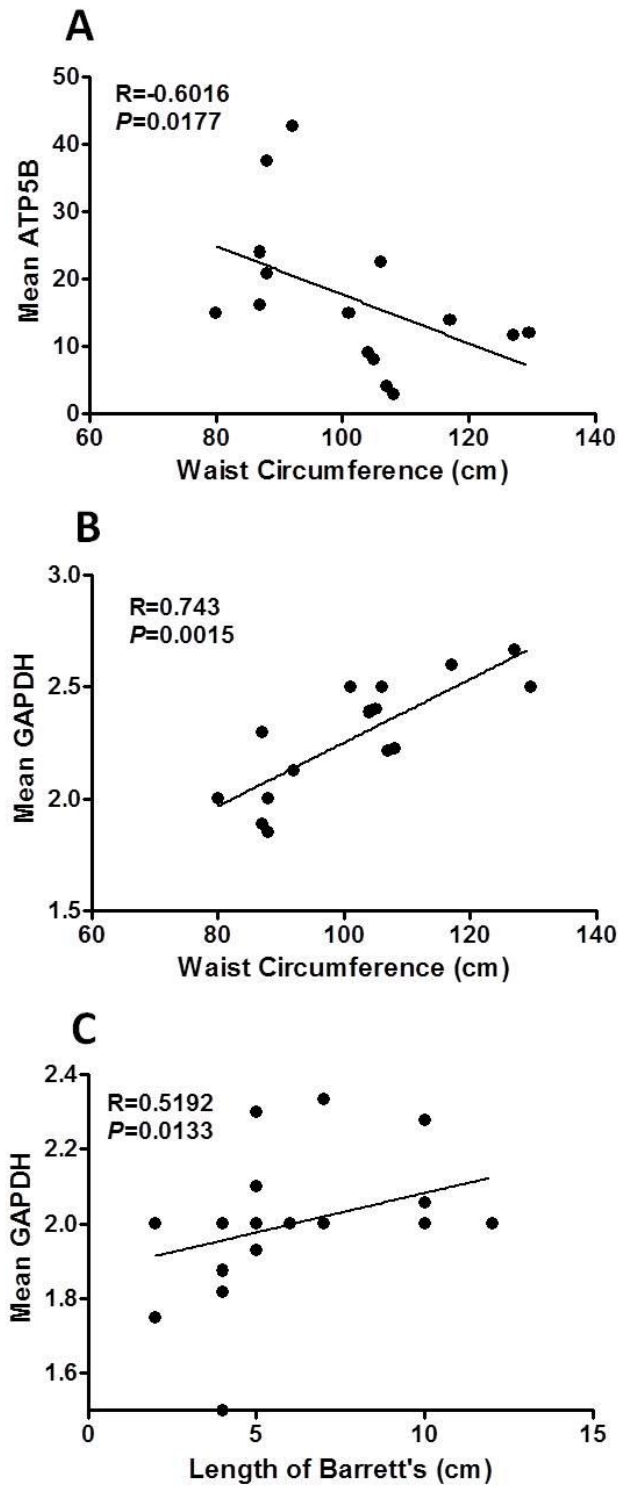


Figure 43. Linking energy metabolism to obesity and to the length of the Barrett's oesophagus *in-vivo*. (A) Stromal ATP5B IxP expression significantly negatively correlated to waist circumference ($R=-0.6016$, $P=0.0177$). (B) Epithelial GAPDH intensity significantly positively correlated to waist circumference ($R=0.743$, $P=0.0015$). (C) Stromal GAPDH intensity significantly positively correlated to the length of the Barrett's segment ($R=0.5192$, $P=0.0133$). Waist circumference and Barrett's segment length demographics were available on 15 and 22 patients respectively from the 29 patients who participated in the study. R denotes Spearman ρ correlation (IxP= intensity by positivity).

5.4.4 Linking energy metabolism to p53, inflammation, hypoxia and angiogenesis in the Barrett's tissue microenvironment ex-vivo

To elucidate the relationship between energy metabolism and these processes, we used Barrett's ex-vivo explant tissue in an effort to utilise a model that mimicked the Barrett's tissue microenvironment linking gene expression profiles and protein secretion profiles associated with the above cellular processes. All nine patients were confirmed for the presence of the intestinal metaplasia molecular marker villin prior to analyses (see appendix V). Table 7 summarises the association between metabolism and inflammation, hypoxia, p53 and angiogenesis in Barrett's ex-vivo explant tissue. *ATP5B* expression significantly positively correlated to TNF α (R= 0.786, P= 0.027), IL-6 (R= 0.93, P= 0.002), *HIF1 α* (R= 0.8833, P= 0.003) and *p53* (R= 0.7167, P= 0.037). *HSP60* expression was significantly positively associated with *HIF1 α* (R= 0.7333, P= 0.031). *GAPDH* expression significantly positively correlated to TNF α (R= 0.81, P= 0.021), IL-6 (R= 0.9, P= 0.004) and *HIF1 α* (R= 0.8667, P= 0.002). *PKM2* expression significantly positively correlated to IL-6 (R= 0.73, P= 0.025), *HIF1 α* (R= 0.9167, P= 0.001) and *p53* (R= 0.9, P= 0.002). Moreover, *HSP60* (R= -0.7, P= 0.036) and *PKM2* (R= -0.683, P= 0.042) were significantly negatively associated with angiogenesis (ANG-1). No significant correlations were found with secreted lactate levels (P>0.05).

5.4.5 Linking inflammation, hypoxia, p53, BMI and angiogenesis in the Barrett's tissue microenvironment ex-vivo

Table 8 summarises the link between inflammation, hypoxia, p53, BMI and angiogenesis in the Barrett's ex-vivo explant tissue. Angiogenesis (ICAM-1) significantly positively correlated to MCP-1 (R= 0.762, P= 0.036), MMP9 (R= 0.717, P= 0.03), IL-2 (R= 0.783, P= 0.013) and TNF α (R= 0.786, P= 0.028). In addition, secreted levels of bFGF significantly positively correlated to IL1 β (R= 0.762, P= 0.036) and IL-10 (R= 0.714, P= 0.047). Moreover, BMI significantly positively correlated to secreted levels of VCAM-1 (R= 0.8, P= 0.01), ICAM-1 (R= 0.733, P= 0.025) and ANG-1 (R= 0.717, P= 0.03). *HIF1 α* significantly positively correlated to expression levels of *p53* (R= 0.8833, P= 0.003), GRO α (R= 0.75, P= 0.025), IL-6 (R= 0.8833, P= 0.003), MIP3 α (R= 0.75, P= 0.025), MMP2 (R= 0.81, P= 0.022), TNF α (R= 0.7167, P= 0.037) and IL1 β (R= 0.6667, P= 0.049). Furthermore, *p53* status significantly positively correlated with IL-6 (R= 0.75, P= 0.025) and MMP2 (R= 0.762, P= 0.037). Analogous associations were discovered linking metabolism, inflammation, angiogenesis and BMI in matched normal adjacent squamous tissue from the same patients (see appendices W and X).

Table 6. Comparing the association between metabolism, inflammation, hypoxia, p53, obesity and the length of the Barrett's segment *in-vivo* using Spearman ρ and multiple regression analyses.

<i>Correlation</i>	<i>Spearman Correlation</i>		<i>Multiple Regression</i>	
	<i>R[#]</i>	<i>P</i>	<i>Estimate</i>	<i>P</i>
<i>Metabolism vs. p53</i>				
ATP5B vs. p53 ^{1A}	0.53	0.0031 **	0.3847	0.0302 *
GAPDH vs. p53 ^{3B}	-0.39	0.0357 *	-3.78245	0.007 **
<i>p53 vs. Inflammation</i>				
p53 vs. IL1 β ^{3A}	0.43	0.02 *	-0.1452	0.464
p53 vs. SERPINA3 ^{2A}	0.536	0.0033 **	0.1397	0.537
<i>Metabolism vs. Inflammation</i>				
ATP5B vs. IL1 β ^{2A}	0.8	<0.0001 ***	0.5118	0.019 *
GAPDH vs. IL1 β ^{2A}	0.43	0.022 *	0.155	0.378
<i>Metabolism vs. Hypoxia</i>				
ATP5B vs. HIF1 α ^{3A}	0.71	<0.0001 ***	0.4838	0.002 **
GAPDH vs. HIF1 α ^{3A}	0.06	0.7	-0.24441	0.112
<i>Hypoxia vs. Inflammation</i>				
HIF1 α vs. SERPINA3 ^{3A}	0.522	0.0044 **	0.08036	0.744
<i>p53 vs. Hypoxia</i>				
p53 vs. HIF1 α ^{3A}	0.455	0.015 *	0.1915	0.253
<i>Metabolism vs. Waist Circumference</i>				
ATP5B ^{3B} vs. Waist Circumference	-0.6016	0.0177 *	-0.89	0.399
ATP5B ^{3A} vs. Waist Circumference	-0.354	0.1952	-2.19	0.059
GAPDH ^{1A} vs. Waist Circumference	0.743	0.0015 **	49.06	0.003 **
<i>Metabolism vs. Length of Barrett's Segment</i>				
GAPDH ^{1B} vs. Barrett's Segment	0.5192	0.0133 *	6.0504	0.181

Correlation Coefficient (R)[#]

Intensity¹ Positivity² Intensity X Positivity³

Epithelium^A Stroma^B

Table 7. The association between metabolism and inflammation, hypoxia, p53 and angiogenesis in Barrett's *ex-vivo* explant tissue.

Correlation	Correlation Coefficient, R	P
<i>Metabolism vs. Inflammation</i>		
<i>ATP5B</i> vs. TNF α *	0.786	0.027
<i>ATP5B</i> vs. IL-6 *	0.93	0.002
<i>GAPDH</i> vs. TNF α *	0.81	0.021
<i>GAPDH</i> vs. IL-6 *	0.9	0.004
<i>PKM2</i> vs. IL-6	0.73	0.025
<i>Metabolism vs. Hypoxia</i>		
<i>ATP5B</i> vs. <i>HIF1α</i>	0.8833	0.003
<i>HSP60</i> vs. <i>HIF1α</i>	0.7333	0.031
<i>GAPDH</i> vs. <i>HIF1α</i>	0.8667	0.002
<i>PKM2</i> vs. <i>HIF1α</i>	0.9167	0.001
<i>Metabolism vs. p53</i>		
<i>ATP5B</i> vs. <i>p53</i>	0.7167	0.037
<i>PKM2</i> vs. <i>p53</i>	0.9	0.002
<i>Metabolism vs. Angiogenesis</i>		
<i>HSP60</i> vs. ANG-1	-0.7	0.036
<i>PKM2</i> vs. ANG-1	-0.683	0.042
Spearman ρ , $n=9$ ($n=8^*$)		

Table 8. The association between inflammation, hypoxia, p53, BMI and angiogenesis in Barrett's ex-vivo explant tissue.

Correlation	Correlation Coefficient, R	P
<i>Inflammation vs. Angiogenesis</i>		
ICAM-1 vs. MCP-1 *	0.762	0.036
ICAM-1 vs. MMP9	0.717	0.03
ICAM-1 vs. IL-2	0.783	0.013
ICAM-1 vs. TNF α *	0.786	0.028
bFGF vs. IL1 β *	0.762	0.036
bFGF vs. IL-10 *	0.714	0.047
<i>Angiogenesis vs. BMI</i>		
VCAM-1 vs. BMI	0.8	0.01
ICAM-1 vs. BMI	0.733	0.025
ANG-1 vs. BMI	0.717	0.03
<i>Hypoxia vs. p53</i>		
HIF1A vs. p53	0.8833	0.003
<i>Hypoxia vs. Inflammation</i>		
HIF1A vs. GRO α	0.75	0.025
HIF1A vs. IL-6	0.8833	0.003
HIF1A vs. MIP3 α	0.75	0.025
HIF1A vs. MMP2 *	0.8095	0.022
HIF1A vs. TNF α	0.7167	0.037
HIF1A vs. IL1 β	0.6667	0.049
<i>p53 vs. Inflammation</i>		
p53 vs. IL-6	0.75	0.025
p53 vs. MMP2 *	0.7619	0.037
Spearman ρ , $n=9$ ($n=8^*$)		

5.5 DISCUSSION

An understanding of the complex processes in the inflammation to tumour model of Barrett's oesophagus and OAC may provide some insight into both biomarkers of risk progression, and the potential for the development of novel targeted therapies. We have shown for the first time that mitochondrial energy metabolism is strongly associated with inflammation and hypoxia in the Barrett's oesophagus tissue microenvironment. The study also highlights that mitochondrial energy metabolism is aligned with p53 status, obesity status and to the length of the Barrett's segment, further demonstrating that various cellular mechanisms may operate mutually, fueling progression and altering cellular processes within the Barrett's microenvironment to HGD and OAC.

In this study, we have shown *in-vivo* and *ex-vivo* that ATP5B, a marker of oxidative phosphorylation, was significantly positively correlated to p53 status in Barrett's oesophagus. We also demonstrate *in-vivo* that GAPDH, a marker of glycolysis, was significantly negatively associated with p53. At the gene level *ex-vivo*, p53 was shown to be positively associated with another marker of glycolysis, PKM2. The aberrant expression of the tumour suppressor protein, p53, commonly associated with aneuploidy is associated with an increased risk of neoplastic progression in Barrett's oesophagus (292). p53 has an important role in cellular metabolism, lowering glycolysis, an anti-Warburg effect, and promoting oxidative phosphorylation (175, 197, 198, 212). p53 promotes oxidative phosphorylation through the p53-inducible protein Miao and also through the master transcription regulator nuclear factor kappa B (NFκB)-mediated upregulation of mitochondrial Synthesis of Cytochrome c Oxidase 2 (SCO2) (201, 223). p53 negatively regulates glycolysis by downregulating key components of glycolysis such as glucose transporter 1 (GLUT1), GLUT3, phosphofructose kinase 1 and PKM2 (197, 208, 209, 222). It may be plausible that the increased oxidative microenvironment that p53 promotes in Barrett's oesophagus supports metaplastic progression as one study has found that oxidative-induced damage in Barrett's patients results in telomere shortening and mutations in the p53 gene itself (202). Therefore, with an oxidative-induced abrogation of p53 function, glycolytic levels are no longer negatively regulated and this may explain why levels of glycolysis may increase early in the progression of OAC (130). Alternatively, p53 may simultaneously promote oxidative phosphorylation producing large amounts of ATP and shunt high energy glycolytic intermediates into the pentose phosphate pathway (207). The NFκB family member RelA is transported into mitochondria and recruited to the mitochondrial genome where it can repress mitochondrial gene expression, oxygen consumption and cellular ATP levels, thereby contributing to the switch to glycolysis. Conversely, upon low cellular ATP levels, NFκB can upregulate mitochondrial

respiration through mitochondrial synthesis of cytochrome c oxidase 2, a key component of complex IV of the electron transport chain (223).

In this study, ATP5B was significantly positively correlated to levels of IL1 β and SERPINA3 *in-vivo*, and with TNF α and IL-6 in Barrett's *ex-vivo* explant tissue. Furthermore, GAPDH was significantly positively correlated to levels of IL1 β , TNF α and IL-6 in *in-vivo* and *ex-vivo* Barrett's tissue. Few studies have investigated the direct association between oxidative phosphorylation and inflammation. NF κ B is a key inflammatory mediator of both oxidative phosphorylation and glycolysis, and promotes IL1 β and TNF α production (221-223). IL1 β , IL-6 and TNF α may have key roles in the development and subsequent progression of OAC, consistent with a murine model where overexpression of IL1 β induced intestinal metaplasia and OAC, an effect abrogated by IL-6 deficiency (69). In this context, the effector functions of IL1 β -dependent T_H17 cells have been shown to be related to their glycolytic capacity (471). TNF α has also been shown to stimulate glycolysis in colorectal cancer cells (468). Moreover, increased expression of the key glycolytic enzymes, 6-phosphofructo-2-kinase/fructose-2,6-bisphosphatase-3 and hexokinase 2, have been shown to be orchestrated by the IL-6-STAT3 pathway further providing a mechanism for inflammation-associated oncogenesis in Barrett's oesophagus (289). Inflammation is also known to mediate metabolism through NF κ B in a p53-dependent manner (221, 223).

Hypoxia and related genes, and their interface with inflammation and metabolism, are also relevant to this model. To assess hypoxia, we examined the expression of HIF1 α , however, we acknowledge limitations in the use of this hypoxic marker. HIF1 α can be upregulated by non-hypoxic pathways, therefore, alternative reliable hypoxia markers, or their combined value, such as carbonic anhydrase 9, VEGF, GLUT1, JMJD1A and erythropoietin may be more hypoxia specific (259, 268, 472-476). Subsequent to demonstrating differential hypoxia-induced effects on inflammation, angiogenesis and metabolism *in-vitro*, we found that both oxidative phosphorylation (ATP5B and HSP60) and glycolysis (GAPDH and PKM2) significantly positively correlated to HIF1 α at the gene level *ex-vivo*. Moreover, *in-vivo* ATP5B protein levels significantly positively correlated with HIF1 α protein expression, however, HIF1 α showed no correlation with GAPDH *in-vivo*. Interestingly, various studies in the cancer setting have implicated glycolysis as one of the main distinctive factors in the adaptation to hypoxic stress, as hypoxia mediates metabolism by inducing the expression of various glycolytic components (180). Few studies to our knowledge have showed a link between hypoxia and oxidative phosphorylation, however, the growth of HeLa cells and breast cancer cells in aglycemia and/or hypoxia has been shown to trigger a compensatory increase in oxidative phosphorylation capacity (163, 167). Even though

this adaptation to oxidative phosphorylation results in the production of large amounts of ATP produced per glucose molecule compared to glycolysis, it is plausible, however, that this positive relationship reflects more of an indirect relationship between hypoxia and other complex constitutive processes in the Barrett's microenvironment, such as inflammation and p53 status. Therefore, we investigated if there was an association between hypoxia, inflammation and p53 status in Barrett's tissue microenvironment. We found that hypoxia significantly positively correlated to levels of p53 *in-vivo* and *ex-vivo*. No studies to our knowledge have linked hypoxia to p53 in the Barrett's setting. Some studies, however, have shown p53 to encompass an important role in hypoxic microenvironments (206, 477). Under hypoxic conditions, the p53-inducible phosphatase, TP53-induced glycolysis and apoptosis regulator, forms a complex with hexokinase 2 at the mitochondria (206). This complex subsequently shunts glycolytic intermediates into the pentose phosphate pathway reducing glycolytic flux and generating NADPH, ribose-5-phosphate and erythrose-4-phosphate for the production of fatty acids, nucleotides, nucleic acids and amino acids (206). In the neoplastic setting, suppression of HIF2 α has been shown to restore p53 activity reversing chemoresistance in renal carcinoma cells (477).

We have further demonstrated that hypoxia significantly positively correlated with inflammation in the Barrett's setting *in-vivo*. *Ex-vivo* we illustrate that HIF1 α is positively associated with various secreted inflammatory proteins including GRO α , IL-6, MIP3 α , MMP2, MMP9, TNF α and IL1 β . HIF1 α protein expression has previously been documented to be associated with inflammation in Barrett's oesophagus, however, this study utilised the Sydney system to assess inflammation and not an inflammatory molecular marker analogous to this current study (176). Another study found increased expression of the hypoxia-inducible proteins across the metaplasia-dysplasia-OAC sequence *in-vivo* (461). Therefore, the greater degree of inflammation known to be associated with the latter stages of the Barrett's sequence may in part be hypoxia-induced inflammation in origin (219, 478). Moreover, T-cells are known to play an important role in the initiation and subsequent progression of Barrett's oesophagus (456). Interestingly, hypoxia is known to stimulate increased levels of IL1 β , IL-10 and IL8 in human CD4⁺ T cells, but the absence of glucose reduces secretions of these cytokines implying that CD4⁺ T cells can be highly metabolically adaptable in highly fluctuating bioenergetic microenvironments (183). Since both oxidative phosphorylation and glycolysis were strongly associated with increased inflammation in the Barrett's tissue microenvironment in this study, hypoxia-induced secretions of various proinflammatory proteins may in theory alter the metabolic profile in the Barrett's microenvironment. In addition to its close link with hypoxia, we have shown *in-vivo* that p53 significantly positively correlated with both IL1 β and SERPINA3 in Barrett's oesophagus. *Ex-vivo*,

we illustrate positive links between *p53*, IL-6 and MMP2. Few studies have linked *p53* to IL1 β and SERPINA3 in the literature but *p53*'s role in the regulation of the key central inflammatory and metabolic regulator, NF κ B, has been documented (221, 222). Consequently, the intrinsic relationship between hypoxia, inflammation and *p53* early in the Barrett's microenvironment may be sufficient to mediate metabolism in support of metaplastic transformation. It is also important to note, however, that the associations linking *p53*, ATP5B and HIF1 α to the cellular processes illustrated here may be time-dependent as the expression of *p53*, ATP5B and HIF1 α were found to be differentially expressed between initial and most recently biopsied matched longitudinal Barrett's tissue.

Obesity is strongly associated with the increase in incidence of Barrett's oesophagus and OAC (82, 83). Detailed studies of the Barrett's and tumour microenvironment in this model are, however, scarce, therefore, we assessed if there was an association between obesity and both oxidative phosphorylation and glycolysis in our Barrett's cohort. Interestingly, we found a significant negative association between waist circumference and ATP5B expression but a significant positive association between waist circumference and GAPDH expression. No studies have shown such a reciprocal association between obesity and metabolism in preneoplastic or cancer tissue. It is possible, however, that such obesity-induced metabolic alterations are the functional result of various adipokines known to be secreted by adipose tissue (479). The fatty acid, palmitic acid, has been shown to increase concentrations of fructose 2,6-biphosphate, a key glycolytic intermediate (480). Obesity has also been shown to promote aerobic glycolysis in prostate cancer cells (481). Conversely, a high fat diet has been shown to downregulate genes required for oxidative phosphorylation (482). Moreover, after a 6-month exercise programme, extensive alterations in the transcriptome profile of healthy human adipose tissue has shown increases in a variety of genes associated with oxidative phosphorylation (483). Adiponectin is also known to promote mitochondrial biogenesis (484). Serum adiponectin levels are known to decline with obesity in Barrett's oesophagus which may decrease mitochondrial biogenesis in the process (479). In addition, it has also been shown that a palmitic acid-induced decrease in adiponectin is responsible for mitochondrial dysfunction in adipocytes (485). The degree of glycolysis may also depend on the oxidative capacity of the tissue, thus increases in glycolysis may be a compensatory mechanism as oxidative metabolism is inhibited. To support this, when we inhibit oxidative phosphorylation *in-vitro* Barrett's cells utilising Seahorse technology, we see a significant compensatory increase in glycolytic levels (see appendix L). We also found a significant positive correlation between GAPDH and the length of the Barrett's segment, previously linked to metaplastic progression in Barrett's oesophagus (10, 469, 470).

Angiogenesis, a key hallmark of cancer, is linked to hypoxia and glycolysis and therefore key to endothelial cell function (226). We found that both *HSP60* and *PKM2* were significantly negatively associated with the angiogenesis marker, ANG-1, in Barrett's *ex-vivo* explant tissue. Although angiogenesis is positively associated with neoplastic progression in some disease entities, these findings may have some significant physiological implications; that is, high energy levels are associated with low angiogenic potential and low energy levels are associated with high angiogenic potential. In addition, we found *ex-vivo* that angiogenesis (ICAM-1 and bFGF) significantly positively correlated with levels of inflammation (MCP-1, MMP9, IL-2, TNF α , IL1 β and IL-10). Moreover, angiogenesis (ICAM-1, VCAM-1 and ANG-1) significantly positively correlated with BMI status *ex-vivo*.

Overall, the *in-vivo* and *ex-vivo* findings in this study, as depicted in figure 44, effectively demonstrate the complexity of the cellular processes activated in the Barrett's tissue microenvironment and give some insight into how these processes could potentially support metaplastic progression through the alteration of cellular energy metabolism. Identifying and exploring the underlying molecular mechanisms that link metabolism to these key cellular processes, and to each other, would significantly aid in understanding how these processes interact and may provide some insight into the development of targeted therapies influencing these processes.

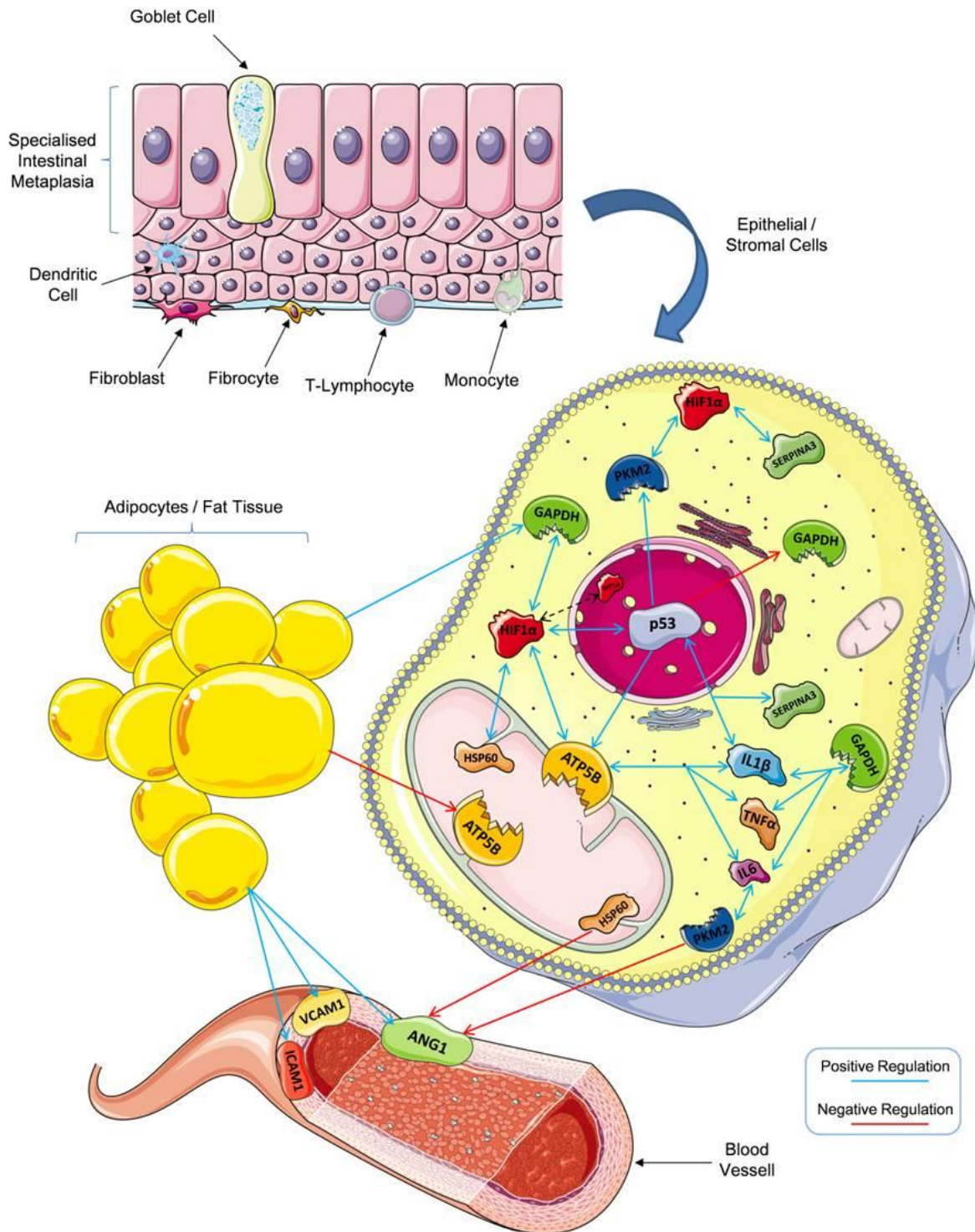


Figure 44. The Barrett's oesophagus microenvironment. The inflamed specialised intestinal metaplasia of Barrett's oesophagus demonstrates many complex interdependencies. Within epithelial and stromal cells, p53 positively associates with ATP5B but negatively with GAPDH. p53 positively correlates with IL1β and SERPINA3. Both ATP5B and GAPDH are positively linked with IL1β, TNFα and IL-6. p53 expression positively correlates with HIF1α expression. HIF1α expression positively correlates with ATP5B, PKM2 and SERPINA3. HSP60 and PKM2 negatively associate with ANG-1, a marker of angiogenesis. Obesity status positively links with GAPDH but negatively with ATP5B. Obesity positively correlates with angiogenesis. Inflammation and angiogenesis are additionally interdependent.

Chapter 6

Investigating the functional effect of IL1 β overexpression and a high fat diet in a transgenic model of Barrett's oesophagus on cellular processes, specifically energy metabolism, p53 and hypoxia.

6.1 INTRODUCTION

In chapter 5, we showed that mitochondrial energy metabolism is strongly linked with inflammation and hypoxia in the Barrett's oesophagus tissue microenvironment. We also demonstrated that mitochondrial energy metabolism is coupled with p53 status, obesity status and to the length of the Barrett's segment, further demonstrating that various cellular mechanisms may operate interdependently, altering cellular processes within the Barrett's microenvironment and thereby promoting disease progression. Central to these intrinsic connections, however, our data indicates that inflammation may play a central role in the Barrett's tissue microenvironment. Examining whether there are functional mechanistic connections between inflammation and these processes, however, requires further investigation.

Chronic inflammation of the oesophagus has been heavily linked to the incidence of OAC (75). Increasing evidence throughout the literature demonstrates that chronic inflammation can modulate the tissue microenvironment further substantiating the role of chronic inflammation in tumourigenesis (288). Moreover, the persistence of an acute inflammatory response can result in a chronic state of inflammation which has the potential to sculpt its microenvironment making it more vulnerable to further disease progression (175, 288). Moreover, various inflammatory mediators link inflammation to Barrett's-associated carcinogenesis (486). Inflammatory-induced ROS-mediated DNA damage can result in altered transcription, genomic instability, replication errors and alterations in DNA repair systems and cell cycle control (486, 487).

Furthermore, various studies highlight Barrett's oesophagus as a state of chronic inflammation. Immunohistochemical analysis reveals that Barrett's tissue contains significantly higher numbers of Th2 effector cells compared to reflux oesophagitis thus suggestive of a humoral immune phenotype (488). In addition, cytokines generated by the activation of immune cells, such as macrophages, are considered important in the orchestration of inflammatory associated carcinogenesis (489). One study demonstrated the link between cytokine gene polymorphisms and a strong proinflammatory response in the development of Barrett's oesophagus (490). To provide further evidence linking inflammation and tumourigenesis in a mouse model of colitis-associated cancer, deletion of I κ B kinase, the kinase responsible for NF κ B activation, results in inactivation of the NF κ B pathway resulting in decreased tumour incidence (491).

Inflammation has long been implicated in disease progression in Barrett's oesophagus. The proinflammatory cytokines IL-8 and IL1 β are significantly elevated in the Barrett's epithelium with expression markedly increased in OAC (219). The activation of NF κ B, known to be increased in

Barrett's oesophagus and OAC, is additionally linked with cytokine activation in patients with OAC further linking inflammatory-induced cytokines to tumourigenesis (219). Inflammation generated through cyclooxygenase-2, induced by prostaglandins, has additionally been implicated as playing an important role between inflammation and tumourigenesis (492). Increased cyclooxygenase-2 expression, therefore, observed during progression from Barrett's to LGD, HGD and OAC may increase the inflammatory burden of Barrett's tissue (492). Interestingly, GORD refluxate is also known to induce cyclooxygenase-2 expression in a ROS-mediated manner (493). In addition, the bile acid DCA also attenuates the inflammatory microenvironment by stimulating the expression of IL-8 and IL1 β through NF κ B (219). Recent research has also shown that the inflammatory C-reactive protein and IL-6 helps to identify persons at higher risk of progression to OAC further implicating inflammation in disease progression (494). It is also known that the frequency of mutations, seen to increase with increasing histological grade, in the tumour suppressor gene *CDKN2A*, are caused by chronic inflammation in Barrett's oesophagus (366). Furthermore, obesity, linked with oesophageal inflammation, metaplasia and neoplastic progression, is now seen as a proinflammatory state that potentially links chronic inflammation to tumourigenesis (495).

In a model of chronic inflammation, targeted overexpression of IL1 β to the oral cavity, oesophagus and forestomach in a transgenic C57/B6 PL2-IL1 β mouse model induces a Barrett's-like metaplasia at the squamocolumnar junction (SCJ) resulting in various histopathological and gene signatures closely resembling human Barrett's oesophagus (69). Interestingly, the development of Barrett's and OAC is inhibited by IL-6 deficiency in the same model (69). Moreover, lineage tracing studies demonstrate in this PL2-IL1 β model the likely origin of metaplastic tissue to be within the gastric cardia (69). The infiltration of immature myeloid cells is additionally observed upon induction of IL1 β in the subsequent development of metaplasia in this model (69). Specific deletion of I κ B kinase within myeloid cells of a mouse model of colitis-associated cancer has been shown to decrease tumour size and diminish the expression of various proinflammatory cytokines (491). Despite various studies implicating a number of cytokines in inflammatory-induced carcinogenesis, more studies need to elucidate if a single cytokine alone can potentiate the development of neoplastic tissue. One such study, using IL1 β transgenic mice deficient in T and B lymphocytes, showed that deficient mice still develop gastric dysplasia accompanied by significant numbers of myeloid-derived suppressor cells demonstrating that pathological elevation of a single proinflammatory cytokine may be sufficient to induce neoplasia and provide a direct link between IL1 β , myeloid cells and tumourigenesis (496).

To build on our previous data and investigate the link between metabolism, inflammation, hypoxia, p53 and obesity in the Barrett's tissue microenvironment presented in chapter 5, utilising

the transgenic PL2-IL1 β mouse model of Barrett's-like metaplasia in collaboration with the Quante lab in the Technical University of Munich, we examined if induction of IL1 β overexpression and a high fat diet could alter metabolism, p53 and hypoxia. We show that induction of inflammation through IL1 β manipulation can modulate glycolysis, oxidative phosphorylation, p53 and HIF1 α . We also demonstrate that a high fat diet can mediate these processes providing further insight into the potential role of obesity in exacerbating disease progression. Our results also imply that columnar cells within the Barrett's microenvironment are more sensitive to inflammatory-induced fluctuations, thereby contributing to further disease progression. These results illustrate that chronic inflammation and a high fat diet may potentially operate independently, or mutually, to support neoplastic progression within the inflammatory microenvironment of Barrett's oesophagus.

6.2 HYPOTHESIS AND AIMS OF CHAPTER SIX

We hypothesise that IL1 β overexpression and a high fat diet can modulate energy metabolism and other key cellular processes to promote disease progression in Barrett's oesophagus.

Specific aims of chapter 6;

- 1) Elucidate the effect of IL1 β overexpression on oxidative phosphorylation and glycolysis in a transgenic mouse model of chronic Barrett's-like oesophageal inflammation.
- 2) Examine the effect of manipulating IL1 β on p53 expression in a transgenic mouse model of chronic Barrett's-like oesophageal inflammation.
- 3) Assess the effect of IL1 β induction on HIF1 α expression in a transgenic mouse model of chronic Barrett-like oesophageal inflammation.
- 4) Investigate the effect of a high fat diet on the expression of same above cellular markers (ATP5B, GAPDH, p53, HIF1 α) in a transgenic mouse model of chronic Barrett's-like oesophageal inflammation.

6.3 MATERIALS AND METHODS

6.3.1 Wild-type and PL2-IL1 β mice

This work was performed in collaboration with Michael Quante (Technical University of Munich). All murine studies and breeding were carried out under the approval of the district government of Upper Bavaria (Regierung von Oberbayern) in the Medical Clinic at the Technical University of Munich. As depicted in figure 45, human *IL1 β* transgenic mice were generated in Columbia University, New York, by targeting the expression of human IL1 β to the oral cavity, oesophagus and forestomach using the Epstein Bar virus promoter. IL1 β cDNA consisted of a constitutively secreted form, not requiring caspase-1 cleavage, of mature human IL1 β fused with the signal sequence derived from structurally related human interleukin-1 receptor antagonist. These sequences were subcloned, along with the hGH/polyadenylation sequence, downstream of the EBV promoter into the pB-KS+ vector, linearised and injected into C57BL/6 x SJL F2 hybrid zygotes to generate two founder mice: wild type and PL2-IL1 β . All transgenic mice were on a pure C57/B6 background after 6 backcrosses. C57/B6 mice were purchased from Jackson Laboratories. Original founder mice were transferred to Munich, Germany from Columbia University, New York, USA. All mice utilised in this study were obtained from the Freising facility. Founder mice for colonies in Freising were originally obtained from Klinikum Rechts der Isar animal facility, Munich, Germany. Mice were introduced into the Freising SPF facility via embryo-transfer.

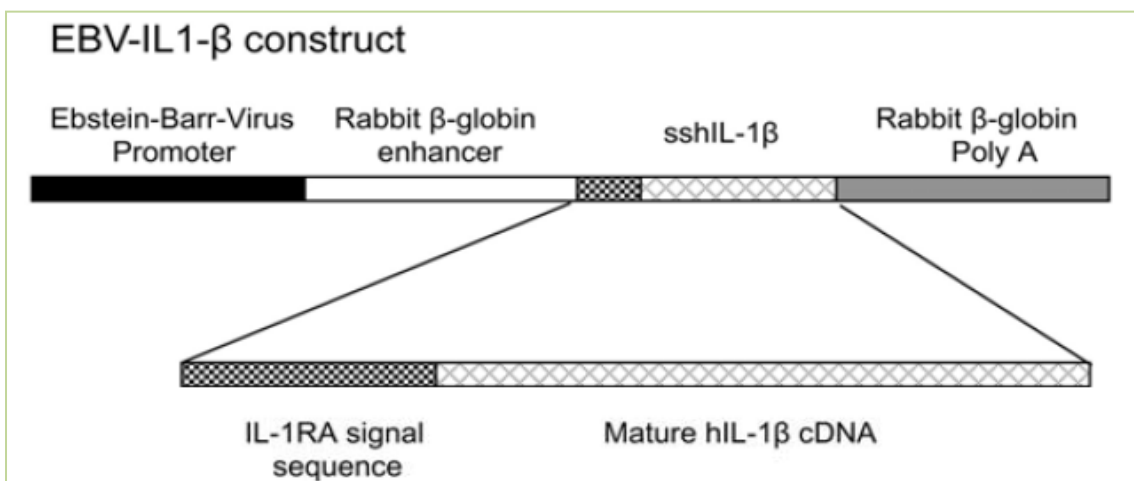


Figure 45. The Epstein Bar virus IL1 β construct. Human *IL1 β* transgenic mice were generated in the laboratory by targeting the expression of human IL1 β to the oral cavity, oesophagus and forestomach using the Epstein Bar virus promoter. Image: Quante *et al.*, 2012. *Cancer Cell* (69).

6.3.2 Maintenance of wild-type and PL2-IL1 β mice

Mice were handled in a sterile laminar flow hood (Interactive SafeChange Station, Tecniplast) within a specific-pathogen-free facility consisting of an animal room fully equipped to carry out the study. The animal room provides housing, breeding space and uses sterile water and food in addition to autoclaved microisolator cages. The entire facility is located behind a strict microbiologic barrier where admittance is strictly limited and all personal must wear sterile coveralls, gloves, masks, footwear covers and hats. Male and female mice were used for experimental and/or phenotyping purposes. All mice were kept at room temperature ($23\text{ }^{\circ}\text{C} \pm 1\text{ }^{\circ}\text{C}$) with an intermittent 12 hour light/dark cycle.

6.3.3 Experimental design

Wild-type and PL2-IL1 β mice were started on either a diet of chow (Ssniff, V1124-000) or on a high fat diet of chow supplemented with 20% palm oil (Ssniff, S5745-E712) from the ages of 6-8 weeks. Mice were allowed a pelleted lab chow diet from birth until weaning and water *ad libitum*. Following weaning between weeks 6 and 8 of age, mice were assigned an experimental or chow diet. Six mice (3 male and 3 female) ($n=6$) were maintained for each treatment group ($n=48$ total). Breeding pairs were also allowed a pelleted lab chow diet and water *ad libitum*. Experimental animals were housed in groups of 4 to 6 animals per cage (Tecniplasta, GM500). Wild-type and PL2-IL1 β were maintained strictly under these sterile and dietary conditions for 9 months (40 ± 2 weeks) and 12 months ($52\pm$ weeks) until mice were sacrificed. This study protocol can be summarised in figure 46. After 9 and/or 12 months, or until tumour progression with noticeable symptoms of disease such as cachexia and/or pain (erected fur and relieve posture), the mice were weighed and euthanized in a CO₂ chamber. The oesophagus and stomach were resected, dissected open exposing the inner part of the stomach and oesophagus, and were subsequently fixed with zinc formalin fixative (Polysciences, Inc.) overnight. Figures 47 and 48 show the anatomy of all male and female mice (48 mice total) respectively within the study post treatment prior to formalin fixation and paraffin embedding. Tissue samples were dehydrated with increasing concentrations of ethanol, xylol and paraffin in a Leica S300 tissue-processing unit. Finally, the formalin fixed organs were embedded in liquid paraffin and allowed to cool and harden. The formalin-fixed, paraffin-embedded (FFPE) blocks were stored at room temperature.

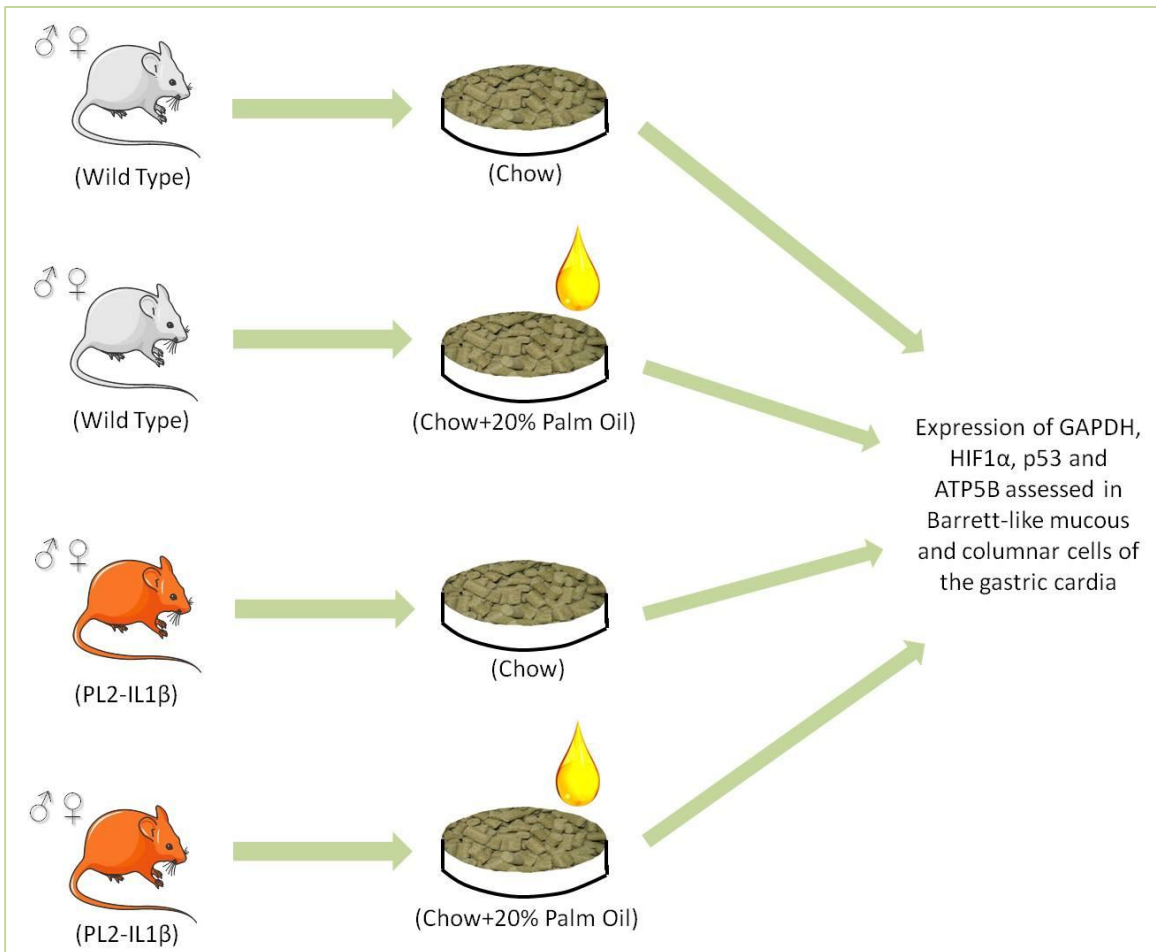


Figure 46. Study protocol. Human IL1 β transgenic C57/B6 mice were generated in the Medical Clinic laboratory at the Technical University of Munich by targeting the expression of human IL1 β to the oral cavity, oesophagus and forestomach using the Epstein Bar virus promoter. Both male and female wild-type and PL2-IL1 β mice were fed chow or a high fat diet consisting of chow supplemented with 20% palm oil for either 9 months (40 \pm 2 weeks) or 12 months (52 \pm 2 weeks) until mice were sacrificed. Subsequently, the expression profiles of the protein markers GAPDH, HIF1 α , p53 and ATP5B were assessed in Barrett-like **mucous** producing and **columnar** cells of the gastric cardia in each treatment group ($n=6$).

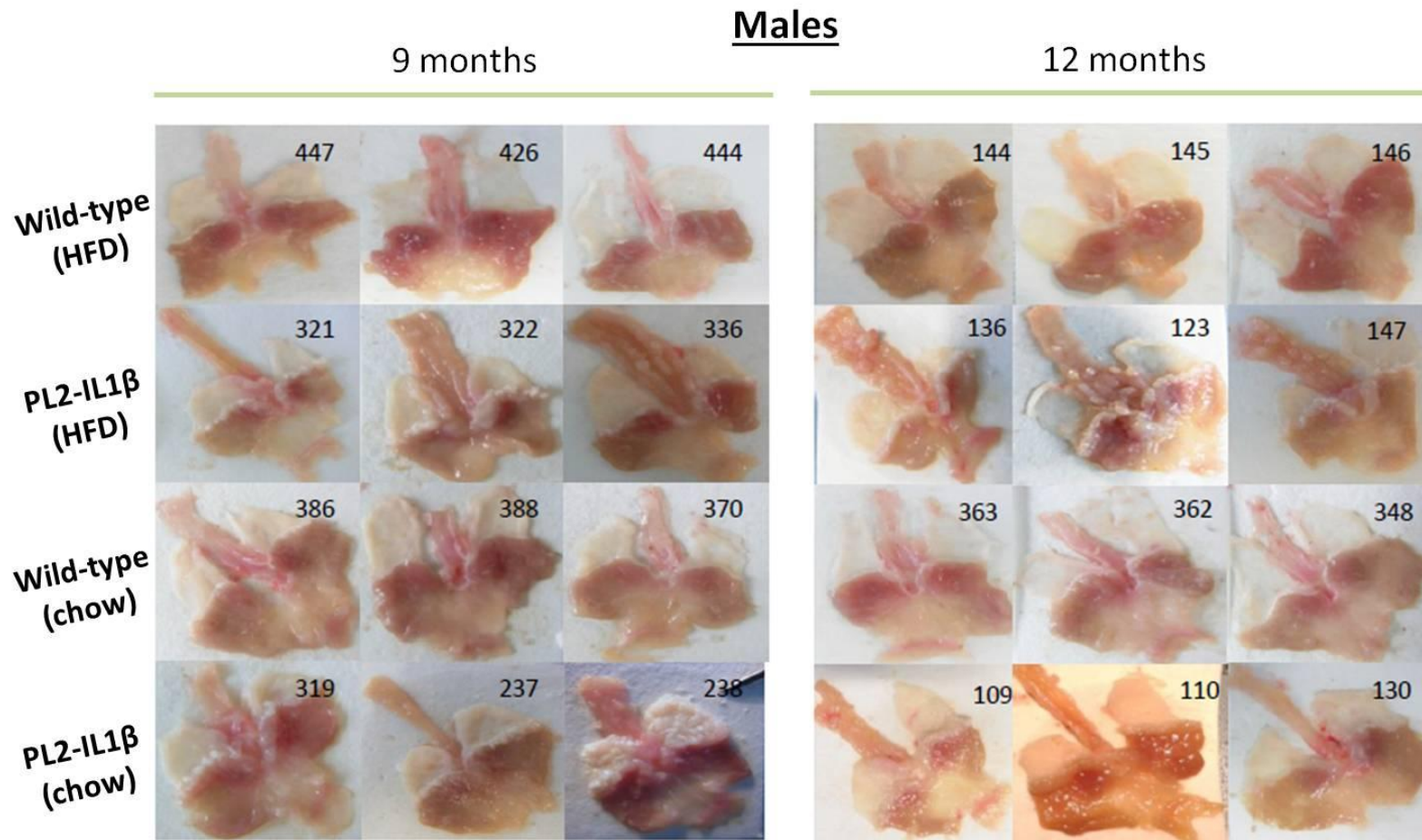


Figure 47. Anatomy of all male mice within the study post treatment prior to formalin fixation and paraffin embedding. Rows 1, 2, 3 and 4 correspond to the treatment groups; wild-type mice on a high fat diet, PL2-IL1 β mice on a high fat diet, wild-type mice on chow and PL2-IL1 β mice on chow respectively. Note the manifestation of neoplasms on the squamocolumnar junctions within mice overexpressing IL1 β (rows 2 and 4), for example mice 123 and 238, and those on a high fat diet (row 2), for example, mouse 322.

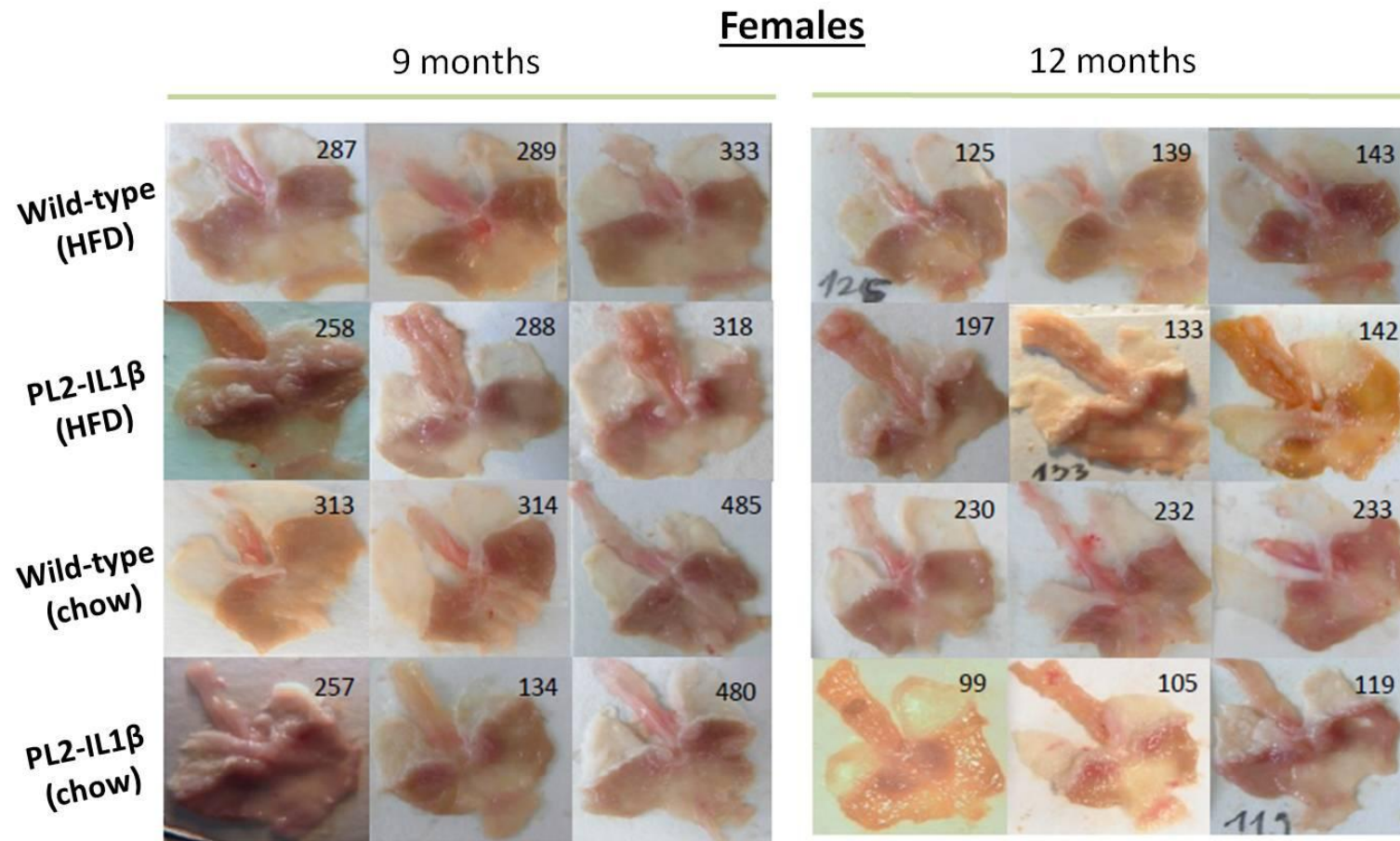


Figure 48. Anatomy of all female mice within the study post treatment prior to formalin fixation and paraffin embedding. Rows 1, 2, 3 and 4 correspond to the treatment groups; wild-type mice on a high fat diet, PL2-IL1 β mice on a high fat diet, wild-type mice on chow and PL2-IL1 β mice on chow respectively. Note the manifestation of neoplasms on the squamocolumnar junctions within mice overexpressing IL1 β (rows 2 and 4), for example mice 133 and 257, and those on a high fat diet (row 2), for example, mouse 258.

6.3.4 *Histopathological analysis*

FFPE-blocks were cut to 2-3 μ m on a microtome (Thermo scientific, Microm HM 355S) and transferred to a 50°C water bath for stretching and collected on microscopic glass slides (Thermo scientific). Sections were allowed to dry overnight. Following drying, slides were heated at 60°C for 60 minutes in a Heraeus Instruments Function line incubator (Thermo Scientific). The stomach and oesophagus from wild-type and PL2-IL1 β mice were subsequently stained with haematoxylin (Merck, Germany), eosin (Morphisto, Germany) and periodic acid Schiff (Roth, Germany). Histopathological features of the SCJ were graded semi-quantitatively by adapting a previously described scoring system for the murine stomach (Fox et al., 2000) by a pathologist who was blinded to the four treatment groups.

6.3.5 *Immunohistochemical analysis of ATP5B, GAPDH, p53 and HIF1 α*

Immunohistochemistry was performed utilising 9 month and 12 month old wild-type mice fed chow ($n=6$), wild-type mice fed a high fat diet of chow supplemented with 20% palm oil ($n=6$), PL2-IL1 β mice fed chow ($n=6$) and PL2-IL1 β mice fed a high fat diet of chow supplemented with 20% palm oil ($n=6$). Immunohistochemistry was performed on the slides utilising the Vectastain Kit (Elite) as described before (see section 3.3.4). Sections containing tissue of the same age were processed and stained on the same day. Primary antibodies included a rabbit anti-ATP5B IgG (SantaCruz Biotechnology), a rabbit anti-GAPDH IgG (AbDserotec Division of MorphoSys), a rabbit anti-p53 IgG (Abcam) and a rabbit anti-HIF1 α IgG (Abcam) diluted 1:200, 1:600, 1:50 and 1:150 in PBS respectively. Slides were scanned (Aperio Scan Scope System 5523-R, Technical University Munich) and immunoreactivity was assessed digitally under 40X magnification in a semi-quantitative manner for each protein by two observers (by James Phelan in Ireland and Natasha Stephens in Germany) who were blinded to the pathology and treatment groups of the study using Image Scope software. Prior to examining the expression of each protein, areas of mucous producing cells and columnar cells specifically within the gastric cardia were marked out on each slide to maintain a standardised immunohistochemical evaluation between observers. Figure 49 demonstrates the histology of wild-type mice (figure 49A) and PL2-IL1 β mice (figure 49B) fed a high fat diet at 12 months. For scoring purposes, we focused on the cardia region which included squamous epithelium, mucous producing cells and columnar epithelium. In wild-type mice, it was rare to see mucous producing cells. For each protein, mucous producing cells and columnar cells were evaluated for both percentage positivity and intensity of cytoplasmic staining. A third score, designated IxP, was obtained by multiplying intensity by positivity. Intensity was graded as 0 (negative), 1 (weak), 2 (moderate) and 3 (strong) and positivity was evaluated between 0-100%.

The scoring was undertaken by consensus evaluation with two replicate tissues scored per slide and the average value was calculated.

6.3.6 *Statistical analyses*

Data were analysed using Graph Pad Prism software (Graph Pad Prism, San Diego, CA). Immunohistochemical expression profiles of ATP5B, GAPDH, p53 and HIF1 α were statistically analysed between treatment groups utilising unpaired *t*-tests. Non-repeated two way ANOVA tests assessed for interactions between diets and mouse models. Differences of $P < 0.05$ (*), $P < 0.01$ (**) and $P < 0.001$ (***) were considered statistically significant.

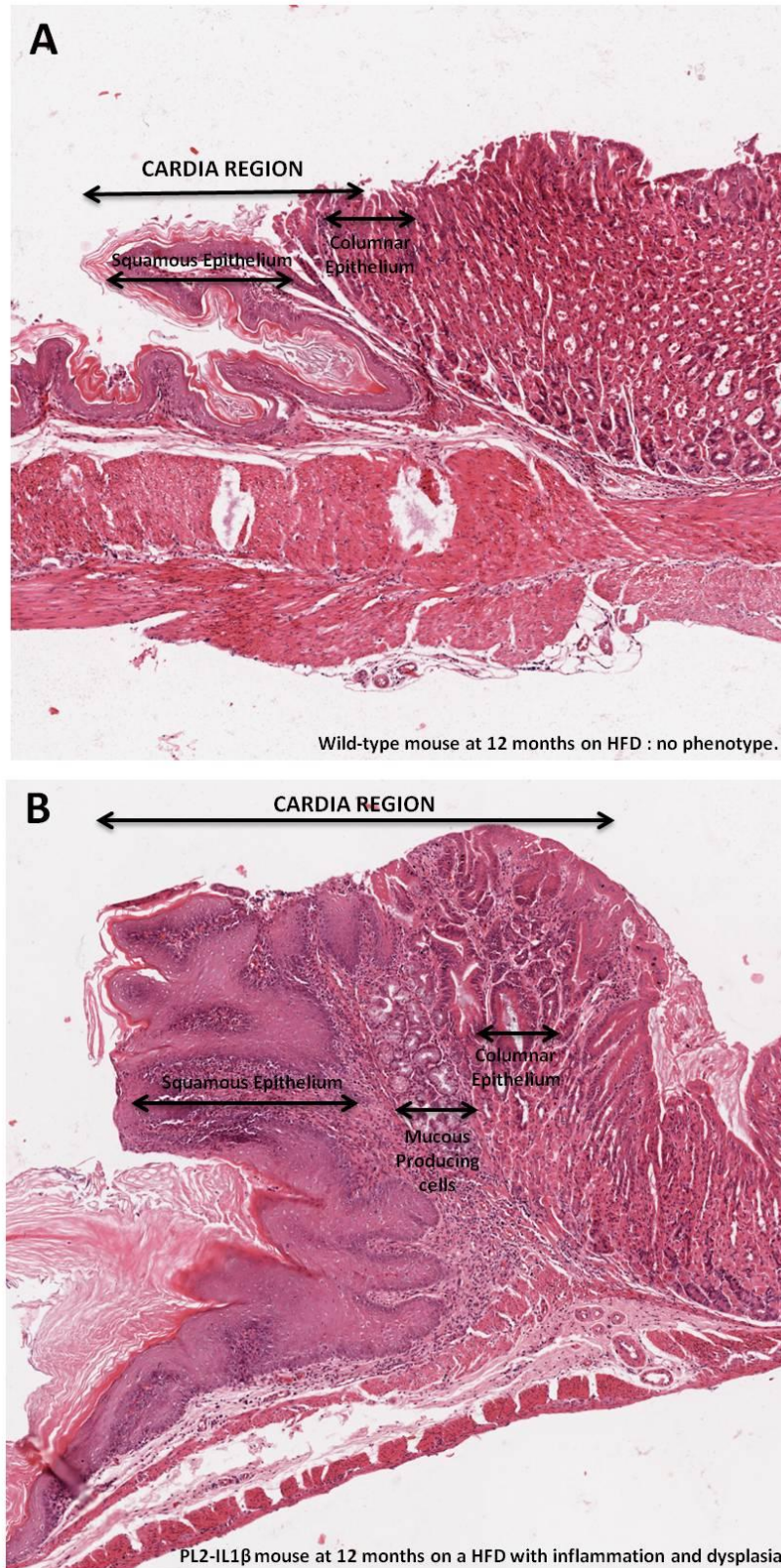


Figure 49. Histology of PL2-IL1 β and wild-type mice. (A) Histopathology of a wild-type mouse on a high fat diet. In wild-type mice, it was rare to see mucous producing cells. This was observed on occasion in high fat fed mice where only a few mucous producing cells were present. **(B)** Histopathology of a PL2-IL1 β mouse on a high fat diet at 12 months. For scoring purposes, we focused on the cardia region. The cardia region included squamous epithelium, mucous producing cells and columnar epithelium. Five columnar epithelial crypts was the cut off for scoring columnar epithelium.

6.4 RESULTS

6.4.1 Examining the effect of IL1 β overexpression and diet on glycolytic profiles in transgenic mice

To assess the effect of IL1 β overexpression on glycolysis, levels of GAPDH were assessed in mucous producing and columnar cells of the gastric cardia at two different time points, in 9 month and 12 month old mice, subsequent to induction of IL1 β expression. Figure 50 examines the functional effect of IL1 β induction on glycolytic profiles between transgenic wild-type and PL2-IL1 β mice. In chow fed mice at 9 months, induction of IL1 β expression had no significant effect on GAPDH IxP expression in mucous producing cells of IL1 β mice compared to wild-type mice (figure 50A) ($P>0.05$), however, induction of IL1 β expression significantly increased GAPDH IxP expression within columnar cells (figure 50B) ($P=0.0007$). Induction of IL1 β expression significantly increased GAPDH intensity in mucous producing cells in mice fed a high fat diet only at 12 months (figure 50C) ($P=0.048$). Overexpression of IL1 β had no significant effect on GAPDH intensity in IL1 β mice compared to wild-type mice in the columnar cells of mice fed a high fat diet at 12 months (figure 50D) ($P>0.05$).

Figure 51 investigates the effect of a high fat diet on glycolytic profiles in transgenic wild-type and PL2-IL1 β mice. A high fat diet had no significant effect on GAPDH positivity in mucous producing cells of wild-type mice at 9 months (figure 51A) ($P>0.05$), however, a high fat diet significantly increased GAPDH positivity in columnar cells (figure 51B) ($P=0.01$). PL2-IL1 β mice on a high fat diet exhibited significantly decreased GAPDH IxP expression (figure 51C) ($P=0.027$) and GAPDH positivity (figure 51D) ($P=0.001$) in mucous producing cells and columnar cells respectively at 9 months only. Supplementation with a high fat diet significantly increased GAPDH IxP expression in mucous producing cells in PL2-IL1 β mice at 12 months only (figure 51E) ($P=0.018$), however, a high fat diet had no significant effect on GAPDH IxP expression in columnar cells (figure 51F) ($P>0.05$). At 12 months, GAPDH expression within mucous producing cells was lower in PL2-IL1 β mice on a chow diet (figure 51G) compared to those on a high fat diet (figure 51H).

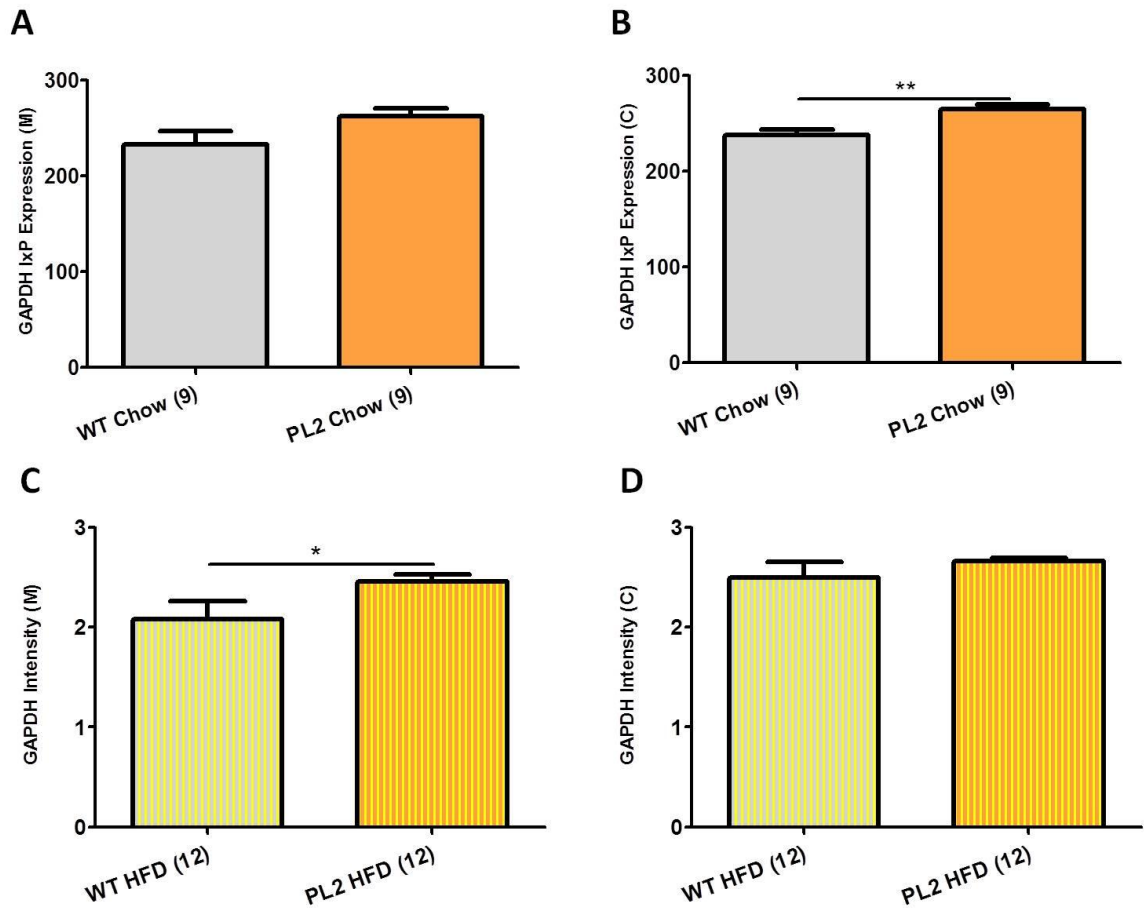


Figure 50. Examining the functional effect of IL1 β induction on glycolytic profiles between transgenic wild-type and IL1 β mice. (A) Induction of IL1 β expression had no significant effect on GAPDH IxP expression in the **mucous** producing cells of chow fed mice at 9 months ($P > 0.05$). **(B)** In **columnar** cells of chow fed mice at 9 months, induction of IL1 β expression significantly increased GAPDH IxP expression ($P = 0.0007$). **(C)** In the **mucous** producing cells of mice fed on a high fat diet at 12 months, induction of IL1 β expression significantly increased GAPDH intensity ($P = 0.048$). **(D)** Induction of IL1 β expression had no significant effect on GAPDH intensity in the **columnar** cells of mice fed a high fat diet at 12 months ($P > 0.05$). Unpaired *t*-tests. Bars denote mean \pm SEM. M=mucous producing cells; C=columnar cells.

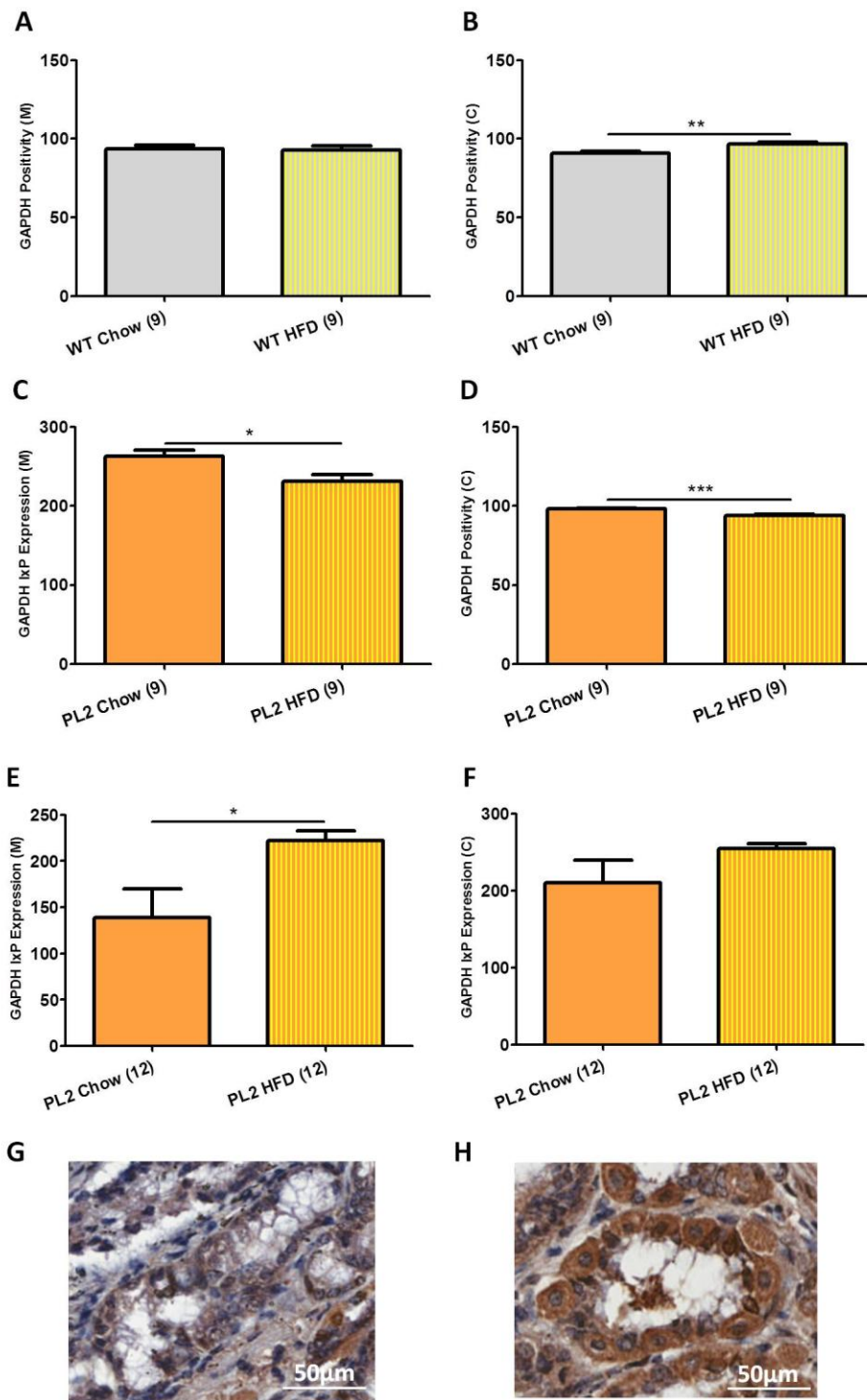


Figure 51. Investigating the effect of a high fat diet on glycolytic profiles in transgenic wild-type and IL1 β mice. (A) A high fat diet had no significant effect on GAPDH positivity in **mucous** producing cells of wild-type mice at 9 months ($P>0.05$). (B) Supplementation with a high fat diet significantly increased GAPDH positivity in the **columnar** cells of wild-type mice at 9 months ($P=0.01$). (C) Supplementation with a high fat diet significantly decreased GAPDH IxP expression in **mucous** producing cells of PL2-IL1 β mice at 9 months ($P=0.027$). (D) Supplementation with a high fat diet significantly decreased GAPDH positivity in **columnar** cells of PL2-IL1 β mice at 9 months ($P=0.001$). (E) Supplementation with a high fat diet significantly increased GAPDH IxP expression in **mucous** producing cells of PL2-IL1 β mice at 12 months ($P=0.018$). (F) A high fat diet had no significant effect on GAPDH IxP expression in **columnar** cells of PL2-IL1 β mice at 12 months ($P>0.05$). (G) GAPDH IxP expression within **mucous** producing cells of mice on a chow diet at 12 months. (H) GAPDH IxP expression within **mucous** producing cells of mice on a high fat diet at 12 months. Unpaired t -tests. Bars denote mean \pm SEM. M=mucous producing cells; C=columnar cells.

6.4.2 Assessing the effect of IL1 β overexpression and diet on oxidative phosphorylation in transgenic mice

Next we investigated the effect of IL1 β overexpression on the alternate energy metabolism pathway, oxidative phosphorylation, by assessing ATP5B expression levels in mucous producing and columnar cells of the gastric cardia at two different time points, in 9 month and 12 month old mice, subsequent to induction of IL1 β expression. Figure 52 examines the effect of IL1 β induction on ATP5B between transgenic wild-type and PL2-IL1 β mice. As the representative figures 52A and 52B respectively show, overexpression of IL1 β decreased ATP5B positivity within mucous producing cells of mice at 12 months. In mucous producing cells (figure 52C) and columnar cells (figure 52D) of mice fed a high fat diet, induction of IL1 β expression significantly decreased ATP5B positivity ($P=0.021$) and ATP5B IxP expression ($P=0.005$) respectively at 12 months. Induction of IL1 β expression had no significant effect on ATP5B intensity within columnar cells of chow fed mice at 9 months (figure 52E) ($P>0.05$), however, induction of IL1 β expression significantly decreased ATP5B intensity in mice at 12 months (figure 52F) ($P=0.018$).

Figure 53 illustrates the effect of a high fat diet on oxidative phosphorylation in transgenic wild-type and PL2-IL1 β mice. We found that supplementation with a high fat diet does not significantly affect ATP5B positivity in the columnar cells of wild-type mice at 9 months (figure 53A) or at 12 months (figure 53B) ($P>0.05$). Interestingly, supplementation with a high fat diet did significantly decrease ATP5B positivity in mucous producing cells of PL2-IL1 β mice only at 12 months (figure 53C) ($P=0.027$). A high fat diet showed no significant effect on ATP5B positivity in columnar cells of PL2-IL1 β mice at 12 months (figure 53D) ($P>0.05$). Figure 54 summarises the effect of IL1 β manipulation on metabolism in wild-type and PL2-IL1 β mice. Moreover, figure 55 summaries the effect of a high fat diet on metabolism in wild-type and PL2-IL1 β mice.

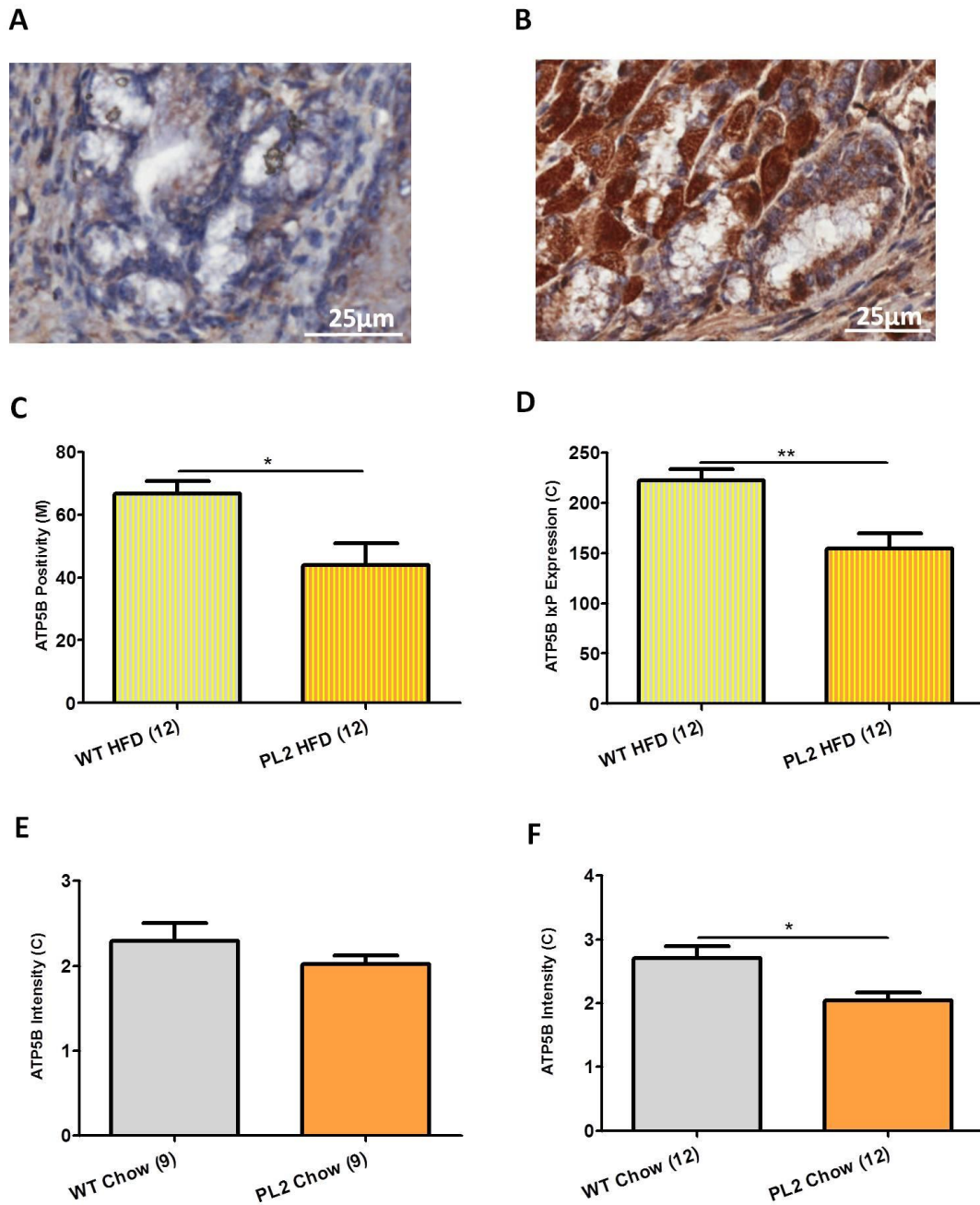


Figure 52. Examining the functional effect of IL1 β induction on oxidative phosphorylation between transgenic wild-type and IL1 β mice. (A) Overexpression of IL1 β decreases ATP5B positivity in **mucous** producing cells of mice fed a high fat diet versus **(B)** wild-type controls at 12 months. **(C)** In the **mucous** producing cells of mice fed a high fat diet, induction of IL1 β expression significantly decreased ATP5B positivity at 12 months ($P=0.021$). **(D)** In the **columnar** cells of mice fed a high fat diet, induction of IL1 β expression significantly decreased ATP5B IxP expression at 12 months ($P=0.005$). **(E)** Induction of IL1 β expression had no significant effect on ATP5B intensity within **columnar** cells of chow fed mice at 9 months ($P>0.05$). **(F)** In the **columnar** cells of chow fed mice, induction of IL1 β expression significantly decreased ATP5B intensity at 12 months ($P=0.018$). Unpaired t -tests. Bars denote mean \pm SEM. M=mucous producing cells; C=columnar cells.

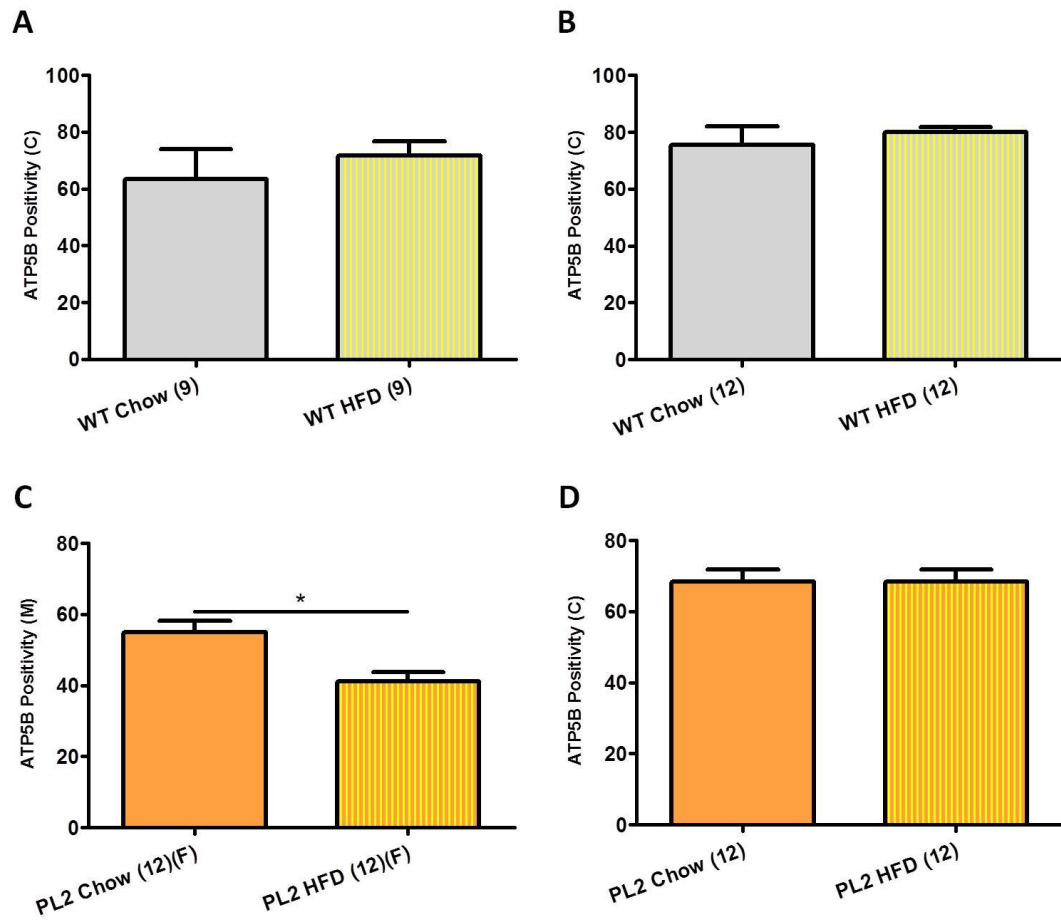


Figure 53. Investigating the effect of a high fat diet on oxidative phosphorylation in transgenic wild-type and IL1 β mice. (A) Supplementation with a high fat diet did not significantly affect ATP5B positivity in the **columnar** cells of wild-type mice at 9 months ($P>0.05$). **(B)** A high fat diet had no significant effect on ATP5B positivity in **columnar** cells of wild-type mice at 12 months ($P>0.05$). **(C)** Supplementation with a high fat diet significantly decreased ATP5B positivity in **mucous** producing cells of female PL2-IL1 β mice at 12 months ($n=3$) ($P=0.027$). **(D)** A high fat diet had no significant effect on ATP5B positivity in **columnar** cells of PL2-IL1 β mice at 12 months ($P>0.05$). Unpaired t -tests. Bars denote mean \pm SEM. M=mucous producing cells; C=columnar cells.

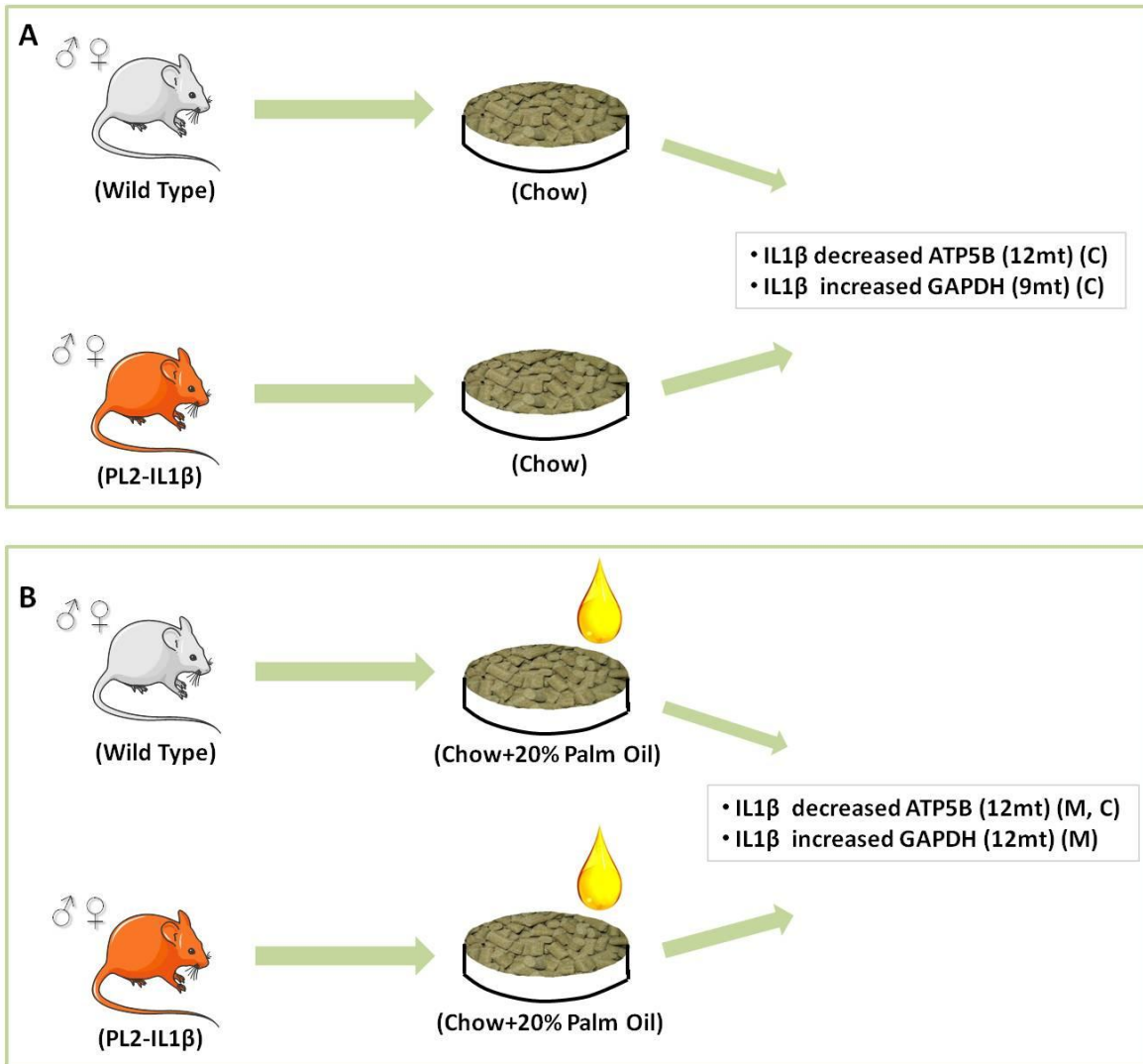


Figure 54. Summarising the effect of IL1 β manipulation on metabolism in mice fed chow (A) and high fat (B) diets. (A) In **columnar** cells, induction of IL1 β expression decreased ATP5B in mice at 12 months and increased GAPDH in mice at 9 months. Induction of IL1 β expression did not affect ATP5B or GAPDH in **mucous** producing cells. **(B)** In both **mucous** producing and **columnar** cells, induction of IL1 β decreased ATP5B expression. Moreover, induction of IL1 β increased GAPDH expression in the **mucous** producing cells of mice at 12 months. M=mucous producing cells; C=columnar cells.

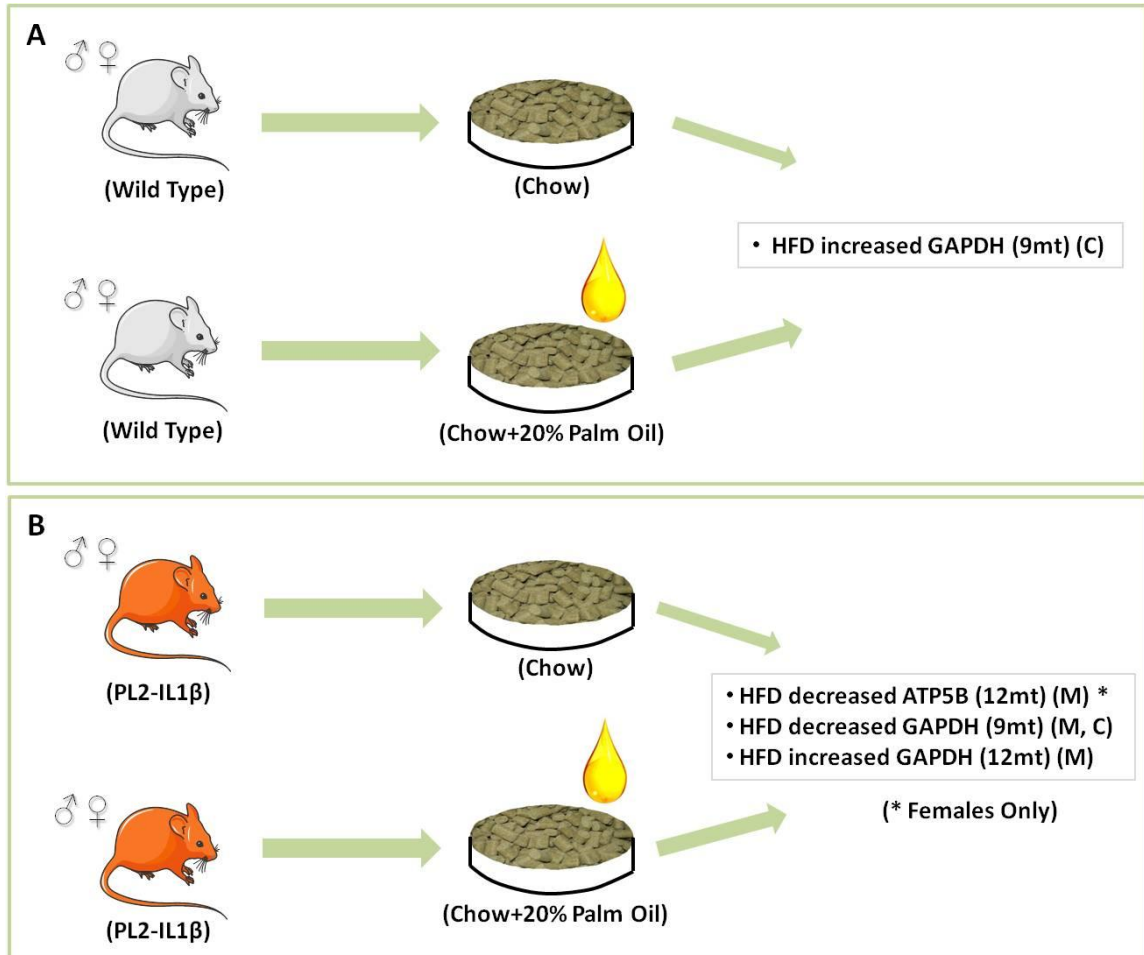


Figure 55. Summarising the effect of a high fat diet on metabolism in wild-type (A) and PL2-IL1β (B) mice. (A) Supplementation with a high fat diet induced higher GAPDH levels within **columnar** cells of mice at 9 months. A high fat diet had no effect on the expression levels of ATP5B. (B) Supplementation with a high fat diet induced higher GAPDH levels in the **mucous** producing cells of mice at 12 months. Moreover, a high fat diet decreased GAPDH expression in **columnar** and **mucous** producing cells of mice at 9 months. In **mucous** producing cells of female mice at 12 months, a high fat diet decreased the expression of ATP5B. M=mucous producing cells; C=columnar cells.

6.4.3 Examining the effect of IL1 β overexpression and diet on p53 expression in transgenic mice

Furthermore, we examined the effect of IL1 β induction on p53 expression in mucous producing and columnar cells of the gastric cardia at two different time points, in 9 month and 12 month old mice. Figure 56 examines the functional effect of IL1 β induction on p53 expression between transgenic wild-type and PL2-IL1 β mice. Despite overexpression of IL1 β having no significant effect on p53 positivity in mucous producing cells of mice fed a high fat diet at 9 months (figure 56A) ($P>0.05$), induction of IL1 β expression significantly decreased p53 intensity in columnar cells (figure 56B) ($P=0.047$). In addition, in mucous producing cells of mice on a high fat diet, induction of IL1 β expression had no significant effect on p53 positivity in wild-type mice at 12 months (figure 56C) ($P>0.05$), however, induction of IL1 β expression significantly decreased p53 positivity in columnar cells (figure 56D) ($P=0.026$). In chow fed mice, induction of IL1 β expression had no significant effect on p53 intensity in mucous producing cells at 9 months (figure 56E) or on p53 positivity at 12 months (figure 56F) ($P>0.05$).

Figure 57 displays the effect of a high fat diet on p53 expression in transgenic wild-type and PL2-IL1 β mice. Supplementation with a high fat diet significantly increased p53 IxP expression in mucous producing cells of PL2-IL1 β mice at 12 months (figure 57A) ($P=0.0496$), however, the high fat diet did not affect p53 IxP expression in columnar cells (figure 57B) ($P>0.05$). As the representative images show, mucous producing cells of PL2-IL1 β mice on a high fat diet exhibited higher p53 intensity levels (figure 57D) than PL2-IL1 β mice on a chow diet at 12 months (figure 57C). Diet had no significant effect on p53 IxP expression levels in columnar cells of wild-type mice at 9 months (figure 57E) or 12 months (figure 57F) ($P>0.05$). Figure 58 summarises the effect of IL1 β overexpression and a high fat diet on p53 expression in wild-type and PL2-IL1 β mice.

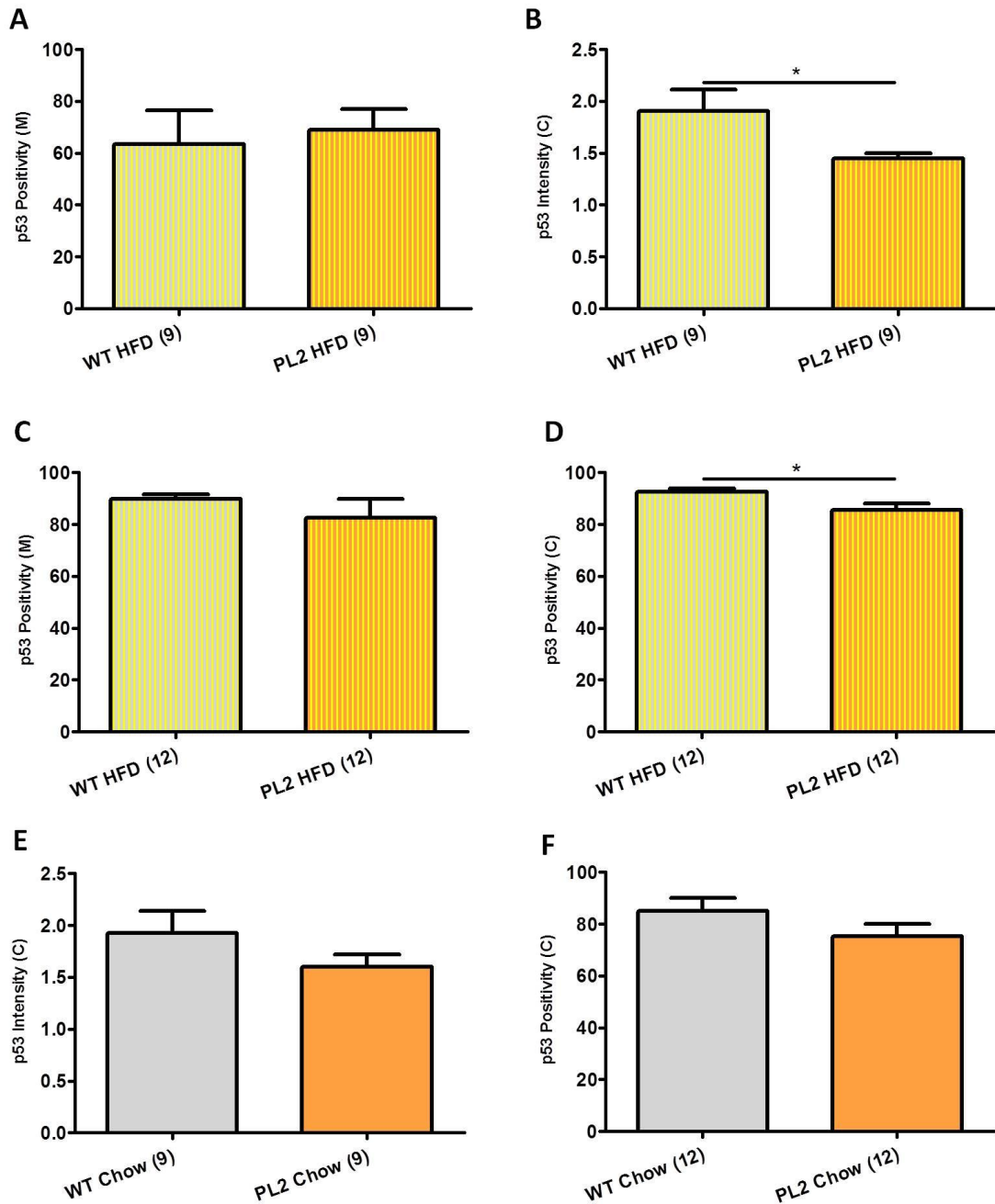


Figure 56. Examining the functional effect of IL1 β induction on p53 expression between transgenic wild-type and IL1 β mice. (A) Induction of IL1 β expression had no significant effect on p53 positivity in **mucous** producing cells of mice fed a high fat diet at 9 months ($P > 0.05$). **(B)** In the **columnar** cells of mice fed a high fat diet, induction of IL1 β expression significantly decreased p53 intensity at 9 months ($P = 0.047$). **(C)** Induction of IL1 β expression had no significant effect on p53 positivity in IL1 β versus wild-type mice within **mucous** producing cells of mice fed a high fat diet at 12 months ($P > 0.05$). **(D)** In the **columnar** cells of mice fed a high fat diet, induction of IL1 β expression significantly decreased p53 positivity at 12 months ($P = 0.026$). In chow fed mice, induction of IL1 β expression had no significant effect on p53 intensity in **mucous** producing cells of mice at 9 months **(E)** or p53 positivity in mice at 12 months **(F)** ($P > 0.05$). Unpaired *t*-tests. Bars denote mean \pm SEM. M=mucous producing cells; C=columnar cells.

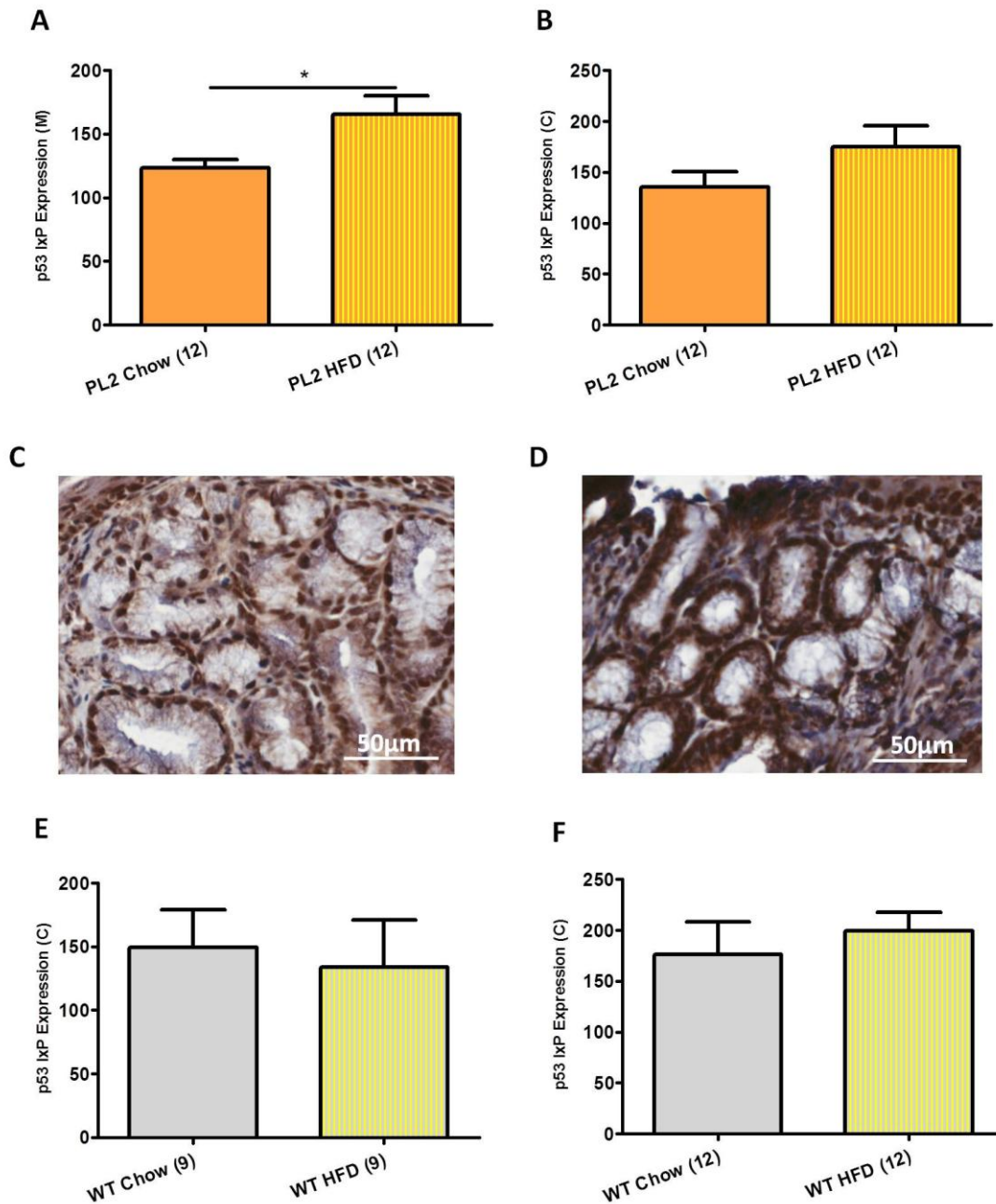


Figure 57. Investigating the effect of a high fat diet on p53 in transgenic wild-type and IL1 β mice. (A) Supplementation with a high fat diet significantly increased p53 IxP expression in **mucous** producing cells of PL2-IL1 β mice at 12 months ($P=0.0496$). **(B)** Supplementation with a high fat diet did not significantly affect p53 IxP expression in **columnar** cells of PL2-IL1 β mice at 12 months ($P>0.05$). PL2-IL1 β mice fed a high fat diet **(D)** exhibited higher p53 intensity levels in **mucous** producing cells versus those PL2-IL1 β mice on a chow diet **(C)** at 12 months. **(E)** Diet had no significant effect on p53 IxP expression levels in **columnar** cells of wild-type mice at 9 months and **(F)** wild-type mice at 12 months ($P>0.05$). Unpaired *t*-tests. Bars denote mean \pm SEM. M=mucous producing cells; C=columnar cells.

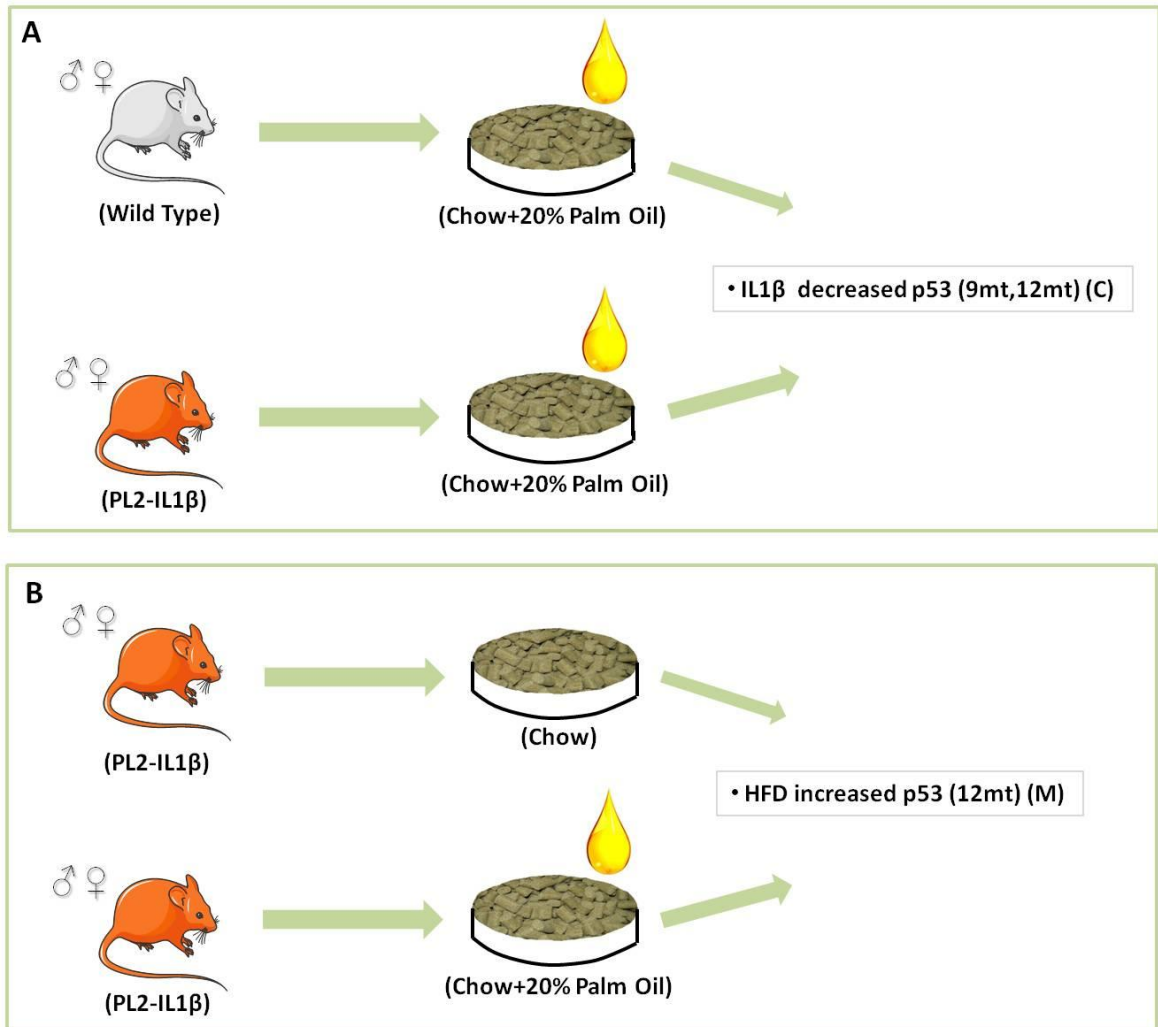


Figure 58. Summarising the effect of IL1 β overexpression and a high fat diet on p53 expression in wild type and PL2-IL1 β mice. (A) Induction of IL1 β decreased p53 expression in the columnar cells of mice at 9 and 12 months. (B) Supplementation with a high fat diet induced higher p53 levels in the mucous producing cells of mice overexpressing IL1 β at 12 months. M=mucous producing cells; C=columnar cells.

6.4.4 Examining the effect of IL1 β overexpression and diet on hypoxia in transgenic mice

To assess the effect IL1 β induction on the levels of HIF1 α , HIF1 α expression was assessed in mucous producing and columnar cells of the gastric cardia at two different time points, in 9 month and 12 month old mice, subsequent to induction of IL1 β expression. Figure 59 examines the functional effect of IL1 β induction on HIF1 α expression between transgenic wild-type and PL2-IL1 β mice. Induction of IL1 β expression had no significant effect on HIF1 α IxP expression in columnar cells of chow fed mice at 9 months (figure 59A) ($P>0.05$). However, in the columnar cells of chow fed mice, induction of IL1 β expression significantly increased HIF1 α IxP expression at 12 months (figure 59B) ($P=0.049$). The representative images illustrate that induction of IL1 β (figure 59D) increases HIF1 α positivity in columnar cells of chow fed mice at 12 months compared to wild-type mice (figure 59C). Moreover, in mucous producing cells (figure 59E) ($P=0.032$) and columnar cells (figure 59F) ($P=0.008$) of mice fed a high fat diet, induction of IL1 β expression significantly increased HIF1 α IxP expression at 12 months.

Figure 60 shows the effect of a high fat diet on HIF1 α expression in transgenic wild-type and PL2-IL1 β mice. Diet had no significant effect on HIF1 α positivity in the columnar cells of mice at 9 months (figure 60A) or at 12 months (figure 60B) ($P>0.05$). Furthermore, diet did not affect HIF1 α positivity in columnar cells (figure 60C) or mucous producing cells (figure 60D) of PL2-IL1 β mice after 12 months ($P>0.05$). Figure 61 summarises the effect of IL1 β overexpression and a high fat diet on HIF1 α expression in wild-type and PL2-IL1 β mice. Statistical analyses detected no significant interactions between mouse models (wild-type/PL2-IL1 β) and diet on ATP5B, p53 or HIF1 α expression profiles throughout the study, however, mouse models and diets were shown to significantly affect GAPDH positivity (figure 62A) ($P=0.0003$) and GAPDH IxP expression (figure 62B) ($P=0.018$) in mice at 9 months.

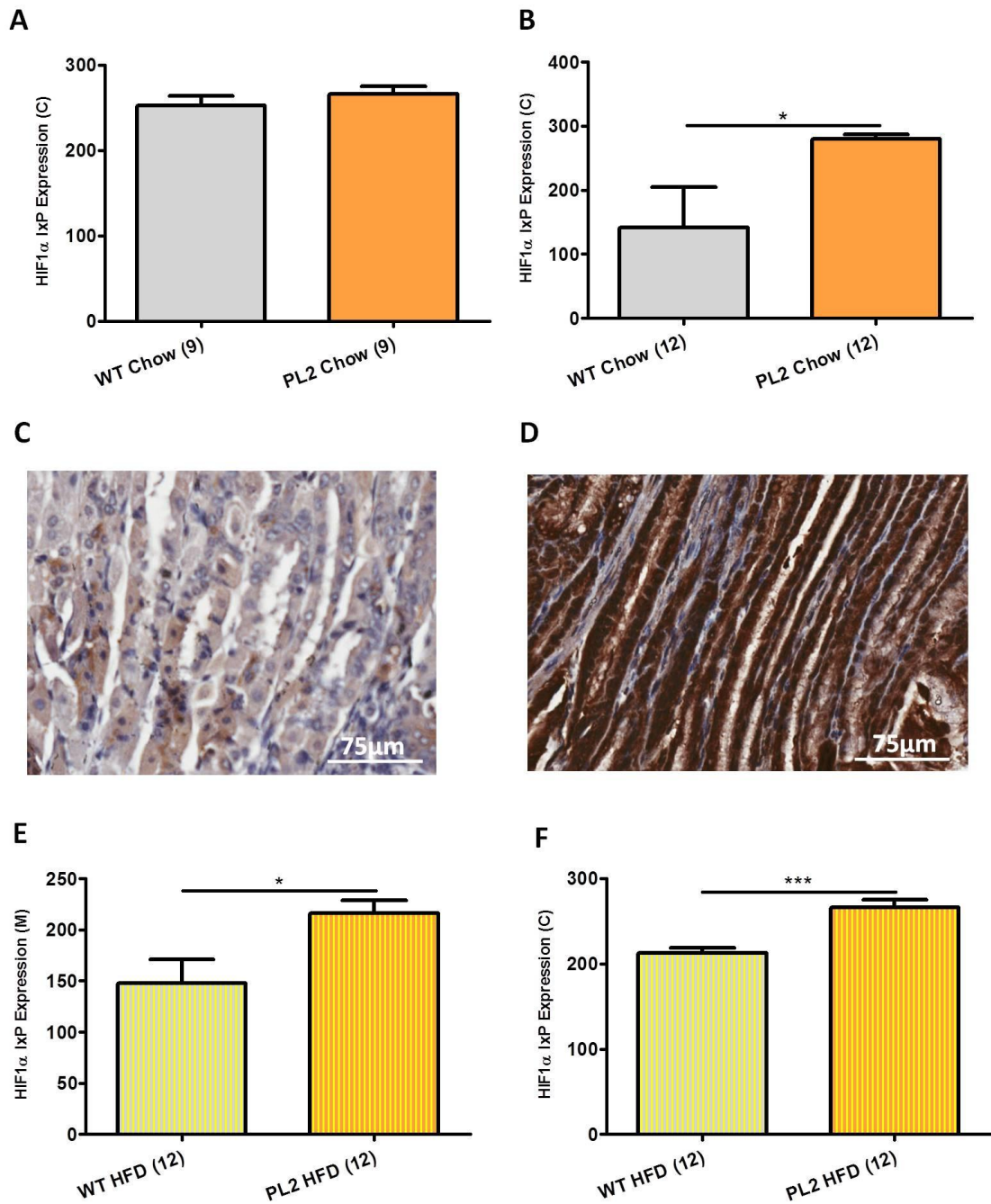


Figure 59. Examining the functional effect of IL1β induction on HIF1α expression between transgenic wild-type and IL1β mice. (A) Induction of IL1β expression had no significant effect on HIF1α IxP expression in **columnar** cells of chow fed mice at 9 months ($P>0.05$). **(B)** In the **columnar** cells of chow fed mice at 12 months, induction of IL1β expression significantly increased HIF1α IxP expression ($P=0.049$). **(C)** HIF1α positivity in the **columnar** cells of chow fed mice is lower in wild-type mice versus **(D)** mice overexpressing IL1β at 12 months. **(E)** In **mucous** producing cells ($P=0.032$) and **(F)** **columnar** cells ($P=0.008$) of mice fed a high fat diet, induction of IL1β expression significantly increased HIF1α IxP expression at 12 months. Unpaired *t*-tests. Bars denote mean \pm SEM. M=mucous producing cells; C=columnar cells.

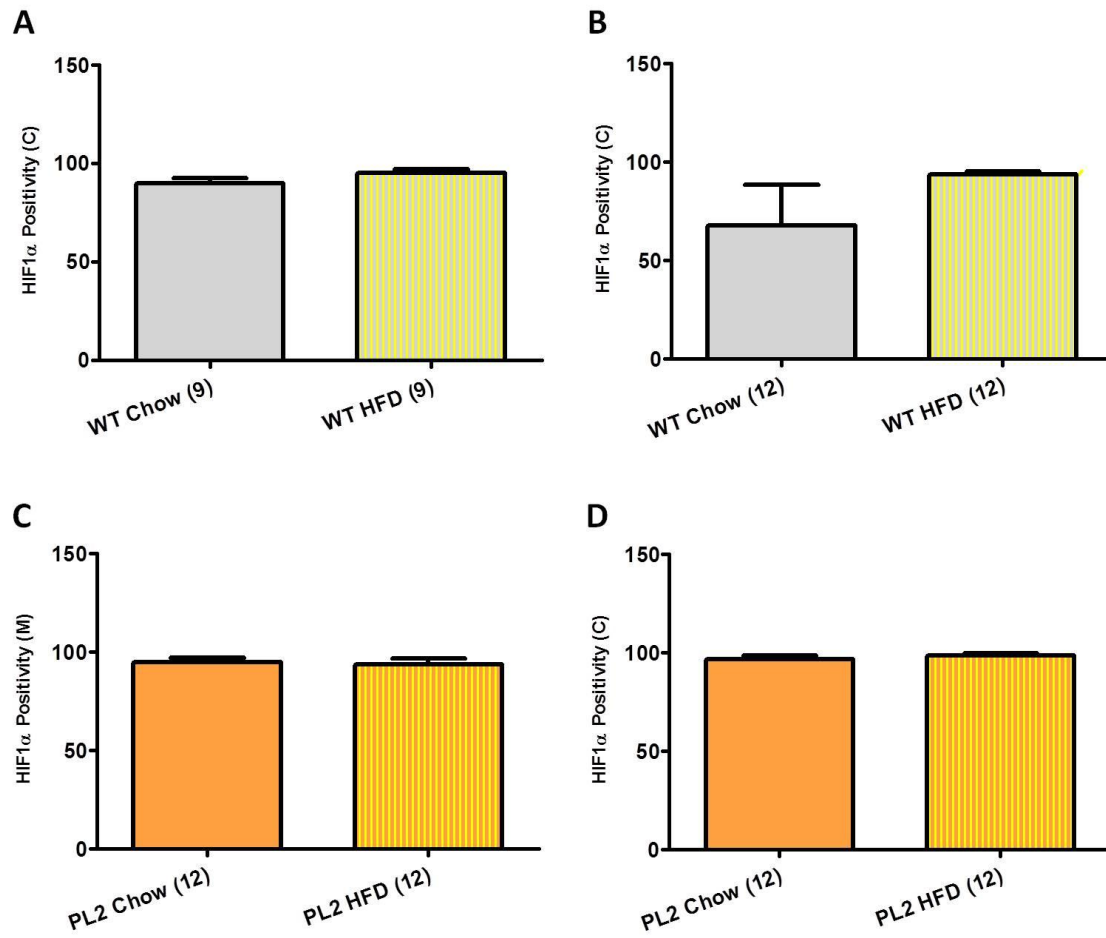


Figure 60. Investigating the effect of a high fat diet on HIF1 α in transgenic wild-type and IL1 β mice. (A) Diet had no significant effect on HIF1 α positivity in **columnar** cells of wild-type mice at 9 months **(B)** or at 12 months ($P>0.05$). Diet had no significant effect on HIF1 α positivity in **(C) columnar** cells and **(D) mucous** producing cells of PL2-IL1 β mice at 12 months ($P>0.05$). Unpaired t -tests. Bars denote mean \pm SEM. M=mucous producing cells; C=columnar cells.

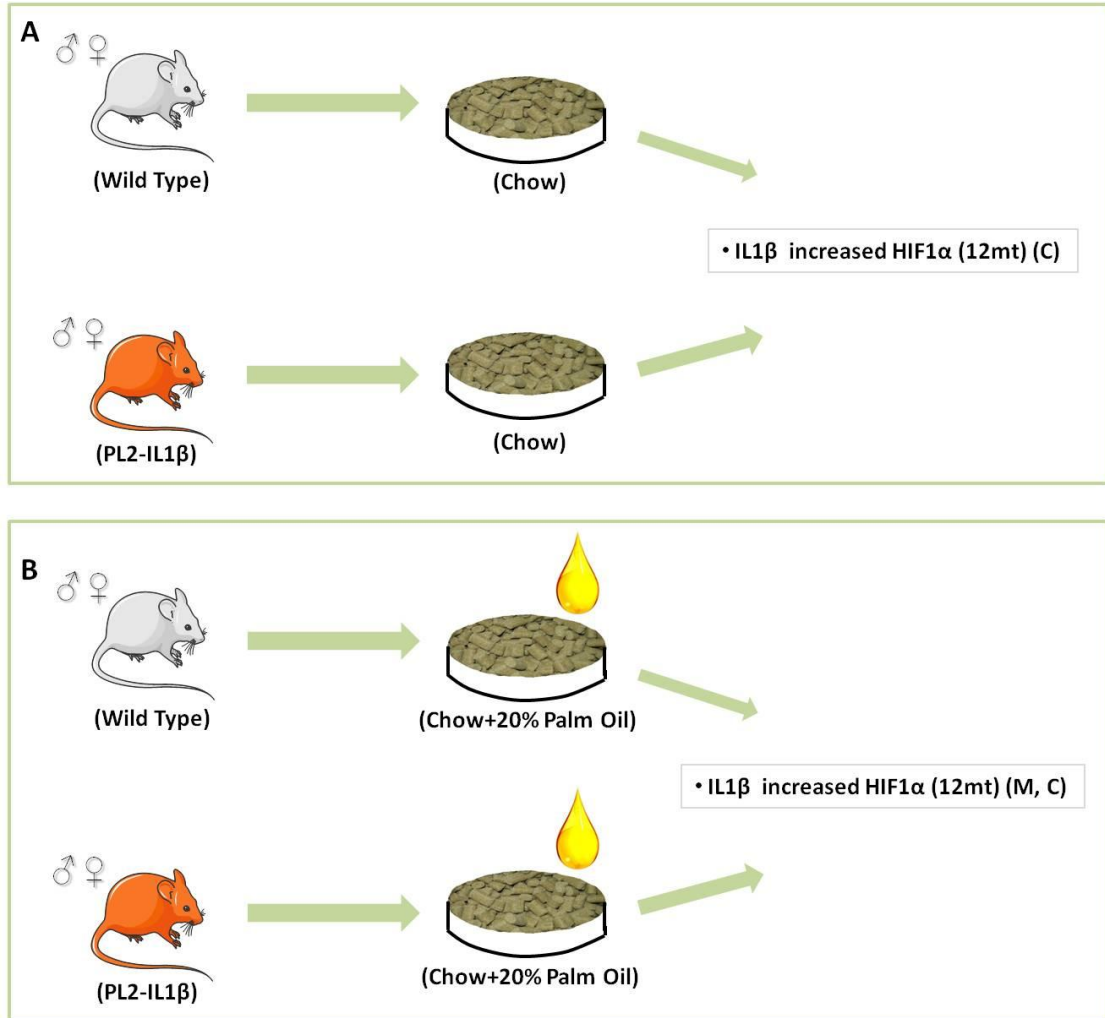


Figure 61. Summarising the effect of IL1 β manipulation and diet on HIF1 α expression in wild type and transgenic mice. (A) In columnar cells, induction of IL1 β expression increased HIF1 α in mice at 12 months. Induction of IL1 β expression did not affect HIF1 α in mucous producing cells. (B) In both mucous producing and columnar cells, induction of IL1 β increased HIF1 α expression in mice at 12 months. Altering diet had no effect on the expression levels of HIF1 α . M=mucous producing cells; C=columnar cells.

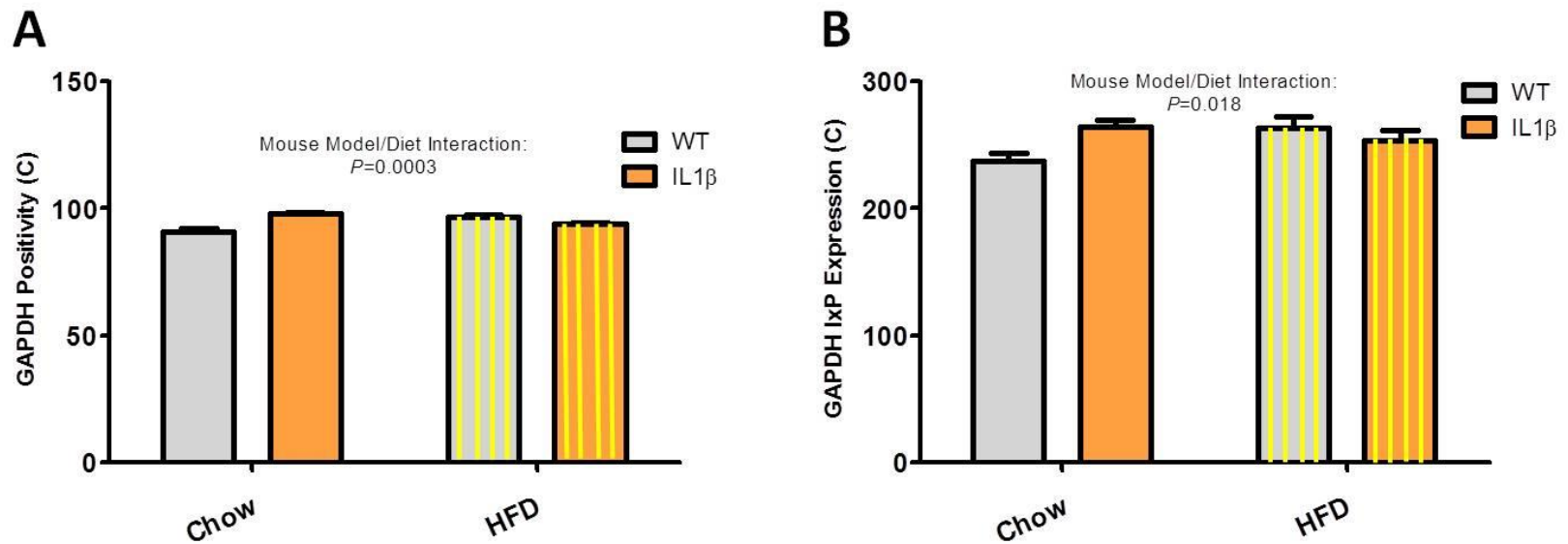


Figure 62. Investigating the interaction between transgenic mouse models and diet and their effect on glycolysis. (A) Interactive analyses between mouse models (wild-type/PL2-IL1 β) and diets were shown to significantly affect GAPDH positivity in mice at 9 months ($P=0.0003$). (B) Interactive analyses between mouse models (wild-type/PL2-IL1 β) and diets were shown to significantly affect GAPDH IxP expression in mice at 9 months ($P=0.018$). Non-repeated measures two-way ANOVA tests. Bars denote mean \pm SEM. C=columnar cells.

6.5 DISCUSSION

Ascertaining the precise mechanisms into how Barrett's oesophagus supports neoplastic progression to OAC may help identify how key cellular processes are modulated within an inflammatory microenvironment to support the development of OAC and may thereby provide better insight into the development of targeted therapies influencing these complex integral cellular processes. Utilising a transgenic mouse model of Barrett's oesophagus, we have shown that induction of inflammation through IL1 β manipulation can specifically modulate glycolysis, oxidative phosphorylation, p53 and HIF1 α . The study also demonstrates that a high fat diet can alter these processes providing further insight into the potential role of obesity in exacerbating disease progression. These results functionally demonstrate that inflammation and a high fat diet may potentially operate independently to support neoplastic progression within the microenvironment of Barrett's oesophagus.

In chapter 5, we showed significant associations between inflammation, energy metabolism, HIF1 α , p53 and obesity status in the Barrett's tissue microenvironment within patients with Barrett's oesophagus. To build on this data and to functionally show a relationship between these processes, we investigated the effect of manipulating IL1 β and diet on energy metabolism, p53 and hypoxia in a transgenic mouse model of chronic oesophageal inflammation in collaboration with the Quante lab in the Technical University of Munich, Germany. Targeted overexpression of IL1 β to the oral cavity, oesophagus and forestomach in this transgenic C57/B6 mouse model induces a Barrett's-like metaplasia at the SCJ that results in various histopathological and gene signatures closely resembling human Barrett's oesophagus (69).

Even though this PL2-IL1 β mouse model doesn't exhibit classical goblet cells, PL2-IL1 β mice develop severe columnar metaplasia along with mucous producing cells at the SCJ consistent with a Barrett's-like metaplasia (69). Barrett's oesophagus does not require classical goblet cells to establish diagnosis (497, 498). Various studies have substantiated this concept by indicating that the risk of progression to OAC is similar in patients with a columnar lined oesophagus without goblet cells and those with Barrett's oesophagus (499-501). Overexpression of IL1 β in this model additionally induces metaplasia of the SCJ through the recruitment of immature myeloid cells (69). Immature myeloid cells have been previously associated with oesophageal and colorectal carcinogenesis in murine studies (496, 502, 503). Moreover, in this model, it is thought that immature myeloid cells contribute to oesophageal inflammation and carcinogenesis through the secretion of the proinflammatory cytokines IL-6 and TNF α and the chemokine stromal cell-derived factor 1 (69).

Our research has shown that glycolysis is differentially expressed across the *in-vitro* and *in-vivo* metaplasia-dysplasia-adenocarcinoma sequence, thereby potentially contributing to the development of OAC (130). Increased IL1 β expression, at the SCJ, is also thought to contribute to inflammatory and malignant complications in Barrett's oesophagus (504). Therefore, we investigated if the induction of IL1 β overexpression could mediate glycolytic profiles in this transgenic model of Barrett's-like metaplasia. We found that IL1 β overexpression significantly increases GAPDH IxP expression in the columnar cells of chow fed mice. Moreover, induction of IL1 β significantly increases GAPDH intensity in the mucous producing cells of mice on a high fat diet. This is the first study to our knowledge that has examined IL1 β -induced alterations in metabolism in a transgenic mouse model.

It has long been known that IL1 β plays a role in promoting glycolysis (505-508). Mechanistically, IL1 β stimulates hexose transport in fibroblasts in normal healthy human chondrocytes by increasing the expression of glucose transporters (506). IL1 β also induces glycolysis by increasing the expression of a GAPDH isoform and another important glycolytic enzyme triosephosphate isomerase (509). IL1 β , along with TNF α , were additionally found to modulate the expression of a total of 18 different proteins with 45% of the proteins involved in the generation of cellular energy and glycolysis (509). Moreover, one study assessed the bioenergetic profile of macrophages generated in the presence of granulocyte macrophage colony-stimulating factor and those macrophages generated in the presence of macrophage colony-stimulating factor, and showed that macrophages treated with the former exhibited significantly increased OCR and ECAR in addition to higher expression of genes encoding glycolytic enzymes (510). In addition, even though glycolysis positively regulated IL1 β and TNF mRNA expression in both macrophage subtypes, mitochondrial respiration negatively affected IL-6, IL1 β and TNF α mRNA expression further showing that metabolism can modulate IL1 β expression (510). Moreover, macrophage inflammasome activation in hyperhomocysteinemia is associated with significantly high IL1 β levels with concomitant increases in ROS production and a switch from oxidative phosphorylation to glycolysis (511). The PL2-IL1 β mouse model in the current study has been shown to recruit a significant number of myeloid cells as it progresses from Barrett's metaplasia to a dysplastic phenotype (69). Macrophages, derived from myeloid cells and implicated in the development of OAC, are functionally heterogeneous cells that can be activated by a variety of microenvironmental stimuli including IL1 β (512-514). These macrophages, once activated, exhibit an M1 phenotype characterised by increased glycolysis, lactate release and decreased oxygen consumption (512). It is possible from these studies linking IL1 β and metabolism, therefore, that IL1 β may promote glycolysis through a macrophage-induced mechanism.

Palm oil is the second largest consumed vegetable oil in the world and contains about 50% saturated fatty acids (515). Despite some benefits, a considerable amount of palm oil, such as vegetable oil commonly found in various Western diets, is processed for use in an oxidized state which poses various biochemical and physiological hazards (515). Obesity is strongly associated with increased incidence of Barrett's oesophagus (82, 83). Moreover, as detailed studies linking obesity to OAC progression in Barrett's oesophagus are scarce, we investigated if induction of a high fat diet could mediate cellular processes such as glycolysis, oxidative phosphorylation, HIF1 α and p53 status in Barrett's-like metaplasia. In this transgenic mouse model, even though mice fed a high fat diet do not become overweight, they display more inflammatory lesions and exhibit an accelerated phenotype as they progress to dysplasia at a faster rate (unpublished data from Michael Quante's laboratory). We demonstrate that wild-type and PL2-IL1 β mice fed high fat diets exhibit significantly higher levels of GAPDH in mucous producing and columnar cells. Despite a high fat diet conversely inducing significant decreases in GAPDH expression in PL2-IL1 β mice at 9 months, this is likely due to the significant interaction we show between PL2-IL1 β mice and mice on a high fat diet. A comparable study showed that rats fed a high fat diet containing mixed lipids akin to the present study also promoted carcinogenesis of the colon (516). Our results show, that a high fat diet and the inflammatory microenvironment in Barrett's oesophagus could potentially promote neoplastic progression, possibly through IL1 β , by supporting glycolytic metabolism, the energy pathway implicated in the extensive transformation, differentiation and aggressive proliferation of various cancers including OAC (130, 385).

As we have previously shown that oxidative phosphorylation could potentially contribute to the development of OAC, we investigated if the induction of IL1 β could mediate oxidative phosphorylation in the same transgenic model of Barrett's-like metaplasia (130). We show that induction of IL1 β in mice at 12 months exhibit significantly reduced levels of ATP5B. Moreover, we found that a high fat diet induced significantly lower levels of ATP5B in PL2-IL1 β mice. These results may suggest that glycolysis is the preferred metabolic pathway in this model, particularly at an early stage, as glycolysis possesses many more advantages due to its role in various anabolic processes. It must also be noted, however, that oxidative phosphorylation produces more ATP per molecule of glucose so high oxidative phosphorylation levels may not be required early in the Barrett's setting and may therefore increase with time to support neoplastic progression, analogous to what has been previously shown (130). It is also plausible that lowering the levels of oxidative phosphorylation allows high energy intermediates to be redirected for anabolic purposes. Direct IL1 β treatment has been previously shown to decrease oxygen consumption in neuronal cells (508). Interestingly, IL1 β treatment also induces changes in MMP and caspase

activation, however, the same cells were partially protected from IL1 β toxicity by the increased presence of glucose (508). Therefore, buildup of cellular glucose could be partially protective in an inflammatory burdened Barrett's microenvironment. M2 macrophages, unlike M1 macrophages that favour glycolysis, employ oxidative metabolism pathways (512). Furthermore, a recent study in a murine model showed that macrophages do indeed infiltrate into the oesophagus, however, it was found that M2 macrophages infiltrate following infiltration of M1 macrophages (514). This may explain in part why we don't observe increased oxidative phosphorylation in conjunction with increased glycolytic levels; 'glycophilic' M1 macrophages infiltrate initially followed by a subsequent infiltration of oxidative M2 macrophages. Consequently, more studies are required, firstly, to further characterize the immune infiltrate in Barrett's oesophagus, secondly, to examine the metabolic profiles associated with these immune phenotypes in greater detail and, thirdly, to interrogate how the metabolism in these resident inflammatory and immune cells promotes a Barrett's microenvironment that is more amenable to cancer progression.

As aberrant expression of p53 is additionally associated with an increased risk of neoplastic progression in Barrett's oesophagus, we investigated if manipulation of inflammation and diet could potentially modulate the expression of p53 (292, 517, 518). We have shown that induction of IL1 β overexpression significantly decreased p53 expression in columnar cells of mice fed on a high fat diet at 9 and 12 months. Furthermore, we show in mucous producing cells that a high fat diet significantly increases p53 expression in PL2-IL1 β mice. Interestingly, even though p53 overexpression is associated with increased risk of developing OAC, the risk is significantly higher with loss of p53 expression (292).

In a transgenic mouse model investigating the effect of IL1 β overexpression in the development of chronic pancreatitis, introduction of a p53 mutator strain leads to the formation of a model consisting of tubular metaplastic complexes making it an ideal model to study its relationship with pancreatic adenocarcinoma (519). In the model used in this study, the development of Barrett's and OAC is inhibited by IL-6 deficiency (69). Moreover, mutations in the p53 gene have been associated with excessive cytokine production in cancer, in particular, by stimulating macrophage colony-stimulating factor, the p53-inducible cytokine known to trigger macrophages to produce large amounts of IL1 β , IL-6 and TNF α (520-522). IL1 β has additionally been identified as a stromal chemokine secreted by cancer cells capable of suppressing p53 protein expression in adjacent stromal cancer-associated fibroblasts (522). As p53 exhibits distinctive pro-oxidative and anti-Warburg effects, it is plausible that the increases and decreases in GAPDH and ATP5B expression profiles demonstrated in this study respectively may be due to the downregulation of p53 (198).

To recall, we also showed that a high fat diet significantly elevated p53 expression levels. p53 expression has indeed been shown to be significantly increased within genetically obese murine adipocytes (523). Furthermore, endothelial expression of p53, upregulated in mice fed on a high calorie diet, was also found to induce various metabolic abnormalities (524). Therefore, high fat diet- and IL1 β -induced alterations in p53 expression, in addition to attenuating cell cycle and apoptosis, may promote an inflammatory laden protumorigenic Barrett's microenvironment.

HIF1 α mediates various key cellular processes including energy metabolism, cell survival, angiogenesis and inflammation, and has previously been linked with the acute and chronic inflammatory reaction in Barrett's oesophagus (176). We have shown that induction of IL1 β significantly increases HIF1 α expression within columnar and mucous producing cells of mice fed both chow and high fat diets. We additionally demonstrate that diet has no significant effect in mediating HIF1 α expression within wild-type and PL2-IL1 β mice. Studies have shown, however, that dietary obesity and adipose tissue itself can positively regulate and induce HIF1 α expression (525, 526). IL1 β and one of its downstream effectors, TNF α , are known to stimulate DNA binding of HIF1 α , with the former increasing HIF1 α protein levels, thereby modulating gene expression during periods of inflammation (527). IL1 β can also mediate the non-hypoxic cytokine-dependent regulation of HIF1 α stabilization and its subsequent nuclear translocation where it elicits additional pathological functions (528). For example, via an NF κ B/cyclooxygenase-2 pathway, IL1 β regulation links HIF1 α -induced inflammation to lung adenocarcinoma (529). IL1 β and HIF1 α also cooperate to induce the expression of adrenomedullin in ovarian carcinoma cells (530). In LPS treated macrophages that switch their metabolism to glycolysis upon activation, inhibition of glycolysis with 2-deoxyglucose suppresses LPS-induced IL1 β (243). Interestingly, however, LPS can increase the levels of the tricarboxylic-acid cycle component succinate which leads to stabilization of HIF1 α and increased production of IL1 β through HIF1 α (243). These studies demonstrate that IL1 β and HIF1 α can function in a biphasic manner; IL1 β can induce increased HIF1 α expression and HIF1 α can stimulate additional IL1 β making them complementary protumorigenic mediators. This suggests, akin to the current study, that IL1 β -induced HIF1 α expression could potentially promote further disease progression in a glycolytic microenvironment, as we additionally show increased glycolysis upon IL1 β induction, however, any disturbances in glycolytic metabolism could still lead to the preservation of an IL1 β milieu through an oxidative pathway such as succinate via the tricarboxylic-acid cycle. It may, therefore, be worthwhile speculating that multi-targeted therapies hold greater promise in the treatment of such unpredictable heterogeneous preneoplastic and neoplastic tissues.

One of the most debated questions in Barrett's oesophagus is the origin of the metaplastic tissue itself. Numerous studies suggest that Barrett's oesophagus originates from a single progenitor cell, transdifferentiation of the squamous epithelium, submucosal glands, residual embryonic cells at the SCJ or the gastric cardia (531-535). In the PL2-IL1 β model used in this study, lineage tracing studies demonstrate the likely origin of some of the metaplastic tissue from within the gastric cardia (69). Despite much attention being attributed to goblet cells within classical intestinal metaplasia, the change in the definition to include a non-goblet columnar lined oesophagus acknowledged the varied histological presentation of Barrett's oesophagus (69). Therefore, we investigated the effect of diet and induction of IL1 β overexpression on GAPDH, ATP5B, p53 and HIF1 α between columnar cells and mucous producing Barrett's-like cells. Despite most of the significant effects occurring in columnar cells, the strongest statistically significant diet and IL1 β -induced alterations also occurred in columnar cells. This may suggest that columnar cells within the Barrett's microenvironment are more sensitive to inflammatory-provoked fluctuations and thereby contribute indirectly by modulating adjacent cells and tissue, or directly, by undergoing further disease progression. Another possibility is that any diet or IL1 β -induced effects elicited within columnar cells may affect linked processes in adjacent mucous producing cells. For example, the large increase in HIF1 α caused by induction of IL1 β in the columnar cells of mice at 12 months may have had a positive feedback effect on HIF1 α and GAPDH expression in adjacent mucous producing cells that were also found to be significantly increased. In this scenario, high-energy nutrients such as ketones, glutamine and L-lactate secreted by highly glycolytic columnar tissue could assist adjacent mucous producing cells akin to the 'reverse Warburg effect' concept established by Lisanti *et al.* (536).

We have shown that IL1 β manipulation can modulate glycolysis, oxidative phosphorylation, p53 and HIF1 α in a transgenic model of Barrett's like-metaplasia. Furthermore, we also demonstrate that a high fat diet can alter these processes providing further insight into the potential role of diet and obesity in exacerbating disease progression. These results demonstrate that inflammation and a high fat diet, possibly through their association with metabolism and hypoxia, may potentially operate to support neoplastic progression within the microenvironment of Barrett's oesophagus.

Chapter 7
General Discussion

7.1 DISCUSSION

In 1956, Warburg proposed that dysfunctional mitochondria were required and necessary to initiate biochemical and pathological events that resulted in cellular transformation to the cancerous state (170). Conversely, twenty years later, Weinhouse argued the reverse was true and that cancer cells have reduced mitochondrial activity as a consequence of enhanced glycolytic flux (537). To this day, the field has not reached a consensus (538). Abnormal mitochondrial function has since been linked with the development and progression of cancer (539). As genomic instability and mutations, tumour-promoting inflammation and the deregulation of cellular energetics are now emerging hallmarks of cancer, mitochondrial associated inflammation, oxidative stress and alterations in cellular metabolism are becoming a more promising target in cancer therapy. In this Ph.D thesis, we investigated the role of mitochondrial metabolism and function in the initiation and progression of Barrett's oesophagus. Through the use of *in-vitro*, *in-vivo* and *ex-vivo* models, we examined mitochondrial function, characterised mitochondrial energy metabolism across the Barrett's disease sequence, assessed if markers of metabolism could identify Barrett's oesophagus patients who progress to OAC and investigated the connection between metabolism and other key cellular processes known to be linked with disease progression in Barrett's oesophagus in patients and using a mouse model of Barrett's oesophagus.

Early studies show that mitochondrial function is altered in Barrett's oesophagus and may play an important role in the subsequent progression to OAC. Mutations in the mtDNA D-loop region have been shown to occur frequently in OAC in Barrett's oesophagus supporting the hypothesis that oxidative damage might be a mechanism for the induction of OAC in Barrett's tissue (116). mtDNA mutations have also been shown to be specific to Barrett's tissue which may support dysplastic progression (115). Mitochondrial-induced oxidative stress and oxidative DNA damage, as measured through the oxidative stress marker 8-hydroxy-deoxyguanosine, are also known to be present in oesophageal tissues and cells exposed to bile acids and low pH (540). No studies, however, have investigated global mitochondrial function across the metaplastic-dysplastic-OAC sequence. In chapter two, through the use of a human PCR microarray, we identified four genes (*BAK1*, *FIS1*, *SFN*, *CDKN2A*) to be differentially expressed across the metaplastic-dysplastic-OAC sequence *in-vitro*. Upon *in-vitro* validation of these four gene targets, we found that all four genes exhibited differential expression profiles in *in-vivo* patient material that were specific to Barrett's tissue compared to matched normal adjacent tissue. These alterations in mitochondrial function within Barrett's tissue, therefore, may play some role in mediating neoplastic progression. For example, the increase in apoptotic resistance exhibited in Barrett's tissue compared to matched

normal adjacent tissue in one study may have been attributed by increased levels of the pro-apoptotic protein *BAK1* that we have shown to be higher in Barrett's tissue compared to normal tissue (541).

Chapter two also demonstrated significant alterations in mitochondrial function upon functional manipulation of the *BAK1*, *FIS1* and *SFN* genes. We showed that knockdown of all gene targets resulted in significant decreases in MMP in Barrett's cells suggestive of a role in apoptosis. Indeed Barrett's oesophagus does exhibit increased apoptotic capability and studies have demonstrated increased MMP in various cancers, therefore, agents that induce apoptosis may have significant clinical promise in both Barrett's oesophagus and OAC tissue (378, 541). We also acknowledge limitations within chapter 2. Our mitochondrial function PCR microarray consisted of gene targets linked with membrane polarisation, membrane potential, small molecule and macromolecule transport, fission and fusion, translocation, targeting proteins to mitochondria, protein influx, mitochondrial localisation and apoptosis. While we chose 4 gene targets, these gene targets do not encompass the entire functional repertoire, therefore, other novel targets from our microarray also warrant further investigation. Moreover, we show different expression patterns between *in-vitro* and *in-vivo* validations, for example, *SFN* decreases between metaplasia and OAC *in-vitro* but increases *in-vivo*. Compared to *in-vitro* cells, however, *in-vivo* samples are complex heterogeneous tissues composed of an assortment of specialised cells which may exhibit differential expression patterns. Therefore, localising *BAK1*, *FIS1* or *SFN* expression profiles specifically within Barrett's epithelium would require alternative analyses, such as immunohistochemistry. Furthermore, we found that functional knockdown of the *BAK1*, *FIS1* and *SFN* genes significantly altered various aspects of cellular metabolism in OAC cells but not in Barrett's cells suggesting agents that target these genes and their associated processes in neoplastic tissue may additionally benefit through the alteration of cellular metabolism. Furthermore, based on previous studies, *BAK1*, *FIS1* and *SFN* may play substantial roles in chemotherapeutic resistance in the setting of OAC further substantiating agents that target *BAK1*, *FIS1* and *SFN* in the modulation of chemoresistance (350, 353, 363, 364).

In the preneoplastic tissue of ulcerative colitis, loss of oxidative phosphorylation precedes the development of dysplasia with restoration of mitochondria noted upon neoplastic progression (286). Over a decade ago, PKM2 was shown to play a pathological role during transformation and proliferation along the metaplasia-dysplasia-OAC sequence (392). Moreover, cell lines derived from patients with more advanced genetically unstable Barrett's oesophagus have up to 2-fold higher glycolytic rates compared to a cell line derived from a patient with early genetically stable

Barrett's oesophagus (391). However, the same cell lines were shown to preserve active mitochondria and demonstrate significant modulation in oxygen consumption as inhibition of glycolysis in the most glycolytic cell lines resulted in compensatory increases in oxidative phosphorylation suggesting a role for oxidative phosphorylation in the development of OAC (391). Therefore, in chapter 3, we characterised mitochondrial energy metabolism across the metaplasia-dysplasia-OAC sequence in *in-vitro* and *in-vivo* models of Barrett's oesophagus. Through the use of a human PCR microarray, we identified three genes (*ATP12A*, *COX4I2*, *COX8C*) associated with oxidative phosphorylation to be differentially expressed across the metaplastic-dysplastic-OAC sequence *in-vitro* (130). Upon *in-vitro* validation of these gene targets, we found that all genes exhibited differential expression profiles in *in-vivo* patient material that were specific to Barrett's tissue compared to matched normal adjacent tissue (130). Moreover, significant increases in both oxidative and glycolytic metabolism were demonstrated in epithelial and stromal tissues across the metaplastic-dysplastic-OAC sequence *in-vivo* implying that both metabolic pathways are important in OAC progression (130). As such, agents that target both metabolic pathways may provide some clinical benefit. Further analysis of oxidative metabolism in Barrett's cells demonstrated that Barrett's cells rely more on oxidative metabolism compared to OAC cells suggesting that the increased preference of oxidative metabolism in Barrett's cells may predispose them to higher levels of oxidative stress, thereby possibly increasing mtDNA mutations, and neoplastic progression (130). We must also acknowledge that our initial primary focus in this chapter was investigating the role of oxidative phosphorylation in Barrett's oesophagus. Therefore, as our metabolic PCR microarray screen focused solely on mitochondrial energy metabolism, that is oxidative phosphorylation, we acknowledge that a PCR microarray screen examining specific aspects of glycolytic metabolism may uncover additional findings. Such studies deciphering key components of glycolysis, for example, rate limiting steps, are thus warranted. Similarly, other metabolic pathways known to play key roles in tumourigenesis, such as the citric acid cycle, glutamine metabolism and the pentose phosphate pathway among others, require further investigation to determine their roles in Barrett's oesophagus and in the progression to OAC (542-544).

Better methods are needed to identify Barrett's oesophagus patients at greater risk of neoplastic progression. Biomarkers possess significant clinical promise in their utilisation to risk stratify those patients with greater risk of progression. Such risk stratification could result in altered surveillance intervals, changes in treatment regimes or enrolment into secondary prevention studies. p53 protein overexpression in LGD is one such example of a risk assessment marker (27, 545, 546). Other promising biomarkers for identifying patients with Barrett's oesophagus at high risk of

developing OAC include aneuploidy, loss of heterozygosity, cyclin A, minichromosome maintenance protein 2, various methylation markers and HGD itself (545, 546). In chapter 3, we show that ATP5B expression in sequential follow up surveillance biopsy material segregated Barrett's non progressors and progressors to HGD and OAC, thereby highlighting its prognostic advantage in these preneoplastic patients, however, additional validation of ATP5B in different patient cohorts within other clinical institutions would potentially strengthen its applicability as a biomarker in the clinical setting (130).

The bile acid DCA is known to play a major role in the development of Barrett's oesophagus and in its subsequent progression to OAC (70-74). In chapter 4, we show that DCA alters mitochondrial energy metabolism across the *in-vitro* squamous-metaplasia-dysplasia-OAC sequence; DCA decreases oxidative phosphorylation in Barrett's cells, increases oxidative metabolism in dysplastic and OAC cells and increases glycolysis in OAC cells. These findings suggest that DCA promotes metabolism in the neoplastic epithelium. Moreover, as decreased oxidative profiles are associated with poor prognosis in IBD, it is possible that reduced oxidative metabolism is linked with poor prognosis in Barrett's epithelial cells (294). Moreover, as DCA is known to alter NFκB and p53 profiles in Barrett's oesophagus, it is plausible that DCA modulates metabolism through these molecular mediators (72, 73). As we chose a single cell line to represent the Barrett's epithelium throughout this Ph.D thesis, this presents a limitation throughout our studies itself. QH cells, which represent genetically stable Barrett's epithelium, may not induce sufficient cellular modifications compared to genetically unstable Barrett's cell lines that are known to exhibit more aggressive metabolic phenotypes (391). To overcome this *in-vitro* limitation, we utilised comparable human *in-vivo* and *ex-vivo* models of Barrett's oesophagus.

In chapter 4, we also demonstrate that DCA treated QH and OE33 cells supplemented with the antioxidant EGCG exhibit significantly lower levels of oxidative phosphorylation and glycolysis respectively. However, supplementation with NAC showed no such metabolic benefits. Analogous to previous studies, this result further supports the role of EGCG as an anti-cancer agent (440). Moreover, as proton pump inhibitors have been documented as having various additional advantages beyond acid repression, we examined their independent effect on metabolic profiles *in-vitro* (442). We demonstrate that the use of lansoprazole significantly reduces glycolysis in Barrett's cells suggesting that in addition to treating reflux, lansoprazole reduces glycolysis and thus lowers the risk of progression. As lansoprazole has previously exhibited anti-inflammatory potential, it may mediate its anti-metabolic effect through one or more inflammatory pathways (447). Moreover, the use of lansoprazole and omeprazole both independently reduce oxidative

metabolism in dysplastic cells, thereby potentially demonstrating a protective role in the neoplastic setting as previously speculated (450). In addition, the supplementation of proton pump inhibitors in OAC patients with Barrett's oesophagus without reflux represents a chemopreventative agent further highlighting its multi-modal use (453).

In chapter 4, we also investigated if Quininib, our patented small molecule anti-metabolic drug, could modulate cellular metabolism across the *in-vitro* sequence. We show that Quininib demonstrates potent anti-oxidative and anti-glycolytic potential in Barrett's and OAC cells *in-vitro*. As Quininib has previously been shown to exhibit anti-inflammatory and anti-angiogenic activity in zebrafish, in *ex-vivo* human colorectal explants and in mice (under review; Murphy *et al.*), these results reflect exciting anti-metabolic potential for Quininib treatment in metaplastic and OAC epithelium. Even though Quininib exhibited differential effects on inflammation, angiogenesis and metabolism in Barrett's explant tissue, such results may be expected due to the heterogeneous complexity of Barrett's tissue. For example, Quininib may exert distinct effects on diverse cell types in explant tissues which may explain the differential responses to Quininib treatment between patients. As the effect of Quininib, and its analogues, may be tissue specific, future studies should examine its potential anti-carcinogenic role in the *ex-vivo* setting of OAC and in other preneoplastic settings. Although chapter 4 investigated the independent effect of lansoprazole, omeprazole and Quininib on metabolism, we acknowledge, however, that in the presence of DCA, both proton pump inhibitors may have induced differential metabolic effects to what we have shown. Furthermore, the effect of additional bile acids in conjunction with DCA may differentially modulate energy metabolism profiles.

Various cellular processes, molecular mediators and metabolic disorders have been implicated in disease progression in Barrett's oesophagus. These encompass inflammation, p53, hypoxia, angiogenesis and obesity (83, 176, 223, 292, 457). Through Spearman and multivariate analyses, we show in chapter 5 that energy metabolism is linked with inflammation and hypoxia in the Barrett's tissue microenvironment *in-vivo*. Our data also highlights that energy metabolism is linked with p53 status, obesity status and to the length of the Barrett's segment *in-vivo*. Utilising *ex-vivo* explant tissue to mimic the Barrett's microenvironment, similar associations between these key processes were established. We acknowledge that these associations do not prove causality. Therefore, to build on these associations and investigate potential functionality, we demonstrate in chapter 6 that induction of inflammation through IL1 β manipulation can modulate glycolysis, oxidative phosphorylation, p53 and hypoxia in a transgenic mouse model of Barrett's oesophagus. Our data indicates that IL1 β , through the modulation of these cellular processes,

could potentially mediate and support neoplastic progression within the microenvironment of Barrett's oesophagus. Moreover, we find that a high fat diet can alter these processes providing further insight into the potential role of obesity in exacerbating disease progression. These novel findings within the inflammatory microenvironment of Barrett's oesophagus may provide some insight into the key mechanisms linking Barrett's oesophagus with neoplastic progression. Consequently, such knowledge may aid in the development of promising multi-targeted therapies with potential translational applicability in other inflammatory disorders. These findings, however, warrant further study to determine if they play specific mechanistic and functional roles in disease progression. We also acknowledge limitations in the use of the surrogate markers chosen. For example, even though GAPDH is central to glycolysis, PKM2 is more abundant during aerobic glycolysis in many tumour types, including the Barrett's-dysplastic-OAC disease sequence (392). Moreover, HIF1 α can be upregulated by non-hypoxic pathways, therefore, alternative reliable hypoxia markers, or their combined value, such as carbonic anhydrase 9, VEGF, GLUT1, JMJD1A and erythropoietin may be more specific (259, 268, 472-476).

In conclusion, this thesis has shown for the first time through the use of *in-vitro*, *in-vivo* and *ex-vivo* models, that oxidative phosphorylation and glycolysis play a central role in disease progression in Barrett's oesophagus. Moreover, a marker of oxidative phosphorylation, ATP5B, exhibits significant promise in segregating those Barrett's patients at higher risk of neoplastic progression. Mitochondrial function, also shown to be altered across the metaplastic-dysplastic-OAC disease sequence and known to induce functional changes in Barrett's and OAC cells *in-vitro*, can indirectly mediate energy metabolism profiles. Endogenous DCA, and the administration of proton pump inhibitors in conjunction with antioxidant supplementation, can additionally modulate cellular oxidative phosphorylation and glycolytic profiles. In addition, oxidative phosphorylation and glycolysis are closely linked with levels of inflammation, hypoxia, p53 and obesity in *in-vivo* and *ex-vivo* tissue from Barrett's oesophagus patients. Furthermore, to prove possible functionality, IL1 β overexpression and manipulation of diet can modulate glycolysis, oxidative phosphorylation, p53 and hypoxia in a transgenic model of Barrett's like-metaplasia, thereby demonstrating the complexity of the Barrett's tissue microenvironment. The findings within this Ph.D thesis give an insight into how energy metabolism and its associated processes could potentially support disease progression in Barrett's oesophagus thereby highlighting future potential therapeutic opportunities in the field.

7.2 FUTURE DIRECTIONS

This Ph.D thesis has revealed many future research possibilities.

1. An *in-vitro* PCR microarray screen examining specific aspects of glycolytic metabolism in QH and OE33 cells may uncover significant findings within Barrett's associated aerobic glycolysis. As oxidative phosphorylation and glycolysis are now known to play possible roles in OAC progression, other metabolic pathways known to play key roles in tumourigenesis, such as glutamine metabolism and the pentose phosphate pathway for example, warrant further study using models of Barrett's oesophagus akin to the models utilised throughout this Ph.D thesis. Furthermore, investigating if ATP5B encompasses prognostic potential in independent cohorts of Barrett's oesophagus patients and examining its potential clinical utility across medical institutions is essential.
2. *In-vitro* cell culture studies linking metabolism to inflammation, HIF1 α , p53 and obesity through precise mechanisms within Barrett's tissue may uncover improved therapeutic potential. Although functionally difficult, investigating whether inflammation is functionally linked to protumourigenic pathways through the mediation of metabolism would be intriguing. For example, examining if IL1 β can induce cell proliferation and/or cell differentiation specifically through metabolic means may further prove causality. Such functional studies may encompass manipulating various genes *in-vitro* to explore any functional effects and/or the antagonism of downstream signalling pathways. Subsequently identifying the molecular mechanisms of such functionality may offer significant therapeutic insights.
3. *In-vitro* analyses examining specific protein-protein interactions and the functional consequences of blocking such interactions would offer further insights. Furthermore, with recent advancements in methodologies such as CRISPR-Cas, exploring the functional effects, for example, of rescuing mutations in p53 in QH cells and thus restoring wild-type p53, would provide a better understanding of the functionality of genes and their links with other cellular mediators in Barrett's oesophagus. Such methods may be beneficial in particular for mtDNA due to its increased susceptibility to damage and mutation. *In-vivo* and *ex-vivo* studies could subsequently be undertaken to validate and explore potential clinical benefits as a result of any potential significant *in-vitro* findings.
4. Through the use of *in-vitro* cell culture techniques, additional insight into how DCA mediates cell function and deciphering the primary molecular processes it utilises to exacerbate disease progression may offer clinical promise. Investigating the role of DCA in Barrett's oesophagus and its role in the modulation of cellular processes, such as energy

metabolism, in an *ex-vivo* setting also warrants further investigation. Quininib has since exhibited potential as an anti-inflammatory, anti-angiogenic and anti-metabolic agent in *ex-vivo* OAC explant tissue (currently being undertaken by Róisín Byrne), however, examining whether Quininib or its associated analogues can recapitulate these effects in preneoplastic Barrett's *ex-vivo* tissue requires further inspection.

5. Micro RNAs have also shown promise at targeting cancer metabolic pathways. A recent study demonstrated that mir-122 targets PKM2 and affects metabolism in hepatocellular carcinoma, therefore, investigating the role of micro RNAs in the modulation of cellular energy metabolism in Barrett's oesophagus and OAC may also offer significant promise (319).
6. In lieu of single gene target knockdown, combined knockdown of the *BAK1*, *FIS1* and *SFN* genes in Barrett's and OAC cells may offer better insight into their role in mitochondrial function in both the preneoplastic and neoplastic settings. Such combined siRNA knockdown or therapeutic inhibition may substantially influence cellular metabolism and induce considerable apoptosis in Barrett's and OAC cells. Based on previous findings of *BAK1*, *FIS1* and *SFN*, another exciting extension of this work would be to investigate their role in chemotherapeutic resistance in QH, GO and OE33 cells through the use of clonogenic assays *in-vitro*. Examining other gene targets from the functional PCR microarray screen using the methods employed in this thesis, such as *AIFM2*, *STARD3*, *DNM1L* and *UCP2*, may also warrant further examination.

Appendices

Appendix A. Mitochondrial function gene microarray screen between GO and QH cell lines

Gene	Expression*	Gene	Expression*	Gene	Expression*
<i>AIFM2</i>	-1.32	<i>NEFL</i>	-1.63	<i>SLC25A4</i>	2.84
<i>AIP</i>	-1.14	<i>OPA1</i>	1.31	<i>SLC25A5</i>	1.20
<i>BAK1</i>	1.61	<i>PMAIP1</i>	1.87	<i>SOD1</i>	1.44
<i>BBC3</i>	1.63	<i>RHOT1</i>	1.76	<i>SOD2</i>	1.19
<i>BCL2</i>	1.66	<i>RHOT2</i>	1.39	<i>STARD3</i>	2.19
<i>BCL2L1</i>	1.86	<i>SFN</i>	6.06	<i>TAZ</i>	1.32
<i>BID</i>	1.14	<i>SH3GLB1</i>	1.35	<i>TIMM10</i>	1.32
<i>BNIP3</i>	-16.32	<i>SLC25A1</i>	-1.11	<i>TIMM17A</i>	1.72
<i>CDKN2A</i>	-30.20	<i>SLC25A10</i>	1.38	<i>TIMM17B</i>	1.34
<i>COX10</i>	2.33	<i>SLC25A12</i>	1.23	<i>TIMM22</i>	1.46
<i>COX18</i>	2.26	<i>SLC25A13</i>	1.93	<i>TIMM23</i>	1.43
<i>CPT1B</i>	-1.09	<i>SLC25A14</i>	1.82	<i>TIMM44</i>	1.63
<i>CPT2</i>	-1.26	<i>SLC25A15</i>	1.55	<i>TIMM50</i>	1.73
<i>DNAJC19</i>	1.32	<i>SLC25A16</i>	1.16	<i>TIMM8A</i>	1.83
<i>DNM1L</i>	1.87	<i>SLC25A17</i>	1.54	<i>TIMM8B</i>	1.10
<i>FIS1</i>	1.57	<i>SLC25A19</i>	2.37	<i>TIMM9</i>	1.34
<i>FXC1</i>	1.37	<i>SLC25A2</i>	1.56	<i>TOMM20</i>	1.15
<i>GRPEL1</i>	2.57	<i>SLC25A20</i>	1.00	<i>TOMM22</i>	1.67
<i>HSP90AA1</i>	1.95	<i>SLC25A21</i>	1.62	<i>TOMM34</i>	1.28
<i>HSPD1</i>	2.30	<i>SLC25A22</i>	2.22	<i>TOMM40</i>	2.15
<i>IMMP1L</i>	1.30	<i>SLC25A23</i>	-4.93	<i>TOMM40L</i>	1.81
<i>IMMP2L</i>	2.44	<i>SLC25A24</i>	1.58	<i>TOMM70A</i>	1.42
<i>LRPPRC</i>	1.70	<i>SLC25A25</i>	1.39	<i>TP53</i>	1.75
<i>MFN1</i>	1.53	<i>SLC25A27</i>	1.45	<i>TSPO</i>	1.93
<i>MFN2</i>	1.61	<i>SLC25A3</i>	-1.13	<i>UCP1</i>	-1.51
<i>MIPEP</i>	1.86	<i>SLC25A30</i>	1.58	<i>UCP2</i>	-2.99
<i>MSTO1</i>	1.62	<i>SLC25A31</i>	-1.40	<i>UCP3</i>	-1.15
<i>MTX2</i>	1.53	<i>SLC25A37</i>	2.09	<i>UXT</i>	1.12

B2M = Endogenous Control Gene

* Relative Expression (e.g. expression of *BAK1* is 1.61 times greater in QH than GO cells)

Appendix B. Mitochondrial function gene microarray screen between GO and OE33 cell lines

Gene	Expression*	Gene	Expression*	Gene	Expression*
<i>AIFM2</i>	3.14	<i>NEFL</i>	4.07	<i>SLC25A4</i>	4.63
<i>AIP</i>	-1.34	<i>OPA1</i>	-54.33	<i>SLC25A5</i>	1.33
<i>BAK1</i>	-33.20	<i>PMAIP1</i>	1.56	<i>SOD1</i>	-1.13
<i>BBC3</i>	-1.31	<i>RHOT1</i>	2.80	<i>SOD2</i>	-1.56
<i>BCL2</i>	2.03	<i>RHOT2</i>	1.22	<i>STARD3</i>	13.45
<i>BCL2L1</i>	2.39	<i>SFN</i>	-1.05	<i>TAZ</i>	2.01
<i>BID</i>	2.06	<i>SH3GLB1</i>	1.34	<i>TIMM10</i>	2.07
<i>BNIP3</i>	-3.64	<i>SLC25A1</i>	-1.98	<i>TIMM17A</i>	1.32
<i>CDKN2A</i>	84.95	<i>SLC25A10</i>	2.13	<i>TIMM17B</i>	1.72
<i>COX10</i>	1.24	<i>SLC25A12</i>	-1.57	<i>TIMM22</i>	-1.76
<i>COX18</i>	1.19	<i>SLC25A13</i>	-14.71	<i>TIMM23</i>	2.18
<i>CPT1B</i>	-1.25	<i>SLC25A14</i>	-2.15	<i>TIMM44</i>	1.69
<i>CPT2</i>	-2.33	<i>SLC25A15</i>	1.30	<i>TIMM50</i>	1.19
<i>DNAJC19</i>	1.36	<i>SLC25A16</i>	1.65	<i>TIMM8A</i>	1.60
<i>DNM1L</i>	-62.51	<i>SLC25A17</i>	1.84	<i>TIMM8B</i>	-1.30
<i>FIS1</i>	-23.70	<i>SLC25A19</i>	4.01	<i>TIMM9</i>	-1.00
<i>FXC1</i>	-1.86	<i>SLC25A2</i>	1.61	<i>TOMM20</i>	-1.86
<i>GRPEL1</i>	1.65	<i>SLC25A20</i>	-1.54	<i>TOMM22</i>	1.32
<i>HSP90AA1</i>	2.41	<i>SLC25A21</i>	3.09	<i>TOMM34</i>	-1.28
<i>HSPD1</i>	3.36	<i>SLC25A22</i>	1.99	<i>TOMM40</i>	2.71
<i>IMMP1L</i>	1.05	<i>SLC25A23</i>	2.77	<i>TOMM40L</i>	1.10
<i>IMMP2L</i>	6.88	<i>SLC25A24</i>	-50.87	<i>TOMM70A</i>	1.10
<i>LRPPRC</i>	-1.34	<i>SLC25A25</i>	2.97	<i>TP53</i>	-1.46
<i>MFN1</i>	1.25	<i>SLC25A27</i>	-2.28	<i>TSPO</i>	1.27
<i>MFN2</i>	-1.57	<i>SLC25A3</i>	-1.20	<i>UCP1</i>	2.20
<i>MIPEP</i>	1.14	<i>SLC25A30</i>	1.90	<i>UCP2</i>	9.48
<i>MSTO1</i>	-1.02	<i>SLC25A31</i>	3.59	<i>UCP3</i>	1.80
<i>MTX2</i>	1.72	<i>SLC25A37</i>	1.62	<i>UXT</i>	-1.03

B2M = Endogenous Control Gene

* Relative Expression (e.g. expression of *AIFM2* is 3.14 times greater in OE33 than GO cells)

Appendix C. Energy Metabolism Gene Microarray Screen between GO and QH Cell Lines

Gene	Expression*	Gene	Expression*	Gene	Expression*
<i>ATP4A</i>	-1.32	<i>COX6B1</i>	1.53	<i>NDUFB8</i>	2.087632837
<i>ATP4B</i>	-1.14	<i>COX6B2</i>	-1.63	<i>NDUFB9</i>	2.844636874
<i>ATP5A1</i>	1.61	<i>COX6C</i>	1.31	<i>NDUFC1</i>	1.195772966
<i>ATP5B</i>	1.63	<i>COX7A2</i>	1.87	<i>NDUFC2</i>	1.442785171
<i>ATP5C1</i>	1.66	<i>COX7A2L</i>	1.76	<i>NDUFS1</i>	1.186150852
<i>ATP5F1</i>	1.86	<i>COX7B</i>	1.39	<i>NDUFS2</i>	2.194229608
<i>ATP5G1</i>	1.14	<i>COX8A</i>	6.06	<i>NDUFS3</i>	1.321997089
<i>ATP5G2</i>	-16.32	<i>COX8C</i>	1.35	<i>NDUFS4</i>	1.315440505
<i>ATP5G3</i>	-30.20	<i>CYC1</i>	-1.11	<i>NDUFS5</i>	1.720803662
<i>ATP5H</i>	2.33	<i>LHPP</i>	1.38	<i>NDUFS6</i>	1.338563425
<i>ATP5I</i>	2.26	<i>NDUFA1</i>	1.23	<i>NDUFS7</i>	1.458616885
<i>ATP5J</i>	-1.09	<i>NDUFA10</i>	1.93	<i>NDUFS8</i>	1.429104585
<i>ATP5J2</i>	-1.26	<i>NDUFA11</i>	1.82	<i>NDUFV1</i>	1.633253238
<i>ATP5L</i>	1.32	<i>NDUFA2</i>	1.55	<i>NDUFV2</i>	1.73205771
<i>ATP5O</i>	1.87	<i>NDUFA3</i>	1.16	<i>NDUFV3</i>	1.827097344
<i>ATP6V0A2</i>	1.57	<i>NDUFA4</i>	1.54	<i>OXA1L</i>	1.104644001
<i>ATP6V0D2</i>	1.37	<i>NDUFA5</i>	2.37	<i>PPA1</i>	1.336093063
<i>ATP6V1C2</i>	2.57	<i>NDUFA6</i>	1.56	<i>PPA2</i>	1.150856137
<i>ATP6V1E2</i>	1.95	<i>NDUFA7</i>	1.00	<i>SDHA</i>	1.671923688
<i>ATP6V1G3</i>	2.30	<i>NDUFA8</i>	1.62	<i>SDHB</i>	1.278780367
<i>ATP12A</i>	0.28	<i>NDUFAB1</i>	2.22	<i>SDHC</i>	2.149186975
<i>BCS1L</i>	1.30	<i>NDUFB10</i>	-4.93	<i>SDHD</i>	1.814056009
<i>COX4I1</i>	2.44	<i>NDUFB2</i>	1.58	<i>UQCR11</i>	1.422928825
<i>COX4I2</i>	1.70	<i>NDUFB3</i>	1.39	<i>UQCRC1</i>	1.746699585
<i>COX5A</i>	1.53	<i>NDUFB4</i>	1.45	<i>UQCRC2</i>	1.932374205
<i>COX5B</i>	1.61	<i>NDUFB5</i>	-1.13	<i>UQCRFS1</i>	-1.506760899
<i>COX6A1</i>	1.86	<i>NDUFB6</i>	1.58	<i>UQCRH</i>	-2.987419835
<i>COX6A2</i>	1.62	<i>NDUFB7</i>	-1.40	<i>UQCRQ</i>	-1.1456648

B2M = Endogenous Control Gene

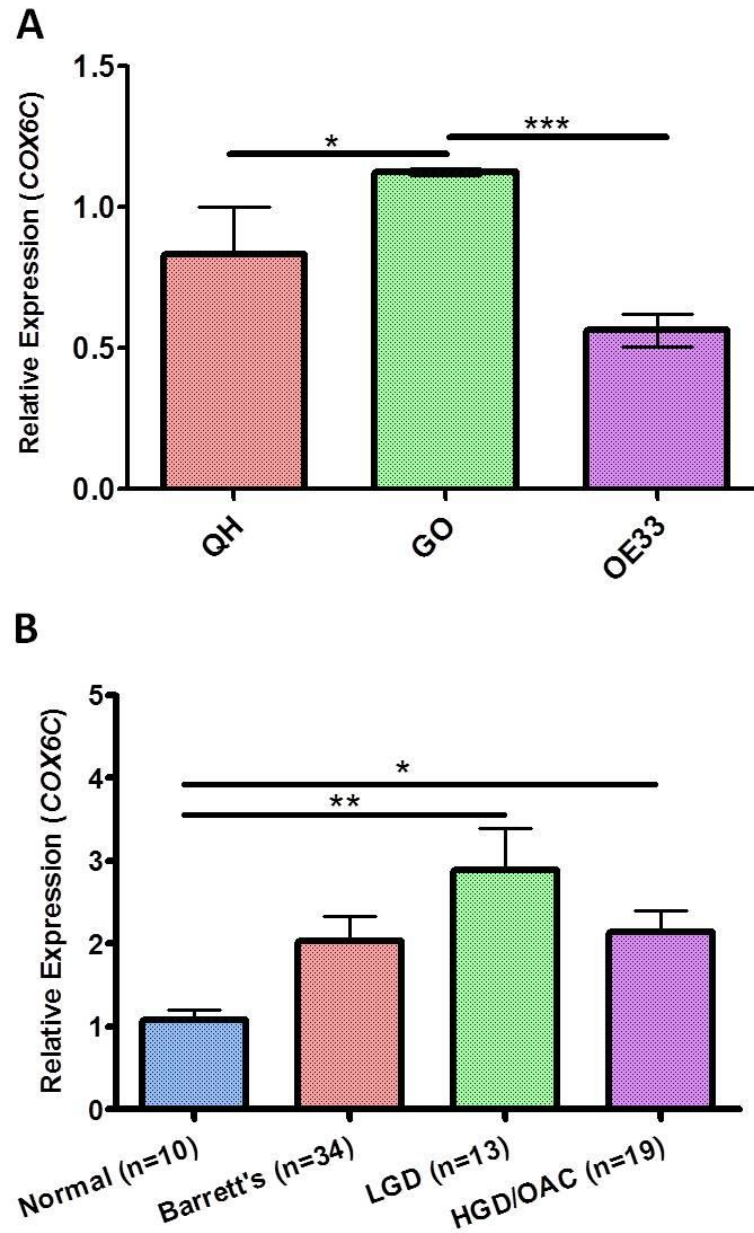
* Relative Expression (e.g. expression of *ATP5A1* is 1.61 times greater in QH than GO cells)

Appendix D. Energy Metabolism Gene Microarray Screen between GO and OE33 Cell Lines

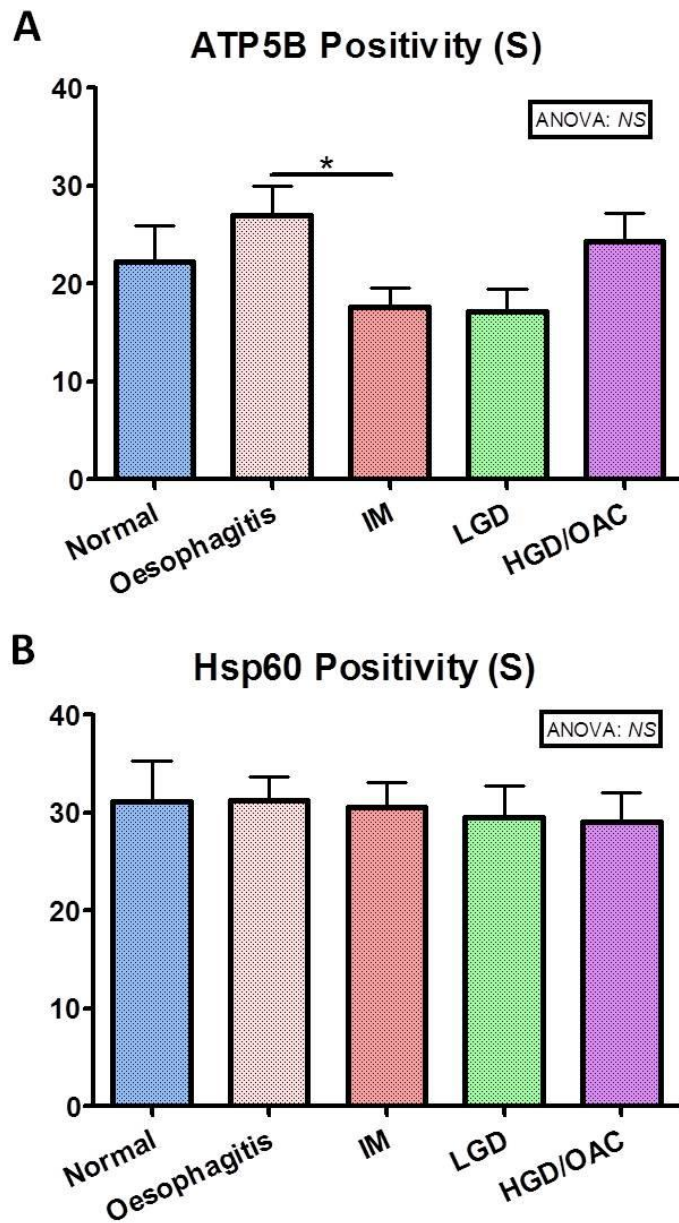
Gene	Expression*	Gene	Expression*	Gene	Expression*
<i>ATP4A</i>	1.79	<i>COX6B1</i>	1.61	<i>NDUFB8</i>	-2.46
<i>ATP4B</i>	1.46	<i>COX6B2</i>	-1.45	<i>NDUFB9</i>	1.14
<i>ATP5A1</i>	1.51	<i>COX6C</i>	1.69	<i>NDUFC1</i>	-1.09
<i>ATP5B</i>	-2.16	<i>COX7A2</i>	1.50	<i>NDUFC2</i>	1.84
<i>ATP5C1</i>	-1.50	<i>COX7A2L</i>	-1.10	<i>NDUFS1</i>	-1.58
<i>ATP5F1</i>	-1.00	<i>COX7B</i>	-1.32	<i>NDUFS2</i>	-1.08
<i>ATP5G1</i>	1.27	<i>COX8A</i>	-1.48	<i>NDUFS3</i>	-1.83
<i>ATP5G2</i>	-2.06	<i>COX8C</i>	-1.16	<i>NDUFS4</i>	1.04
<i>ATP5G3</i>	-2.13	<i>CYC1</i>	1.32	<i>NDUFS5</i>	1.26
<i>ATP5H</i>	-1.96	<i>LHPP</i>	-1.39	<i>NDUFS6</i>	-1.64
<i>ATP5I</i>	-1.24	<i>NDUFA1</i>	-2.00	<i>NDUFS7</i>	1.75
<i>ATP5J</i>	-1.12	<i>NDUFA10</i>	4.67	<i>NDUFS8</i>	-4.06
<i>ATP5J2</i>	-1.83	<i>NDUFA11</i>	-1.25	<i>NDUFV1</i>	1.07
<i>ATP5L</i>	3.52	<i>NDUFA2</i>	-2.28	<i>NDUFV2</i>	1.30
<i>ATP5O</i>	-1.99	<i>NDUFA3</i>	-1.58	<i>NDUFV3</i>	-1.83
<i>ATP6VOA2</i>	1.32	<i>NDUFA4</i>	1.03	<i>OXA1L</i>	1.76
<i>ATP6VOD2</i>	2.66	<i>NDUFA5</i>	1.10	<i>PPA1</i>	-1.24
<i>ATP6V1C2</i>	1.46	<i>NDUFA6</i>	-1.46	<i>PPA2</i>	2.80
<i>ATP6V1E2</i>	3.55	<i>NDUFA7</i>	-1.87	<i>SDHA</i>	2.09
<i>ATP6V1G3</i>	1.86	<i>NDUFA8</i>	-1.61	<i>SDHB</i>	1.61
<i>ATP12A</i>	1.79	<i>NDUFAB1</i>	-1.39	<i>SDHC</i>	-2.12
<i>BCS1L</i>	1.31	<i>NDUFB10</i>	2.24	<i>SDHD</i>	-1.79
<i>COX4I1</i>	-1.08	<i>NDUFB2</i>	-1.15	<i>UQCR11</i>	-3.20
<i>COX4I2</i>	-1.95	<i>NDUFB3</i>	-1.51	<i>UQCRC1</i>	-1.49
<i>COX5A</i>	1.87	<i>NDUFB4</i>	-1.39	<i>UQCRC2</i>	-2.84
<i>COX5B</i>	-1.71	<i>NDUFB5</i>	1.21	<i>UQCRCF1</i>	1.23
<i>COX6A1</i>	-1.21	<i>NDUFB6</i>	-1.51	<i>UQCRH</i>	-1.32
<i>COX6A2</i>	-1.35	<i>NDUFB7</i>	1.79	<i>UQCRQ</i>	-2.49

B2M = Endogenous Control Gene

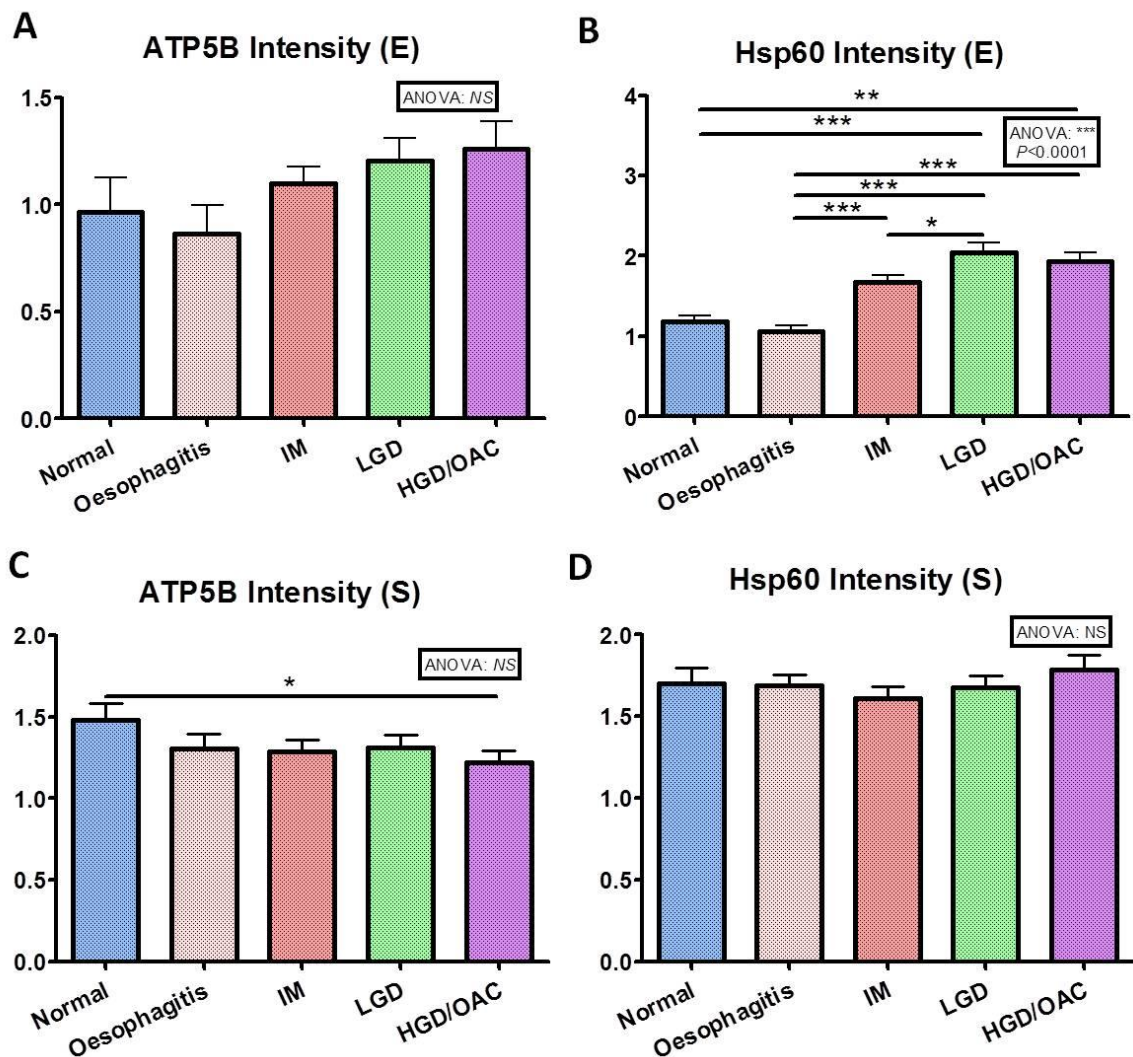
* Relative Expression (e.g. expression of *ATP4A* is 1.79 times greater in OE33 than GO cells)



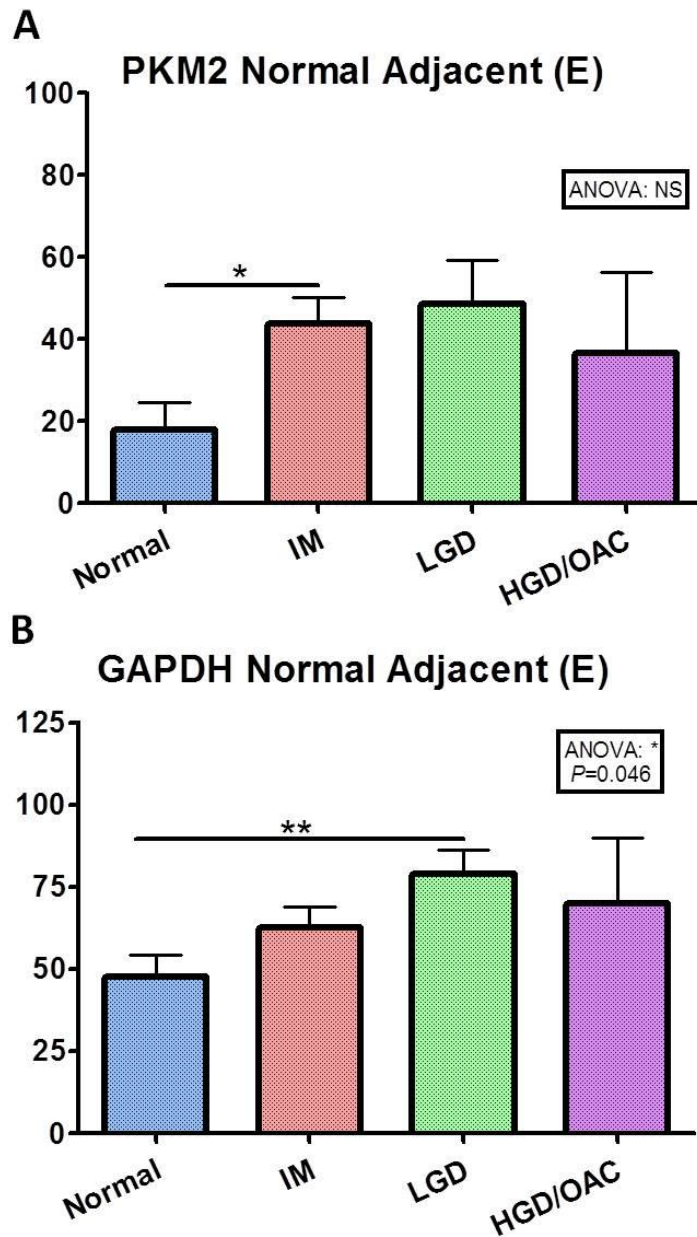
Appendix E. *In-vitro* and *in-vivo* validation of COX6C. (A) COX6C ($P < 0.05$) was differentially expressed between the *in-vitro* Barrett's cell lines (unpaired *t*-test) (Bonferroni post-hoc test). One-way ANOVA was used to investigate differences across the *in-vitro* Barrett's sequence for COX6C *in-vitro* ($P = 0.003$). (B) COX6C ($P < 0.05$) was differentially expressed across the Barrett's disease sequence (Mann-Whitney U). A Kruskal-Wallis test was used to investigate differences across the Barrett's sequence for COX6C *in-vivo* ($P = 0.013$). Bars denote mean \pm SEM.



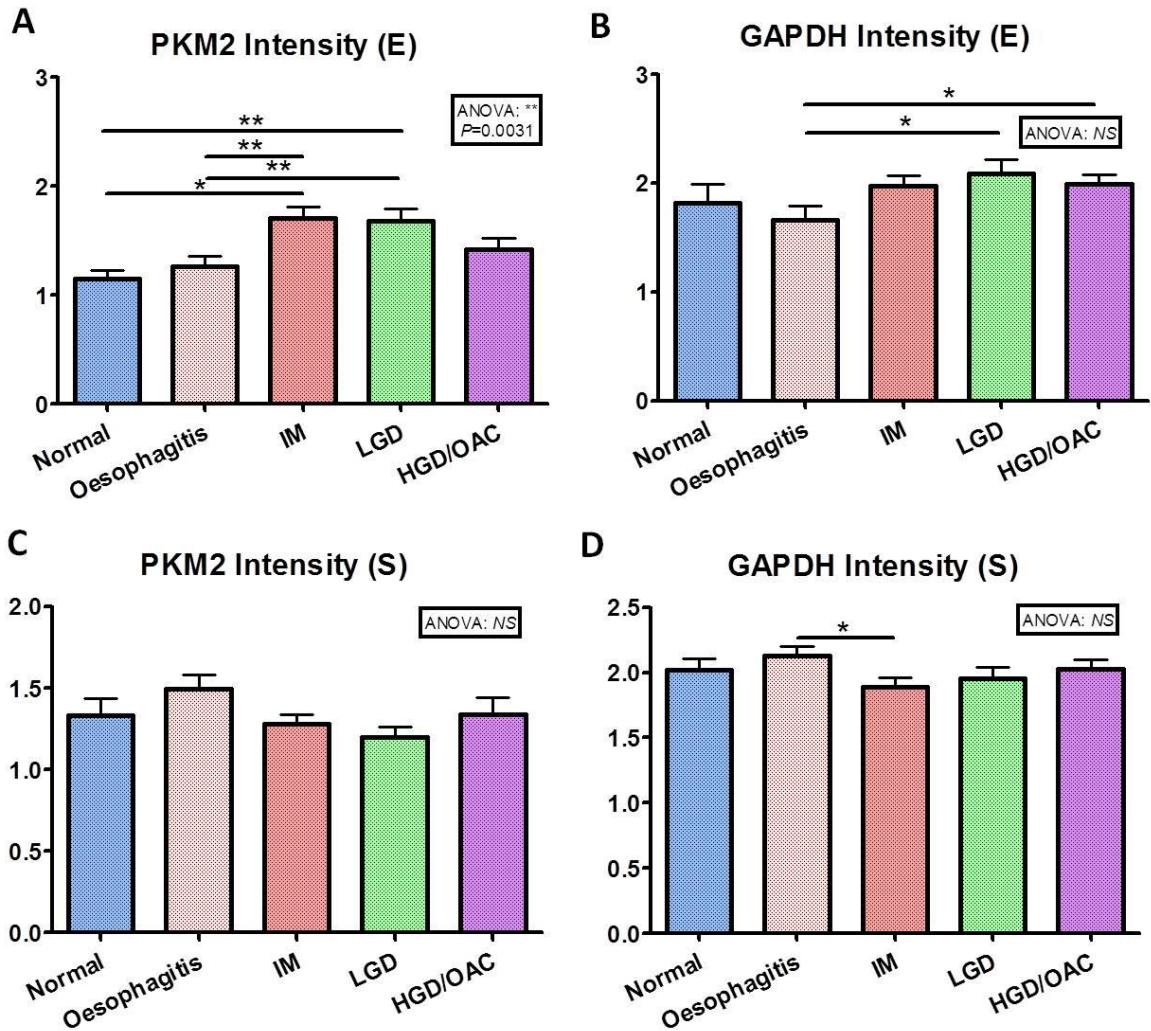
Appendix F. Stromal immunohistochemical tissue expression of the oxidative phosphorylation protein markers, ATP5B and HSP60, across the metaplasia-dysplasia-adenocarcinoma disease sequence. (A) Stromal ATP5B positivity was unchanged across the Barrett's disease sequence (Kruskal Wallis test) ($P>0.05$). ATP5B positivity was significantly increased between oesophagitis and intestinal metaplasia subgroups ($P=0.042$) (Dunn's post hoc test; Mann Whitney U test). **(B)** Stromal HSP60 positivity was unchanged across the Barrett's disease sequence (Kruskal-Wallis test) ($P>0.05$). Bars denote mean \pm SEM.



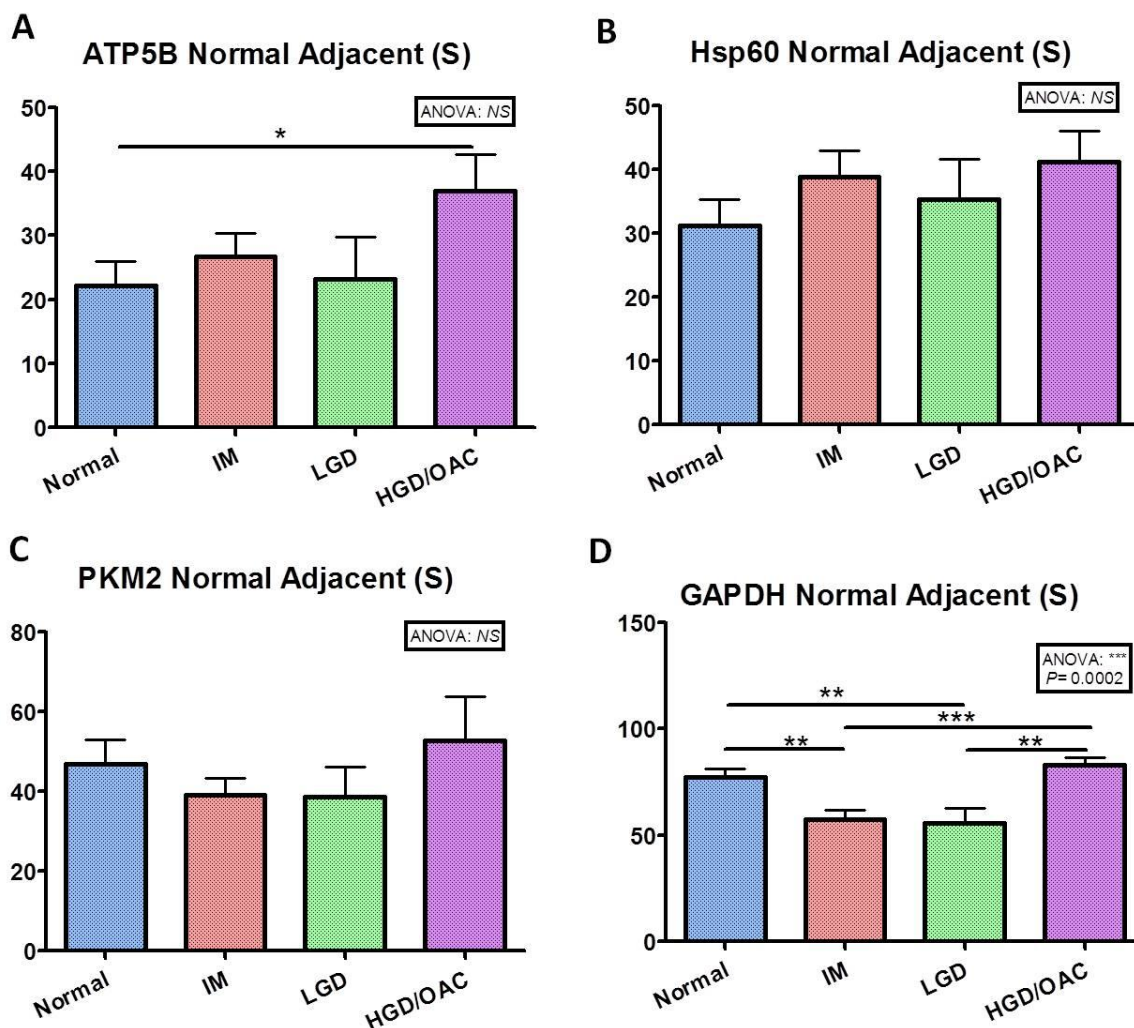
Appendix G. Epithelial and stromal immunohistochemical tissue intensity of the oxidative phosphorylation protein markers, ATP5B and HSP60, across the metaplasia-dysplasia-adenocarcinoma disease sequence. (A) Epithelial ATP5B intensity was unchanged across the Barrett's disease sequence (Kruskal-Wallis test) ($P>0.05$). **(B)** Epithelial HSP60 intensity significantly increased across the Barrett's disease sequence (Kruskal-Wallis test) ($P<0.0001$) (Dunn's post hoc tests; Mann Whitney U tests). **(C)** Stromal ATP5B intensity was unchanged across the Barrett's disease sequence (Kruskal Wallis test; Mann Whitney U test) ($P>0.05$). **(D)** Stromal HSP60 intensity was unchanged across the Barrett's disease sequence (Kruskal Wallis test; Mann Whitney U test) ($P>0.05$). Bars denote mean \pm SEM.



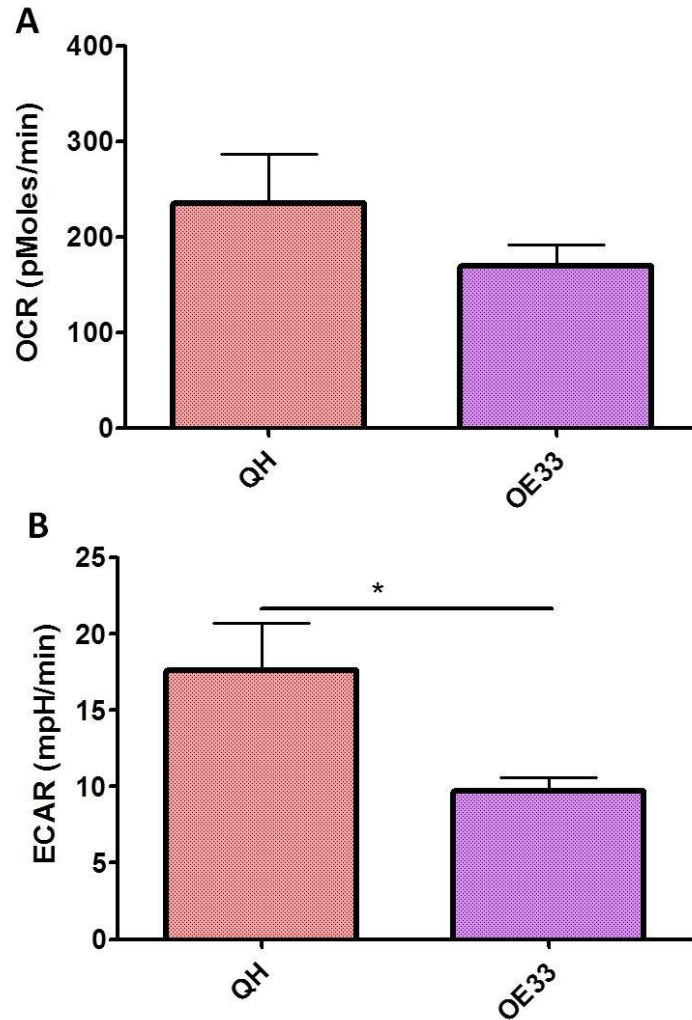
Appendix H. Epithelial immunohistochemical tissue expression of the glycolytic protein biomarkers, PKM2 and GAPDH, across the metaplasia-dysplasia-adenocarcinoma disease sequence in matched normal adjacent tissue. (A) Epithelial PKM2 positivity was unchanged across the Barrett's disease sequence in matched normal adjacent tissue (Kruskal-Wallis test) ($P>0.05$). PKM2 positivity was significantly increased between squamous and intestinal metaplasia subgroups ($P=0.027$) (Dunn's post hoc test; Mann Whitney U test). **(B)** Epithelial GAPDH positivity was unchanged across the Barrett's disease sequence in matched normal adjacent tissue (Kruskal-Wallis test) ($P>0.05$). GAPDH positivity was significantly increased between squamous and LGD subgroups ($P=0.007$) (Dunn's post hoc test; Mann Whitney U test). Bars denote mean \pm SEM.



Appendix I. Epithelial and stromal immunohistochemical tissue intensity of the glycolytic protein biomarkers, PKM2 and GAPDH, across the metaplasia-dysplasia-adenocarcinoma disease sequence. (A) Epithelial PKM2 intensity was significantly increased across the Barrett’s disease sequence (Kruskal-Wallis test) ($P=0.0031$) (Dunn’s post hoc tests; Mann Whitney U tests). **(B)** Epithelial GAPDH intensity was unchanged across the Barrett’s disease sequence (Kruskal-Wallis test; Mann Whitney U tests) ($P>0.05$). **(C)** Stromal PKM2 intensity was unchanged across the Barrett’s disease sequence (Kruskal Wallis test) ($P>0.05$). **(D)** Stromal GAPDH intensity was unchanged across the Barrett’s disease sequence (Kruskal Wallis test; Mann Whitney U test) ($P>0.05$). Bars denote mean \pm SEM.

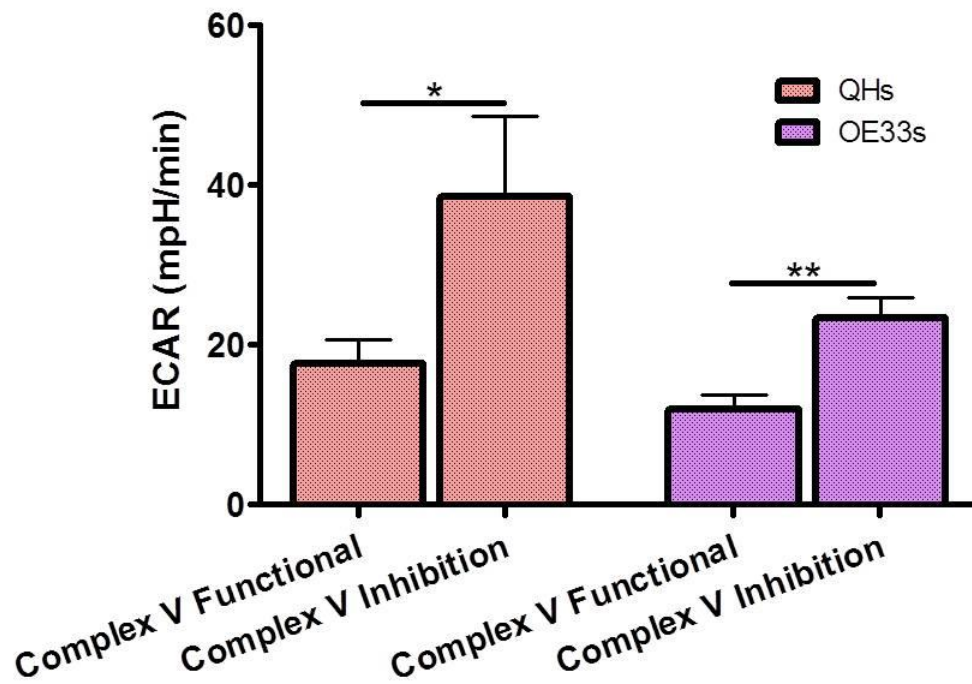


Appendix J. Stromal immunohistochemical positivity of the oxidative phosphorylation protein markers, ATP5B and HSP60, and the glycolytic protein biomarkers, PKM2 and GAPDH, across the metaplasia-dysplasia-adenocarcinoma disease sequence in matched normal adjacent tissue. (A) Stromal ATP5B positivity was unchanged across the Barrett’s disease sequence (Kruskal-Wallis test; Mann Whitney U test) ($P>0.05$). **(B)** Stromal HSP60 positivity was unchanged across the Barrett’s disease sequence (Kruskal-Wallis test) ($P>0.05$). **(C)** Stromal PKM2 positivity was unchanged across the Barrett’s disease sequence (Kruskal-Wallis test) ($P>0.05$). **(D)** Stromal GAPDH positivity was significantly altered across the Barrett’s disease sequence in matched normal adjacent tissue (Kruskal Wallis test; Dunn’s post hoc tests; Mann Whitney U tests) ($P=0.0002$). Bars denote mean \pm SEM.

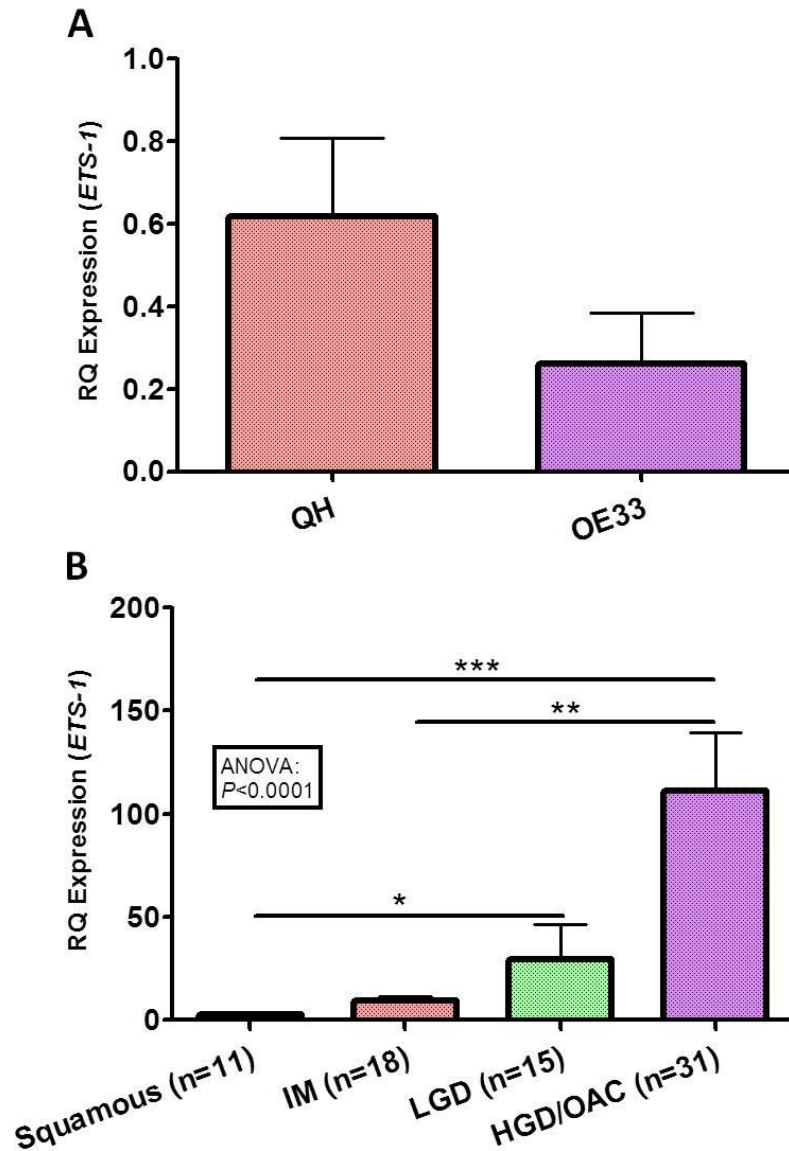


Appendix K. Characterising realtime metabolism at baseline in QH and OE33 cell lines. (A) No significant changes in the levels of OCR were exhibited between QH and OE33 cell lines at baseline ($P=0.276$) (unpaired t -test). **(B)** Levels of ECAR were significantly higher in the Barrett's QH cells compared to the OE33 adenocarcinoma cells at baseline ($P=0.04$) (unpaired t -test). Bars denote mean \pm SEM ($n=5$).

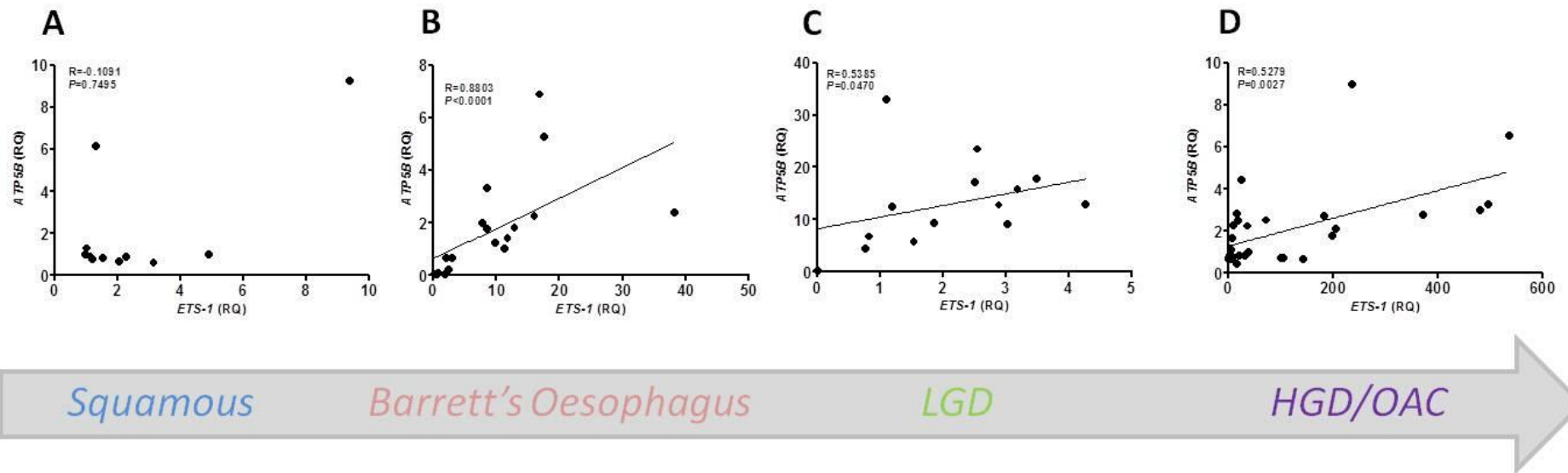
Glycolytic Compensation



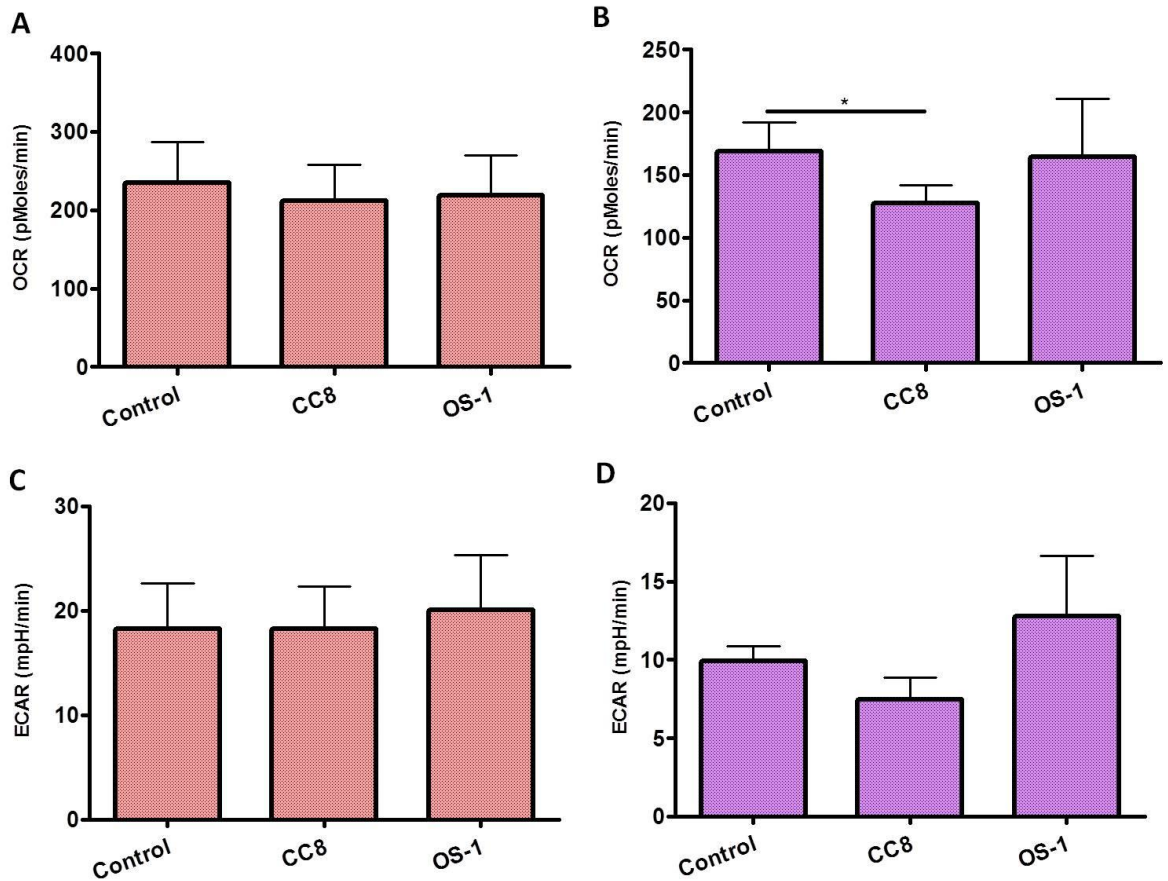
Appendix L. Investigating the realtime effect of complex V (ATP synthase) inhibition on glycolysis in the Barrett's (QH) and adenocarcinoma (OE33) cell lines *in-vitro*. ECAR, reflecting glycolysis, was significantly increased in QH ($P=0.044$) and OE33 ($P=0.005$) cell lines subsequent to oligomycin-induced complex V inhibition using Seahorse technology (paired *t*-tests). Bars denote mean \pm SEM ($n=5$).



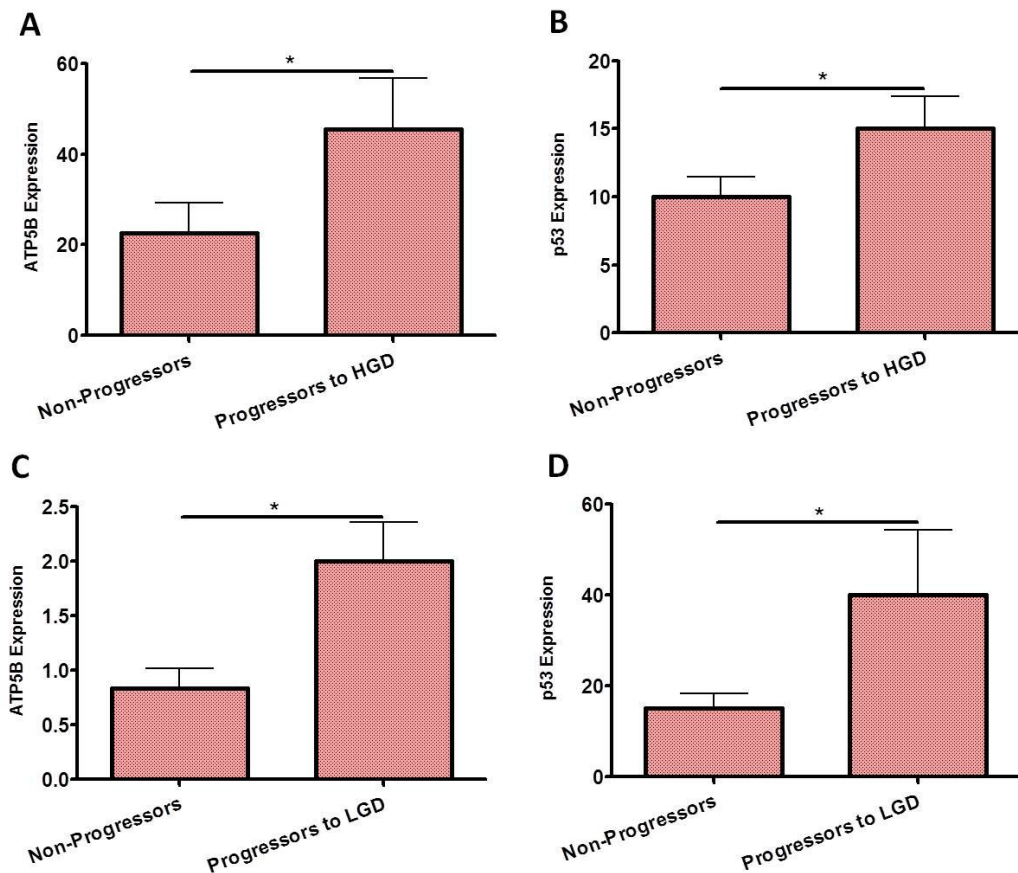
Appendix M. *In-vitro* and *in-vivo* validation of *ETS-1*. (A) No significant difference in *ETS-1* expression was found between Barrett's and OAC cell lines (unpaired *t*-test) ($n=3$) ($P>0.05$). (B) *ETS-1* ($P<0.0001$) expression was significantly increased across the squamous-metaplasia-dysplasia-OAC sequence *in-vivo* (Kruskal-Wallis test; Dunn's post hoc tests). Bars denote mean \pm SEM.



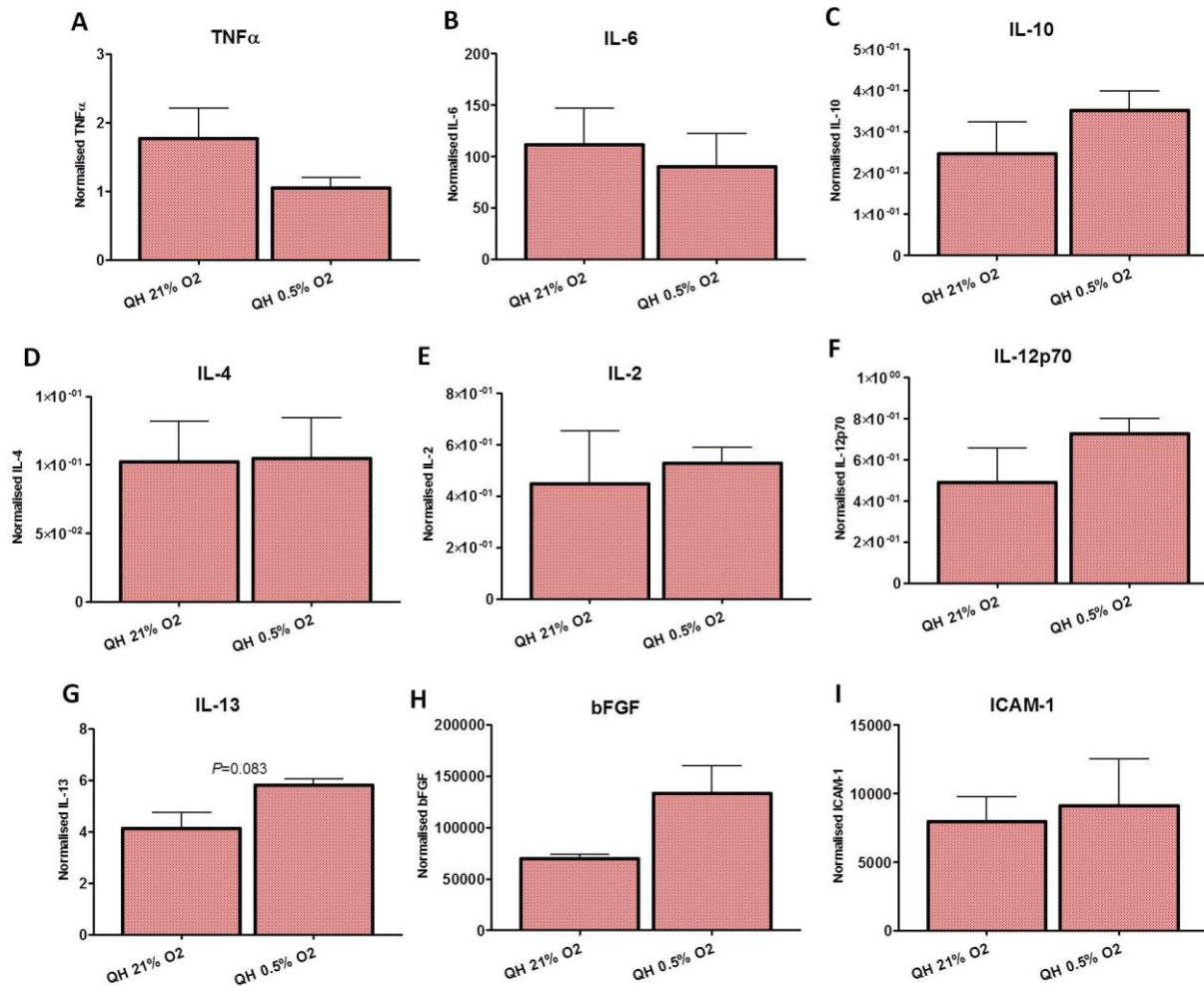
Appendix N. Investigating the association between ATP5B and the transcription factor *ETS-1* across the squamous-metaplasia-dysplasia-adenocarcinoma disease sequence *in-vivo*. (A) No link was found between *ATP5B* and *ETS-1* in normal squamous tissue ($R = -0.109$, $P = 0.7495$) ($n = 11$). (B) A strong significant positive association was found between *ATP5B* and *ETS-1* in Barrett's tissue ($R = 0.88$, $P < 0.0001$) ($n = 18$). (C) A significant positive relationship was found between *ATP5B* and *ETS-1* in LGD tissue ($R = 0.539$, $P = 0.047$) ($n = 14$). (D) A significant positive link was found between *ATP5B* and *ETS-1* in HGD/OAC tissue ($R = 0.528$, $P = 0.0027$) ($n = 30$). R denotes Spearman ρ correlation. Note that two outliers, one in the LGD and one in the HGD/OAC analyses, were removed.



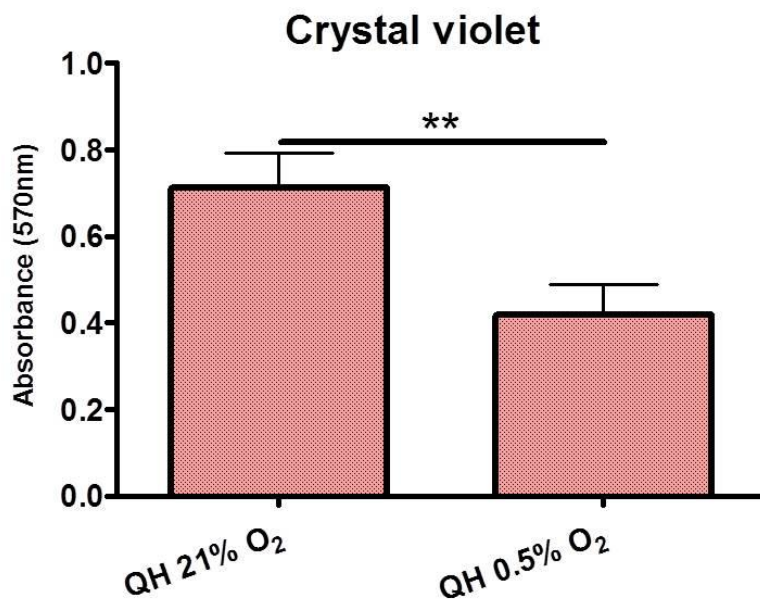
Appendix O. Investigating the effect of two Quinib analogues, CC8 and OS-1, on metabolism between metaplasia and adenocarcinoma cell lines *in-vitro*. (A) CC8 and OS-1 treated QH cells demonstrated no significant alterations in OCR versus untreated QH cells ($P>0.05$). (B) CC8 treated OE33 cells exhibited significantly lower levels of OCR compared to untreated OE33 cells ($P=0.01$). (C) CC8 and OS-1 treated QH cells demonstrated no significant alterations in ECAR in QH cells ($P>0.05$). (D) CC8 and OS-1 treated OE33 cells exhibited no significant alterations in ECAR in OE33 cells ($P>0.05$). Paired *t*-tests assessed differences between treatment groups ($n=5$). Bars denote mean \pm SEM.



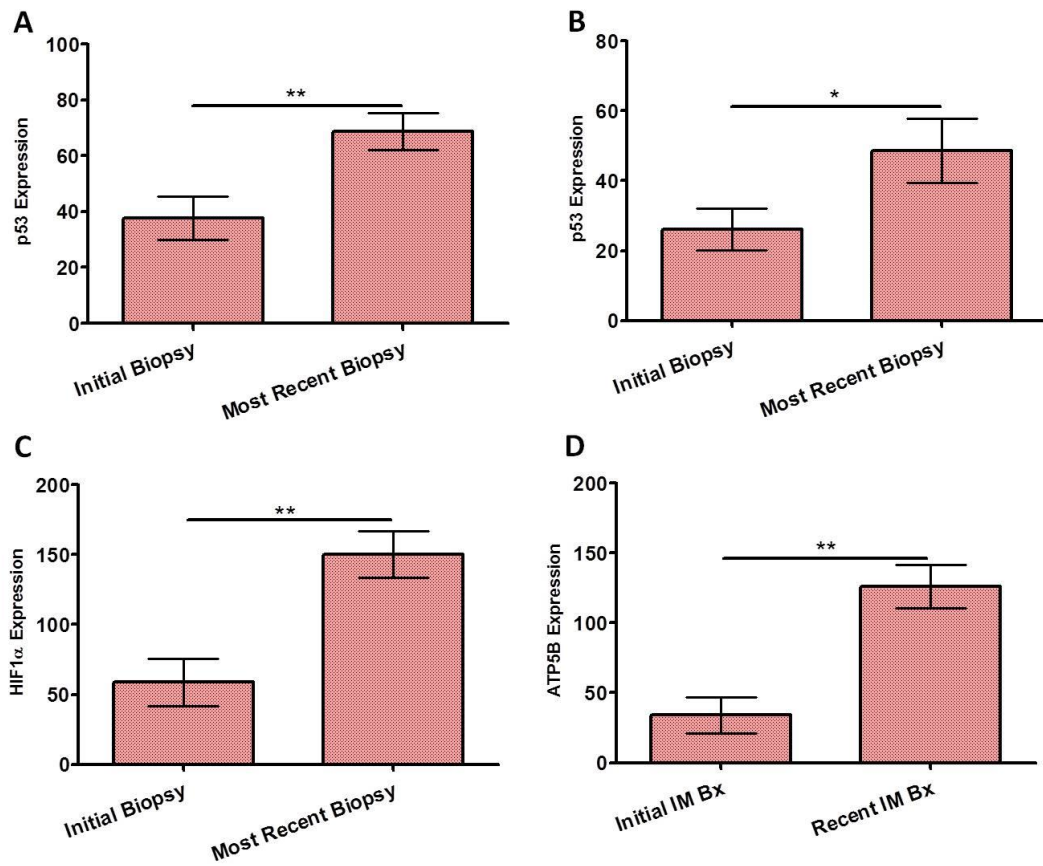
Appendix P. Longitudinal immunohistochemical assessment of p53 and ATP5B expression in Barrett's non-progressors and progressors to LGD and HGD. (A) Barrett's patients who prospectively progressed to HGD ($n=9$) exhibited significantly higher epithelial cytoplasmic ATP5B positivity versus Barrett's non-progressors ($n=18$) ($P=0.046$). (B) Barrett's patients who progressed to HGD ($n=9$) exhibited significantly higher stromal cytoplasmic p53 IxP expression versus Barrett's non-progressors ($n=17$) ($P=0.027$). (C) Barrett's patients who prospectively progressed to LGD ($n=4$) exhibited significantly higher epithelial cytoplasmic ATP5B intensity versus Barrett's non-progressors ($n=18$) ($P=0.028$). (D) Barrett's patients who progressed to LGD ($n=4$) exhibited significantly higher epithelial cytoplasmic p53 positivity versus Barrett's non-progressors ($n=18$) ($P=0.039$). (Mann Whitney U tests). Bars denote mean \pm SEM.



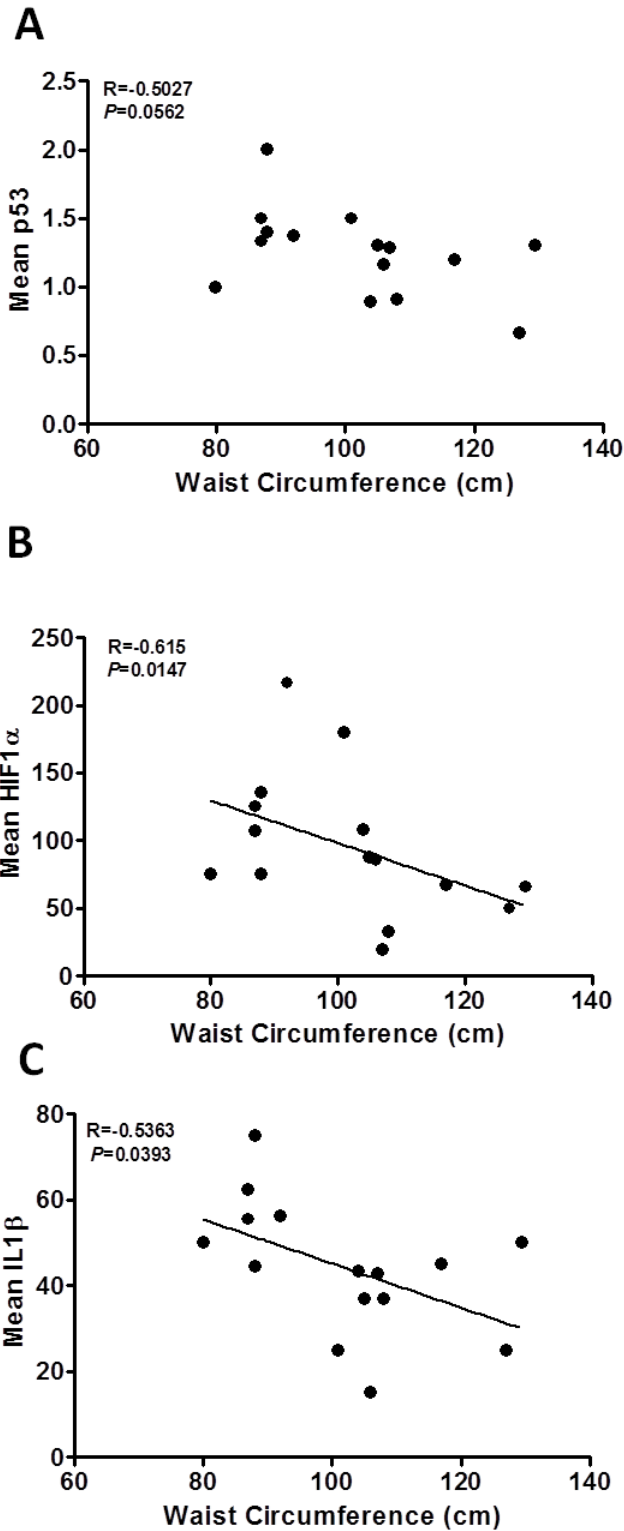
Appendix Q. Investigating the effect of hypoxia on inflammatory and angiogenic profiles in an *in-vitro* model of Barrett's oesophagus. No significant difference in the secreted levels of TNF α (A), IL-6 (B), IL-10 (C), IL-4 (D), IL-2 (E), IL-12p70 (F), IL-13 (G), bFGF (H) and ICAM-1 (I) were found in Barrett's cells exposed to normoxia (21% oxygen) and hypoxia (0.5% hypoxia) ($P > 0.05$; paired t -test; $n = 3-7$). Bars denote mean \pm SEM.



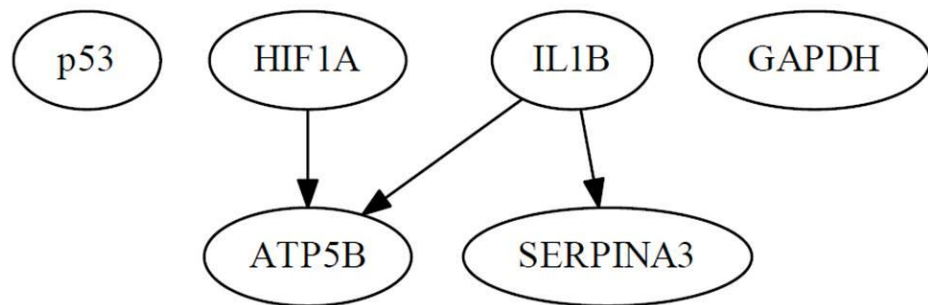
Appendix R. Investigating the effect of hypoxia on cell number in the Barrett's QH cell line *in-vitro*. Cell numbers were significantly altered in Barrett's cells exposed to normoxia (21% oxygen) and hypoxia (0.5% hypoxia) as demonstrated by crystal violet assay (paired *t*-test; *n*=3). Bars denote mean ± SEM.



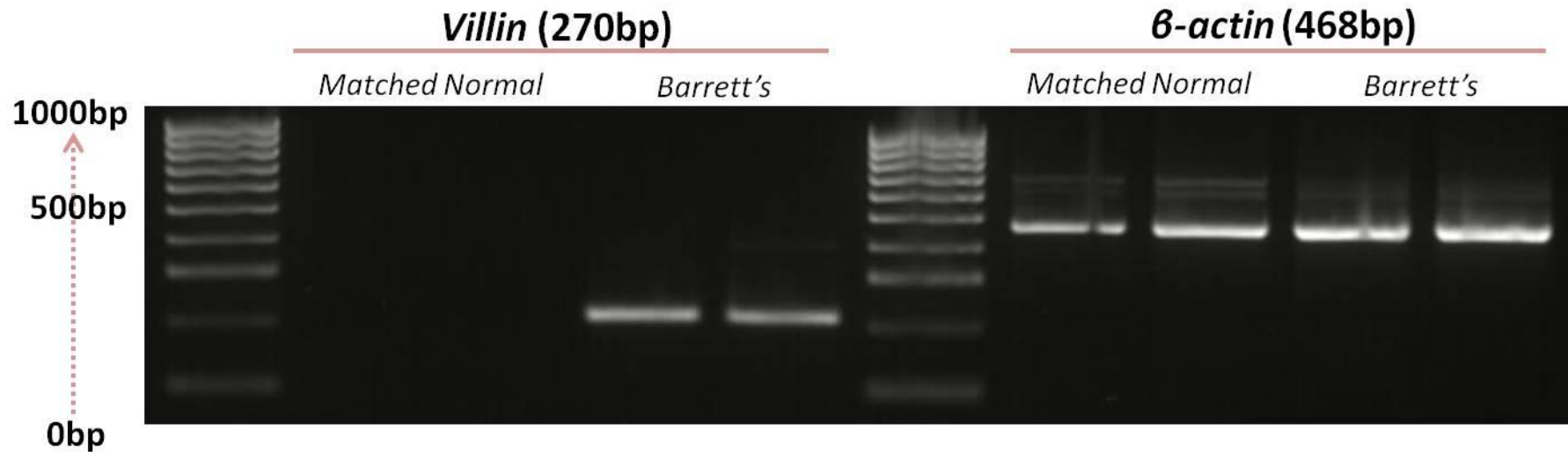
Appendix S. Examining the expression of p53, HIF1α and ATP5B in initial and most recent matched longitudinal Barrett's tissues. (A) Epithelial nuclear p53 positivity was significantly increased in most recently biopsied Barrett's tissue compared to initial tissue ($P=0.007$) ($n=19$). (B) Epithelial cytoplasmic p53 IxP expression was significantly increased in most recently biopsied Barrett's tissue compared to initial tissue ($P=0.042$) ($n=19$). (C) Epithelial cytoplasmic HIF1α IxP expression was significantly increased in most recently biopsied Barrett's tissue compared to initial tissue ($P=0.002$) ($n=18$). (D) Epithelial cytoplasmic ATP5B IxP expression was significantly increased in most recently biopsied Barrett's tissue compared to initial tissue ($P=0.002$) ($n=19$) (Wilcoxon signed rank tests). Bars denote mean \pm SEM.



Appendix T. Linking obesity to p53 status, HIF1 α and IL1 β in Barrett's oesophagus *in-vivo*. (A) Stromal cytoplasmic p53 intensity showed no significant association with waist circumference ($R=-0.503$, $P=0.056$). (B) Epithelial cytoplasmic HIF1 α IxP expression significantly negatively correlated with waist circumference ($R=-0.615$, $P=0.015$). (C) Stromal cytoplasmic IL1 β positivity significantly negatively correlated to waist circumference ($R=-0.536$, $P=0.039$). Waist circumference was available on 15 patients from the 29 patients who participated in the study. R denotes Spearman ρ correlation (IxP= intensity by positivity).

A**B**

Appendix U. Assessing the dependencies between factors taking into account the combined effect of all factors *in-vivo*. (A) Positivity data revealed that ATP5B expression is directly interdependent with HIF1 α , IL1 β and indirectly with SERPINA3 expression within epithelial compartments. (B) Positivity data revealed that GAPDH expression is directly interdependent with p53 expression within stromal compartments. All links function reciprocally and thus are not one-way.



Appendix V. Characterisation of matched normal adjacent and Barrett's tissue. A representative image from a RT-PCR gel showing the absence of the intestinal metaplasia molecular marker, villin (270bp), in matched normal adjacent tissue and the presence of the same marker in Barrett's tissue. Both tissue types were simultaneously confirmed for the presence of β -actin (468bp). Upon synthesis of cDNA from mRNA, villin and β -actin were amplified in a PCR reaction utilising 2 μ L of cDNA with the melting temperatures (T_m) of 62° and 58° respectively for 38 cycles. Primer sequences were as follows: **Villin forward** - 5'-AATGCCACCATGGAGAACA-3'; **Villin reverse** - 5'-ACCACAATTCTGTCTTTCACGG-3'; β -actin forward – 5'-TGAGAGGGAAATCGTGCGTG-3'; β -actin reverse – 5'-TGCTTGCTGATCCACATCTGC-3'. Each PCR reaction contained 10 μ L of 1x Mangomix (Bioline), 2 μ L 10 μ M forward primer, 2 μ L 10 μ M reverse primer, 5 μ L RNase/DNase free dH₂O and 2 μ L cDNA. PCR was performed for 95°C for 5 minutes, followed by 38 cycles of 95°C for 1 minute, 62°C for 1 minute (58°C for β -actin) and 72°C for 1 minute. Lastly, PCR was heated to 72°C for 10 minutes and PCR products ran on a 2% agarose gel containing 10mg/mL ethidium bromide at 80V for 1 hour and the gel imaged through UV exposure. Analogous images were obtained for all 9 *ex-vivo* Barrett's explant tissues used throughout this study.

Appendix W. The association between metabolism, inflammation, angiogenesis and BMI in matched normal adjacent *ex-vivo* explant tissue from patients with Barrett's oesophagus.

Correlation	Correlation Coefficient, r	P
<i>Metabolism vs. Inflammation</i>		
ATP5B vs. IL1 β *	0.762	0.036
GAPDH vs. IL1 β	0.883	0.002
GAPDH vs. IL-2 *	0.785	0.027
HSP60 vs. IL1 β *	0.8	0.01
HSP60 vs. IL-2	0.767	0.016
PKM2 vs. IL1 β *	0.683	0.04
<i>Metabolism vs. Angiogenesis</i>		
ATP5B vs. ICAM-1 *	0.8	0.02
GAPDH vs. ICAM-1 *	0.928	0.002
HSP60 vs. ICAM-1 *	0.7381	0.045
<i>Metabolism vs. BMI</i>		
GAPDH vs. BMI	0.833	0.005
HSP60 vs. BMI	0.967	0.0001
ATP5B vs. BMI	0.78	0.013
PKM2 vs. BMI	0.833	0.002
<i>Inflammation vs. BMI</i>		
IL-2 vs. BMI	0.783	0.013
Spearman ρ , n=9 (n=8*)		

Appendix X. The association between angiogenesis, inflammation and SMAC/Diablo in matched normal adjacent *ex-vivo* explant tissue from patients with Barrett's oesophagus.

Correlation	Correlation Coefficient, r	P
<i>Angiogenesis vs. Inflammation</i>		
ANG-1 vs. IL1 β	0.767	0.016
ANG-1 vs. TNF α	0.8	0.01
ANG-1 vs. IL-2	0.717	0.03
bFGF vs. GRO α *	0.77	0.02
bFGF vs. MMP9 *	0.833	0.0005
bFGF vs. MMP2 *	0.883	0.004
bFGF vs. MIP3 α *	0.762	0.03
bFGF vs. MCP-1 *	0.857	0.011
PAI-1 vs. GRO α *	0.96	0.0001
PAI-1 vs. MMP2 *	0.778	0.028
PAI-1 vs. MIP3 α *	0.81	0.022
PAI-1 vs. MCP-1 *	0.883	0.002
VCAM-1 vs. IL-2	0.75	0.02
<i>SMAC/Diablo vs. Angiogenesis</i>		
SMAC/Diablo vs. bFGF *	0.95	0.001
SMAC/Diablo vs. VEGF	0.683	0.042
SMAC/Diablo vs. MMP9	0.7	0.036
SMAC/Diablo vs. MCP-1 *	0.715	0.046
Spearman ρ , $n=9$ ($n=8^*$)		

References

1. Vizcaino AP, Moreno V, Lambert R, Parkin DM. Time trends incidence of both major histologic types of esophageal carcinomas in selected countries, 1973-1995. *International journal of cancer*. 2002 Jun 20;99(6):860-8. PubMed PMID: 12115489. Epub 2002/07/13. eng.
2. Pennathur A, Gibson MK, Jobe BA, Luketich JD. Oesophageal carcinoma. *Lancet (London, England)*. 2013 Feb 2;381(9864):400-12. PubMed PMID: 23374478. Epub 2013/02/05. eng.
3. Simard EP, Ward EM, Siegel R, Jemal A. Cancers with increasing incidence trends in the United States: 1999 through 2008. *CA: a cancer journal for clinicians - Cancer J Clin*. 2012 Mar-Apr;62(2):118-28. PubMed PMID: 22281605. Epub 2012/01/28. eng.
4. Ireland NCR. Incidence and 5-year survival rates 2015 [cited 2015 2nd-September-2015]. Incidence and 5-year survival rate of those with oesophageal cancer in the Irish population]. Available from: <http://www.ncri.ie/>.
5. Hvid-Jensen F, Pedersen L, Drewes AM, Sorensen HT, Funch-Jensen P. Incidence of adenocarcinoma among patients with Barrett's esophagus. *The New England journal of medicine*. 2011 Oct 13;365(15):1375-83. PubMed PMID: 21995385. Epub 2011/10/15. eng.
6. Sharma P. Clinical practice. Barrett's esophagus. *The New England journal of medicine*. 2009 Dec 24;361(26):2548-56. PubMed PMID: 20032324. Epub 2009/12/25. eng.
7. Hayeck TJ, Kong CY, Spechler SJ, Gazelle GS, Hur C. The prevalence of Barrett's esophagus in the US: estimates from a simulation model confirmed by SEER data. *Diseases of the esophagus*. 2010 Aug;23(6):451-7. PubMed PMID: 20353441. Pubmed Central PMCID: PMC2896446. Epub 2010/04/01. eng.
8. Rex DK, Cummings OW, Shaw M, Cumings MD, Wong RK, Vasudeva RS, et al. Screening for Barrett's esophagus in colonoscopy patients with and without heartburn. *Gastroenterology*. 2003 Dec;125(6):1670-7. PubMed PMID: 14724819. Epub 2004/01/16. eng.
9. Sharma P, McQuaid K, Dent J, Fennerty MB, Sampliner R, Spechler S, et al. A critical review of the diagnosis and management of Barrett's esophagus: the AGA Chicago Workshop. *Gastroenterology*. 2004 Jul;127(1):310-30. PubMed PMID: 15236196. Epub 2004/07/06. eng.
10. Anaparthi R, Gaddam S, Kanakadandi V, Alsop BR, Gupta N, Higbee AD, et al. Association between length of Barrett's esophagus and risk of high-grade dysplasia or adenocarcinoma in patients without dysplasia. *Clinical gastroenterology and hepatology : the official clinical practice journal of the American Gastroenterological Assoc*. 2013 Nov;11(11):1430-6. PubMed PMID: 23707463. Epub 2013/05/28. eng.
11. Naini BV, Chak A, Ali MA, Odze RD. Barrett's oesophagus diagnostic criteria: endoscopy and histology. *Best practice & research Clinical gastroenterology*. 2015 Feb;29(1):77-96. PubMed PMID: 25743458. Epub 2015/03/07. eng.
12. Cohen J, Safdi MA, Deal SE, Baron TH, Chak A, Hoffman B, et al. Quality indicators for esophagogastroduodenoscopy. *Gastrointestinal endoscopy*. 2006 Apr;63(4 Suppl):S10-5. PubMed PMID: 16564907. Epub 2006/03/28. eng.
13. Riddell RH, Odze RD. Definition of Barrett's esophagus: time for a rethink--is intestinal metaplasia dead? *The American journal of gastroenterology*. 2009 Oct;104(10):2588-94. PubMed PMID: 19623166. Epub 2009/07/23. eng.

14. Wang DH, Souza RF. Biology of Barrett's esophagus and esophageal adenocarcinoma. *Gastrointestinal endoscopy clinics of North America*. 2011 Jan;21(1):25-38. PubMed PMID: 21112495. Pubmed Central PMCID: PMC3052949. Epub 2010/11/30. eng.
15. Fitzgerald RC, di Pietro M, Ragnath K, Ang Y, Kang JY, Watson P, et al. British Society of Gastroenterology guidelines on the diagnosis and management of Barrett's oesophagus. *Gut*. 2014 Jan;63(1):7-42. PubMed PMID: 24165758. Epub 2013/10/30. eng.
16. Liu W, Hahn H, Odze RD, Goyal RK. Metaplastic esophageal columnar epithelium without goblet cells shows DNA content abnormalities similar to goblet cell-containing epithelium. *The American journal of gastroenterology*. 2009 Apr;104(4):816-24. PubMed PMID: 19293780. Pubmed Central PMCID: PMC2722438. Epub 2009/03/19. eng.
17. Chaves P, Crespo M, Ribeiro C, Laranjeira C, Pereira AD, Suspiro A, et al. Chromosomal analysis of Barrett's cells: demonstration of instability and detection of the metaplastic lineage involved. *Modern Pathology*. 2007 Jul;20(7):788-96. PubMed PMID: 17529926. Epub 2007/05/29. eng.
18. Bhat S, Coleman HG, Yousef F, Johnston BT, McManus DT, Gavin AT, et al. Risk of malignant progression in Barrett's esophagus patients: results from a large population-based study. *Journal of the National Cancer Institute*. 2011 Jul 6;103(13):1049-57. PubMed PMID: 21680910. Pubmed Central PMCID: PMC3632011. Epub 2011/06/18. eng.
19. Chaves P, Cruz C, Dias Pereira A, Suspiro A, de Almeida JC, Leitao CN, et al. Gastric and intestinal differentiation in Barrett's metaplasia and associated adenocarcinoma. *Diseases of the esophagus*. 2005;18(6):383-7. PubMed PMID: 16336609. Epub 2005/12/13. eng.
20. Hahn HP, Blount PL, Ayub K, Das KM, Souza R, Spechler S, et al. Intestinal differentiation in metaplastic, nongoblet columnar epithelium in the esophagus. *The American journal of surgical pathology*. 2009 Jul;33(7):1006-15. PubMed PMID: 19363439. Pubmed Central PMCID: PMC2807916. Epub 2009/04/14. eng.
21. Spechler SJ. Barrett's esophagus and esophageal adenocarcinoma: pathogenesis, diagnosis, and therapy. *The Medical clinics of North America*. 2002 Nov;86(6):1423-45, vii. PubMed PMID: 12510459. Epub 2003/01/04. eng.
22. Edge SB, Compton CC. The American Joint Committee on Cancer: the 7th edition of the AJCC cancer staging manual and the future of TNM. *Ann Surg Oncol*. 2010 Jun;17(6):1471-4. PubMed PMID: 20180029. Epub 2010/02/25. eng.
23. Schmidt HG, Riddell RH, Walther B, Skinner DB, Riemann JF. Dysplasia in Barrett's esophagus. *Journal of cancer research and clinical oncology*. 1985;110(2):145-52. PubMed PMID: 4044629. Epub 1985/01/01. eng.
24. Jagadeshram VP, Kely CJ. Low grade dysplasia in Barrett's esophagus: Should we worry? *World journal of gastrointestinal pathophysiology*. 2014 May 15;5(2):91-9. PubMed PMID: 24891980. Pubmed Central PMCID: PMC4025077. Epub 2014/06/04. eng.
25. Odze RD. Diagnosis and grading of dysplasia in Barrett's oesophagus. *Journal of clinical pathology*. 2006 Oct;59(10):1029-38. PubMed PMID: 17021130. Pubmed Central PMCID: PMC1861756. Epub 2006/10/06. eng.
26. Skacel M, Petras RE, Gramlich TL, Sigel JE, Richter JE, Goldblum JR. The diagnosis of low-grade dysplasia in Barrett's esophagus and its implications for disease progression. *The American journal of gastroenterology*. 2000 Dec;95(12):3383-7. PubMed PMID: 11151865. Epub 2001/01/11. eng.

27. Weston AP, Banerjee SK, Sharma P, Tran TM, Richards R, Cherian R. p53 protein overexpression in low grade dysplasia (LGD) in Barrett's esophagus: immunohistochemical marker predictive of progression. *The American journal of gastroenterology*. 2001 May;96(5):1355-62. PubMed PMID: 11374668. Epub 2001/05/26. eng.
28. Schulmann K, Sterian A, Berki A, Yin J, Sato F, Xu Y, et al. Inactivation of p16, RUNX3, and HPP1 occurs early in Barrett's-associated neoplastic progression and predicts progression risk. *Oncogene*. 2005 Jun 9;24(25):4138-48. PubMed PMID: 15824739. Epub 2005/04/13. eng.
29. Reid BJ, Levine DS, Longton G, Blount PL, Rabinovitch PS. Predictors of progression to cancer in Barrett's esophagus: baseline histology and flow cytometry identify low- and high-risk patient subsets. *The American journal of gastroenterology*. 2000 Jul;95(7):1669-76. PubMed PMID: 10925966. Pubmed Central PMCID: PMC1783835. Epub 2000/08/05. eng.
30. Rabinovitch PS, Longton G, Blount PL, Levine DS, Reid BJ. Predictors of progression in Barrett's esophagus III: baseline flow cytometric variables. *The American journal of gastroenterology*. 2001 Nov;96(11):3071-83. PubMed PMID: 11721752. Pubmed Central PMCID: PMC1559994. Epub 2001/11/28. eng.
31. Booth CL, Thompson KS. Barrett's esophagus: A review of diagnostic criteria, clinical surveillance practices and new developments. *Journal of gastrointestinal oncology*. 2012 Sep;3(3):232-42. PubMed PMID: 22943014. Pubmed Central PMCID: PMC3418534. Epub 2012/09/04. eng.
32. Peters JH, Clark GW, Ireland AP, Chandrasoma P, Smyrk TC, DeMeester TR. Outcome of adenocarcinoma arising in Barrett's esophagus in endoscopically surveyed and nonsurveyed patients. *The Journal of thoracic and cardiovascular surgery*. 1994 Nov;108(5):813-21; discussion 21-2. PubMed PMID: 7967662. Epub 1994/11/01. eng.
33. Fountoulakis A, Zafirellis KD, Dolan K, Dexter SP, Martin IG, Sue-Ling HM. Effect of surveillance of Barrett's oesophagus on the clinical outcome of oesophageal cancer. *The British journal of surgery*. 2004 Aug;91(8):997-1003. PubMed PMID: 15286961. Epub 2004/08/03. eng.
34. Roberts KJ, Harper E, Alderson D, Hallissey M. Long-term survival and cost analysis of an annual Barrett's surveillance programme. *European journal of gastroenterology & hepatology*. 2010 Apr;22(4):399-403. PubMed PMID: 19858726. Epub 2009/10/28. eng.
35. Corley DA, Levin TR, Habel LA, Weiss NS, Buffler PA. Surveillance and survival in Barrett's adenocarcinomas: a population-based study. *Gastroenterology*. 2002 Mar;122(3):633-40. PubMed PMID: 11874995. Epub 2002/03/05. eng.
36. Spechler SJ, Sharma P, Souza RF, Inadomi JM, Shaheen NJ. American Gastroenterological Association medical position statement on the management of Barrett's esophagus. *Gastroenterology*. 2011 Mar;140(3):1084-91. PubMed PMID: 21376940. Epub 2011/03/08. eng.
37. Wang KK, Sampliner RE. Updated guidelines 2008 for the diagnosis, surveillance and therapy of Barrett's esophagus. *The American journal of gastroenterology*. 2008 Mar;103(3):788-97. PubMed PMID: 18341497. Epub 2008/03/18. eng.
38. Rees JR, Lao-Sirieix P, Wong A, Fitzgerald RC. Treatment for Barrett's oesophagus. *The Cochrane database of systematic reviews*. 2010 (1):CD004060. PubMed PMID: 20091557. Epub 2010/01/22. eng.
39. Kahrilas PJ. Clinical practice. Gastroesophageal reflux disease. *The New England journal of medicine*. 2008 Oct 16;359(16):1700-7. PubMed PMID: 18923172. Pubmed Central PMCID: PMC3058591. Epub 2008/10/17. eng.

40. Attwood SE, Lundell L, Hatlebakk JG, Eklund S, Junghard O, Galmiche JP, et al. Medical or surgical management of GERD patients with Barrett's esophagus: the LOTUS trial 3-year experience. *Journal of gastrointestinal surgery : official journal of the Society for Surgery of the Alimentary Tract*. 2008 Oct;12(10):1646-54; discussion 54-5. PubMed PMID: 18709511. Epub 2008/08/19. eng.
41. El-Serag HB, Aguirre TV, Davis S, Kuebler M, Bhattacharyya A, Sampliner RE. Proton pump inhibitors are associated with reduced incidence of dysplasia in Barrett's esophagus. *The American journal of gastroenterology*. 2004 Oct;99(10):1877-83. PubMed PMID: 15447744. Epub 2004/09/28. eng.
42. Hillman LC, Chiragakis L, Shadbolt B, Kaye GL, Clarke AC. Proton-pump inhibitor therapy and the development of dysplasia in patients with Barrett's oesophagus. *The Medical journal of Australia*. 2004 Apr 19;180(8):387-91. PubMed PMID: 15089728. Epub 2004/04/20. eng.
43. Sharma P, Sampliner RE, Camargo E. Normalization of esophageal pH with high-dose proton pump inhibitor therapy does not result in regression of Barrett's esophagus. *The American journal of gastroenterology*. 1997 Apr;92(4):582-5. PubMed PMID: 9128303. Epub 1997/04/01. eng.
44. Corey KE, Schmitz SM, Shaheen NJ. Does a surgical antireflux procedure decrease the incidence of esophageal adenocarcinoma in Barrett's esophagus? A meta-analysis. *The American journal of gastroenterology*. 2003 Nov;98(11):2390-4. PubMed PMID: 14638338. Epub 2003/11/26. eng.
45. Rice TW, Murthy SC, Mason DP, Rybicki LA, Yerian LM, Dumot JA, et al. Esophagectomy for clinical high-grade dysplasia. *European journal of cardio-thoracic surgery*. 2011 Jul;40(1):113-9. PubMed PMID: 21277216. Epub 2011/02/01. eng.
46. Wani S, Sayana H, Sharma P. Endoscopic eradication of Barrett's esophagus. *Gastrointestinal endoscopy*. 2010 Jan;71(1):147-66. PubMed PMID: 19879565. Epub 2009/11/03. eng.
47. Konda VJ, Ross AS, Ferguson MK, Hart JA, Lin S, Naylor K, et al. Is the risk of concomitant invasive esophageal cancer in high-grade dysplasia in Barrett's esophagus overestimated? *Clinical gastroenterology and hepatology : the official clinical practice journal of the American Gastroenterological Association*. 2008 Feb;6(2):159-64. PubMed PMID: 18096439. Epub 2007/12/22. eng.
48. O'Farrell NJ, Reynolds JV, Ravi N, Larkin JO, Malik V, Wilson GF, et al. Evolving changes in the management of early oesophageal adenocarcinoma in a tertiary centre. *Irish journal of medical science*. 2013 Sep;182(3):363-9. PubMed PMID: 23242575. Epub 2012/12/18. eng.
49. Overholt BF, Lightdale CJ, Wang KK, Canto MI, Burdick S, Haggitt RC, et al. Photodynamic therapy with porfimer sodium for ablation of high-grade dysplasia in Barrett's esophagus: international, partially blinded, randomized phase III trial. *Gastrointestinal endoscopy*. 2005 Oct;62(4):488-98. PubMed PMID: 16185958. Epub 2005/09/28. eng.
50. Shaheen NJ, Sharma P, Overholt BF, Wolfsen HC, Sampliner RE, Wang KK, et al. Radiofrequency ablation in Barrett's esophagus with dysplasia. *The New England journal of medicine*. 2009 May 28;360(22):2277-88. PubMed PMID: 19474425. Epub 2009/05/29. eng.
51. Pech O, Behrens A, May A, Nachbar L, Gossner L, Rabenstein T, et al. Long-term results and risk factor analysis for recurrence after curative endoscopic therapy in 349 patients with high-grade intraepithelial neoplasia and mucosal adenocarcinoma in Barrett's oesophagus. *Gut*. 2008 Sep;57(9):1200-6. PubMed PMID: 18460553. Epub 2008/05/08. eng.

52. Allum WH, Blazeby JM, Griffin SM, Cunningham D, Jankowski JA, Wong R. Guidelines for the management of oesophageal and gastric cancer. *Gut*. 2011 Nov;60(11):1449-72. PubMed PMID: 21705456. Epub 2011/06/28. eng.
53. Group. MRCOCW. Surgical resection with or without preoperative chemotherapy in oesophageal cancer: a randomised controlled trial. *Lancet (London, England)*. 2002 May 18;359(9319):1727-33. PubMed PMID: 12049861. Epub 2002/06/07. eng.
54. Cunningham D, Allum WH, Stenning SP, Thompson JN, Van de Velde CJ, Nicolson M, et al. Perioperative chemotherapy versus surgery alone for resectable gastroesophageal cancer. *The New England journal of medicine*. 2006 Jul 6;355(1):11-20. PubMed PMID: 16822992. Epub 2006/07/11. eng.
55. Schneider JL, Corley DA. A review of the epidemiology of Barrett's oesophagus and oesophageal adenocarcinoma. *Best practice & research Clinical gastroenterology*. 2015 Feb;29(1):29-39. PubMed PMID: 25743454. Epub 2015/03/07. eng.
56. Wong A, Fitzgerald RC. Epidemiologic risk factors for Barrett's esophagus and associated adenocarcinoma. *Clinical gastroenterology and hepatology : the official clinical practice journal of the American Gastroenterological Association*. 2005 Jan;3(1):1-10. PubMed PMID: 15645398. Epub 2005/01/13. eng.
57. Vaezi MF, Richter JE. Role of acid and duodenogastroesophageal reflux in gastroesophageal reflux disease. *Gastroenterology*. 1996 Nov;111(5):1192-9. PubMed PMID: 8898632. Epub 1996/11/01. eng.
58. Fennerty MB. Barrett's-related esophageal cancer: has the final hurdle been cleared, now paving the way for human chemoprevention trials? *Gastroenterology*. 2002 Apr;122(4):1172-5. PubMed PMID: 11910370. Epub 2002/03/23. eng.
59. Cook MB, Corley DA, Murray LJ, Liao LM, Kamangar F, Ye W, et al. Gastroesophageal reflux in relation to adenocarcinomas of the esophagus: a pooled analysis from the Barrett's and Esophageal Adenocarcinoma Consortium (BEACON). *PloS one*. 2014;9(7):e103508. PubMed PMID: 25075959. Pubmed Central PMCID: PMC4116205. Epub 2014/07/31. eng.
60. Reid BJ, Kostadinov R, Maley CC. New strategies in Barrett's esophagus: integrating clonal evolutionary theory with clinical management. *Clinical cancer research*. 2011 Jun 1;17(11):3512-9. PubMed PMID: 21498395. Pubmed Central PMCID: PMC3119197. Epub 2011/04/19. eng.
61. Lagergren J, Bergstrom R, Lindgren A, Nyren O. Symptomatic gastroesophageal reflux as a risk factor for esophageal adenocarcinoma. *The New England journal of medicine*. 1999 Mar 18;340(11):825-31. PubMed PMID: 10080844. Epub 1999/03/18. eng.
62. Lieberman DA, Oehlke M, Helfand M. Risk factors for Barrett's esophagus in community-based practice. GORGE consortium. Gastroenterology Outcomes Research Group in Endoscopy. *The American journal of gastroenterology*. 1997 Aug;92(8):1293-7. PubMed PMID: 9260792. Epub 1997/08/01. eng.
63. Orenstein SR, Shalaby TM, Barmada MM, Whitcomb DC. Genetics of gastroesophageal reflux disease: a review. *Journal of pediatric gastroenterology and nutrition*. 2002 May;34(5):506-10. PubMed PMID: 12050574. Epub 2002/06/07. eng.
64. Souza RF. The role of acid and bile reflux in oesophagitis and Barrett's metaplasia. *Biochemical Society transactions*. 2010 Apr;38(2):348-52. PubMed PMID: 20298181. Pubmed Central PMCID: PMC3072824. Epub 2010/03/20. eng.

65. Livstone EM, Sheahan DG, Behar J. Studies of esophageal epithelial cell proliferation in patients with reflux esophagitis. *Gastroenterology*. 1977 Dec;73(6):1315-9. PubMed PMID: 913973. Epub 1977/12/01. eng.
66. Karin M. The regulation of AP-1 activity by mitogen-activated protein kinases. *Philosophical transactions of the Royal Society of London Series B, Biological sciences*. 1996 Feb 29;351(1336):127-34. PubMed PMID: 8650258. Epub 1996/02/29. eng.
67. Souza RF, Shewmake KL, Shen Y, Ramirez RD, Bullock JS, Hladik CL, et al. Differences in ERK activation in squamous mucosa in patients who have gastroesophageal reflux disease with and without Barrett's esophagus. *The American journal of gastroenterology*. 2005 Mar;100(3):551-9. PubMed PMID: 15743351. Epub 2005/03/04. eng.
68. Souza RF, Huo X, Mittal V, Schuler CM, Carmack SW, Zhang HY, et al. Gastroesophageal reflux might cause esophagitis through a cytokine-mediated mechanism rather than caustic acid injury. *Gastroenterology*. 2009 Nov;137(5):1776-84. PubMed PMID: 19660463. Epub 2009/08/08. eng.
69. Quante M, Bhagat G, Abrams JA, Marache F, Good P, Lee MD, et al. Bile acid and inflammation activate gastric cardia stem cells in a mouse model of Barrett-like metaplasia. *Cancer cell*. 2012 Jan 17;21(1):36-51. PubMed PMID: 22264787. Pubmed Central PMCID: PMC3266546. Epub 2012/01/24. eng.
70. Burnat G, Rau T, Elshimi E, Hahn EG, Konturek PC. Bile acids induce overexpression of homeobox gene CDX-2 and vascular endothelial growth factor (VEGF) in human Barrett's esophageal mucosa and adenocarcinoma cell line. *Scandinavian journal of gastroenterology*. 2007 Dec;42(12):1460-5. PubMed PMID: 17852856. Epub 2007/09/14. eng.
71. Huo X, Juergens S, Zhang X, Rezaei D, Yu C, Strauch ED, et al. Deoxycholic acid causes DNA damage while inducing apoptotic resistance through NF-kappaB activation in benign Barrett's epithelial cells. *American journal of physiology Gastrointestinal and liver physiology*. 2011 Aug;301(2):G278-86. PubMed PMID: 21636532. Pubmed Central PMCID: PMC3154602. Epub 2011/06/04. eng.
72. Jenkins GJ, Cronin J, Alhamdani A, Rawat N, D'Souza F, Thomas T, et al. The bile acid deoxycholic acid has a non-linear dose response for DNA damage and possibly NF-kappaB activation in oesophageal cells, with a mechanism of action involving ROS. *Mutagenesis*. 2008 Sep;23(5):399-405. PubMed PMID: 18515815. Epub 2008/06/03. eng.
73. Jenkins GJ, D'Souza FR, Suzen SH, Eltahir ZS, James SA, Parry JM, et al. Deoxycholic acid at neutral and acid pH, is genotoxic to oesophageal cells through the induction of ROS: The potential role of anti-oxidants in Barrett's oesophagus. *Carcinogenesis*. 2007 Jan;28(1):136-42. PubMed PMID: 16905748. Epub 2006/08/15. eng.
74. Jenkins GJ, Harries K, Doak SH, Wilmes A, Griffiths AP, Baxter JN, et al. The bile acid deoxycholic acid (DCA) at neutral pH activates NF-kappaB and induces IL-8 expression in oesophageal cells in vitro. *Carcinogenesis*. 2004 Mar;25(3):317-23. PubMed PMID: 14656946. Epub 2003/12/06. eng.
75. Corley DA, Kubo A, Levin TR, Block G, Habel L, Rumore G, et al. Race, ethnicity, sex and temporal differences in Barrett's oesophagus diagnosis: a large community-based study, 1994-2006. *Gut*. 2009 Feb;58(2):182-8. PubMed PMID: 18978173. Pubmed Central PMCID: PMC2671084. Epub 2008/11/04. eng.
76. El-Serag HB, Mason AC, Petersen N, Key CR. Epidemiological differences between adenocarcinoma of the oesophagus and adenocarcinoma of the gastric cardia in the USA. *Gut*.

2002 Mar;50(3):368-72. PubMed PMID: 11839716. Pubmed Central PMCID: PMC1773122. Epub 2002/02/13. eng.

77. Picardo SL, O'Brien MP, Feighery R, O'Toole D, Ravi N, O'Farrell NJ, et al. A Barrett's esophagus registry of over 1000 patients from a specialist center highlights greater risk of progression than population-based registries and high risk of low grade dysplasia. *Diseases of the esophagus*. 2015 Feb-Mar;28(2):121-6. PubMed PMID: 24428806. Epub 2014/01/17. eng.

78. Rogers EL, Goldkind SF, Iseri OA, Bustin M, Goldkind L, Hamilton SR, et al. Adenocarcinoma of the lower esophagus. A disease primarily of white men with Barrett's esophagus. *Journal of clinical gastroenterology*. 1986 Dec;8(6):613-8. PubMed PMID: 3805655. Epub 1986/12/01. eng.

79. Cook MB, Wild CP, Forman D. A systematic review and meta-analysis of the sex ratio for Barrett's esophagus, erosive reflux disease, and nonerosive reflux disease. *American journal of epidemiology*. 2005 Dec 1;162(11):1050-61. PubMed PMID: 16221805. Epub 2005/10/14. eng.

80. Younes M, Henson DE, Ertan A, Miller CC. Incidence and survival trends of esophageal carcinoma in the United States: racial and gender differences by histological type. *Scandinavian journal of gastroenterology*. 2002 Dec;37(12):1359-65. PubMed PMID: 12523583. Epub 2003/01/14. eng.

81. Yeh C, Hsu CT, Ho AS, Sampliner RE, Fass R. Erosive esophagitis and Barrett's esophagus in Taiwan: a higher frequency than expected. *Digestive diseases and sciences*. 1997 Apr;42(4):702-6. PubMed PMID: 9125635. Epub 1997/04/01. eng.

82. Thrift AP, Shaheen NJ, Gammon MD, Bernstein L, Reid BJ, Onstad L, et al. Obesity and risk of esophageal adenocarcinoma and Barrett's esophagus: a mendelian randomization study. *Journal of the National Cancer Institute*. 2014 Nov;106(11). PubMed PMID: 25269698. Pubmed Central PMCID: PMC4200028. Epub 2014/10/02. eng.

83. Kendall BJ, Macdonald GA, Prins JB, O'Brien S, Whiteman DC. Total body fat and the risk of Barrett's oesophagus - a bioelectrical impedance study. *Cancer epidemiology*. 2014 Jun;38(3):266-72. PubMed PMID: 24726825. Pubmed Central PMCID: PMC4180020. Epub 2014/04/15. eng.

84. Murray L, Johnston B, Lane A, Harvey I, Donovan J, Nair P, et al. Relationship between body mass and gastro-oesophageal reflux symptoms: The Bristol Helicobacter Project. *International journal of epidemiology*. 2003 Aug;32(4):645-50. PubMed PMID: 12913045. Epub 2003/08/13. eng.

85. Kulig M, Nocon M, Vieth M, Leodolter A, Jaspersen D, Labenz J, et al. Risk factors of gastroesophageal reflux disease: methodology and first epidemiological results of the ProGERD study. *Journal of clinical epidemiology*. 2004 Jun;57(6):580-9. PubMed PMID: 15246126. Epub 2004/07/13. eng.

86. Edelstein ZR, Farrow DC, Bronner MP, Rosen SN, Vaughan TL. Central adiposity and risk of Barrett's esophagus. *Gastroenterology*. 2007 Aug;133(2):403-11. PubMed PMID: 17681161. Epub 2007/08/08. eng.

87. Su Z, Gay LJ, Strange A, Palles C, Band G, Whiteman DC, et al. Common variants at the MHC locus and at chromosome 16q24.1 predispose to Barrett's esophagus. *Nature genetics*. 2012 Sep 9;44(10):1131-6. PubMed PMID: 22961001. Pubmed Central PMCID: PMC3459818. Epub 2012/09/11. Eng.

88. Kubo A, Levin TR, Block G, Rumore GJ, Quesenberry CP, Jr., Buffler P, et al. Dietary antioxidants, fruits, and vegetables and the risk of Barrett's esophagus. *The American journal of*

gastroenterology. 2008 Jul;103(7):1614-23; quiz 24. PubMed PMID: 18494834. Pubmed Central PMCID: PMC2735568. Epub 2008/05/23. eng.

89. Kubo A, Block G, Quesenberry CP, Jr., Buffler P, Corley DA. Effects of dietary fiber, fats, and meat intakes on the risk of Barrett's esophagus. *Nutrition and cancer*. 2009;61(5):607-16. PubMed PMID: 19838934. Pubmed Central PMCID: PMC2765669. Epub 2009/10/20. eng.

90. Kubo A, Levin TR, Block G, Rumore GJ, Quesenberry CP, Jr., Buffler P, et al. Dietary patterns and the risk of Barrett's esophagus. *American journal of epidemiology*. 2008 Apr 1;167(7):839-46. PubMed PMID: 18218607. Epub 2008/01/26. eng.

91. Kubo A, Corley DA, Jensen CD, Kaur R. Dietary factors and the risks of oesophageal adenocarcinoma and Barrett's oesophagus. *Nutrition research reviews*. 2010 Dec;23(2):230-46. PubMed PMID: 20624335. Pubmed Central PMCID: PMC3062915. Epub 2010/07/14. eng.

92. Jiao L, Kramer JR, Ruge M, Parente P, Verstovsek G, Alsarraj A, et al. Dietary intake of vegetables, folate, and antioxidants and the risk of Barrett's esophagus. *Cancer causes & control : CCC*. 2013 May;24(5):1005-14. PubMed PMID: 23420329. Pubmed Central PMCID: PMC3633655. Epub 2013/02/20. eng.

93. Rudolph RE, Vaughan TL, Kristal AR, Blount PL, Levine DS, Galipeau PC, et al. Serum selenium levels in relation to markers of neoplastic progression among persons with Barrett's esophagus. *Journal of the National Cancer Institute*. 2003 May 21;95(10):750-7. PubMed PMID: 12759393. Pubmed Central PMCID: PMC1939970. Epub 2003/05/22. eng.

94. Caygill CP, Johnston DA, Lopez M, Johnston BJ, Watson A, Reed PI, et al. Lifestyle factors and Barrett's esophagus. *The American journal of gastroenterology*. 2002 Jun;97(6):1328-31. PubMed PMID: 12094845. Epub 2002/07/04. eng.

95. Kabat GC, Ng SK, Wynder EL. Tobacco, alcohol intake, and diet in relation to adenocarcinoma of the esophagus and gastric cardia. *Cancer causes & control : CCC*. 1993 Mar;4(2):123-32. PubMed PMID: 8481491. Epub 1993/03/01. eng.

96. Lagergren J, Bergstrom R, Adami HO, Nyren O. Association between medications that relax the lower esophageal sphincter and risk for esophageal adenocarcinoma. *Annals of internal medicine*. 2000 Aug 1;133(3):165-75. PubMed PMID: 10906830. Epub 2000/07/25. eng.

97. Xu Q, Guo W, Shi X, Zhang W, Zhang T, Wu C, et al. Association Between Alcohol Consumption and the Risk of Barrett's Esophagus: A Meta-Analysis of Observational Studies. *Medicine*. 2015 Aug;94(32):e1244. PubMed PMID: 26266354. Epub 2015/08/13. eng.

98. Cook MB, Shaheen NJ, Anderson LA, Giffen C, Chow WH, Vaughan TL, et al. Cigarette smoking increases risk of Barrett's esophagus: an analysis of the Barrett's and Esophageal Adenocarcinoma Consortium. *Gastroenterology*. 2012 Apr;142(4):744-53. PubMed PMID: 22245667. Pubmed Central PMCID: PMC3321098. Epub 2012/01/17. eng.

99. Andrici J, Cox MR, Eslick GD. Cigarette smoking and the risk of Barrett's esophagus: a systematic review and meta-analysis. *Journal of gastroenterology and hepatology*. 2013 Aug;28(8):1258-73. PubMed PMID: 23611750. Epub 2013/04/25. eng.

100. Cook MB, Kamangar F, Whiteman DC, Freedman ND, Gammon MD, Bernstein L, et al. Cigarette smoking and adenocarcinomas of the esophagus and esophagogastric junction: a pooled analysis from the international BEACON consortium. *Journal of the National Cancer Institute*. 2010 Sep 8;102(17):1344-53. PubMed PMID: 20716718. Pubmed Central PMCID: PMC2935475. Epub 2010/08/19. eng.

101. Gray MR, Donnelly RJ, Kingsnorth AN. The role of smoking and alcohol in metaplasia and cancer risk in Barrett's columnar lined oesophagus. *Gut*. 1993 Jun;34(6):727-31. PubMed PMID: 8314502. Pubmed Central PMCID: PMC1374251. Epub 1993/06/01. eng.
102. Wang C, Yuan Y, Hunt RH. Helicobacter pylori infection and Barrett's esophagus: a systematic review and meta-analysis. *The American journal of gastroenterology*. 2009 Feb;104(2):492-500; quiz 491, 501. PubMed PMID: 19174811. Epub 2009/01/29. eng.
103. Fischbach LA, Nordenstedt H, Kramer JR, Gandhi S, Dick-Onuoha S, Lewis A, et al. The association between Barrett's esophagus and Helicobacter pylori infection: a meta-analysis. *Helicobacter*. 2012 Jun;17(3):163-75. PubMed PMID: 22515353. Pubmed Central PMCID: PMC3335759. Epub 2012/04/21. eng.
104. Corley DA, Kubo A, Levin TR, Block G, Habel L, Rumore G, et al. Helicobacter pylori and gastroesophageal reflux disease: a case-control study. *Helicobacter*. 2008 Oct;13(5):352-60. PubMed PMID: 19250510. Pubmed Central PMCID: PMC2714194. Epub 2009/03/03. eng.
105. Richter JE. Effect of Helicobacter pylori eradication on the treatment of gastro-oesophageal reflux disease. *Gut*. 2004 Feb;53(2):310-1. PubMed PMID: 14724170. Pubmed Central PMCID: PMC1774927. Epub 2004/01/16. eng.
106. Ford AC, Forman D, Reynolds PD, Cooper BT, Moayyedi P. Ethnicity, gender, and socioeconomic status as risk factors for esophagitis and Barrett's esophagus. *American journal of epidemiology*. 2005 Sep 1;162(5):454-60. PubMed PMID: 16076833. Epub 2005/08/04. eng.
107. Gammon MD, Schoenberg JB, Ahsan H, Risch HA, Vaughan TL, Chow WH, et al. Tobacco, alcohol, and socioeconomic status and adenocarcinomas of the esophagus and gastric cardia. *Journal of the National Cancer Institute*. 1997 Sep 3;89(17):1277-84. PubMed PMID: 9293918. Epub 1997/09/18. eng.
108. Brown LM, Silverman DT, Pottern LM, Schoenberg JB, Greenberg RS, Swanson GM, et al. Adenocarcinoma of the esophagus and esophagogastric junction in white men in the United States: alcohol, tobacco, and socioeconomic factors. *Cancer causes & control : CCC*. 1994 Jul;5(4):333-40. PubMed PMID: 8080945. Epub 1994/07/01. eng.
109. Sui G, Zhou S, Wang J, Canto M, Lee EE, Eshleman JR, et al. Mitochondrial DNA mutations in preneoplastic lesions of the gastrointestinal tract: a biomarker for the early detection of cancer. *Molecular cancer therapeutics*. 2006;5:73. PubMed PMID: 17166268. Pubmed Central PMCID: PMC1764424. Epub 2006/12/15. eng.
110. Wilson DM, 3rd, Brooks PJ. The mitochondrial genome: dynamics, mechanisms of repair, and a target in disease and therapy. *Environmental and molecular mutagenesis*. 2010 Jun;51(5):349-51. PubMed PMID: 20544877. Pubmed Central PMCID: PMC2940707. Epub 2010/06/15. eng.
111. Carew JS, Huang P. Mitochondrial defects in cancer. *Molecular cancer*. 2002 Dec 9;1:9. PubMed PMID: 12513701. Pubmed Central PMCID: PMC149412. Epub 2003/01/07. eng.
112. Holt IJ, Reyes A. Human mitochondrial DNA replication. *Cold Spring Harbor perspectives in biology*. 2012 Dec;4(12). PubMed PMID: 23143808. Pubmed Central PMCID: PMC3504440. Epub 2012/11/13. eng.
113. Zastawny TH, Dabrowska M, Jaskolski T, Klimarczyk M, Kulinski L, Koszela A, et al. Comparison of oxidative base damage in mitochondrial and nuclear DNA. *Free radical biology & medicine*. 1998 Mar 15;24(5):722-5. PubMed PMID: 9586801. Epub 1998/05/20. eng.
114. Chatterjee A, Mambo E, Sidransky D. Mitochondrial DNA mutations in human cancer. *Oncogene*. 2006 Aug 7;25(34):4663-74. PubMed PMID: 16892080. Epub 2006/08/08. eng.

115. Lee S, Han MJ, Lee KS, Back SC, Hwang D, Kim HY, et al. Frequent occurrence of mitochondrial DNA mutations in Barrett's metaplasia without the presence of dysplasia. *PLoS one*. 2012;7(5):e37571. PubMed PMID: 22629421. Pubmed Central PMCID: PMC3358277. Epub 2012/05/26. eng.
116. Miyazono F, Schneider PM, Metzger R, Warnecke-Eberz U, Baldus SE, Dienes HP, et al. Mutations in the mitochondrial DNA D-Loop region occur frequently in adenocarcinoma in Barrett's esophagus. *Oncogene*. 2002 May 23;21(23):3780-3. PubMed PMID: 12032845. Epub 2002/05/29. eng.
117. Stachler MD, Taylor-Weiner A, Peng S, McKenna A, Agoston AT, Odze RD, et al. Paired exome analysis of Barrett's esophagus and adenocarcinoma. *Nature genetics*. 2015 Sep;47(9):1047-55. PubMed PMID: 26192918. Pubmed Central PMCID: PMC4552571. Epub 2015/07/21. eng.
118. Eluri S, Brugge WR, Daglilar ES, Jackson SA, Styn MA, Callenberg KM, et al. The Presence of Genetic Mutations at Key Loci Predicts Progression to Esophageal Adenocarcinoma in Barrett's Esophagus. *The American journal of gastroenterology*. 2015 Jun;110(6):828-34. PubMed PMID: 26010308. Pubmed Central PMCID: PMC4471888. Epub 2015/05/27. eng.
119. Tan BH, Skipworth RJ, Stephens NA, Wheelhouse NM, Gilmour H, de Beaux AC, et al. Frequency of the mitochondrial DNA 4977bp deletion in oesophageal mucosa during the progression of Barrett's oesophagus. *European journal of cancer*. 2009 Mar;45(5):736-40. PubMed PMID: 19211242. Epub 2009/02/13. eng.
120. Croft J, Parry EM, Jenkins GJ, Doak SH, Baxter JN, Griffiths AP, et al. Analysis of the premalignant stages of Barrett's oesophagus through to adenocarcinoma by comparative genomic hybridization. *European journal of gastroenterology & hepatology*. 2002 Nov;14(11):1179-86. PubMed PMID: 12439111. Epub 2002/11/20. eng.
121. Nishikawa M, Oshitani N, Matsumoto T, Nishigami T, Arakawa T, Inoue M. Accumulation of mitochondrial DNA mutation with colorectal carcinogenesis in ulcerative colitis. *British journal of cancer*. 2005 Aug 8;93(3):331-7. PubMed PMID: 15956973. Pubmed Central PMCID: PMC2361569. Epub 2005/06/16. eng.
122. Warburg O. On respiratory impairment in cancer cells. *Science (New York, NY)*. 1956 Aug 10;124(3215):269-70. PubMed PMID: 13351639. Epub 1956/08/10. eng.
123. Sharma LK, Fang H, Liu J, Vartak R, Deng J, Bai Y. Mitochondrial respiratory complex I dysfunction promotes tumorigenesis through ROS alteration and AKT activation. *Human molecular genetics*. 2011 Dec 1;20(23):4605-16. PubMed PMID: 21890492. Pubmed Central PMCID: PMC3209831. Epub 2011/09/06. eng.
124. Lu J, Sharma LK, Bai Y. Implications of mitochondrial DNA mutations and mitochondrial dysfunction in tumorigenesis. *Cell research*. 2009 Jul;19(7):802-15. PubMed PMID: 19532122. Epub 2009/06/18. eng.
125. Park JS, Sharma LK, Li H, Xiang R, Holstein D, Wu J, et al. A heteroplasmic, not homoplasmic, mitochondrial DNA mutation promotes tumorigenesis via alteration in reactive oxygen species generation and apoptosis. *Human molecular genetics*. 2009 May 1;18(9):1578-89. PubMed PMID: 19208652. Pubmed Central PMCID: PMC2733816. Epub 2009/02/12. eng.
126. DeHaan C, Habibi-Nazhad B, Yan E, Salloum N, Parliament M, Allalunis-Turner J. Mutation in mitochondrial complex I ND6 subunit is associated with defective response to hypoxia in human glioma cells. *Mol Cancer*. 2004 Jul 12;3:19. PubMed PMID: 15248896. Pubmed Central PMCID: PMC481082. Epub 2004/07/14. eng.

127. Yu AK, Song L, Murray KD, van der List D, Sun C, Shen Y, et al. Mitochondrial complex I deficiency leads to inflammation and retinal ganglion cell death in the Ndufs4 mouse. *Human molecular genetics*. 2015 May 15;24(10):2848-60. PubMed PMID: 25652399. Pubmed Central PMCID: PMC4406296. Epub 2015/02/06. eng.
128. Ishikawa K, Takenaga K, Akimoto M, Koshikawa N, Yamaguchi A, Imanishi H, et al. ROS-generating mitochondrial DNA mutations can regulate tumor cell metastasis. *Science (New York, NY)*. 2008 May 2;320(5876):661-4. PubMed PMID: 18388260. Epub 2008/04/05. eng.
129. Zhang J, Gao Q, Zhou Y, Dier U, Hempel N, Hochwald SN. Focal adhesion kinase-promoted tumor glucose metabolism is associated with a shift of mitochondrial respiration to glycolysis. *Oncogene*. 2015 Jun 29. PubMed PMID: 26119934. Pubmed Central PMCID: PMC4486081. Epub 2015/06/30. Eng.
130. Phelan JJ, MacCarthy F, Feighery R, O'Farrell NJ, Lynam-Lennon N, Doyle B, et al. Differential expression of mitochondrial energy metabolism profiles across the metaplasia-dysplasia-adenocarcinoma disease sequence in Barrett's oesophagus. *Cancer letters*. 2014 Aug 10. PubMed PMID: 25107643. Epub 2014/08/12. Eng.
131. Luengo A, Sullivan LB, Heiden MG. Understanding the complex-ity of metformin action: limiting mitochondrial respiration to improve cancer therapy. *BMC biology*. 2014;12:82. PubMed PMID: 25347702. Pubmed Central PMCID: PMC4207883. Epub 2014/10/28. eng.
132. Orecchioni S, Reggiani F, Talarico G, Mancuso P, Calleri A, Gregato G, et al. The biguanides metformin and phenformin inhibit angiogenesis, local and metastatic growth of breast cancer by targeting both neoplastic and microenvironment cells. *International journal of cancer*. 2015 Mar 15;136(6):E534-44. PubMed PMID: 25196138. Epub 2014/09/10. eng.
133. Laskov I, Drudi L, Beauchamp MC, Yasmeen A, Ferenczy A, Pollak M, et al. Anti-diabetic doses of metformin decrease proliferation markers in tumors of patients with endometrial cancer. *Gynecologic oncology*. 2014 Sep;134(3):607-14. PubMed PMID: 24972190. Epub 2014/06/28. eng.
134. Mitsuhashi A, Kiyokawa T, Sato Y, Shozu M. Effects of metformin on endometrial cancer cell growth in vivo: a preoperative prospective trial. *Cancer*. 2014 Oct 1;120(19):2986-95. PubMed PMID: 24917306. Epub 2014/06/12. eng.
135. Becker C, Jick SS, Meier CR, Bodmer M. Metformin and the risk of head and neck cancer: a case-control analysis. *Diabetes, obesity & metabolism*. 2014 Nov;16(11):1148-54. PubMed PMID: 25041125. Epub 2014/07/22. eng.
136. Fasano M, Della Corte CM, Capuano A, Sasso FC, Papaccio F, Berrino L, et al. A multicenter, open-label phase II study of metformin with erlotinib in second-line therapy of stage IV non-small-cell lung cancer patients: treatment rationale and protocol dynamics of the METAL trial. *Clinical lung cancer*. 2015 Jan;16(1):57-9. PubMed PMID: 25242667. Epub 2014/09/23. eng.
137. Pusceddu S, de Braud F, Concas L, Bregant C, Leuzzi L, Formisano B, et al. Rationale and protocol of the MetNET-1 trial, a prospective, single center, phase II study to evaluate the activity and safety of everolimus in combination with octreotide LAR and metformin in patients with advanced pancreatic neuroendocrine tumors. *Tumori*. 2014 Nov-Dec;100(6):e286-9. PubMed PMID: 25688512. Epub 2015/02/18. eng.
138. Kluckova K, Bezawork-Geleta A, Rohlena J, Dong L, Neuzil J. Mitochondrial complex II, a novel target for anti-cancer agents. *Biochimica et biophysica acta*. 2013 May;1827(5):552-64. PubMed PMID: 23142170. Epub 2012/11/13. eng.
139. Janeway KA, Kim SY, Lodish M, Nose V, Rustin P, Gaal J, et al. Defects in succinate dehydrogenase in gastrointestinal stromal tumors lacking KIT and PDGFRA mutations. *Proceedings*

of the National Academy of Sciences of the United States of America. 2011 Jan 4;108(1):314-8. PubMed PMID: 21173220. Pubmed Central PMCID: PMC3017134. Epub 2010/12/22. eng.

140. Pollard PJ, Briere JJ, Alam NA, Barwell J, Barclay E, Wortham NC, et al. Accumulation of Krebs cycle intermediates and over-expression of HIF1alpha in tumours which result from germline FH and SDH mutations. *Human molecular genetics*. 2005 Aug 1;14(15):2231-9. PubMed PMID: 15987702. Epub 2005/07/01. eng.

141. Favier J, Briere JJ, Burnichon N, Riviere J, Vescovo L, Benit P, et al. The Warburg effect is genetically determined in inherited pheochromocytomas. *PloS one*. 2009;4(9):e7094. PubMed PMID: 19763184. Pubmed Central PMCID: PMC2738974. Epub 2009/09/19. eng.

142. Pasini B, Stratakis CA. SDH mutations in tumorigenesis and inherited endocrine tumours: lesson from the phaeochromocytoma-paraganglioma syndromes. *Journal of internal medicine*. 2009 Jul;266(1):19-42. PubMed PMID: 19522823. Pubmed Central PMCID: PMC3163304. Epub 2009/06/16. eng.

143. van Nederveen FH, Gaal J, Favier J, Korpershoek E, Oldenburg RA, de Bruyn EM, et al. An immunohistochemical procedure to detect patients with paraganglioma and phaeochromocytoma with germline SDHB, SDHC, or SDHD gene mutations: a retrospective and prospective analysis. *Lancet Oncology*. 2009 Aug;10(8):764-71. PubMed PMID: 19576851. Epub 2009/07/07. eng.

144. Ni Y, Eng C. Vitamin E protects against lipid peroxidation and rescues tumorigenic phenotypes in cowden/cowden-like patient-derived lymphoblast cells with germline SDHx variants. *Clinical cancer research*. 2012 Sep 15;18(18):4954-61. PubMed PMID: 22829200. Pubmed Central PMCID: PMC3445717. Epub 2012/07/26. eng.

145. Huang LS, Sun G, Cobessi D, Wang AC, Shen JT, Tung EY, et al. 3-nitropropionic acid is a suicide inhibitor of mitochondrial respiration that, upon oxidation by complex II, forms a covalent adduct with a catalytic base arginine in the active site of the enzyme. *The Journal of biological chemistry*. 2006 Mar 3;281(9):5965-72. PubMed PMID: 16371358. Pubmed Central PMCID: PMC1482830. Epub 2005/12/24. eng.

146. Gomez-Lazaro M, Galindo MF, Melero-Fernandez de Mera RM, Fernandez-Gomez FJ, Concannon CG, Segura MF, et al. Reactive oxygen species and p38 mitogen-activated protein kinase activate Bax to induce mitochondrial cytochrome c release and apoptosis in response to malonate. *Molecular pharmacology*. 2007 Mar;71(3):736-43. PubMed PMID: 17172466. Epub 2006/12/19. eng.

147. Boitier E, Merad-Boudia M, Guguen-Guillouzo C, Defer N, Ceballos-Picot I, Leroux JP, et al. Impairment of the mitochondrial respiratory chain activity in diethylnitrosamine-induced rat hepatomas: possible involvement of oxygen free radicals. *Cancer research*. 1995 Jul 15;55(14):3028-35. PubMed PMID: 7606723. Epub 1995/07/15. eng.

148. Benit P, Lebon S, Rustin P. Respiratory-chain diseases related to complex III deficiency. *Biochimica et biophysica acta*. 2009 Jan;1793(1):181-5. PubMed PMID: 18601960. Epub 2008/07/08. eng.

149. Liu VW, Shi HH, Cheung AN, Chiu PM, Leung TW, Nagley P, et al. High incidence of somatic mitochondrial DNA mutations in human ovarian carcinomas. *Cancer research*. 2001 Aug 15;61(16):5998-6001. PubMed PMID: 11507041. Epub 2001/08/17. eng.

150. Tseng LM, Yin PH, Chi CW, Hsu CY, Wu CW, Lee LM, et al. Mitochondrial DNA mutations and mitochondrial DNA depletion in breast cancer. *Genes, chromosomes & cancer*. 2006 Jul;45(7):629-38. PubMed PMID: 16568452. Epub 2006/03/29. eng.

151. Polyak K, Li Y, Zhu H, Lengauer C, Willson JK, Markowitz SD, et al. Somatic mutations of the mitochondrial genome in human colorectal tumours. *Nature genetics*. 1998 Nov;20(3):291-3. PubMed PMID: 9806551. Epub 1998/11/07. eng.
152. Abnet CC, Huppi K, Carrera A, Armistead D, McKenney K, Hu N, et al. Control region mutations and the 'common deletion' are frequent in the mitochondrial DNA of patients with esophageal squamous cell carcinoma. *BMC cancer*. 2004 Jul 1;4:30. PubMed PMID: 15230979. Pubmed Central PMCID: PMC459226. Epub 2004/07/03. eng.
153. Kato S, Miyabayashi S, Ohi R, Nakagawa H, Abe J, Yamamoto K, et al. Chronic pancreatitis in muscular cytochrome c oxidase deficiency. *Journal of pediatric gastroenterology and nutrition*. 1990 Nov;11(4):549-52. PubMed PMID: 2175784. Epub 1990/11/01. eng.
154. Muller-Hocker J, Schafer S, Krebs S, Blum H, Zsurka G, Kunz WS, et al. Oxyphil cell metaplasia in the parathyroids is characterized by somatic mitochondrial DNA mutations in NADH dehydrogenase genes and cytochrome c oxidase activity-impairing genes. *The American journal of pathology*. 2014 Nov;184(11):2922-35. PubMed PMID: 25418474. Epub 2014/11/25. eng.
155. Bernstein C, Facista A, Nguyen H, Zaitlin B, Hassounah N, Loustaunau C, et al. Cancer and age related colonic crypt deficiencies in cytochrome c oxidase I. *World journal of gastrointestinal oncology*. 2010 Dec 15;2(12):429-42. PubMed PMID: 21191537. Pubmed Central PMCID: PMC3011097. Epub 2010/12/31. eng.
156. Petros JA, Baumann AK, Ruiz-Pesini E, Amin MB, Sun CQ, Hall J, et al. mtDNA mutations increase tumorigenicity in prostate cancer. *Proceedings of the National Academy of Sciences of the United States of America*. 2005 Jan 18;102(3):719-24. PubMed PMID: 15647368. Pubmed Central PMCID: PMC545582. Epub 2005/01/14. eng.
157. Kruse JP, Gu W. p53 aerobics: the major tumor suppressor fuels your workout. *Cell metabolism*. 2006 Jul;4(1):1-3. PubMed PMID: 16814724. Epub 2006/07/04. eng.
158. Lynam-Lennon N, Maher SG, Maguire A, Phelan J, Muldoon C, Reynolds JV, et al. Altered mitochondrial function and energy metabolism is associated with a radioresistant phenotype in oesophageal adenocarcinoma. *PloS one*. 2014;9(6):e100738. PubMed PMID: 24968221. Pubmed Central PMCID: PMC4072695. Epub 2014/06/27. eng.
159. Imad Al Ghoul NKHK, Ulla G. Knaus, Kathy K. Griendling, Rhian M. Touyz, Victor J. Thannickal, Aaron Barchowsky, William M. Nauseef, Eric E. Kelley, Phillip M. Bauer, Victor Darley-Usmar, Sruti Shiva, Eugenia Cifuentes-Pagano, Bruce A. Freeman, Mark T. Gladwin and Patrick J. Pagano. *Oxidases and Peroxidases in Cardiovascular and Lung Disease: New Concepts in Reactive Oxygen Species Signaling*. Free radical biology & medicine. 2011.
160. Lu J, Tan M, Cai Q. The Warburg effect in tumor progression: mitochondrial oxidative metabolism as an anti-metastasis mechanism. *Cancer letters*. 2015 Jan 28;356(2 Pt A):156-64. PubMed PMID: 24732809. Pubmed Central PMCID: PMC4195816. Epub 2014/04/16. eng.
161. Vander Heiden MG, Lunt SY, Dayton TL, Fiske BP, Israelsen WJ, Mattaini KR, et al. Metabolic pathway alterations that support cell proliferation. *Cold Spring Harbor symposia on quantitative biology*. 2011;76:325-34. PubMed PMID: 22262476. Epub 2012/01/21. eng.
162. Vander Heiden MG, Cantley LC, Thompson CB. Understanding the Warburg effect: the metabolic requirements of cell proliferation. *Science (New York, NY)*. 2009 May 22;324(5930):1029-33. PubMed PMID: 19460998. Pubmed Central PMCID: PMC2849637. Epub 2009/05/23. eng.

163. Jose C, Bellance N, Rossignol R. Choosing between glycolysis and oxidative phosphorylation: a tumor's dilemma? *Biochimica et biophysica acta*. 2011 Jun;1807(6):552-61. PubMed PMID: 20955683. Epub 2010/10/20. eng.
164. Bellance N, Benard G, Furt F, Begueret H, Smolkova K, Passerieux E, et al. Bioenergetics of lung tumors: alteration of mitochondrial biogenesis and respiratory capacity. *The international journal of biochemistry & cell biology*. 2009 Dec;41(12):2566-77. PubMed PMID: 19712747. Epub 2009/08/29. eng.
165. Rodriguez-Enriquez S, Carreno-Fuentes L, Gallardo-Perez JC, Saavedra E, Quezada H, Vega A, et al. Oxidative phosphorylation is impaired by prolonged hypoxia in breast and possibly in cervix carcinoma. *The international journal of biochemistry & cell biology*. 2010 Oct;42(10):1744-51. PubMed PMID: 20654728. Epub 2010/07/27. eng.
166. Griguer CE, Oliva CR, Gillespie GY. Glucose metabolism heterogeneity in human and mouse malignant glioma cell lines. *Journal of neuro-oncology*. 2005 Sep;74(2):123-33. PubMed PMID: 16193382. Epub 2005/09/30. eng.
167. Smolkova K, Bellance N, Scandurra F, Genot E, Gnaiger E, Plecita-Hlavata L, et al. Mitochondrial bioenergetic adaptations of breast cancer cells to aglycemia and hypoxia. *Journal of bioenergetics and biomembranes*. 2010 Feb;42(1):55-67. PubMed PMID: 20084539. Epub 2010/01/20. eng.
168. Funes JM, Quintero M, Henderson S, Martinez D, Qureshi U, Westwood C, et al. Transformation of human mesenchymal stem cells increases their dependency on oxidative phosphorylation for energy production. *Proceedings of the National Academy of Sciences of the United States of America*. 2007 Apr 10;104(15):6223-8. PubMed PMID: 17384149. Pubmed Central PMCID: PMC1851087. Epub 2007/03/27. eng.
169. Moiseeva O, Bourdeau V, Roux A, Deschenes-Simard X, Ferbeyre G. Mitochondrial dysfunction contributes to oncogene-induced senescence. *Molecular and cellular biology*. 2009 Aug;29(16):4495-507. PubMed PMID: 19528227. Pubmed Central PMCID: PMC2725737. Epub 2009/06/17. eng.
170. Warburg O. On the origin of cancer cells. *Science (New York, NY)*. 1956 Feb 24;123(3191):309-14. PubMed PMID: 13298683. Epub 1956/02/24. eng.
171. Hanahan D, Weinberg RA. The hallmarks of cancer. *Cell*. 2000 Jan 7;100(1):57-70. PubMed PMID: 10647931. Epub 2000/01/27. eng.
172. Hanahan D, Weinberg RA. Hallmarks of cancer: the next generation. *Cell*. 2011 Mar 4;144(5):646-74. PubMed PMID: 21376230. Epub 2011/03/08. eng.
173. Weinberg F, Chandel NS. Mitochondrial metabolism and cancer. *Annals of the New York Academy of Sciences*. 2009 Oct;1177:66-73. PubMed PMID: 19845608. Epub 2009/10/23. eng.
174. Tennant DA, Duran RV, Gottlieb E. Targeting metabolic transformation for cancer therapy. *Nature reviews Cancer*. 2010 Apr;10(4):267-77. PubMed PMID: 20300106. Epub 2010/03/20. eng.
175. Phelan JJ, O'Hanlon, C., Reynolds, J.V., and O'Sullivan, J. The Role of Energy Metabolism in Driving Disease Progression in Inflammatory, Hypoxic and Angiogenic Microenvironments. *Gastro Open Journal*. 2015;Volume 1(Issue 2).
176. Ling FC, Khochfar J, Baldus SE, Brabender J, Drebber U, Bollschweiler E, et al. HIF-1alpha protein expression is associated with the environmental inflammatory reaction in Barrett's metaplasia. *Diseases of the esophagus : official journal of the International Society for Diseases of the Esophagus / ISDE*. 2009;22(8):694-9. PubMed PMID: 19302222. Epub 2009/03/24. eng.

177. Schmalz C, Hardenbergh PH, Wells A, Fisher DE. Regulation of proliferation-survival decisions during tumor cell hypoxia. *Molecular and cellular biology*. 1998 May;18(5):2845-54. PubMed PMID: 9566903. Pubmed Central PMCID: PMC110663. Epub 1998/05/05. eng.
178. Brizel DM, Scully SP, Harrelson JM, Layfield LJ, Bean JM, Prosnitz LR, et al. Tumor oxygenation predicts for the likelihood of distant metastases in human soft tissue sarcoma. *Cancer research*. 1996 Mar 1;56(5):941-3. PubMed PMID: 8640781. Epub 1996/03/01. eng.
179. Casey TM, Pakay JL, Guppy M, Arthur PG. Hypoxia causes downregulation of protein and RNA synthesis in noncontracting Mammalian cardiomyocytes. *Circulation research*. 2002 Apr 19;90(7):777-83. PubMed PMID: 11964370. Epub 2002/04/20. eng.
180. Semenza GL. Regulation of metabolism by hypoxia-inducible factor 1. *Cold Spring Harbor symposia on quantitative biology*. 2011;76:347-53. PubMed PMID: 21785006. Epub 2011/07/26. eng.
181. Zheng Y, Delgoffe GM, Meyer CF, Chan W, Powell JD. Anergic T cells are metabolically anergic. *Journal of immunology (Baltimore, Md : 1950)*. 2009 Nov 15;183(10):6095-101. PubMed PMID: 19841171. Pubmed Central PMCID: PMC2884282. Epub 2009/10/21. eng.
182. Fox CJ, Hammerman PS, Thompson CB. Fuel feeds function: energy metabolism and the T-cell response. *Nature reviews Immunology*. 2005 Nov;5(11):844-52. PubMed PMID: 16239903. Epub 2005/10/22. eng.
183. Dziurla R, Gaber T, Fangradt M, Hahne M, Tripmacher R, Kolar P, et al. Effects of hypoxia and/or lack of glucose on cellular energy metabolism and cytokine production in stimulated human CD4+ T lymphocytes. *Immunology letters*. 2010 Jun 15;131(1):97-105. PubMed PMID: 20206208. Epub 2010/03/09. eng.
184. Dang EV, Barbi J, Yang HY, Jinasena D, Yu H, Zheng Y, et al. Control of T(H)17/T(reg) balance by hypoxia-inducible factor 1. *Cell*. 2011 Sep 2;146(5):772-84. PubMed PMID: 21871655. Pubmed Central PMCID: PMC3387678. Epub 2011/08/30. eng.
185. Shi LZ, Wang R, Huang G, Vogel P, Neale G, Green DR, et al. HIF1alpha-dependent glycolytic pathway orchestrates a metabolic checkpoint for the differentiation of TH17 and Treg cells. *The Journal of experimental medicine*. 2011 Jul 4;208(7):1367-76. PubMed PMID: 21708926. Pubmed Central PMCID: PMC3135370. Epub 2011/06/29. eng.
186. Finlay DK, Rosenzweig E, Sinclair LV, Feijoo-Carnero C, Hukelmann JL, Rolf J, et al. PDK1 regulation of mTOR and hypoxia-inducible factor 1 integrate metabolism and migration of CD8+ T cells. *The Journal of experimental medicine*. 2012 Dec 17;209(13):2441-53. PubMed PMID: 23183047. Pubmed Central PMCID: PMC3526360. Epub 2012/11/28. eng.
187. Dandapani M, Hardie DG. AMPK: opposing the metabolic changes in both tumour cells and inflammatory cells? *Biochemical Society transactions*. 2013 Apr;41(2):687-93. PubMed PMID: 23514177. Pubmed Central PMCID: PMC3638122. Epub 2013/03/22. eng.
188. Merrill GF, Kurth EJ, Hardie DG, Winder WW. AICA riboside increases AMP-activated protein kinase, fatty acid oxidation, and glucose uptake in rat muscle. *The American journal of physiology*. 1997 Dec;273(6 Pt 1):E1107-12. PubMed PMID: 9435525. Epub 1998/01/22. eng.
189. Zong H, Ren JM, Young LH, Pypaert M, Mu J, Birnbaum MJ, et al. AMP kinase is required for mitochondrial biogenesis in skeletal muscle in response to chronic energy deprivation. *Proceedings of the National Academy of Sciences of the United States of America*. 2002 Dec 10;99(25):15983-7. PubMed PMID: 12444247. Pubmed Central PMCID: PMC138551. Epub 2002/11/22. eng.

190. Winder WW, Holmes BF, Rubink DS, Jensen EB, Chen M, Holloszy JO. Activation of AMP-activated protein kinase increases mitochondrial enzymes in skeletal muscle. *Journal of applied physiology* (Bethesda, Md : 1985). 2000 Jun;88(6):2219-26. PubMed PMID: 10846039. Epub 2000/06/14. eng.
191. Hardie DG, Ross FA, Hawley SA. AMPK: a nutrient and energy sensor that maintains energy homeostasis. *Nature reviews Molecular cell biology*. 2012 Apr;13(4):251-62. PubMed PMID: 22436748. Epub 2012/03/23. eng.
192. Hoppe S, Bierhoff H, Cado I, Weber A, Tiebe M, Grummt I, et al. AMP-activated protein kinase adapts rRNA synthesis to cellular energy supply. *Proceedings of the National Academy of Sciences of the United States of America*. 2009 Oct 20;106(42):17781-6. PubMed PMID: 19815529. Pubmed Central PMCID: PMC2764937. Epub 2009/10/10. eng.
193. Shackelford DB, Vasquez DS, Corbeil J, Wu S, Leblanc M, Wu CL, et al. mTOR and HIF-1alpha-mediated tumor metabolism in an LKB1 mouse model of Peutz-Jeghers syndrome. *Proceedings of the National Academy of Sciences of the United States of America*. 2009 Jul 7;106(27):11137-42. PubMed PMID: 19541609. Pubmed Central PMCID: PMC2708689. Epub 2009/06/23. eng.
194. Krawczyk CM, Holowka T, Sun J, Blagih J, Amiel E, DeBerardinis RJ, et al. Toll-like receptor-induced changes in glycolytic metabolism regulate dendritic cell activation. *Blood*. 2010 Jun 10;115(23):4742-9. PubMed PMID: 20351312. Pubmed Central PMCID: PMC2890190. Epub 2010/03/31. eng.
195. Sag D, Carling D, Stout RD, Suttles J. Adenosine 5'-monophosphate-activated protein kinase promotes macrophage polarization to an anti-inflammatory functional phenotype. *Journal of immunology* (Baltimore, Md : 1950). 2008 Dec 15;181(12):8633-41. PubMed PMID: 19050283. Pubmed Central PMCID: PMC2756051. Epub 2008/12/04. eng.
196. Rolf J, Zarrouk M, Finlay DK, Foretz M, Viollet B, Cantrell DA. AMPKalpha1: a glucose sensor that controls CD8 T-cell memory. *European journal of immunology*. 2013 Apr;43(4):889-96. PubMed PMID: 23310952. Pubmed Central PMCID: PMC3734624. Epub 2013/01/12. eng.
197. Berkers CR, Maddocks OD, Cheung EC, Mor I, Vousden KH. Metabolic regulation by p53 family members. *Cell metabolism*. 2013 Nov 5;18(5):617-33. PubMed PMID: 23954639. Pubmed Central PMCID: PMC3824073. Epub 2013/08/21. eng.
198. Vousden KH, Ryan KM. p53 and metabolism. *Nature reviews Cancer*. 2009 Oct;9(10):691-700. PubMed PMID: 19759539. Epub 2009/09/18. eng.
199. Kulawiec M, Ayyasamy V, Singh KK. p53 regulates mtDNA copy number and mitochekpoint pathway. *Journal of carcinogenesis*. 2009;8:8. PubMed PMID: 19439913. Pubmed Central PMCID: PMC2687143. Epub 2009/05/15. eng.
200. Sahin E, Colla S, Liesa M, Moslehi J, Muller FL, Guo M, et al. Telomere dysfunction induces metabolic and mitochondrial compromise. *Nature*. 2011 Feb 17;470(7334):359-65. PubMed PMID: 21307849. Pubmed Central PMCID: PMC3741661. Epub 2011/02/11. eng.
201. Kitamura N, Nakamura Y, Miyamoto Y, Miyamoto T, Kabu K, Yoshida M, et al. Mieap, a p53-inducible protein, controls mitochondrial quality by repairing or eliminating unhealthy mitochondria. *PloS one*. 2011;6(1):e16060. PubMed PMID: 21264228. Pubmed Central PMCID: PMC3022033. Epub 2011/01/26. eng.
202. Cardin R, Piciocchi M, Tieppo C, Maddalo G, Zaninotto G, Mescoli C, et al. Oxidative DNA damage in Barrett mucosa: correlation with telomeric dysfunction and p53 mutation. *Annals of surgical oncology*. 2013 Dec;20 Suppl 3:S583-9. PubMed PMID: 23744553. Epub 2013/06/08. eng.

203. Matoba S, Kang JG, Patino WD, Wragg A, Boehm M, Gavrilova O, et al. p53 regulates mitochondrial respiration. *Science (New York, NY)*. 2006 Jun 16;312(5780):1650-3. PubMed PMID: 16728594. Epub 2006/05/27. eng.
204. Okamura S, Ng CC, Koyama K, Takei Y, Arakawa H, Monden M, et al. Identification of seven genes regulated by wild-type p53 in a colon cancer cell line carrying a well-controlled wild-type p53 expression system. *Oncology research*. 1999;11(6):281-5. PubMed PMID: 10691030. Epub 2000/02/26. eng.
205. Stambolsky P, Weisz L, Shats I, Klein Y, Goldfinger N, Oren M, et al. Regulation of AIF expression by p53. *Cell death and differentiation*. 2006 Dec;13(12):2140-9. PubMed PMID: 16729031. Epub 2006/05/27. eng.
206. Cheung EC, Ludwig RL, Vousden KH. Mitochondrial localization of TIGAR under hypoxia stimulates HK2 and lowers ROS and cell death. *Proceedings of the National Academy of Sciences of the United States of America*. 2012 Dec 11;109(50):20491-6. PubMed PMID: 23185017. Pubmed Central PMCID: PMC3528527. Epub 2012/11/28. eng.
207. Li H, Jogl G. Structural and biochemical studies of TIGAR (TP53-induced glycolysis and apoptosis regulator). *The Journal of biological chemistry*. 2009 Jan 16;284(3):1748-54. PubMed PMID: 19015259. Pubmed Central PMCID: PMC2615519. Epub 2008/11/19. eng.
208. Contractor T, Harris CR. p53 negatively regulates transcription of the pyruvate dehydrogenase kinase Pdk2. *Cancer research*. 2012 Jan 15;72(2):560-7. PubMed PMID: 22123926. Epub 2011/11/30. eng.
209. Schwartzberg-Bar-Yoseph F, Armoni M, Karnieli E. The tumor suppressor p53 down-regulates glucose transporters GLUT1 and GLUT4 gene expression. *Cancer research*. 2004 Apr 1;64(7):2627-33. PubMed PMID: 15059920. Epub 2004/04/03. eng.
210. Boidot R, Vegran F, Meulle A, Le Breton A, Dessy C, Sonveaux P, et al. Regulation of monocarboxylate transporter MCT1 expression by p53 mediates inward and outward lactate fluxes in tumors. *Cancer research*. 2012 Feb 15;72(4):939-48. PubMed PMID: 22184616. Epub 2011/12/21. eng.
211. Mathupala SP, Heese C, Pedersen PL. Glucose catabolism in cancer cells. The type II hexokinase promoter contains functionally active response elements for the tumor suppressor p53. *The Journal of biological chemistry*. 1997 Sep 5;272(36):22776-80. PubMed PMID: 9278438. Epub 1997/09/05. eng.
212. Maddocks OD, Vousden KH. Metabolic regulation by p53. *Journal of molecular medicine (Berlin, Germany)*. 2011 Mar;89(3):237-45. PubMed PMID: 21340684. Pubmed Central PMCID: PMC3043245. Epub 2011/02/23. eng.
213. Hotamisligil GS, Erbay E. Nutrient sensing and inflammation in metabolic diseases. *Nature reviews Immunology*. 2008 Dec;8(12):923-34. PubMed PMID: 19029988. Pubmed Central PMCID: PMC2814543. Epub 2008/11/26. eng.
214. Solinas G, Karin M. JNK1 and IKKbeta: molecular links between obesity and metabolic dysfunction. *FASEB journal : official publication of the Federation of American Societies for Experimental Biology*. 2010 Aug;24(8):2596-611. PubMed PMID: 20371626. Epub 2010/04/08. eng.
215. Tornatore L, Thotakura AK, Bennett J, Moretti M, Franzoso G. The nuclear factor kappa B signaling pathway: integrating metabolism with inflammation. *Trends in cell biology*. 2012 Nov;22(11):557-66. PubMed PMID: 22995730. Epub 2012/09/22. eng.

216. Marusawa H, Jenkins BJ. Inflammation and gastrointestinal cancer: an overview. *Cancer letters*. 2014 Apr 10;345(2):153-6. PubMed PMID: 23981579. Epub 2013/08/29. eng.
217. DiDonato JA, Mercurio F, Karin M. NF-kappaB and the link between inflammation and cancer. *Immunological reviews*. 2012 Mar;246(1):379-400. PubMed PMID: 22435567. Epub 2012/03/23. eng.
218. Grivennikov SI, Greten FR, Karin M. Immunity, inflammation, and cancer. *Cell*. 2010 Mar 19;140(6):883-99. PubMed PMID: 20303878. Pubmed Central PMCID: PMC2866629. Epub 2010/03/23. eng.
219. O'Riordan JM, Abdel-latif MM, Ravi N, McNamara D, Byrne PJ, McDonald GS, et al. Proinflammatory cytokine and nuclear factor kappa-B expression along the inflammation-metaplasia-dysplasia-adenocarcinoma sequence in the esophagus. *The American journal of gastroenterology*. 2005 Jun;100(6):1257-64. PubMed PMID: 15929754. Epub 2005/06/03. eng.
220. Abdel-Latif MM, Kelleher D, Reynolds JV. Molecular mechanisms of constitutive and inducible NF-kappaB activation in oesophageal adenocarcinoma. *European journal of cancer*. 2015 Mar;51(4):464-72. PubMed PMID: 25596807. Epub 2015/01/19. eng.
221. Johnson RF, Witzel, II, Perkins ND. p53-dependent regulation of mitochondrial energy production by the RelA subunit of NF-kappaB. *Cancer research*. 2011 Aug 15;71(16):5588-97. PubMed PMID: 21742773. Pubmed Central PMCID: PMC3379538. Epub 2011/07/12. eng.
222. Kawachi K, Araki K, Tobiume K, Tanaka N. p53 regulates glucose metabolism through an IKK-NF-kappaB pathway and inhibits cell transformation. *Nature cell biology*. 2008 May;10(5):611-8. PubMed PMID: 18391940. Epub 2008/04/09. eng.
223. Mauro C, Leow SC, Anso E, Rocha S, Thotakura AK, Tornatore L, et al. NF-kappaB controls energy homeostasis and metabolic adaptation by upregulating mitochondrial respiration. *Nature cell biology*. 2011 Oct;13(10):1272-9. PubMed PMID: 21968997. Pubmed Central PMCID: PMC3462316. Epub 2011/10/05. eng.
224. Eelen G, Cruys B, Welte J, De Bock K, Carmeliet P. Control of vessel sprouting by genetic and metabolic determinants. *Trends in endocrinology and metabolism: TEM*. 2013 Dec;24(12):589-96. PubMed PMID: 24075830. Epub 2013/10/01. eng.
225. De Bock K, Georgiadou M, Carmeliet P. Role of endothelial cell metabolism in vessel sprouting. *Cell metabolism*. 2013 Nov 5;18(5):634-47. PubMed PMID: 23973331. Epub 2013/08/27. eng.
226. De Bock K, Georgiadou M, Schoors S, Kuchnio A, Wong BW, Cantelmo AR, et al. Role of PFKFB3-driven glycolysis in vessel sprouting. *Cell*. 2013 Aug 1;154(3):651-63. PubMed PMID: 23911327. Epub 2013/08/06. eng.
227. Potente M, Gerhardt H, Carmeliet P. Basic and therapeutic aspects of angiogenesis. *Cell*. 2011 Sep 16;146(6):873-87. PubMed PMID: 21925313. Epub 2011/09/20. eng.
228. Sonveaux P, Copetti T, De Saedeleer CJ, Vegran F, Verrax J, Kennedy KM, et al. Targeting the lactate transporter MCT1 in endothelial cells inhibits lactate-induced HIF-1 activation and tumor angiogenesis. *PloS one*. 2012;7(3):e33418. PubMed PMID: 22428047. Pubmed Central PMCID: PMC3302812. Epub 2012/03/20. eng.
229. Hunt TK, Aslam RS, Beckert S, Wagner S, Ghani QP, Hussain MZ, et al. Aerobically derived lactate stimulates revascularization and tissue repair via redox mechanisms. *Antioxidants & redox signaling*. 2007 Aug;9(8):1115-24. PubMed PMID: 17567242. Pubmed Central PMCID: PMC2443402. Epub 2007/06/15. eng.

230. Vegran F, Boidot R, Michiels C, Sonveaux P, Feron O. Lactate influx through the endothelial cell monocarboxylate transporter MCT1 supports an NF-kappaB/IL-8 pathway that drives tumor angiogenesis. *Cancer research*. 2011 Apr 1;71(7):2550-60. PubMed PMID: 21300765. Epub 2011/02/09. eng.
231. Hao Q, Wang L, Tang H. Vascular endothelial growth factor induces protein kinase D-dependent production of proinflammatory cytokines in endothelial cells. *American journal of physiology Cell physiology*. 2009 Apr;296(4):C821-7. PubMed PMID: 19176759. Epub 2009/01/30. eng.
232. Wright GL, Maroulakou IG, Eldridge J, Liby TL, Sridharan V, Tsihchlis PN, et al. VEGF stimulation of mitochondrial biogenesis: requirement of AKT3 kinase. *FASEB journal : official publication of the Federation of American Societies for Experimental Biology*. 2008 Sep;22(9):3264-75. PubMed PMID: 18524868. Pubmed Central PMCID: PMC2518259. Epub 2008/06/06. eng.
233. Elmasri H, Karaaslan C, Teper Y, Ghelfi E, Weng M, Ince TA, et al. Fatty acid binding protein 4 is a target of VEGF and a regulator of cell proliferation in endothelial cells. *FASEB journal : official publication of the Federation of American Societies for Experimental Biology*. 2009 Nov;23(11):3865-73. PubMed PMID: 19625659. Pubmed Central PMCID: PMC2775007. Epub 2009/07/25. eng.
234. Hagberg CE, Mehlem A, Falkevall A, Muhl L, Fam BC, Ortsater H, et al. Targeting VEGF-B as a novel treatment for insulin resistance and type 2 diabetes. *Nature*. 2012 Oct 18;490(7420):426-30. PubMed PMID: 23023133. Epub 2012/10/02. eng.
235. Xu X, Ye L, Araki K, Ahmed R. mTOR, linking metabolism and immunity. *Seminars in immunology*. 2012 Dec;24(6):429-35. PubMed PMID: 23352227. Pubmed Central PMCID: PMC3582734. Epub 2013/01/29. eng.
236. Thomson AW, Turnquist HR, Raimondi G. Immunoregulatory functions of mTOR inhibition. *Nature reviews Immunology*. 2009 May;9(5):324-37. PubMed PMID: 19390566. Pubmed Central PMCID: PMC2847476. Epub 2009/04/25. eng.
237. Buller CL, Loberg RD, Fan MH, Zhu Q, Park JL, Vesely E, et al. A GSK-3/TSC2/mTOR pathway regulates glucose uptake and GLUT1 glucose transporter expression. *American journal of physiology Cell physiology*. 2008 Sep;295(3):C836-43. PubMed PMID: 18650261. Pubmed Central PMCID: PMC2544442. Epub 2008/07/25. eng.
238. Duvel K, Yecies JL, Menon S, Raman P, Lipovsky AI, Souza AL, et al. Activation of a metabolic gene regulatory network downstream of mTOR complex 1. *Molecular cell*. 2010 Jul 30;39(2):171-83. PubMed PMID: 20670887. Pubmed Central PMCID: PMC2946786. Epub 2010/07/31. eng.
239. Wang R, Dillon CP, Shi LZ, Milasta S, Carter R, Finkelstein D, et al. The transcription factor Myc controls metabolic reprogramming upon T lymphocyte activation. *Immunity*. 2011 Dec 23;35(6):871-82. PubMed PMID: 22195744. Pubmed Central PMCID: PMC3248798. Epub 2011/12/27. eng.
240. Araki K, Turner AP, Shaffer VO, Gangappa S, Keller SA, Bachmann MF, et al. mTOR regulates memory CD8 T-cell differentiation. *Nature*. 2009 Jul 2;460(7251):108-12. PubMed PMID: 19543266. Pubmed Central PMCID: PMC2710807. Epub 2009/06/23. eng.
241. Selak MA, Armour SM, MacKenzie ED, Boulahbel H, Watson DG, Mansfield KD, et al. Succinate links TCA cycle dysfunction to oncogenesis by inhibiting HIF-alpha prolyl hydroxylase. *Cancer cell*. 2005 Jan;7(1):77-85. PubMed PMID: 15652751. Epub 2005/01/18. eng.

242. Pistollato F, Abbadi S, Rampazzo E, Viola G, Della Puppa A, Cavallini L, et al. Hypoxia and succinate antagonize 2-deoxyglucose effects on glioblastoma. *Biochemical pharmacology*. 2010 Nov 15;80(10):1517-27. PubMed PMID: 20705058. Epub 2010/08/14. eng.
243. Tannahill GM, Curtis AM, Adamik J, Palsson-McDermott EM, McGettrick AF, Goel G, et al. Succinate is an inflammatory signal that induces IL-1beta through HIF-1alpha. *Nature*. 2013 Apr 11;496(7444):238-42. PubMed PMID: 23535595. Pubmed Central PMCID: PMC4031686. Epub 2013/03/29. eng.
244. Qi QR, Yang ZM. Regulation and function of signal transducer and activator of transcription 3. *World journal of biological chemistry*. 2014 May 26;5(2):231-9. PubMed PMID: 24921012. Pubmed Central PMCID: PMC4050116. Epub 2014/06/13. eng.
245. Haigis MC, Deng CX, Finley LW, Kim HS, Gius D. SIRT3 is a mitochondrial tumor suppressor: a scientific tale that connects aberrant cellular ROS, the Warburg effect, and carcinogenesis. *Cancer research*. 2012 May 15;72(10):2468-72. PubMed PMID: 22589271. Pubmed Central PMCID: PMC3354726. Epub 2012/05/17. eng.
246. Tateno T, Asa SL, Zheng L, Mayr T, Ullrich A, Ezzat S. The FGFR4-G388R polymorphism promotes mitochondrial STAT3 serine phosphorylation to facilitate pituitary growth hormone cell tumorigenesis. *PLoS genetics*. 2011 Dec;7(12):e1002400. PubMed PMID: 22174695. Pubmed Central PMCID: PMC3234213. Epub 2011/12/17. eng.
247. Gough DJ, Corlett A, Schlessinger K, Wegrzyn J, Lerner AC, Levy DE. Mitochondrial STAT3 supports Ras-dependent oncogenic transformation. *Science (New York, NY)*. 2009 Jun 26;324(5935):1713-6. PubMed PMID: 19556508. Pubmed Central PMCID: PMC2840701. Epub 2009/06/27. eng.
248. Gough DJ, Marie IJ, Lobry C, Aifantis I, Levy DE. STAT3 supports experimental K-RasG12D-induced murine myeloproliferative neoplasms dependent on serine phosphorylation. *Blood*. 2014 Aug 22. PubMed PMID: 25150294. Epub 2014/08/26. Eng.
249. Henderson B, Bitensky L, Chayen J. Glycolytic activity in human synovial lining cells in rheumatoid arthritis. *Annals of the rheumatic diseases*. 1979 Feb;38(1):63-7. PubMed PMID: 434949. Pubmed Central PMCID: PMC1000321. Epub 1979/02/01. eng.
250. Chang X, Wei C. Glycolysis and rheumatoid arthritis. *International journal of rheumatic diseases*. 2011 Aug;14(3):217-22. PubMed PMID: 21816017. Epub 2011/08/06. eng.
251. Ciurtin C, Cojocaru VM, Miron IM, Preda F, Milicescu M, Bojinca M, et al. Correlation between different components of synovial fluid and pathogenesis of rheumatic diseases. *Romanian journal of internal medicine = Revue roumaine de medecine interne*. 2006;44(2):171-81. PubMed PMID: 17236298. Epub 2007/01/24. eng.
252. Biniiecka M, Fox E, Gao W, Ng CT, Veale DJ, Fearon U, et al. Hypoxia induces mitochondrial mutagenesis and dysfunction in inflammatory arthritis. *Arthritis and rheumatism*. 2011 Aug;63(8):2172-82. PubMed PMID: 21484771. Epub 2011/04/13. eng.
253. Moran EM, Heydrich R, Ng CT, Saber TP, McCormick J, Sieper J, et al. IL-17A expression is localised to both mononuclear and polymorphonuclear synovial cell infiltrates. *PloS one*. 2011;6(8):e24048. PubMed PMID: 21887369. Pubmed Central PMCID: PMC3161104. Epub 2011/09/03. eng.
254. Biniiecka M, Kennedy A, Ng CT, Chang TC, Balogh E, Fox E, et al. Successful tumour necrosis factor (TNF) blocking therapy suppresses oxidative stress and hypoxia-induced mitochondrial mutagenesis in inflammatory arthritis. *Arthritis research & therapy*.

- 2011;13(4):R121. PubMed PMID: 21787418. Pubmed Central PMCID: PMC3239359. Epub 2011/07/27. eng.
255. Kennedy A, Ng CT, Chang TC, Biniiecka M, O'Sullivan JN, Heffernan E, et al. Tumor necrosis factor blocking therapy alters joint inflammation and hypoxia. *Arthritis and rheumatism*. 2011 Apr;63(4):923-32. PubMed PMID: 21225682. Epub 2011/01/13. eng.
256. Ng CT, Biniiecka M, Kennedy A, McCormick J, Fitzgerald O, Bresnihan B, et al. Synovial tissue hypoxia and inflammation in vivo. *Annals of the rheumatic diseases*. 2010 Jul;69(7):1389-95. PubMed PMID: 20439288. Pubmed Central PMCID: PMC2946116. Epub 2010/05/05. eng.
257. Hollander AP, Corke KP, Freemont AJ, Lewis CE. Expression of hypoxia-inducible factor 1alpha by macrophages in the rheumatoid synovium: implications for targeting of therapeutic genes to the inflamed joint. *Arthritis and rheumatism*. 2001 Jul;44(7):1540-4. PubMed PMID: 11465705. Epub 2001/07/24. eng.
258. Giatromanolaki A, Sivridis E, Maltezos E, Athanassou N, Papazoglou D, Gatter KC, et al. Upregulated hypoxia inducible factor-1alpha and -2alpha pathway in rheumatoid arthritis and osteoarthritis. *Arthritis research & therapy*. 2003;5(4):R193-201. PubMed PMID: 12823854. Pubmed Central PMCID: PMC165055. Epub 2003/06/26. eng.
259. Mobasheri A, Richardson S, Mobasheri R, Shakibaei M, Hoyland JA. Hypoxia inducible factor-1 and facilitative glucose transporters GLUT1 and GLUT3: putative molecular components of the oxygen and glucose sensing apparatus in articular chondrocytes. *Histology and histopathology*. 2005 Oct;20(4):1327-38. PubMed PMID: 16136514. Epub 2005/09/02. eng.
260. Gaber T, Dziurla R, Tripmacher R, Burmester GR, Buttgereit F. Hypoxia inducible factor (HIF) in rheumatology: low O2! See what HIF can do! *Annals of the rheumatic diseases*. 2005 Jul;64(7):971-80. PubMed PMID: 15800008. Pubmed Central PMCID: PMC1755583. Epub 2005/04/01. eng.
261. Bodamyali T, Stevens CR, Billingham ME, Ohta S, Blake DR. Influence of hypoxia in inflammatory synovitis. *Annals of the rheumatic diseases*. 1998 Dec;57(12):703-10. PubMed PMID: 10070268. Pubmed Central PMCID: PMC1752510. Epub 1999/03/10. eng.
262. Distler JH, Wenger RH, Gassmann M, Kurowska M, Hirth A, Gay S, et al. Physiologic responses to hypoxia and implications for hypoxia-inducible factors in the pathogenesis of rheumatoid arthritis. *Arthritis and rheumatism*. 2004 Jan;50(1):10-23. PubMed PMID: 14730595. Epub 2004/01/20. eng.
263. Taylor PC, Sivakumar B. Hypoxia and angiogenesis in rheumatoid arthritis. *Current opinion in rheumatology*. 2005 May;17(3):293-8. PubMed PMID: 15838239. Epub 2005/04/20. eng.
264. Firestein GS, Echeverri F, Yeo M, Zvaifler NJ, Green DR. Somatic mutations in the p53 tumor suppressor gene in rheumatoid arthritis synovium. *Proceedings of the National Academy of Sciences of the United States of America*. 1997 Sep 30;94(20):10895-900. PubMed PMID: 9380731. Pubmed Central PMCID: PMC23522. Epub 1997/10/06. eng.
265. Reme T, Travaglio A, Gueydon E, Adla L, Jorgensen C, Sany J. Mutations of the p53 tumour suppressor gene in erosive rheumatoid synovial tissue. *Clinical and experimental immunology*. 1998 Feb;111(2):353-8. PubMed PMID: 9486403. Pubmed Central PMCID: PMC1904928. Epub 1998/03/05. eng.
266. Kullmann F, Judex M, Neudecker I, Lechner S, Justen HP, Green DR, et al. Analysis of the p53 tumor suppressor gene in rheumatoid arthritis synovial fibroblasts. *Arthritis and rheumatism*. 1999 Aug;42(8):1594-600. PubMed PMID: 10446856. Epub 1999/08/14. eng.

267. Kawauchi K, Araki K, Tobiume K, Tanaka N. Loss of p53 enhances catalytic activity of IKKbeta through O-linked beta-N-acetyl glucosamine modification. *Proceedings of the National Academy of Sciences of the United States of America*. 2009 Mar 3;106(9):3431-6. PubMed PMID: 19202066. Pubmed Central PMCID: PMC2651314. Epub 2009/02/10. eng.
268. Biniiecka M, Connolly M, Gao W, Ng CT, Balogh E, Gogarty M, et al. Redox mediated angiogenesis in the hypoxic joint of inflammatory arthritis. *Arthritis & rheumatology (Hoboken, NJ)*. 2014 Aug 22. PubMed PMID: 25155522. Epub 2014/08/27. Eng.
269. Yang M, Guo M, Hu Y, Jiang Y. Scube regulates synovial angiogenesis-related signaling. *Medical hypotheses*. 2013 Nov;81(5):948-53. PubMed PMID: 24084593. Epub 2013/10/03. eng.
270. Bailey SM, Udoh US, Young ME. Circadian regulation of metabolism. *The Journal of endocrinology*. 2014 Aug;222(2):R75-96. PubMed PMID: 24928941. Pubmed Central PMCID: PMC4109003. Epub 2014/06/15. eng.
271. Langmesser S, Albrecht U. Life time-circadian clocks, mitochondria and metabolism. *Chronobiology international*. 2006;23(1-2):151-7. PubMed PMID: 16687289. Epub 2006/05/12. eng.
272. Nikonova EV, Vijayarathy C, Zhang L, Cater JR, Galante RJ, Ward SE, et al. Differences in activity of cytochrome C oxidase in brain between sleep and wakefulness. *Sleep*. 2005 Jan;28(1):21-7. PubMed PMID: 15700717. Epub 2005/02/11. eng.
273. Jordan SD, Lamia KA. AMPK at the crossroads of circadian clocks and metabolism. *Molecular and cellular endocrinology*. 2013 Feb 25;366(2):163-9. PubMed PMID: 22750052. Pubmed Central PMCID: PMC3502724. Epub 2012/07/04. eng.
274. Sancar A. Regulation of the mammalian circadian clock by cryptochrome. *The Journal of biological chemistry*. 2004 Aug 13;279(33):34079-82. PubMed PMID: 15123698. Epub 2004/05/05. eng.
275. Busino L, Bassermann F, Maiolica A, Lee C, Nolan PM, Godinho SI, et al. SCFFbx13 controls the oscillation of the circadian clock by directing the degradation of cryptochrome proteins. *Science (New York, NY)*. 2007 May 11;316(5826):900-4. PubMed PMID: 17463251. Epub 2007/04/28. eng.
276. Lamia KA, Sachdeva UM, DiTacchio L, Williams EC, Alvarez JG, Egan DF, et al. AMPK regulates the circadian clock by cryptochrome phosphorylation and degradation. *Science (New York, NY)*. 2009 Oct 16;326(5951):437-40. PubMed PMID: 19833968. Pubmed Central PMCID: PMC2819106. Epub 2009/10/17. eng.
277. Etchegaray JP, Machida KK, Noton E, Constance CM, Dallmann R, Di Napoli MN, et al. Casein kinase 1 delta regulates the pace of the mammalian circadian clock. *Molecular and cellular biology*. 2009 Jul;29(14):3853-66. PubMed PMID: 19414593. Pubmed Central PMCID: PMC2704743. Epub 2009/05/06. eng.
278. Um JH, Yang S, Yamazaki S, Kang H, Viollet B, Foretz M, et al. Activation of 5'-AMP-activated kinase with diabetes drug metformin induces casein kinase Iepsilon (CKIepsilon)-dependent degradation of clock protein mPer2. *The Journal of biological chemistry*. 2007 Jul 20;282(29):20794-8. PubMed PMID: 17525164. Epub 2007/05/26. eng.
279. Vieira E, Nilsson EC, Nerstedt A, Ormestad M, Long YC, Garcia-Roves PM, et al. Relationship between AMPK and the transcriptional balance of clock-related genes in skeletal muscle. *American journal of physiology Endocrinology and metabolism*. 2008 Nov;295(5):E1032-7. PubMed PMID: 18728219. Epub 2008/08/30. eng.

280. Canto C, Gerhart-Hines Z, Feige JN, Lagouge M, Noriega L, Milne JC, et al. AMPK regulates energy expenditure by modulating NAD⁺ metabolism and SIRT1 activity. *Nature*. 2009 Apr 23;458(7241):1056-60. PubMed PMID: 19262508. Pubmed Central PMCID: PMC3616311. Epub 2009/03/06. eng.
281. Lan F, Cacicedo JM, Ruderman N, Ido Y. SIRT1 modulation of the acetylation status, cytosolic localization, and activity of LKB1. Possible role in AMP-activated protein kinase activation. *The Journal of biological chemistry*. 2008 Oct 10;283(41):27628-35. PubMed PMID: 18687677. Pubmed Central PMCID: PMC2562073. Epub 2008/08/09. eng.
282. Walker JW, Jijon HB, Madsen KL. AMP-activated protein kinase is a positive regulator of poly(ADP-ribose) polymerase. *Biochemical and biophysical research communications*. 2006 Mar 31;342(1):336-41. PubMed PMID: 16480959. Epub 2006/02/17. eng.
283. Fulco M, Cen Y, Zhao P, Hoffman EP, McBurney MW, Sauve AA, et al. Glucose restriction inhibits skeletal myoblast differentiation by activating SIRT1 through AMPK-mediated regulation of Nampt. *Developmental cell*. 2008 May;14(5):661-73. PubMed PMID: 18477450. Pubmed Central PMCID: PMC2431467. Epub 2008/05/15. eng.
284. Zhang X, Xu L, Shen J, Cao B, Cheng T, Zhao T, et al. Metabolic signatures of esophageal cancer: NMR-based metabolomics and UHPLC-based focused metabolomics of blood serum. *Biochimica et biophysica acta*. 2013 Aug;1832(8):1207-16. PubMed PMID: 23524237. Epub 2013/03/26. eng.
285. Abbassi-Ghadi N, Kumar S, Huang J, Goldin R, Takats Z, Hanna GB. Metabolomic profiling of oesophago-gastric cancer: a systematic review. *European journal of cancer*. 2013 Nov;49(17):3625-37. PubMed PMID: 23896378. Epub 2013/07/31. eng.
286. Ussakli CH, Ebaee A, Binkley J, Brentnall TA, Emond MJ, Rabinovitch PS, et al. Mitochondria and tumor progression in ulcerative colitis. *Journal of the National Cancer Institute*. 2013 Aug 21;105(16):1239-48. PubMed PMID: 23852949. Pubmed Central PMCID: PMC3748006. Epub 2013/07/16. eng.
287. Gruno M, Peet N, Tein A, Salupere R, Sirotkina M, Valle J, et al. Atrophic gastritis: deficient complex I of the respiratory chain in the mitochondria of corpus mucosal cells. *Journal of gastroenterology*. 2008;43(10):780-8. PubMed PMID: 18958547. Epub 2008/10/30. eng.
288. O'Sullivan KE, Phelan JJ, O'Hanlon C, Lysaght J, O'Sullivan JN, Reynolds JV. The role of inflammation in cancer of the esophagus. *Expert review of gastroenterology & hepatology*. 2014 Sep;8(7):749-60. PubMed PMID: 24857183. Epub 2014/05/27. eng.
289. Ando M, Uehara I, Kogure K, Asano Y, Nakajima W, Abe Y, et al. Interleukin 6 enhances glycolysis through expression of the glycolytic enzymes hexokinase 2 and 6-phosphofructo-2-kinase/fructose-2,6-bisphosphatase-3. *Journal of Nippon Medical School = Nippon Ika Daigaku zasshi*. 2010 Apr;77(2):97-105. PubMed PMID: 20453422. Epub 2010/05/11. eng.
290. Catarzi S, Favilli F, Romagnoli C, Marcucci T, Picariello L, Tonelli F, et al. Oxidative state and IL-6 production in intestinal myofibroblasts of Crohn's disease patients. *Inflammatory bowel diseases*. 2011 Aug;17(8):1674-84. PubMed PMID: 21744422. Epub 2011/07/12. eng.
291. Dvorakova K, Payne CM, Ramsey L, Holubec H, Sampliner R, Dominguez J, et al. Increased expression and secretion of interleukin-6 in patients with Barrett's esophagus. *Clinical cancer research : an official journal of the American Association for Cancer Research*. 2004 Mar 15;10(6):2020-8. PubMed PMID: 15041721. Epub 2004/03/26. eng.
292. Kastelein F, Biermann K, Steyerberg EW, Verheij J, Kalisvaart M, Looijenga LH, et al. Aberrant p53 protein expression is associated with an increased risk of neoplastic progression in

patients with Barrett's oesophagus. *Gut*. 2013 Dec;62(12):1676-83. PubMed PMID: 23256952. Epub 2012/12/22. eng.

293. Angelo LS, Talpaz M, Kurzrock R. Autocrine interleukin-6 production in renal cell carcinoma: evidence for the involvement of p53. *Cancer research*. 2002 Feb 1;62(3):932-40. PubMed PMID: 11830554. Epub 2002/02/07. eng.

294. Bar F, Bochmann W, Widok A, von Medem K, Pagel R, Hirose M, et al. Mitochondrial gene polymorphisms that protect mice from colitis. *Gastroenterology*. 2013 Nov;145(5):1055-63 e3. PubMed PMID: 23872498. Epub 2013/07/23. eng.

295. Gruno M, Peet N, Seppet E, Kadaja L, Paju K, Eimre M, et al. Oxidative phosphorylation and its coupling to mitochondrial creatine and adenylate kinases in human gastric mucosa. *American journal of physiology Regulatory, integrative and comparative physiology*. 2006 Oct;291(4):R936-46. PubMed PMID: 16741143. Epub 2006/06/03. eng.

296. Puurand M, Peet N, Piirsoo A, Peetsalu M, Soplepmann J, Sirotkina M, et al. Deficiency of the complex I of the mitochondrial respiratory chain but improved adenylate control over succinate-dependent respiration are human gastric cancer-specific phenomena. *Molecular and cellular biochemistry*. 2012 Nov;370(1-2):69-78. PubMed PMID: 22821176. Epub 2012/07/24. eng.

297. Chan AW, Gill RS, Schiller D, Sawyer MB. Potential role of metabolomics in diagnosis and surveillance of gastric cancer. *World journal of gastroenterology : WJG*. 2014 Sep 28;20(36):12874-82. PubMed PMID: 25278684. Pubmed Central PMCID: PMC4177469. Epub 2014/10/04. eng.

298. Li H, Wang J, Xu H, Xing R, Pan Y, Li W, et al. Decreased fructose-1,6-bisphosphatase-2 expression promotes glycolysis and growth in gastric cancer cells. *Molecular cancer*. 2013;12(1):110. PubMed PMID: 24063558. Pubmed Central PMCID: PMC3849177. Epub 2013/09/26. eng.

299. Liu X, Wang X, Zhang J, Lam EK, Shin VY, Cheng AS, et al. Warburg effect revisited: an epigenetic link between glycolysis and gastric carcinogenesis. *Oncogene*. 2010 Jan 21;29(3):442-50. PubMed PMID: 19881551. Epub 2009/11/03. eng.

300. Kwon OH, Kang TW, Kim JH, Kim M, Noh SM, Song KS, et al. Pyruvate kinase M2 promotes the growth of gastric cancer cells via regulation of Bcl-xL expression at transcriptional level. *Biochemical and biophysical research communications*. 2012 Jun 22;423(1):38-44. PubMed PMID: 22627140. Epub 2012/05/26. eng.

301. Zhou CF, Li XB, Sun H, Zhang B, Han YS, Jiang Y, et al. Pyruvate kinase type M2 is upregulated in colorectal cancer and promotes proliferation and migration of colon cancer cells. *IUBMB life*. 2012 Sep;64(9):775-82. PubMed PMID: 22807066. Epub 2012/07/19. eng.

302. Hur H, Xuan Y, Kim YB, Lee G, Shim W, Yun J, et al. Expression of pyruvate dehydrogenase kinase-1 in gastric cancer as a potential therapeutic target. *International journal of oncology*. 2013 Jan;42(1):44-54. PubMed PMID: 23135628. Pubmed Central PMCID: PMC3583751. Epub 2012/11/09. eng.

303. Giatromanolaki A, Sivridis E, Maltezos E, Papazoglou D, Simopoulos C, Gatter KC, et al. Hypoxia inducible factor 1alpha and 2alpha overexpression in inflammatory bowel disease. *Journal of clinical pathology*. 2003 Mar;56(3):209-13. PubMed PMID: 12610101. Pubmed Central PMCID: PMC1769899. Epub 2003/03/01. eng.

304. Vermeulen N, Vermeire S, Arijis I, Michiels G, Ballet V, Derua R, et al. Seroreactivity against glycolytic enzymes in inflammatory bowel disease. *Inflammatory bowel diseases*. 2011 Feb;17(2):557-64. PubMed PMID: 20629101. Epub 2010/07/16. eng.

305. Bobarykina AY, Minchenko DO, Opentanova IL, Moenner M, Caro J, Esumi H, et al. Hypoxic regulation of PFKFB-3 and PFKFB-4 gene expression in gastric and pancreatic cancer cell lines and expression of PFKFB genes in gastric cancers. *Acta biochimica Polonica*. 2006;53(4):789-99. PubMed PMID: 17143338. Epub 2006/12/05. eng.
306. Tong M, McHardy I, Ruegger P, Goudarzi M, Kashyap PC, Haritunians T, et al. Reprogramming of gut microbiome energy metabolism by the FUT2 Crohn's disease risk polymorphism. *The ISME journal*. 2014 Nov;8(11):2193-206. PubMed PMID: 24781901. Epub 2014/05/02. eng.
307. Engelman JA, Chen L, Tan X, Crosby K, Guimaraes AR, Upadhyay R, et al. Effective use of PI3K and MEK inhibitors to treat mutant Kras G12D and PIK3CA H1047R murine lung cancers. *Nature medicine*. 2008 Dec;14(12):1351-6. PubMed PMID: 19029981. Pubmed Central PMCID: PMC2683415. Epub 2008/11/26. eng.
308. Libby G, Donnelly LA, Donnan PT, Alessi DR, Morris AD, Evans JM. New users of metformin are at low risk of incident cancer: a cohort study among people with type 2 diabetes. *Diabetes care*. 2009 Sep;32(9):1620-5. PubMed PMID: 19564453. Pubmed Central PMCID: PMC2732153. Epub 2009/07/01. eng.
309. Hawley SA, Fullerton MD, Ross FA, Schertzer JD, Chevtzoff C, Walker KJ, et al. The ancient drug salicylate directly activates AMP-activated protein kinase. *Science (New York, NY)*. 2012 May 18;336(6083):918-22. PubMed PMID: 22517326. Pubmed Central PMCID: PMC3399766. Epub 2012/04/21. eng.
310. Beckers A, Organe S, Timmermans L, Vanderhoydonc F, Deboel L, Derua R, et al. Methotrexate enhances the antianabolic and antiproliferative effects of 5-aminoimidazole-4-carboxamide riboside. *Molecular cancer therapeutics*. 2006 Sep;5(9):2211-7. PubMed PMID: 16985054. Epub 2006/09/21. eng.
311. Xuan Y, Hur H, Ham IH, Yun J, Lee JY, Shim W, et al. Dichloroacetate attenuates hypoxia-induced resistance to 5-fluorouracil in gastric cancer through the regulation of glucose metabolism. *Experimental cell research*. 2014 Feb 15;321(2):219-30. PubMed PMID: 24342832. Epub 2013/12/18. eng.
312. Maschek G, Savaraj N, Priebe W, Braunschweiger P, Hamilton K, Tidmarsh GF, et al. 2-deoxy-D-glucose increases the efficacy of adriamycin and paclitaxel in human osteosarcoma and non-small cell lung cancers in vivo. *Cancer research*. 2004 Jan 1;64(1):31-4. PubMed PMID: 14729604. Epub 2004/01/20. eng.
313. Singh D, Banerji AK, Dwarakanath BS, Tripathi RP, Gupta JP, Mathew TL, et al. Optimizing cancer radiotherapy with 2-deoxy-d-glucose dose escalation studies in patients with glioblastoma multiforme. *Strahlentherapie und Onkologie : Organ der Deutschen Rontgengesellschaft [et al]*. 2005 Aug;181(8):507-14. PubMed PMID: 16044218. Epub 2005/07/27. eng.
314. Nelson JA, Falk RE. Phloridzin and phloretin inhibition of 2-deoxy-D-glucose uptake by tumor cells in vitro and in vivo. *Anticancer research*. 1993 Nov-Dec;13(6A):2293-9. PubMed PMID: 8297149. Epub 1993/11/01. eng.
315. Nelson JA, Falk RE. The efficacy of phloridzin and phloretin on tumor cell growth. *Anticancer research*. 1993 Nov-Dec;13(6A):2287-92. PubMed PMID: 8297148. Epub 1993/11/01. eng.
316. Liu W, Fang Y, Wang XT, Liu J, Dan X, Sun LL. Overcoming 5-Fu resistance of colon cells through inhibition of Glut1 by the specific inhibitor WZB117. *Asian Pacific journal of cancer prevention : APJCP*. 2014;15(17):7037-41. PubMed PMID: 25227787. Epub 2014/09/18. eng.

317. Clem B, Telang S, Clem A, Yalcin A, Meier J, Simmons A, et al. Small-molecule inhibition of 6-phosphofructo-2-kinase activity suppresses glycolytic flux and tumor growth. *Molecular cancer therapeutics*. 2008 Jan;7(1):110-20. PubMed PMID: 18202014. Epub 2008/01/19. eng.
318. Nebeling LC, Miraldi F, Shurin SB, Lerner E. Effects of a ketogenic diet on tumor metabolism and nutritional status in pediatric oncology patients: two case reports. *Journal of the American College of Nutrition*. 1995 Apr;14(2):202-8. PubMed PMID: 7790697. Epub 1995/04/01. eng.
319. Liu AM, Xu Z, Shek FH, Wong KF, Lee NP, Poon RT, et al. miR-122 targets pyruvate kinase M2 and affects metabolism of hepatocellular carcinoma. *PloS one*. 2014;9(1):e86872. PubMed PMID: 24466275. Pubmed Central PMCID: PMC3900676. Epub 2014/01/28. eng.
320. Jankowski J, Barr H, Wang K, Delaney B. Diagnosis and management of Barrett's oesophagus. *BMJ (Clinical research ed)*. 2010;341:c4551. PubMed PMID: 20833742. Pubmed Central PMCID: PMC3230123. Epub 2010/09/14. eng.
321. Reynolds JV, Donohoe CL, McGillicuddy E, Ravi N, O'Toole D, O'Byrne K, et al. Evolving progress in oncologic and operative outcomes for esophageal and junctional cancer: lessons from the experience of a high-volume center. *The Journal of thoracic and cardiovascular surgery*. 2012 May;143(5):1130-7 e1. PubMed PMID: 22244551. Epub 2012/01/17. eng.
322. Malik AN, Czajka A. Is mitochondrial DNA content a potential biomarker of mitochondrial dysfunction? *Mitochondrion*. 2013 Sep;13(5):481-92. PubMed PMID: 23085537. Epub 2012/10/23. eng.
323. Brahim-Horn MC, Mazure NM. Hypoxic VDAC1: a potential mitochondrial marker for cancer therapy. *Advances in experimental medicine and biology*. 2014;772:101-10. PubMed PMID: 24272356. Epub 2013/11/26. eng.
324. Jakupciak JP, Dakubo GD, Maragh S, Parr RL. Analysis of potential cancer biomarkers in mitochondrial DNA. *Current opinion in molecular therapeutics*. 2006 Dec;8(6):500-6. PubMed PMID: 17243485. Epub 2007/01/25. eng.
325. Amoedo ND, Rodrigues MF, Rumjanek FD. Mitochondria: are mitochondria accessory to metastasis? *The international journal of biochemistry & cell biology*. 2014 Jun;51:53-7. PubMed PMID: 24661997. Epub 2014/03/26. eng.
326. Sonveaux P, Vegran F, Schroeder T, Wergin MC, Verrax J, Rabbani ZN, et al. Targeting lactate-fueled respiration selectively kills hypoxic tumor cells in mice. *The Journal of clinical investigation*. 2008 Dec;118(12):3930-42. PubMed PMID: 19033663. Pubmed Central PMCID: PMC2582933. Epub 2008/11/27. eng.
327. Sotgia F, Whitaker-Menezes D, Martinez-Outschoorn UE, Salem AF, Tsigos A, Lamb R, et al. Mitochondria "fuel" breast cancer metabolism: fifteen markers of mitochondrial biogenesis label epithelial cancer cells, but are excluded from adjacent stromal cells. *Cell cycle (Georgetown, Tex)*. 2012 Dec 1;11(23):4390-401. PubMed PMID: 23172368. Pubmed Central PMCID: PMC3552922. Epub 2012/11/23. eng.
328. Bhandary B, Marahatta A, Kim HR, Chae HJ. Mitochondria in relation to cancer metastasis. *Journal of bioenergetics and biomembranes*. 2012 Dec;44(6):623-7. PubMed PMID: 22914881. Epub 2012/08/24. eng.
329. Santhanam S, Venkatraman A, Ramakrishna BS. Impairment of mitochondrial acetoacetyl CoA thiolase activity in the colonic mucosa of patients with ulcerative colitis. *Gut*. 2007 Nov;56(11):1543-9. PubMed PMID: 17483192. Pubmed Central PMCID: PMC2095666. Epub 2007/05/08. eng.

330. Sifroni KG, Damiani CR, Stoffel C, Cardoso MR, Ferreira GK, Jeremias IC, et al. Mitochondrial respiratory chain in the colonic mucosal of patients with ulcerative colitis. *Molecular and cellular biochemistry*. 2010 Sep;342(1-2):111-5. PubMed PMID: 20440543. Epub 2010/05/05. eng.
331. Damiani CR, Benetton CA, Stoffel C, Bardini KC, Cardoso VH, Di Giunta G, et al. Oxidative stress and metabolism in animal model of colitis induced by dextran sulfate sodium. *Journal of gastroenterology and hepatology*. 2007 Nov;22(11):1846-51. PubMed PMID: 17489966. Epub 2007/05/11. eng.
332. Santhanam S, Rajamanickam S, Motamarry A, Ramakrishna BS, Amirtharaj JG, Ramachandran A, et al. Mitochondrial electron transport chain complex dysfunction in the colonic mucosa in ulcerative colitis. *Inflammatory bowel diseases*. 2012 Nov;18(11):2158-68. PubMed PMID: 22374887. Epub 2012/03/01. eng.
333. Brentnall TA, Pan S, Bronner MP, Crispin DA, Mirzaei H, Cooke K, et al. Proteins That Underlie Neoplastic Progression of Ulcerative Colitis. *Proteomics Clinical applications*. 2009 Sep 14;3(11):1326. PubMed PMID: 20098637. Pubmed Central PMCID: PMC2809935. Epub 2010/01/26. Eng.
334. Ostuni MA, Issop L, Peranzi G, Walker F, Fasseu M, Elbim C, et al. Overexpression of translocator protein in inflammatory bowel disease: potential diagnostic and treatment value. *Inflammatory bowel diseases*. 2010 Sep;16(9):1476-87. PubMed PMID: 20222126. Pubmed Central PMCID: PMC2930116. Epub 2010/03/12. eng.
335. Guaragnella N, Giannattasio S, Moro L. Mitochondrial dysfunction in cancer chemoresistance. *Biochemical pharmacology*. 2014 Nov 1;92(1):62-72. PubMed PMID: 25107705. Epub 2014/08/12. eng.
336. Hail N, Jr., Chen P, Kepa JJ. Selective apoptosis induction by the cancer chemopreventive agent N-(4-hydroxyphenyl)retinamide is achieved by modulating mitochondrial bioenergetics in premalignant and malignant human prostate epithelial cells. *Apoptosis : an international journal on programmed cell death*. 2009 Jul;14(7):849-63. PubMed PMID: 19421858. Pubmed Central PMCID: PMC2891029. Epub 2009/05/08. eng.
337. Moro L, Arbini AA, Marra E, Greco M. Mitochondrial DNA depletion reduces PARP-1 levels and promotes progression of the neoplastic phenotype in prostate carcinoma. *Cellular oncology : the official journal of the International Society for Cellular Oncology*. 2008;30(4):307-22. PubMed PMID: 18607066. Epub 2008/07/09. eng.
338. Biswas G, Anandatheerthavarada HK, Avadhani NG. Mechanism of mitochondrial stress-induced resistance to apoptosis in mitochondrial DNA-depleted C2C12 myocytes. *Cell death and differentiation*. 2005 Mar;12(3):266-78. PubMed PMID: 15650755. Epub 2005/01/15. eng.
339. Trachootham D, Alexandre J, Huang P. Targeting cancer cells by ROS-mediated mechanisms: a radical therapeutic approach? *Nature reviews Drug discovery*. 2009 Jul;8(7):579-91. PubMed PMID: 19478820. Epub 2009/05/30. eng.
340. Fulda S, Galluzzi L, Kroemer G. Targeting mitochondria for cancer therapy. *Nature reviews Drug discovery*. 2010 Jun;9(6):447-64. PubMed PMID: 20467424. Epub 2010/05/15. eng.
341. Shidara Y, Yamagata K, Kanamori T, Nakano K, Kwong JQ, Manfredi G, et al. Positive contribution of pathogenic mutations in the mitochondrial genome to the promotion of cancer by prevention from apoptosis. *Cancer research*. 2005 Mar 1;65(5):1655-63. PubMed PMID: 15753359. Epub 2005/03/09. eng.

342. Mizumachi T, Suzuki S, Naito A, Carcel-Trullols J, Evans TT, Spring PM, et al. Increased mitochondrial DNA induces acquired docetaxel resistance in head and neck cancer cells. *Oncogene*. 2008 Jan 31;27(6):831-8. PubMed PMID: 17637738. Pubmed Central PMCID: PMC2268644. Epub 2007/07/20. eng.
343. Guerra F, Perrone AM, Kurelac I, Santini D, Ceccarelli C, Cricca M, et al. Mitochondrial DNA mutation in serous ovarian cancer: implications for mitochondria-coded genes in chemoresistance. *Journal of clinical oncology : official journal of the American Society of Clinical Oncology*. 2012 Dec 20;30(36):e373-8. PubMed PMID: 23150702. Epub 2012/11/15. eng.
344. Wenner CE. Targeting mitochondria as a therapeutic target in cancer. *Journal of cellular physiology*. 2012 Feb;227(2):450-6. PubMed PMID: 21503875. Epub 2011/04/20. eng.
345. Tong QS, Zheng LD, Wang L, Liu J, Qian W. BAK overexpression mediates p53-independent apoptosis inducing effects on human gastric cancer cells. *BMC cancer*. 2004 Jul 12;4:33. PubMed PMID: 15248898. Pubmed Central PMCID: PMC481072. Epub 2004/07/14. eng.
346. Luger A, Schmidt M, Luger N, Pauels HG, Domschke W, Kucharzik T. Infliximab induces apoptosis in monocytes from patients with chronic active Crohn's disease by using a caspase-dependent pathway. *Gastroenterology*. 2001 Nov;121(5):1145-57. PubMed PMID: 11677207. Epub 2001/10/26. eng.
347. Skender B, Hofmanova J, Slavik J, Jelinkova I, Machala M, Moyer MP, et al. DHA-mediated enhancement of TRAIL-induced apoptosis in colon cancer cells is associated with engagement of mitochondria and specific alterations in sphingolipid metabolism. *Biochimica et biophysica acta*. 2014 Sep;1841(9):1308-17. PubMed PMID: 24953781. Epub 2014/06/24. eng.
348. Worsham MJ, Lu M, Chen KM, Stephen JK, Havard S, Schweitzer VP. Malignant and nonmalignant gene signatures in squamous head and neck cancer. *Journal of oncology*. 2012;2012:752860. PubMed PMID: 22570652. Pubmed Central PMCID: PMC3335248. Epub 2012/05/10. eng.
349. Hikita H, Kodama T, Shimizu S, Li W, Shigekawa M, Tanaka S, et al. Bak deficiency inhibits liver carcinogenesis: a causal link between apoptosis and carcinogenesis. *Journal of hepatology*. 2012 Jul;57(1):92-100. PubMed PMID: 22414765. Epub 2012/03/15. eng.
350. Chen ZX, Pervaiz S. Bcl-2 induces pro-oxidant state by engaging mitochondrial respiration in tumor cells. *Cell death and differentiation*. 2007 Sep;14(9):1617-27. PubMed PMID: 17510660. Epub 2007/05/19. eng.
351. Tian Y, Huang Z, Wang Z, Yin C, Zhou L, Zhang L, et al. Identification of novel molecular markers for prognosis estimation of acute myeloid leukemia: over-expression of PDCD7, FIS1 and Ang2 may indicate poor prognosis in pretreatment patients with acute myeloid leukemia. *PloS one*. 2014;9(1):e84150. PubMed PMID: 24416201. Pubmed Central PMCID: PMC3885535. Epub 2014/01/15. eng.
352. Hsiao CP, Wang D, Kaushal A, Saligan L. Mitochondria-Related Gene Expression Changes Are Associated With Fatigue in Patients With Nonmetastatic Prostate Cancer Receiving External Beam Radiation Therapy. *Cancer nursing*. 2012 Oct 5. PubMed PMID: 23047795. Epub 2012/10/11. Eng.
353. Fan S, Chen WX, Lv XB, Tang QL, Sun LJ, Liu BD, et al. miR-483-5p determines mitochondrial fission and cisplatin sensitivity in tongue squamous cell carcinoma by targeting FIS1. *Cancer letters*. 2015 Jul 1;362(2):183-91. PubMed PMID: 25843291. Epub 2015/04/07. eng.

354. Mao K, Klionsky DJ. Participation of mitochondrial fission during mitophagy. *Cell cycle* (Georgetown, Tex). 2013 Oct 1;12(19):3131-2. PubMed PMID: 24013417. Pubmed Central PMCID: PMC3865006. Epub 2013/09/10. eng.
355. Nacht M, Ferguson AT, Zhang W, Petroziello JM, Cook BP, Gao YH, et al. Combining serial analysis of gene expression and array technologies to identify genes differentially expressed in breast cancer. *Cancer research*. 1999 Nov 1;59(21):5464-70. PubMed PMID: 10554019. Epub 1999/12/20. eng.
356. Akahira J, Sugihashi Y, Suzuki T, Ito K, Niikura H, Moriya T, et al. Decreased expression of 14-3-3 sigma is associated with advanced disease in human epithelial ovarian cancer: its correlation with aberrant DNA methylation. *Clinical cancer research : an official journal of the American Association for Cancer Research*. 2004 Apr 15;10(8):2687-93. PubMed PMID: 15102672. Epub 2004/04/23. eng.
357. Deng J, Gao G, Wang L, Wang T, Yu J, Zhao Z. Stratifin expression is a novel prognostic factor in human gliomas. *Pathology, research and practice*. 2011 Nov 15;207(11):674-9. PubMed PMID: 21940111. Epub 2011/09/24. eng.
358. Urano T, Takahashi S, Suzuki T, Fujimura T, Fujita M, Kumagai J, et al. 14-3-3sigma is down-regulated in human prostate cancer. *Biochemical and biophysical research communications*. 2004 Jul 2;319(3):795-800. PubMed PMID: 15184053. Epub 2004/06/09. eng.
359. Perathoner A, Pirkebner D, Brandacher G, Spizzo G, Stadlmann S, Obrist P, et al. 14-3-3sigma expression is an independent prognostic parameter for poor survival in colorectal carcinoma patients. *Clinical cancer research : an official journal of the American Association for Cancer Research*. 2005 May 1;11(9):3274-9. PubMed PMID: 15867223. Epub 2005/05/04. eng.
360. Ren HZ, Wang JS, Pan GQ, Lv H, Wen JF, Luo GQ, et al. Comparative proteomic analysis of beta-catenin-mediated malignant progression of esophageal squamous cell carcinoma. *Diseases of the esophagus : official journal of the International Society for Diseases of the Esophagus / ISDE*. 2010 Feb;23(2):175-84. PubMed PMID: 19664078. Epub 2009/08/12. eng.
361. Zhang J, Wang K, Zhang J, Liu SS, Dai L, Zhang JY. Using proteomic approach to identify tumor-associated proteins as biomarkers in human esophageal squamous cell carcinoma. *Journal of proteome research*. 2011 Jun 3;10(6):2863-72. PubMed PMID: 21517111. Pubmed Central PMCID: PMC3119842. Epub 2011/04/27. eng.
362. Okumura H, Kita Y, Yokomakura N, Uchikado Y, Setoyama T, Sakurai H, et al. Nuclear expression of 14-3-3 sigma is related to prognosis in patients with esophageal squamous cell carcinoma. *Anticancer research*. 2010 Dec;30(12):5175-9. PubMed PMID: 21187508. Epub 2010/12/29. eng.
363. Okumura H, Natsugoe S, Matsumoto M, Yokomakura N, Uchikado Y, Takatori H, et al. Predictive value of p53 and 14-3-3sigma for the effect of chemoradiation therapy on esophageal squamous cell carcinoma. *Journal of surgical oncology*. 2005 Jul 1;91(1):84-9. PubMed PMID: 15999354. Epub 2005/07/07. eng.
364. Ren HZ, Pan GQ, Wang JS, Wen JF, Wang KS, Luo GQ, et al. Reduced stratifin expression can serve as an independent prognostic factor for poor survival in patients with esophageal squamous cell carcinoma. *Digestive diseases and sciences*. 2010 Sep;55(9):2552-60. PubMed PMID: 20108042. Epub 2010/01/29. eng.
365. Barrett MT, Sanchez CA, Galipeau PC, Neshat K, Emond M, Reid BJ. Allelic loss of 9p21 and mutation of the CDKN2/p16 gene develop as early lesions during neoplastic progression in Barrett's esophagus. *Oncogene*. 1996 Nov 7;13(9):1867-73. PubMed PMID: 8934532. Epub 1996/11/07. eng.

366. Paulson TG, Galipeau PC, Xu L, Kissel HD, Li X, Blount PL, et al. p16 mutation spectrum in the premalignant condition Barrett's esophagus. *PLoS one*. 2008;3(11):e3809. PubMed PMID: 19043591. Pubmed Central PMCID: PMC2585012. Epub 2008/12/02. eng.
367. Wang JS, Guo M, Montgomery EA, Thompson RE, Cosby H, Hicks L, et al. DNA promoter hypermethylation of p16 and APC predicts neoplastic progression in Barrett's esophagus. *The American journal of gastroenterology*. 2009 Sep;104(9):2153-60. PubMed PMID: 19584833. Pubmed Central PMCID: PMC3090447. Epub 2009/07/09. eng.
368. Wong DJ, Paulson TG, Prevo LJ, Galipeau PC, Longton G, Blount PL, et al. p16(INK4a) lesions are common, early abnormalities that undergo clonal expansion in Barrett's metaplastic epithelium. *Cancer research*. 2001 Nov 15;61(22):8284-9. PubMed PMID: 11719461. Epub 2001/11/24. eng.
369. Galipeau PC, Li X, Blount PL, Maley CC, Sanchez CA, Odze RD, et al. NSAIDs modulate CDKN2A, TP53, and DNA content risk for progression to esophageal adenocarcinoma. *PLoS medicine*. 2007 Feb;4(2):e67. PubMed PMID: 17326708. Pubmed Central PMCID: PMC1808095. Epub 2007/03/01. eng.
370. Brankley SM, Fritcher EG, Smyrk TC, Keeney ME, Campion MB, Voss JS, et al. Fluorescence in situ hybridization mapping of esophagectomy specimens from patients with Barrett's esophagus with high-grade dysplasia or adenocarcinoma. *Human pathology*. 2012 Feb;43(2):172-9. PubMed PMID: 21820152. Epub 2011/08/09. eng.
371. Milde-Langosch K, Bamberger AM, Rieck G, Kelp B, Loning T. Overexpression of the p16 cell cycle inhibitor in breast cancer is associated with a more malignant phenotype. *Breast cancer research and treatment*. 2001 May;67(1):61-70. PubMed PMID: 11518467. Epub 2001/08/24. eng.
372. Romagosa C, Simonetti S, Lopez-Vicente L, Mazo A, Lleonart ME, Castellvi J, et al. p16(Ink4a) overexpression in cancer: a tumor suppressor gene associated with senescence and high-grade tumors. *Oncogene*. 2011 May 5;30(18):2087-97. PubMed PMID: 21297668. Epub 2011/02/08. eng.
373. Pavlov K, Maley CC. New models of neoplastic progression in Barrett's oesophagus. *Biochemical Society transactions*. 2010 Apr;38(2):331-6. PubMed PMID: 20298178. Pubmed Central PMCID: PMC2866622. Epub 2010/03/20. eng.
374. Ohashi S, Natsuzaka M, Wong GS, Michaylira CZ, Grugan KD, Stairs DB, et al. Epidermal growth factor receptor and mutant p53 expand an esophageal cellular subpopulation capable of epithelial-to-mesenchymal transition through ZEB transcription factors. *Cancer Res*. 2010 May 15;70(10):4174-84. PubMed PMID: 20424117. Pubmed Central PMCID: PMC3007622. Epub 2010/04/29. eng.
375. Harada H, Nakagawa H, Oyama K, Takaoka M, Andl CD, Jacobmeier B, et al. Telomerase induces immortalization of human esophageal keratinocytes without p16INK4a inactivation. *Molecular cancer research : MCR*. 2003 Aug;1(10):729-38. PubMed PMID: 12939398. Epub 2003/08/27. eng.
376. Hong J, Resnick M, Behar J, Wang LJ, Wands J, DeLellis RA, et al. Acid-induced p16 hypermethylation contributes to development of esophageal adenocarcinoma via activation of NADPH oxidase NOX5-S. *Am J Physiol Gastrointest Liver Physiol*. 2010 Sep;299(3):G697-706. PubMed PMID: 20576920. Pubmed Central PMCID: PMC2950676. Epub 2010/06/26. eng.
377. Modica-Napolitano JS, Aprille JR. Delocalized lipophilic cations selectively target the mitochondria of carcinoma cells. *Advanced drug delivery reviews*. 2001 Jul 2;49(1-2):63-70. PubMed PMID: 11377803. Epub 2001/05/30. eng.

378. Indran IR, Tufo G, Pervaiz S, Brenner C. Recent advances in apoptosis, mitochondria and drug resistance in cancer cells. *Biochimica et biophysica acta*. 2011 Jun;1807(6):735-45. PubMed PMID: 21453675. Epub 2011/04/02. eng.
379. Modica-Napolitano JS, Nalbandian R, Kidd ME, Nalbandian A, Nguyen CC. The selective in vitro cytotoxicity of carcinoma cells by AZT is enhanced by concurrent treatment with delocalized lipophilic cations. *Cancer letters*. 2003 Jul 30;198(1):59-68. PubMed PMID: 12893431. Epub 2003/08/02. eng.
380. Mai S, Klinkenberg M, Auburger G, Bereiter-Hahn J, Jendrach M. Decreased expression of Drp1 and Fis1 mediates mitochondrial elongation in senescent cells and enhances resistance to oxidative stress through PINK1. *Journal of cell science*. 2010 Mar 15;123(Pt 6):917-26. PubMed PMID: 20179104. Epub 2010/02/25. eng.
381. Pelissier-Rota MA, Pelosi L, Meresse P, Jacquier-Sarlin MR. Nicotine-induced cellular stresses and autophagy in human cancer colon cells: A supportive effect on cell homeostasis via up-regulation of Cox-2 and PGE production. *The international journal of biochemistry & cell biology*. 2015 Jun 19;65:239-56. PubMed PMID: 26100595. Epub 2015/06/24. Eng.
382. Gottlieb E, Armour SM, Harris MH, Thompson CB. Mitochondrial membrane potential regulates matrix configuration and cytochrome c release during apoptosis. *Cell death and differentiation*. 2003 Jun;10(6):709-17. PubMed PMID: 12761579. Epub 2003/05/23. eng.
383. Bersani C, Xu LD, Vilborg A, Lui WO, Wiman KG. Wig-1 regulates cell cycle arrest and cell death through the p53 targets FAS and 14-3-3sigma. *Oncogene*. 2014 Aug 28;33(35):4407-17. PubMed PMID: 24469038. Pubmed Central PMCID: PMC4150987. Epub 2014/01/29. eng.
384. Lee JJ, Lee JS, Cui MN, Yun HH, Kim HY, Lee SH, et al. BIS targeting induces cellular senescence through the regulation of 14-3-3 zeta/STAT3/SKP2/p27 in glioblastoma cells. *Cell death & disease*. 2014;5:e1537. PubMed PMID: 25412315. Pubmed Central PMCID: PMC4260756. Epub 2014/11/21. eng.
385. Gogvadze V, Zhivotovsky B, Orrenius S. The Warburg effect and mitochondrial stability in cancer cells. *Molecular aspects of medicine*. 2010 Feb;31(1):60-74. PubMed PMID: 19995572. Epub 2009/12/10. eng.
386. Isidoro A, Martinez M, Fernandez PL, Ortega AD, Santamaria G, Chamorro M, et al. Alteration of the bioenergetic phenotype of mitochondria is a hallmark of breast, gastric, lung and oesophageal cancer. *The Biochemical journal*. 2004 Feb 15;378(Pt 1):17-20. PubMed PMID: 14683524. Pubmed Central PMCID: PMC1223948. Epub 2003/12/20. eng.
387. Cairns RA, Harris IS, Mak TW. Regulation of cancer cell metabolism. *Nature reviews Cancer*. 2011 Feb;11(2):85-95. PubMed PMID: 21258394. Epub 2011/01/25. eng.
388. Cuezva JM, Krajewska M, de Heredia ML, Krajewski S, Santamaria G, Kim H, et al. The bioenergetic signature of cancer: a marker of tumor progression. *Cancer research*. 2002 Nov 15;62(22):6674-81. PubMed PMID: 12438266. Epub 2002/11/20. eng.
389. Fogal V, Richardson AD, Karmali PP, Scheffler IE, Smith JW, Ruoslahti E. Mitochondrial p32 protein is a critical regulator of tumor metabolism via maintenance of oxidative phosphorylation. *Molecular and cellular biology*. 2010 Mar;30(6):1303-18. PubMed PMID: 20100866. Pubmed Central PMCID: PMC2832503. Epub 2010/01/27. eng.
390. Ericson NG, Kulawiec M, Vermulst M, Sheahan K, O'Sullivan J, Salk JJ, et al. Decreased mitochondrial DNA mutagenesis in human colorectal cancer. *PLoS genetics*. 2012;8(6):e1002689. PubMed PMID: 22685414. Pubmed Central PMCID: PMC3369930. Epub 2012/06/12. eng.

391. Suchorolski MT, Paulson TG, Sanchez CA, Hockenbery D, Reid BJ. Warburg and Crabtree effects in premalignant barrett's esophagus cell lines with active mitochondria. *PloS one*. 2013;8(2):e56884. PubMed PMID: 23460817. Pubmed Central PMCID: PMC3584058. Epub 2013/03/06. eng.
392. Koss K, Harrison RF, Gregory J, Darnton SJ, Anderson MR, Jankowski JA. The metabolic marker tumour pyruvate kinase type M2 (tumour M2-PK) shows increased expression along the metaplasia-dysplasia-adenocarcinoma sequence in Barrett's oesophagus. *Journal of clinical pathology*. 2004 Nov;57(11):1156-9. PubMed PMID: 15509675. Pubmed Central PMCID: PMC1770481. Epub 2004/10/29. eng.
393. Hjerpe E, Brage SE, Frostvik Stolt M, Johansson H, Shoshan M, Avall-Lundqvist E. Metabolic markers and HSP60 in chemo-naive serous solid ovarian cancer versus ascites. *International journal of gynecological cancer : official journal of the International Gynecological Cancer Society*. 2014 Oct;24(8):1389-94. PubMed PMID: 25188891. Epub 2014/09/05. eng.
394. De Meirleir L, Seneca S, Lissens W, De Clercq I, Eyskens F, Gerlo E, et al. Respiratory chain complex V deficiency due to a mutation in the assembly gene ATP12. *Journal of medical genetics*. 2004 Feb;41(2):120-4. PubMed PMID: 14757859. Pubmed Central PMCID: PMC1735674. Epub 2004/02/06. eng.
395. Streif D, Iglseider E, Hauser-Kronberger C, Fink KG, Jakab M, Ritter M. Expression of the non-gastric H⁺/K⁺ ATPase ATP12A in normal and pathological human prostate tissue. *Cellular physiology and biochemistry : international journal of experimental cellular physiology, biochemistry, and pharmaco*. 2011;28(6):1287-94. PubMed PMID: 22179016. Epub 2011/12/20. eng.
396. Huttemann M, Lee I, Gao X, Pecina P, Pecinova A, Liu J, et al. Cytochrome c oxidase subunit 4 isoform 2-knockout mice show reduced enzyme activity, airway hyporeactivity, and lung pathology. *FASEB journal : official publication of the Federation of American Societies for Experimental Biology*. 2012 Sep;26(9):3916-30. PubMed PMID: 22730437. Pubmed Central PMCID: PMC3425824. Epub 2012/06/26. eng.
397. Baracca A, Chiaradonna F, Sgarbi G, Solaini G, Alberghina L, Lenaz G. Mitochondrial Complex I decrease is responsible for bioenergetic dysfunction in K-ras transformed cells. *Biochimica et biophysica acta*. 2010 Feb;1797(2):314-23. PubMed PMID: 19931505. Epub 2009/11/26. eng.
398. Bonora E, Porcelli AM, Gasparre G, Biondi A, Ghelli A, Carelli V, et al. Defective oxidative phosphorylation in thyroid oncocyctic carcinoma is associated with pathogenic mitochondrial DNA mutations affecting complexes I and III. *Cancer research*. 2006 Jun 15;66(12):6087-96. PubMed PMID: 16778181. Epub 2006/06/17. eng.
399. Simonnet H, Alazard N, Pfeiffer K, Gallou C, Beroud C, Demont J, et al. Low mitochondrial respiratory chain content correlates with tumor aggressiveness in renal cell carcinoma. *Carcinogenesis*. 2002 May;23(5):759-68. PubMed PMID: 12016148. Epub 2002/05/23. eng.
400. Simonnet H, Demont J, Pfeiffer K, Guenaneche L, Bouvier R, Brandt U, et al. Mitochondrial complex I is deficient in renal oncocytomas. *Carcinogenesis*. 2003 Sep;24(9):1461-6. PubMed PMID: 12844484. Epub 2003/07/08. eng.
401. Hudson EK, Hogue BA, Souza-Pinto NC, Croteau DL, Anson RM, Bohr VA, et al. Age-associated change in mitochondrial DNA damage. *Free radical research*. 1998 Dec;29(6):573-9. PubMed PMID: 10098461. Epub 1999/03/31. eng.

402. Ortega AD, Sanchez-Arago M, Giner-Sanchez D, Sanchez-Cenizo L, Willers I, Cuezva JM. Glucose avidity of carcinomas. *Cancer letters*. 2009 Apr 18;276(2):125-35. PubMed PMID: 18790562. Epub 2008/09/16. eng.
403. Isidoro A, Casado E, Redondo A, Acebo P, Espinosa E, Alonso AM, et al. Breast carcinomas fulfill the Warburg hypothesis and provide metabolic markers of cancer prognosis. *Carcinogenesis*. 2005 Dec;26(12):2095-104. PubMed PMID: 16033770. Epub 2005/07/22. eng.
404. Whitaker-Menezes D, Martinez-Outschoorn UE, Flomenberg N, Birbe RC, Witkiewicz AK, Howell A, et al. Hyperactivation of oxidative mitochondrial metabolism in epithelial cancer cells in situ: visualizing the therapeutic effects of metformin in tumor tissue. *Cell cycle (Georgetown, Tex)*. 2011 Dec 1;10(23):4047-64. PubMed PMID: 22134189. Pubmed Central PMCID: PMC3272287. Epub 2011/12/03. eng.
405. Cornford PA, Dodson AR, Parsons KF, Desmond AD, Woolfenden A, Fordham M, et al. Heat shock protein expression independently predicts clinical outcome in prostate cancer. *Cancer research*. 2000 Dec 15;60(24):7099-105. PubMed PMID: 11156417. Epub 2001/01/13. eng.
406. Ruan W, Wang Y, Ma Y, Xing X, Lin J, Cui J, et al. HSP60, a protein downregulated by IGFBP7 in colorectal carcinoma. *Journal of experimental & clinical cancer research : CR*. 2010;29:41. PubMed PMID: 20433702. Pubmed Central PMCID: PMC2873425. Epub 2010/05/04. eng.
407. Thomas X, Campos L, Mounier C, Cornillon J, Flandrin P, Le QH, et al. Expression of heat-shock proteins is associated with major adverse prognostic factors in acute myeloid leukemia. *Leukemia research*. 2005 Sep;29(9):1049-58. PubMed PMID: 16038731. Epub 2005/07/26. eng.
408. Yao F, Zhao T, Zhong C, Zhu J, Zhao H. LDHA is necessary for the tumorigenicity of esophageal squamous cell carcinoma. *Tumour biology : the journal of the International Society for Oncodevelopmental Biology and Medicine*. 2013 Feb;34(1):25-31. PubMed PMID: 22961700. Epub 2012/09/11. eng.
409. Liu J, Wang LD, Sun YB, Li EM, Xu LY, Zhang YP, et al. Deciphering the signature of selective constraints on cancerous mitochondrial genome. *Molecular biology and evolution*. 2012 Apr;29(4):1255-61. PubMed PMID: 22130971. Epub 2011/12/02. eng.
410. Villena JA, Martin I, Vinas O, Cormand B, Iglesias R, Mampel T, et al. ETS transcription factors regulate the expression of the gene for the human mitochondrial ATP synthase beta-subunit. *The Journal of biological chemistry*. 1994 Dec 23;269(51):32649-54. PubMed PMID: 7798271. Epub 1994/12/23. eng.
411. Verschoor ML, Wilson LA, Verschoor CP, Singh G. Ets-1 regulates energy metabolism in cancer cells. *PloS one*. 2010;5(10):e13565. PubMed PMID: 21042593. Pubmed Central PMCID: PMC2962648. Epub 2010/11/03. eng.
412. Drahos J, Xiao Q, Risch HA, Freedman ND, Abnet CC, Anderson LA, et al. Age-specific risk factor profiles of adenocarcinomas of the esophagus: A pooled analysis from the international BEACON consortium. *International journal of cancer Journal international du cancer*. 2015 Jul 14. PubMed PMID: 26175109. Epub 2015/07/16. Eng.
413. Burnat G, Majka J, Konturek PC. Bile acids are multifunctional modulators of the Barrett's carcinogenesis. *Journal of physiology and pharmacology : an official journal of the Polish Physiological Society*. 2010 Apr;61(2):185-92. PubMed PMID: 20436219. Epub 2010/05/04. eng.
414. Liu X, Wong A, Kadri SR, Corovic A, O'Donovan M, Lao-Sirieix P, et al. Gastro-esophageal reflux disease symptoms and demographic factors as a pre-screening tool for Barrett's esophagus.

PloS one. 2014;9(4):e94163. PubMed PMID: 24736597. Pubmed Central PMCID: PMC3988048. Epub 2014/04/17. eng.

415. Falk GW. Gastroesophageal reflux disease and Barrett's esophagus. *Endoscopy*. 2001 Feb;33(2):109-18. PubMed PMID: 11272213. Epub 2001/03/29. eng.

416. Flejou JF. Barrett's oesophagus: from metaplasia to dysplasia and cancer. *Gut*. 2005 Mar;54 Suppl 1:i6-12. PubMed PMID: 15711008. Pubmed Central PMCID: PMC1867794. Epub 2005/02/16. eng.

417. Menges M, Muller M, Zeitz M. Increased acid and bile reflux in Barrett's esophagus compared to reflux esophagitis, and effect of proton pump inhibitor therapy. *The American journal of gastroenterology*. 2001 Feb;96(2):331-7. PubMed PMID: 11232672. Epub 2001/03/10. eng.

418. Martinez JD, Stratagoules ED, LaRue JM, Powell AA, Gause PR, Craven MT, et al. Different bile acids exhibit distinct biological effects: the tumor promoter deoxycholic acid induces apoptosis and the chemopreventive agent ursodeoxycholic acid inhibits cell proliferation. *Nutrition and cancer*. 1998;31(2):111-8. PubMed PMID: 9770722. Epub 1998/10/15. eng.

419. Peng S, Huo X, Rezaei D, Zhang Q, Zhang X, Yu C, et al. In Barrett's esophagus patients and Barrett's cell lines, ursodeoxycholic acid increases antioxidant expression and prevents DNA damage by bile acids. *American journal of physiology Gastrointestinal and liver physiology*. 2014 Jul 15;307(2):G129-39. PubMed PMID: 24852569. Pubmed Central PMCID: PMC4101678. Epub 2014/05/24. eng.

420. Capello A, Moons LM, Van de Winkel A, Siersema PD, van Dekken H, Kuipers EJ, et al. Bile acid-stimulated expression of the farnesoid X receptor enhances the immune response in Barrett esophagus. *The American journal of gastroenterology*. 2008 Jun;103(6):1510-6. PubMed PMID: 18510604. Epub 2008/05/31. eng.

421. Dunbar KB, Souza RF, Spechler SJ. The Effect of Proton Pump Inhibitors on Barrett's Esophagus. *Gastroenterology clinics of North America*. 2015 Jun;44(2):415-24. PubMed PMID: 26021202. Epub 2015/05/30. eng.

422. Singh S, Garg SK, Singh PP, Iyer PG, El-Serag HB. Acid-suppressive medications and risk of oesophageal adenocarcinoma in patients with Barrett's oesophagus: a systematic review and meta-analysis. *Gut*. 2014 Aug;63(8):1229-37. PubMed PMID: 24221456. Pubmed Central PMCID: PMC4199831. Epub 2013/11/14. eng.

423. Nguyen DM, Richardson P, El-Serag HB. Medications (NSAIDs, statins, proton pump inhibitors) and the risk of esophageal adenocarcinoma in patients with Barrett's esophagus. *Gastroenterology*. 2010 Jun;138(7):2260-6. PubMed PMID: 20188100. Pubmed Central PMCID: PMC2883678. Epub 2010/03/02. eng.

424. Hillman LC, Chiragakis L, Shadbolt B, Kaye GL, Clarke AC. Effect of proton pump inhibitors on markers of risk for high-grade dysplasia and oesophageal cancer in Barrett's oesophagus. *Alimentary pharmacology & therapeutics*. 2008 Feb 15;27(4):321-6. PubMed PMID: 18047565. Epub 2007/12/01. eng.

425. van Staa TP, de Vries F, Leufkens HG. Gastric acid-suppressive agents and risk of *Clostridium difficile*-associated disease. *Jama*. 2006 Jun 14;295(22):2599; author reply 600-1. PubMed PMID: 16772618. Epub 2006/06/15. eng.

426. Corley DA, Kubo A, Zhao W, Quesenberry C. Proton pump inhibitors and histamine-2 receptor antagonists are associated with hip fractures among at-risk patients. *Gastroenterology*.

- 2010 Jul;139(1):93-101. PubMed PMID: 20353792. Pubmed Central PMCID: PMC2902649. Epub 2010/04/01. eng.
427. Marino ML, Fais S, Djavaheri-Mergny M, Villa A, Meschini S, Lozupone F, et al. Proton pump inhibition induces autophagy as a survival mechanism following oxidative stress in human melanoma cells. *Cell death & disease*. 2010;1:e87. PubMed PMID: 21368860. Pubmed Central PMCID: PMC3035900. Epub 2011/03/04. eng.
428. Phelan JJ, O'Hanlon C, Reynolds JV, O'Sullivan J. The role of energy metabolism in driving disease progression in inflammatory, hypoxic and angiogenic microenvironments. *Gastro Open Journal*. 2015;1(2):44-58.
429. Filiberti R, Fontana V, De Ceglie A, Bianchi S, Grossi E, Della Casa D, et al. Smoking as an independent determinant of Barrett's esophagus and, to a lesser degree, of reflux esophagitis. *Cancer causes & control : CCC*. 2015 Mar;26(3):419-29. PubMed PMID: 25555994. Epub 2015/01/04. eng.
430. Agrawal S, Patel P, Agrawal A, Makhijani N, Markert R, Deidrich W. Metformin use and the risk of esophageal cancer in Barrett esophagus. *Southern medical journal*. 2014 Dec;107(12):774-9. PubMed PMID: 25502158. Epub 2014/12/17. eng.
431. Yang L, Chaudhary N, Baghdadi J, Pei Z. Microbiome in reflux disorders and esophageal adenocarcinoma. *Cancer journal (Sudbury, Mass)*. 2014 May-Jun;20(3):207-10. PubMed PMID: 24855009. Pubmed Central PMCID: PMC4120752. Epub 2014/05/24. eng.
432. Gutierrez-Escobar AJ, Bayona-Rojas M, Barragan-Vidal C, Rojas-Lara S, Oliveros R. Metagenomic analysis of the gastric microbiota cultivable from a patient with gastritis concomitant with Barrett's esophagus. *Revista de gastroenterologia del Peru*. 2014 Jul;34(3):229-35. PubMed PMID: 25293992. Epub 2014/10/09. eng.
433. Amir I, Konikoff FM, Oppenheim M, Gophna U, Half EE. Gastric microbiota is altered in oesophagitis and Barrett's oesophagus and further modified by proton pump inhibitors. *Environmental microbiology*. 2014 Sep;16(9):2905-14. PubMed PMID: 24112768. Epub 2013/10/12. eng.
434. Horna Strand A, Franzen T. Influence of Life Style Factors on Barrett's Oesophagus. *Gastroenterology research and practice*. 2014;2014:408470. PubMed PMID: 24971090. Pubmed Central PMCID: PMC4058172. Epub 2014/06/28. eng.
435. Thrift AP, Cook MB, Vaughan TL, Anderson LA, Murray LJ, Whiteman DC, et al. Alcohol and the risk of Barrett's esophagus: a pooled analysis from the International BEACON Consortium. *The American journal of gastroenterology*. 2014 Oct;109(10):1586-94. PubMed PMID: 25047401. Pubmed Central PMCID: PMC4189971. Epub 2014/07/23. eng.
436. Lou Z, Xing H, Li D. Alcohol consumption and the neoplastic progression in Barrett's esophagus: a systematic review and meta-analysis. *PloS one*. 2014;9(10):e105612. PubMed PMID: 25299129. Pubmed Central PMCID: PMC4191954. Epub 2014/10/10. eng.
437. Nunez D, Chacin J. Effects of bile salts on energy metabolism and acid secretion by the isolated toad gastric mucosa. *Gastroenterology*. 1989 Jan;96(1):130-8. PubMed PMID: 2491820. Epub 1989/01/01. eng.
438. Sayin VI, Ibrahim MX, Larsson E, Nilsson JA, Lindahl P, Bergo MO. Science translational medicine. *Science translational medicine*. 2014 Jan 29;6(221):221ra15. PubMed PMID: 24477002. Epub 2014/01/31. eng.

439. Hwang JT, Kwon DY, Yoon SH. AMP-activated protein kinase: a potential target for the diseases prevention by natural occurring polyphenols. *New biotechnology*. 2009 Oct 1;26(1-2):17-22. PubMed PMID: 19818314. Epub 2009/10/13. eng.
440. Beltz LA, Bayer DK, Moss AL, Simet IM. Mechanisms of cancer prevention by green and black tea polyphenols. *Anti-cancer agents in medicinal chemistry*. 2006 Sep;6(5):389-406. PubMed PMID: 17017850. Epub 2006/10/05. eng.
441. Watson JT, Moawad FJ, Veerappan GR, Bassett JT, Maydonovitch CL, Horwhat JD, et al. The dose of omeprazole required to achieve adequate intraesophageal acid suppression in patients with gastroesophageal junction specialized intestinal metaplasia and Barrett's esophagus. *Digestive diseases and sciences*. 2013 Aug;58(8):2253-60. PubMed PMID: 23824407. Epub 2013/07/05. eng.
442. Miyashita T, Shah FA, Harmon JW, Marti GP, Matsui D, Okamoto K, et al. Do proton pump inhibitors protect against cancer progression in GERD? *Surgery today*. 2013 Aug;43(8):831-7. PubMed PMID: 23111465. Epub 2012/11/01. eng.
443. de Jonge PJ, Spaander MC, Bruno MJ, Kuipers EJ. Acid suppression and surgical therapy for Barrett's oesophagus. *Best practice & research Clinical gastroenterology*. 2015 Feb;29(1):139-50. PubMed PMID: 25743462. Epub 2015/03/07. eng.
444. Lapenna D, de Gioia S, Ciofani G, Festi D, Cuccurullo F. Antioxidant properties of omeprazole. *FEBS letters*. 1996 Mar 11;382(1-2):189-92. PubMed PMID: 8612750. Epub 1996/03/11. eng.
445. Blandizzi C, Fornai M, Colucci R, Natale G, Lubrano V, Vassalle C, et al. Lansoprazole prevents experimental gastric injury induced by non-steroidal anti-inflammatory drugs through a reduction of mucosal oxidative damage. *World journal of gastroenterology : WJG*. 2005 Jul 14;11(26):4052-60. PubMed PMID: 15996031. Pubmed Central PMCID: PMC4502102. Epub 2005/07/05. eng.
446. Yoshida N, Yoshikawa T, Tanaka Y, Fujita N, Kassai K, Naito Y, et al. A new mechanism for anti-inflammatory actions of proton pump inhibitors--inhibitory effects on neutrophil-endothelial cell interactions. *Alimentary pharmacology & therapeutics*. 2000 Apr;14 Suppl 1:74-81. PubMed PMID: 10807407. Epub 2000/05/12. eng.
447. Takagi T, Naito Y, Okada H, Ishii T, Mizushima K, Akagiri S, et al. Lansoprazole, a proton pump inhibitor, mediates anti-inflammatory effect in gastric mucosal cells through the induction of heme oxygenase-1 via activation of NF-E2-related factor 2 and oxidation of kelch-like ECH-associating protein 1. *The Journal of pharmacology and experimental therapeutics*. 2009 Oct;331(1):255-64. PubMed PMID: 19628634. Epub 2009/07/25. eng.
448. Maity P, Bindu S, Choubey V, Alam A, Mitra K, Goyal M, et al. Lansoprazole protects and heals gastric mucosa from non-steroidal anti-inflammatory drug (NSAID)-induced gastropathy by inhibiting mitochondrial as well as Fas-mediated death pathways with concurrent induction of mucosal cell renewal. *The Journal of biological chemistry*. 2008 May 23;283(21):14391-401. PubMed PMID: 18375387. Epub 2008/04/01. eng.
449. Ohta T, Tajima H, Yachie A, Yokoyama K, Elnemr A, Fushida S, et al. Activated lansoprazole inhibits cancer cell adhesion to extracellular matrix components. *International journal of oncology*. 1999 Jul;15(1):33-9. PubMed PMID: 10375591. Epub 1999/06/22. eng.
450. De Milito A, Marino ML, Fais S. A rationale for the use of proton pump inhibitors as antineoplastic agents. *Current pharmaceutical design*. 2012;18(10):1395-406. PubMed PMID: 22360553. Epub 2012/03/01. eng.

451. Zhang S, Wang Y, Li SJ. Lansoprazole induces apoptosis of breast cancer cells through inhibition of intracellular proton extrusion. *Biochemical and biophysical research communications*. 2014 Jun 13;448(4):424-9. PubMed PMID: 24802401. Epub 2014/05/08. eng.
452. Olsen LF, Andersen AZ, Lunding A, Brasen JC, Poulsen AK. Regulation of glycolytic oscillations by mitochondrial and plasma membrane H⁺-ATPases. *Biophysical journal*. 2009 May 6;96(9):3850-61. PubMed PMID: 19413991. Pubmed Central PMCID: PMC2711425. Epub 2009/05/06. eng.
453. Sharaiha RZ, Freedberg DE, Abrams JA, Wang YC. Cost-effectiveness of chemoprevention with proton pump inhibitors in Barrett's esophagus. *Digestive diseases and sciences*. 2014 Jun;59(6):1222-30. PubMed PMID: 24795040. Pubmed Central PMCID: PMC4315516. Epub 2014/05/06. eng.
454. Lee ES, Kim N, Lee SH, Park YS, Kim JW, Jeong SH, et al. Comparison of risk factors and clinical responses to proton pump inhibitors in patients with erosive oesophagitis and non-erosive reflux disease. *Alimentary pharmacology & therapeutics*. 2009 Jul 1;30(2):154-64. PubMed PMID: 19392871. Epub 2009/04/28. eng.
455. Murphy A. Development and functional validation of novel anti-angiogenic compounds for use in colorectal cancer using ex vivo human colorectal explants, zebrafish and mice: University College Dublin; 2013.
456. Collepriest BJ, Ward SG, Tosh D. How does inflammation cause Barrett's metaplasia? *Current opinion in pharmacology*. 2009 Dec;9(6):721-6. PubMed PMID: 19828375. Epub 2009/10/16. eng.
457. Torres C, Wang H, Turner J, Shahsafaei A, Odze RD. Prognostic significance and effect of chemoradiotherapy on microvessel density (angiogenesis) in esophageal Barrett's esophagus-associated adenocarcinoma and squamous cell carcinoma. *Human pathology*. 1999 Jul;30(7):753-8. PubMed PMID: 10414493. Epub 1999/07/22. eng.
458. Taddei A, Fabbroni V, Pini A, Lucarini L, Ringressi MN, Fantappie O, et al. Cyclooxygenase-2 and inflammation mediators have a crucial role in reflux-related esophageal histological changes and Barrett's esophagus. *Digestive diseases and sciences*. 2014 May;59(5):949-57. PubMed PMID: 24357184. Epub 2013/12/21. eng.
459. Zhang Q, Yu C, Peng S, Xu H, Wright E, Zhang X, et al. Autocrine VEGF signaling promotes proliferation of neoplastic Barrett's epithelial cells through a PLC-dependent pathway. *Gastroenterology*. 2014 Feb;146(2):461-72 e6. PubMed PMID: 24120473. Pubmed Central PMCID: PMC3899829. Epub 2013/10/15. eng.
460. Zampeli E, Karamanolis G, Morfopoulos G, Xirouchakis E, Kalampoki V, Michopoulos S, et al. Increased expression of VEGF, COX-2, and Ki-67 in Barrett's esophagus: does the length matter? *Digestive diseases and sciences*. 2012 May;57(5):1190-6. PubMed PMID: 22147251. Epub 2011/12/08. eng.
461. Griffiths EA, Pritchard SA, McGrath SM, Valentine HR, Price PM, Welch IM, et al. Increasing expression of hypoxia-inducible proteins in the Barrett's metaplasia-dysplasia-adenocarcinoma sequence. *British journal of cancer*. 2007 May 7;96(9):1377-83. PubMed PMID: 17437013. Pubmed Central PMCID: PMC2360174. Epub 2007/04/18. eng.
462. Zhang HY, Zhang Q, Zhang X, Yu C, Huo X, Cheng E, et al. Cancer-related inflammation and Barrett's carcinogenesis: interleukin-6 and STAT3 mediate apoptotic resistance in transformed Barrett's cells. *American journal of physiology Gastrointestinal and liver physiology*. 2011 Mar;300(3):G454-60. PubMed PMID: 21148399. Pubmed Central PMCID: PMC3064115. Epub 2010/12/15. eng.

463. Moriyama N, Amano Y, Mishima Y, Okita K, Takahashi Y, Yuki T, et al. What is the clinical significance of stromal angiogenesis in Barrett's esophagus? *Journal of gastroenterology and hepatology*. 2008 Dec;23 Suppl 2:S210-5. PubMed PMID: 19120900. Epub 2009/01/16. eng.
464. Duggan C, Onstad L, Hardikar S, Blount PL, Reid BJ, Vaughan TL. Association between markers of obesity and progression from Barrett's esophagus to esophageal adenocarcinoma. *Clinical gastroenterology and hepatology : the official clinical practice journal of the American Gastroenterological Association*. 2013 Aug;11(8):934-43. PubMed PMID: 23466711. Pubmed Central PMCID: PMC3722274. Epub 2013/03/08. eng.
465. Rubenstein JH, Dahlkemper A, Kao JY, Zhang M, Morgenstern H, McMahon L, et al. A pilot study of the association of low plasma adiponectin and Barrett's esophagus. *The American journal of gastroenterology*. 2008 Jun;103(6):1358-64. PubMed PMID: 18510610. Epub 2008/05/31. eng.
466. Cheng KK, Sharp L, McKinney PA, Logan RF, Chilvers CE, Cook-Mozaffari P, et al. A case-control study of oesophageal adenocarcinoma in women: a preventable disease. *British journal of cancer*. 2000 Jul;83(1):127-32. PubMed PMID: 10883680. Pubmed Central PMCID: PMC2374528. Epub 2000/07/07. eng.
467. Wei EK, Giovannucci E, Fuchs CS, Willett WC, Mantzoros CS. Low plasma adiponectin levels and risk of colorectal cancer in men: a prospective study. *Journal of the National Cancer Institute*. 2005 Nov 16;97(22):1688-94. PubMed PMID: 16288122. Epub 2005/11/17. eng.
468. Straus DS. TNFalpha and IL-17 cooperatively stimulate glucose metabolism and growth factor production in human colorectal cancer cells. *Molecular cancer*. 2013;12:78. PubMed PMID: 23866118. Pubmed Central PMCID: PMC3725176. Epub 2013/07/20. eng.
469. Avidan B, Sonnenberg A, Schnell TG, Chejfec G, Metz A, Sontag SJ. Hiatal hernia size, Barrett's length, and severity of acid reflux are all risk factors for esophageal adenocarcinoma. *The American journal of gastroenterology*. 2002 Aug;97(8):1930-6. PubMed PMID: 12190156. Epub 2002/08/23. eng.
470. Gatenby PA, Caygill CP, Ramus JR, Charlett A, Fitzgerald RC, Watson A. Short segment columnar-lined oesophagus: an underestimated cancer risk? A large cohort study of the relationship between Barrett's columnar-lined oesophagus segment length and adenocarcinoma risk. *European journal of gastroenterology & hepatology*. 2007 Nov;19(11):969-75. PubMed PMID: 18049166. Epub 2007/12/01. eng.
471. Chatterjee S, Thyagarajan K, Kesarwani P, Song JH, Soloshchenko M, Fu J, et al. Reducing CD73 expression by IL1beta-Programmed Th17 cells improves immunotherapeutic control of tumors. *Cancer research*. 2014 Nov 1;74(21):6048-59. PubMed PMID: 25205101. Pubmed Central PMCID: PMC4216762. Epub 2014/09/11. eng.
472. Swinson DE, Jones JL, Richardson D, Wykoff C, Turley H, Pastorek J, et al. Carbonic anhydrase IX expression, a novel surrogate marker of tumor hypoxia, is associated with a poor prognosis in non-small-cell lung cancer. *Journal of clinical oncology*. 2003 Feb 1;21(3):473-82. PubMed PMID: 12560438. Epub 2003/02/01. eng.
473. Mimura I, Tanaka T, Wada Y, Kodama T, Nangaku M. Pathophysiological response to hypoxia - from the molecular mechanisms of malady to drug discovery: epigenetic regulation of the hypoxic response via hypoxia-inducible factor and histone modifying enzymes. *Journal of pharmacological sciences*. 2011;115(4):453-8. PubMed PMID: 21422728. Epub 2011/03/23. eng.
474. Baltaziak M, Wincewicz A, Kanczuga-Koda L, Lotowska JM, Koda M, Sulkowska U, et al. The relationships between hypoxia-dependent markers: HIF-1alpha, EPO and EPOR in colorectal cancer. *Folia histochemica et cytobiologica*. 2013;51(4):320-5. PubMed PMID: 24497137. Epub 2014/02/06. eng.

475. Mayer A, Schmidt M, Seeger A, Serras AF, Vaupel P, Schmidberger H. GLUT-1 expression is largely unrelated to both hypoxia and the Warburg phenotype in squamous cell carcinomas of the vulva. *BMC cancer*. 2014;14:760. PubMed PMID: 25306097. Pubmed Central PMCID: PMC4210616. Epub 2014/10/13. eng.
476. Jomrich G, Jesch B, Birner P, Schwameis K, Paireder M, Asari R, et al. Stromal expression of carbonic anhydrase IX in esophageal cancer. *Clinical & translational oncology*. 2014 Nov;16(11):966-72. PubMed PMID: 24737069. Epub 2014/04/17. eng.
477. Roberts AM, Watson IR, Evans AJ, Foster DA, Irwin MS, Ohh M. Suppression of hypoxia-inducible factor 2alpha restores p53 activity via Hdm2 and reverses chemoresistance of renal carcinoma cells. *Cancer research*. 2009 Dec 1;69(23):9056-64. PubMed PMID: 19920202. Pubmed Central PMCID: PMC2789194. Epub 2009/11/19. eng.
478. Bobryshev YV, Tran D, Killingsworth MC, Buckland M, Lord RV. Dendritic cells in Barrett's esophagus and esophageal adenocarcinoma. *Journal of gastrointestinal surgery : official journal of the Society for Surgery of the Alimentary Tract*. 2009 Jan;13(1):44-53. PubMed PMID: 18685901. Epub 2008/08/08. eng.
479. Mokrowiecka A, Daniel P, Jasinska A, Pietruczuk M, Pawlowski M, Szczesniak P, et al. Serum adiponectin, resistin, leptin concentration and central adiposity parameters in Barrett's esophagus patients with and without intestinal metaplasia in comparison to healthy controls and patients with GERD. *Hepato-gastroenterology*. 2012 Nov-Dec;59(120):2395-9. PubMed PMID: 22944288. Epub 2012/09/05. eng.
480. Blackard WG, Clore JN, Powers LP. A stimulatory effect of FFA on glycolysis unmasked in cells with impaired oxidative capacity. *The American journal of physiology*. 1990 Sep;259(3 Pt 1):E451-6. PubMed PMID: 2169202. Epub 1990/09/01. eng.
481. Cavazos DA, deGraffenried MJ, Apte SA, Bowers LW, Whelan KA, deGraffenried LA. Obesity promotes aerobic glycolysis in prostate cancer cells. *Nutrition and cancer*. 2014;66(7):1179-86. PubMed PMID: 25264717. Pubmed Central PMCID: PMC4198485. Epub 2014/09/30. eng.
482. Sparks LM, Xie H, Koza RA, Mynatt R, Hulver MW, Bray GA, et al. A high-fat diet coordinately downregulates genes required for mitochondrial oxidative phosphorylation in skeletal muscle. *Diabetes*. 2005 Jul;54(7):1926-33. PubMed PMID: 15983191. Epub 2005/06/29. eng.
483. Ronn T, Volkov P, Tornberg A, Elgzyri T, Hansson O, Eriksson KF, et al. Extensive changes in the transcriptional profile of human adipose tissue including genes involved in oxidative phosphorylation after a 6-month exercise intervention. *Acta physiologica (Oxford, England)*. 2014 May;211(1):188-200. PubMed PMID: 24495239. Epub 2014/02/06. eng.
484. Qiao L, Kinney B, Yoo HS, Lee B, Schaack J, Shao J. Adiponectin increases skeletal muscle mitochondrial biogenesis by suppressing mitogen-activated protein kinase phosphatase-1. *Diabetes*. 2012 Jun;61(6):1463-70. PubMed PMID: 22415879. Pubmed Central PMCID: PMC3357265. Epub 2012/03/15. eng.
485. Jeon MJ, Leem J, Ko MS, Jang JE, Park HS, Kim HS, et al. Mitochondrial dysfunction and activation of iNOS are responsible for the palmitate-induced decrease in adiponectin synthesis in 3T3L1 adipocytes. *Experimental & molecular medicine*. 2012 Sep 30;44(9):562-70. PubMed PMID: 22809900. Pubmed Central PMCID: PMC3465750. Epub 2012/07/20. eng.
486. Poehlmann A, Kuester D, Malfertheiner P, Guenther T, Roessner A. Inflammation and Barrett's carcinogenesis. *Pathology, research and practice*. 2012 May 15;208(5):269-80. PubMed PMID: 22541897. Epub 2012/05/01. eng.

487. Kawanishi S, Hiraku Y. Oxidative and nitrative DNA damage as biomarker for carcinogenesis with special reference to inflammation. *Antioxidants & redox signaling*. 2006 May-Jun;8(5-6):1047-58. PubMed PMID: 16771694. Epub 2006/06/15. eng.
488. Moons LM, Kusters JG, Bultman E, Kuipers EJ, van Dekken H, Tra WM, et al. Barrett's oesophagus is characterized by a predominantly humoral inflammatory response. *The Journal of pathology*. 2005 Nov;207(3):269-76. PubMed PMID: 16177953. Epub 2005/09/24. eng.
489. Lin WW, Karin M. A cytokine-mediated link between innate immunity, inflammation, and cancer. *The Journal of clinical investigation*. 2007 May;117(5):1175-83. PubMed PMID: 17476347. Pubmed Central PMCID: PMC1857251. Epub 2007/05/04. eng.
490. Moons LM, Kusters JG, van Delft JH, Kuipers EJ, Gottschalk R, Geldof H, et al. A pro-inflammatory genotype predisposes to Barrett's esophagus. *Carcinogenesis*. 2008 May;29(5):926-31. PubMed PMID: 18192685. Epub 2008/01/15. eng.
491. Greten FR, Eckmann L, Greten TF, Park JM, Li ZW, Egan LJ, et al. IKKbeta links inflammation and tumorigenesis in a mouse model of colitis-associated cancer. *Cell*. 2004 Aug 6;118(3):285-96. PubMed PMID: 15294155. Epub 2004/08/06. eng.
492. Morris CD, Armstrong GR, Bigley G, Green H, Attwood SE. Cyclooxygenase-2 expression in the Barrett's metaplasia-dysplasia-adenocarcinoma sequence. *The American journal of gastroenterology*. 2001 Apr;96(4):990-6. PubMed PMID: 11316217. Epub 2001/04/24. eng.
493. Song S, Guha S, Liu K, Buttar NS, Bresalier RS. COX-2 induction by unconjugated bile acids involves reactive oxygen species-mediated signalling pathways in Barrett's oesophagus and oesophageal adenocarcinoma. *Gut*. 2007 Nov;56(11):1512-21. PubMed PMID: 17604323. Pubmed Central PMCID: PMC2095641. Epub 2007/07/03. eng.
494. Hardikar S, Onstad L, Song X, Wilson AM, Montine TJ, Kratz M, et al. Inflammation and oxidative stress markers and esophageal adenocarcinoma incidence in a Barrett's esophagus cohort. *Cancer epidemiology, biomarkers & prevention*. 2014 Nov;23(11):2393-403. PubMed PMID: 25106775. Pubmed Central PMCID: PMC4221307. Epub 2014/08/12. eng.
495. Singh S, Sharma AN, Murad MH, Buttar NS, El-Serag HB, Katzka DA, et al. Central adiposity is associated with increased risk of esophageal inflammation, metaplasia, and adenocarcinoma: a systematic review and meta-analysis. *Clinical gastroenterology and hepatology : the official clinical practice journal of the American Gastroenterological Association*. 2013 Nov;11(11):1399-412 e7. PubMed PMID: 23707461. Pubmed Central PMCID: PMC3873801. Epub 2013/05/28. eng.
496. Tu S, Bhagat G, Cui G, Takaishi S, Kurt-Jones EA, Rickman B, et al. Overexpression of interleukin-1beta induces gastric inflammation and cancer and mobilizes myeloid-derived suppressor cells in mice. *Cancer cell*. 2008 Nov 4;14(5):408-19. PubMed PMID: 18977329. Pubmed Central PMCID: PMC2586894. Epub 2008/11/04. eng.
497. Ogiya K, Kawano T, Ito E, Nakajima Y, Kawada K, Nishikage T, et al. Lower esophageal palisade vessels and the definition of Barrett's esophagus. *Diseases of the esophagus*. 2008;21(7):645-9. PubMed PMID: 18459993. Epub 2008/05/08. eng.
498. Playford RJ. New British Society of Gastroenterology (BSG) guidelines for the diagnosis and management of Barrett's oesophagus. *Gut*. 2006 Apr;55(4):442. PubMed PMID: 16531521. Pubmed Central PMCID: PMC1856188. Epub 2006/03/15. eng.
499. DeMeester SR. Letter to the editor regarding "Definition of Barrett's esophagus: time for a rethink-is intestinal metaplasia dead?". *The American journal of gastroenterology*. 2010 May;105(5):1201-2; author reply 2-3. PubMed PMID: 20445513. Epub 2010/05/07. eng.

500. Odze RD, Maley CC. Neoplasia without dysplasia: lessons from Barrett esophagus and other tubal gut neoplasms. *Archives of pathology & laboratory medicine*. 2010 Jun;134(6):896-906. PubMed PMID: 20524867. Epub 2010/06/09. eng.
501. Takubo K, Aida J, Naomoto Y, Sawabe M, Arai T, Shiraishi H, et al. Cardiac rather than intestinal-type background in endoscopic resection specimens of minute Barrett adenocarcinoma. *Human pathology*. 2009 Jan;40(1):65-74. PubMed PMID: 18755496. Epub 2008/08/30. eng.
502. Stairs DB, Bayne LJ, Rhoades B, Vega ME, Waldron TJ, Kalabis J, et al. Deletion of p120-catenin results in a tumor microenvironment with inflammation and cancer that establishes it as a tumor suppressor gene. *Cancer cell*. 2011 Apr 12;19(4):470-83. PubMed PMID: 21481789. Pubmed Central PMCID: PMC3077713. Epub 2011/04/13. eng.
503. Yang XD, Ai W, Asfaha S, Bhagat G, Friedman RA, Jin G, et al. Histamine deficiency promotes inflammation-associated carcinogenesis through reduced myeloid maturation and accumulation of CD11b+Ly6G+ immature myeloid cells. *Nature medicine*. 2011 Jan;17(1):87-95. PubMed PMID: 21170045. Pubmed Central PMCID: PMC3075560. Epub 2010/12/21. eng.
504. Fitzgerald RC, Abdalla S, Onwuegbusi BA, Sirieix P, Saeed IT, Burnham WR, et al. Inflammatory gradient in Barrett's oesophagus: implications for disease complications. *Gut*. 2002 Sep;51(3):316-22. PubMed PMID: 12171950. Pubmed Central PMCID: PMC1773354. Epub 2002/08/13. eng.
505. Taylor DJ, Whitehead RJ, Evanson JM, Westmacott D, Feldmann M, Bertfield H, et al. Effect of recombinant cytokines on glycolysis and fructose 2,6-bisphosphate in rheumatoid synovial cells in vitro. *The Biochemical journal*. 1988 Feb 15;250(1):111-5. PubMed PMID: 3128273. Pubmed Central PMCID: PMC1148822. Epub 1988/02/15. eng.
506. Bird TA, Davies A, Baldwin SA, Saklatvala J. Interleukin 1 stimulates hexose transport in fibroblasts by increasing the expression of glucose transporters. *The Journal of biological chemistry*. 1990 Aug 15;265(23):13578-83. PubMed PMID: 2380175. Epub 1990/08/15. eng.
507. Berg S, Sappington PL, Guzik LJ, Delude RL, Fink MP. Proinflammatory cytokines increase the rate of glycolysis and adenosine-5'-triphosphate turnover in cultured rat enterocytes. *Critical care medicine*. 2003 Apr;31(4):1203-12. PubMed PMID: 12682494. Epub 2003/04/19. eng.
508. Abcouwer SF, Shanmugam S, Gomez PF, Shushanov S, Barber AJ, Lanoue KF, et al. Effect of IL-1beta on survival and energy metabolism of R28 and RGC-5 retinal neurons. *Investigative ophthalmology & visual science*. 2008 Dec;49(12):5581-92. PubMed PMID: 19037001. Epub 2008/11/28. eng.
509. Cillero-Pastor B, Ruiz-Romero C, Carames B, Lopez-Armada MJ, Blanco FJ. Proteomic analysis by two-dimensional electrophoresis to identify the normal human chondrocyte proteome stimulated by tumor necrosis factor alpha and interleukin-1beta. *Arthritis and rheumatism*. 2010 Mar;62(3):802-14. PubMed PMID: 20131227. Epub 2010/02/05. eng.
510. Izquierdo E, Cuevas VD, Fernandez-Arroyo S, Riera-Borrull M, Orta-Zavalza E, Joven J, et al. Reshaping of Human Macrophage Polarization through Modulation of Glucose Catabolic Pathways. *Journal of immunology (Baltimore, Md : 1950)*. 2015 Sep 1;195(5):2442-51. PubMed PMID: 26209622. Epub 2015/07/26. eng.
511. Sun W, Pang Y, Liu Z, Sun L, Liu B, Xu M, et al. Macrophage inflammasome mediates hyperhomocysteinemia-aggravated abdominal aortic aneurysm. *Journal of molecular and cellular cardiology*. 2015 Apr;81:96-106. PubMed PMID: 25680906. Epub 2015/02/15. eng.

512. Zhu L, Zhao Q, Yang T, Ding W, Zhao Y. Cellular metabolism and macrophage functional polarization. *International reviews of immunology*. 2015 Jan;34(1):82-100. PubMed PMID: 25340307. Epub 2014/10/24. eng.
513. Bobryshev YV, Lu J, Lord RV. Expression of C1q complement component in Barrett's esophagus and esophageal adenocarcinoma. *Journal of gastrointestinal surgery : official journal of the Society for Surgery of the Alimentary Tract*. 2010 Aug;14(8):1207-13. PubMed PMID: 20496011. Epub 2010/05/25. eng.
514. Miyashita T, Tajima H, Shah FA, Oshima M, Makino I, Nakagawara H, et al. Impact of inflammation-metaplasia-adenocarcinoma sequence and inflammatory microenvironment in esophageal carcinogenesis using surgical rat models. *Annals of surgical oncology*. 2014 Jun;21(6):2012-9. PubMed PMID: 24526548. Epub 2014/02/15. eng.
515. Edem DO. Palm oil: biochemical, physiological, nutritional, hematological, and toxicological aspects: a review. *Plant foods for human nutrition*. 2002 Fall;57(3-4):319-41. PubMed PMID: 12602939. Epub 2003/02/27. eng.
516. Rao CV, Hirose Y, Indranie C, Reddy BS. Modulation of experimental colon tumorigenesis by types and amounts of dietary fatty acids. *Cancer research*. 2001 Mar 1;61(5):1927-33. PubMed PMID: 11280748. Epub 2001/03/31. eng.
517. Davelaar AL, Calpe S, Lau L, Timmer MR, Visser M, Ten Kate FJ, et al. Aberrant TP53 detected by combining immunohistochemistry and DNA-FISH improves Barrett's esophagus progression prediction: a prospective follow-up study. *V*. 2015 Feb;54(2):82-90. PubMed PMID: 25284618. Epub 2014/10/07. eng.
518. Yu C, Huo X, Agoston AT, Zhang X, Theiss AL, Cheng E, et al. Mitochondrial STAT3 contributes to transformation of Barrett's epithelial cells that express oncogenic Ras in a p53-independent fashion. *American journal of physiology*. 2015 Aug 1;309(3):G146-61. PubMed PMID: 26045618. Pubmed Central PMCID: PMC4525109. Epub 2015/06/06. eng.
519. Marrache F, Tu SP, Bhagat G, Pendyala S, Osterreicher CH, Gordon S, et al. Overexpression of interleukin-1beta in the murine pancreas results in chronic pancreatitis. *Gastroenterology*. 2008 Oct;135(4):1277-87. PubMed PMID: 18789941. Pubmed Central PMCID: PMC2707078. Epub 2008/09/16. eng.
520. Asschert JG, Vellenga E, Hollema H, van der Zee AG, de Vries EG. Expression of macrophage colony-stimulating factor (M-CSF), interleukin-6, (IL-6), interleukin-1 beta (IL-1 beta), interleukin-11 (IL-11) and tumour necrosis factor-alpha (TNF-alpha) in p53-characterised human ovarian carcinomas. *European journal of cancer*. 1997 Nov;33(13):2246-51. PubMed PMID: 9470814. Epub 1998/02/21. eng.
521. Li BY, Mohanraj D, Olson MC, Moradi M, Twiggs L, Carson LF, et al. Human ovarian epithelial cancer cells cultures in vitro express both interleukin 1 alpha and beta genes. *Cancer Res*. 1992 Apr 15;52(8):2248-52. PubMed PMID: 1559228. Epub 1992/04/15. eng.
522. Schauer IG, Zhang J, Xing Z, Guo X, Mercado-Urbe I, Sood AK, et al. Interleukin-1beta promotes ovarian tumorigenesis through a p53/NF-kappaB-mediated inflammatory response in stromal fibroblasts. *Neoplasia (New York, NY)*. 2013 Apr;15(4):409-20. PubMed PMID: 23555186. Pubmed Central PMCID: PMC3612913. Epub 2013/04/05. eng.
523. Yahagi N, Shimano H, Matsuzaka T, Najima Y, Sekiya M, Nakagawa Y, et al. p53 Activation in adipocytes of obese mice. *The Journal of biological chemistry*. 2003 Jul 11;278(28):25395-400. PubMed PMID: 12734185. Epub 2003/05/08. eng.

524. Yokoyama M, Okada S, Nakagomi A, Moriya J, Shimizu I, Nojima A, et al. Inhibition of endothelial p53 improves metabolic abnormalities related to dietary obesity. *Cell reports*. 2014 Jun 12;7(5):1691-703. PubMed PMID: 24857662. Epub 2014/05/27. eng.
525. He Q, Gao Z, Yin J, Zhang J, Yun Z, Ye J. Regulation of HIF-1{alpha} activity in adipose tissue by obesity-associated factors: adipogenesis, insulin, and hypoxia. *American journal of physiology* 2011 May;300(5):E877-85. PubMed PMID: 21343542. Pubmed Central PMCID: PMC3093977. Epub 2011/02/24. eng.
526. Krishnan J, Danzer C, Simka T, Ukropec J, Walter KM, Kumpf S, et al. Dietary obesity-associated Hif1alpha activation in adipocytes restricts fatty acid oxidation and energy expenditure via suppression of the Sirt2-NAD+ system. *Genes & development*. 2012 Feb 1;26(3):259-70. PubMed PMID: 22302938. Pubmed Central PMCID: PMC3278893. Epub 2012/02/04. eng.
527. Hellwig-Burgel T, Rutkowski K, Metzen E, Fandrey J, Jelkmann W. Interleukin-1beta and tumor necrosis factor-alpha stimulate DNA binding of hypoxia-inducible factor-1. *Blood*. 1999 Sep 1;94(5):1561-7. PubMed PMID: 10477681. Epub 1999/09/09. eng.
528. Haddad JJ. Recombinant human interleukin (IL)-1 beta-mediated regulation of hypoxia-inducible factor-1 alpha (HIF-1 alpha) stabilization, nuclear translocation and activation requires an antioxidant/reactive oxygen species (ROS)-sensitive mechanism. *European cytokine network*. 2002 Apr-Jun;13(2):250-60. PubMed PMID: 12101082. Epub 2002/07/09. eng.
529. Jung YJ, Isaacs JS, Lee S, Trepel J, Neckers L. IL-1beta-mediated up-regulation of HIF-1alpha via an NFkappaB/COX-2 pathway identifies HIF-1 as a critical link between inflammation and oncogenesis. *FASEB journal*. 2003 Nov;17(14):2115-7. PubMed PMID: 12958148. Epub 2003/09/06. eng.
530. Frede S, Freitag P, Otto T, Heilmaier C, Fandrey J. The proinflammatory cytokine interleukin 1beta and hypoxia cooperatively induce the expression of adrenomedullin in ovarian carcinoma cells through hypoxia inducible factor 1 activation. *Cancer research*. 2005 Jun 1;65(11):4690-7. PubMed PMID: 15930287. Epub 2005/06/03. eng.
531. Barbera M, Fitzgerald RC. Cellular origin of Barrett's metaplasia and oesophageal stem cells. *Biochemical Society transactions*. 2010 Apr;38(2):370-3. PubMed PMID: 20298185. Epub 2010/03/20. eng.
532. Wang X, Ouyang H, Yamamoto Y, Kumar PA, Wei TS, Dagher R, et al. Residual embryonic cells as precursors of a Barrett's-like metaplasia. *Cell*. 2011 Jun 24;145(7):1023-35. PubMed PMID: 21703447. Pubmed Central PMCID: PMC3125107. Epub 2011/06/28. eng.
533. Leedham SJ, Preston SL, McDonald SA, Elia G, Bhandari P, Poller D, et al. Individual crypt genetic heterogeneity and the origin of metaplastic glandular epithelium in human Barrett's oesophagus. *Gut*. 2008 Aug;57(8):1041-8. PubMed PMID: 18305067. Pubmed Central PMCID: PMC2564832. Epub 2008/02/29. eng.
534. Kalabis J, Oyama K, Okawa T, Nakagawa H, Michaylira CZ, Stairs DB, et al. A subpopulation of mouse esophageal basal cells has properties of stem cells with the capacity for self-renewal and lineage specification. *The Journal of clinical investigation*. 2008 Dec;118(12):3860-9. PubMed PMID: 19033657. Pubmed Central PMCID: PMC2579884. Epub 2008/11/27. eng.
535. Yu WY, Slack JM, Tosh D. Conversion of columnar to stratified squamous epithelium in the developing mouse oesophagus. *Developmental biology*. 2005 Aug 1;284(1):157-70. PubMed PMID: 15992795. Epub 2005/07/05. eng.
536. Pavlides S, Whitaker-Menezes D, Castello-Cros R, Flomenberg N, Witkiewicz AK, Frank PG, et al. The reverse Warburg effect: aerobic glycolysis in cancer associated fibroblasts and the

tumor stroma. *Cell cycle* (Georgetown, Tex). 2009 Dec;8(23):3984-4001. PubMed PMID: 19923890. Epub 2009/11/20. eng.

537. Weinhouse S. The Warburg hypothesis fifty years later. *Zeitschrift fur Krebsforschung und klinische Onkologie Cancer research and clinical oncology*. 1976;87(2):115-26. PubMed PMID: 136820. Epub 1976/01/01. eng.

538. Senyilmaz D, Teleman AA. Chicken or the egg: Warburg effect and mitochondrial dysfunction. *F1000prime reports*. 2015;7:41. PubMed PMID: 26097714. Pubmed Central PMCID: PMC4447048. Epub 2015/06/23. eng.

539. Ferreira A, Serafim TL, Sardao VA, Cunha-Oliveira T. Role of mtDNA-related mitoeipigenetic phenomena in cancer. *European journal of clinical investigation*. 2015 Jan;45 Suppl 1:44-9. PubMed PMID: 25524586. Epub 2014/12/20. eng.

540. Dvorak K, Payne CM, Chavarria M, Ramsey L, Dvorakova B, Bernstein H, et al. Bile acids in combination with low pH induce oxidative stress and oxidative DNA damage: relevance to the pathogenesis of Barrett's oesophagus. *Gut*. 2007 Jun;56(6):763-71. PubMed PMID: 17145738. Pubmed Central PMCID: PMC1954874. Epub 2006/12/06. eng.

541. Dvorakova K, Payne CM, Ramsey L, Bernstein H, Holubec H, Chavarria M, et al. Apoptosis resistance in Barrett's esophagus: ex vivo bioassay of live stressed tissues. *The American journal of gastroenterology*. 2005 Feb;100(2):424-31. PubMed PMID: 15667503. Epub 2005/01/26. eng.

542. Patra KC, Hay N. The pentose phosphate pathway and cancer. *Trends in biochemical sciences*. 2014 Aug;39(8):347-54. PubMed PMID: 25037503. Pubmed Central PMCID: PMC4329227. Epub 2014/07/20. eng.

543. Raimundo N, Baysal BE, Shadel GS. Revisiting the TCA cycle: signaling to tumor formation. *Trends in molecular medicine*. 2011 Nov;17(11):641-9. PubMed PMID: 21764377. Pubmed Central PMCID: PMC3205302. Epub 2011/07/19. eng.

544. Ruiz-Perez MV, Sanchez-Jimenez F, Alonso FJ, Segura JA, Marquez J, Medina MA. Glutamine, glucose and other fuels for cancer. *Current pharmaceutical design*. 2014;20(15):2557-79. PubMed PMID: 23859613. Epub 2013/07/19. eng.

545. Bansal A, Fitzgerald RC. Biomarkers in Barrett's Esophagus: Role in Diagnosis, Risk Stratification, and Prediction of Response to Therapy. *Gastroenterology clinics of North America*. 2015 Jun;44(2):373-90. PubMed PMID: 26021200. Epub 2015/05/30. eng.

546. Ong CA, Lao-Sirieix P, Fitzgerald RC. Biomarkers in Barrett's esophagus and esophageal adenocarcinoma: predictors of progression and prognosis. *World journal of gastroenterology*. 2010 Dec 7;16(45):5669-81. PubMed PMID: 21128316. Pubmed Central PMCID: PMC2997982. Epub 2010/12/04. eng.